From Glycosylations to Peptide Bond Formation: Studies Towards the Total Syntheses of the Nucleoside Antibiotic Amicetin and the Cyclopeptide Alkaloid Nummularine H

Lukas Leu

Diss. ETH No. 26234

Zurich 2019

DISS. ETH NO. 26234

From Glycosylations to Peptide Bond Formation: Studies Towards the Total Syntheses of the Nucleoside Antibiotic Amicetin and the Cyclopeptide Alkaloid Nummularine H

A thesis submitted to attain the degree of

DOCTOR OF SCIENCES of ETH ZURICH

(Dr. sc. ETH Zurich)

presented by

Lukas Leu

MSc ETH Zurich

born on 19.09.1989

citizen of Hohenrain LU, Switzerland

accepted on the recommendation of

Prof. Dr. Karl-Heinz Altmann

Prof. Dr. Antonio Togni

2019

“Curiosity is, in great and generous minds, the first passion and the last.”

William Samuel Johnson

DANKSAGUNG

Ich möchte mich ganz herzlich bei Herrn Prof. Dr. Karl-Heinz Altmann bedanken. Dank Ihm durfte ich mich während meinem Doktorat in einer spannenden Thematik vertiefen, mich selbständig weiterentwickeln und stets in einem guten Umfeld bewegen. Danke für die tolle Zeit.

Ich bedanke mich herzlich bei Herrn Prof. Dr. Togni für die Übernahmen des Korreferats und für die Examination meiner Dissertation.

Ein grosses Dankeschön geht an Kurt Hauenstein. Er bildet wortwörtlich das Rückgrat unserer Labors, hat stets alles im Griff und weiss für alles eine sichere und elegante technische Lösung. Nicht zu vergessen sind an dieser Stelle die Himbeer-Tiramisu, die seine Ehefrau Claudia uns ab und an vergönnte.

Während meines Doktorats durfte ich mit einer Handvoll tollen Leuten zusammen arbeiten und Freundschaften schliessen. Zu erwähnen sind hier die Mitstreiter aus dem H496: Adriana Edenharter, Leo Betschart und Patrick Eisenring. Wir haben viel geteilt - die Musik, die Leiden, die Freuden, den Kaffee und die Stunden. Eine Zeit, die mir immer in guter Erinnerung bleiben wird. Herzlichen Dank euch allen.

Die Jungs von der Rad-Front: Simon Glauser, Raffael Schrof und Simone Berardozzi waren nebst der Zeit im Labor auch auf der Strasse während einigen Stunden und Kilometern an meiner Seite. Dank euch weiss ich nun, wie man einen Schlauch wechselt, ich kann mir endlich die Schweizer Pässe merken, kenne den Hunger nach zwei Portionen Pasta und so vieles mehr. Wir hatten unglaublich gute Zeiten und ich freue mich auf zukünftige Ausfahrten mit euch allen!

Meine Dissertation durfte ich im Schreibraum H468 mit den Damen Maryline Dong und Melanie Zechner geniessen. Danke euch für die lebhaften Diskussionen, die gute Stimmung und das gemeinsame Durchhalten.

Ein weiteres Dankeschön geht an den ganzen hervorragenden Rest der Altmann-Gruppe. Ihr alle wart immer eine gute Gesellschaft, dank euch habe ich viel gelacht, Kuchen gegessen und gegen den Eich im Armdrücken verloren.

Nicht zu vergessen sind die Leute aus der Togni Gruppe, die einen grossen Anteil an meiner Zeit hier an der ETH mitgestaltet haben. So ist dies Jedi Meister Remo Senn, Barbara NMR Czarniecki und mein guter Boulder-Freund Carl-Philipp Rosenau.

Wegweisend und immer ein guter Freund war Gabriel Schäfer. Herzlichen Dank für deine Ratschläge und dein Wissen.

Ebenfalls bedanken möchte ich mich bei meinen fleissigen Studenten Viktoria Gerken und Yulia Yuts für ihre Bemühungen im Reich der Zucker-Synthese.

Ausserhalb der hochschulischen Gefielden gibt es einige Personen denen ein Dank an dieser Stelle zugesprochen werden soll. Meine Eltern Vreni und Josef Leu hatten mich während meinem ganzen «Studi-Leben» halbwegs durchgefüttert (den anderen Teil musste ich selbst beitragen). Mein Bruder Raffael hat stets dafür gesorgt, dass ich, wie er immer so schön sagte, sozialisiert bleibe und hat mich zu allen guten Taten immer mitgenommen. Ganz herzlichen Dank euch allen. Ebenfalls zur Familie gehören die Freunde Tarkan Özküp und Matthias Bürgler. Ihr beide habt die Zeit während meinem Doktorat äusserst bereichert, mitgelebt und zu einer wunderbaren Erfahrung gemacht. Eine bessere Unterstützung kann man sich nicht wünschen.

A special thank goes to Malu. You accompanied me in the most intense phase of my PhD, enriched my days, were always supportive and gave me many moments of joy. For this I am extremely thankful. Yellow Ledbetter.

Contents

1 Studies Towards the Total Synthesis of Amicetin (**A-1**) 1

1.1 Introduction 2

1.1.1 Isolation of Amicetin and First Biological Testing Results 2

1.1.2 Biosynthesis of Amicetin (**A-1**) 3

1.1.3 Tuberculosis 5

1.1.4 Natural Products in Drug Discovery 16

1.1.5 Natural Products in TB Drug Research 17

1.1.6 The Bacterial Ribosome as Target for Antibiotics 18

1.1.7 Nucleoside Antibiotics 26

1.1.8 Amicetin (**A-1**): Mode of Action 27

1.1.9 Relevant Synthetic Work 30

1.2 Aims and Scope 35

1.3 Results and Discussion 36

1.3.1 General Retrosynthetic Considerations 36

1.3.2 Oxazolidine Fragment **A-55** 38

1.3.3 Pyrimidylbenzamide Fragment **A-75** 39

1.3.4 Ullmann Coupling and Deprotection to Access Cytimidine (**A-53**) 42

1.3.5 Sequential Approach 43

1.3.6 Disaccharide Approach 68

1.3.7 Ester Analogues of Amicetin (**A-1**) 81

1.4 Conclusion and Outlook 85

1.4.1 Future Potential 86

2 Studies Towards the Total Synthesis of Nummularine H (**N-1**) 89

2.1 Introduction 90

2.1.1 Cyclopeptide Alkaloids 90

2.1.2 Isolation of Nummularine H (**N-1**) and Biological Activity 91

2.1.3 Relevant Synthetic Work 92
2.2 Aims and Scope 97
2.3 Results and Discussion 98
2.3.1 Ynamide Approach 98
2.3.2 Late Stage Dehydration Approach 106
2.4 Conclusion and Outlook 114
3 Experimental 117
3.1 General Methods 118
3.2 Preparations and Analytical Data 120
3.2.1 Amicetin (**A-1**) 120
3.2.2 Nummularine H (**N-1**) 298
4 Bibliography 343
5 Curriculum Vitae 361

ABSTRACT

The nucleoside antibiotic amicetin (**I**) was first isolated in 1953 from *Streptomyces vinaceus-drappus* by *DeBoer*. In a first *in vitro* testing, the compound was shown to inhibit the growth of certain acid-fast and Gram-positive bacteria. Follow-up studies also demonstrated that **I** was active *in vivo* against *Mycobacterium tuberculosis* H37Rv in mice. Amicetin (**I**) inhibits protein biosynthesis through binding to the 23S rRNA region within the peptidyl transferase centre (PTC) located at the large prokaryotic ribosomal subunit. A recently published crystal structure of the antibiotic bound to the 70S ribosome unambiguously established its binding site.

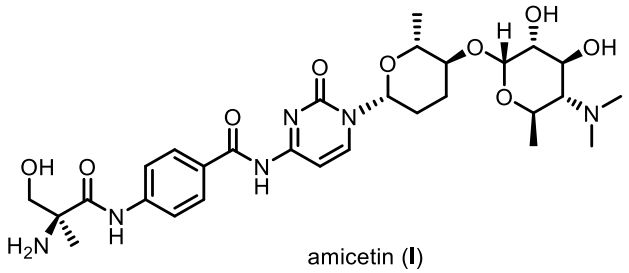

amicetin (**I**)

It was both its the biological activity and its intriguing structural features that led us to embark on the total synthesis of **I**. The synthesis commenced with the elaboration of building blocks **IV**, **V**, and various mono- or disaccharide derivatives (Scheme 1 and 2), which were subsequently assembled. Amide **IV** was synthesised in 6 steps from L-serine, entailing a selective condensation/protection to form the oxazolidine ring, followed by a substrate controlled alkylation. Solubility issues with the cytosine moiety were overcome by use of a PMB-protecting group on the pyrimidine ring, which was introduced by reaction of PMB-OH with the sulfone obtained by oxidation of thioether **III**.

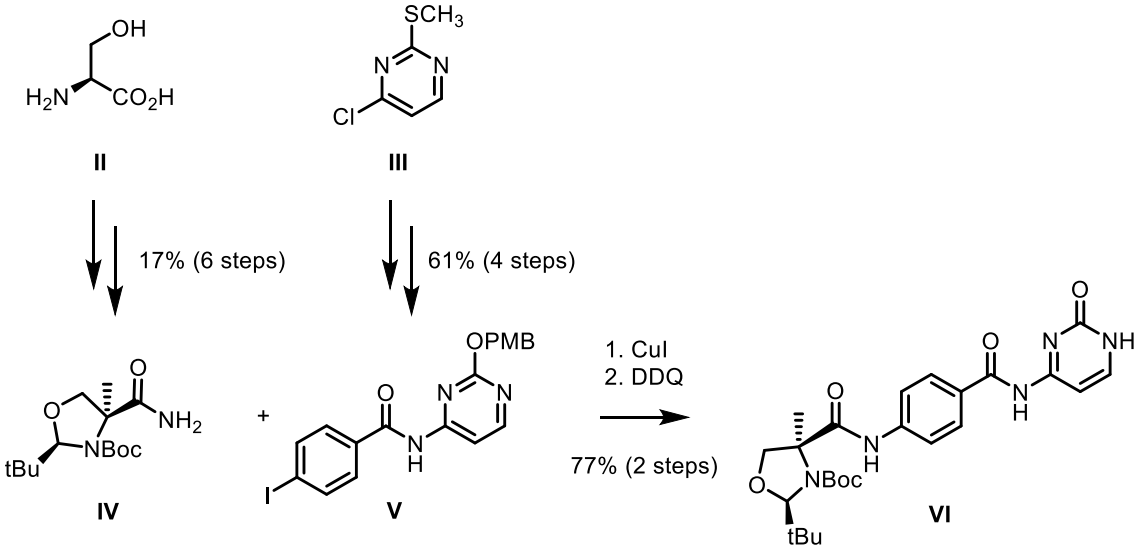

Scheme 1 Synthesis of aglycone **VI**.

The exocyclic nitrogen of the cytosine moiety originates from *p*-iodobenzylamide, which was introduced by an *Ullmann* coupling to give **V**. Building blocks **IV** and **V** were joined in a copper-catalysed coupling reaction and oxidative removal of the PMB group from the coupling product gave the aglycone **VI**.

The amicetose sugar **VIII** was accessed by *de novo* chemical synthesis, departing from (+)-ethyl D-lactate and establishing the tetrahydropyran ring by ring-closing olefin metathesis (RCM). In contrast, the amosamine derivative **X** was obtained from pyranose **IX**.

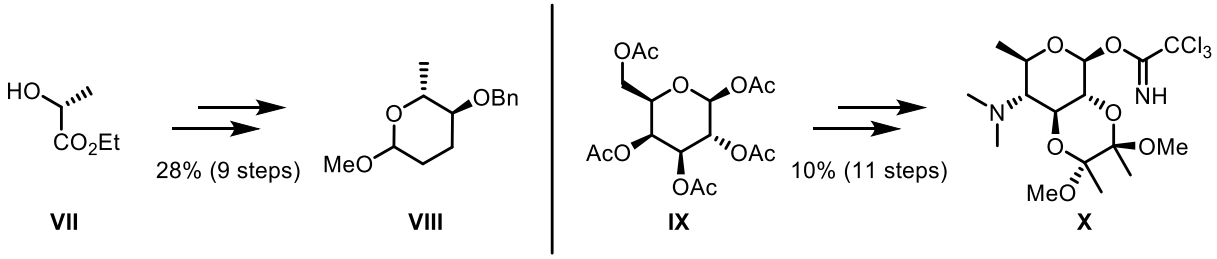

VII **VIII** **IX** **X**

Scheme 2 Synthesis of the pyranose derivatives amicetose and amosamine.

A key challenge for the synthesis of amicetin is the stereoselective introduction of the two glycosidic bonds. Amicetose derivative **VIII** was found to efficiently react under *Vorbrüggen* conditions with aglycone **VI** to give exclusive formation of the desired β-linked nucleoside **XI** (Scheme 3). The latter was then envisioned to be elaborated into fully protected amicetin (or an appropriate precursor) by glycosylation with a suitable glycosyl donor such as **XIII** (Scheme 3). In an alternative approach, **VI** was planned to be glycosylated directly with disaccharide **XII** which was accessed by a *Schmidt* glycosylation in excellent yields with 4:1 α:β-selectivity. Analysis of glycosylation reactions conducted with **XIII** and **XII** indicated that the desired glycosylation products were indeed formed, but, unfortunately these products could never be isolated in pure form. Various other glycosyl donor/acceptor systems investigated failed to deliver any product.

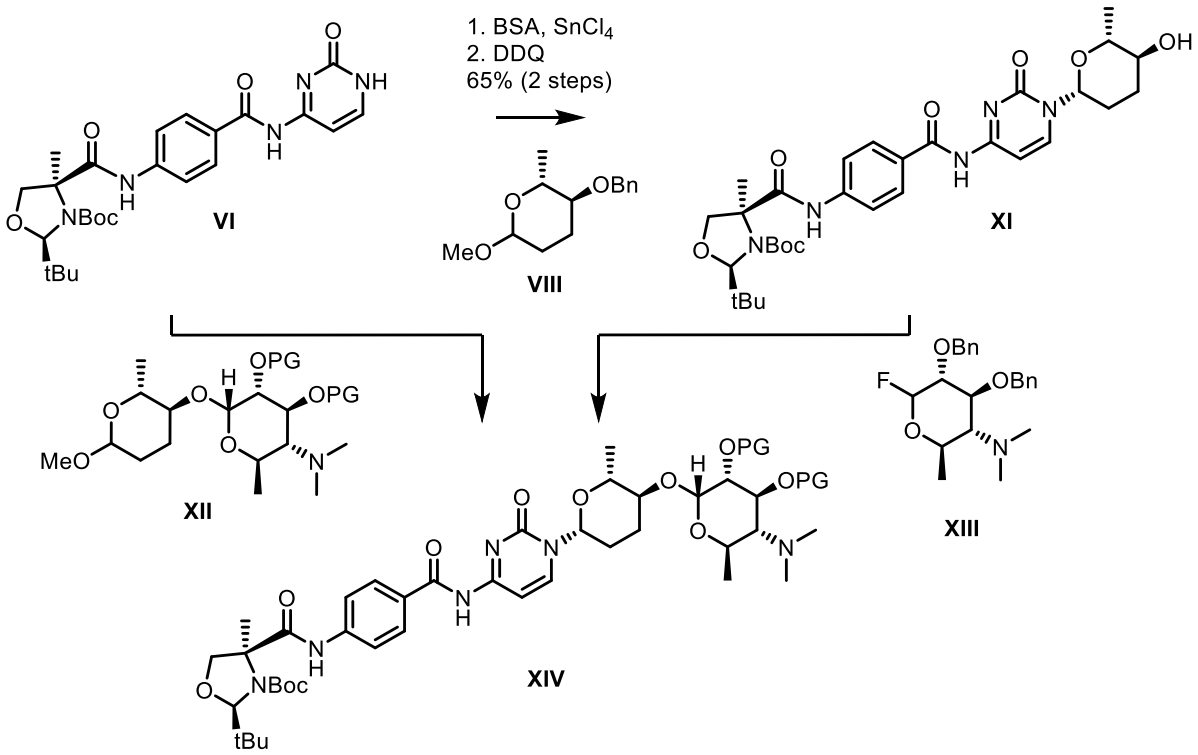

Scheme 3 Endgame towards amicetin comprising pivotal glycosylation reactions.

Monoglycoside **XI** could be successfully elaborated into ester analogues **XV** and **XVI**, thus demonstrating the feasibility of acid-promoted oxazolidine cleavage in the presence of the more labile glycosidic bond. Analog **XV** showed weak antimycobacterial activity, but given the flexible nature of the ester appendix there may be substantial room for improvement with more rigid structures.

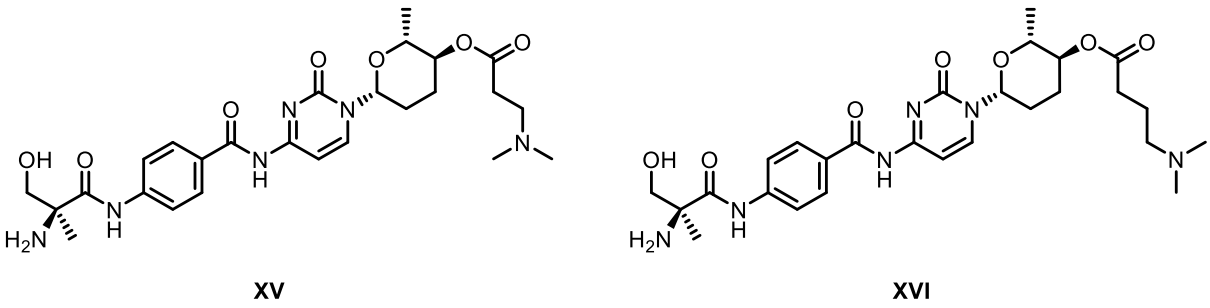

Figure 1 Accessed ester analogues exhibiting the free serine moiety.

The natural product nummularine H (**XVII**) belongs to the family of cyclopeptide alkaloids and comprises a 13-membered macrocyclic core structure. Its isolation from *Ziziphus nummularia* dates back to 1976, as part of a comprehensive isolation campaign for various cyclopeptide alkaloids. Nummularine H (**XVII**) was found to be active against *Mycobacterium tuberculosis* with an MIC value of 4.5 µM.

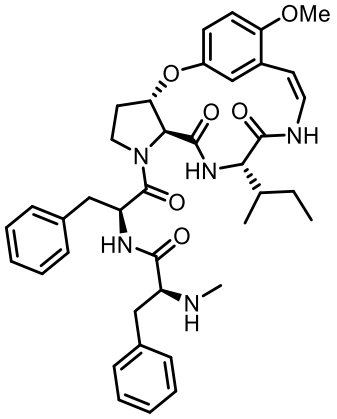

nummularine H (**XVII**)

The total synthesis of nummularine H (**XVII**) was a second objective of this PhD thesis, in order to enable its biological assessment and confirm its antimycobacterial activity as a basis for the potential synthesis of analogues and structure-activity-relationship studies. Two different approaches to form the macrocyclic core structure of **XVII** were examined which envisioned macrocyclic ring-closure through formation of the phenyl ether linkage either by *Mitsunobu* reaction (for **XIX**) or by nucleophilic aromatic substitution for (**XXI**) (Scheme 4).

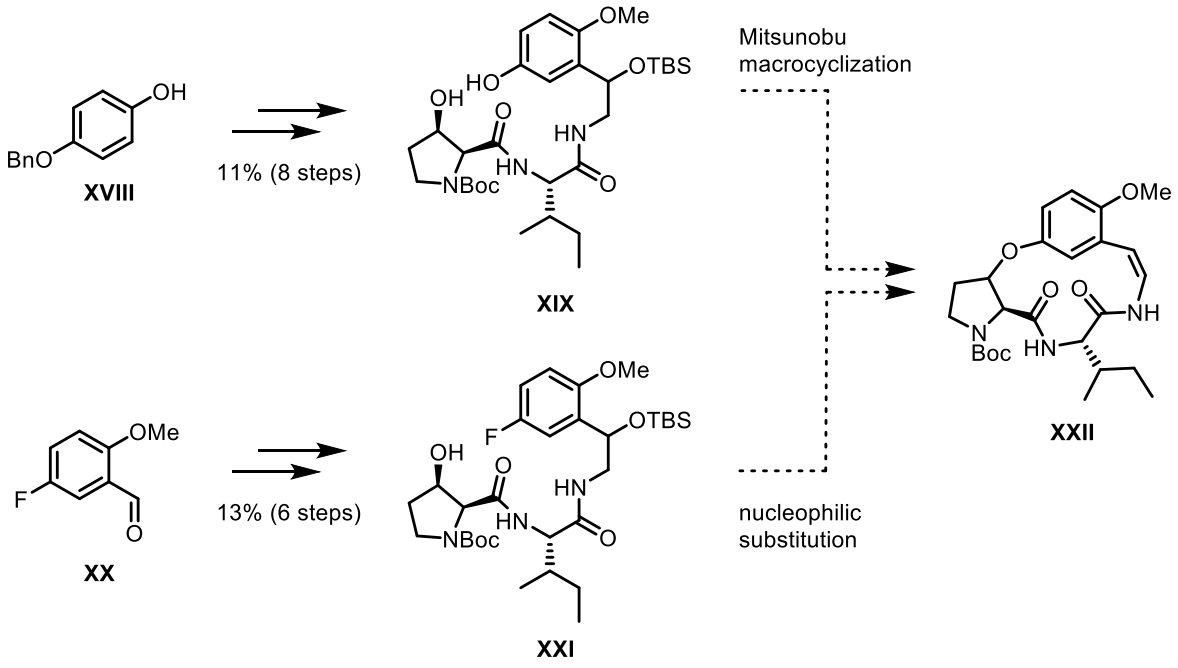

Scheme 4 Synthesis of the linear precursors and macrocyclization attempts.

In both cases, the requisite linear precursors were efficiently accessed departing from the substituted benzenes **XVIII** or **XX**. Despite various conditions analysed, a successful macrocyclization was shown to be unfeasible under the chosen conditions.

ZUSAMMENFASSUNG

Das Nukleosid Antibiotikum Amicetin (**I**) wurde 1953 erstmals aus *Streptomyces vinaceus-drappus* von *DeBoer* isoliert. In ersten *in vitro* Studien konnte gezeigt werden, dass die Verbindung das Wachstum bestimmter säurefester und grampositiver Bakterien hemmt. Nachfolgende *in vivo* Studien in Mäusen zeigten, dass **I** wirksam gegen *Mycobacterium tuberculosis* H37Rv ist. Amicetin (**I**) hemmt die Proteinbiosynthese durch Bindung an die 23S rRNA-Region innerhalb der Peptidyltransferase in der grossen prokaryotischen ribosomalen Untereinheit. Eine kürzlich veröffentlichte Kristallstruktur des an das 70S-Ribosom gebundenen Antibiotikums stellte eindeutig seine Bindungsstelle fest.

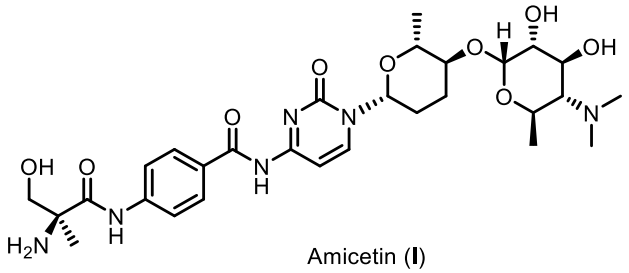

Amicetin (**I**)

Es waren sowohl die biologische Aktivität, als auch die faszinierenden strukturellen Eigenschaften, die uns zur Totalsynthese von **I** bewegt haben. Die Synthese begann mit der Ausarbeitung der Bausteine **IV**, **V** und verschiedener Mono-, oder Disaccharid Derivate (Schema 1 und Schema 2). Das Amid **IV** wurde in sechs Schritten, ausgehend von L-Serin, über eine selektive Kondensation/Schützung gefolgt von einer substrat-kontrollierten Alkylierung synthetisiert. Löslichkeitsprobleme mit dem Cytosin-Teil wurden durch die Verwendung einer PMB-Schutzgruppe am Pyrimidin-Ring umgangen. Die Schutzgruppe wurde durch die Reaktion zwischen PMB-OH und dem Sulfons, welches nach der Oxidation des Thioethers **III** erhalten wurde, eingebracht. Der exozyklische Stickstoff des Cytosins stammt aus *p*-Iodobenzylamid, das durch eine *Ullmann*-Kopplung eingeführt wurde. Dies führte erfolgreich zu Produkt **V**. Die Bausteine **IV** und **V** wurden durch eine kupferkatalysierte Kopplungreaktion verbunden und eine darauffolgende oxidative Entfernung der PMB-Schutzgruppe ergab das gewünschte Aglykon **VI**.

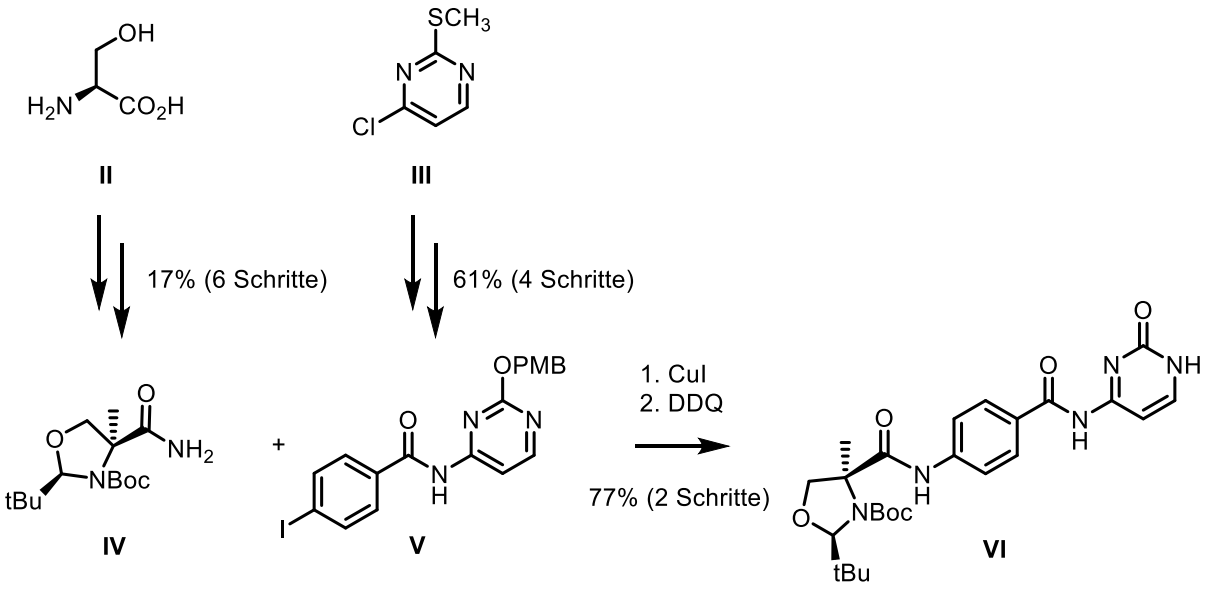

Schema 1 Synthese des Aglycons **VI**.

Amicetose **VIII** wurde durch eine *de novo* Synthese, ausgehend von (+)-Ethyl D-lactat erhalten, wobei der Tetrahydropyran Ring durch eine Ringschlussmetathese synthetisiert wurde. Im Gegensatz dazu, wurde Amosamine **X** aus der Pyranose **IX** hergestellt.

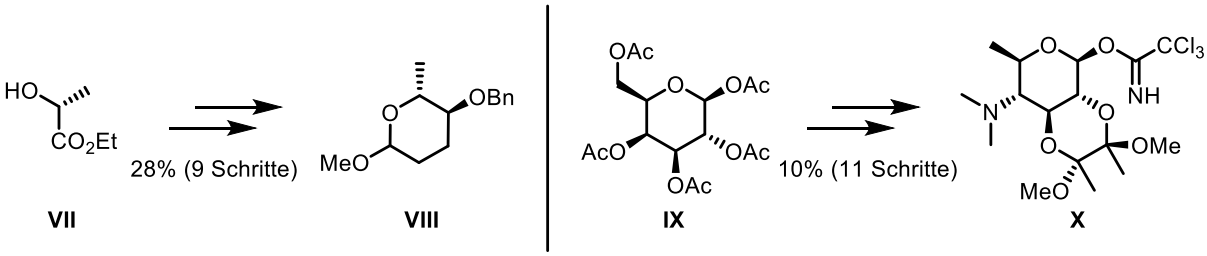

Schema 2 Synthese der Pyranose Derivate Amicetose und Amosamine.

Eine zentrale Herausforderung in der Synthese von Amicetin ist die stereoselektive Einführung der beiden glykosidischen Bindungen. Amicetose Derivat **VIII** konnte wirksam mittels *Vorbrüggen* Konditionen mit dem Aglykon **VI** verknüpft werden und gab ausschliesslich das gewünschte β-Nukleosid **XI** (Schema 3). Letzeres sollte durch eine weitere Glykosylierung mit einem geeigneten Baustein wie **XIII**, in das geschützte Amicetin (oder einen geeignetem Vorläufer) überführt werden (Schema 3). In einem alternativen Ansatz sollte **VI** direkt mit dem Disaccharid Baustein **XII** glykosyliert werden. Das erwähnte Disaccharid **XII** wurde erfolgreich durch eine *Schmidt* Glykosylierung in hervorragender Ausbeute und einer α:β-Selektivität von 4:1 hergestellt. Ein genäueres Betrachten der Glykosylierungsreaktionen, welche mit **XII** und **XIII** durchgeführt wurden, wies auf die Entstehung der gewünschten Produkte hin, welche leider jedoch nie in reiner Form isoliert werden konnten. Verschiedene andere untersuchte Glykosyl Donor/Acceptor Systeme scheiterten ebenfalls um **XIV** zu liefern.

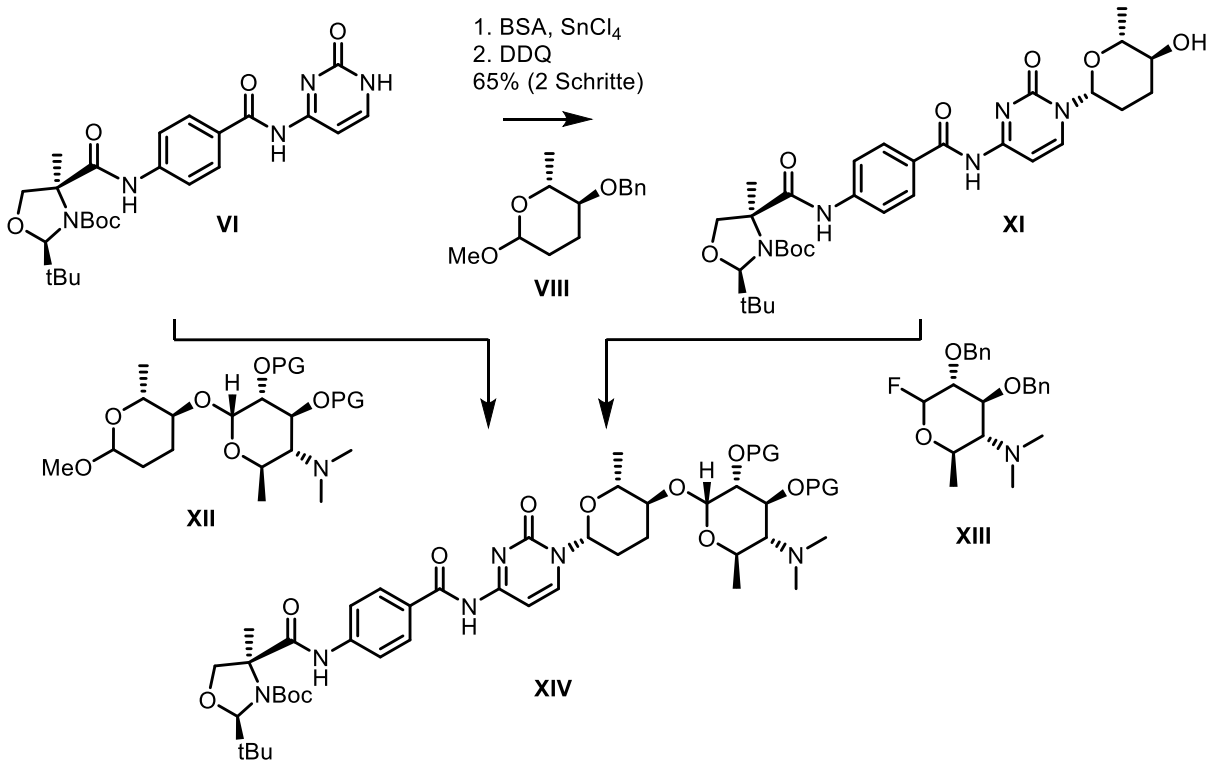

Schema 3 Endphase der Synthese von Amicetin und deren Glykosylierungen als Schlüsselschritte.

Das Monoglykosid **XI** konnte erfolgreich in die beiden Ester-Analoga **XV** und **XVI** überführt werden und demonstrierte damit die Umsetzbarkeit einer Säuren-basierten Entschützung des Oxazolidins in Gegenwart der eher labilen glykosidischen Bindungen. Erste biologische Tests der Verbindungen **XV** und **XVI** gegen den Bakterienstamm H37Rv zeigten, dass die Verbindung **XV** eine zwar schwache, aber dennoch vorhandene antimykobakterielle Wirkung aufweist. In Anbetracht der Flexibilität des Esters lässt dieser Befund auf Verbesserungspotential für rigidere Strukturen hoffen und spornt zur Synthese weiterer Analoga an.

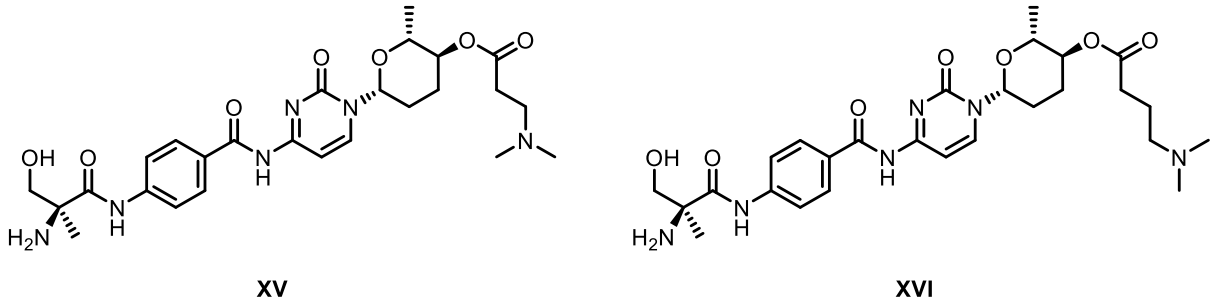

Abbildung 1 Vervollständigte Synthese zweier Ester-Analoga mit freigesetztem Serin Rest.

Der Naturstoff Nummularin H (**XVII**) gehört zur Familie der Cyclopeptid-Alkaloide und umfasst eine 13-gliedrige makrozyklische Grundstruktur. Die Isolierung aus *Ziziphus nummularia* geht auf das Jahr 1976 zurück und war Teil einer umfassenden Isolationsstudie für verschiedene Cyclopeptid-Alkaloide. Nummularin H (**XVII**) zeigte gewisse Aktivität gegen *Mycobacterium tuberculosis* mit einem MHK-Wert von 4.5 µM.

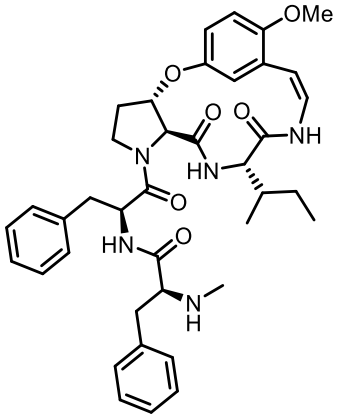

Nummularine H (**XVII**)

Die Totalsynthese von **XVII**, war ein zweites Ziel dieser Dissertation und diente dazu die biologische Aktivität von Nummularine H zu untersuchen, dessen antimykobakterielle Wirkung zu bestätigen und eine Grundlage für eine Struktur-Wirkungs-Beziehungs Studie zu schaffen. Zwei verschiedene Ansätze zur Bildung der makrozyklischen Grundstruktur von **XVII** wurden dabei untersucht. Ein makrozyklischer Ringschluss durch Bildung einer Phenylether Bindung wurde entweder anhand einer *Mitsunobu* Reaktion (für **XIX**) oder durch eine nukleophile aromatische Substitution (für **XXI**) für möglich gehalten (Schema 4).

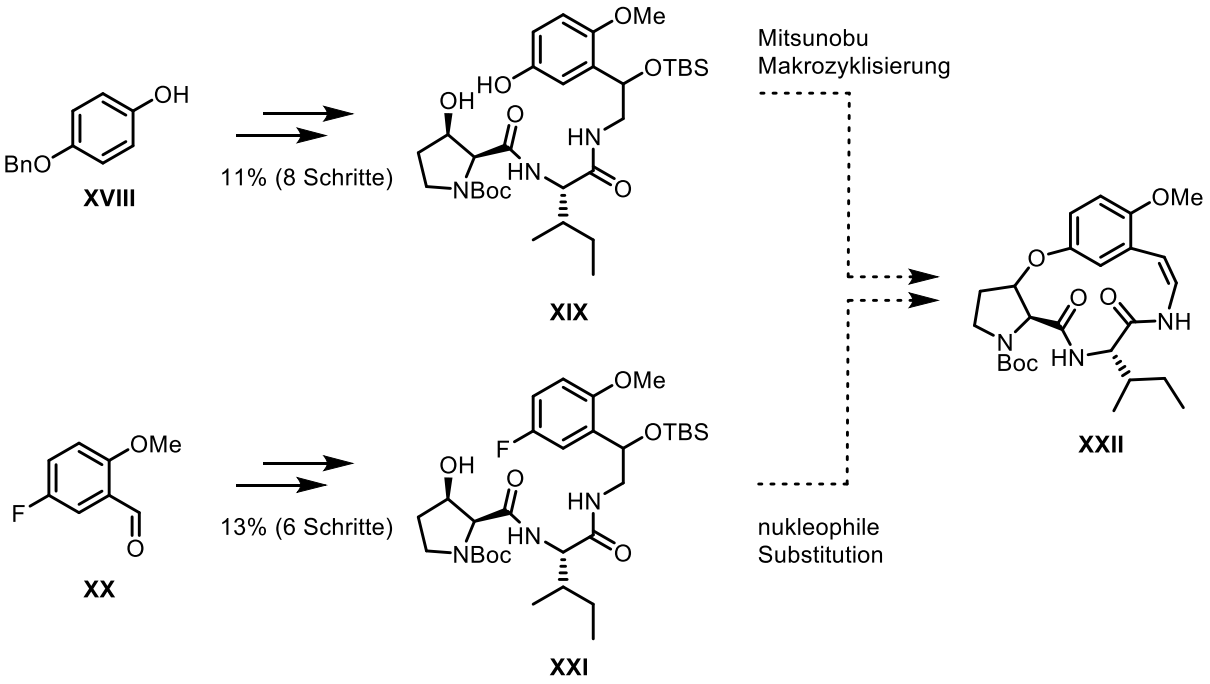

Schema 4 Synthese der linearen Vorläufer **XIX**, **XXI** und Makrozyclisierungs Versuche.

In beiden Fällen konnten die entsprechenden linearen Vorläufer ausgehend von den substituierten Benzolen **XVIII** und **XX** effizient hergestellt werden. Trotz einer Vielzahl an untersuchten Bedingungen, verliefen die Versuche zur Makrocyclisierung jedoch erfolgslos.

List of Abbreviations, Acronyms and Symbols

A

$[\alpha]_D^T$	specific rotation at temperature T at the sodium D line
Å	Ångstrom
Ac	acetyl
ADDP	1,1'-(azodicarbonyl)dipiperidine
aq.	aqueous

B

BEMP	2-tert-Butylimino-2-diethylamino-1,3-dimethylperhydro-1,3,2-diazaphosphorine
Bn	benzyl
Bz	benzoyl
brsm	by recovery of starting material
BSA	bis(trimethylsilyl)acetamide

C

ca.	approximately
cat.	catalytic
CoA	coenzyme A
CSA	camphorsulfonic acid
°C	degree centigrade
CNS	central nervous system

D

δ	NMR chemical shift in ppm
d	doublet
DCC	N,N'-dicyclohexylcarbodiimide
1,2-DCE	1,2-dichloroethane
DCM	dichloromethane
DDQ	2,3-dichloro-5,6-dicyano-1,4-benzoquinone
DEAD	diethyl diazenedicarboxylate
DIAD	diisopropyl azodicarboxylate
DIBALH	diisobutylaluminum hydride
DIPEA	diisopropylethylamin
DMAP	4-dimethylamino pyridine
DMEDA	N,N'-dimethylethylenediamine
DMF	N,N-dimethylformamide
DMS	dimethylsulfide
DMSO	dimethyl sulfoxide
DNA	deoxyribonucleic acid
dr	diastereomeric ratio

E

EDC	1-(3-dimethylaminopropyl)-3-ethylcarbodiimide
EDCI	1-(3-dimethylaminopropyl)-3-ethylcarbodiimide hydrochloride
ee	enantiomeric excess
EI	electron ionization
EMEA	European Medicines Agency
ESI	electrospray ionization
equiv	equivalent

Et	ethyl
F	
FC	flash chromatography
FDA	US Food and Drug Administration
FDPP	pentafluorophenyl diphenylphosphinate
G	
g	gram
GDP	guanosine diphosphate
H	
h	hour
Hal	halogen
HATU	1-[Bis(dimethylamino)methylene]-1*H*-1,2,3-triazolo[4,5-*b*]pyridinium 3-oxid hexafluorophosphate
HCTU	2-(6-Chloro-1*H*-benzotriazole-1-yl)-1,1,3,3-tetramethylaminium hexafluorophosphate
HIV	Human Immunodeficiency Virus
HOBt	1-hydroxybenzotriazole
HPLC	high-performance liquid chromatography
HR	high resolution
HRMS	high resolution mass spectrometry
Hyf	hydroxy Phe
Hyl	hydroxy Leu
Hyp	hydroxy Pro
Hz	Hertz (s^{-1})
I	
i	*iso*
IC_{50}	half maximal inhibitory concentration
IM	imidazole
*i*Pr	isopropyl
IR	infrared
J	
J	coupling constant
K	
kcal	kilocalorie
k	kilo
KHMDS	potassium bis(trimethylsilyl)amide
kd	kilo dalton
L	
LDA	lithium diisopropylamide
LiHMDS	lithium bis(trimethylsilyl)amide
M	
m	multiplet
m	*meta*
M	molarity (moles per liter)
MALDI	matrix-assisted laser desorption/ionization
m-CPBA	*meta*-chloroperoxybenzoic acid

MDR	multidrug-resistant
Me	methyl
MEM	2-methoxyethoxymethyl
mg	milligram
MHz	Megahertz
MIC	minimum inhibitory concentration
min	minute
mL	milliliter
mmol	millimole
µL	microliter
mol.	molecular
mol-%	mole percent
m.p.	melting point
mRNA	messenger RNA
MS	mass spectrometry
Ms	methanesulfonyl
Mtb	*Mycobacterium tuberculosis*

N

ng	nanogram
n. d.	not determined
NDP	nucleoside diphosphate
NMP	nucleoside monophosphate
NMM	N-methylmorpholine
NMO	N-methylmorpholine N-oxide
NMR	nuclear magnetic resonance
NOE	nuclear Overhauser effect
NTP	nucleoside triphosphate
nuc	nucleophile

O

o	*ortho*

P

p	*para*
PG	protecting group
Ph	phenyl
PhD	doctor of philosophy
1,10-phen	1,10-phenanthroline
PMB	4-methoxybenzyl
ppm	parts per million
PPTS	pyridinium *para*-toluenesulfonate
Pr	propyl
pyr	pyridine

Q

q	quartet
quant.	quantitative

R

RCM	ring-closing metathesis
Red-Al®	sodium bis(2-methoxyethoxy)aluminumhydride
R_f	retention factor

RNA	ribonucleic acid
RNAP	ribonucleic acid polymerase
rRNA	ribosomal RNA
rsm	recovered starting material
rt	room temperature
S	
s	second or singlet
SAR	structure-activity relationship
sec	*secondary*
sm	starting material
T	
t	triplet
t	*tert*
T	temperature
TB	tuberculosis
TBAF	tetra-*n*-butylammonium fluoride
TBAI	tetra-*n*-butylammonium iodide
TBS	*tert*-butyldimethylsilyl
TES	triethylsilyl
TfO	triflate = trifluoromethanesulfonate
TFA	trifluoroacetic acid
THF	tetrahydrofuran
TLC	thin layer chromatography
TMS	trimethylsilyl
TNF	tumor necrosis factor
Tol	tolyl
Ts	*p*-toluene sulfonyl
U	
µ	micro
US	United States (of America)
UV	ultraviolet
V	
VIS	visible
W	
WHO	World Health Organization
X	
XDR	extensively drug-resistance

1 Studies Towards the Total Synthesis of Amicetin (**A-1**)

1.1 Introduction

1.1.1 Isolation of Amicetin and First Biological Testing Results

Amicetin (**A-1**), a member of the group of disaccharide nucleoside antibiotics, was first isolated in 1953 from *Streptomyces vinaceus-drappus*, obtained from a soil sample collected in Michigan.[1] The isolate was tested against *Mycobacterium tuberculosis* (*Mtb*), *Bacillus subtilis*, *Escherichia coli, Proteus vulgaris* and *Staphylococcus aureus*. The fermentation broth was found to inhibit the growth of certain mycobacteria as well as Gram-negative and Gram-positive bacteria.

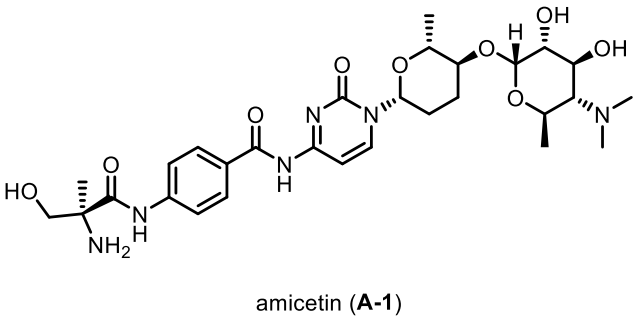

Figure 2 Structure of amicetin.

The isolation process involved the extraction of the fermentation broth with n-butanol at a pH of 7.5, distilling off the solvents, washing the residues with water and lyophilizing the aqueous solution. Distribution of the freeze-dried sample between water and methylene chloride and finally crystallization from water gave **A-1** as a pure crystalline product.[1] The activity of the crystalline material was tested in first *in vitro* experiments (Table 1) and compared to a streptomycin standard.

Table 1 Antibacterial activity of amicetin (**A-1**) compared to streptomycin. Values are given in µg per ml required for complete growth inhibition.[1]

Organism	Amicetin	Streptomycin
Mycobacterium tuberculosis (H37Rv)	0.5	1.0
Mycobacterium tuberculosis (ATCC-607)	1.0	1.0
Staphylococcus aureus (FDA-209)	2.0	0.2
Bacillus subtilis (III.)	4.0	0.1
Escherichia coli (ATCC-26)	>20.0	1.0

Growth inhibition was detected for certain acid-fast and Gram-positive bacteria but not so for the Gram-negative bacterium *E. coli*. Of particular importance in the context of this PhD thesis is the fact that first *in vivo* experiments performed in mice infected with *Mycobacterium tuberculosis* H37Rv showed a certain activity, which, unfortunately, is not further specified in reference [1]. Nevertheless, its reported potent *in vitro* activity against two strains of *Mtb*, which is comparable with that of

streptomycin, makes amicetin (**A-1**) a highly interesting lead structure for the development of new antimycobacterial agents.

The structure of amicetin (**A-1**) was elucidated through various degradation and transformation studies around 1960.[2–5] The compound was reported to be highly unstable in alkaline solution at pH 8 or higher, based on an observed loss of activity of the corresponding solutions.[6] The unambiguous structure elucidation followed in 1981 by X-ray diffraction analysis.[7] Later, in 2006, a solution state NMR structure determination[8] was performed. Amicetin (**A-1**) consists of a disaccharide pyrimidine nucleoside, in which the terminal amino sugar amosamine is α-(1 → 4)-linked to amicetose, which is β-(1 → N^1)-linked to a cytosine motif forming together cytosamine. Two amide bonds are present in the western-part of **A-1** connecting the pyrimidine moiety to a *p*-aminobenzoic acid, which is bound to (+)-α-methylserine building the aglycone designated cytimidine.

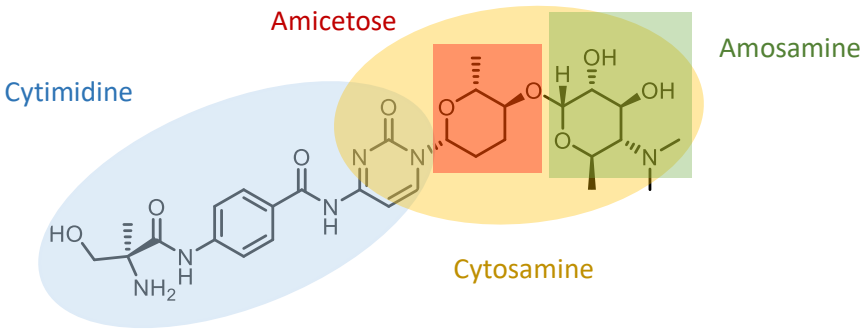

1.1.2 Biosynthesis of Amicetin (A-1)

The amicetin (**A-1**) gene cluster (*ami*) was identified and cloned from *Streptomyces vinaceus-drappus* NRRL 2363.[9] Its unambiguous confirmation was achieved by heterologous expression in *Streptomyces lividans* TK64, which indeed resulted in the biosynthesis of **A-1** and its analogues. It was revealed that 21 genes were putatively involved in amicetin (**A-1**) production, spanning a DNA region of approximately 37 kilobases.

The proposed biosynthetic pathway of the two pyranose moieties from D-glucose-1-phosphate **A-2** is depicted in Scheme 5. Thus, AmiE was identified to catalyse the formation of thymidine diphosphate (TDP)-D-glucose (**A-3**), which is further converted to the 4-keto derivative **A-4** by the TDP-glucose 4,6-dehydratase AmiU. Interestingly, compound **A-4** is found in many other deoxysugar pathways.[10] At this point, the pathway is believed to diverge towards **A-10** and **A-11**, respectively. The aminotransferase AmiB converts **A-4** to **A-5**. AmiH, which carries a methyltransferase domain will then alkylate the free amino group to give TDP-D-amosamine (**A-11**). The pathway from **A-4** to TDP-D-amicetose (**A-10**) comprises four enzymes. The formation of the diketo compound **A-6** is believed to be catalysed by the dehydratase AmiC and subsequent oxidation. AmiD may reduce the C3-keto

group to give **A-7**. Another dehydratase, AmiN, then creates the 3-deoxy compound **A-9** which is reduced to **A-10**.

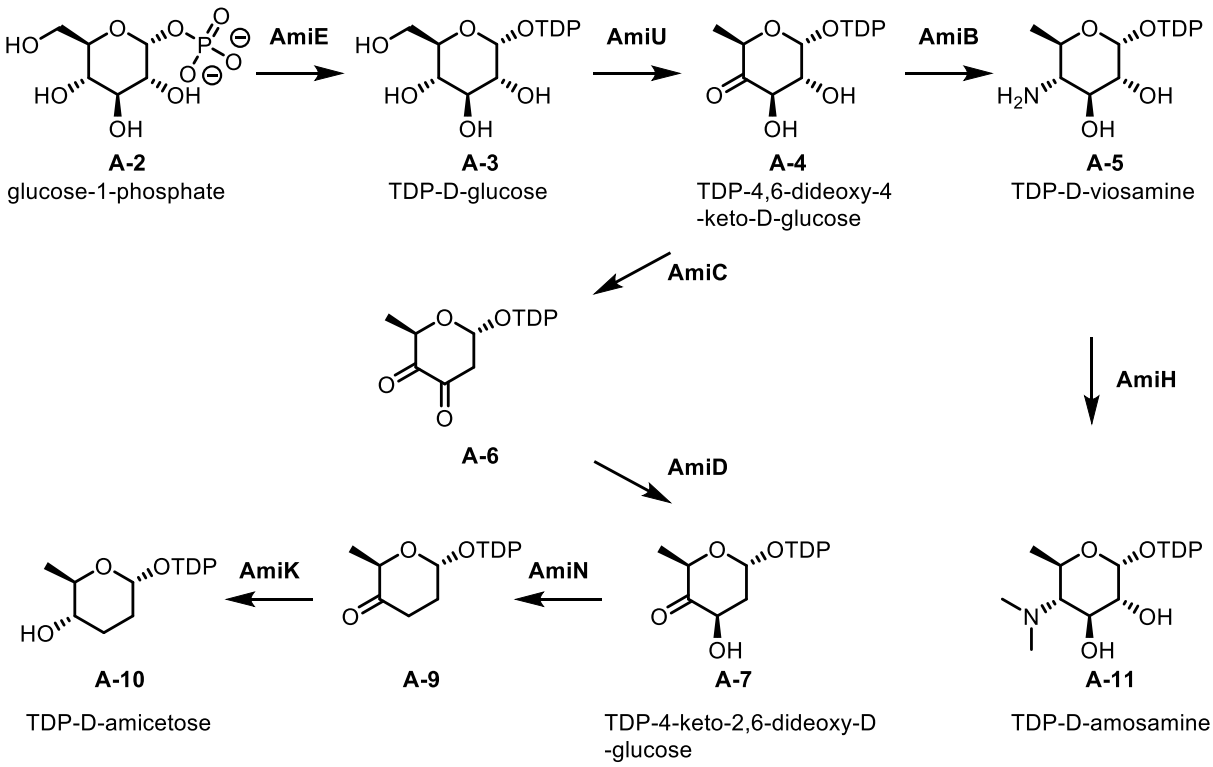

Scheme 5 Proposed biosynthesis of the amosamine and amicetose moieties in amicetin (**A-1**). TDP: thymidine diphosphate.

Two probable glycosyltransferases AmiJ and AmiG might then catalyse the sequential attachment of both sugar moieties to cytosine. In a BLAST search, AmiJ was found to exhibit 39% sequence similarity to the cytosylglucuronic acid synthase BlsD, which catalyses the attachment of glucuronic acid to cytosine in the blasticidin S pathway.[11,12] Analysis of the *amiF* gene revealed that AmiF contains a conserved domain for the *N*-acetyltransferase superfamily enzymes and was thus hypothesized to be responsible for amide bond formation between cytosamine (**A-15**) and PABA **A-16** to give **A-17**. Finally, AmiR was assigned to be responsible for the formation of the amide bond between **A-18** and the *p*-amino group of **A-17** to give amicetin (**A-1**).

The various enzymes were not only assigned bioinformatically by BLAST search but also by knockout experiments, which were performed on the genes *amiF*, *amiI* and *amiR*. For the *amiI* mutant, no biosynthesis of amicetin (**A-1**) was detectable. When *amiF* was inactivated and the mutant was fermented on large scale, cytosamine (**A-15**) was isolated but not **A-1**. Upon the silencing of *amiR,* only plicacetin was isolated. In later studies,[12] AmiH was confirmed to be an *N*-methyltransferase and AmiG the amosaminyltransferase. Upon silencing the *amiH* gene, compounds incorporating a primary instead of a tertiary amino group were isolated and characterized.

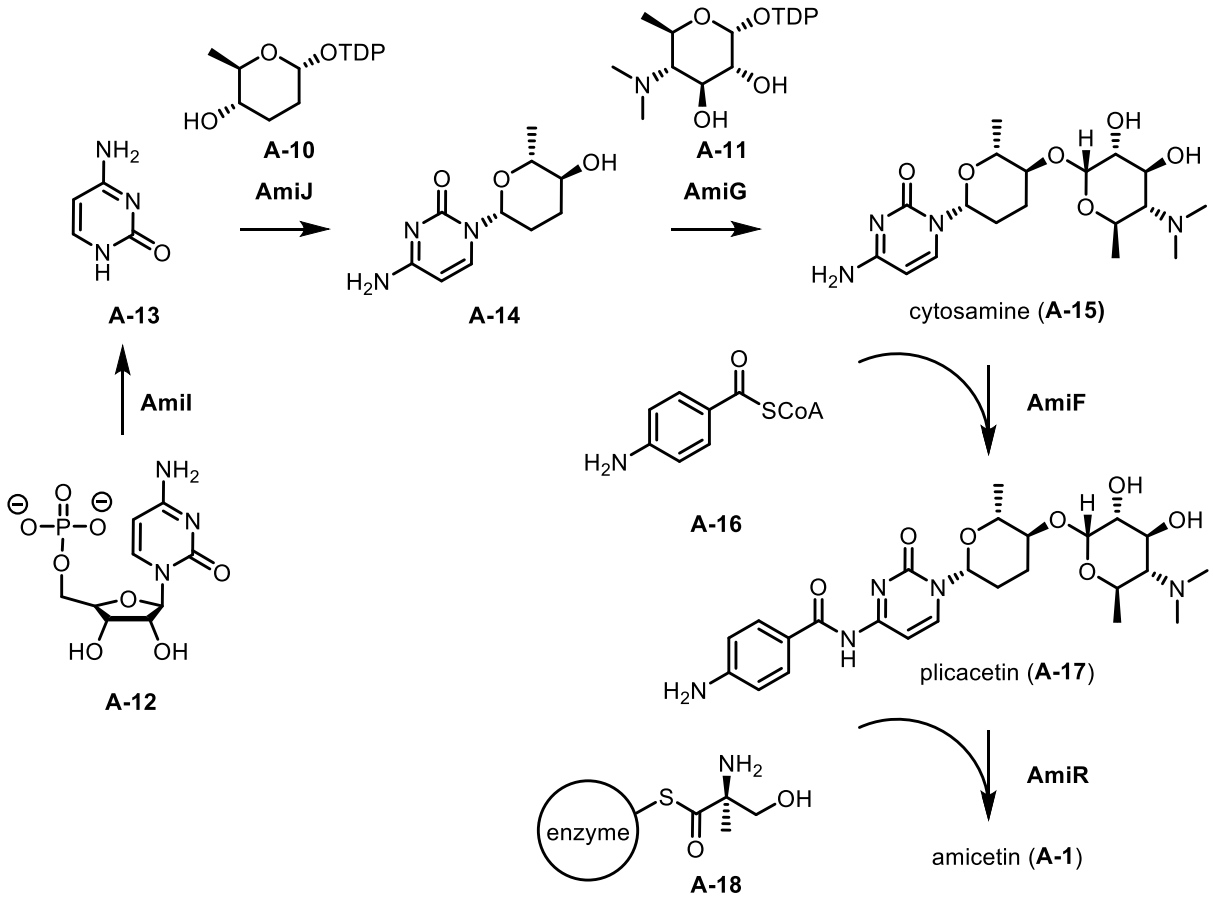

Scheme 6 Putative biosynthetic pathway to amicetin. CoA: coenzyme A.

In light of the biological activity of amicetin (**A-1**) and its potential as a promising lead structure for the discovery of new antimycobacterial agents, the following section will cover an introduction to tuberculosis (TB) and the importance of natural products in drug discovery.

1.1.3 Tuberculosis

1.1.3.1 Epidemiology

The Global Tuberculosis Report 2018[13] by the World Health Organization (WHO) summarises the ongoing global health threat posed by tuberculosis. The infection was the reason for an estimated 1.3 million deaths among HIV-negative people and another 300'000 deaths among HIV-positive individuals in 2017. These numbers underline the severity of TB and establish the disease to be the leading cause of mortality by a single infectious agent. With the massive morbidity toll taken by TB, it ranks prominently amongst the top ten causes of death worldwide.[14]

Fortunately, since the turn of the millennium, global TB incidence has been declining continuously at an average rate of 1.5% per year (Figure 3). As depicted in Figure 3B, the TB mortality rate among HIV-negative people is falling at about 3% per year. The WHO reports an overall reduction of TB cases

in the time between 2000 and 2017 of 42%. Most significant reductions were achieved in the regions of Europe and Africa.[13] Timely disease detection and effective drug treatments along with the general development of various countries were fundamental in the efforts against TB over the past years.

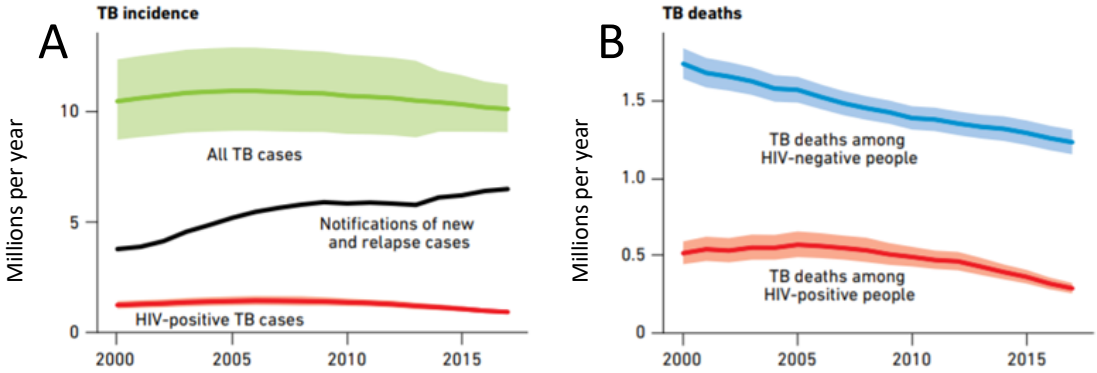

Figure 3 Global trends of estimated number of incident TB cases and the number of TB deaths from 2000 to 2017.[13]

Despite these encouraging trends, there are still 10 million people suffering from TB each year. A significant share of the global incidence in 2017 was associated with the twenty countries with the highest estimated numbers of TB cases. Remarkably, eight of these countries, *i.e.* India, China, Indonesia, the Philippines, Pakistan, Nigeria, Bangladesh and South Africa, accounted for 66% of global TB cases.[13]

While the absolute number of new TB cases is decreasing, the number of recorded incidents of drug-resistant *Mycobacterium tuberculosis* (*Mtb*) strains is on the rise (Figure 4). The incidence of rifampicin-resistant (RR) as well as multidrug-resistant TB (MDR-TB), which is defined by resistance of *Mtb* against at least isoniazid and rifampicin, increase annually. While in 2013 a total number of 450'000 RR-TB cases were reported, this number increased by 24% within the following four years. In 2017, 558'000 new cases of rifampicin-resistant TB were reported and among them were 457'560 that were found to have MDR-TB.[13]

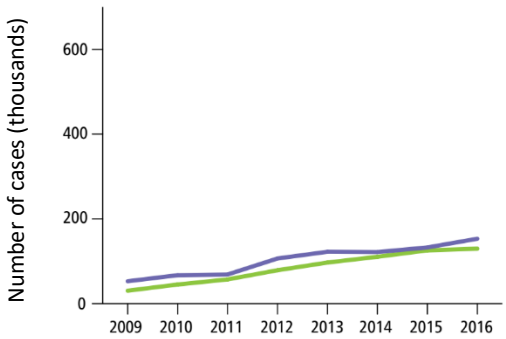

Figure 4 RR/MDR-TB cases detected (in purple) and number of people being enrolled on MDR-treatment (in green).

Geographically, the occurrence of RR/MDR-TB is particularly alarming in countries of Eastern Europe and Western Asia with a recorded increase of over 18% per year (Figure 5).

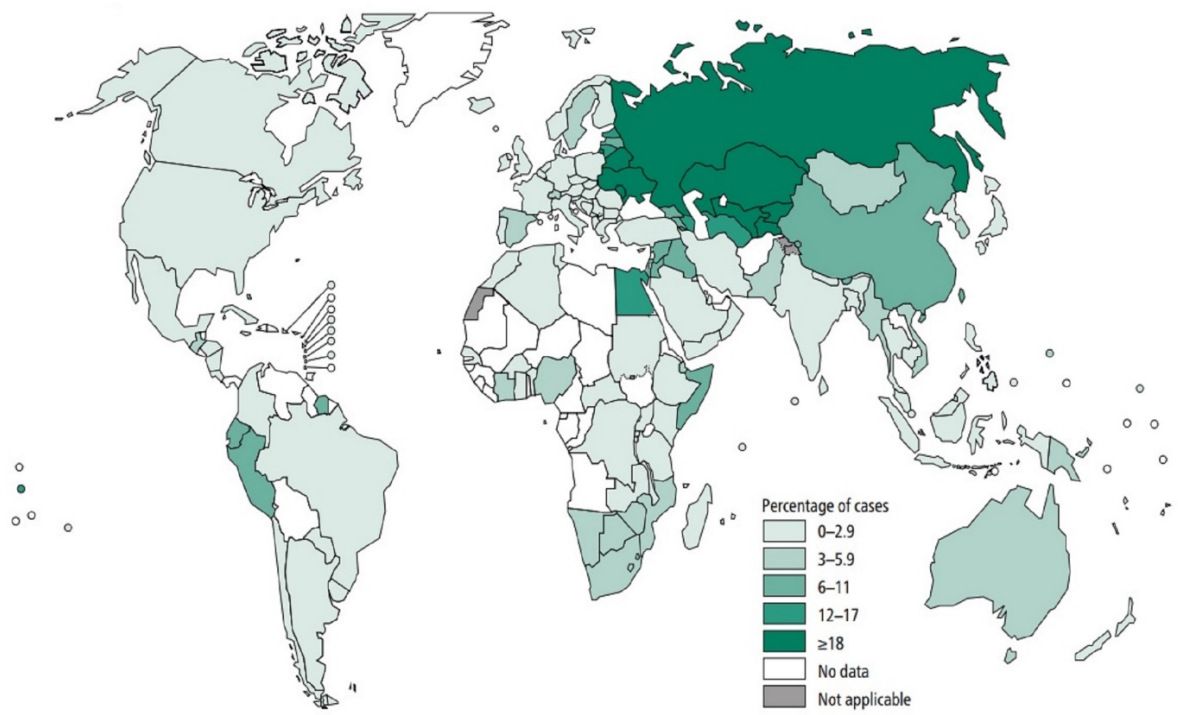

Figure 5 Percentage of new TB cases with RR/MDR-TB in 2017.[13]

An additional problem is the occurrence of extensively-drug resistant TB (XDR-TB), which is defined as MDR-TB plus resistance to any fluoroquinolone (a group of second line TB drugs, for further explanation see Chapter 1.1.3.5) and additional resistance against at least one of the second-line injectable drugs.[13] The treatment success rate for XDR-TB is roughly at 34% at the current time.

It is estimated that about one third of the world's population is latently infected with *Mtb*, but thereof only 5 - 15% will develop active disease during their lifetime.[14] Immunocompromised individuals (e.g. people infected with HIV) suffer from a 10% higher probability of an active TB outburst compared to non-compromised persons, fortunately, a decline of the number of HIV/TB-co-infected patients is recorded in the developed countries, due to improved infection-control practices as well as the availability of more sophisticated treatments for both HIV and TB infections. Worldwide, roughly 90% of people suffering from active TB are adults and among these are twice as many men affected as women.

Efforts have been made to reduce TB burden and certainly, there have been many successes. Nonetheless, the global health threat due to TB remains severe and new antimycobacterial agents are urgently needed. In particular, drug-resistant TB that has to be addressed along with disease

control in the low- and middle-income countries, which account for the majority of all recorded incidents.

1.1.3.2 Pathogenesis

Human infection by the causative pathogen is initiated through the inhalation of aerosol droplets containing *Mtb* that are expectorated from individuals having active TB.[15] The *mycobacteria* reach the alveoli, as depicted in Figure 6, where they are recognized and attacked by the host's innate immune system. Macrophages engulf the bacilli by phagocytosis and start to proteolytically digest the pathogen. The following immune response consists of the release of cytokines and chemokines, which attract other lymphocytes, macrophages and dendritic cells.[16] In immunocompetent individuals this process might lead to the complete elimination of *Mtb*.[17]

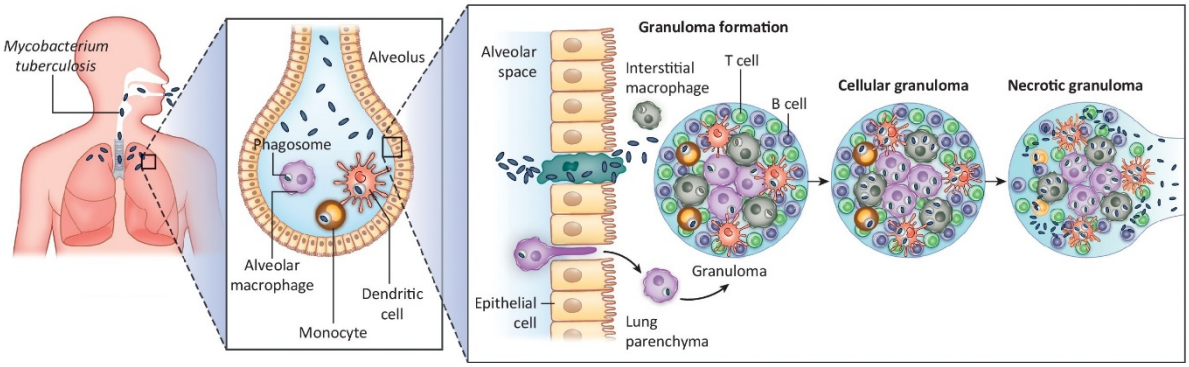

Figure 6 Pathogenesis of *Mtb.*

In the course of the immune response, an aggregation of densely organized mature macrophages is formed. These collections of immune cells are designated as granuloma;[18] within a granuloma macrophages can fuse into multinucleated giant cells, referred to *Langhans* giant cells, differentiate into foam cells or comprise B- or T-cells.[19] The underlying purpose of such spherical arrangements is to establish a physical barrier to control the infection and to sequester and eradicate the pathogen. However, in the case of TB, the granuloma provides bacteria with a natural habitat for their dormant state. Within the granuloma, *Mtb* is shielded physically from antibiotics and immune-based attacks and can successfully survive.[20] The dormant state of *Mtb* is characterized by a reduced active replication, an increased cell wall thickness and an altered metabolism of complex fatty acids.[21] Over time, the granulomas increase in size and form a caseum, a cellular structure containing necrotic material that is rich in lipids, is hypoxic, has a low pH and a limited amount of nutrients.[16] By cunning biological mechanisms, *Mtb* can survive in some cases these hostile conditions. Over progression of TB disease the granuloma undergoes a structural remodelling: the spherical arrangement loses structural integrity and eventually results in granuloma lesions, which allows the infectious bacteria to evade and re-infect the host.[22]

1.1.3.3 Mycobacterium Tuberculosis and Immunity

Mtb is an acid-fast, non-motile, non-sporulating pathogenic bacterium of the *Actinomycete* family (Figure 7).[17] Due to its highly aerobic physiology, it preferentially affects tissues with high oxygen levels such as the lungs.[17]

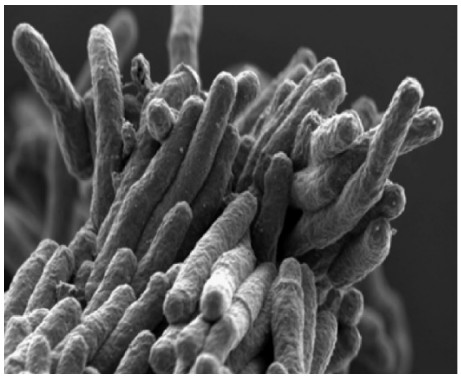

Figure 7 Rod shaped M*ycobacterium tuberculosis*.

The cell wall of *Mtb* shows neither clear Gram-positive nor Gram-negative characteristics. Like all *mycobacteria*, *Mtb* shows a high percentage of lipids integrated in their cell wall, which makes them resistant to commonly used staining methods.[17,23] Therefore, the family of *mycobacteria* are usually stained and identified by the *Ziehl-Neelsen* stain[24] and are thus categorized as acid-fast organisms.

The core cell wall of *Mtb* encompasses three major components (Figure 8): an inner mesh-like layer of peptidoglycan (PG), a densely branched arabinogalactan (AG) polysaccharide layer and on the outer part long-chain mycolic acids.[25] The PG layer confers rigidity to the cell through its cross-linked structure and is essential to withstand osmotic pressure.[26] Together with PG, the AG forms a vast macro-polymer. The mycolate layer is of asymmetric nature and is intercalated by glycolipids and inert waxy components.[25]

Mycobacteria are relatively slow-growing with a doubling time of about 20 hours.[27] *Mtb* represents the most prominent pathogen amongst a handful of mycobacterial species grouped in the *Mycobacterium tuberculosis* complex (MTBC). Other pathogens are *Mycobacterium africanum*, *Mycobacterium bovis, Mycobacterium caprae* or *Mycobacterium microti*.[28]

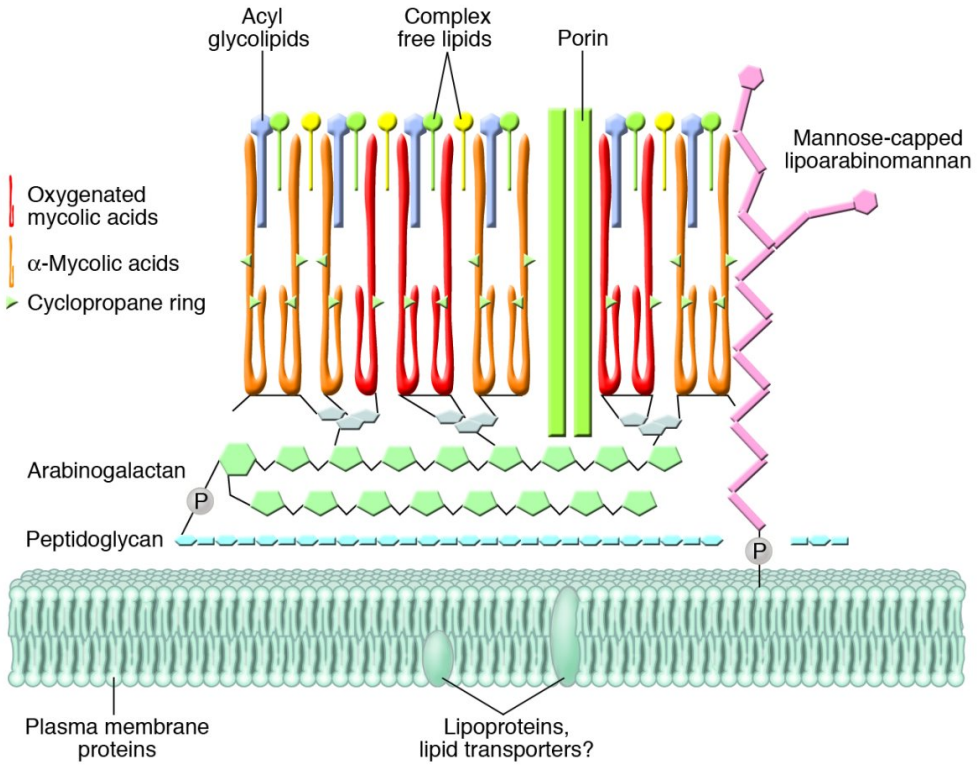

Figure 8 Schematic illustration of the mycobacterial cell wall.

The obligate human pathogen, *Mtb*, stands out from other bacteria considered as microbial threats in several aspects. One of these oddities is that *Mtb* does not exchange DNA via horizontal gene transfer (HGT), a trait typically associated with antimicrobial resistance. *Mtb* strains have extremely low levels of diversity (*i. e.* they are monomorphic bacteria) and they have a strictly clonal reproduction.[29] Besides this, the bacterium is intrinsically resistant to a variety of antibiotics due to its shielding and impermeable mycolic acid-rich cell envelope. Further, the bacteria's ability to hide in pulmonary cavities, where low drug permeation prevails complicates efficient targeting.[30] Pharmacokinetic studies highlighted the difference of anti-tuberculosis medications (moxiflacin and isoniazid) regarding their distribution and abilities to penetrate the lung tissue. For example, moxiflacin permeates well the cavities, whereas first-line drugs isoniazid, rifampicin and pyrazinamide are less efficient.[31]

Other complications in the fight against *Mtb* arise from its unusual life cycle and the long latency period. The complete eradication of the bacterium is hampered by the accessibility of a dormant state.

Finally, a poor patient compliance is a serious issue in TB treatment. On one hand the severe and unpleasant side-effects of the drugs make people abandon treatment prematurely, on the other hand the sense of well-being that begins shortly after the first treatment can mistakenly lead patients to believe that the infection has vanished.[32] This elongates the phases were people stay

infected and increases the likelihood of a relapse. People that have active TB will approximately infect ten to fifteen persons a year.[33]

In order to address the issue above, the WHO has established a cost-effective TB treatment strategy known as directly observed treatment, short course (DOTS),[33] which has contributed significantly to improved patient compliance. DOTS comprises a standardized treatment regimen of six to eight months with directly observed treatment (DOT) for at least the initial two months.[33] Further, it ensures a non-interrupted supply of the essential anti-TB drugs and allows recording and reporting of TB cases.

1.1.3.4 TB detection

The diagnosis of TB can be performed based on different methods. The most relevant ones are briefly discussed in this section.

Culturing *Mycobacterium tuberculosis*: This is the gold standard of laboratory diagnosis of TB. However, it entails a rather lengthy process of sample collection and transport to the laboratory, inoculation and incubation of the media, growth detection and mycobacteria identification.[34]

Rapid molecular tests: The WHO recommends Xpert® MTB/RIF as a first-line diagnostic testing for TB, which provides rapid DNA-based detection of the causative pathogen.[35] It is a fully automated, cartridge-based nucleic acid amplification test. The test is capable to give results within 2 hours and is informative about both general TB infection and whether the strain is resistance to rifampicin.[13] There has been a recent advent of a re-engineered Xpert® Ultra test with a lower limit of detection and better performance.[36,37] Xpert® Ultra has been shown to be substantially more sensitive than the commonly used Xpert®, especially for smear-negative specimens and specimens from HIV-positive individuals.[36,38]

Sputum smear microscopy: A small sample of sputum is collected on a glass slide (smear) and analysed by microscopy. The test is inexpensive, provides results within hours and does not require any sophisticated laboratory devices. The drawback is its low accuracy compared to Xpert®, especially for people being co-infected with HIV, who tend to show low numbers of TB bacteria in their sputum.[13]

1.1.3.5 Current Treatment Options

The effective use of antimicrobials against TB has started in the middle of the 20th century with the discovery of streptomycin[39] and continued with the development of the synthetic drug *para*-aminosalicylic acid (PAS) only four years later. In 1952, Sir *John Crofton* reported the first regimen based on streptomycin, PAS, and isoniazid for the effective treatment of TB.[40] These findings paved the way for further discoveries and laid the foundation for today's treatment options.

In principle, a TB patient can be treated effectively by chemotherapy. The therapeutic approach includes first-, second- and third-line medication depending on the drug-susceptibility of the bacteria. In an initial phase, the bactericidal phase, *mycobacteria* with a high replication rate are targeted. This may result in the eradication of clinical symptoms. A second phase, the continuation phase, aims at the elimination of persistent or dormant bacteria, which survived the initial phase .[41]

Current treatment of **drug-susceptible (DS)-TB** consists in the administration of the first line drugs isoniazid, rifampicin, pyrazinamide and ethambutol for an initial two-month phase, which is followed by a second four-month-phase of isoniazid and rifampicin treatment (Figure 9). According to the WHO, the treatment success rate is at least 85% for DS-TB and the treatment can be used for both pulmonary and extra pulmonary TB.[13,42]

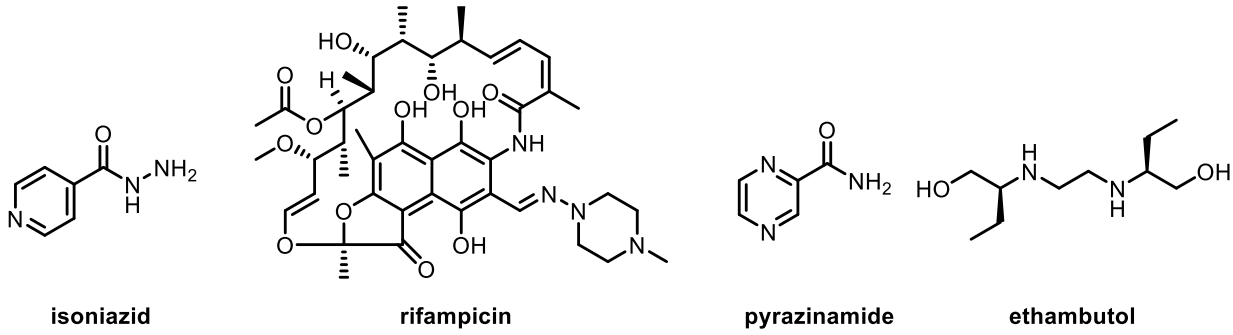

Figure 9 First-line TB drugs.

All of the first-line antimicrobial drugs can induce mild or severe side effects. Possible adverse drug reactions are hepatotoxicity for isoniazid, rifampicin and pyrazinamide,[43] gastrointestinal disorders arise from rifampicin and cutaneous side effects are reported for isoniazid, pyrazinamide and ethambutol.[44,45] In previous studies,[45] 23% of the participants had to terminate their intake of either isoniazid, rifampicin or pyrazinamide due to unbearable side effects.

Table 2 First-line TB drugs, their targets, inhibition and the recommended daily dosage.[46]

Drug	Target	Inhibition	Daily dose
isoniazid	enoyl-[acyl-carrier-protein] reductase	mycolic acid synthesis	5 mg/kg
rifampicin	RNA polymerase	RNA synthesis	10 mg/kg
pyrazinamide	arabinosyl transferase	arabinogalactan synthesis	25 mg/kg
ethambutol	arabinosyl transferase	bacterial cell wall complex	15-20 mg/kg

If a patient is not responding to at least rifampicin and isoniazid, he or she will be declared as MDR-TB (see chapter 1.1.3.1) and **second-line drugs** are administered (Table 3 and Figure 9). Treatment for drug-resistant (MDR- and RR-TB) cases gets very costly and prolonged. Regimens for second-line TB treatment consist of more toxic drugs and are therefore associated with higher rates of drug-related side effects.[13,17] The WHO recommends an intensive phase of at least five effective anti-TB medications, including pyrazinamide and four core second-line TB drugs: one each from group A and B and two from group C[47] (Table 3). The current success rate for the treatment of MDR-TB is reported to be about 55%. As the most relevant components of second-line TB treatment regimens, the fluoroquinolones (group A) are recommended to always be used in MDR-TB treatment. All of them target the bacterial topoisomerase, encoded by the *gyrA* gene,[48] and inhibit DNA supercoiling. In general, the have a good safety profile. Injectable anti-tuberculosis drugs (group B), on the other hand, inhibit bacterial protein synthesis and are associated with an increased probability of treatment success when included in the treatment regimen.[47] The mode of action of group C drugs is more diverse compared to fluoroquinolones and injectable agents. Thus, ethionamide is a prodrug that is believed to act by inhibiting mycolic acid synthesis, similar to isoniazid.[49] The cyclic D-serine derivative cycloserine inhibits bacterial cell-wall biosynthesis by targeting two enzymes involved in the cytosolic stages of peptidoglycan synthesis.[50] Linezolid disrupts the translation of mRNA and therefore acts as a bacterial protein synthesis inhibitor.[51] Clofazimine is another prodrug that gets reduced by type 2 NADH-quinone oxidoreductase followed by a non-enzymatic oxidation of the reduced clofazimine through O_2, thereby generating reactive oxygen species, which affect the cell growth.[52,53]

As mentioned previously, the second-line regimens are more toxic and accompanied by various adverse side effects, which affect a remarkable 86% of patients. While the safety profile of fluoroquinolones is relatively good, careful monitoring is needed when applying second-line injectable agents. Most frequently observed adverse effects for group B drugs are hearing loss and nephrotoxicity. Other effects such as skin rash, hypersensitivity and peripheral neuropathy have been described as well.[47,55] The side effects for group C drugs range from skin discoloration (clofazimine)[52] to anaemia, peripheral and/or optical neuropathy (linezolid),[56] gastrointestinal irritation (ethionamide),[57] and neurological reactions for cycloserine[57].

Table 3 Second-line (according to guidelines 2016 WHO) TB drugs.

Drug	Target	Inhibition	Daily dose[54]
Group A Fluoroquinolones			
levofloxacin	DNA gyrase and topoisomerase	DNA supercoiling	15 mg/kg
moxifloxacin	DNA gyrase and topoisomerase	DNA supercoiling	7.5-10 mg/kg
gatifloxacin	DNA gyrase and topoisomerase	DNA supercoiling	15 mg/kg
Group B Second-line Injectable Agents			
amikacin	30S ribosomal subunit	protein synthesis	15 mg/kg
capreomycin	interbridges 30S and 50S ribosomal subunit	protein synthesis	15 mg/kg
kanamycin	30S ribosomal subunit	protein synthesis	15 mg/kg
streptomycin	16S rRNA of 30S ribosomal subunits	protein synthesis	15 mg/kg
Group C Other Core Second-line Agents			
ethionamide	enoyl-[acyl-carrier-protein] reductase	mycolic acid synthesis	15 mg/kg
cycloserine	D-alanine racemase/ligase	peptidoglycan synthesis	15 mg/kg
linezolide	23S portion of the 50S subunit	protein synthesis	600-300 mg daily
clofazimine	competes with menaquinone (MK-4)	electron transfer chain	

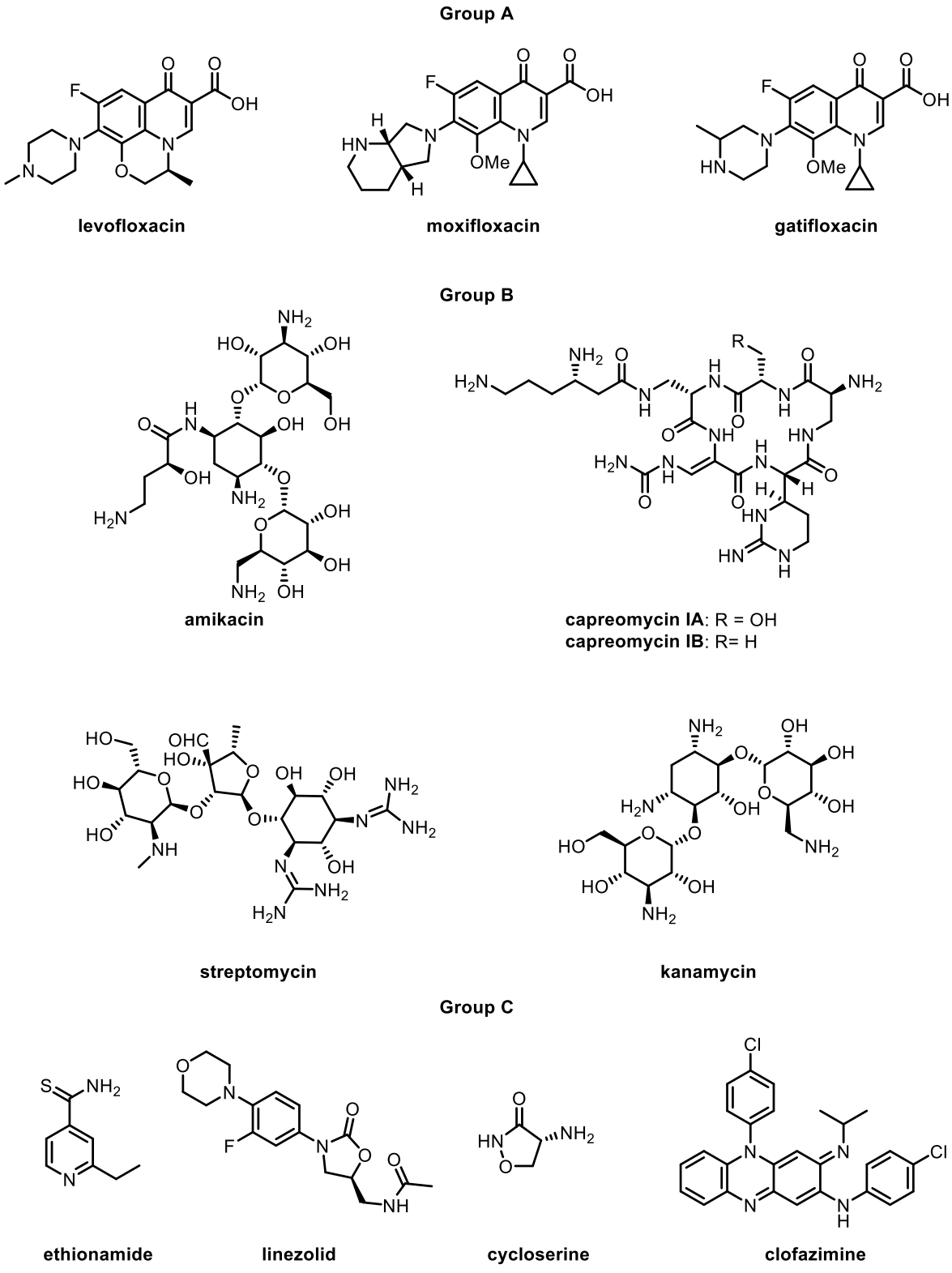

Figure 10 Second-line TB drugs.

Compounds belonging to **group D** (Table 4) are not core second-line agents. Group D1 drugs are usually added to core second-line medications and are first-line drugs. Group D2 drugs include bedaquiline and delamanid, which were both approved only recently (bedaquiline in 2012 and delamanid in 2014 by FDA).[58,59] Recent case studies have shown the effective and safe use of

bedaquiline up to a treatment time of 18 months.[60,61] However, some reservation has been expressed regarding the use of bedaquiline in connection with potential cross-resistance with clofazimine.[62]

Table 4 Group D Add-on agents.

Group D Add-on agents		
D1	**D2**	**D3**
pyrazinamide ethambutol high-dose isoniazid	bedaquiline delamanid	*p*-Aminosalicylic acid imipenem-cilastatin meropenem amoxicilin-clavulanate

Delamanid exhibits good bactericidal and sterilizing activity and, in contrast to bedaquiline, shows no cross-resistance with any other TB drug.[63] Both bedaquiline and delamanid are administered only for the first six months in the treatment of XDR-TB patients, which sets clear limitations for both compounds.[64] In more recent studies, carbapenems (ertapenem, imipenem, meropenem) were tested to be included in new TB drug combination trials.[65] In particular, the combination of meropenem and clavulanate has recently gained attention; these compounds are currently considered as possible second-line core drugs.

1.1.4 Natural Products in Drug Discovery

Natural products (NPs) served as a vital source of molecules that have played pivotal roles in pharmacy, biology and medicine.[66] History is full of exceptional scientific discoveries where a natural product profoundly impacted progress in medicine and overall human well-being. To name only a few, the discovery of penicillin, streptomycin, salicin, morphine, digitoxin, vancomycin or taxol were milestones in the history of natural product drug discovery.

For many years NPs and their molecular architectures have played a significant role as lead structure for drug discovery or as actual drug candidates. They have greatly contributed in the past and continue to contribute today to the landscape of new molecular entities (NME) that have been approved for clinical use in humans, as highlighted in a number of extensive reviews of *Newman* and *Cragg*.[67–71] Secondary metabolites produced by enzymatic machineries have been structurally fine-tuned during evolution to serve a specific biological purpose and to interact with macromolecular targets.[72] The sheer size of this reservoir of compounds remains an unparalleled source of chemical and biological diversity and inspiration. Compared to synthetic molecules, NPs often deviate from a "flat" scaffold structure and can exhibit highly complex molecular architectures.[73] They frequently

embody a large fraction of sp^3-hybridized bridgehead atoms and chiral centres compared to synthetic molecules.[74]

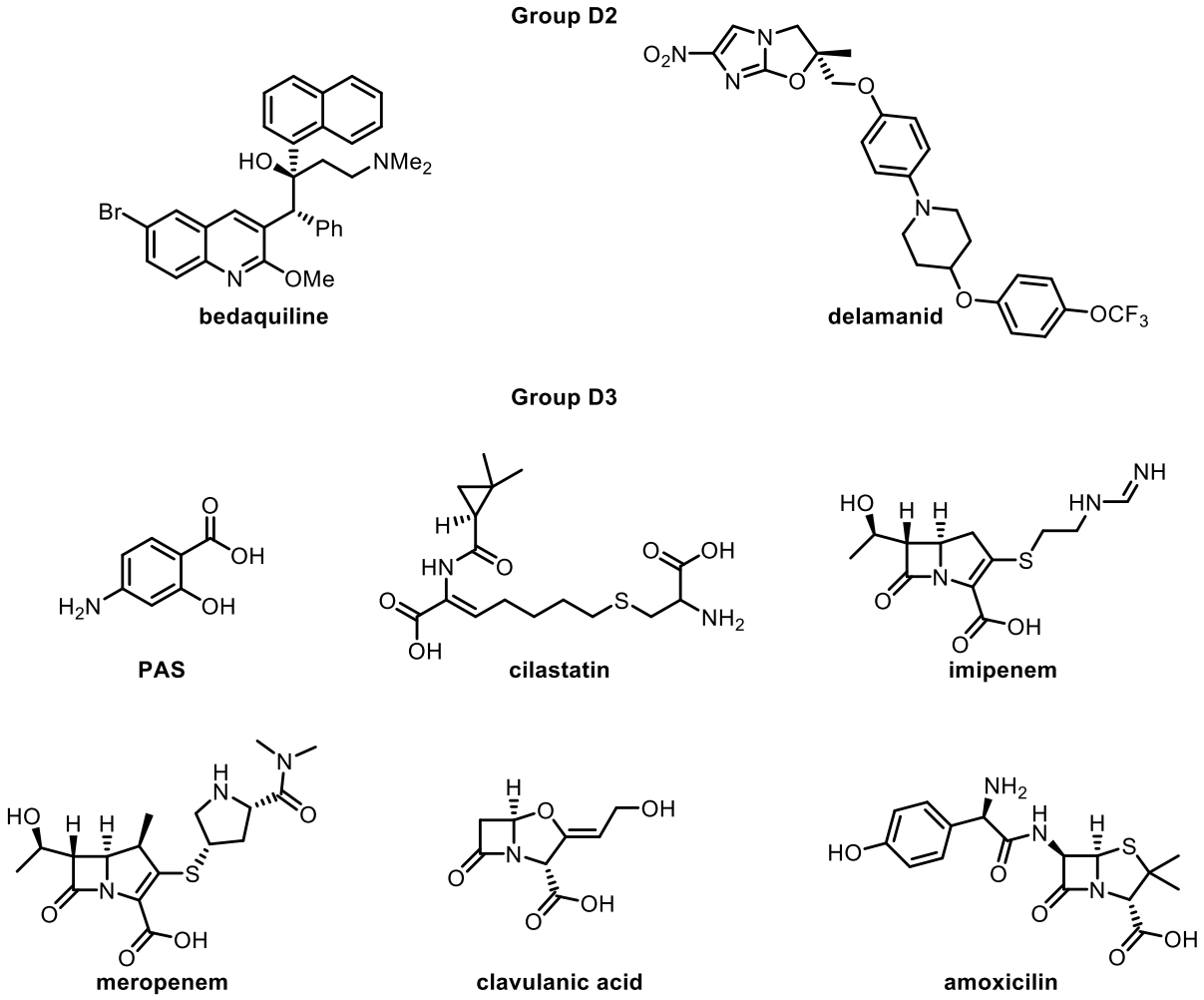

Figure 11 Group D2 and D3 add-on agents.

The continuous advances in NP research such as combinatorial biosynthesis, selective activation of gene clusters, superior isolation techniques and outstanding synthetic methodologies will help to exploit the potential of NPs to explore novel chemical space and unveil interesting biological activity.[75–77]

1.1.5 Natural Products in TB Drug Research

NPs have played a particularly important role in the field of antimicrobial agents and the majority of clinically used antibiotics are NPs or NP derivatives.[76]

In the context of anti-TB drug discovery, it was the isolation of the aminoglycoside streptomycin in 1944 that enabled the first effective pharmacotherapy of TB.[39] As discussed in section 1.1.3.5 streptomycin today is one of the core second-line injectable agents, which are used in the treatment

of MDR-TB patients. Roughly ten years after the discovery of streptomycin, the macrolactam rifamycin B (Figure 12) was isolated from *Streptomyces mediterrranei*.

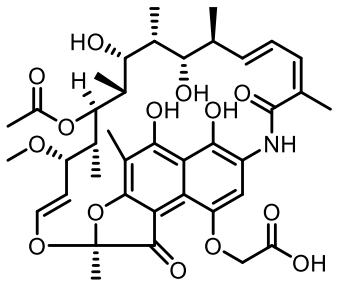

Figure 12 The natural product rifamycin B.

This compound served as the structural basis for the development of the first-line TB drug rifampicin. Rifampicin was the result of efforts by a group of the Dow-Lepetit Research Laboratories in Milan, Italy, who transformed rifamycin B into a handful of derivatives with increased stability and oral availability. The discovery of rifampicin was accomplished in 1965 and only shortly after this, the drug was included in the first-line treatment regimen for TB.[78] Other second-line TB drugs that are natural product derivatives include the aminoglycosides amikacin and kanamycin, the polypeptide antibiotic capreomycin and cycloserine (Figure 10).

While NP (derivatives) are well represented in the current anti-TB regimens, NMEs based on NPs are conspicuous by their absence from TB drug development over the last fifty years. Since the advent of rifampicin treatment, there have been little efforts made to populate the TB drug pipeline in general. Despite this rather unpromising environment, several compounds have been found in recent years with interesting activity against *Mtb* and with reasonable efforts one of them might make it to a marketable therapeutic.[76]

1.1.6 The Bacterial Ribosome as Target for Antibiotics

Amicetin's (**A-1**) putative mode of action (*vide infra* Section *1.1.8*) as an antibacterial agent is believed to be based on the interference with the bacterial ribosome. To cover the fundamental concept of the biosynthesis of proteins and the role of antibiotics, the following section will give a brief outline on this subject.

1.1.6.1 Structure of the Bacterial Ribosome and Protein Synthesis

The ribosome is a complex machinery responsible for the biosynthesis of proteins (Figure 13). The bacterial ribosome in particular consists of a small subunit (30S) and a large subunit (50S) that form the complete 70S ribosome.[79] It comprises three rRNA chains (16S, 23S, 5S) (65% of the complete ribosome) and different ribosomal proteins (35%),[80] with most of the biological function relying on the rRNA. The small 30S subunit is involved in the interaction between the coding mRNA and the

tRNA anticodons,[81] while the large subunit includes the pivotal peptidyl transferase centre and catalyses peptide bond formation. The fully assembled 70S ribosome has three binding sites for tRNA; the A-site, which binds the aminoacylated tRNA; the P-site, which holds the tRNA bound to the nascent peptide chain, and the E-site that binds the free deacylated tRNA before exiting the ribosome.[82]

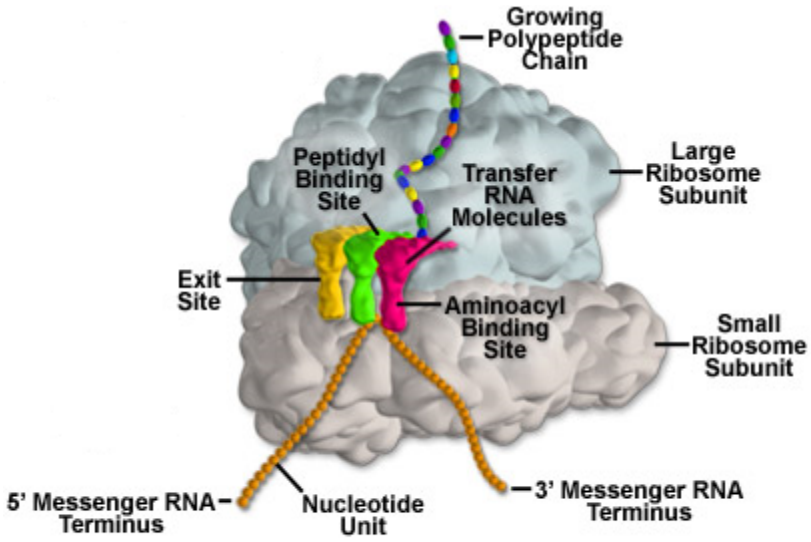

Figure 13 Schematic drawing of a prokaryotic ribosome.

The process of translation is initiated by the binding of the small subunit to a *Shine-Dalgarno* sequence on the mRNA, involving three initiation factors (IF1, IF2 and IF3), followed by the binding of an initiator formyl-methionine transfer RNA (fMet-tRNA$_i^{fMet}$).[82] In a next step, the large subunit associates to the acceptor arm of the tRNA associated with the small subunit to form the 70S initiation complex. The end of the initiation phase leaves the ribosome with an empty A-site and a P-site occupied by the initiation tRNA. The ribosome is now "ready" to accept the incoming aminoacyl tRNA, carrying an amino acid (aa) and the anticodon triplet that is complementary to the codon of the mRNA. The next incoming aminoacylated tRNA reaches the A-site as a complex together with an elongation factor (EF-Tu) and GTP. If the codon is correctly matched by the anticodon of the tRNA, the ribosome undergoes a conformational change that triggers the hydrolysis of GTP by EF-Tu. With both, the A- and the P-site occupied, the peptide chain (or aa, for the first one) attached to the tRNA in the P-site is transferred to the amino terminus of the next amino acid, which is attached to the tRNA occupying the A-site. Both translocation of the two tRNAs as well as the mRNA is catalysed by EF-G, another GTPase. This transformation leaves the ribosome with an occupied E-site (deacylated tRNA) and a peptidyl tRNA in the P-site, while the A-site is ready to receive the next tRNA. Iterative repetition of this process occurs until a stop codon is encountered on the mRNA, which initiates the termination of the translation process. The termination sequence involves two release factors, RF1 and RF2, that facilitate the hydrolysis of the ester bond between the peptide chain and the tRNA

located in the P-site.[83] The disassembly of the complete machinery involves yet a third release factor (RF3), whose function remains to be further clarified.

1.1.6.2 Ribosomal Peptidyl Transferase Centre

The ribosomal peptidyl transferase centre (PTC) represents the catalytic heart of the ribosome and is responsible for catalysis of both peptide bond formation and peptide release (*vide supra*) during the translation process.[84] The X-ray crystallographic elucidation of the structure of the ribosome on an atomic level[81] confirmed the PTC to be an RNA enzyme within the large 50S subunit. Firstly, the peptidyl transferase promotes the aminolysis of the ester bond that links the nascent peptide chain to the 3'-hydroxy group of the 3'-terminal ribose in the P-site by an attack of the α-amino group of the A-site aminoacyl tRNA (Figure 14). The enzyme achieves an impressive synthesis rate of up to 50 peptide bonds per second.[85] An uncatalysed reaction between an ester and an amine proceeds at a rate of about 10^{-4} M^{-1} s^{-1} at ambient temperature, meaning that the enzyme accelerates the reaction by six to seven orders of magnitude.[86] It is assumed that the catalysis is almost entirely based on proper substrate positioning within the active site.[87,88]

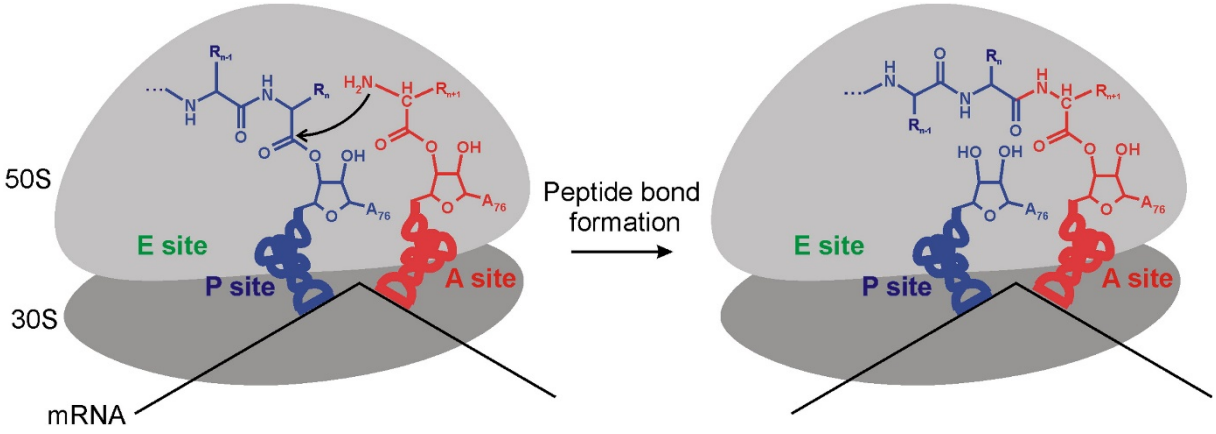

Figure 14 Peptide bond forming process within the PTC.

Secondly, the PTC catalyses the hydrolysis of the peptidyl-tRNA in the termination step (see section 1.1.6.1), which is needed to release the fully assembled polypeptide.[84] The hydrolysis involves the nucleophilic attack of a water molecule on the P-site-located peptidyl-tRNA, thereby breaking the ester bond between the peptide and the tRNA.[89] The hydrolysis of the peptide bond is more challenging than the formation of the amide bond. The PTC must be capable of switching between amide bond formation and ester bond hydrolysis. The switch to "hydrolysis mode" is induced by the binding of a release factor.[84]

1.1.6.3 Antibiotics Acting on the Bacterial Ribosome

During the past two decades, the structural sophistication of the ribosomal machinery complex has been elucidated by X-ray crystallography and cryoelectron microscopy (Cryo-EM), providing a good

understanding of the full translation mechanism.[90,91] In this section I will discuss antibiotics that inhibit protein synthesis, with a special focus on some prominent antibiotics targeting the large ribosomal subunit. For the sake of brevity, circular peptides and macrolides are not included in this discussion.

Antibiotics that target the 50S subunit. The peptidyl transferase centre is one of the most prominent targets for antibiotics that interfere with the large ribosomal subunit. The PTC contains two hydrophobic crevices that play a pivotal role in the interaction with antibiotics.[92] One of them, designated the A-site crevice, is located in the active site of the PTC. It is this crevice that interacts with the amino acid side chains of the incoming aa-tRNAs and this is where competing interaction with antibiotics can take place.[93] A prominent example of a compound interacting with the A-site crevice is the broad-spectrum antibiotic chloramphenicol that inhibits protein synthesis in a wide range of Gram-positive and Gram-negative bacteria (Figure 15).[94–97]

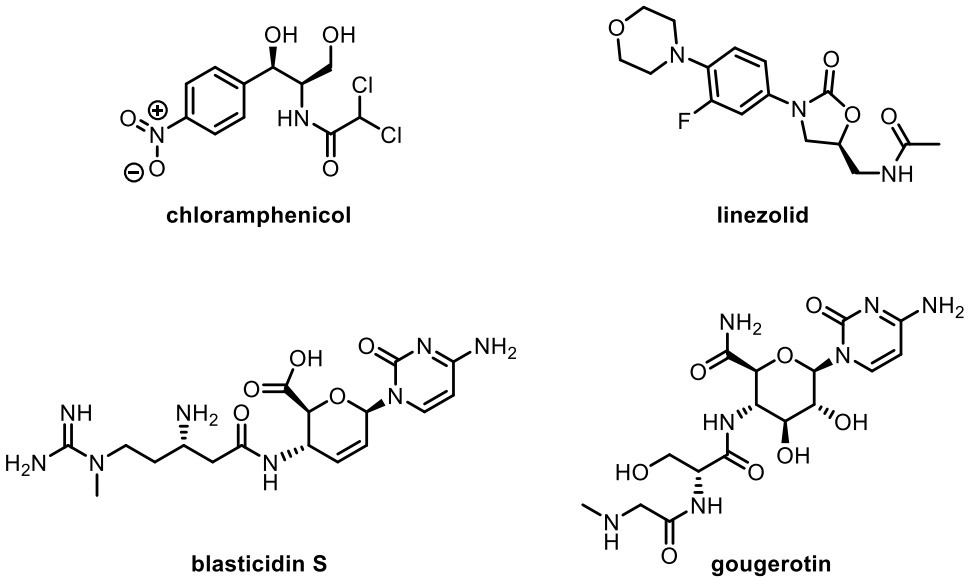

Figure 15 A selection of antibiotics that target the large ribosomal subunit.

The nitrophenyl ring of chloramphenicol is involved in π-stacking interactions with nucleotides of the 23S rRNA (Figure 16).[92]

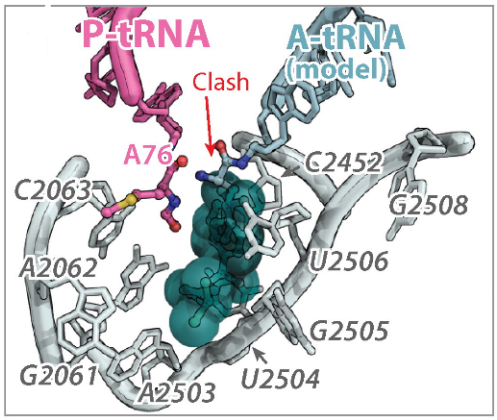

Figure 16 Interaction of chloramphenicol (in cyan) with the PTC A-site crevice (in grey).

While it had been believed for a long time that chloramphenicol was a universal inhibitor of peptide bond formation, recent studies have shown that the activity of chloramphenicol is dependent on the aa-sequence of the nascent peptide chain and therefore is context-dependent.[98]

The 50S subunit is also the target of linezolid (Figure 15), which belongs to the oxazolidinone family and is active against Gram-positive bacteria. It is one of the core second-line agents in the treatment of TB. As for chloramphenicol, the binding site of linezolid is the PTC. The crystal structure of linezolid bound to the *Haloarcula marismortui* 50S subunit has shown that the oxazolidinone ring interacts with the nucleotides of the A-site cleft (Figure 17).[99] It is assumed, that the antibiotic clashes with part of the aa-tRNA and thereby inhibit its placement within the ribosome.

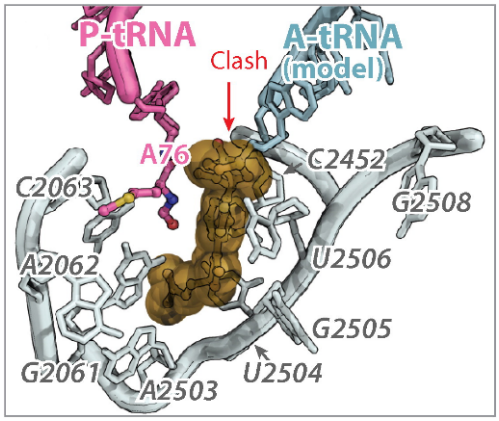

Figure 17 Interaction of linezolid (in brown) with the PTC A-site crevice (in grey).

Blasticidin S is a potent inhibitor of eukaryotic and prokaryotic protein synthesis (Figure 15). It was first isolated from *Streptomyces griseochromogenes* in 1958 by *Takeuchi*.[100] It bears a cytosine linked to a dideoxyhexose that is bound to a modified arginine. This nucleoside antibiotic was the first successfully utilized microbial fungicide and it has been widely used in Japan against the virulent fungus *Pyricularia oryzae*, in order to control rice blast disease.[101] While other peptidyl transferase inhibitors, such as chloramphenicol or linezolid bind to the A site of the large ribosomal subunit,[102]

blasticidin S binds to the P site. By binding of the nucleoside antibiotic in the P-loop of the 23S rRNA, it distorts the 3'-terminus of the P-site tRNA and displaces C75 from its usual position (Figure 18).[103] These crystallography-based conclusions however stand somewhat in contrast with the fact that blasticidin S competes for binding with puromycin, an antibiotic that is known to bind the A-site cleft.[104] Further biochemical experiments revealed that upon binding of blasticidin S and distortion of the P-site tRNA, the RF1-mediated release of the peptidyl-tRNA is nearly abolished.

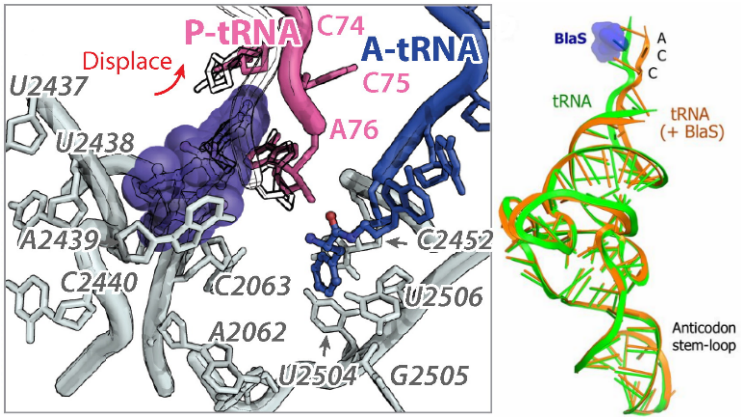

Figure 18 Displacement and distortion of the P-site located tRNA through blasticidin S (in purple). On the right side, an overlay of the free tRNA (in green) and a blasticidin S bound tRNA (in gold) is shown. Clearly, a displacement of the tRNA is visible.

Gougerotin is an aminoacyl-nucleoside antibiotic and consists of a cytosine, 4-amino-4-deoxyglucuronamide and a sarcosyl-D-serine dipeptide unit (Figure 15). It was first isolated from *Streptomyces gougerotii* in 1962 (as No. 21544) by *Kanzaki* in Osaka, Japan,[105] and found to exhibit broad-spectrum antibiotic as well as antiviral and antitumor activities. Unfortunately, a certain toxicity to mammalian systems (LD_{50} in mice is 57 mg/kg) was reported. The structure elucidation of gougerotin followed in 1964. While initial studies showed that gougerotin is an inhibitor of protein synthesis, this effect is not detectable in intact cells due to the inability of the compound to cross the plasma membrane. In cell free assays or virally infected cells the nucleoside antibiotic shows activity.[106]

Antibiotics that target the 30S subunit. The small ribosomal subunit is especially involved in the initiation of the translation process, as discussed above. The binding of the 30S subunit to tRNA and mRNA assures, through a complex decoding mechanism, a correct recognition of each A-site codon of the mRNA by the corresponding anticodon of the aa-tRNA. This specific part of the 30S subunit involved in the proof-reading process is also referred as the decoding centre (DC) and is targeted by several classes of antibiotics. In the following section the mechanisms of action of four prominent antibiotics will be outlined, starting with the most prominent of those drugs, namely streptomycin (Figure 19).

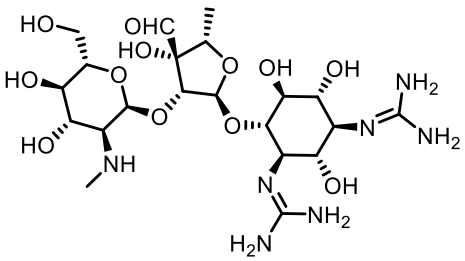

streptomycin

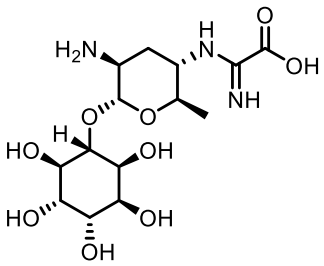

kasugamycin

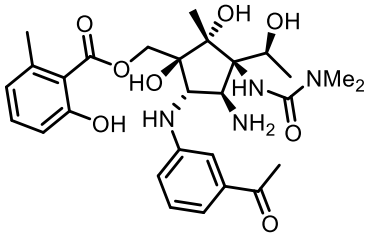

pactamycin

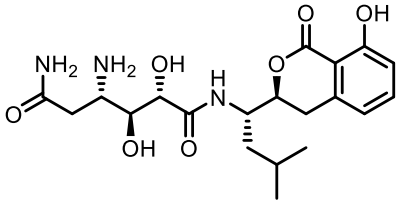

amicoumacin A

Figure 19 A handful of antibiotics that target the small ribosomal subunit.

Whereas initial investigations of its mode of action indicated that streptomycin rendered the ribosome more error-prone by affecting the proof-reading mechanism,[107] more recent work showed that it also induces miscoding by interacting with the minor groove of the codon anticodon helix.[108,109] It causes distortions within the A-site of the 30S subunit upon binding, which increase the level of miscoding by favouring the binding of non-cognate tRNAs.[110]

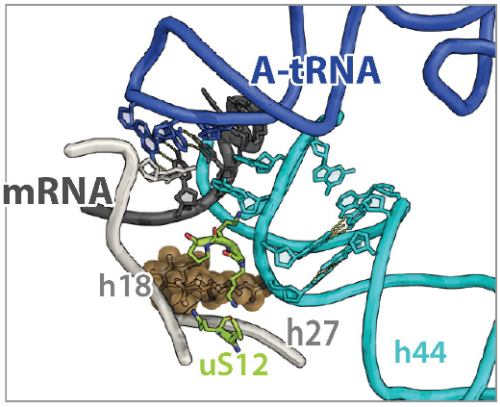

Figure 20 Crystal structure of streptomycin (in brown) bound to the 30S subunit (in grey, cyan and light green).

Not only the A-site of the small subunit can be targeted by antibiotics but also the P- and the E-site. Antibiotics that bind to the P- and E-sites are commonly referred to as translation initiation inhibitors but they can also affect the translocation of the mRNA and tRNA.[93]

The aminoglycoside antibiotic kasugamycin (Figure 19) binds the 30S subunit in a manner that it spans over the binding site of the E-site into the P-site region of the mRNA. It thereby distorts the designated space for the mRNA and inhibits the recognition of the start codon by the initiator fMet-$tRNA_i^{Met}$.[98]

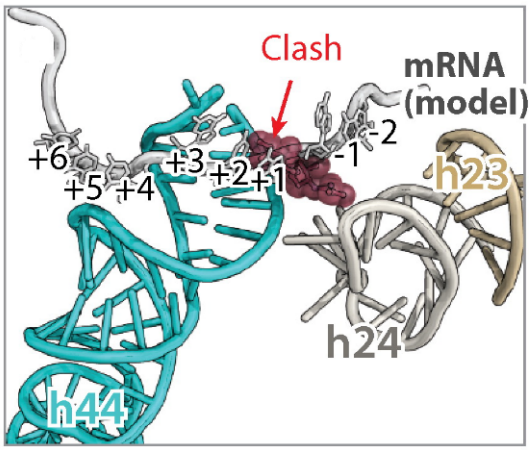

Figure 21 Overlap of the kasugamycin (in dark red) and the distorted mRNA recognition site.

Pactamycin (Figure 19) inhibits protein synthesis in bacteria, archaea and eukaryotes. It acts similar to kasugamycin, in the sense that it disturbs the binding of the mRNA and inhibits the formation of the initiation complex.[111] Strangely, the activity of pactamycin relies on the nature of the A-site substrate. The structural data currently available do not allow to explain such a context-dependency.[111]

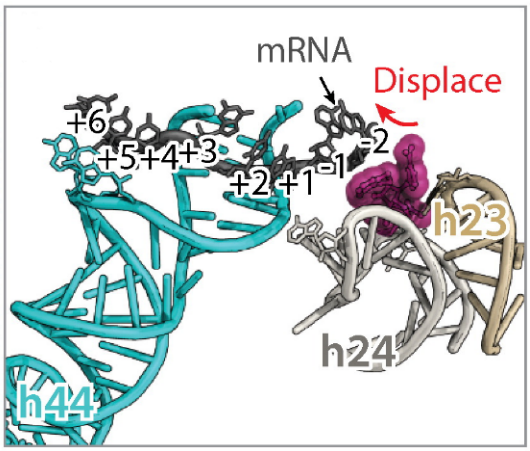

Figure 22 Pactamycin (in purple) bound to the 30S subunit and its induced mRNA displacement.

As the last example to be discussed here, amicoumacin A (Figure 19) tethers the backbone of mRNA and conserved nucleotides of the E-site 16S rRNA together. The mRNA is therefore incapable of moving, which finally results in the abortion of the translation process.

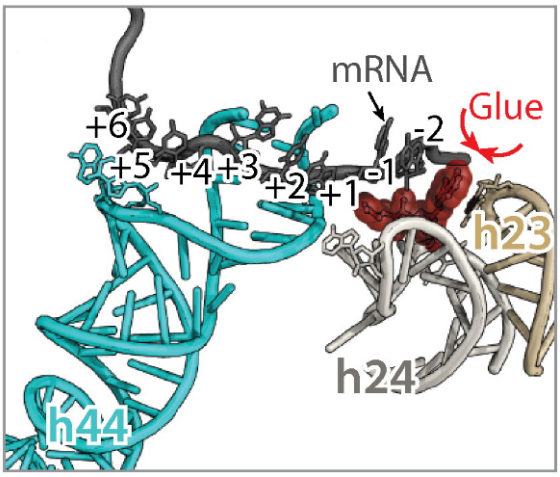

Figure 23 Amicoumacin (in red) binds between mRNA and the rRNA of the 30S subunit.

A fundamental requirement for all ribosomal antibiotics is the ability to discriminate between the prokaryotic and eukaryotic ribosomes.[112] Some noteworthy differences between the two ribosomes are important to briefly point out. **Structure**: The eukaryotic ribosome consists of a 60S large subunit and a 40S small subunit forming together the 80S ribosome with a mass of 4200 kd. The bacterial 70S ribosome has a significantly smaller mass of 2700 kd.[113] **Initiation**: The initiating amino acid in eukaryotes is methionine rather than *N*-formylmethionine and the exclusive initiation codon AUG exists in almost all cases only once. In contrast, prokaryotic mRNA has multiple *Shine-Dalgarno* sequences. Further, the eukaryotic machinery relies on more initiation factors than the prokaryotic. **Elongation and termination**: The elongation factors of the bacterial and mammalian cells are not the same and the termination is induced by a single release factor in eukaryotes compared with two counterparts in prokaryotes. [79,93,113]

1.1.7 Nucleoside Antibiotics

Nucleoside antibiotics (NA) represent a large family of natural products with immensely diverse biological activities, such as antibacterial,[114,115] antiviral,[116] antifungal,[117] antitumor[116] and insecticidal effects. They are of microbial origin and produced as secondary metabolites. It is not surprising that NAs often exhibit a broad spectrum of activities, since nucleosides and nucleotides play fundamental roles in cellular processes, such as storage of genetic information, embodying of metabolites, providing energy sources, being involved in cell signalling and representing cofactors for various enzymes.[118]

Categorizing NAs by their biological function, it is reasonable to organize them into three major groups. Firstly, NAs that target bacterial cell wall biosynthesis and inhibit the bacterial enzyme MraY (phospo-MurNAc-pentapeptide translocase), which is an integral membrane protein that catalyses the first step of the lipid cycle of bacterial peptidoglycan biosynthesis.[119] Secondly, the antifungal

NAs that inhibit the chitin synthesis by directly acting as a competitive chitin synthase inhibitors. Thirdly, the NAs, which block protein synthesis by inhibiting the peptidyl transferase.[120]

Alternatively, one can classify them by their chemical structure, as suggested by *Isono*, who is one of the pioneers in the field. According to *Isono* NAs can be grouped by their molecular architecture. Due to the extensiveness of this classification we would like to refer to the references [118,121].

1.1.8 Amicetin (**A-1**): Mode of Action

To the best of our knowledge, the first studies trying to determine amicetin's (**A-1**) mode of action were performed in 1966. The addition of the compound was shown to immediately stop protein synthesis in growing cultures of *E. coli* but did not affect the formation of RNA and DNA.[122] These findings clearly indicated an interference with the protein synthesis machinery and paved the way for further research. It was hypothesized, that amicetin (**A-1**) blocks the transfer of an amino acid from the aminoacyl-tRNA to the ribosomal peptide, in analogy to the nucleoside antibiotics puromycin, gougerotin and, blasticidin S.

Some 20 years later, the exact binding site of amicetin (**A-1**) was deciphered, based on site-directed mutagenesis and chemical footprinting studies.[108] *Halobacterium halobium* were exposed to sub-inhibitory concentrations of amicetin (**A-1**) for 1.5 months. After this period, the bacteria isolated were substantially more resistant to **A-1** than the original wild type. RNA sequencing revealed a particular ribosomal point mutation, U2457 → C, that was located in the 23S rRNA region at a crucial site within the PTC. No other mutations were detected in the central circle of region V (Figure 24). In previous studies, single-site mutations in this specific region of the rRNA led to resistance to known peptidyl transferase inhibitors such as chloramphenicol.[123]

Mutant plasmids were designed by the group of *Garret* with specific mutations at position 2457 (all three possibilities) by site-directed mutagenesis.[108] Each mutation was transferred, via plasmid transformation, into the wild-type, to the single chromosomal 23S rRNA gene by homologous recombination along with a specific anisomycin resistance mutation. Based on the selection of anisomycin resistant bacteria, the mutants were analysed and sequencing confirmed that only the U2457 → C mutation produced resistance against amicetin (**A-1**).

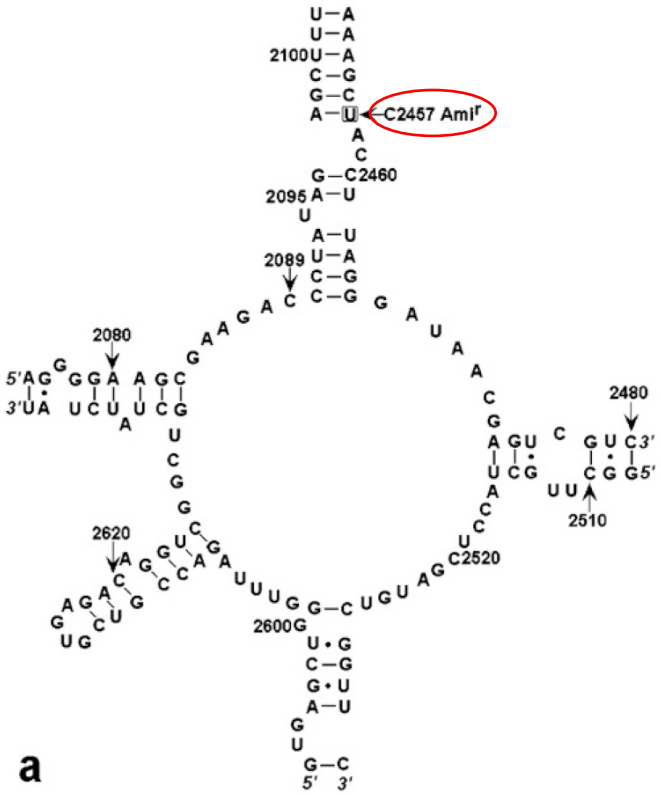

Figure 24 Schematic drawing of the secondary structure of the peptidyl transferase centre, domain V, of the 23S rRNA and the amicetin induced point mutation C2457 Ami^r.

Together with the results of previous investigations on other pyranosyl-cytosine derivatives drugs, which had been shown not to be simple analogues of A-site-bound aminoacyl tRNAs,[108,124] *Garret*'s findings suggested that amicetin (**A-1**) may interfere with the movement of the aminoacyl group towards the P-site-bound peptidyl tRNA. This hypothesis is also supported by the fact that amicetin (**A-1**) does not effectively compete with chloramphenicol. However, all these efforts notwithstanding, the precise mode of inhibition of protein synthesis by amicetin (**A-1**) remains to be elucidated.

Most recently, the solution structure of amicetin (**A-1**) has been determined by the group of *Ramesh.*[125–128] Initially, they investigated the interaction of the 23S ribosomal RNAs of *Halobacterium halobium* and *E. coli* with **A-1** by proton NMR spectroscopy and additional molecular modelling studies.[128] Synthetic 35-mer RNA motifs were scrutinized for changes in their spectral features upon the addition of amicetin (**A-1**). By titration of **A-1** to the 35-mer RNA sample in H_2O, shifts and selective line broadening of the bases located in the highly conserved region of the PTC were observed (loop nucleotides remain unaffected).

In further work,[126] they used experimentally determined ROE-based distances as input for a three-dimensional structure determination protocol and on that basis calculated an energy-minimised structure of amicetin (**A-1**) in solution (Figure 25). As depicted below, in solution, **A-1** adopts a folded

conformation exhibiting three distinct intramolecular hydrogen bonds that hold together the bent structure. Hydrogen bonds are formed between the nitrogen- and carbonyl-moieties of the serine-amide and the 5-OH and 6-OH groups present in the amosamine sugar. The amosamine adopts a chair-type conformation with a slight rotation in the direction of the serine amide, which is essential for the hydrogen bonding. In contrast to the reported crystal structure of amicetin (**A-1**),[7] where the amicetose sugar is found in a (slightly distorted) chair conformation, it assumes a twisted chair conformation.

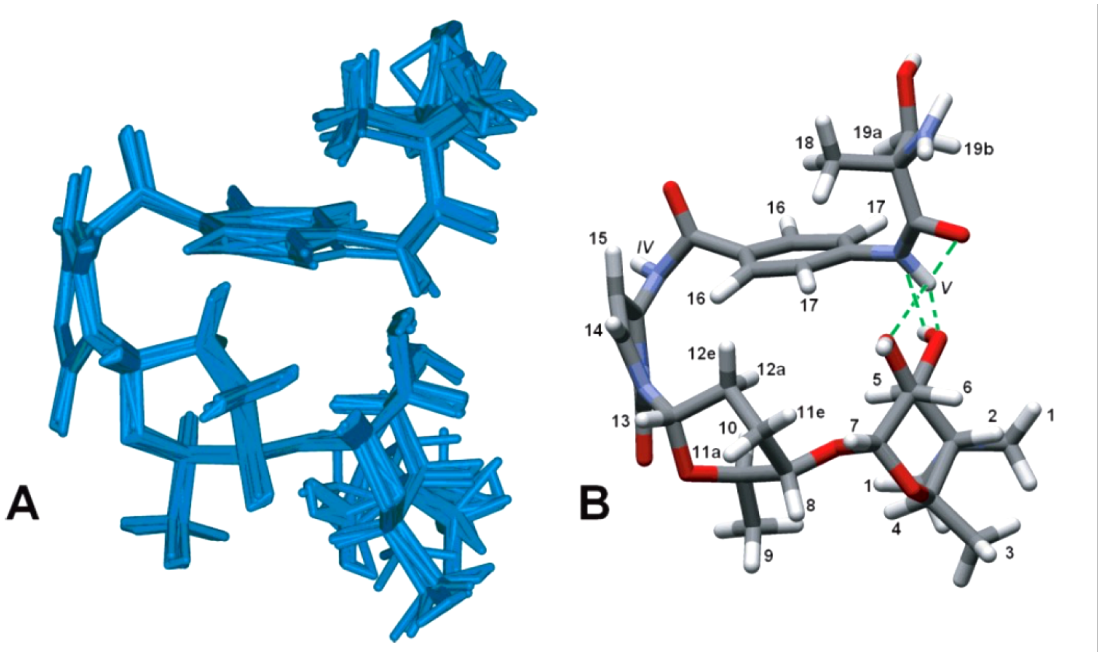

Figure 25 Solution state NMR structure of amicetin **(A-1)**. A) Describes the overlay of the ten energy-minimised structures of amicetin **(A-1)** in solution. Calculations were done using NMR constraints (total of 18 NOEs were measured and categorised into either strong 1.8 - 2.5 Å, medium 1.8 - 3.3 Å or weak 1.8 - 5 Å). B) Describes an averaged structure derived from the ten calculated structures. The green dotted lines indicate hydrogen bonding interactions.

As a closing remark, the group speculates about the functionally important conformation of the cytosine motif for the assumed interaction with the peptidyl transferase RNA motif of the 23S rRNA. The critical turn position within the folded structure is assumed to allow the cytosine moiety to make potential hydrogen bonding interactions with the ribosomal RNA.[129]

Over the past years, the structure of several antibiotics bound either to the peptidyl transferase centre or the small subunit of the bacterial ribosome has been determined by X-ray crystallography.[92,130,131] A recently published crystal structure of amicetin (**A-1**) bound to the 70S ribosome (PDB-code 6CZR), which has yet not been further discussed by the authors, might deepen our understanding of the molecular detail of the antibiotic interaction with the ribosome in the near future.

1.1.9 Relevant Synthetic Work

*1.1.9.1 Stevens' Synthesis of Plicacetin (**A-17**)*

The first total synthesis of a disaccharide pyrimidine nucleoside antibiotic was reported 19 years after the isolation of amicetin (**A-1**) in 1953.[1] In 1972, *Stevens* and co-workers published their work on plicacetin (**A-17**), which paved the way for further studies towards the total synthesis of **A-1** (Scheme 7).[132] The key step of their synthesis was the stereospecific formation of the α-disaccharide linkage between amosamine and amicetose. They reacted the β-chloro azido sugar **A-20** with the nucleoside **A-19** under basic conditions to form the acetal **A-21** in 38% yield.

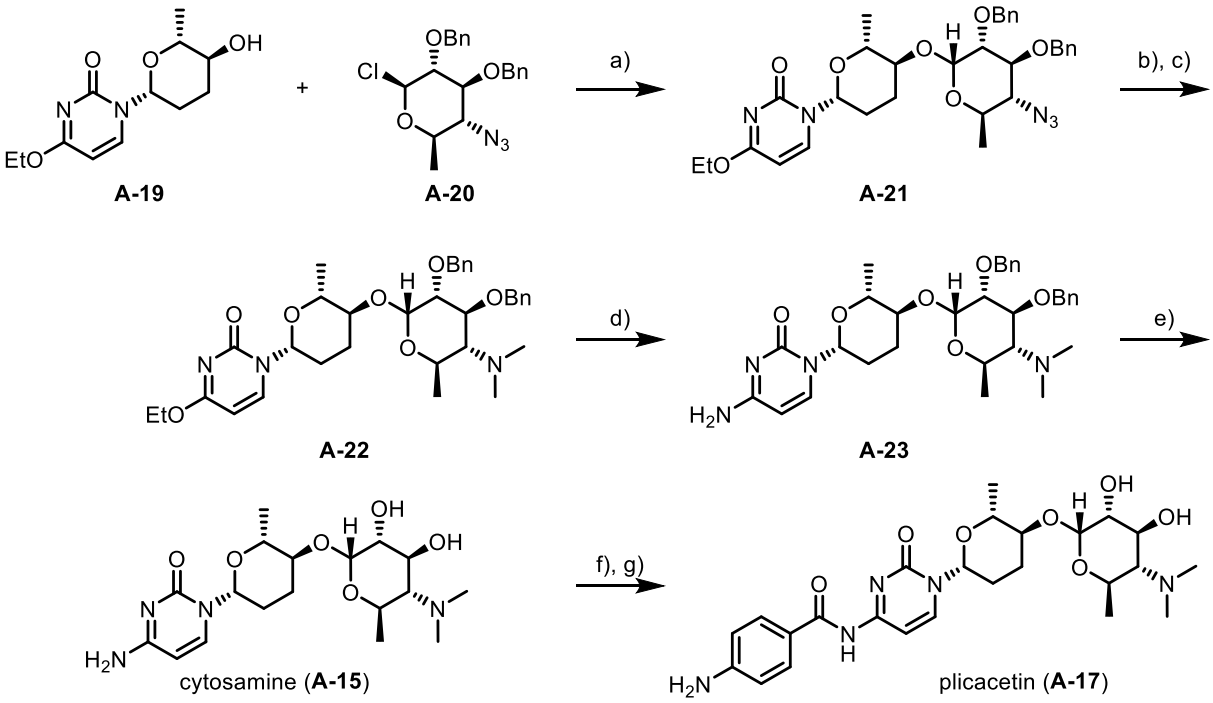

Scheme 7 *Stevens*' total synthesis of plicacetin (**A-17**). Reagents and conditions: a) Dowex 1-X2 (OH^-), 38%; b) Pd/C, H_2; c) HCHO, H_2, Pd/C, EtOH, 84% over two steps; d) ammonia-ethanol, 110 °C, 88%; e) Pd/C, H_2, cat. HCl; f) *p*-nitrobenzoyl chloride, $CHCl_3$, reflux; g) Pd/C, H_2. No yields were reported for the steps f) and g).

After preparative thin-layer chromatography and two recrystallizations, they obtained the solely α-linked disaccharide, which was confirmed by the vicinal coupling constant of the anomeric proton (J = 3 Hz). Unfortunately, no explicit information is provided in *Steven*'s report if they obtained or isolated any of the β-configured disaccharide side product. The synthesis was continued by a reduction of the azide moiety of **A-21** with hydrogen over palladium on charcoal, followed by a reductive methylation with formaldehyde to give **A-22** in good 84% yield over two steps. The free amino group of the cytosine moiety was introduced by boiling the compound in an ammonia-ethanol mixture at 110 °C to yield **A-23**. Finally, the benzyl protecting groups were removed under reductive conditions with HCl as acid catalyst to give the free cytosamine (**A-15**). The formation of plicacetin (**A-17**) starting from **A-15** was performed according a protocol, which was first reported by *Haskell*[133]; cytosamine was reacted with *p*-nitrobenzoyl chloride to give the pure product after recrystallization.

The nitro moiety was then reduced with hydrogen over palladium on charcoal to give plicacetin (**A-17**).

1.1.9.2 Sugimura's Formal Synthesis of Cytosamine

In 2001, *Sugimura* reported the formal synthesis of cytosamine[134] (Scheme 8). They used glycosyl fluoride **A-35** to establish the α-configured glycosydic bond in the disaccharide unit. Further, a stereoselective route to trideoxyhexopyranosyl nucleoside **A-34** via an intramolecular glycosylation reaction was showcased.

The synthesis commenced with commercially available glycal **A-24**, which delivered the thioglycoside **A-25** via a sequence of seven steps. Treatment of **A-24** with boron trifluoride etherate in methanol gave rise to a *Ferrier* rearrangement[135] yielding the 2,3-unsaturated 1-methyoxy pyranose. The double bond was reduced under conventional hydrogenation conditions to give the fully saturated derivative. The use of trimethyl(phenylthio)silane and $BF_3 \cdot Et_2O$ as first reported by *Nicolaou*[136] gave rise to the anomeric thiophenyl moiety. A sequence of deprotection, selective protection of the primary alcohol, protection of the secondary and liberation of the primary alcohol finally delivered **A-25** in good overall yields. The thioglycoside was reacted with **A-26** to give precursor **A-27** for the intramolecular glycosylation reaction. Treatment of the pyranosyl nucleoside with $Me_2S(SMe)BF_4$ at -20 °C generated the oxonium **A-28** and the cyclic pyrimidinium intermediate **A-29**, respectively. Hydrolysis of **A-29** was achieved using aqueous NaOH to yield the desired β-nucleoside **A-30** in reasonable 56% yield, together with 23% of the C-1 hydrolysed side product **A-31**. It is worth noting that a change from the benzyl protecting group at C-4 to a PMB group increased the yield of the desired β-glycoside to 79%. For the deoxygenation of **A-30**, a thiophenyl moiety was first installed in excellent yield and the desulfurization of **A-32** was attempted. Raney Ni was found to be capable of producing **A-33**, however, only in low yields. An alternative route via a radical reduction of a 6-iodo derivative using tributyltin hydride was also established, which provided **A-33** in 48% yield over two steps. During the endgame, screening for optimal benzyl-removal conditions were made to liberate the alcohol moiety in **A-33**. However, several hydrogenation conditions, including transfer hydrogenation and acid-catalysed reactions were unsuccessful. Under all conditions, starting material was fully recovered. Finally, BCl_3 provided the desired product **A-34**, but only in poor 10% yield.

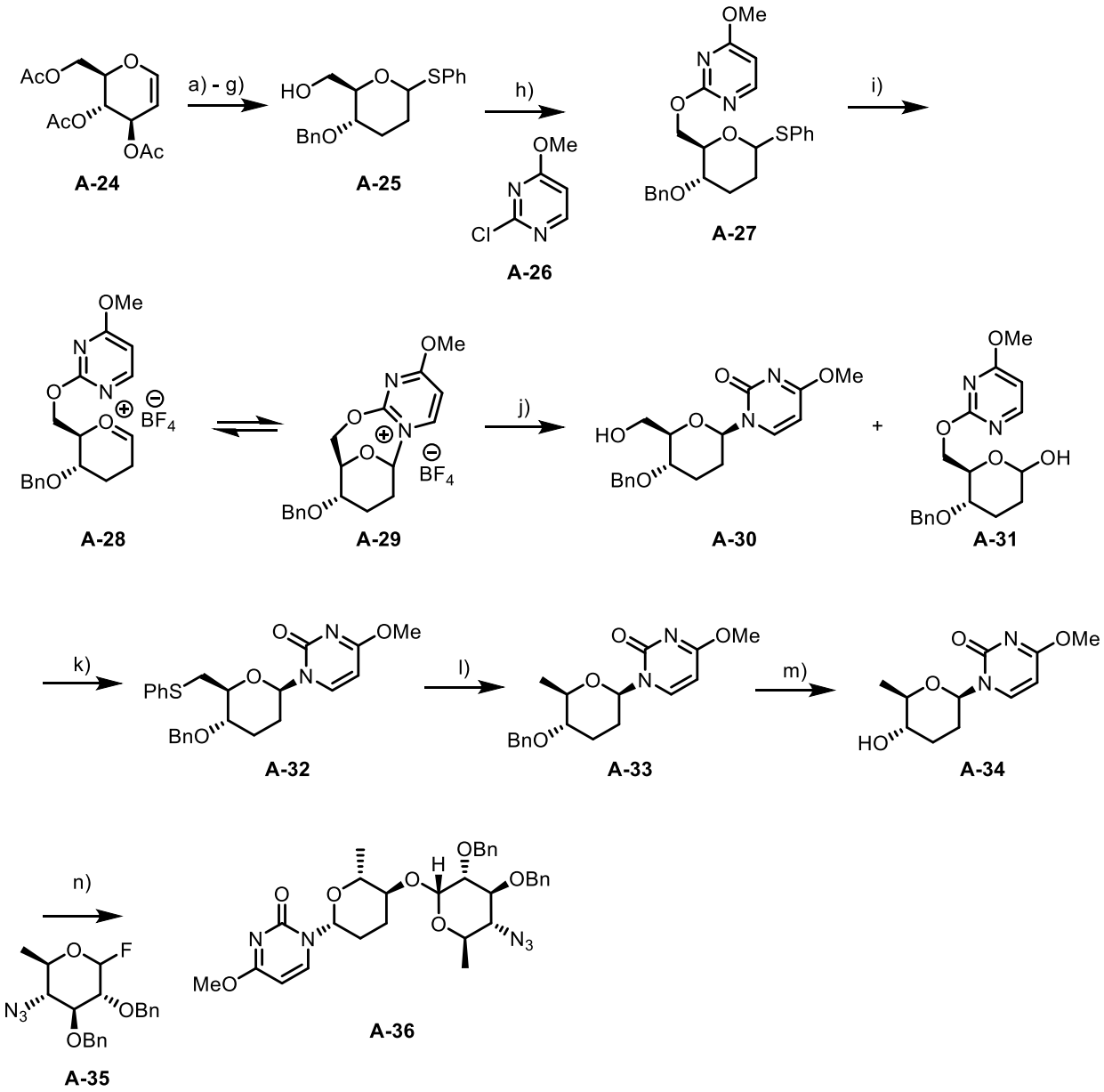

Scheme 8 *Sugimura*'s synthesis of **A-36**. Reagents and conditions: a) MeOH, $BF_3O{\cdot}Et_2O$; b) H_2, Pd/C, 85% over two steps; c) $PhSSiMe_3$, $BF_3O{\cdot}Et_2O$, 81%; d) NaOH, MeOH; e) TrCl, pyridine, 83% over two steps; f) BnBr, NaH, DMF; g) TFA, butanol, 88% over two steps; h) NaH, DMF, -50 to -20 °C, 77%; i) $Me_2S(SMe)BF_4$, MeCN, -20 °C; j) NaOH (1 M), 0 °C, 56% for **A-30** and 23% for **A-31**; k) PhSSPh-Bu_3P, pyridine, 98%; l) Raney Ni, 26%; m) BCl_3, 10%; n) AgOTf, $SnCl_2$, Et_2O:DCE (9:1), 52%.

The second glycosylation was achieved by the activation of glycosyl fluoride **A-35** with silver triflate and stannous chloride, which successfully glycosylated **A-34** to furnish disaccharide **A-36**. The desired α-glycosidic bond was obtained in 52% yield; in addition, 11% of the β-product was isolated. Initially, *Sugimura*'s group investigated the activation of a thioglycoside under conditions reported by *Fukase*,[137] utilizing a mixture of NBS and $LiClO_4$. These efforts remained ineffective though and starting material was reisolated, indicating that the glycosyl donor had not even been activated. They further examined the use of $Me_2S(SMe)BF_4$ and indeed obtained **A-36**, but in low yields and with poor anomeric selectivity (11% and a ratio of α:β = 2).

1.1.9.3 Yu's Synthesis of Plicacetin and Streptcytosine A

Early in 2018, Y*u* and co-workers published the total synthesis of plicacetin (**A-17**) and streptcytosine A (**A-49**) (Scheme 9 and Scheme 10).[138] Their work is centred on a gold-catalysed glycosylation of the cytosine base with an advanced disaccharide moiety. At that time, our synthetic efforts towards **A-1** were already advanced and only the ultimate glycosylation was missing.

Yu's synthesis commenced with the preparation of glycosyl donor **A-38**, which was accessed in 11 steps from commercially available penta-O-acetyl-β-D-galactopyranose. The glycosyl acceptor **A-37**, was synthesised in 6 steps departing from a 3,4,6-tri-O-acetyl-D-glucal. With this building blocks in hand, disaccharide **A-39** was successfully obtained by means of a *Schmidt* glycosylation promoted by TBSOTf at -60 °C in diethyl ether. The reaction showed excellent α-selectivity (α:β = 8:1) and was very high yielding (92%). The anomers were readily separated via silica gel chromatography. A TBAF-mediated desilylation, followed by installation of the *o*-hexynylbenzoate moiety gave the desired donor **A-40**. The reaction with silylated cytosine under $Ph_3PAuNTf_2$ catalysis in acetonitrile gave nucleoside **A-42** in good yield (77%) and excellent β-selectivity (α:β = 1:10). The gold(I)-catalysed glycosylation using an *o*-hexynylbenzoate donor had been developed previously in *Yu*'s laboratory (for more details *vide infra* in sub-chapter *1.3.5.12*).[139–142]

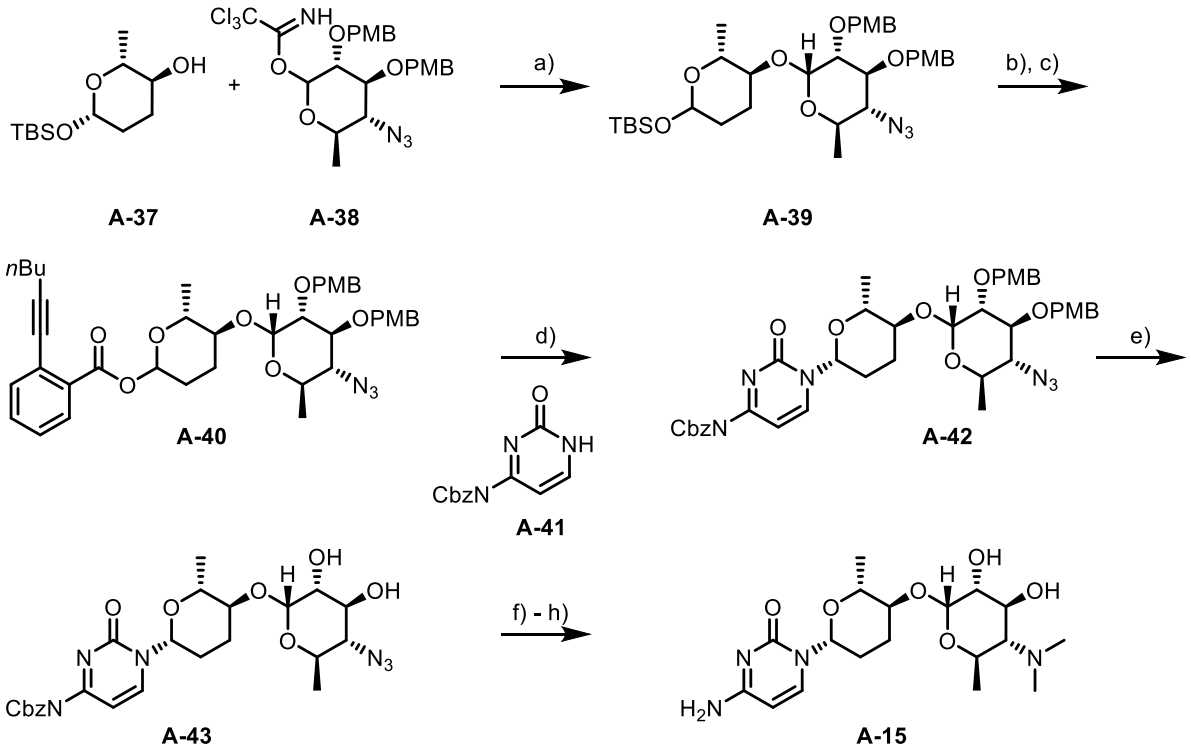

Scheme 9 Synthesis of cytosamine (**A-15**). Reagents and conditions: a) TBSOTf, Et_2O, -60 °C, 92%, α:β = 8:1; b) TBAF, THF; c) *o*-hexynylbenzoic acid, EDCl, DIPEA, DMAP, CH_2Cl_2, 84% over two steps; d) BSTFA, $Ph_3PAuNTf_2$, CH_3CN, 77%, α:β = 1:10; e) TFA, CH_2Cl_2, 83%; f) $P(CH_3)_3$, NEt_3, THF, H_2O, 50 °C; g) $(CH_2O)n$, $NaBH_3CN$, AcOH, CH_3OH; h) H_2 (1 atm), Pd/C, CH_3OH, 64% over three steps.

Both PMB-protecting groups were removed with TFA and the azide moiety of **A-43** was submitted to a reduction/alkylation sequence. Finally, the reductive cleavage of the Cbz-group gave cytosamine (**A-15**) in good yields (64% over the last 3 steps).

The endgame of the synthesis of **A-49** commenced with the HATU-promoted amide coupling of oxazolidine **A-44** with benzyl 4-aminobenzoate (**A-45**) at 80 °C. Opening of the oxazolidine under forcing conditions and subsequent TBS-protection of the primary alcohol gave amine **A-47** in 75% over two steps. Next, formation of the imidazolidine ring was performed by reacting **A-47** with paraformaldehyde and $NaHCO_3$ and the acid functionality was obtained after removal of the benzyl ester to give **A-48** in 81% yield over both steps. Coupling of the acid **A-48** with **A-15** was performed with HATU in pyridine. The final TBS-removal was achieved with HF·pyridine and additional pyridine as buffer to give the natural product streptcytosine A (**A-49**).

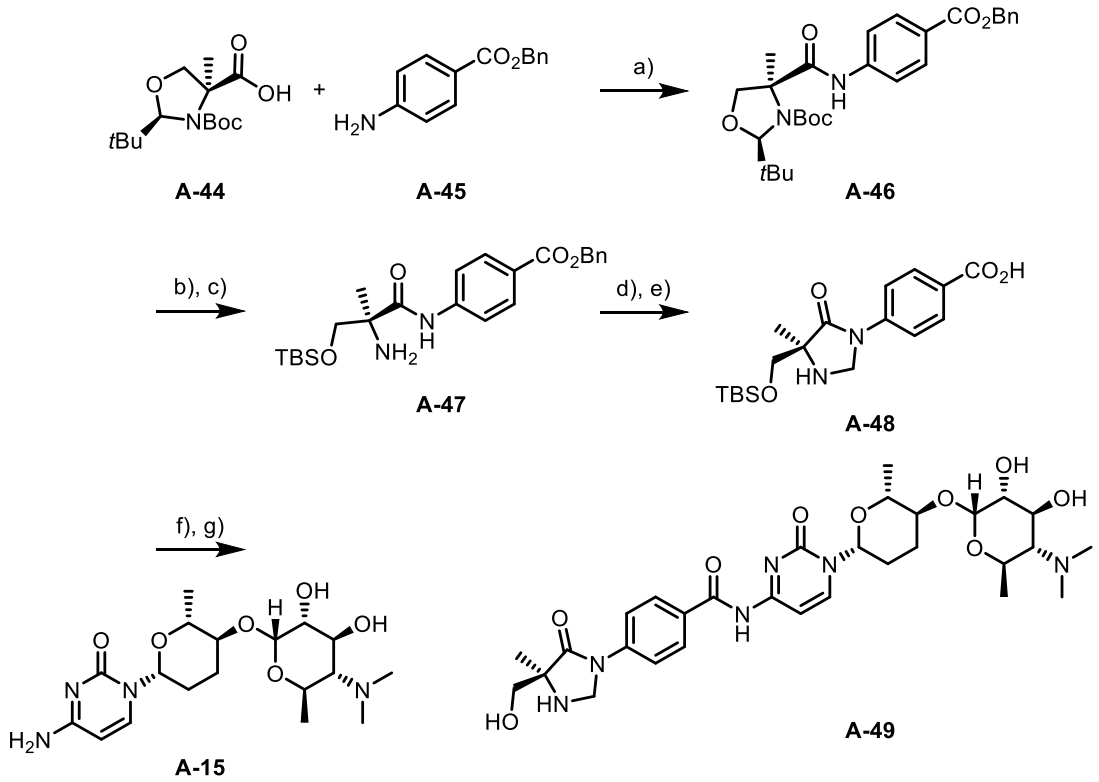

Scheme 10 Synthesis of streptcytosine A. Reagents and conditions: a) HATU, DIPEA, DMF, 80 °C, 67%, b) HCl (6 M), BnOH, 80 °C; c) TBSCl, imidazole, DMF, 75% over two steps; d) $(CH_2O)n$, $NaHCO_3$, MeCN, 60 °C; e) H_2 (1 atm), Pd/C, CH_3OH, 81% over two steps; f) HATU, pyridine, 80 °C; g) HF·pyridine, pyridine, 65% over two steps.

1.2 Aims and Scope

Based on the discussion in section 1.1.1, it is clear that amicetin (**A-1**) represents a potentially promising lead structure for the discovery of new antibiotics, including and in particular for the development of new antimycobacterial agents. At the same time, while some limited work had been reported on the chemistry of disaccharide-based cytosine nucleoside antibiotics, no total synthesis of amicetin (**A-1**) had been reported in the literature at the outset of this PhD project. Prior work had included the synthesis of each of the sugar moieties amosamine (**A-52**)[2,3] and amicetose (**A-51**)[143], along with efforts towards the cytosine nucleoside,[144] the amicetin (**A-1**) aglycone cytimidine (**A-50**)[145] and the nucleoside antibiotic plicacetin (**A-17**)[138,146]. Importantly, the work by *Yu* discussed in section 1.1.9.3 was only published when our synthetic efforts had already advanced to the stage, where only a final glycosylation was required to complete the synthesis.

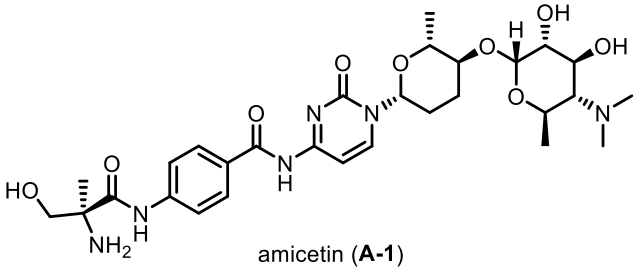

amicetin (**A-1**)

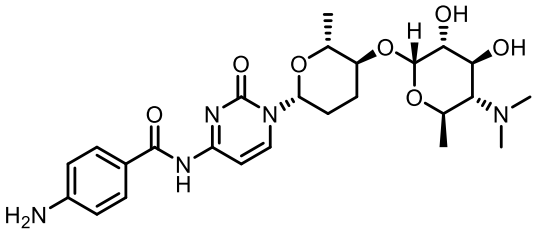

plicacetin (**A-17**)

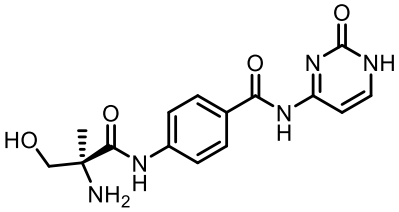

cytimidine (**A-50**)

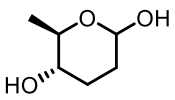

amicetose (**A-51**)

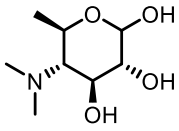

amosamine (**A-52**)

In light of the above, the primary goal of this PhD thesis was the development of a first total synthesis of **A-1**. In subsequent steps, the chemistry developed in the course of the total synthesis work was planned to be exploited for the synthesis of structural analogues of amicetin (**A-1**) for structure-activity relationship (SAR) studies. In particular, these studies should shed light on the importance of the specific disaccharide moiety in amicetin (**A-1**) for its biological activity. No SAR studies around amicetin (**A-1**) can be found in the literature so far.

1.3 Results and Discussion

1.3.1 General Retrosynthetic Considerations

In principle, two distinct pathways could be envisioned for the elaboration of protected cytimidine **A-53** into amicetin (**A-1**) (Scheme 11): **A-53** could be glycosylated with the fully decorated disaccharide **A-54** (pathway A) or a sequential route could be followed, in which glycosyl donors **A-58** and **A-59** are reacted sequentially (pathway B).

While glycosylation of **A-53** was planned to be performed by a *Vorbrüggen* glycosylation, independent of the specific pathway to be followed, several options were considered to establish the glycosidic bond between **A-58** and **A-59**. In general, the disaccharide approach offered a higher degree of flexibility with regard to the amosamine donor system to be employed, which could be a glycosyl fluoride,[147] thioglycoside[148] or trichloroacetimidate,[149–151] to name only three possible options. In addition, precursors of compound **A-54** would allow functional group manipulations, especially the formation of the dimethylamine moiety at the disaccharide stage. As for the sequential route, the more elaborated intermediate **A-60** was anticipated to be more sensitive than **A-53**, thus leading to a limited choice of glycosylation conditions for the establishment of the glycosidic bond between the amicetose and amosamine moieties. Mild activation conditions for the glycosylation should be chosen for the glycosylation of the acceptor **A-60**. In light of the essential *Vorbrüggen* glycosylation in both strategies, we planned to examine the sequential approach first, based on the use of simpler glycosyl donor **A-58**. The expertise gained in this reaction can be employed for the disaccharide route in a second stage.

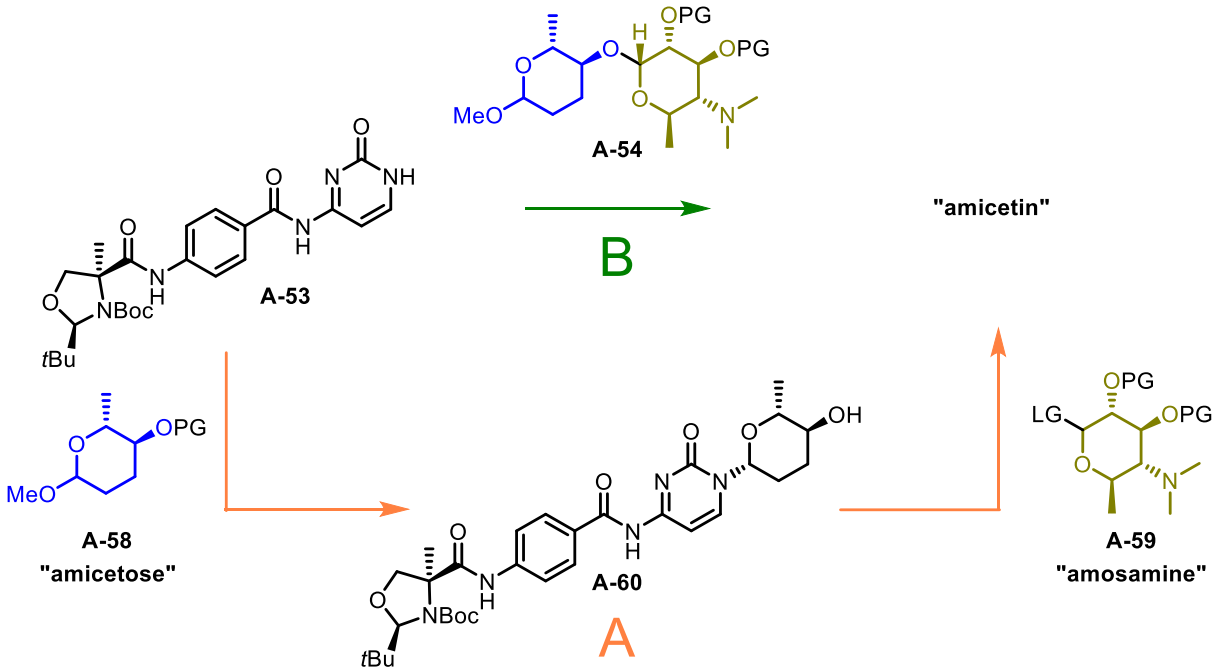

Scheme 11 The two plausible pathways A and B towards amicetin (**A-1**). PG: protecting group, LG: leaving group.

Among the different options for the order of fragment assembly, we felt it sensible to pursue a late stage aglycone glycosylation approach, in order to minimize the number of steps subsequent the incorporation of the sensitive sugar moieties. Therefore, we envisioned to complete the basic scaffold of **A-1** by a *Vorbrüggen* glycosylation of protected cytimidine **A-53** with the disaccharide donor **A-54** in a β-selective fashion (Scheme 12). Compound **A-54**, in which amosamine is α(1 → 4)-linked to amicetose, represents a retron for an α-selective *Schmidt* or *Mukaiyama* glycosylation between the glycosyl donor **A-59** and the scarcely decorated 2,3,6-deoxy sugar **A-58**.

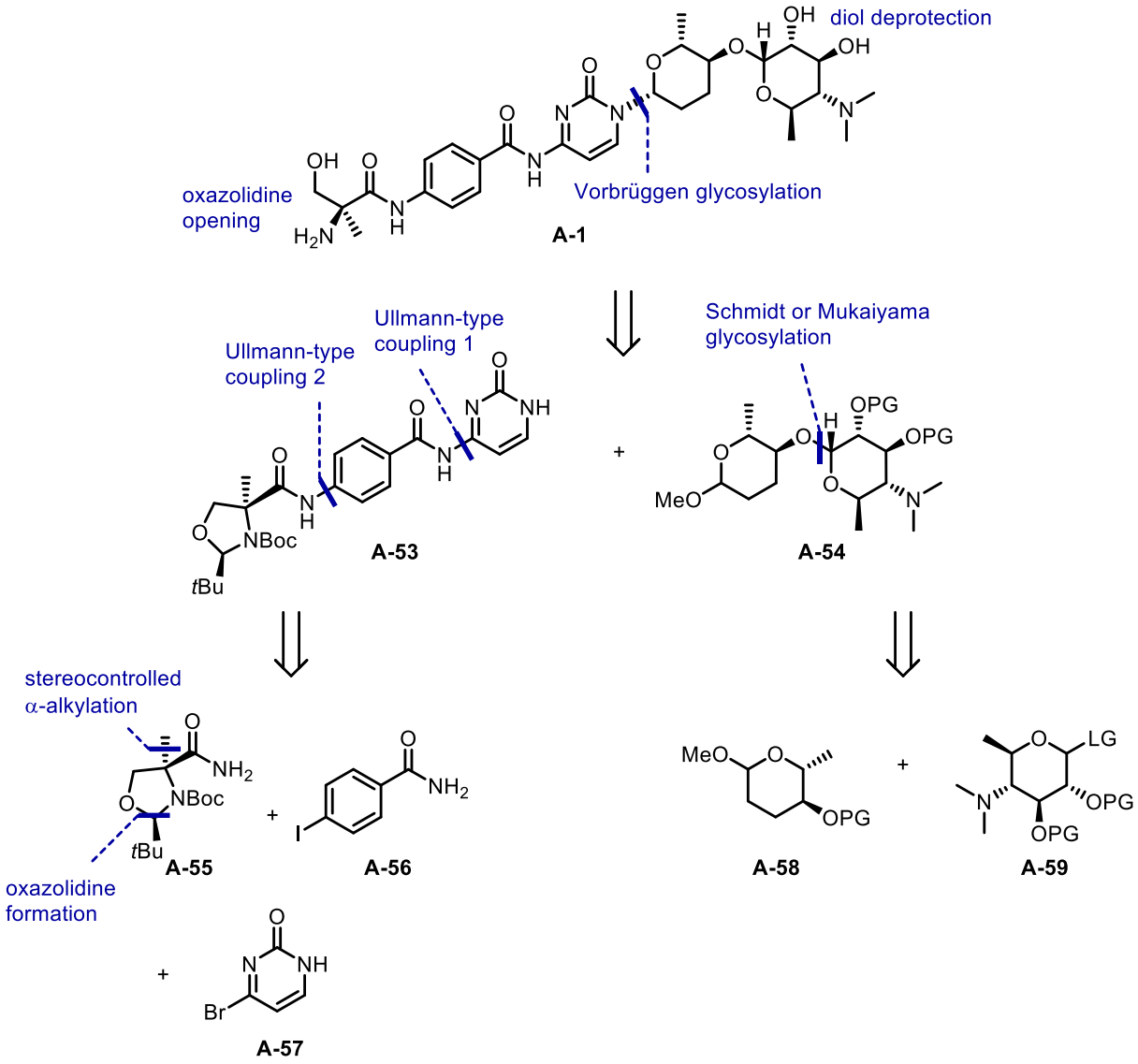

Scheme 12 Retrosynthesis of **A-1**. PG: Protecting group; LG: Leaving group.

The protected aglycone, *i.e.* cytimidine derivative (**A-53**) was to result from two successive *Ullmann*-type couplings involving the halogenated pyrimidinone **A-57**, *para*-iodobenzamide (**A-56**) and oxazolidine fragment **A-55**.

1.3.2 Oxazolidine Fragment A-55

The syntheses of acid **A-44**[152] and amide **A-55**[145] have been described in the literature (Scheme 13). In essence, the published procedures were followed with only minor changes. Thus, *L*-serine (**A-61**) was converted into its methyl ester **A-62** using thionyl chloride/methanol. The ester was condensed with pivalaldehyde under *Dean-Stark*[153] conditions and the resulting cyclic hemiaminal was directly Boc-protected to give oxazolidine **A-64** as a single diastereomer in 17% yield from *L*-serine.[154]

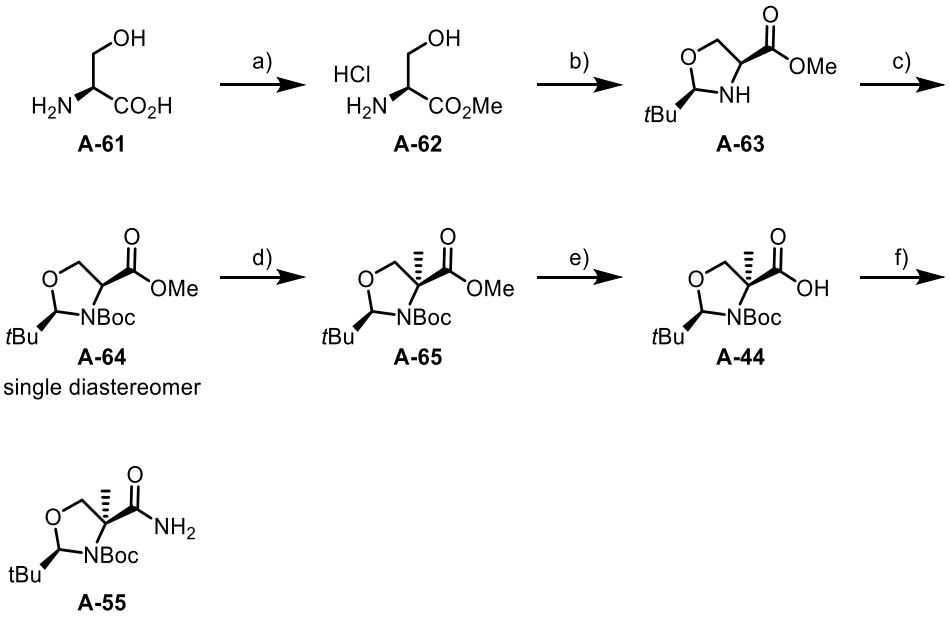

Scheme 13 Synthesis of **A-55**. Reagents and conditions: a) $SOCl_2$, MeOH, 0 - 25 °C, 20 h, quant.; b) $(CH_3)_3CHO$, NEt_3, pentane, reflux, 3.5 h; c) Boc_2O, K_2CO_3, THF, rt, 16 h, 61% over two steps; d) LiHMDS, MeI, THF, -78 °C, 6 h, 70%, dr: 10:1; e) $LiOH \cdot H_2O$, THF, 50 °C, 48 h, 75%; f) $(COCl)_2$, NEt_3, cat. DMF, CH_2Cl_2, NH_4OH (aq.), 0 °C to rt, 16 h, 54%.

The exclusive formation of the *cis*-configurated oxazolidine is in full agreement with published work.[154] As depicted in Scheme 14, the reaction of **A-62** with pivalaldehyde leads to a mixture of an open-chain imine, and *cis* or *trans* oxazolidine forms which can be observed by ^1H NMR. The ring-chain tautomerism of oxazolidines derived from serine esters has been described in detail by *Fülöp* and *Pihlaja*.[155] After the addition of Boc-anhydride, a shift of the equilibrium towards the ring form results in a selective protection of the *cis*-isomer.[156,157]

Alkylation of **A-64** was performed by enolate formation with LiHMDS and reaction with methyl iodide, which gave the desired product **A-65** with an excellent *dr* of 10:1 and in 70% yield. The selective methylation of **A-64** has been described previously by *Seebach*[158]. The enolate derived from **A-64** is still chiral due to the temporary centre of chirality at the acetal-C-atom, which bears the stereoinformation. Saponification of the ester moiety in **A-65** gave the free acid **A-44** in 75% yield. Surprisingly, the conversion of **A-44** into amide **A-55** was more cumbersome than expected. The best

results were obtained by forming the acid chloride, which was subsequently treated with aqueous ammonia giving amide **A-55** in 50% yield.

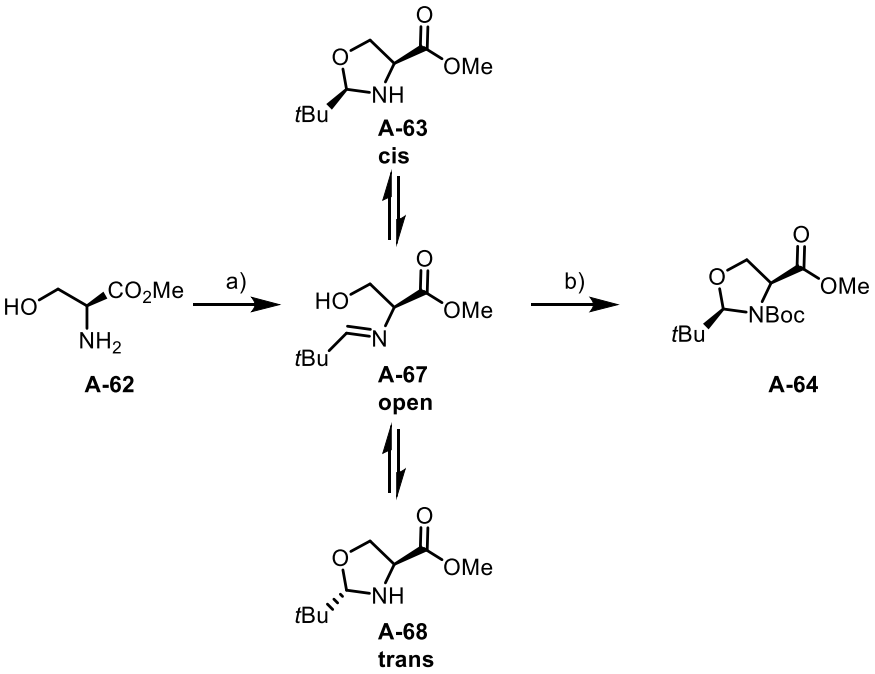

Scheme 14 Formation of N-Boc *cis*-oxazolidine. a) $(CH_3)_3COH$, NEt_3, pentane, reflux, 3.5 h. b) Boc_2O, K_2CO_3, THF, rt, 16 h.

1.3.3 Pyrimidylbenzamide Fragment A-75

1.3.3.1 Synthesis of A-72

Rather than trying to work with the barely soluble nucleobase cytosine, we planned to base our synthesis of the centre section of amicetin (**A-1**) on the use of a cytosine precursor or surrogate such as **A-71** (Scheme 15) that would facilitate handling. 4-Bromopyrimidine **A-70** was easily accessible from the commercially available thiopyrimidine **A-69** via a halogen exchange[159] followed by oxidation of the thioether linkage to the sulfone oxidation state[160] and a subsequent nucleophilic aromatic substitution.

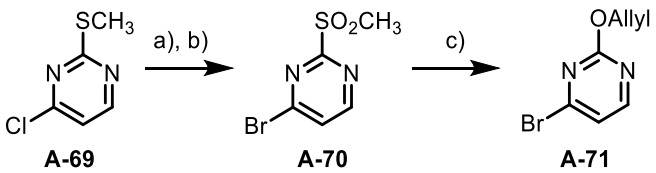

Scheme 15 Reagents and conditions: a) TMSBr, MeCN, 40 °C, 24 h, 97%; b) $(NH_4)_6Mo_7O_{24}$ $4H_2O$, H_2O_2, 0 °C, 24 h, 95%; c) KOtBu, allyl alcohol, THF, 0 °C then -78 °C, 7 h, 88%.

Bromo-pyrimidine **A-71** was coupled with 4-iodobenzamide (**A-56**) in a copper-catalysed N-aryl amidation reaction[161,162] (Scheme 16). Despite the elevated reaction temperature of 120 °C and a

reaction time of 19 h, full conversion of starting material was not achieved for the coupling (67% yield and 13% recovered starting material).

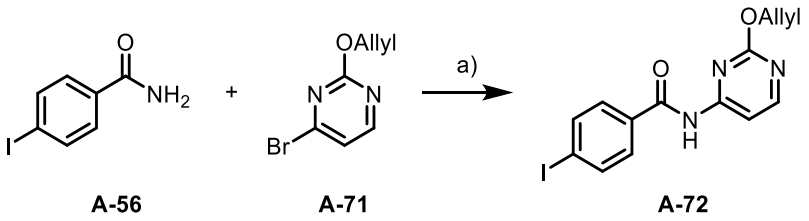

Scheme 16 Reagents and conditions: a) CuI, 1,10-phen, K_3PO_4, dioxane, 120 °C, 19 h, 67%.

*1.3.3.2 Allyl-deprotection of **A-72***

The deprotection of pyrimidylbenzamide **A-72** (Scheme 17) was investigated under various conditions (Table 5).

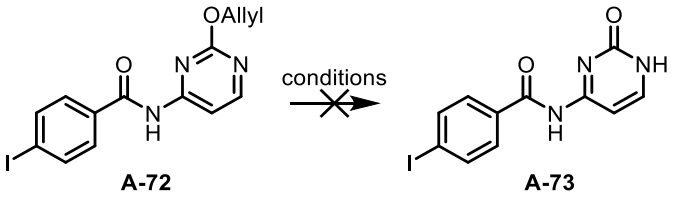

Scheme 17 Screening experiments for deprotection conditions for **A-72.**

In light of the presence of an aryliodide, our investigation started with the treatment of **A-72** with acid instead of transition metal-based catalyst systems with the propensity for metal-halogen insertion. Unfortunately, when **A-72** was simply stirred in a solution of HCl 4 M under microwave irradiation no cleavage of the allyl ether was observed and only starting material was recovered. When the temperature was raised, the compound started to decompose (entry **1**). A palladium mediated protocol was then examined,[163] but the only isolated product was methyl 4-iodobenzoate (entry **2**). These finding prompted us to change the solvent to THF and use morpholine as a base, but only starting material was recovered under those conditions (entry **4**). Finally, we turned our attention to a rhodium catalyst system (entry **3,5,6**), which has been well studied in the literature[164,165]. However, the reported reaction conditions, unfortunately, did not lead to the formation of the desired product. Isomerisation to the enol ether was not achieved and at higher reaction temperatures compound **A-72** either decomposed or the amide bond was cleaved. Eventually, we abandoned the strategy and examined another route (*vide infra*).

Table 5 Screening of allyl deprotection conditions for **A-72**.

Entry	Conditions	Outcome	Enol ether in crude
1	4 M HCl, microwave, 70 °C	recovered starting material	no
2	$Pd(PPh_3)_4$, K_2CO_3, MeOH, rt	formation of methyl 4-iodobenzoate	no
3	1) $RhCl(PPh_3)_3$, DABCO EtOH, H_2O, 80 °C	formation of methyl 4-iodobenzoate	n.d.
4	$Pd(PPh_3)_4$, morpholine, THF	recovered starting material	no
5	$RhCl(PPh_3)_3$, DABCO THF	recovered starting material	no
6	$RhCl(PPh_3)_3$, DABCO EtOH, 80°C	decomposition	n.d.

*1.3.3.3 Synthesis of PMB Derivative **A-75** and Deprotection to Access **A-73***

Confronted with deprotection issues for allyl ether **A-72**, the synthesis of the required pyrimidin-iodobenzamide was slightly adjusted such that sulfone **A-70** was reacted with *p*-methoxybenzyl alcohol, rather than allyl alcohol, under the same conditions, *i.e.* with KO*t*Bu as the base and THF as solvent at -78 °C (Scheme 18). The corresponding PMB-ether **A-74** was obtained in excellent yield (96%) and underwent successful *Ullmann*-type coupling with amide **A-56**, to give **A-75** in 69% yield.

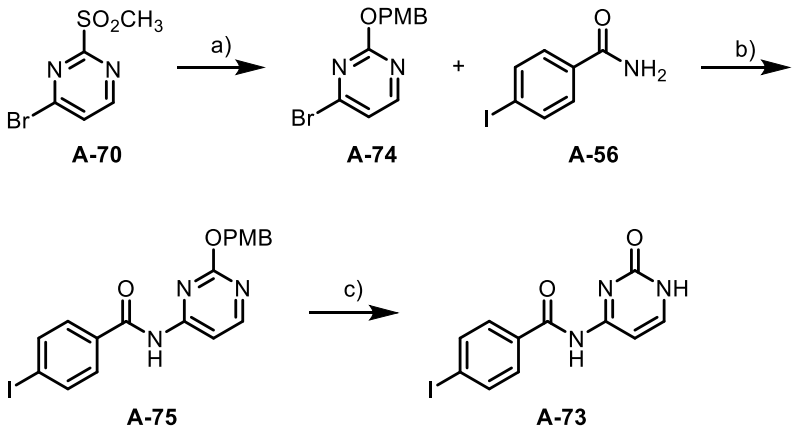

Scheme 18 Reagents and conditions: **a**) KOtBu, *p*-methoxybenzyl alcohol, THF, 0 °C then -78 °C, 7 h, 96%; b) CuI, 1,10-phen, K_3PO_4, dioxane, 120 °C, 21 h, 69%; c) DDQ, CH_2Cl_2, 24 h, 50%.

PMB-ether **A-75** could be successfully deprotected with an excess of DDQ and a reaction time of at least 24 h. The resulting cytosine derivative **A-73** was hardly soluble (even in DMSO) and could be

collected by simple filtration and washed with H_2O and EtOAc to give pure material. It is worth pointing out that NMR spectra of **A-73** had to be measured in deuterated trifluoroacetic acid (TFA)!

As an alternative route to **A-73**, cytosine (**A-13**) can be reacted with benzoyl chloride **A-76** to obtain compound **A-73** directly. Pyrimidinone **A-73** was silylated using N,O-bis(trimethylsilyl)acetamide) and directly, from Schlenk-to-Schlenk, distilled to confirm product formation by NMR analysis.

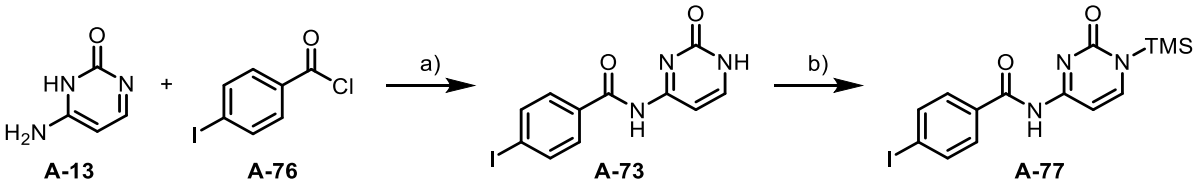

Scheme 19 Reagents and conditions: **a**) pyridine, 0 °C, 4 h, 64%; b) BSA, MeCN, rt, 30 min, yield not calculated.

1.3.4 Ullmann Coupling and Deprotection to Access Cytimidine (A-53)

With building blocks **A-55** and **A-75** in hand, the stage was set for the first phase of the fragment assembly process, which began with a second *Ullmann*-type reaction between the two fragments (Scheme 20). Compared to the coupling between **A-56** and **A-74** (Scheme 18), a different catalyst system was employed, consisting of CuI, DMEDA as a ligand and potassium carbonate in dioxane.[145] The reaction needed 60 h at 100 °C to reach completion and the desired product **A-78**was obtained in 80% yield. It may be hypothesised that in comparison to the more rigid phenanthroline ligand, which was used in the coupling reaction between **A-56** and **A-74**, the DMEDA ligand is more flexible and thus more favourable for the already sterically demanding oxazolidine carboxamide.[166] Usage of freshly distilled DMEDA was beneficial for the reaction yield.

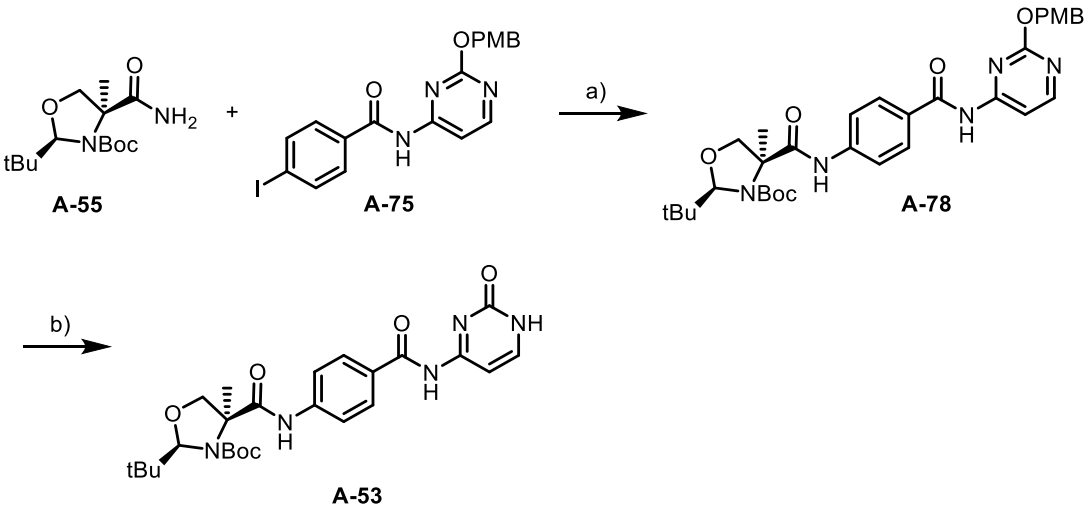

Scheme 20 Reagents and conditions: a) CuI, DMEDA, K_2CO_3, dioxane, 100 °C, 60 h, 80% brsm; b) DDQ, CH_2Cl_2, pH 7 buffer, rt, 67 h, 96%.

As for **A-75**, the successful removal of the PMB-protecting group from pyrimidinone **A-78** was affected by means of an oxidative cleavage with DDQ, to furnish advanced intermediate **A-53** in

excellent yield. Similar to **A-73**, intermediate **A-53** was hardly soluble and, therefore, purification was only possible by filtration and repetitive washings.

1.3.5 Sequential Approach

1.3.5.1 Synthesis of 2,3,6-deoxy sugar A-79

Pyranose **A-79** was envisioned to be obtained by an acid-catalysed methanol addition to glycal **A-81** (Scheme 21). The stereochemistry at the anomeric position of **A-79** is irrelevant due to its erosion at a later stage. The cyclic enol ether **A-81** would be accessed according to an established ring closing metathesis-isomerization approach (*vide infra*) using diene **A-82** as a precursor.[167] A synthetic route to allylic alcohol **A-83** has been described in the literature,[168] departing from commercially available (+)-ethyl D-lactate (**A-84**).

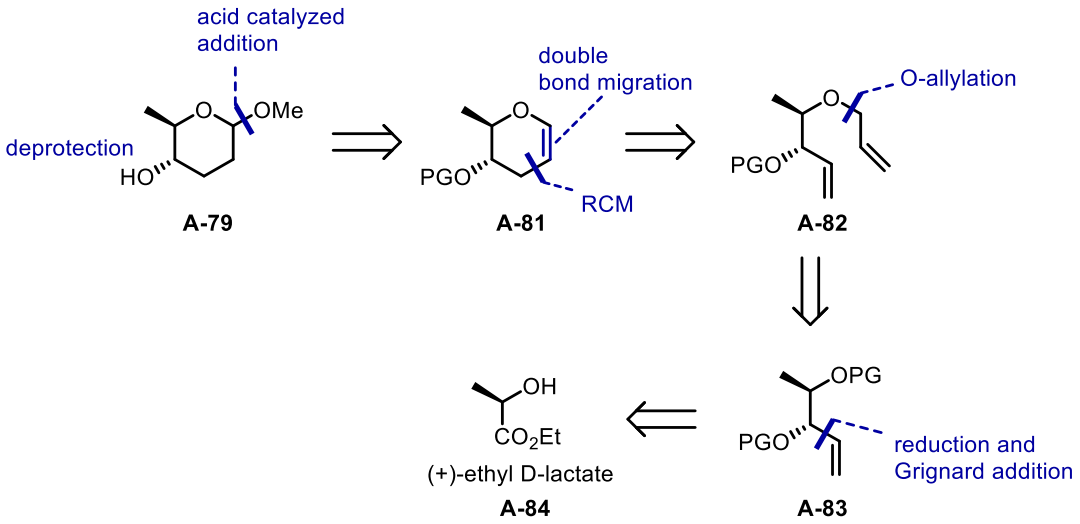

Scheme 21 Retrosynthesis of **A-79**. PG: Protecting group.

The synthesis of amicetose derivative **A-91** (Scheme 23) started with the TBS-protection of (+)-ethyl D-lactate (**A-84**), which proceeded in excellent yield (Scheme 22). Subsequent reduction of ester **A-85** to the aldehyde with DIBALH, followed by reaction of the aldehyde with vinylmagnesium bromide yielded the desired allylic alcohol **A-86** with a *dr* of 7:1.

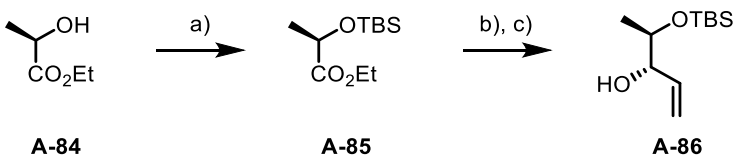

Scheme 22 Synthesis of **A-86**. Reagents and conditions: a) TBSCl, imidazole, CH_2Cl_2, 0 °C – rt, 16 h, 98%; b) DIBALH, Et_2O, -78 °C, 15 min; c) vinylmagnesium bromide, -78 °C, 20 min, 40% over two steps, dr 7:1.

In previous studies, it had been demonstrated that O-silylated lactaldehydes react with organometallic reagents predominantly in a *Felkin-Anh* manner.[169–173] In the *Felkin-Anh* model, the largest group is oriented perpendicular to the carbonyl axis provided there is no heteroatom present

adjacent to the carbonyl.[174] The attack of the nucleophile preferably takes place at an angle close to the ideal tetrahedral bond angle, designated as the *Bürgi-Dunitz*[175] trajectory, and the electrophilic carbonyl is approached over the smallest substituent (Figure 26).

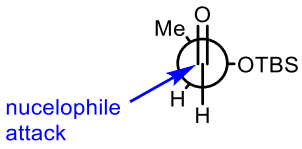

Figure 26 *Felkin-Anh* addition to the obtained lactaldehyde.

The two-step procedure to obtain allylic alcohol **A-86** needed optimization and was initially hampered by low yields. The *Grignard* reagent was always freshly prepared and titrated, to ensure accurate knowledge of the concentration employed. Nevertheless, a substantial amount of lactaldehyde (20 - 40%) was always reisolated after flash column chromatography. The aldehyde is not prone to epimerization during purification as confirmed by $[\alpha]^{20}_{D}$ measurements, which gave values in line with the literature data[176].

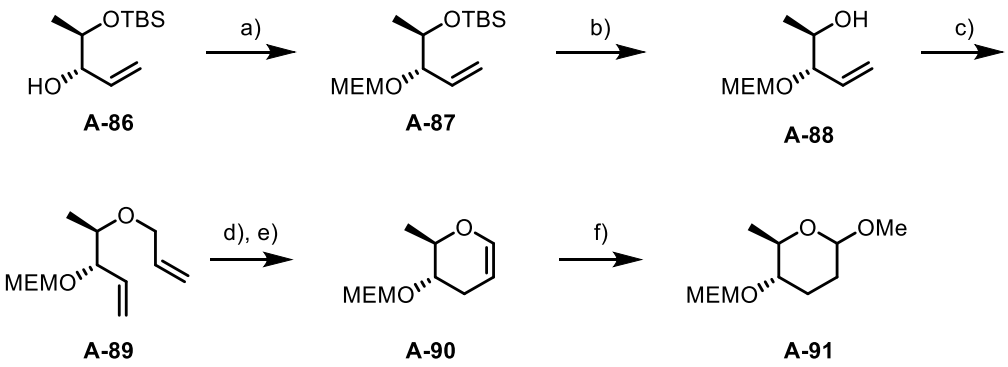

Scheme 23 a) MEM-chloride, DIPEA, CH_2Cl_2, 0 °C – rt, 36 h, 66%; b) TBAF, THF, rt, 16 h, 80%; c) NaH, allyl bromide, THF, 40 °C, 45 min, 67%; d) Grubbs catalyst first generation, toluene, rt, 22 h; e) NaOH, iPrOH, 110 °C, 2 h, 85% over two steps; f) CSA, MeOH, MeCN, rt, 1 h, 78%.

At this stage the two diastereomers were not separated (due to an almost identical R_f value), but the reaction sequence was continued with MEM-protection of alcohol **A-86**, followed by TBAF-mediated deprotection to obtain **A-88**. Allylation of the latter with allyl bromide to access the RCM precursor **A-89** worked smoothly within 45 min; at this point, the two diastereomers were separable by FC. Next, a one-pot ring closing metathesis (RCM) / double bond isomerization was performed to furnish glycal **A-90**. The RCM of functionalized dienes has been described in the literature[177]. Noteworthy, *Snapper*[178] and *Schmidt*[179] were the first to report a metathesis-isomerization sequence without isolating the primary metathesis product. It is believed that a metathesis-active ruthenium catalyst (in our case the 1st generation *Grubbs* catalyst **A-92**) is converted *in situ*[180,181] into an isomerization-active ruthenium-hydride species, such as **A-93**[182–184] (Scheme 24).

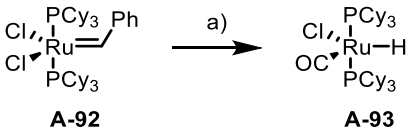

A-92 **A-93**

Scheme 24 Reagents and conditions: 2-propanol, MeOH, reflux.

An established pathway for transition-metal-catalysed olefin isomerization is outlined in Scheme 25. The olefin **A-94** coordinates to a kinetically long-lived metal hydride species, which has been characterized by *Grubbs*[185]. Subsequent insertion into the metal-hydride bond yields metal alkyl intermediate **A-96**. β-elimination and subsequent dissociation of the resulting metal hydride complex **A-97** then yields glycal **A-98** and regenerates the metal-hydride.[186]

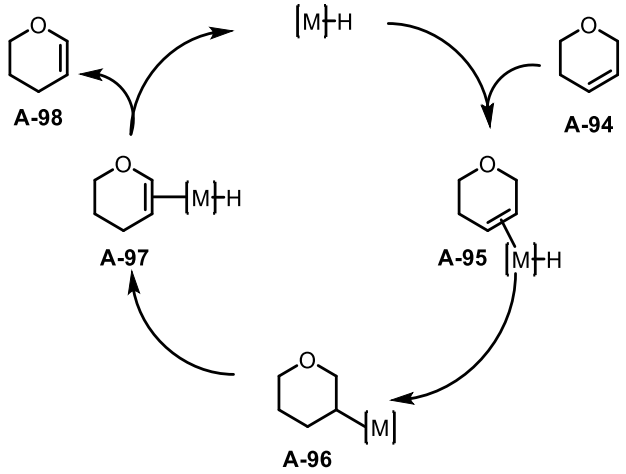

Scheme 25 Metal hydride addition-elimination mechanism.

During the initial step, the diene **A-89** was fully converted into the intermediate RCM product within 22 h at ambient temperature. After the addition of isopropanol and sodium hydroxide, the reaction was refluxed for 2 h, in order to obtain the isomerized glycal **A-90**. During the second step, the reaction had to be carefully monitored by TLC, due to undesired reduction of **A-90** by the ruthenium hydride complex. Hydrogen transfer occurs as a competing reaction with or subsequent to double bond isomerisation. Treatment of **A-90** with camphorsulfonic acid and methanol in dry acetonitrile gave the final amicetose fragment **A-91** as a mixture of anomers. Unfortunately, the final deprotection of **A-91** was low yielding (Scheme 26). In the best case, treatment of **A-91** with zinc bromide in dichloromethane gave **A-79** in 48% yield, while magnesium bromide in diethyl ether only produced uncharacterized side products.

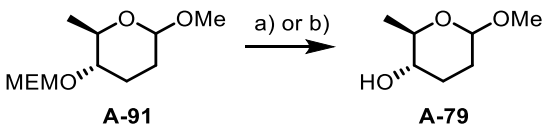

A-91 **A-79**

Scheme 26 Reagents and conditions: a) $ZnBr_2$, CH_2Cl_2, rt, 6 h, 48%; b) $MgBr_2$,Et_2O, rt, 24 h, 0%.

The issues with the final deprotection of **A-91** prompted us to rethink our initial strategy towards the required amicetose building block. In a second generation approach, a benzyl group was chosen to protect the OH group at C4 instead of the previously used MEM protecting group (Scheme 27). Conditions for most of the steps were kept the same as for the synthesis of **A-91**. Unfortunately, the separation of diastereomers after the *Grignard* addition turned out to be more cumbersome than with the MEM-derivative. Various solvent mixtures were tested for optimal chromatographic purification at the stage of **A-86**, with EtOAc:hexane 2:98 emerging as the most promising system. Finally, however, it was most practical to perform the separation of diastereomers at the stage of the alcohol **A-100**. Finally, the synthesis of **A-103** was carried out in a total number of 9 steps and an overall yield of 28%.

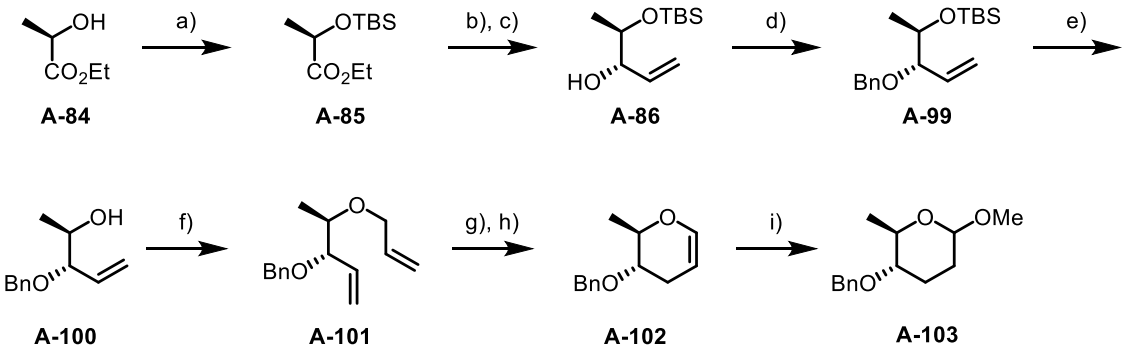

Scheme 27 Synthesis of **A-103**. Reagents and conditions: a) TBSCl, imidazole, CH_2Cl_2, 0 °C – rt, 16 h, 97%; b) DIBAL-H, Et_2O, -78 °C, 15 min; c) vinylmagnesium bromide, -78 °C, 20 min, 68% over two steps, dr 7:1; d) NaH, BnBr, THF, 0 °C – rt, 36 h, 88%; e) TBAF, THF, rt, 16 h, 76%; f) NaH, allyl bromide, THF, 40 °C, 45 min, 85%; g) *Grubbs* catalyst first generation, toluene, rt, 22 h; h) NaOH, iPrOH, 110 °C, 2 h, 82% over two steps; i) CSA, MeOH, MeCN, rt, 1 h, 90%.

In contrast to **A-91**, the deprotection of **A-103** was readily achieved under standard debenzylation conditions with hydrogen over palladium on charcoal in excellent yield (89%).

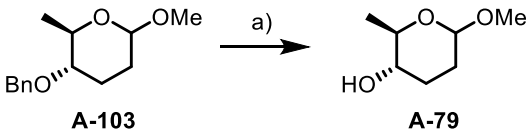

Scheme 28 Reagents and conditions: a) Pd/C, H_2 (balloon pressure), EtOH, rt, 1.5 h, 89%.

*1.3.5.2 Glycosylation of Aglycones **A-53** and **A-73** with Glycosyl Donor **A-103***

Next, we turned our attention to the glycosylation of **A-53** and **A-73** with the simplest glycosyl donor **A-73**, which was expected to be challenging for several reasons. Firstly, **A-103** features a 2,3,6-deoxypyranose ring and, therefore, harbours no inherent stereoinformation on the C-atom next to the anomeric centre, which could direct the attack at the anomeric carbon. The neighbouring group participation of a 2-O-X functionality[187] is usually a reliable promoter of stereoselective glycosylations (Scheme 29).

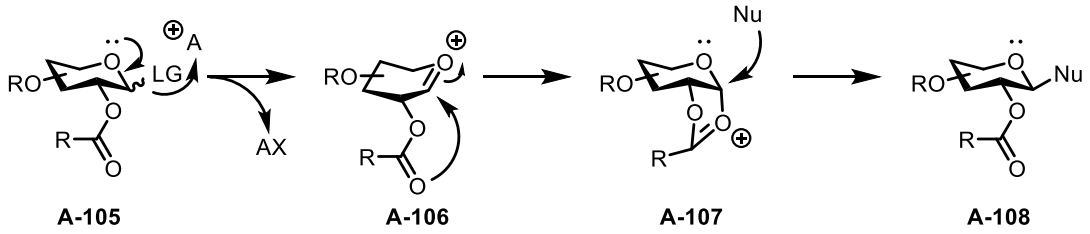

Scheme 29 Neighbouring group participation by a C-2 ester.

Secondly, the β-(1→N[1]) linkage to the cytosine nucleus is possibly not favoured over the axial configuration due to a gauche effect that exists in the case of an axial positioning of the cytosine base (Figure 27).

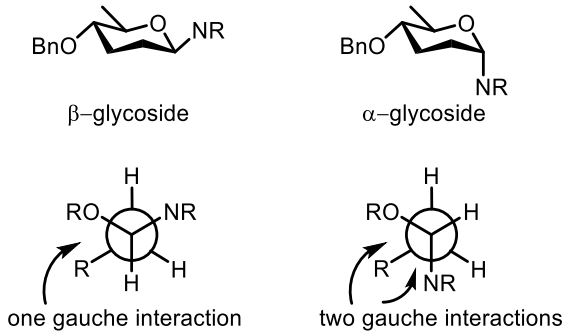

Figure 27 Possible *Gauche* interactions in the α-, β-glycosides.

Thirdly, glycosyl acceptor **A-53** is hardly soluble, which severely limits the choice of solvent systems that can be used for the reaction. Last but not least, one has to consider the anomeric effect, as first described by *Edward* and *Lemieux,*[188,189] which must be more stabilizing then the sum of all the steric factors to effect the conformation of the pyranose.

Literature precedence for the glycosylation of nucleobases goes back to the synthesis of pyrimidine nucleosides by *Hilbert* and *Johnson,*[190,191] who reacted 2,4-dialkoxypyrimidines or 2,4-bis-trimethylsilyl derivatives of uracils, cytosines and their 2-thio analogues with protected 1-halo sugars to give predominantly the *N*[1]-nucleosides. Further studies by *Nishimura*[192] and *Birkofer*[193] then paved the way for the *Vorbrüggen* procedure[194–196] (also known as silyl *Hilbert-Johnson* reaction). *Vorbrüggen* used a *Lewis*-acid catalyst together with per-silylated bases under mild conditions to obtain the desired nucleosides.

Based on these findings along with the results of work by *Eschenmoser,*[197] we attempted the glycosylation of **A-73** and **A-53** with glycosyl donor **A-103** by the use of (N,O-bis(trimethylsilyl)acetamide) and $SnCl_4$ in dry acetonitrile at ambient temperature (Scheme 30).

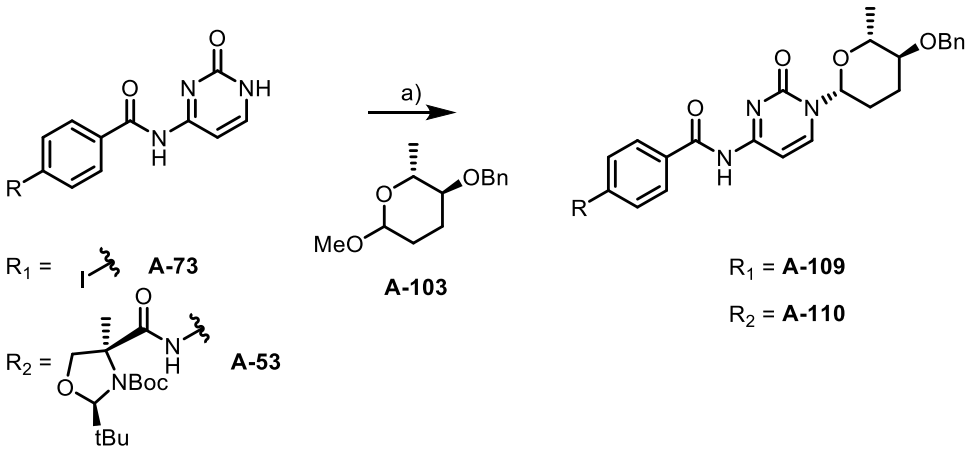

Scheme 30 Glycosylation of pyrimidine nucleoside. Reagents and conditions: a) BSA, $SnCl_4$, MeCN, rt, 45 min, 53% (for **A-109**) and 72% (for **A-110**).

The glycosylation reaction was found to be highly air- and water-sensitive and completely failed in the first few trials. Product formation started to be observed only when a stock solution of $SnCl_4$ in dry acetonitrile was prepared and molecular sieves were used to thoroughly desiccate the reaction mixture. If $SnCl_4$ was used without being premixed with dry acetonitrile, the reaction mixture instantly turned deep red and the starting material was found to be decomposed. For optimal reaction conditions it was beneficial if the solvent and the $SnCl_4$ were freshly distilled and both the starting material **A-53** or **A-73** and **A-103** were co-evaporated with benzene.

Once initial handling-related hurdles had been overcome, we were delighted to see product formation in good yields (up to 72%) and exclusively giving the desired diastereomer. The β-anomeric linkage between amicetose and the cytosine base was evidenced by the coupling constant of the anomeric proton, which was measured to be *J* = 8.4 Hz and thus strongly indicated the desired axial-axial coupling.

In theory, for an α-configured pyranose a characteristic coupling constant is around *J* = 3 Hz and the one for a β-configured linkage roughly *J* = 7.5 Hz. The difference in coupling constants arises from the coupling of the anomeric proton to the vicinal proton(s). In case of the β-anomer, the larger torsion angle between these protons is approximately ϕ = 180° (Figure 28). On the other hand, the torsion angle in the case of an α-anomer is ϕ = 60°. Based on the *Karplus* equation,[198] which describes the correlation between the torsion angle and the NMR coupling constants, the magnitude of the coupling constant increases the closer the torsion angle is to 180° or 0° respectively. This is well visualised by the *Karplus* curve (*vide infra*).

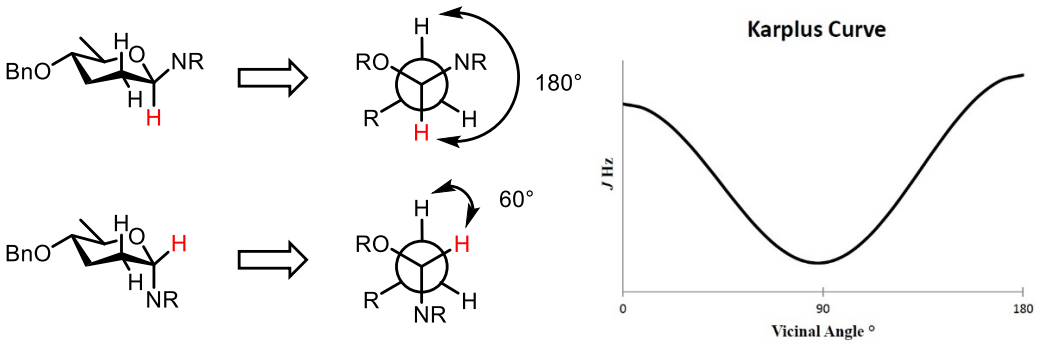

Figure 28 Relationship between the configuration at C1 and measured coupling constants for the anomeric proton.

Further evidence came from NOESY experiments that were measured for both glycosylation products **A-109** and **A-110** (Figure 29).

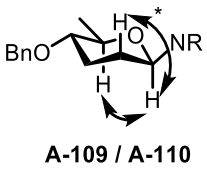

A-109 / A-110

Figure 29 Confirmed NOE signal to the axial H-C5. *: COSY artefact.

A possible explanation for the excellent β-selectivity in the reaction can be given by a solvent effect of acetonitrile that could form an α-nitrilium glucopyranosyl ion by complexation of the nitrile to the activated acceptor (Scheme 31). The attack of the incoming base would take place from the top face and hence giving the β-anomer **A-112**.[199,200]

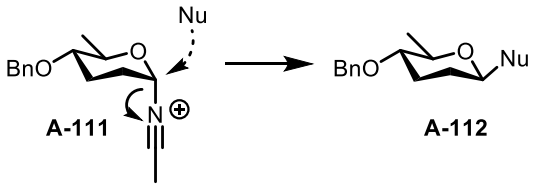

Scheme 31 Proposed solvent participation in glycosylation reaction.

Recent studies by *Codée*[201] mapped the conformational energy landscapes of S_N1-type glycosylation reactions and firmly indicate glycosyl cations as true reaction intermediates. Assuming that the reaction proceeds via an oxocarbenium ion, the two possible conformations **A-113** and **A-114** (Scheme 32) have to be considered. **A-113** is believed to be more favoured through stabilizing effects on the oxocarbenium ion by through space electrostatic interactions effected by the C4-OBn substituent (based on close proximity between the partially negatively charged hydroxyl group).[202–205] The benzyl ether would not obstruct the approach of the incoming nucleophile from the top face resulting in the β-product.

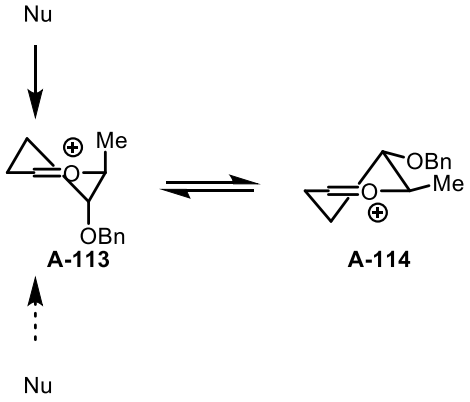

Scheme 32 Two possible oxocarbenium conformations, which are attacked by the nucleophile.

*1.3.5.3 Glycosylation of Aglycone **A-53** with Alternative Donors **A-115** and **A-116***

In further studies, we examined the glycosylation of **A-53** under the same *Vorbrüggen* conditions that had delivered **A-109** and **A-110** with glycosyl donors **A-115** and **A-116** (Scheme 34). Both glycosyl donors were synthesised by protection of **A-79** (Scheme 33).

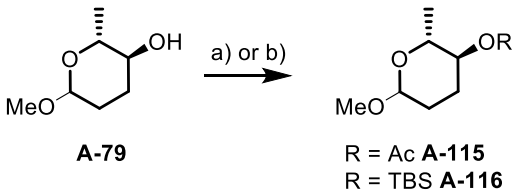

Scheme 33 Synthesis of **A-115** and **A-116**. Reagents and conditions: a) Ac_2O, DMAP, NEt_3, CH_2Cl_2, 85% for **A-115** b) TBSCl, imidazole, DMAP, CH_2Cl_2, 89% for **A-116**.

Intriguingly, the associated change of the protecting group on the distant 4-hydroxy group of the glycosyl donor led to a drastic erosion in yields (15 – 30%). Both reactions were carried out at least five times to ensure that no handling issues occurred, but similarly poor results were obtained in all cases.

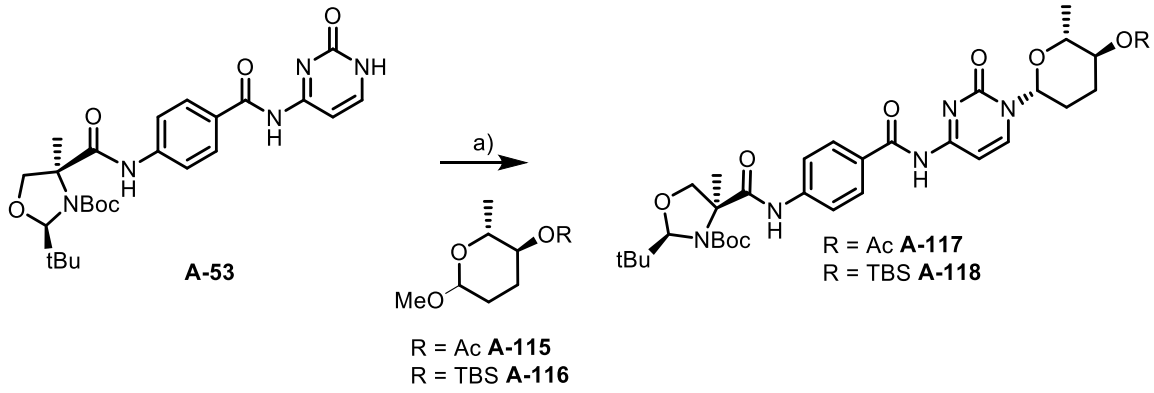

Scheme 34 Glycosylation of pyrimidine nucleoside. Reagents and conditions: a) BSA, $SnCl_4$, MeCN, rt, 45 min, 0-10% (for **A-117**) and 17-30% (for **A-118**).

The reason for the differences in the reaction with **A-103** and **A-115**/**A-116** is not clear at this point. It can only be speculated, that neither the TBS nor the acetyl-protecting group is fully compatible with the tin tetrachloride as part of the activation system.

*1.3.5.4 Benzyl-removal from **A-110***

After the successful glycosylation, the debenzylation of the amicetose hydroxy group in **A-110** by means of catalytic hydrogenation over palladium was examined. As has been shown in section 1.3.5.1 (*vide supra*), the benzyl-protected amicetose sugar **A-103** itself could be deprotected by this method within 90 min. Thus, the debenzylation of **A-110** looked deceptively simple, but turned out to be exactly the opposite (Scheme 35). Under standard hydrogenation conditions (catalytic hydrogenation over palladium at ambient temperature in methanol), a new product was observed (less polar on TLC) within minutes. After isolation and purification, this compound could be identified as the reduced pyrimidinone derivative **A-119**, which still contains the benzyl ether moiety (Figure 30).

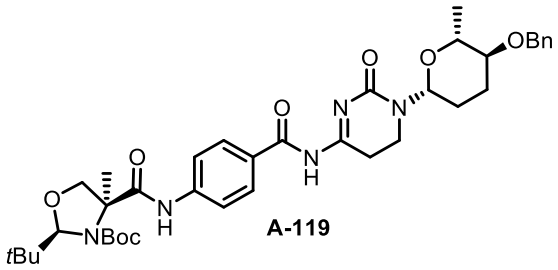

Figure 30 Reduced pyrimidinone **A-119** after attempted debenzylation through catalytic hydrogenation.

This unexpected finding then triggered a screening for suitable conditions for the removal of the benzyl protecting group (Table 6).

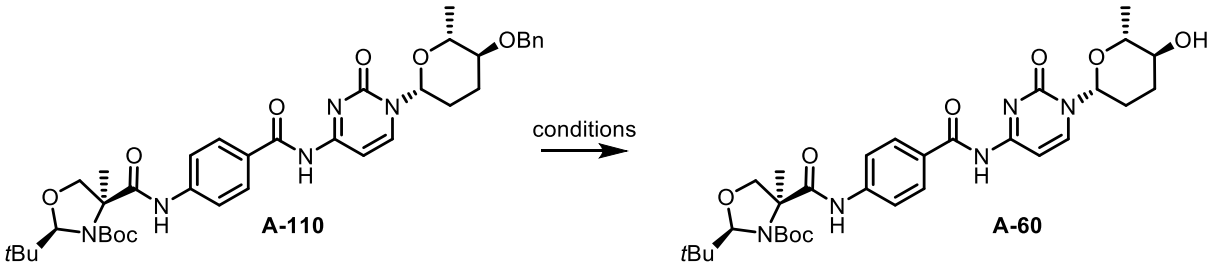

Scheme 35 Screening of benzyl deprotection conditions for **A-110**.

Changing the solvent from methanol to ethanol exclusively led to deglycosylation under catalytic hydrogenation conditions (entry **2**). Boron trichloride, which had been successfully used on amosamine derivative **A-126** (see section 1.3.5.6), turned out to be too harsh for the more elaborate nucleoside **A-110** and resulted in cleavage of the glycosidic bond (entry **3**). When applying milder hydrogenation conditions, such as the use of *Pearlman's* catalyst or transfer-hydrogenation

conditions, no conversion was observed. As the reductive cleavage of benzyl ether groups had been successfully achieved under *Birch* conditions[206,207] as part of the synthesis of glycosyl fluoride **A-130** (see section 1.3.5.7), these conditions were also applied to **A-110**. Unfortunately, this led to exclusive deglycosylation. Eventually, we were delighted to find that an excess of DDQ would give the desired product in good yields without affecting the glycosidic bond.

Table 6 Screening of benzyl deprotection conditions for **A-110**.[a]

Entry	Conditions	Observation
1	Pd/C, H_2, MeOH	reduction of pyrimidinone
2	Pd/C, H_2, EtOH	deglycosylation
3	BCl_3·DMS, CH_2Cl_2	deglycosylation, Boc-deprotection
4	*Pearlman*'s cat., H_2, EtOAc:EtOH	no product formation, potential decomposition
5	Pd/C, cyclohexadiene, DMF, rt	no conversion of starting material
6	Na/NH_3, THF, -78°C	deglycosylation, decomposition
7	DDQ, CH_2Cl_2, rt	slow reaction, excess of DDQ needed, reaction time of 66 h, 90% isolated product

[a] Balloon-hydrogen pressure applied for all hydrogenation reactions.

*1.3.5.5 Desilylation of **A-118***

Quite surprisingly, difficulties were also encountered upon attempted removal of the TBS protecting group from **A-118** (Scheme 36).

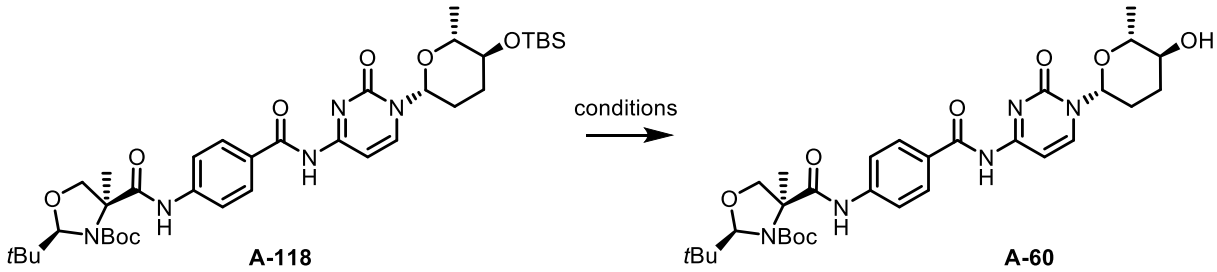

Scheme 36 Desilylation of **A-118**.

Thus, treatment of the latter with triethylamine trihydrofluoride at 0 °C (entry **1**, Table 7) did not produce any conversion. When the reaction temperature was raised to 23 °C, the starting material

was found to be consumed after three days, according to TLC analysis (entry **2**). However, **A-60** could be isolated only in 16% yield. More stringent conditions, *i.e.* HF·pyridine gave a clean reaction and fast conversion of **A-118**, but only traces of **A-60** were finally obtained (entry **3**). In this first experiment, the product may have been lost during workup, when the solution turned too basic. The final key to success was the use of a buffered TBAF solution (with AcOH), which provided **A-60** in 67% yield. The reaction needed to be conducted at 40 °C, otherwise no deprotection took place.

Table 7 Screening of desilylation conditions to free **A-118**.

Entry	Conditions	Observation
1	NEt_3·3HF, THF, 0 °C	no reaction
2	NEt_3·3HF, THF, rt	reaction extremely slow, after stirring for 72 h product was isolated in 16% yield
3	HF·pyridine, THF, 0 °C -rt	clean reaction, quenched after 1.5 h, after workup and FC only traces obtained
4	TBAF (2.2 equiv), AcOH as buffer, THF, rt – 40 °C	no consumption of starting material after 24 h, reaction was then warmed up to 40 °C, full consumption after 4 h -> 67%

*1.3.5.6 Synthesis of Glycosyl Fluoride **A-129***

In the course of this PhD project, a number of different amosamine donors were synthesised as possible building blocks for either the "disaccharide strategy" or the "sequential – glycosylation – strategy". This section discusses the synthesis of the individual donor systems, that were primarily intended to be used for the sequential glycosylation strategy.

Mukaiyama has reported the use of glycosyl fluorides as donors for the preparation of α-glycosides under conditions that involved activation of the fluorides with stannous chloride and silver perchlorate in an ethereal solvent.[208][209] Glycosyl fluorides are chemically more stable than other glycosyl halides, which were reported by *Koenigs* and *Knorr*[210]. C-F bonds have a higher bond-dissociation energy (552 kJ mol^{-1}) in comparison to C-Cl (397±29 kJ mol^{-1}) or C-Br bonds (280±21 kJ mol^{-1}) and can seamlessly be purified by column chromatography and carried through a synthesis under various conditions.[211]

The synthesis of the glycosyl fluoride **A-129** departed from tetra *O*-acetyl thiogalactoside **A-120**, which was globally deprotected with sodium methoxide/methanol (Scheme 37). Contrary to the literature report,[134] a purification by column chromatography of the highly polar sugar had to be performed to ensure a smooth subsequent reaction step. The 4,6-diol moiety was selectively protected as a benzylidene acetal to obtain **A-122**. The reaction can be catalysed either by $BF_3 \cdot Et_2O$, leading to longer reaction times, or by tosic acid, in which case the resulting product can be filtered off easily. The remaining free hydroxy groups were benzyl protected to furnish compound **A-123** in 84% overall yield from **A-120**. Subsequent acetal cleavage was initially performed with aqueous tetrafluoroboric acid, which resulted in poor yields of about 35%. More suitable reaction conditions were found to involve the use of camphor sulfonic acid in methanol, which furnished the free diol in 86% yield. Selective tosylation of the primary alcohol moiety using freshly washed tosyl chloride worked smoothly under basic conditions and gave tosylate **A-125** in 92% yield.

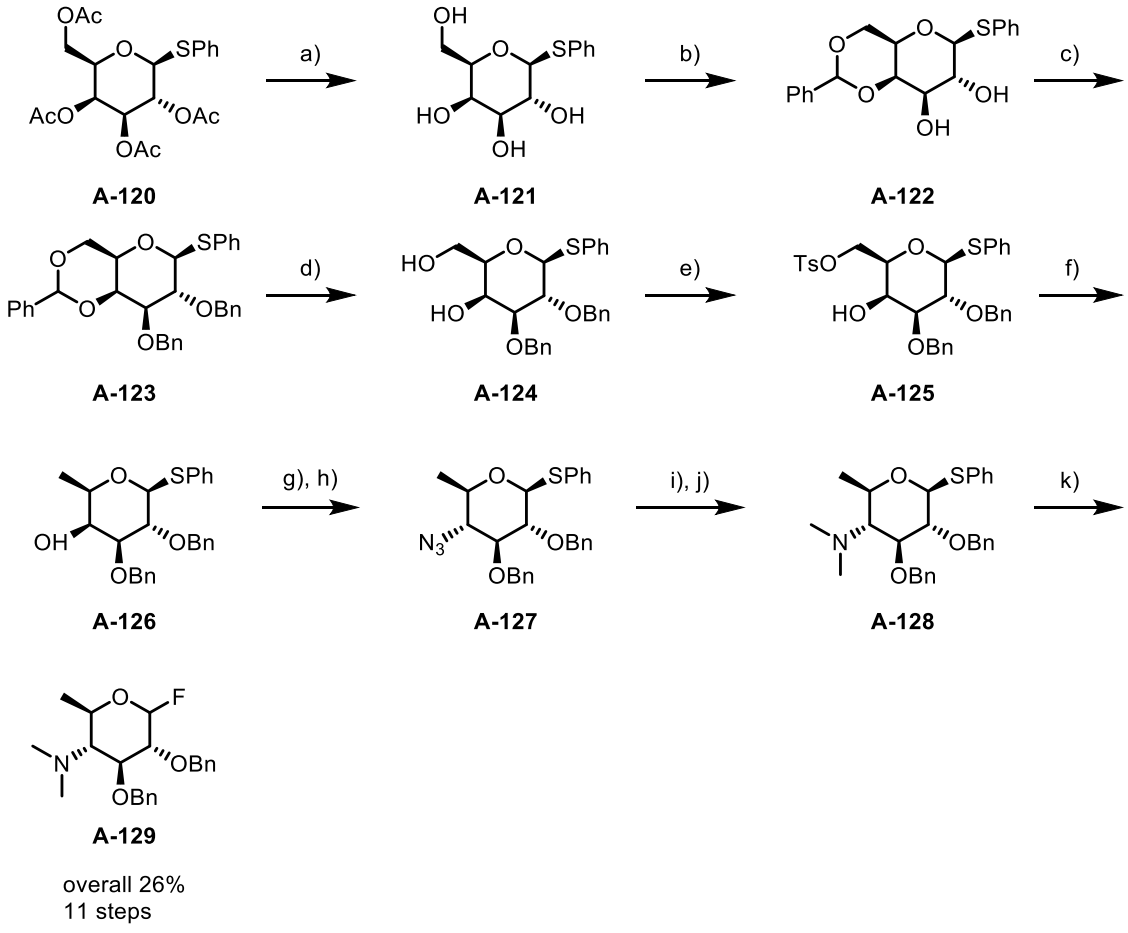

Scheme 37 Synthesis of **A-129**. Reagents and conditions: a) 25% NaOMe, MeOH, 0 °C, 20 min, quant.; b) $PhCH(OMe)_2$, TsOH, MeCN, rt, 2 h, 93%; c) BnBr, NaH, DMF, rt, 17 h, 90%; d) CSA, MeOH:CH_2Cl_2 1:1, rt, 72 h, 86%; e) TsCl, pyridine, 0 °C - rt, 24 h, 92%; f) $LiBEt_3$, THF, rt, 2.5 h, 83%; g) MsCl, pyridine, 0 °C, 3 h; h) NaN_3, DMF, 100 °C, 30 h, 64% over two steps; i) Pd/C, H_2, MeOH, rt; j) Pd/C, H_2, formaldehyde, EtOH, rt, 89% over two steps; k) HF·pyridine, NBS, CH_2Cl_2, -35 °C - 0°C, 1 h, 83%.

Tosylate **A-125** was found to be unstable upon storage even at -20 °C under argon. In one instance this led to decomposition of a gram scale batch of material. Continuing the synthesis, **A-125** was reduced with Super-Hydride in THF at ambient temperature. While performing this reaction, I found that the removal of even the smallest traces of pyridine from the previous reaction step was absolutely crucial. If traces of base were present, the nucleophilic displacement of the tosyloxy group occurred by the neighbouring secondary hydroxy nucleophile and not by the hydride ion, resulting in the formation of an oxetane. The structure of the oxetane side-product was confirmed by single crystal X-ray diffraction analysis (Figure 31).

In light of the base sensitivity of **A-125**, the crude tosylate was purified by means of extraction of a solution in EtOAc with either aqueous HCl or copper sulfate solution and subsequent FC purification before being submitted to reduction. With these precautions, the conversion of **A-125** into **A-126** could be performed without problems and in high yield of 83%

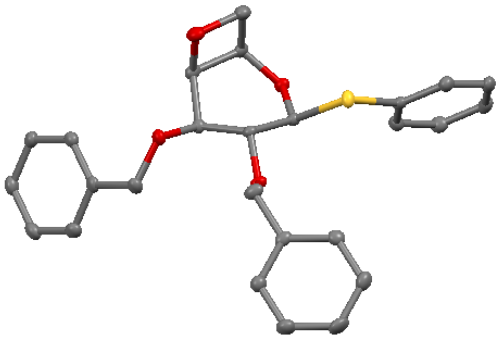

Figure 31 Oxetane crystal structure obtained as a side product during the formation of **A-126**.

The reduction product **A-126** was then converted into azide **A-127** via mesylate formation and subsequent treatment with sodium azide. Mesylate formation was straightforward and purification of the mesylate was not required. The introduction of the azide group with inversion of the stereocentre required extended reaction times (up to 72 h) and elevated temperature (100 °C). Reductive methylation of the azide under *Eschweiler-Clarke*[212,213] conditions then yielded the desired dimethylamine **A-128**. At this point, we considered it prudent to convert part of this material into the corresponding glycosyl fluoride under conditions reported by *Nicolau*[214]. In case of potential stability issues with either **A-128** or **A-129** we would not lose all our material. Treatment of thioglycoside **A-128** with *N*-bromosuccinimide, generated a bromosulfonium ion which upon attack by the fluoride anion (HF·pyridine as the fluoride source) gave the glycosyl fluoride **A-129**. The synthesis of **A-129** was accomplished in 9 steps and 26% overall yield.

With both the thioglycoside **A-128** and the glycosyl fluoride **A-129** in hand we could choose between two different types of glycosyl donors in the future synthesis.

1.3.5.7 Preliminary Debenzylation Studies

In order to establish conditions for the deprotection of a benzyl-protected amicetin (**A-1**) variant, obtained with either of the amosamine intermediates **A-128** or **A-129**, we embarked on preliminary studies on the debenzylation of the diol moiety (Scheme 38).

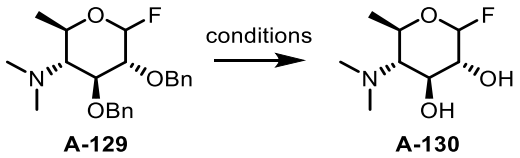

A-129 **A-130**

Scheme 38 Debenzylation of **A-129**.

We commenced with glycosyl fluoride **A-129**, but unfortunately, the deprotection was more challenging than expected. Commonly used protocols using hydrogen over palladium on charcoal[215,216] (entry **1**-**3**,**6**, Table 8) as well as transfer hydrogenation[217] (entry **7**, **8**) did not lead to any conversion. Equally unfruitful was the use of oxidative conditions (DDQ over prolonged time periods)[218] (entry **4**).

Table 8 Screening of debenzylation conditions for **A-129**.[a]

Entry	Conditions	Observation
1	Pd/C, H_2, EtOH	no reaction
2	*Pearlman*'s cat., H_2, EtOAc:EtOH	no reaction
3	Pd/C, H_2, THF	no reaction
4	DDQ, CH_2Cl_2, pH 7 buffer, rt - 40 °C	no reaction
5	BCl_3·DMS, CH_2Cl_2, -78 °C - rt	mono-debenzylation, side products[b]
6	Pd/C, H_2, cat. HCl, EtOH	no reaction
7	Pd/C, cyclohexadiene, THF, 55 - 65 °C	no reaction
8	Pd/C, cyclohexadiene, 2,6-lutidine, MeOH, 45 °C	no reaction
9	$AlCl_3$, N,N-dimethylaniline, CH_2Cl_2	side products[b]

10	$BF_3{\cdot}Et_2O$, NaI, MeCN, 0 °C	side products[b]
11	BCl_3, CH_2Cl_2, -78 °C - rt	side products[b]
12	Na/NH_3, THF, -78 °C	quantitative based on crude

[a] Balloon-hydrogen pressure applied for all hydrogenation reactions. Reactions were carried out on a 1 - 5 mg scale. [b] n.d.: not determined.

Likewise, *Lewis* acid-based conditions for the cleavage of benzyl ethers, such as exposure of **A-129** to BCl_3[219] or $AlCl_3$[220] were unsuccessful and resulted mostly in decomposition (entry **5**, **9**-**11**). $BCl_3{\cdot}DMS$[221] in dichloromethane gave the mono-debenzylated product along with several side products. Finally, we were delighted to find that the exposure of **A-129** to *Birch* conditions[222] delivered the desired diol within seconds and in excellent yields.

The debenzylation was also evaluated on the less advanced intermediate **A-126** (Scheme 39).

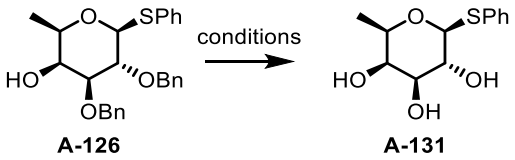

A-126 **A-131**

Scheme 39 Debenzylation conditions for **A-126**.

Again, palladium mediated approaches, *i.e.* transfer hydrogenation and classic catalytic hydrogenations were unsuccessful (entry **1**-**3**, Table 9). Under mildly acidic hydrogenation conditions **A-126** decomposed slowly over time (entry **5**). A reagent system composed of NaI-$BF_3{\cdot}OEt_2$ led to full consumption of the starting material and gave the mono-debenzylated product exclusively (entry **4**). An ammonia-free Li/DBB protocol[207] gave no reaction (entry **6**), while iron trichloride led to decomposition at a reaction temperature of -3 °C. Finally, the use of a 1 M boron trichloride solution in dichloromethane at -78 °C gave the desired product in 17% isolated yield (entry **8**).

Table 9 Screening of debenzylation conditions for **A-126**.[a]

Entry	Conditions	Observation
1	Pd/C, cyclohexadiene, THF, 55 - 65 °C	no reaction
2	Pd/C, cyclohexadiene, 2,6-lutidine, MeOH, 45°C	no reaction
3	Pd/C, H_2, EtOH, rt	no reaction
4	$BF_3{\cdot}Et_2O$, NaI, MeCN, 0°C - rt	mono-debenzylation
5	Pd/C, H_2, MeOH:H_2O:AcOH, rt	side products[b]

6	LiDBB (4.0 equiv), THF, -20 °C	no reaction
7	$FeCl_3$, CH_2Cl_2, -3 °C	decomposition, side products[b]
8	BCl_3, CH_2Cl_2, -78 °C	17% yield, side products[b]

[a] Balloon-hydrogen pressure applied for all hydrogenation reactions. Reactions were carried out on a 5 mg scale. [b] n.d.: not determined.

*1.3.5.8 Protecting Group Exchange for **A-129***

After having established that both benzyl ether moieties in **A-129** can be cleaved under *Birch* conditions, we sought to identify suitable protecting groups for the reprotection of the diol moiety that would be susceptible to cleavage under mild conditions to release amicetin (**A-1**) in the final step of the synthesis (Scheme 40).

Our efforts commenced with attempts to access 1,2-diacetal **A-133** by treatment of **A-130** with dimethylglyoxal and trimethyl orthoformate in the presence of catalytic amounts of camphorsulfonic acid, a protocol well established in carbohydrate chemistry (see, for example reference [223]). Regrettably, these attempts were unsuccessful. Likewise, it was not possible to access acetal **A-134** under *Lewis* acidic reaction conditions. Three different reaction conditions were examined for the possible conversion of **A-130** into dimethylacetal **A-135**, but none of them led to any conversion of starting material. The last unsuccessful attempt at the reprotection of **A-130** involved treatment with PMBCl, to provide a compound close to benzyl derivative **A-129**.

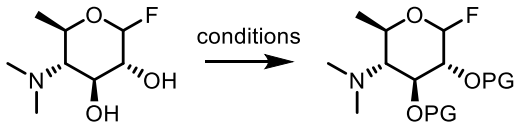

A-130 **A-132**

Scheme 40 Reprotection of **A-130**.

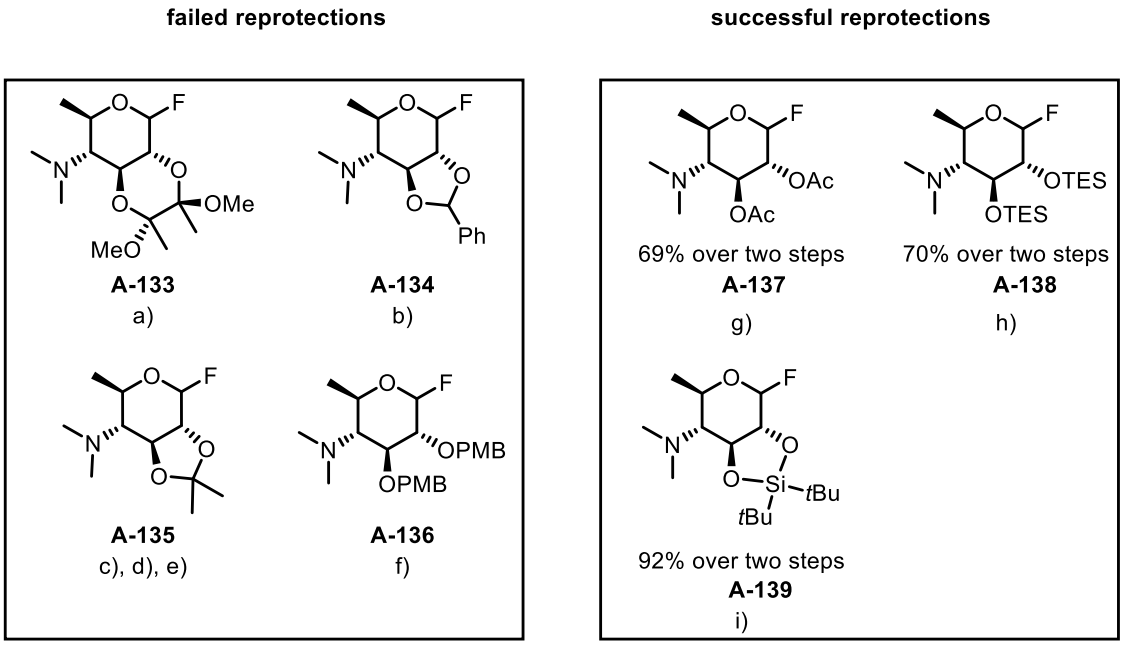

Scheme 41 Envisioned and/or accessed substrates after reprotection of **A-132**. Reagents and conditions: a) dimethylglyoxal, cat. CSA, $CH(OMe)_3$, MeOH, reflux; b) benzaldehyde dimethylacetal, $HBF_4{\cdot}OEt_2$, DMF, rt; c) dimethoxypropane, *p*TsOH, acetone, reflux; d) dimethoxypropane, *p*TsOH, DMF, rt; e) dimethoxypropane, CSA, DMF, rt; f) PMBCl, NaH, THF, 0 °C – rt; g) Ac_2O, DMAP, NEt_3, CH_2Cl_2, 69%*; TES triflate, NEt_3, CH_2cl_2, -78 °C, 70%*; $tBu_2Si(OTf)_2$, pyridine, CH_2Cl_2, 0 °C – rt, 92%*. *) yields are calculated over two steps including *Birch*-mediated deprotection.

Diol **A-130** could be successfully converted into diacetate **A-137** by reaction with acetic anhydride and catalytic amounts of DMAP. TES-triflate masked the free diol within min at -78 °C to provide **A-138** in good yield. Finally, the cyclic silylether **A-139** was synthesised in excellent yield (92%) by treatment of **A-130** with di-*tert*-butylsilyl bistriflate and pyridine in dichloromethane. These protecting groups were assumed to be readily cleaved on the completed amicetin (**A-1**) scaffold and in the same time compatible with the activation conditions used during the glycosylation reaction.

1.3.5.9 Late Stage Glycosylation with Glycosyl Fluorides

With intermediate **A-60** in hand, what was required for the completion of the synthesis of amicetin (**A-1**) was the attachment of the terminal amosamine sugar and final deprotection. In this section, the chemistry that was investigated to establish the α(1→4)-linkage between the two sugar units is discussed. Due to the 1,2-*cis* configuration in the amosamine sugar, the formation of this bond is a particularly challenging problem.

Our experiments were started with glycosyl fluorides **A-129**, **A-138**, and **A-139** and the glycosyl acceptor **A-60** using the before described procedure reported by *Mukaiyama* (see section 1.3.5.6). When applying these (or closely related) conditions (stannous chloride, silver triflate or silver perchlorate, ethereal solvent) to the reaction of **A-60** with our different amosamine-derived glycosyl fluorides, only the bis-benzyl protected derivative **A-129** gave at least traces of the desired product **A-140** (Scheme 42).

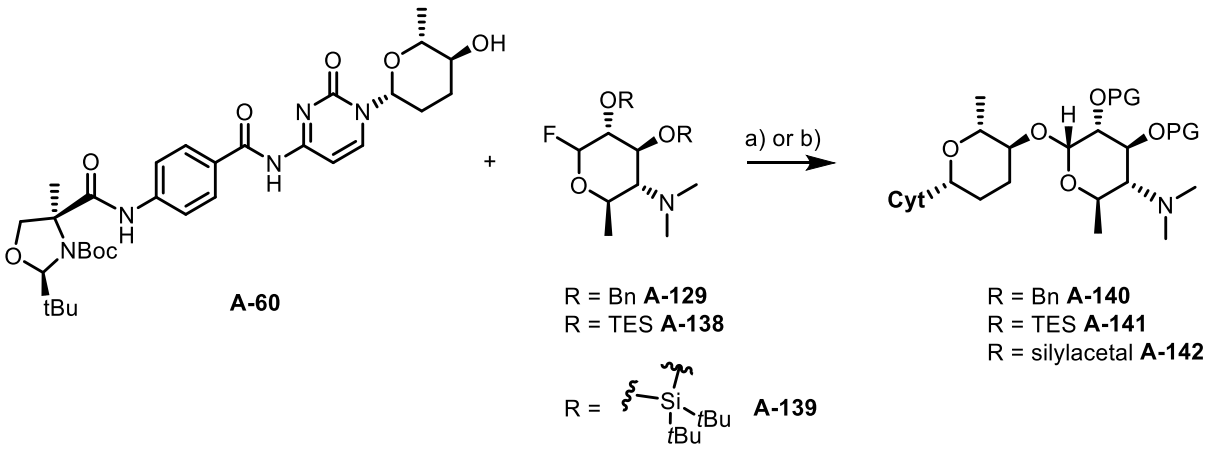

Scheme 42 Reagents and conditions: a) AgOTf, $SnCl_2$, MS 4 Å, Et_2O, DCE, 0 °C – rt, 96 h, 5% (for **A-140**); b) only tested for donor **A-138**: $SnCl_2$, $AgClO_4$, Et_2O, 0 °C – rt, 0%.

The product **A-140** was purified by column chromatography and analysed by ^{1}H-NMR. The coupling constant measured for the anomeric proton of the amosamine unit with the vicinal proton was J = 3.6 Hz (doublet at δ 5.08 ppm; Figure 32). This strongly indicated that the newly formed glycosidic linkage had the desired α-configuration.

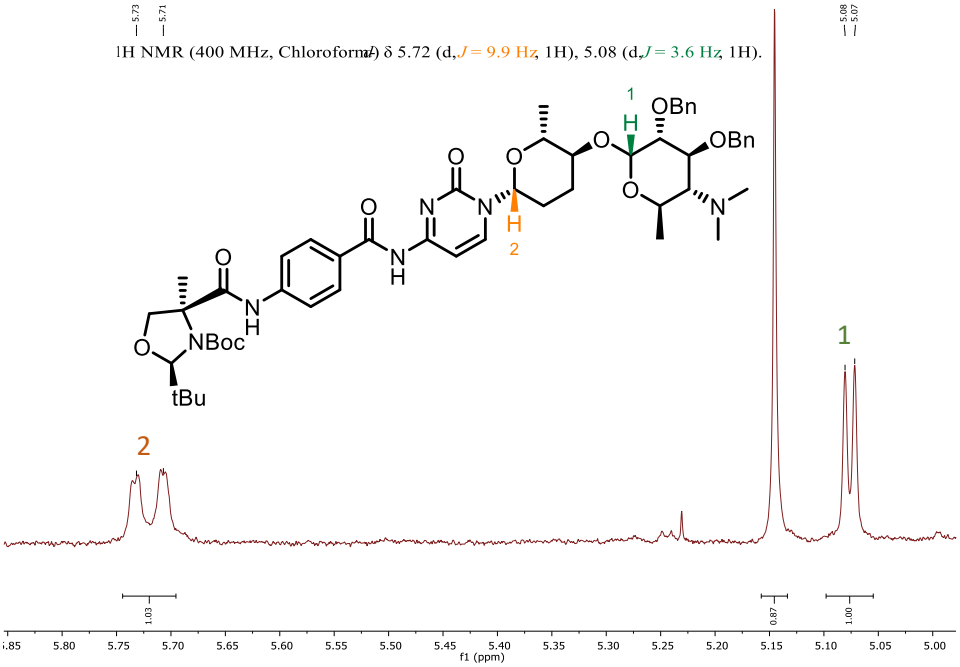

Figure 32 Vicinal coupling constants for both anomeric protons of the isolated product **A-140**.

The formation of **A-140** was extremely slow. According to LC-MS the glycosyl fluoride was detected after setting up the reaction, which indicated that the activation of the glycosyl donor was not immediately taking place and that other protocols should be evaluated (see chapter 1.4 for further discussions). Interestingly, while monitoring the formation of **A-140** by means of LC-MS (Figure 33), two closely eluting peaks of similar intensities were detected that both gave the mass of the desired product **A-140** (product mass: 966 m/z). This observation is likely indicative for the formation of both the α- and the β-glycoside during the reaction. Unfortunately, NMR analysis of the crude product mixture obtained after extractive work-up did not allow to either confirm or refute this hypothesis.

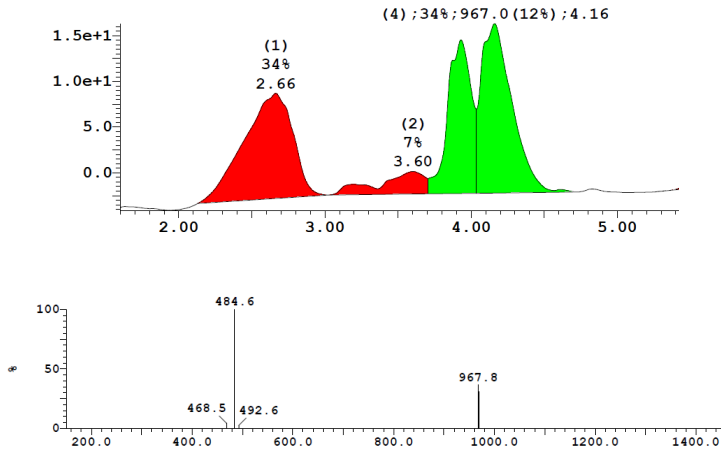

Figure 33 LC-MS run on a C18 column as a reaction control sample. Peak (1) represents the starting material **A-60**, whereas peaks (3) and (4) are associated with the mass of the desired product.

Given the lack of product formation/low yield for the attempted glycosylation of **A-60** with glycosyl fluorides **A-129**, **A-138**, or **A-139** in combination with the precious nature of the starting materials as well as uncertainties about the clean removal of the benzyl protecting groups at the final stage of the synthesis, the sequential glycosylation approach with glycosyl fluorides was not further pursued at this point.

*1.3.5.10 Deprotection of **A-140***

Fully protected amicetin **A-140**, which derived from the *Mukaiyama* glycosylation of **A-60** with **A-129** (see section 1.3.5.9), was subjected to debenzylation conditions (Scheme 43).

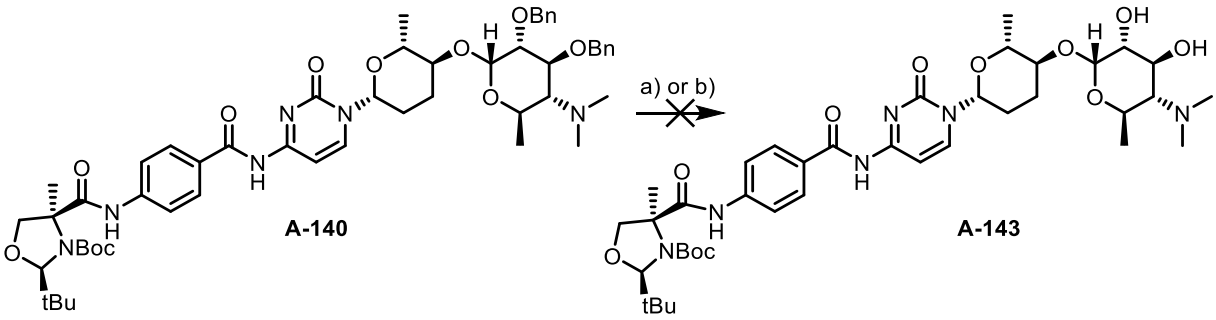

Scheme 43 Benzyl ether cleavage on the amosamine diol motif. Reagents and conditions: a) Na/NH_3, THF, - 78 °C, full decomposition; b) Pd/C, H_2, cat. HCl, ethanol, rt, 0%.

Unfortunately, *Birch* conditions led to full decomposition of the starting material within seconds, while catalytic hydrogenation conditions (H_2 over Pd/C, catalytic amounts of HCl) led to the rapid formation of a new product (not quantified), which however, was not the desired **A-143**. While the structure of this new product could not be elucidated, its ^{1}H-NMR spectrum suggests that it is structurally related to **A-144** due to the missing characteristic anomeric protons arising from the glycosidic bonds (Figure 34).

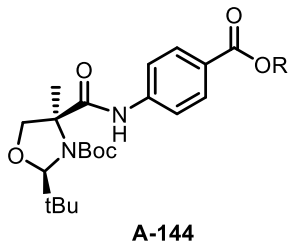

A-144

Figure 34 Proposed structure of the obtained side product **A-144**.

This can be concluded based on spectral data obtained after flash column chromatography of the side product (Figure 35). A comparison of the spectral data of the side product (bottom spectra, dark red) with the mono-glycosylated intermediate **A-60** (top spectrum, turquoise) shows the presence of the characteristic peaks from proton H10 and H11 belonging to the oxazolidine moiety together with the aromatic protons H3-H6. However, the signals H1, H2 of the pyrimidine and H7-H9 of the amosamine were missing. These findings clearly evidenced the cleavage of the eastern part of the molecule.

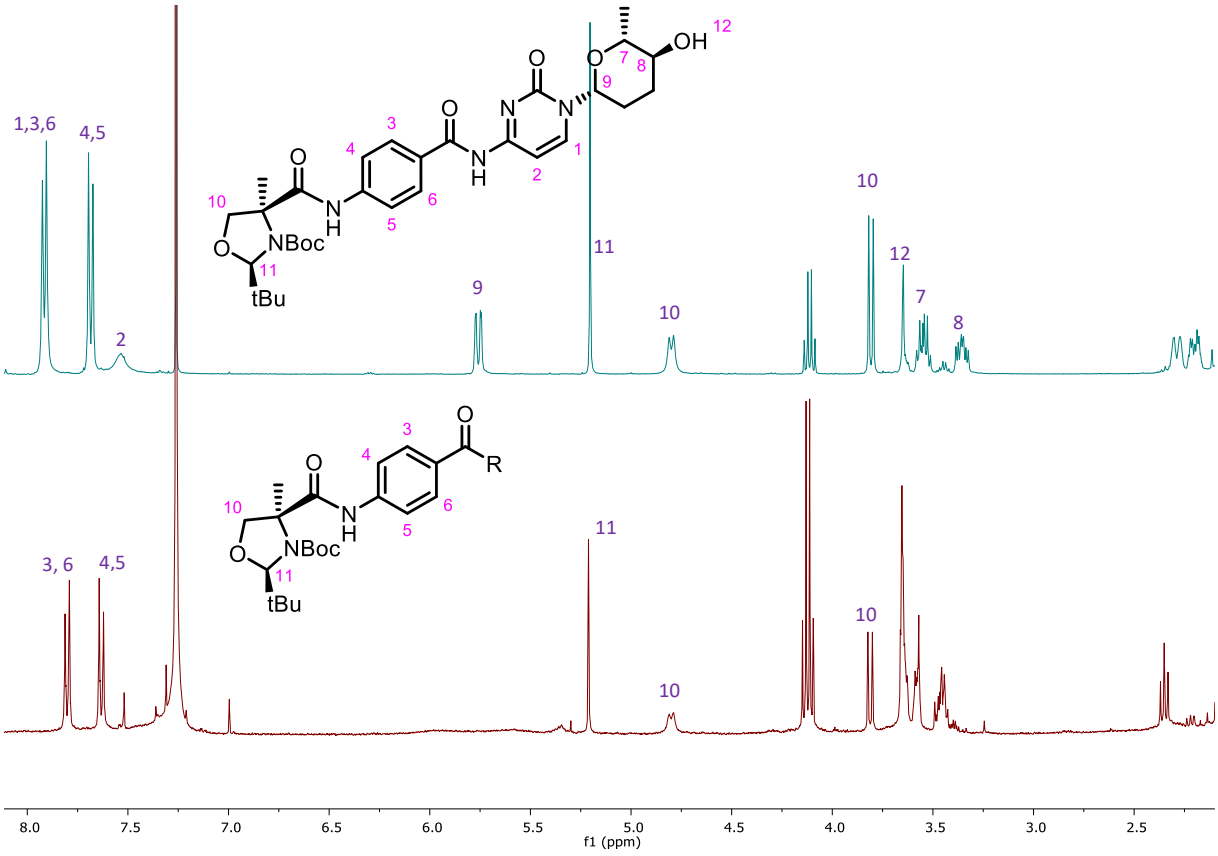

Figure 35 Spectral data of the obtained side product under hydrogenation reaction conditions. Measured in $CDCl_3$, 400 MHz.

It is worth mentioning that *Stevens* applied the exact same conditions to debenzylate the diol system of **A-23** in his total synthesis of plicacetin,[146] as discussed in section 1.1.9.1. *Stevens* reported no problems for the reaction.

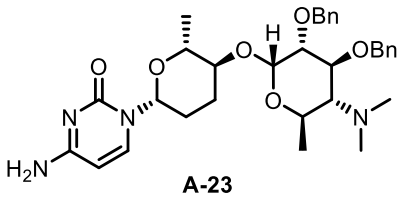

Figure 36 Substrate **A-23** for *Stevens* successful debenzylation in his synthesis of plicacetin (**A-17**).

1.3.5.11 Trichloroacetimidates for Late Stage Glycosylation

In light of the failure to achieve glycosylation of **A-60** with glycosyl fluorides **A-129**, **A-138**, and **A-139**, we turned our attention to the activation of the amosamine building blocks as trichloroacetimidates. The synthesis of the trichloroacetimidates is discussed in section 1.3.6 (*vide infra*).

Glycosylation reactions of **A-60** with the various trichloroacetimidates were carried out at -78 °C under mild activation with catalytic amounts of TMS-triflate in dichloromethane (Scheme 44).

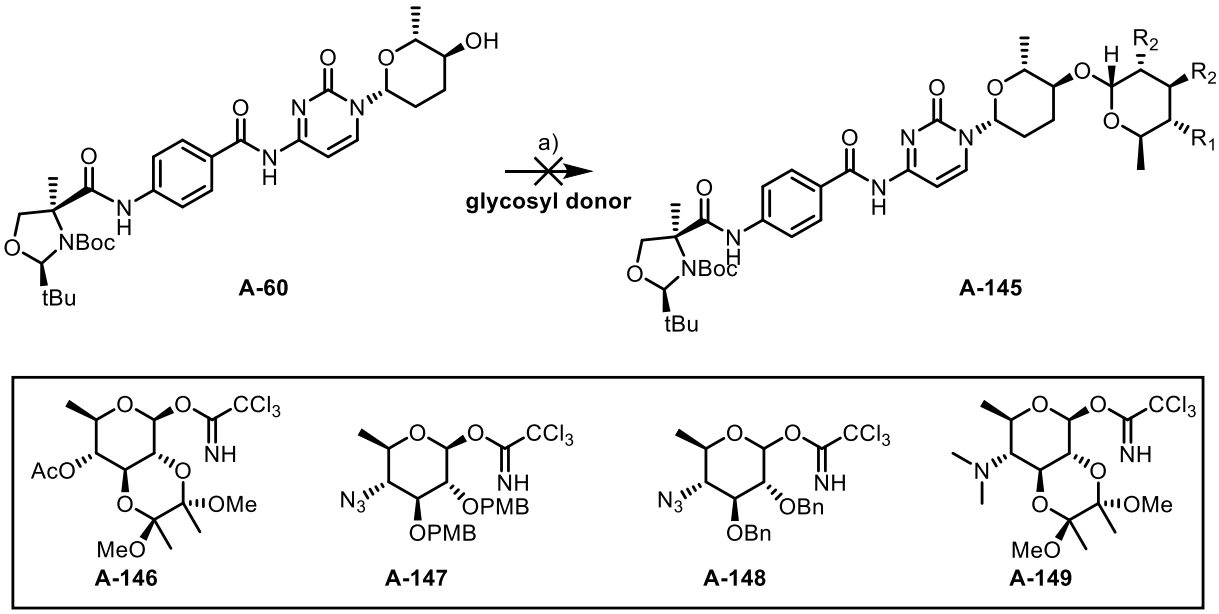

Scheme 44 Glycosylation attempts using various trichloroacetimidates as glycosyl donors. Reagents and conditions: a) TMSOTf, CH_2Cl_2, -78 °C - rt.

Slight modifications were made for the individual reactions, including changes in reaction temperature from -78 to 23 °C, an increase in the amount of TMSOTf, different equivalents of glycosyl donor, reaction time, work-up procedures and the use of molecular sieves (or not) (Table 10). However, under no conditions could even traces of product be isolated. Therefore, this strategy was discontinued.

1.3.5.12 Attempts Towards an o*-Alkynylbenzoate Donor*

In our efforts to identify suitable glycosyl donors, we did not want to miss the opportunity to explore the full richness of methodologies available in the field of carbohydrate chemistry. Therefore, the synthesis of *ortho*-alkynyl benzoates **A-154** and **A-155** (Scheme 45), the same donor type that had been described by the group of *Yu*[138] in their synthesis of **A-40** (see chapter 1.2.3.) was also pursued. In this context, it is important to note that the use of these type of donors, in the synthesis of plicacetin had not been reported in the literature at the outset of this PhD project. The corresponding publication by *Yu* and co-workers appeared only when our own work had been ongoing for some time.

Glycosidic esters **A-154** and **A-155** were to be obtained by coupling of glycoside **A-152** and **A-153**, respectively, and acid **A-151**. The latter was obtained through *Sonogashira* coupling between iodobenzoate **A-150** and 1-hexyne and subsequent saponification of the methyl ester. To our disappointment the coupling between acid **A-151** and the advanced intermediates **A-152** or **A-153** was not feasible with DCC/DMAP in dichloromethane (no conversion). Importantly, however, due to the precious nature of **A-152** and **A-153**, no other coupling methods were investigated.

Table 10 Various conditions tested for glycosylation of **A-60** with different glycosyl donors.[a]

Entry	Donor	Temp. [°C]	Time [h]	Remark	Observation
1	**A-149** (1.0 equiv)	-78 - 23	3 at -78 °C, 13 at 23 °C		no reaction at -78 °C, donor still detected, P detected by LC-MS at rt
2	**A-149** (1.3 equiv)	-78 - 23	3 at -78 °C, 13 at 23 °C	reaction mixture directly filtered over silica	no reaction at -78 °C, donor still detected, no P detected by LC-MS at rt after 13 h
3	**A-149** (8.0 equiv)	-78	2	reaction mixture directly filtered over silica	very little P formation (according to LC-MS)
4	**A-149** (7.5 equiv)	-78	20	reaction mixture directly filtered over silica, after FC additional HPLC	little P formation (according to LC-MS), ratio between SM and P stayed the same after a while, no P after HPLC
5	**A-149** (5.0 equiv)	-78	4	additional 0.3 equiv of TMSOTf after 3 h	no P isolated after FC
6	**A-149** (5.0 equiv)	0	16	aqueous work-up	no P isolated after two FCs
7	**A-147** (1.05 equiv)	-78	4	filter directly over Alox	potential P formation observed (LC-MS), no P isolated after FC
8	**A-148** (1.0 equiv)	-78	1		reaction hard to follow by TLC, no P isolated after FC
9	**A-146** (1.80 equiv)	-78 - 23	1 at -78 °C, 13 at 23 °C	no molecular sieves, reaction mixture directly filtered over silica	P formation observed by LC-MS, HRMS obtained
10	**A-146** (2.0 equiv)	-78 – 23	3	only addition of TMSOTf at -78 °C then directly to rt	several side-P, probable P isolated after FC

[a] All reactions were carried out in dry CH_2Cl_2 in a *Schlenk* tube fitted with a teflon screw cap and pre-dried molecular sieves. TMSOTf was distilled over P_2O_5 under normal pressure at 155 °C and prepared as a stock solution. 0.3 equiv TMSOTf was used. Prior to the addition of the TMSOTf, both compounds were pre-stirred with the previously activated molecular sieves for 1 h. Both compounds were azeotropically dried with benzene prior to be used. Reactions were quenched by NEt_3 if not otherwise stated. SM: starting material. P: product.

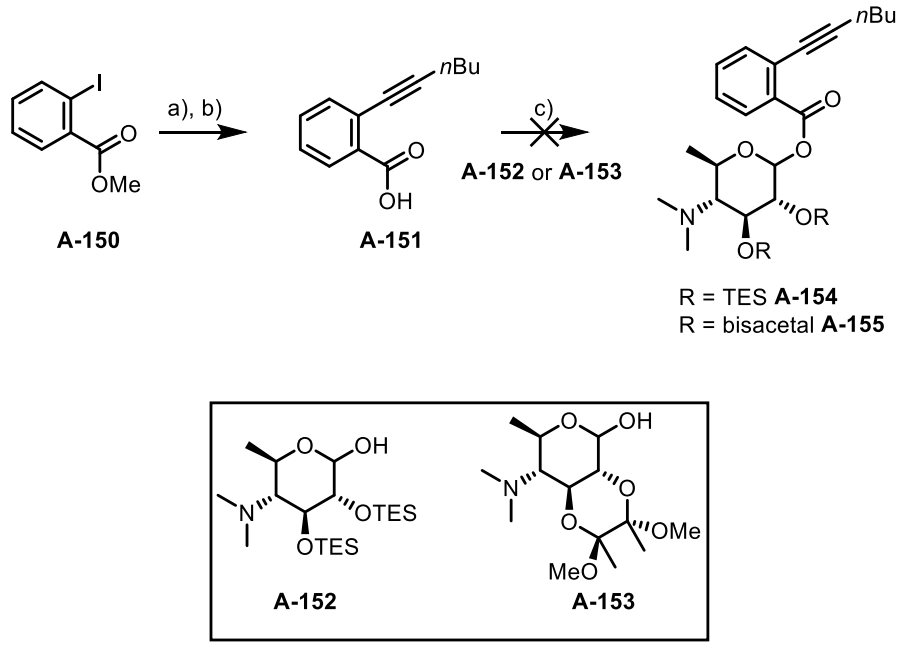

Scheme 45 Attempt of synthesising **A-154** / **A-155** as an alternative glycosyl donor. Reagent and conditions: a) 1-Hexyne, $PdCl_2(PPh_3)_2$, CuI, NEt_3, MeCN, 0 °C –rt, 16 h; b) NaOH 1 M, THF, 50 °C, 12 h, 62% over two steps; c) DCC, DMAP, CH_2Cl_2.

Notwithstanding the lack of success in the synthesis of **A-154** and **A-155**, it is worth to briefly describe the activation mechanism of these putative glycosyl donors (Figure 37). The initiation takes place by an activation of the benzylic triple bond through coordination to an Au(I) catalyst (e.g. $Ph_3PAuOTf$). This triggers a cascade of transformations; an oxocarbenium species **A-156** is likely to be generated by the cleavage of the glycosidic bond and the attack of the triple bond through the adjacent carbonyl moiety. Intermediate **A-156** is attacked by the incoming nucleophile (actual glycosylation) and the carbon-Au(I) bond in **A-157** is cleaved by protonolysis to regenerate the gold-catalyst and form isocoumarin **A-159**.

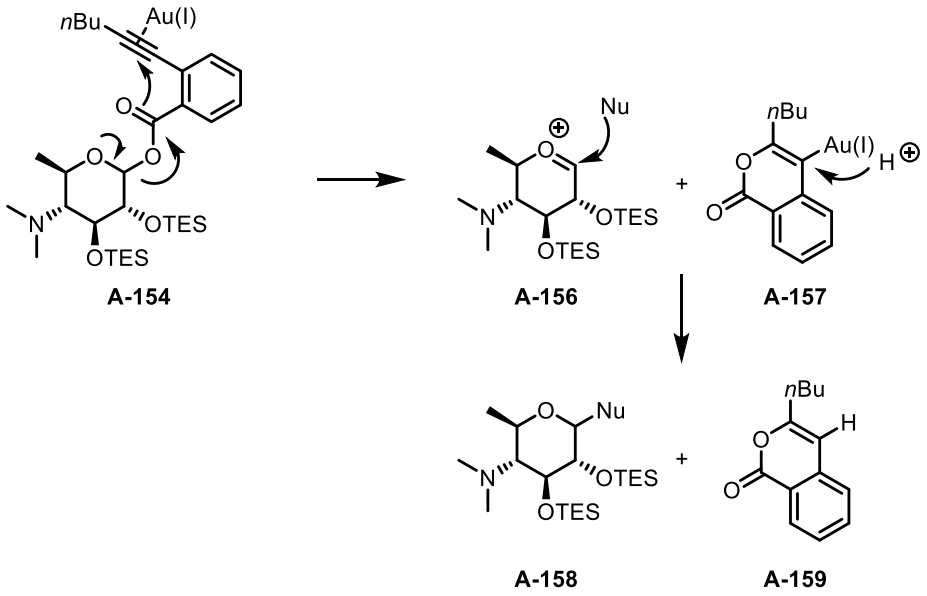

Figure 37 Gold-catalysed glycosylation with an *o*-alkynyl benzoate as a donor.

*1.3.5.13 Alternative Glycosylation Attempts with Trichloroacetimidate ß-D-Glucopyranose Donors **A-159**, **A-160** and **A-161***

As discussed in section 1.1.9.2, *Sugimura* and co-workers have reported a formal total synthesis of cytosamine,[134] which involved a final glycosylation with an azide precursor of the amosamine sugar. Likewise, *Yu* and co-workers, in their total synthesis of plicacetin (**A-17**)[138] (section 1.1.9.3), employing azido sugar **A-38** to glycosylate the TBS-protected amicetose **A-37**. In both cases, the azido group was converted into the required dimethylamino group only subsequent to the formation of the disaccharide moiety. While neither group comments on whether glycosylations were also attempted with a protected amosamine sugar directly, the use of azido sugars as glycosyl donors may in fact indicate that such glycosylations may be difficult to achieve. In this context, it should be noted that no single literature report exists for the use of an amosamine derivative as a glycosyl donor.

In light of these considerations, we decided to investigate the feasibility of the glycosylation of **A-60** with a number of differently protected D-glucose derivatives **A-160** – **A-162** as amosamine surrogates (Scheme 46). If successful, this approach could be of interest for the future synthesis of analogues and it allowed to test reaction conditions with a less valuable donor.

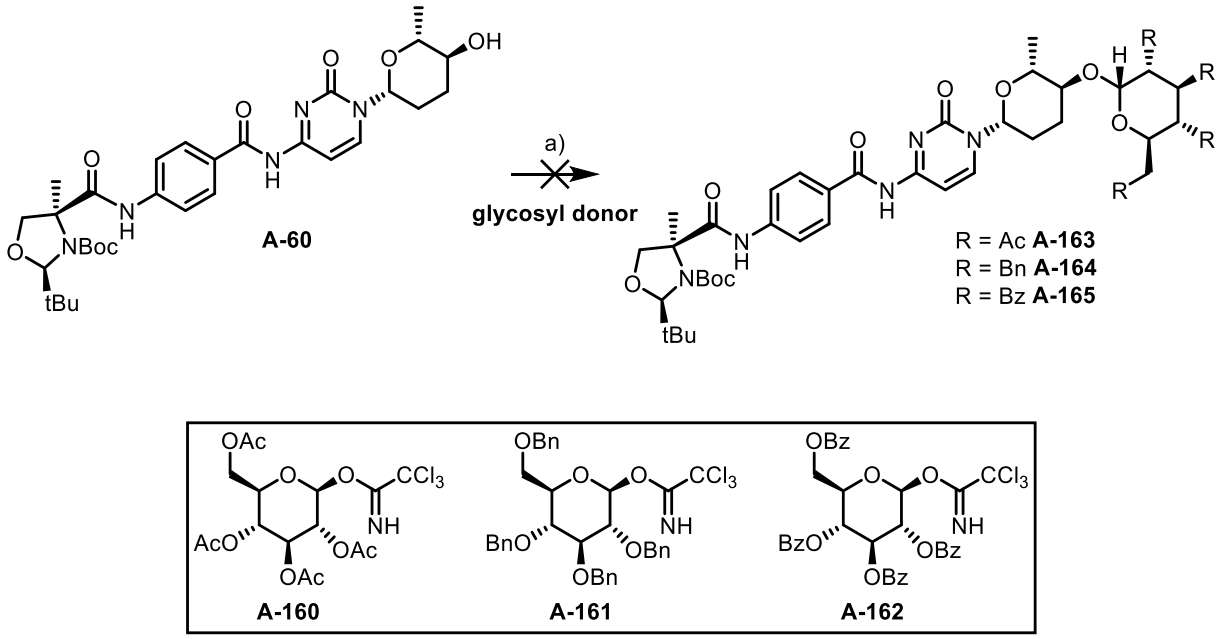

Scheme 46 Reagents and conditions: a) TMSOTf, CH_2Cl_2, -78 °C.

Keeping the same reaction conditions (for detailed reaction setup see Table 10, section 1.3.5.11) as in previous glycosylation attempts, neither of these donors produced the desired products **A-163** – **A-165** in isolable quantities, which, unfortunately, was in line with the results from previous experiments.

1.3.6 Disaccharide Approach

1.3.6.1 Glycosyl Fluorides for Disaccharide Formation

The synthesis of disaccharide building blocks for the implementation of the disaccharide strategy in a first phase involved the evaluation of glycosyl fluorides as glycosyl donors in the reaction with amicetose glycoside **A-79**, as illustrated in Scheme 47 for glycosyl fluoride **A-138**. To our disappointment, the desired disaccharide **A-166** was not obtained upon activation of **A-138** with tin (II) chloride and silver triflate. The glycosyl donor was not activated under these conditions and both starting materials were recovered unchanged for a temperature range from 0 to 24 °C.

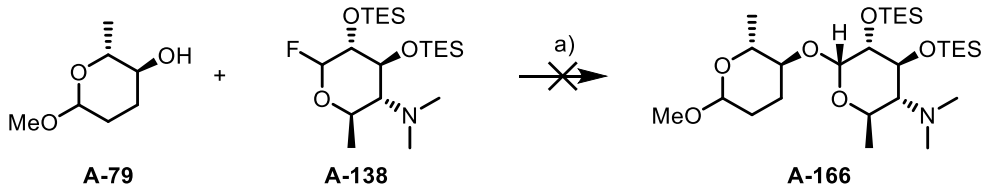

Scheme 47 Reagents and conditions: a) AgOTf, $SnCl_2$, MS 4 Å, Et_2O, DCE, 0 °C – rt.

In order to exclude handling issue, a set of model experiments were conducted with glycosyl fluoride **A-138** and benzyl alcohol as the glycosyl acceptor (Scheme 48).

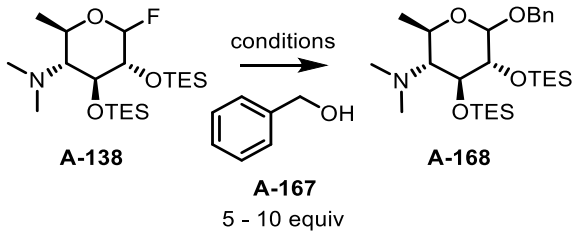

Scheme 48 Activation experiments for glycosyl fluoride **A-138**.

Different conditions were investigated (Table 11) and in contrast to the reaction with **A-79** or **A-60** as glycosyl acceptors, good to high yield of the expected benzyl glycoside could be obtained under appropriate conditions. This finding clearly indicates that the lack of product formation in the attempted reactions of **A-138** with **A-79** or **A-60** is related to the structure of these glycosyl acceptors.

Table 11 Activation conditions for a series of test reactions of **A-138** with benzyl alcohol.[a]

Entry	Conditions	Observation
1	$SnCl_2$, Et_2O, 0 -25 °C	50% isolated product
2	$SnCl_2$, $AgClO_4$, Et_2O, 0 -25 °C	80% isolated product
3	Cp_2ZrCl_2, $AgClO_4$, Et_2O, -78 °C	20% isolated product
4	Cp_2HfCl_2, $AgClO_4$, Et_2O, -78 °C	traces of product

[a] Anomeric mixtures of 1:1 for all of them obtained. The reactions were carried out on a scale of 10 – 90 mg.

1.3.6.2 Thioglycoside for Disaccharide Formation

Thioglycosides as glycosyl donors were first reported by *Ferrier*[224] in combination with mercury (II) salts as promoters. Ever since, thioglycosides have been used in carbohydrate chemistry and the promoter systems have been continuously refined. The promoters can be categorized into four major classes: (1) metal salts; (2) halonium reagents; (3) organosulfur reagents; (4) single electron transfer (SET) reagents/methods.[148]

A series of thioglycosides were investigated as glycosyl donors for the reaction with amicetose glycoside **A-79** to provide a set of building blocks (Scheme 49) for the glycosylation of **A-53** as part of the disaccharide approach A towards amicetin (**A-1**). The hydroxy groups of the 2,3-diol moiety in these amosamine derivatives were protected either as benzyl- or as PMB-ethers (**A-128** and **A-169**, respectively). In addition to the actual amosamine glycosides, incorporating a dimethylamino group on C4, the corresponding 4-azido derivatives (**A-127** and **A-170**, respectively) were also evaluated as potential glycosyl donors; the resulting glycosylation products could serve as precursors for amicetin (**A-1**).

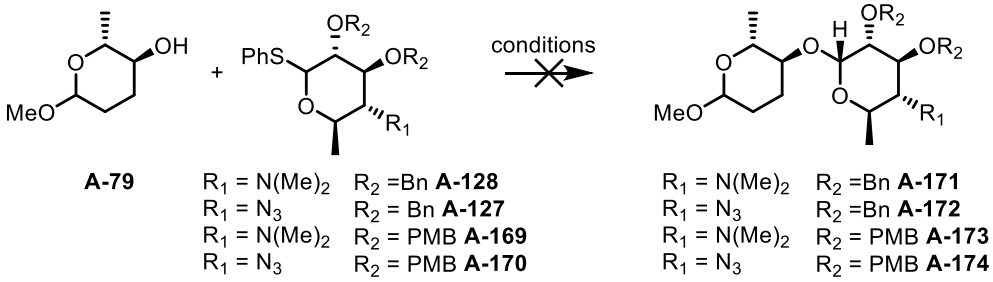

A-79

R_1 = N(Me)$_2$	R_2 =Bn **A-128**	R_1 = N(Me)$_2$	R_2 =Bn **A-171**
R_1 = N_3	R_2 = Bn **A-127**	R_1 = N_3	R_2 =Bn **A-172**
R_1 = N(Me)$_2$	R_2 = PMB **A-169**	R_1 = N(Me)$_2$	R_2 = PMB **A-173**
R_1 = N_3	R_2 = PMB **A-170**	R_1 = N_3	R_2 = PMB **A-174**

Scheme 49 Thioglycosides as glycosyl donors for the reaction with acceptor **A-79**. For conditions see **).**

Table 12.

First experiments were conducted with **A-169** and **A-170** and an activation system composed of AgOTf and NIS (Table 12). This system seemed not to be sufficiently reactive at temperatures of -40°C, but gave decomposed products as soon as the temperature was raised (entry **1** and **2**). Changing from silver triflate to trimethylsilyl triflate gave a red solution immediately after addition of the *Lewis* acid and provided a complex reaction mixture (entry **3**). The activation of phenyl thioglycosides with NBS has been described by *Nicolaou.*[225] Unfortunately, no product formation was observed under these conditions between 0 °C and room temperature; at some point the glycosyl donor started to decompose (entry **4**). The use of NBS was also evaluated for benzyl-protected derivatives **A-127** and **A-128**, but again without any success (entry **5** and **6**).

Table 12 Glycosylation attempts with various thioglycosides as glycosyl donors.[a]

Entry	Compound	Conditions	Observation
1	**A-169**	AgOTf, NIS, CH_2Cl_2, -40 – 24 °C	no product formation, no reaction at low temp., decomposition at 24 °C
2	**A-170**	AgOTf, NIS, CH_2Cl_2, -40 – 0°C	no reaction at low temp., decomposition at 0 °C
3	**A-170**	TMSOTf, NIS, CH_2Cl_2, 0 °C	no product formation, reaction turns red, decomposition
4	**A-170**	NBS, CH_2Cl_2, 0 °C -rt	no product formation, 16 h at 24 °C gave complex reaction mixture
5	**A-128**	NBS, CH_2Cl_2, -78 °C	no product formation
6	**A-127**	NBS, CH_2Cl_2, -78 °C	no product formation

[a] Both pyranoses were co-evaporated with benzene prior to be used. NBS was freshly recrystallized. Reactions from entry **1** – **3** were carried out with additional molecular sieves. TMSOTf was added as a stock solution in CH_2Cl_2.

Facile hydrolysis of **A-127** was observed when activated with NBS and stirred in a mixture of CH_2Cl_2 and H_2O (Scheme 50). These findings could indicate that a reaction temperature higher than -78 °C is

a prequisite for an activation of **A-127** and/or that glycosyl donor **A-79** is not withstanding or suitable for these reaction conditions.

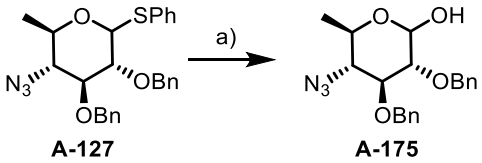

A-127 **A-175**

Scheme 50 Hydrolysis of **A-127**. Reagents and conditions: NBS, CH_2Cl_2:H_2O (9:1), 0 – 5 °C, 2.5 h, 58%. NBS was added to a solution of **A-127** in CH_2Cl_2:H_2O at 0 °C.

1.3.6.3 Trichloroacetimidates for Disaccharide Formation

1. Synthesis of Trichloroacetimidates A-148 and A-177

In order to preempt potential difficulties in the removal of the benzyl-protecting group on the fully assembled amicetin core, in parallel with the use of a new type of donors (experiments described in section 1.3.5.13 were performed afterwards) we pursued a novel strategy that would involve trichloroacetimidates **A-148** or **A-177** as amosamine donors (Scheme 51). Compound **A-148** was envisioned to be coupled to the amicetose acceptor and deprotected at the disaccharide stage, followed by reprotection. The TBS-groups in **A-177** were anticipated to be cleavable on the fully assembled amicetin skeleton.

Trichloroacetimidates as glycosyl donors were first reported by *Schmidt*[149] and have developed into one of the most commonly used donor types in carbohydrate chemistry. They are easy to access and are activated under mild conditions by *Lewis* or *Brønsted* acids, resulting in stereoselective glycoside bond formation.

Compound **A-148** (Scheme 51) was readily synthesised from **A-127** (synthesis is described in section 1.3.5.6). Thus, treatment of thioglycoside **A-127** with NBS in aqueous solution gave the desired pyranose, which was purified by FC. Reaction of the latter with trichloroacetonitrile then yielded the desired acetimidate **A-148** as an anomeric mixture of α:β = 1:5.

The analogous compound **A-177**, to our disappointment, could not be accessed, due to the instability of tosylate **A-176**, which rapidly decomposed even at -4 °C under argon. Intermediate **A-176** was obtained using the chemistry that had been developed for the synthesis of tosylate **A-125** (cf. Scheme 9) with some minor adjustments. *E.g.*, minor changes were made for the benzylidene deprotection of the diol, where acidic conditions were avoided, to not lose the TBS groups. Instead, mild *Lewis* acidic conditions in combination with ethanethiol as a scavenger were successfully applied.

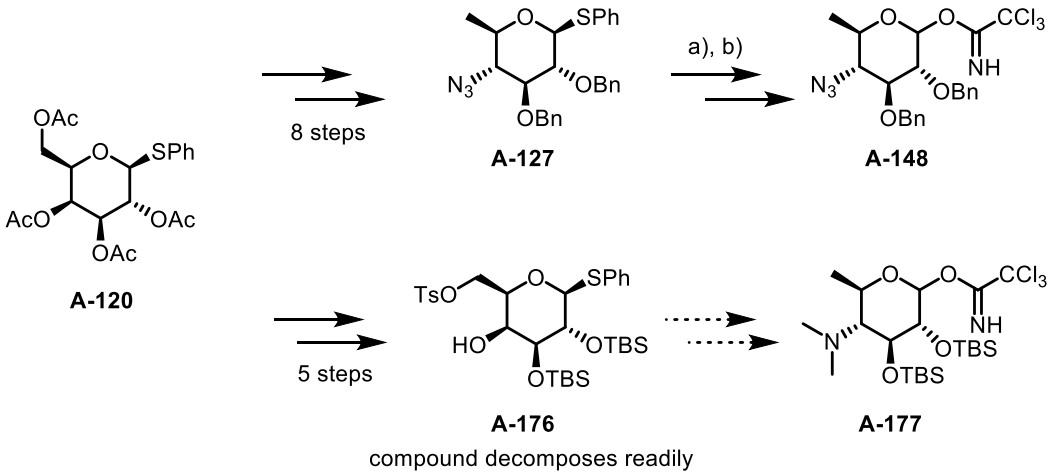

Scheme 51 Synthesis of **A-38** and failed attempt to **A-176**. Reagents and conditions: a) NBS, CH_2Cl_2:H_2O (9:1), 0 °C, 5.5 h, 59%; b) Cl_3CCN, K_2CO_3, CH_2Cl_2, 0 °C – rt, 9 h, 70% as an anomeric mixture α:β = 1:5.

1.3.6.3.1. Synthesis of Trichloroacetimidate A-149

As a possible alternative to **A-148** as a glycosyl donor, we embarked on the synthesis of trichloroacetimidate **A-149**, which incorporates a diacetal protecting group for the diol moiety (Scheme 52). Starting with inexpensive penta-acetyl β-D-glucose (**A-178**), *Lewis* acid-catalyzed installation of the anomeric benzyloxy group,[226] followed by global deacetylation afforded benzyl pyranoside **A-179** in good yields (66% over two steps). The following selective protection of the *trans*-diol motif[223] to provide diacetal **A-180** worked smoothly in the presence of catalytic amounts of boron trifluoride etherate. A sequence of previously discussed transformations then led to glycosyl donor **A-149**. It is worth to note that during debenzylation of the anomeric hydroxy group under catalytic hydrogenation conditions over palladium, an anomeric mixture of **A-153** is obtained.

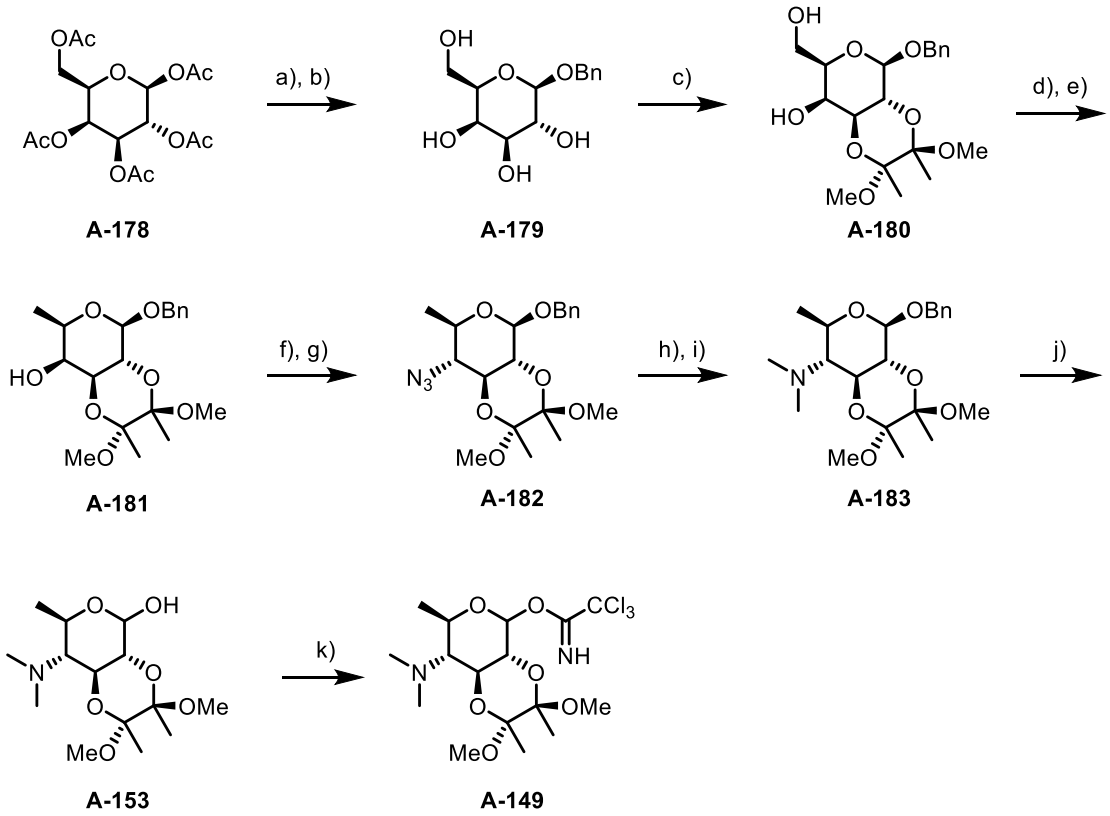

Scheme 52 Synthesis of **A-149**. Reagents and conditions: a) BnOH, $BF_3{\cdot}OEt$, CH_2Cl_2, 0 °C - rt; b) 25% NaOMe, MeOH, 0 °C, 20 min, 66% over two steps; c) butanedione, trimethyl orthoformate, cat. $BF_3{\cdot}OEt_2$, MeOH, rt, 72 h, 75%; d) TsCl, pyridine, 0 °C - rt, 24 h, 79%; e) $LiBEt_3$, THF, rt, 2.5 h, 89%; f) MsCl, pyridine, 0 °C, 3 h; g) NaN_3, DMF, 100 °C, 52 h, 75% over two steps; h) Pd/C, H_2, MeOH, rt; i) Pd/C, H_2, formaldehyde, EtOH, rt, 75% over two steps; j) Pd/C, H_2, MeOH, rt, 85%; k) Cl_3CCN, K_2CO_3, CH_2Cl_2, 0 °C - rt, 61%

We also found that compound **A-153** can directly be obtained from **A-182** by concomitant anomeric debenzylation and azide reduction by means of prolonged catalytic hydrogenation followed by *Eschweiler-Clarke* methylation of the primary amino group. Finally, treatment of **A-153** with trichloroacetonitrile gave the glycosyl donor **A-149**.

1.3.6.3.2. Synthesis of Trichloroacetimidate A-38

Trichloroacetimidate **A-38**, bearing a bis-PMB-protected diol functionality, was considered an attractive glycosyl donor, as the azide group should be readily convertible into the required dimethylamino group without affecting the diol protecting groups (Scheme 53). The PMB-protecting groups, in turn, were expected to be readily cleaved after successful glycosylation, while being stable under the *Lewis* acidic conditions to be employed in the planned *Vorbrüggen* glycosylation of the cytosine moiety. The synthesis of **A-38** departed from alcohol **A-181**, which was first treated with MsCl in dry pyridine at 0 °C and, after an aqueous work-up, stirred under catalytic hydrogenation over palladium to remove the benzyl protecting group. Pyranose **A-185** was smoothly converted into allyl glycoside **A-186** by etherification of the anomeric hydroxy group with allyl bromide under basic conditions (81% yield). Treatment of **A-186** with a mixture of TFA and H_2O at ambient temperature

successfully removed the bisacetal protecting group. Reprotection of the free diol **A-187** was then achieved by reaction with PMBCl, which gave the fully protected glycoside **A-188** in 82% yield. Subsequent palladium-catalysed cleavage of the allyl ether moiety furnished glycoside **A-189**, which was converted into an anomeric mixture of the desired trichloroacetimidates **A-38** under standard conditions (trichloroacetonitrile and potassium carbonate in CH_2Cl_2). **A-38** was obtained in 76% overall yield from **A-188**.

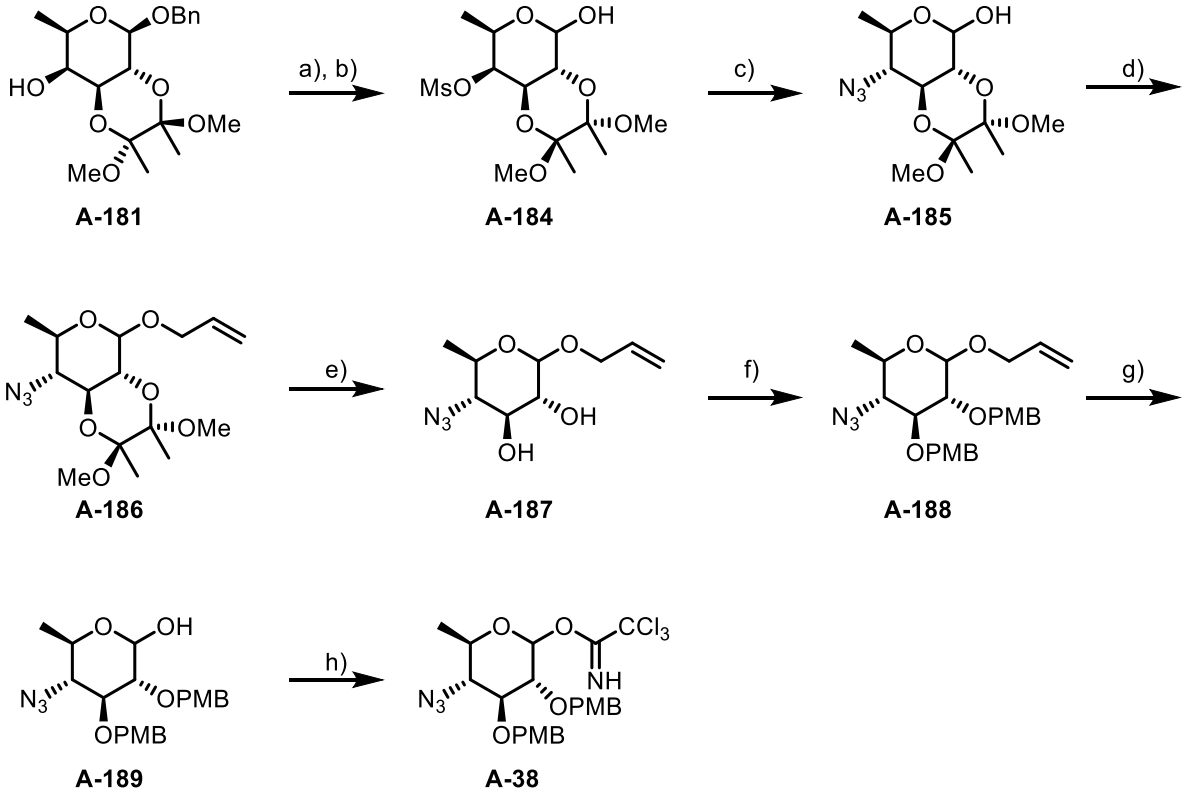

Scheme 53 Reagents and conditions: a) MsCl, pyridine, 0 °C 6 h; b) Pd/C, H_2, MeOH, 14 h, 81% over two steps; c) NaN_3, DMF, 100 °C, 76%; d) Allylbromide, NaH, THF, 50 °C, 13 h, 81%; e) TFA/H_2O, CH_2Cl_2, rt, 18 h, 76%; f) PMBCl, NaH, DMF, 0 °C - rt, 18 h, 82%; g) $PdCl_2$, MeOH/CH_2Cl_2, rt, 5 h; h) Cl_3CCN, K_2CO_3, CH_2Cl_2, 0 °C - rt, 19 h, 76% over two steps.

1.3.6.3.3. Disaccharide Formation

As illustrated in Scheme 54, the reaction of trichloroacetimidate **A-148** with glycosyl acceptor **A-79** at -78 °C in the presence of catalytic amounts of TMS-triflate gave an excellent total yield of 91% of a 4:1 mixture of anomers with the desired α-anomer as the major product. After separation of the anomers, reduction of the azide moiety under catalytic hydrogenation over palladium and methylation of the resulting amine furnished **A-171** in 73% overall yield. Pleasingly, the deprotection was effective under *Birch* conditions and gave sufficiently clean product for use in the following step without further purification. Finally, reprotection of the hydroxy groups either as silyl-ethers or acetate-esters successfully gave **A-166** and **A-191**, respectively, in yields of 61% and 69%. It should be

re-emphasised that this deprotection-protection sequence was needed due to the persistence of the benzyl groups and concerns about their successful removal late in the synthesis.

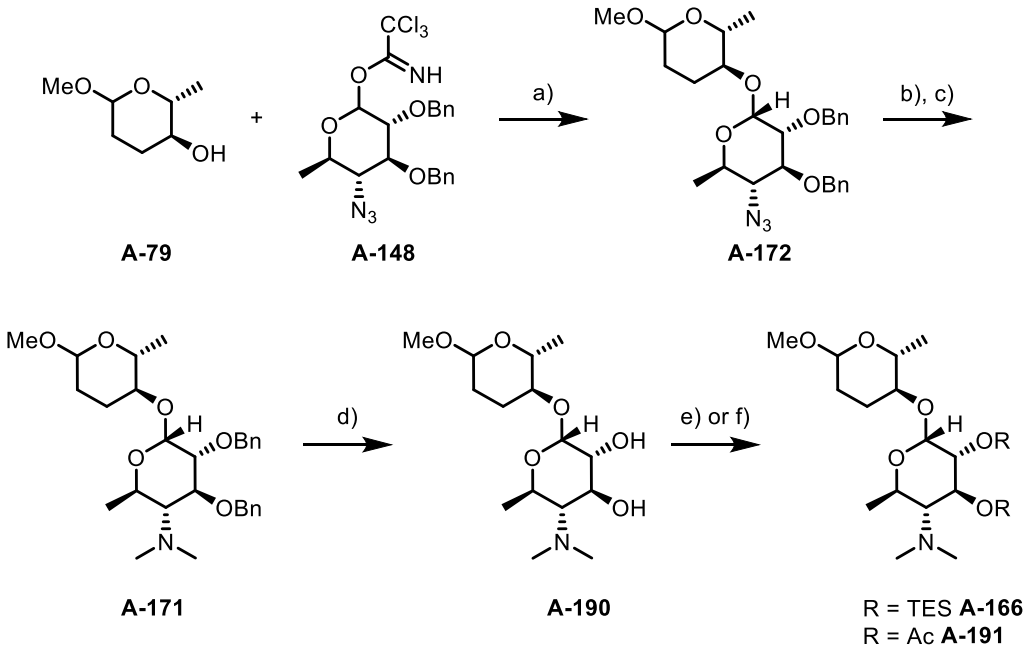

Scheme 54 Reagents and conditions: a) TMSOTf, CH_2Cl_2, -78 °C, 91%, α:β-glycoside (4:1); b) Pd/C, H_2, MeOH, rt; c) Pd/C, H_2, formaldehyde, EtOH, rt, 73% over two steps; d) Na/NH_3, THF, -78 °C, quant. crude; e) TES triflate, NEt_3, CH_2Cl_2, -78 °C, 61%; f) Ac_2O, DMAP, NEt_3, CH_2Cl_2, rt, 69%.

In further efforts, we expanded the synthetic disaccharide feed stock with the substrates shown below. As illustrated in Scheme 55, the same sequence of reactions that led to **A-166** and **A-191** also provided access to disaccharides **A-173** and **A-192** by reprotecting the diol motif in **A-190**.

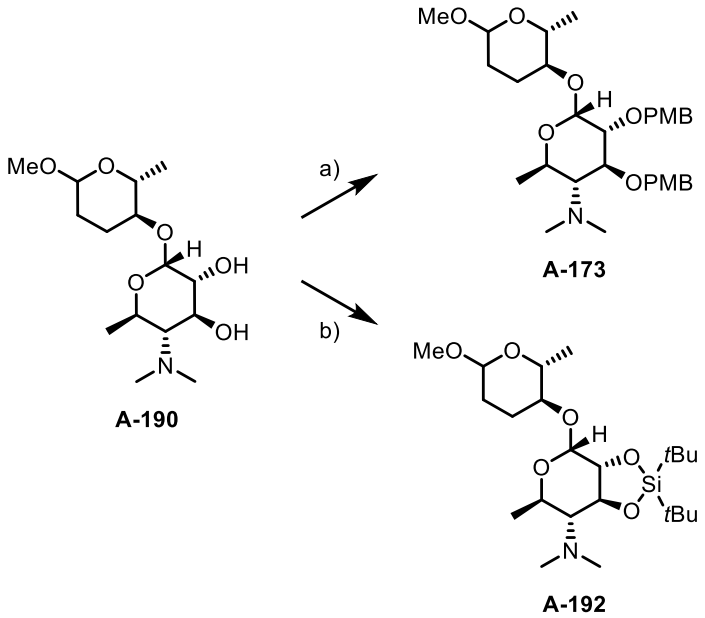

Scheme 55 Reprotection of **A-190**. Reagents and conditions: a) PMBCl, NaH, DMF, 0 °C – rt, 67%; b) $t$$Bu_2Si(OTf)_2$, pyridine, CH_2Cl_2, 0 °C –rt, quant. based on crude.

Disaccharide **A-196** was accessed via trichloroacetimidate **A-146** (Scheme 56), which was synthesis according to similar procedures as reported in section 1.3.5.6. Unfortunately, purification of disaccharide **A-196** was somehow difficult and gave the product only in moderate purity.

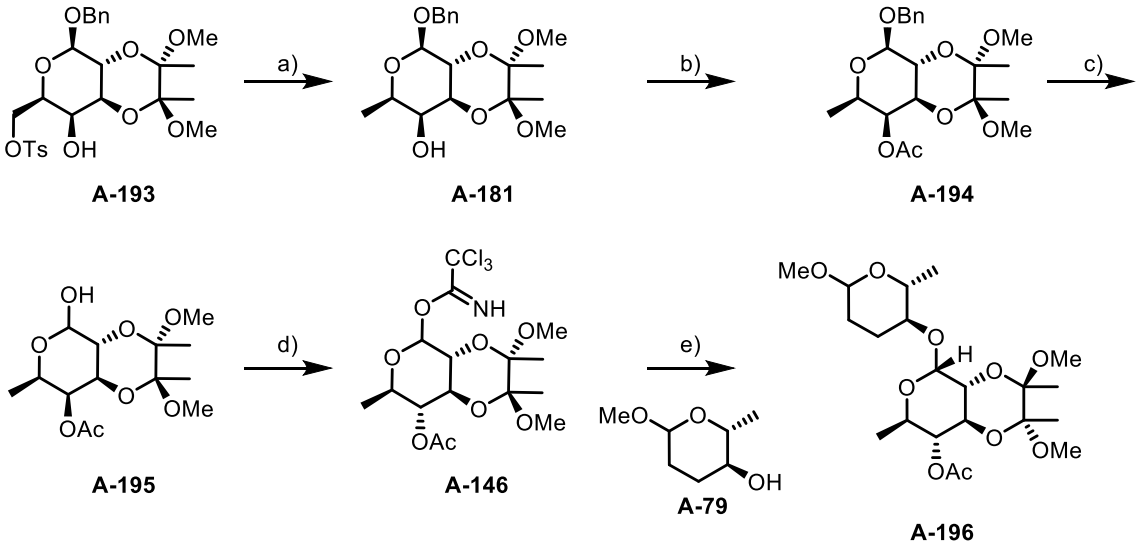

Scheme 56 Reagents and conditions: a) $LiBEt_3H$, THF then H_2O_2, rt, 92%; b) Ac_2O, pyridine, rt, crude; c) Pd/C, H_2, MeOH, rt, 72% over two steps; d) Cl_3CCN, K_2CO_3, CH_2Cl_2, 0 °C – rt, 93% as a mixture of anomers; e) TMSOTf, CH_2Cl_2, -78 °C, 62% (impure).

In contrast, the preparation of disaccharide **A-198** was unsuccessful from both trichloroacetimidate **A-149** and trifluoroacetimidate **A-197**[227] (Scheme 57), with no product formation being observed.

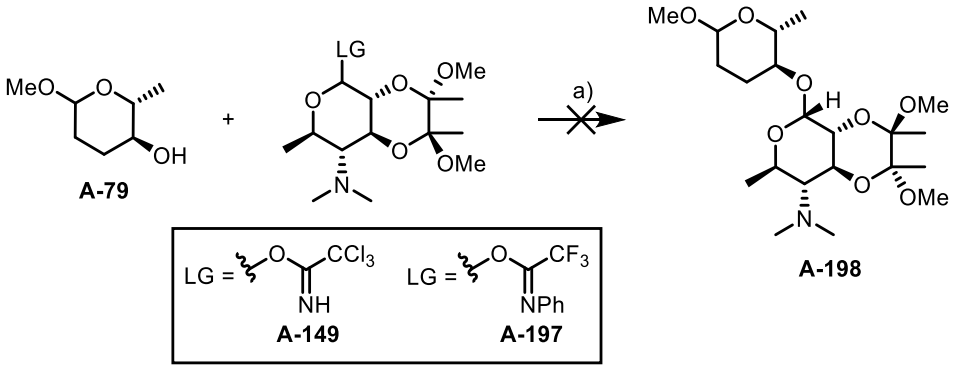

Scheme 57 Failed glycosylation attempts using *Schmidt* donors. Reagents and conditions: a) TMSOTf, CH_2Cl_2, -78 °C.

Interestingly, the azide derivative **A-200** was readily accessed under the exact same *Schmidt* conditions. Eventually, dimethylamino derivative **A-198** could be accessed in traces by the reduction of azide **A-200** and subsequent methylation under the previously described *Eschweiler-Clarke* conditions (Scheme 58).

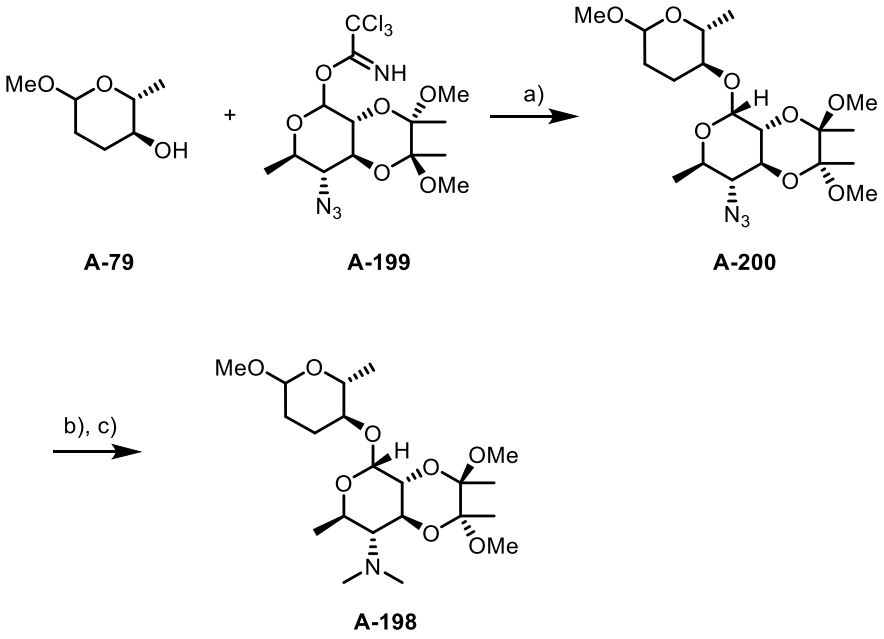

A-79 **A-199** **A-200**

A-198

Scheme 58 Reagents and conditions: a) TMSOTf, CH_2Cl_2, -78 °C, 2 h, 96% (slightly impure); b) Pd/C, H_2, MeOH, rt; c) Pd/C, H_2, formaldehyde, EtOH, rt, traces.

*1.3.6.4 Vorbrüggen Glycosylation Attempts with Disaccharides **A-166, A-173, A-191**, and **A-196***

With disaccharides **A-166**, **A-173, A-191**, and **A-196** in hand, we embarked on the glycosylation of nucleoside **A-53** under the previously described *Vorbrüggen* conditions that had been successfully employed in the glycosylation of **A-53** (section 1.3.5.2; Scheme 59).

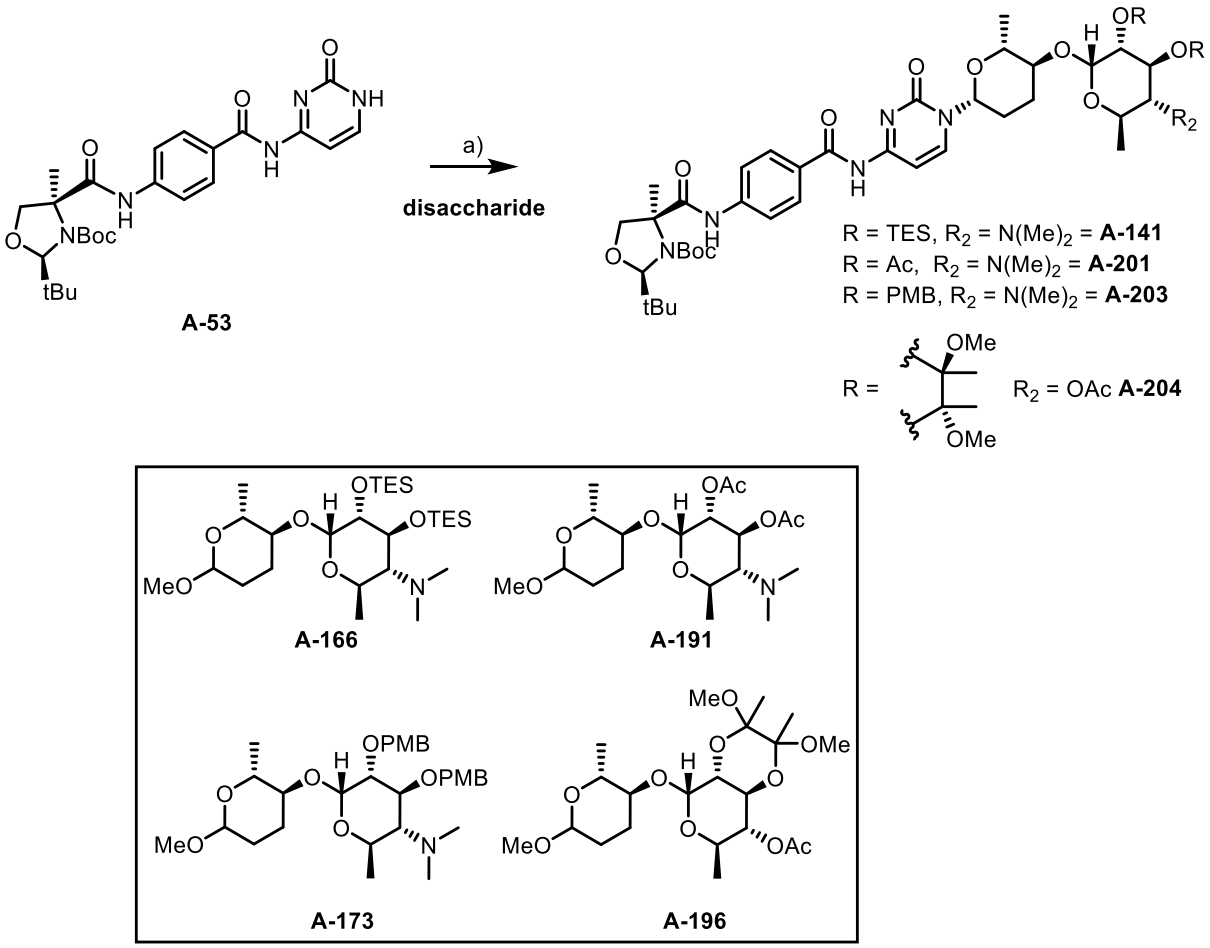

Scheme 59 Reagents and conditions: a) BSA, $SnCl_4$, MeCN, rt – 40 °C. For exact conditions see **Table 13**

Various experiments have been performed with slight variation of reaction conditions (Table 13).The reactions had to be carried out under strictly anhydrous conditions and both the acceptor **A-53** and the respective disaccharide were co-evaporated from toluene immediately prior to use. Solvents were freshly distilled and $SnCl_4$ was distilled over phosphorous pentoxide. Additionally, molecular sieves were added to the reaction mixture to capture residual water.

For disaccharide **A-166**, no consumption of starting material was observed after 150 min at ambient temperature; this did not change when the temperature was raised to 45 °C and another aliquot of tin (IV) chloride was added. Unfortunately, only decomposition of the glycosyl donor was observed.

Next, the acetyl protected disaccharide **A-191** was examined. In this reaction, formation of the desired product was observed (confirmed only by LC-MS) within 60 min. However, the reaction stalled at some point and either heating the reaction mixture to 40 °C or successively increasing the equivalents of $SnCl_4$ only led to decomposition. Despite all efforts to fine-tune the reaction conditions and while clearly detecting the desired product by mass spectrometry, no pure product could be isolated in several experiments.

Table 13 Reaction conditions screened for the glycosylation of **A-53** with the different disaccharide donors.[a]

Entry	Donor	$SnCl_4$ [equiv]	Temp. [°C]	Time [h]	Remark	Observation
1	**A-166**	1.5	23 - 45	1.5 at 23 °C, 13 at 45 °C	when temp. was raised to 45 °C another 1.5 equiv of $SnCl_4$ was added	no consumption of **A-53**, no P isolated after FC, donor fully consumed
2	**A-191**	1.5	23	4.5		**A-53** still present after 4.5 h, P isolated (impure)
3	**A-191**	1.5	23 - 40	1 at 23 °C, then 2 at 40 °C		**A-53** present at rt, decomposition at 40 °C
4	**A-191**	2.7	23	4	started with 1.5 equiv $SnCl_4$ then another 1.5 equiv added	sudden decomposition upon adding more $SnCl_4$
5	**A-191**	1.5	23	3.5		little P formation & isolated, still lot of **A-53** present
6	**A-191**	1.5	23	26		reaction stops at some point, P isolated after FC (impure)
7	**A-173**	1.5	23	4	direct filtration of crude over Alox	P isolated after FC (impure)
8	**A-173**	3.0	23	16	$SnCl_4$ was added in two portions of 1.5 equiv (after 3 h)	no P formation observed
9	**A-173**	1.5	23	5	another drop of $SnCl_4$ (pure) was added after 4	no P formation observed
10	**A-196**	1.5	23	2	direct filtration of crude over Alox	no P formation observed

[a] All reactions were carried out in dry MeCN and pre-dried molecular sieves. $SnCl_4$ was prepared as a stock solution. 2.0 equiv BSA was used to silylate **A-53**. If not otherwise state an aqueous work-up was performed. Both compounds were azeotropically dried with toluene prior to be used. SM: starting material. P: product.

Best results were obtained for the PMB-protected compound **A-173**, although problems were faced with reproducibility. The desired product **A-203** was formed within a few hours (according to mass spectrometry) and was isolated by filtering the crude reaction mixture over a short plug of aluminium oxide. However, this material still contained a significant amount of impurities, as indicated by its proton and carbon NMR spectra.

Bisacetal **A-196** was submitted to the glycosylation procedure without success. The expected product was neither detected by mass analysis nor by ^{1}H-NMR analysis. In this case, the *Lewis* acid could potentially cleave the bisacetal, which had been observed in previous studies when **A-182** was treated with $SnCl_4$ (Scheme 60).

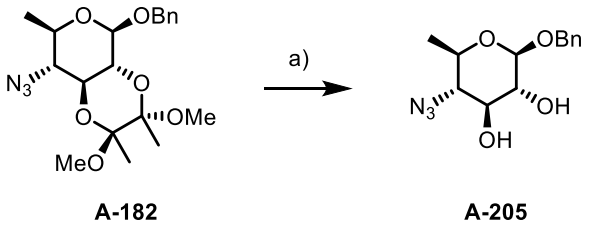

A-182 **A-205**

Scheme 60 Reagents and conditions: a) $SnCl_4$, CH_2Cl_2, 0 °C, 30 min, not isolated.

*1.3.6.5 Deprotection of **A-201***

With small amounts of **A-201** in hand, we embarked on the cleavage of the acetyl groups. The result obtained in these trial experiments have to be treated with some caution, due to the small scale of the reactions which were carried out with 0.3, 0.5 and 0.7 µmol of **A-201**, respectively.

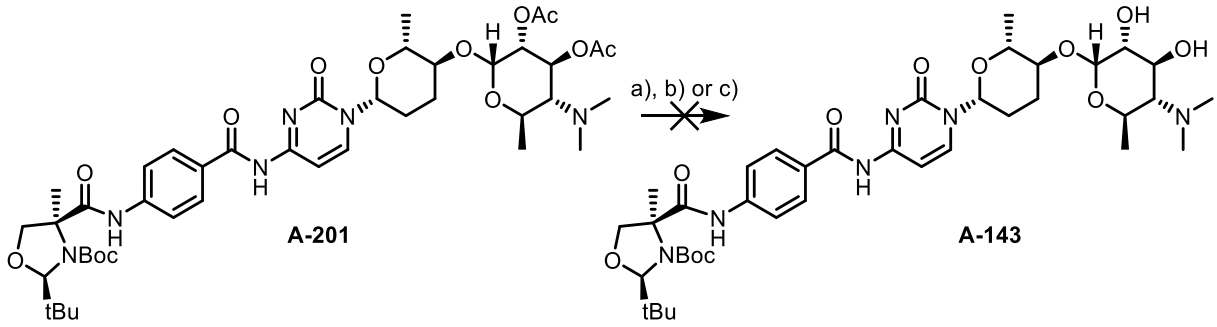

A-201 **A-143**

Scheme 61 Final amosamine deprotection attempts. Reagents and conditions a) NaOMe (0.1 equiv), MeOH, rt; b) NaOMe (30.0 equiv), MeOH, rt; c) K_2CO_3, MeOH, rt, decomposition.

When **A-201** was treated with 0.1 equiv of sodium methoxide in methanol at ambient temperature the reaction proceeded extremely slowly with conversion of starting material after 22 h. In a second experiment, **A-201** was mixed with 10 equiv of sodium methoxide, with the amount being gradually increased to 30 equiv. LC-MS of the reaction mixture clearly indicated the formation of deacetylated product along with a mono-deprotected species and remaining starting material. The addition of additional 10 equiv of sodium methoxide instantly led to decomposition. In a third experiment, potassium carbonate (3.0 equiv) was used as the base, which led to full consumption of starting material within 30 minutes. Unfortunately, LC-MS showed the presence of the same decomposition product as for large quantities of sodium methoxide. Owing to the very small quantities of **A-201** available, we were not able to perform any further reactions.

1.3.7 Ester Analogues of Amicetin (A-1)

As discussed in previous sections, our efforts towards the synthesis of the natural product amicetin (**A-1**) produced a series of various glycosyl donors, but the final glycosylation remained an insurmountable obstacle. Neither of the two pathways, the sequential approach or the disaccharide route, allowed us to isolate substantial amounts of the complete amicetin scaffold.

In order to capitalize on the synthesis of the desamosamine-amicetin derivative and for a preliminary assessment of the importance of the amosamine moiety for the anti-*Mtb* activity of amicetin (**A-1**), we embarked on the synthesis of the two simplified ester analogues **A-208** and **A-209** (Scheme 62). With the purpose to retain a certain degree of resemblance to the natural product, we chose 3-dimethylaminopropanoic acid **A-206** and 4-dimethylaminobutyric acid **A-207** as amosamine replacements, which both incorporate a dimethylamino moiety.

1.3.7.1 Ester Bond Formation

Ester bond formation for both compounds was successfully accomplished with DCC and DMAP in dichloromethane and furnished the desired products **A-208** and **A-209** in 32% and 64% yield, respectively.

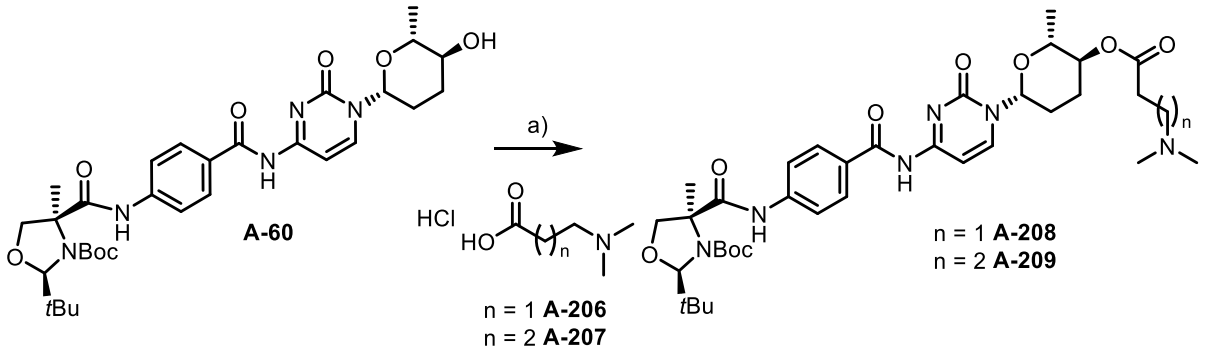

Scheme 62 Reagents and conditions: a) DCC, DMAP, CH_2Cl_2, rt, for **A-206** 6 h, 32%; for **A-207** 18 h, 64%.

Further, we wanted to prepare the two cyclic ester analogues **A-210** and **A-211 (**Figure 38**)**, but unfortunately, the ester bond formation did not work for these substrates with DCC/DMAP. No other conditions were investigated in these cases.

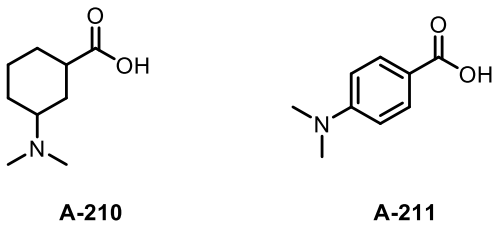

Figure 38 Further carboxylic acids that failed in the coupling reaction.

1.3.7.2 Oxazolidine Opening and Boc-removal of Ester Analogues A-208 and A-209 Including Preliminary Test Reactions

At the outset of our work towards the synthesis of amicetin (**A-1**), we had critically considered a suitable protection strategy for the oxazolidine moiety. As the cleavage of the aminal moiety of a typical *Seebach* oxazolidine is performed under strongly acidic conditions (anhydrous HCl,[228] tosic acid,[229] TFA[230]), we had concerns about the stability of the acid-labile glycosidic bonds in the final deprotection step. However, a group at *GlaxoSmithKline* has reported a protocol to efficiently cleave oxazolidines with potassium trimethylsilanolate to obtain the free amino acids.[231] *Corey* and *Reichard* have described a protocol that uses only slightly acidic conditions (2% HCl) for the oxazolidine opening by a transfer of the methylene unit to 1,3-propanedithiol in TFE at 50 °C. With these options available and in light of the ease of the synthesis of oxazolidines such as **7** (as described in chapter 1.4.4.), we had felt that the synthetic strategy outlined in section 1.3.1 was indeed a viable option.

In order to establish suitable conditions for oxazolidine cleavage in ester analogues **A-208** and **A-209**, we first investigated oxazolidine ring opening for a series of intermediates described in previous sections. Compound **A-65**, was readily cleaved with an excess (43 equiv) of TFA in dichloromethane at ambient temperature to give methyl 2-amino-3-hydroxypropanoate (**A-212**) (Figure 39). LC-MS indicated that the opening of the aminal was faster than the Boc-deprotection of the amino group.

When the cytimidine precursor **A-53** was subjected to these same conditions aminal opening and Boc-deprotection proceeded much more slowly than for **A-65**. The fully deprotected α-methyl serine was obtained after stirring the reaction mixture for 16 hours at ambient temperature.

In order to assess the stability of the glycosidic bond between cytosine and amicetose to the above deprotection conditions, compound **A-109** was exposed to a solution of TFA in dichloromethane and the rate of the glycosidic bond cleavage was measured by LC-MS over a course of 17 hours. At this point, 9% of sugar amicetose cleavage was detected.

Advanced intermediate **A-60** was scrutinised more carefully: We started with a lower amount of TFA (12.36 equiv) and monitored the reaction over 24 h. Direct evaporation of the solvent under reduced pressure at 40 °C without prior aqueous workup showed the formation of the free serine moiety along with the intermediate where the aminal was opened but the Boc-protecting group was still present (according to NMR) and the glycosidic bond was still intact. In a second trial, the excess of TFA was increased (36.0 equiv), which led to complete consumption of starting material within 30 min, but the Boc-protected intermediate turned out to be more stable than anticipated (roughly 90% still present according to LC-MS). Finally, with a large excess of TFA (74.0 equiv) the product was formed within 7 h without any Boc-protected intermediate being left. Unpleasingly, we observed

deglycosylation (below 15%, quantified by LC-MS). The product was purified by HPLC and its structure unambiguously confirmed by NMR spectroscopy.

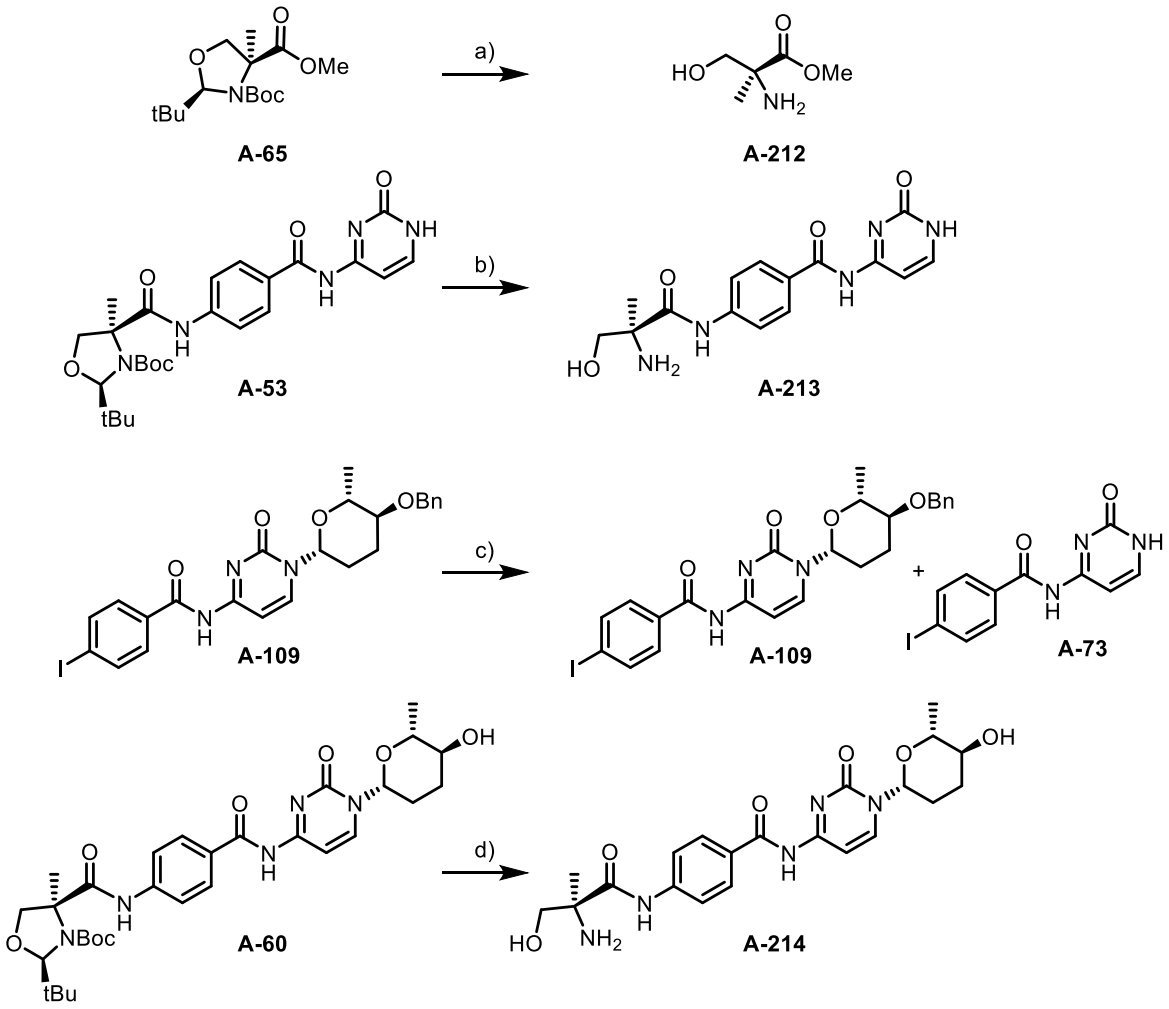

Figure 39 Acid-mediated oxazolidine opening and Boc-deprotection and additional stability test for the glycosidic bond in **A-109**. Reagents and conditions: a) TFA (43 equiv), CH_2Cl_2, rt, SM consumed after 48 h, product formation confirmed by LC-MS; b) TFA (43 equiv), CH_2Cl_2, rt, n.d.; c) TFA (1.5 equiv), CH_2Cl_2, rt, after 17 h were 9% of **47** detected by LC-MS; d) TFA (72 equiv), CH_2Cl_2, rt, 7 h, n.d.

Finally, the deprotection of esters **A-208** and **A-209** was investigated under acidic conditions (Scheme 63, Table 14).

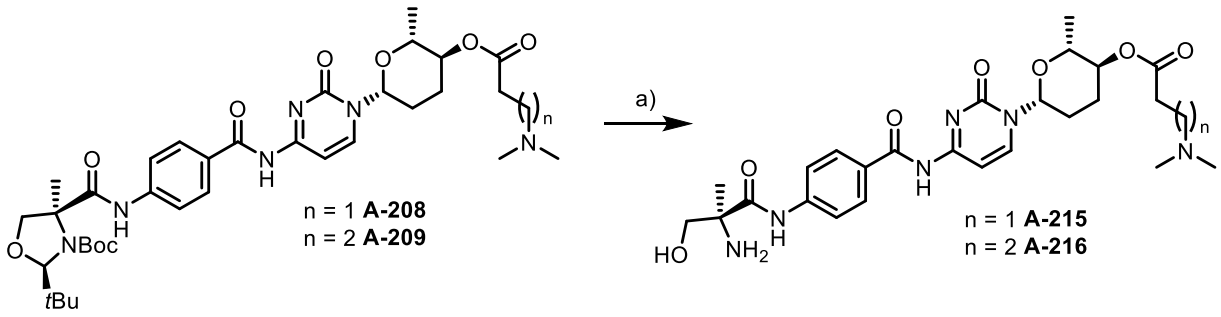

Scheme 63 Oxazolidine deprotection of **A-208** and **A-209**. Reagents and conditions: a) acid, CH_2Cl_2, rt. See Table 14 for details.

Table 14 Screening for suitable oxazolidine opening and Boc deprotection conditions.

Entry	Temp. [°C]	Acid	Equiv	Time [h]	Observation
1	rt	HCl 6 M	37	24	slow reaction, product formation along with various side product
2	rt	HCl 6 M	74	24	full decomposition
3	rt	TFA	12.36	24	aminal opening, Boc not cleaved
4	rt	TFA plus 1 drop of H_2O	37	3.5	starting material consumed within 30 min, Boc not cleaved
5	rt	TFA	74	4	full conversion to product

As can be seen from Table 14, the use of a 74-fold excess of TFA in CH_2Cl_2 for both esters resulted in complete conversion of starting material within 4 h. Purification of the materials thus obtained by preparative RP-HPLC gave the desired amicetin analogues **A-215** and **A-216** in very satisfactory yields of 51% and 70%, respectively.

1.4 Conclusion and Outlook

In the course of this PhD project a number of advanced intermediates were successfully prepared as potential precursors for the natural product amicetin. While fully protected variants of amicetin (**A-1**) could be detected analytically, the isolation of these materials in pure form has remained elusive and the total synthesis of the natural product could not be completed. However, two ester analogues (**A-215** and **A-216**) could be synthesised and submitted for biological testing. Despite all the efforts made since the early 1960's, the first total synthesis of amicetin (**A-1**) remains to be accomplished.

Antimycobacterial activity for both the esters **A-215** and **A-216** was not very high but nevertheless, a certain level of activity was confirmed (Figure 40). These results encourage for the synthesis of more rigid (cyclic) analogues. The bacterial viability (*Mtb* strain H37Rv) was determined using the redox dye resazurin.

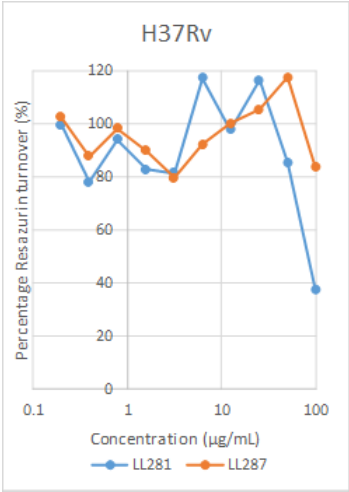

Figure 40 Biological testing results for esters **A-215** (LL281) and **A-216** (LL287).

The major hurdle in the synthesis of amicetin (**A-1**) was the glycosylation of either **A-53** or **A-60**. While **A-53** could be monoglycosylated with amicetose in good yields and excellent anomeric selectivity, the second glycosylation to establish the disaccharide unit consistently failed to provide isolable quantities of clean material. The same was true for attempts at the direct glycosylation of **A-53** with a preformed disaccharide unit. For some donor/acceptor systems, LC-MS of reaction mixtures indicated formation of the fully assembled amicetin skeleton and in one case NMR data could be obtained on a crude product that pointed to the correct configuration of the anomeric centres. Unfortunately, the compound was obtained only in very low yield and purity.

In general, the handling and set-up of the glycosylation reactions was extremely challenging. Small changes in reaction conditions drastically affected the outcome. Therefore, the careful adjustment of reaction parameters was necessary in each individual case. What is still not fully understood at this point, is the possible interference of the dimethylamino motif on the amosamine sugar with the

glycosylation reaction. While attempts to glycosylate **A-60** with glycosyl donors incorporating the dimethylamino group uniformly failed, glycosyl donor **A-148** (which does contain the dimethylamino group) was successfully used for the glycosylation of the methyl glycoside of amicetose. Thus, it seems unlikely that the dimethylamino moiety is the sole reason for glycosylation failure. Given the fact that attempts to glycosylate **A-60** with glucopyranose-derived trichloroacetimidates **A-160**, **A-161**, or **A-162** were unsuccessful, it appears that the glycosylation of **A-60** is generally not feasible under *Schmidt* conditions.

1.4.1 Future Potential

This thesis discloses major issues with protecting group strategies and glycosylation methods, which could be resolved for a successful future total synthesis of amicetin. The chemistry know-how accumulated during this project now allows fast access to advanced intermediates as a basis for the optimization and implementation of the final steps of a total synthesis.

I believe that the problems with the final glycosylation of **A-60** can be overcome by a comprehensive screening of donor systems by a person experienced in the handling of glycosylation reactions. The activation of glycosyl fluoride **A-129** is worth to be reassessed, including an expansion of the range of activation methods beyond those investigated in this thesis. Further, the examination of thioglycosides could be considered (which was only done as part of the disaccharide strategy). The synthesis of thioglycoside **A-128** is disclosed in section 1.3.5.6 and could be readily tested to react with **A-60** under suitable conditions.

Following the disaccharide pathway, it might well be worth to change from a *Vorbrüggen* protocol (silylation and activation by $SnCl_4$) to the glycosylation protocol developed by *Yu*, *i.e.* the activation of a glycosyl *o*-alkynylbenzoate with $Ph_3PAuNTf_2$ at the stage of a disaccharide (Scheme 64). A pivotal decision will be the timing of azide reduction and alkylation. While literature precedence[138] indicates that this transformation might have to be performed after the coupling to the cytosine moiety, performing this transformation before the glycosylation could still be an option that would make the synthesis more convergent.

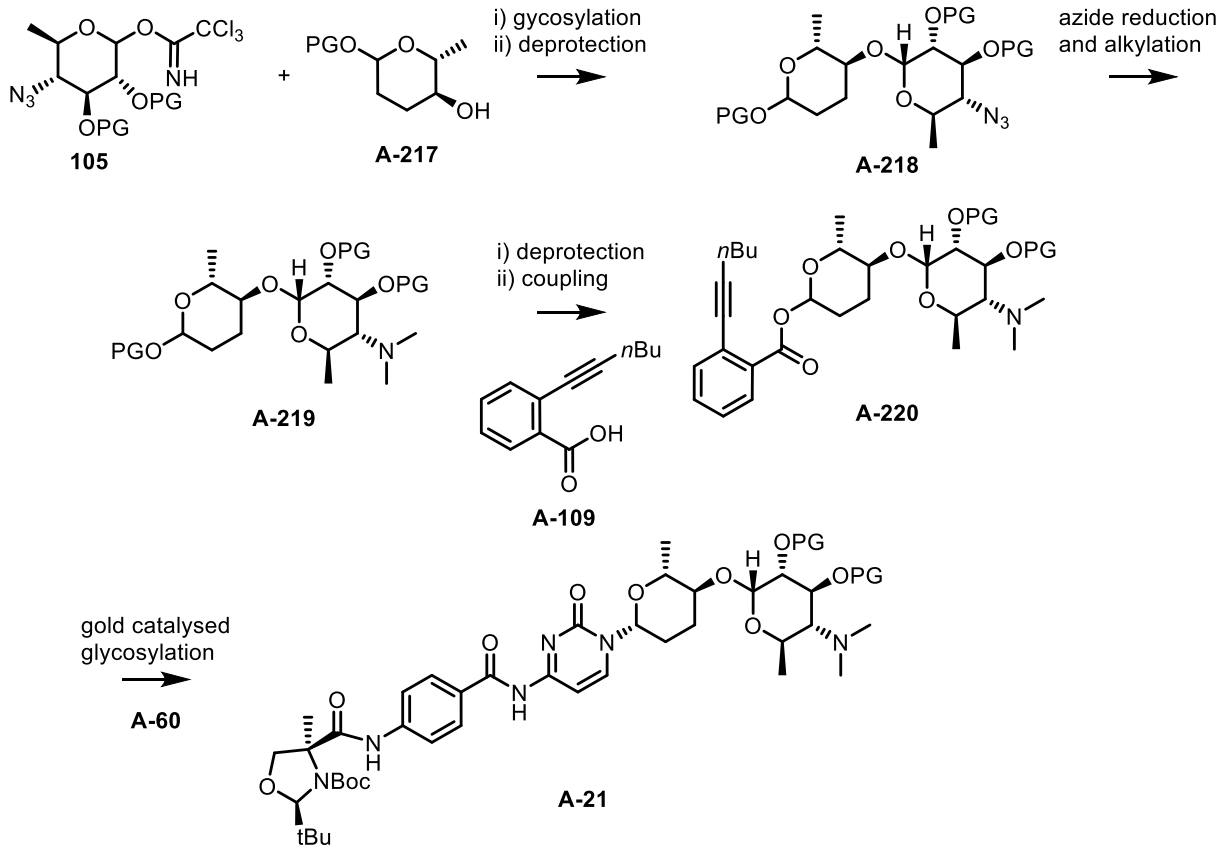

Scheme 64 Alternative route to amicetin via gold-catalysed activation of disaccharide **A-220**.

2 Studies Towards the Total Synthesis of Nummularine H (**N-1**)

2.1 Introduction

2.1.1 Cyclopeptide Alkaloids

Cyclopeptide alkaloids are a class of macrocyclic natural products featuring 13-, 14- or 15-membered ring systems. The macrocycle is comprised of a characteristic hydroxystyrylamine unit, α-amino acid and a β-hydroxy α-amino acid. The term "cyclopeptide" is derived from a characteristic structural feature of the compound class: the bridging of the phenol ring by a peptide-type chain, either at the 1,3-positions for 13-membered rings or at the 1,4-positions for 14-membered macrocycles. The term "alkaloids" refers to the nitrogenous and basic nature of the isolates.[232] Further diversification arises from one or two linearly appended units, which are often other amino acids. Figure 41 illustrates these general structural features for cyclopeptide alkaloids with a 13-membered core structure.

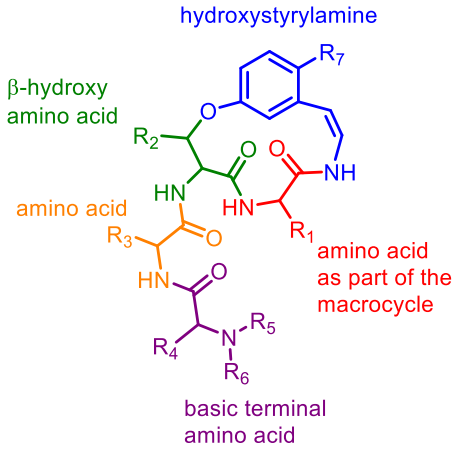

Figure 41 General structure of a 13-membered cyclopeptide alkaloid.

The basicity of the compounds arises from a characteristic primary amino group at the terminus of the side chain, in individual cases, this group can also be mono- or dimethylated.[232,233]

Cyclopeptide alkaloids can be categorized (Figure 42) according to the ring size and the number of incorporated building blocks (either 4 or 5). Due to their rare occurrence, the 15-membered macrocycles are not included in this general classification. In their abbreviated form these categories are referred to 4(13), 5(13), 4(14) or 5(14).[234] The name of each group is based on the first representative that was isolated for each category.[234] Due to the size of the group 4(14) alkaloids are subdivided further according to their β-hydroxy α-amino acid unit.

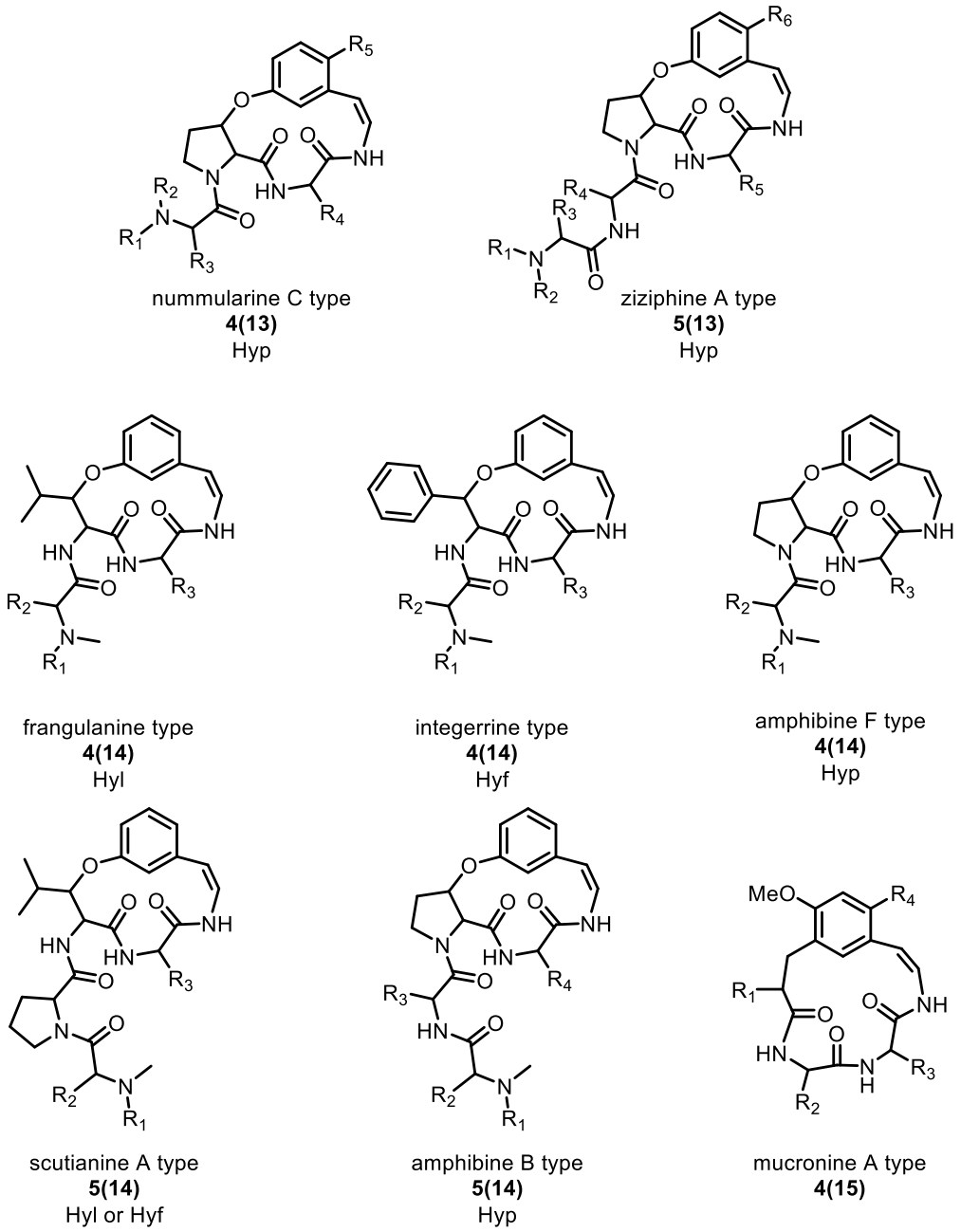

Figure 42 Common structure of cyclopeptide alkaloids. The β-hydroxy amino acid is indicated by its three letter code. Hyl: hydroxy Leu. Hyp: hydroxy Pro. Hyf. hydroxy Phe.

2.1.2 Isolation of Nummularine H (**N-1**) and Biological Activity

Cyclopeptide alkaloids have been extracted from various plant families such as *Acanthaceae*, *Malvaceae, Phyllanthaceae*, *Rubicaceae*, and most frequently, from *Rhamnaceae*.[233] Notably, the genus *Ziziphus* serves as a rich herbal source of the macrocyclic alkaloids.

Nummularine H (**N-1**) (Figure 43) was isolated in 1976 from *Ziziphus nummularia* along with two other peptide alkaloids as part of a comprehensive isolation campaign of members of the nummularine family.[235] The isolation was based on the extraction of the dried tree bark with a mixture of aqueous ammonia and methanol. After concentration of the primary extract followed by

several extraction and washing steps, nummularine H (**N-1**) was finally obtained from the crude alkaloid mixture as colourless needles after extensive column chromatography, with 4.3 kg of dried bark furnishing 110 mg of nummularine H (**N-1**).

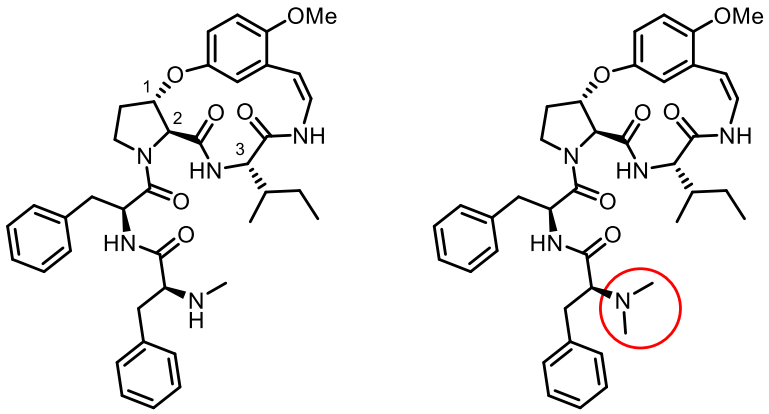

Figure 43 Structures of nummularine H (**N-1**) and the closely related jubanin A (**N-2**).

While the isolation group was able to establish the constitution of the compound as a desmethyl variant of the known jubanin A (**N-2**), the structure of nummularine H (**N-1**) was fully elucidated only 24 years later by the group of *Shoei-Sheng*.[236] Based on CD data and comparison with the previously synthesised zizyphine A,[237] the configuration of **N-1** could be assigned as 1*S*,2*S*,3*S*. This was further supported by the characteristic coupling pattern of H_1 (in $CDCl_3$; δ 4.39, d, *J* = 3.1) and H_2 (in $CDCl_3$; δ 5.40, ddd or dt, *J* = 3.1, 7.3) for a 3*S*-β-hydroxyproline.

Nummularine H (**N-1**) not only caught our attention by its interesting chemical architecture but also by its biological function. Studies have shown, that **N-1** exhibits antiplasmodial activity with an IC_{50} value of 4.2 µM against *P. falciparum* and further activity against *Mycobacterium tuberculosis* with a reported MIC value of 4.5 µM.[238]

2.1.3 Relevant Synthetic Work

As the first total syntheses of a cyclopeptide alkaloids, *Schmidt* described the synthesis of the 13-membered zizyphine A[237] and the 14-membered mucronine B[239] in 1983. A few years later the same group reported a first total synthesis of frangulanine,[240] another 14-membered cyclopeptide. Ever since, seminal contributions from various groups, notably those of *Rapoport*,[241] *Joullié*,[242] *Lipshutz*,[243] and *Evano*[244,245] have been made to the total synthesis of cyclopeptide alkaloids.

2.1.3.1 Schmidt's Total Synthesis of Zizyphine A

Schmidt's total synthesis of zizyphine A[237] (**N-7**) involved formation of the macrocycle by macrolactamization of an activated ω-amino acid ester (Scheme 65).

Hydrogenolytic removal of the Cbz-protecting group in **N-3** smoothly induced the intramolecular attack of the amino group on the pentafluorophenyl ester, leading to the formation of the desired macrocycle in 63% yield. The free alcohol of **N-4** was reacted with tributylphosphine and *p*-nitrophenyl selenocyanate to give selenide **N-5**. H_2O_2-mediated oxidation and subsequent β-elimination gave the *Z*-configured enamide **N-6** in excellent yield (65% over two steps).

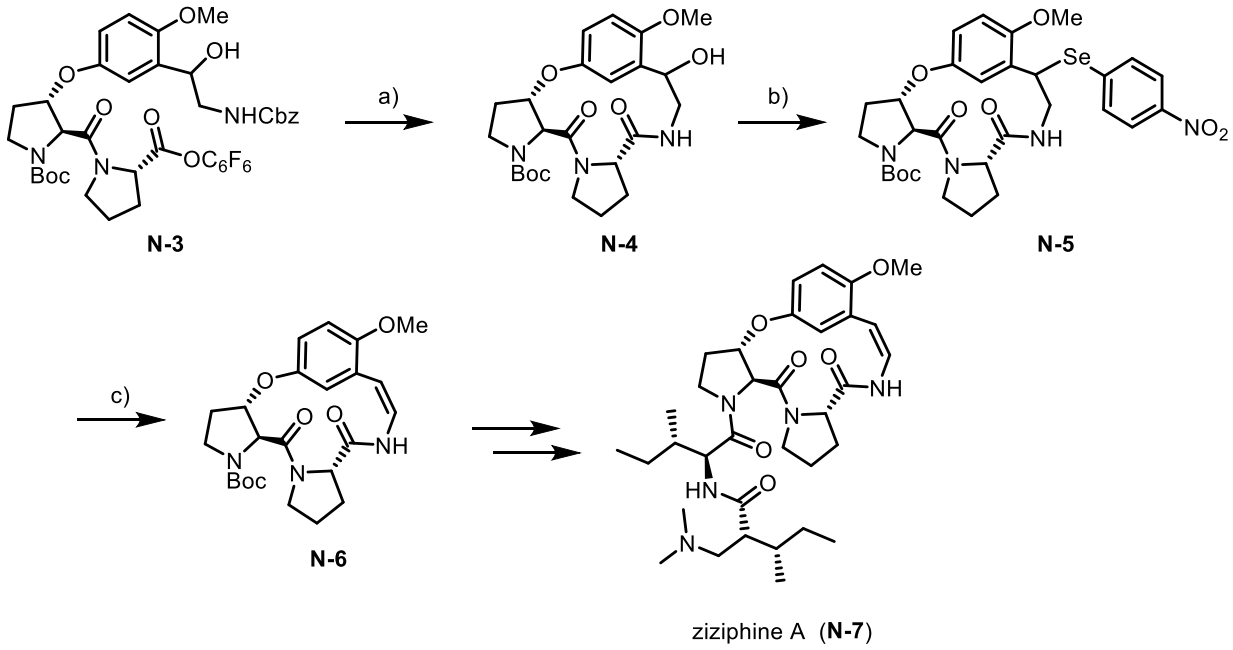

Scheme 65 *Schmidt*'s total synthesis of zizyphine A. Reagents and conditions: a) 4-pyrrolidinopyridine, Pd/C, H_2, dioxane, 4 h, 63%; b) $P(Bn)_3$, *p*-nitrophenyl selenocyanate, THF, 2 h, 72%; c) pyridine, H_2O_2, CH_2Cl_2, 1 h, 90%.

Boc-removal from the β-hydroxy proline moiety, DCC-mediated amide bond formation with Boc-L-isoleucine, followed by a second cycle of deprotection and amide bond formation with the pentafluorophenyl ester of *N,N*-(dimethyl)-L-isoleucine finally furnished zizyphine A (**N-7**).

2.1.3.2 *Ma*'s Total Synthesis of Ziziphine N

In 2007, *Ma* and co-workers reported the successful total synthesis of ziziphine N,[246] employing an intermolecular, Cu-catalysed cross coupling reaction to access the macrocyclization precursor **N-10** (Scheme 66).

Thus, vinyl iodide **N-8** was reacted with the protected proline amide **N-9** using copper iodide, *N*,*N*-dimethylglycine and Cs_2CO_3 in dry dioxane, which gave rise to the enamide **N-10** in 75% yield. The TBS-protected alcohol was treated with TBAF and the resulting free alcohol was subsequently oxidized to the acid employing a *Swern*/*Pinnick* sequence. The free amino acid **N-11** was obtained after Alloc deprotection with $(Ph_3P)_4Pd$ and diethylamine in a yield of 56% over two steps. The stage was set for the formation of the macrocycle, which was performed by the aid of pentafluorophenyl diphenylphosphinate[247] and *Hünig*'s base. The endgame to ziziphine N was comprised of a $ZnBr_2$-

promoted Boc-removal and subsequent coupling of dipeptide **N-12** using HATU in 22% yield over two steps.

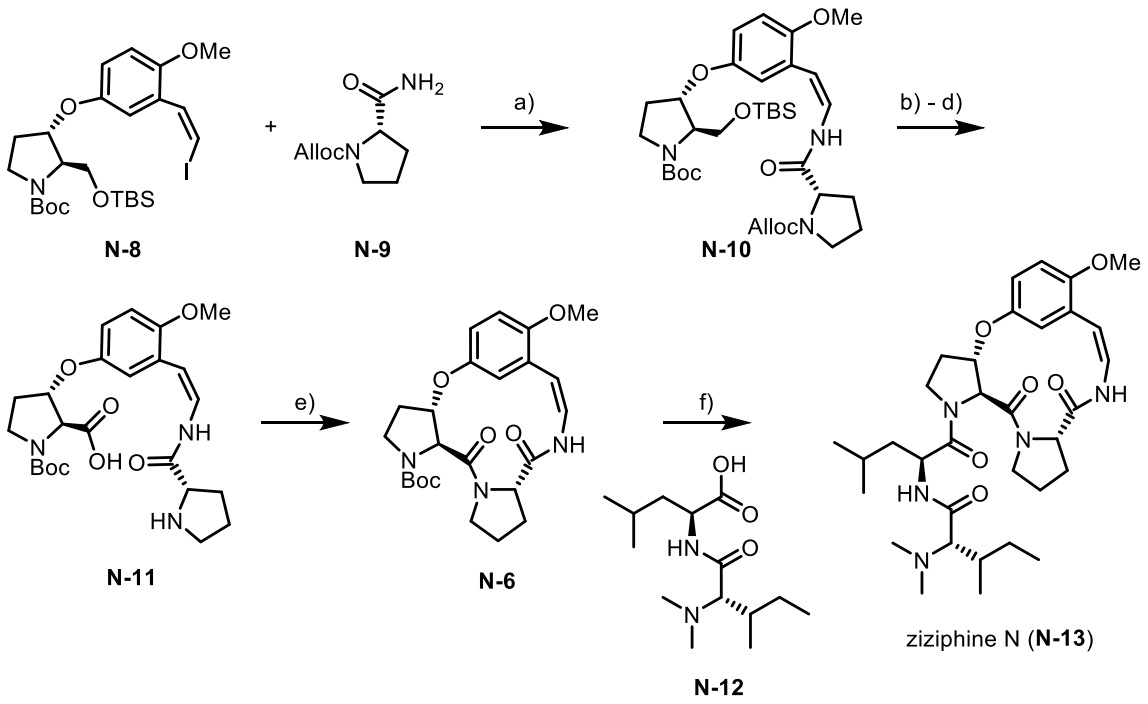

Scheme 66 *Ma*'s total synthesis of ziziphine N. Reagents and conditions: a) CuI, $Me_2NCH_2CO_2H$, Cs_2CO_3, dioxane, 80 °C, 75%; b) TBAF, THF, 95%; c) i) DMP, CH_2Cl_2, ii) $NaClO_2$, NaH_2PO_4, *t*BuOH, MeCN, 2-methyl-1-butene, 0 °C; d) $Pd(PPh_3)_4$, Et_2NH, CH_2Cl_2, 56%; e) FDPP, DIPEA, DMF, 66%; f) i) $ZnBr_2$, CH_2Cl_2, ii) HATU, K_2CO_3, 0 °C, 22%.

2.1.3.3 Evano's Unifying Synthesis of Paliurine E and F

The total syntheses of the cyclopeptide alkaloids paliurine E and F, ziziphine N and Q, abyssenine A, mucronine E and other variants were disclosed by *Evano* and co-workers.[248] A unifying route, involving an intramolecular amidation of a vinyl iodide as the macrocyclization step, allowed for the homologous synthesis of six different cyclopeptide alkaloids. This sub-section will only cover the synthesis of paliurine F (**N-21**) (Scheme 67).

The sequence started from the protected β-hydroxy proline **N-14** and iodobenze **N-15**, which were reacted under copper catalysis to give aryl ether **N-16**. The aldehyde was converted to the *Z*-vinyl iodide **N-18** using conditions reported by *Stork* and *Zhao*[249] in excellent yield and diastereoselectivity (97%, dr. >95:5). TBAF-mediated deprotection of the TBS group yielded the primary alcohol, which was converted to the acid via a *Swern*/*Pinnick* sequence and the isoleucinamide was coupled by an EDC/HOBt coupling-reaction to give **N-19** in 68% over 3 steps. The intramolecular amidation reaction closed the ring and gave **N-20** in good 70% yield. While conventional Boc-removal protocols failed, the use of TMS-triflate and 2,6-lutidine in dichloromethane allowed ready deprotection of the proline moiety.

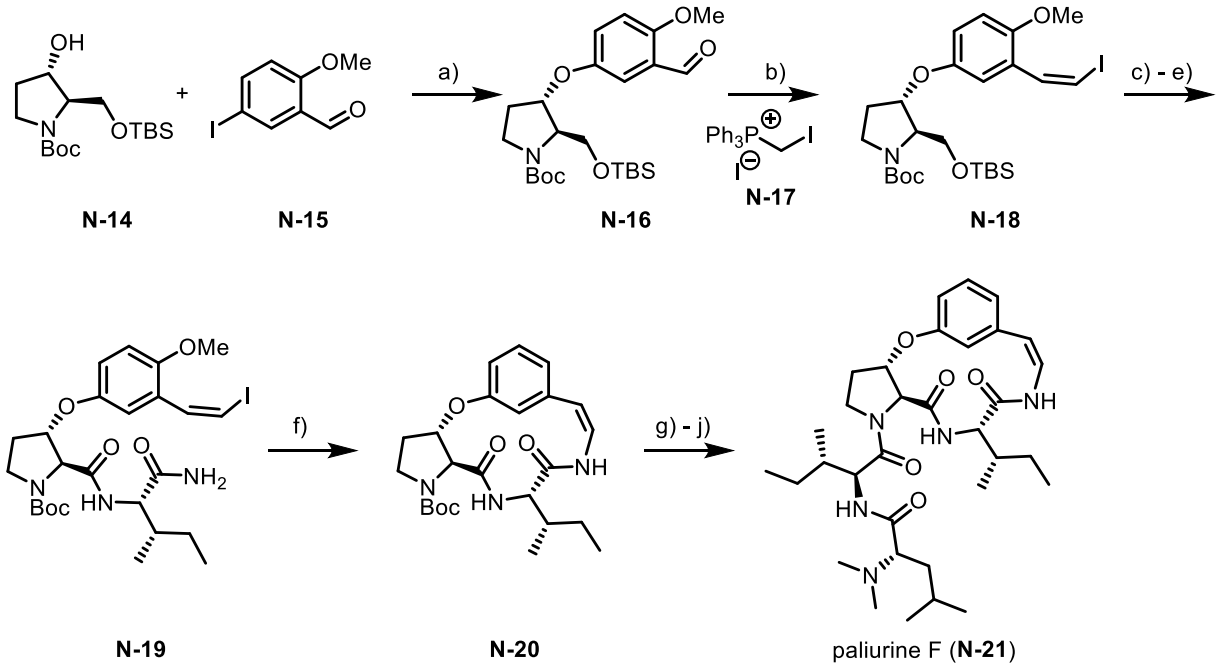

Scheme 67 Total synthesis of Paliurine F. Reagents and conditions: a) CuI (10%), 1,10-phen (20%), Cs_2CO_3, toluene, 125 °C; 75%; b) NaHMDS, THF/HMPA, -78 °C, 97%, dr. > 95:5; c) TBAF, THF, -10 – 25 °C; d) $(COCl)_2$, DMSO, Et_3N, CH_2Cl_2, -78 °C – 10 °C then NaH_2PO_4, 2-methylbut-2-ene, *t*BuOH/THF/H_2O, 68% over three steps; e) L-isoleucinamide·AcOH, EDC, HOBt, NMM, DMF, 75%; f) CuI (10%), DMEDA (20%), Cs_2CO_3, THF, 60 °C, 70%; g) TMSOTf, 2,6-lutidine, CH_2Cl_2, 0 °C, 80% h) *N*-Fmoc-L-isoleucine, HATU, HOAt, *i*Pr_2NEt, DMF; i) Et_2NH, MeCN, j) *N,N*-dimethyl-L-leucine, HATU, HOAt, *i*Pr_2NEt, DMF, 57% over three steps.

Interestingly, the attachment of the dipeptide side chain had to be performed stepwise. None of the following conditions HATU/K_2CO_3, HATU/*i*Pr_2NEt, DCC/HOBt/*i*Pr_2NEt or EDC/HOAt/*i*Pr_2NEt enabled successful attachment of the dipeptide directly. On the other hand, the sequential coupling of the individual amino acids, which was performed with HATU/HOAt, *i*Pr_2NEt, was successful and led to the desired paliurine F in 57% yield from **N-20**.

In the course of their work on the total synthesis of paliurine F, *Evano* and co-workers also examined the feasibility of four different macrocyclization approaches (Scheme 68).

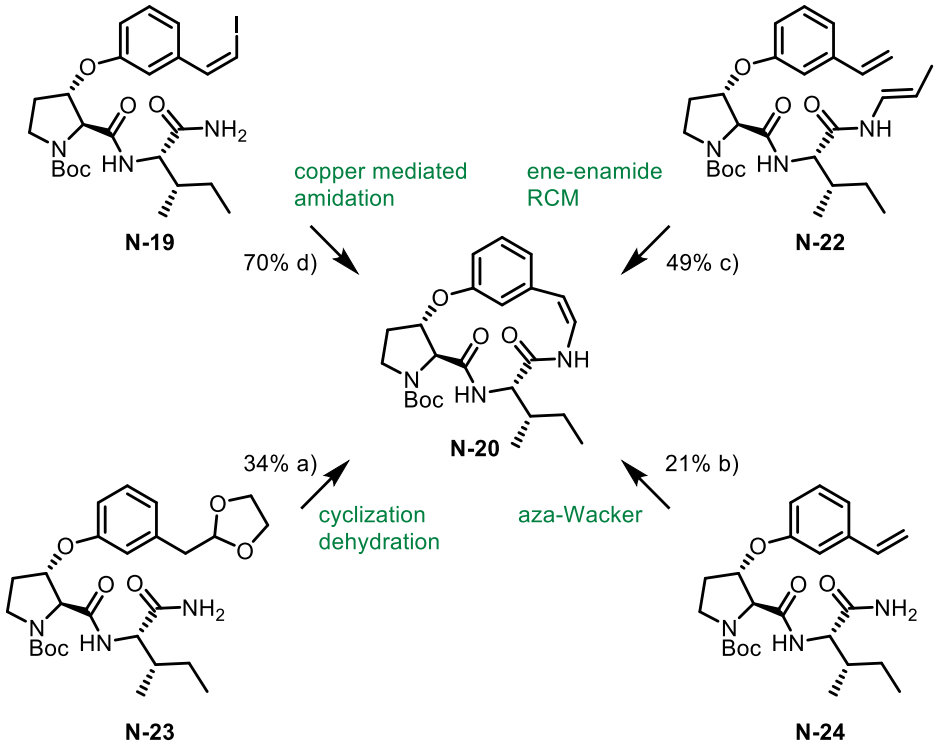

Scheme 68 Different macrocyclization attempts to access the paliurine F main core. Reagents and conditions: a) *p*TsOH, toluene, H_2O, 100 °C, 34%; b) $PdCl_2(CH_3CN)_2$, $CuCl_2$, O_2, DME, 60 °C, 21%; c) Grubbs second generation, 1,2-DCE, reflux, 49%; d) CuI, DMEDA, Cs_2CO_3, 60 °C, 70%.

For the cyclization/dehydration pathway various promoters, such as TsOH, HCl, oxalic acid or iodine were investigated for acetal deprotection/activation, which revealed that the cyclodehydration of **N-23** was best performed with 60 mol% *p*TsOH in a mixture of toluene and water to give **N-20** in 34% yield. The intramolecular aza-*Wacker* reaction was best performed with bis(acetonitrile)dichloropalladium and copper chloride to close the ring in 21% yield. The ene-enamide RCM reaction had been thoroughly analysed by *Evano* in previous studies.[250] The enamide substitution pattern as well as the reaction conditions were extensively optimised to finally achieve a moderately successful cyclization of **N-22**, using *Grubbs* second-generation catalyst in 1,2-dichloroethane. Overall, the best results for the macrocyclization were obtained with the copper-mediated amidation reaction, which was thus employed for the synthesis of the six cyclopeptide alkaloids.

2.2 Aims and Scope

The primary goal of this project was the development of a total synthesis of nummularine H (**N-1**) using a new macrocyclization approach that would involve the formation of the ether bond as the cyclization step. No such approach has yet been described to access the macrocyclic core structure. Additionally, we wanted to showcase a new approach to access the enamide functionality.

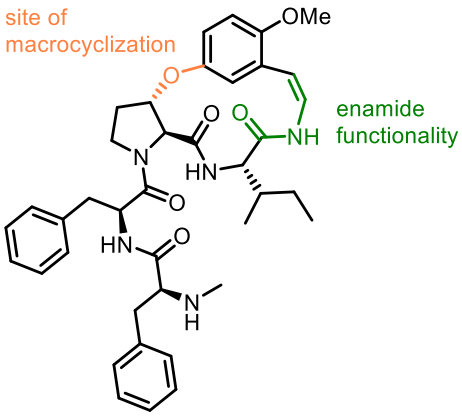

nummularine H (**N-1**)

In subsequent steps, biological testing and verification of the antimycobacterial activity of **N-1** was planned to be done and the chemistry developed was to be exploited for the synthesis of structural analogues of nummularine H (**N-1**) for structure-activity relationship (SAR) studies.

2.3 Results and Discussion

2.3.1 Ynamide Approach

2.3.1.1 Retrosynthetic Considerations

Our first generation retrosynthesis of nummularine H (**N-1**) is shown in Scheme 69. Target structure **N-1** was planned to be accessed via late stage amide bond formation between the proline moiety and the side chain. The two amino acids were envisioned to be attached sequentially or, preferably, as a pre-assembled dipeptide fragment.

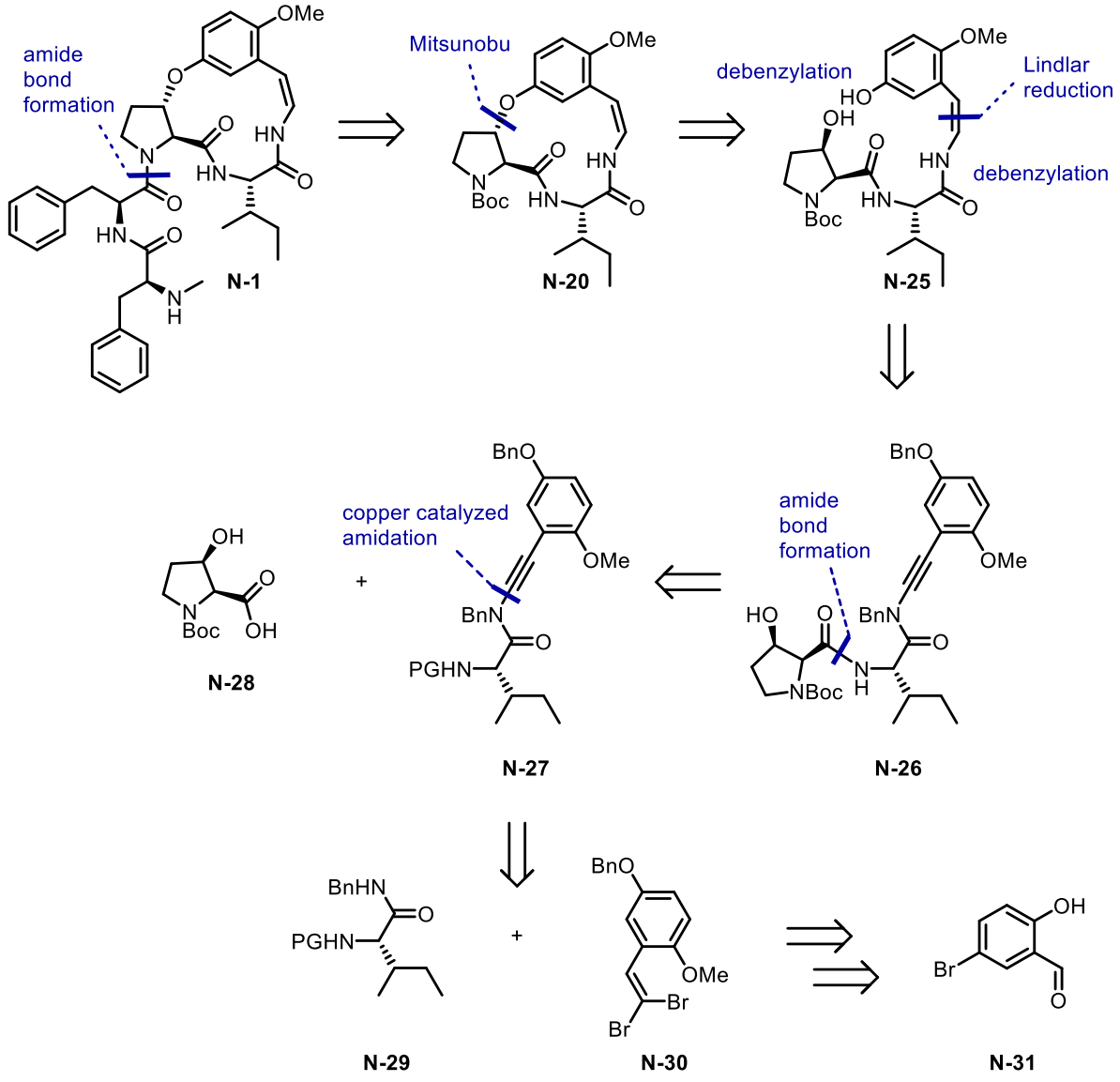

Scheme 69 Retrosynthesis of nummularine H.

The core macrocycle **N-20** was envisioned to be accessed by a *Mitsunobu* reaction between the phenolic hydroxy group and the activated hydroxy group of the β-hydroxyproline unit with inversion of stereochemistry. Linear precursor **N-25** represents a retron, which was to be accessed from **N-26** via a *Z*-selective *Lindlar* reduction and concomitant benzyl removal from the phenolic hydroxy group

and the protected amide nitrogen. Ynamide **N-26** should be accessible via coupling of **N-27** with the protected β-hydroxyproline derivative **N-28**. The pivotal copper-catalysed amidation reaction between **N-29** and dibromoalkene **N-30**, was envisioned to lead to **N-27**. The dibromoalkene **N-30** was planned to be obtained from **N-31** via a sequence of phenol formation, protection of the phenolic hydroxy group and *Corey-Fuchs* homologation.

*2.3.1.2 Synthesis of **N-30** and **N-34***

Inspired by recent work by *Buchwald* and co-workers[251] on the selective reaction of aryl halides with KOH to form phenols, we started our efforts with the conversion of bromobenzaldehyde **N-31** into phenol **N-32** (Scheme 70). Using the monodentate $Me_4tBuXphos$ ligand, $Pd_2(dba)_3$ and KOH in a mixture of dioxane and H_2O, the desired **N-32** was eventually obtained in 40% yield. Alkali hydroxides (KOH, NaOH) were found to be essential as the source of the nucleophiles. When other inorganic bases such as Cs_2CO_3 or K_2CO_3 where used, none of the desired phenol was observed, instead exclusive formation of the symmetrical diaryl compounds occurred. Despite significant efforts, the yield of the reaction could not be increased above 40%, measures such as degassing the solvent and/or varying the reaction temperature and the reaction time were all ineffective. The problem was additionally exacerbated by an impurity that had to be tediously removed by FC and that was observed in all the experiments.

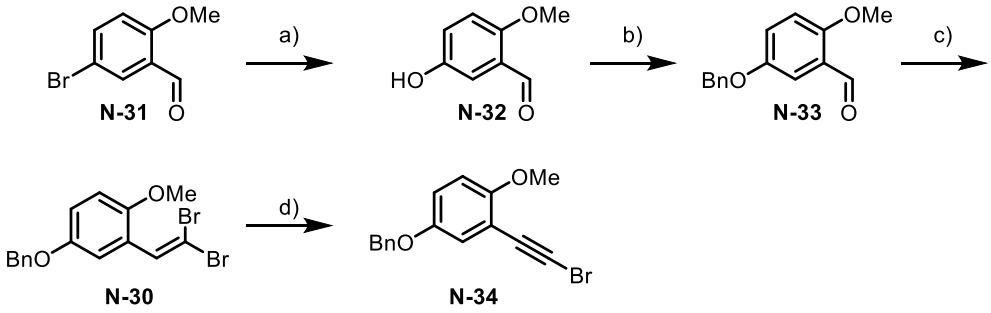

Scheme 70 Reagents and conditions: a) KOH, $Pd_2(dba)_3$, $Me_4tBuXphos$, H_2O:dioxane (1:1), 80 °C, 18 h, 40%; b) NaOMe, MeOH, 23 °C, 1 h then BnBr, DMF, 23 °C, 3 h, 78 % over two steps; c) CBr_4, PPh_3, CH_2Cl_2, 0 - 23 °C, 1.5 h, 74%; d) Cs_2CO_3, DMA, 50 °C, 16 h, 44%.

The transformation of **N-32** into its benzyl ether **N-33** followed a reported procedure.[252] In a first step, the sodium phenolate was formed and isolated as a crude, which was then dissolved in DMF and treated with benzyl bromide to give **N-33** in good 78% yield. Performing a *Corey-Fuchs* homologation gave the dibromoalkene **N-30**. Optionally, compound **N-30** could be further transformed into the terminal bromoethyne **N-34** by treatment it with Cs_2CO_3 in DMA.

Initial difficulties to form **N-32** from aryl halide **N-31** had also urged us to investigate an alternative strategy to access **N-33**. Therefore, we attempted to directly introduce the benzyloxy group in **N-35** by means of copper or transition metal catalysis (Scheme 71).

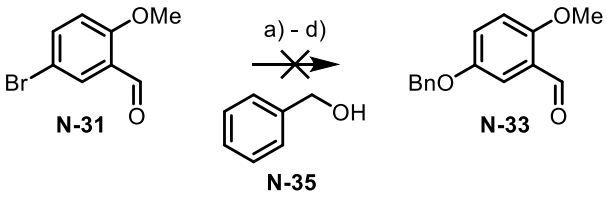

Scheme 71 Reagents and conditions: a) CuI, 1,10-phen, Cs_2CO_3, toluene, 125 °C; b) CuI, 1,10-phen, Cs_2CO_3, dioxane, 125 °C c) Cs_2CO_3, $Pd(OAc)_2$, Me_4*t*BuXPhos, dioxane, 70 °C; d) Cs_2CO_3, $Pd(OAc)_2$, Me_4*t*BuXPhos, toluene, 70 °C.

Coupling experiments between **N-31** and **N-35** were performed with copper iodide, phenanthroline, cesium carbonate and either toluene or dioxane as solvent in microwave tubes under pressure. However, not even traces of the desired product could be detected. Further experiments were based on palladium catalysis using $Pd(OAc)_2$, Cs_2CO_3, and Me_4*t*BuXPhos in either dioxane or toluene at 70 °C. The reactions were followed by means of TLC-, LC-MS- and NMR-analysis, but unfortunately no product formation was observed. Clearly, we did not exhaust the plethora of existing coupling conditions, however, we decided not to perform extensive screening efforts for this initial reaction step and concluded to use the previously described approach (as shown in Scheme 70).

*2.3.1.3 Copper-Catalysed Amidation of **N-30** and **N-34***

Having intermediates **N-30** and **N-34** in hand, we turned our attention towards the synthesis of the ynamide moiety. The increasing interest that these functionalities gained in recent years, triggered the advent of novel synthetic strategies. There are mainly two approaches that shall be highlighted at this point:

In 2006, *Hsung* and co-workers disclosed a copper(II)-catalysed amidation of simple alkynyl bromides to access ynamides and *Z*-enamides after selective reduction.[253] They found that a catalyst system composed of $CuSO_4 \cdot 5H_2O$, 1,10-phen and K_3PO_4 in toluene at elevated temperatures was active on a variety of substrates. It is worth mentioning though that their protocol was effective for the use of sulfonamides or oxazolidinones, whereas only a limited number of very simple amide structures were successfully used.

A second protocol was disclosed by *Evano* in 2009, which involves a copper mediated coupling of 1,1-dibromo-1-alkenes with different nitrogen nucleophiles.[254] They effectively used CuI, DMEDA and Cs_2CO_3 in dioxane to yield various ynamides. Strikingly, while variations in the dibromoalkene system seem to be well tolerated, the amide partner was limited to sulfonamides or oxazolidinones.

Inspired by the above reports, we embarked on the coupling of **N-30** and **N-34** and tested both conditions on a variety of amine and amide substrates (Scheme 72). It soon became clear that a direct coupling of *L*-isoleucine amide was not feasible under the conditions screened. Neither substrate **N-42** nor the benzyl-protected variant **N-43** gave any conversion. We further examined the

coupling of benzylamine (**N-44**), dibenzylamine (**N-45**) and sulfonamide **N-46** under copper catalysis no conversion of starting material was observed.

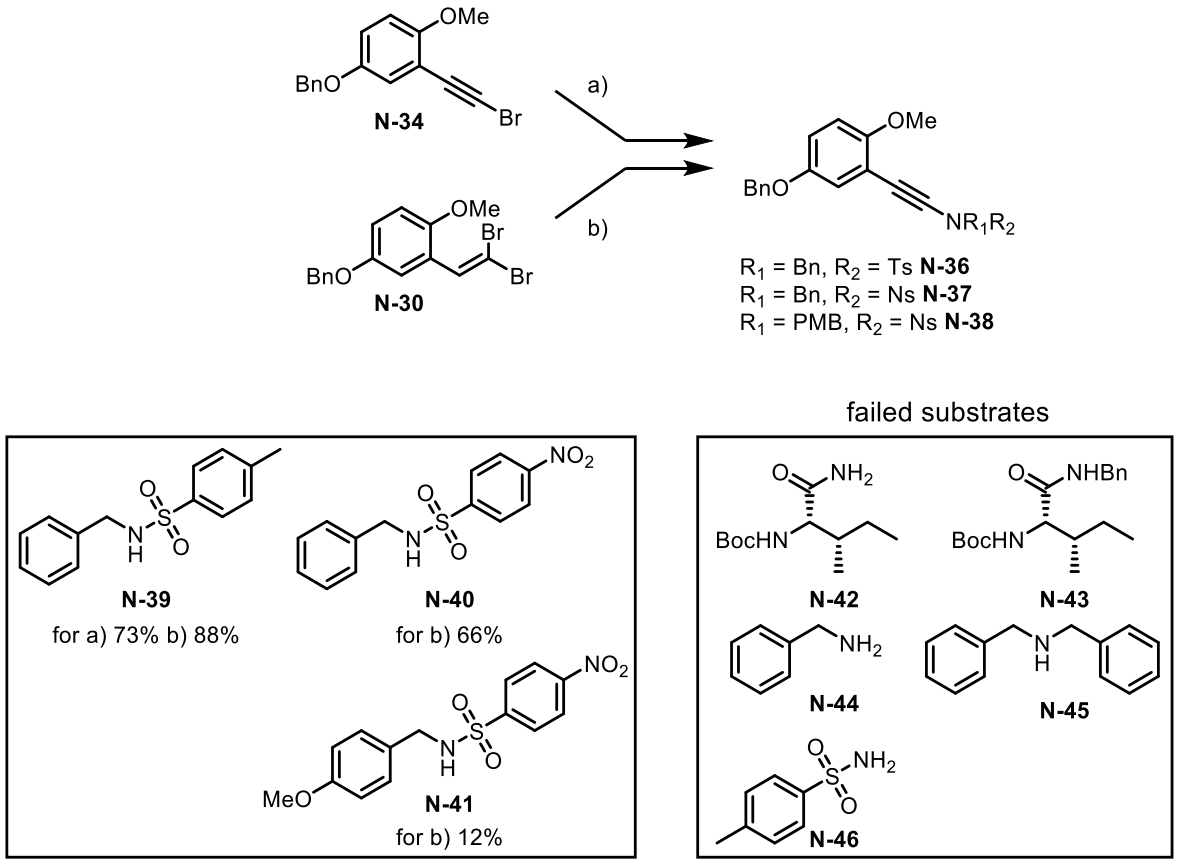

Scheme 72 Reagents and conditions: a) CuI, DMEDA, Cs_2CO_3, THF, 60 °C; b) $CuSO_4 \cdot 5H_2O$, 1,10-phen, K_3PO_4, toluene, 75 °C.

In contrast, sulfonamides **N-39**, **N-40,** and **N-41** readily reacted under the described conditions to give ynamides **N-36** – **N-38**. These findings confirmed the rather narrow substrate scope, which had been reported by *Hsung* and *Evano* for their investigations in which mainly tosylated amines were used as substrates. The following plausible mechanism for the formation of ynamides from 1,1-dibromo-1-alkenes was proposed (Scheme 73).[254]

The oxidative insertion of the copper-nitrogen complex **N-49** takes place at the more reactive *trans* C-Br bond, as shown by *Zapata* and *Ruiz.*[255] Finally, reductive elimination yields the *Z*-configured product **N-51**, which after treatment with Cs_2CO_3 gives the desired ynamide **N-52**.

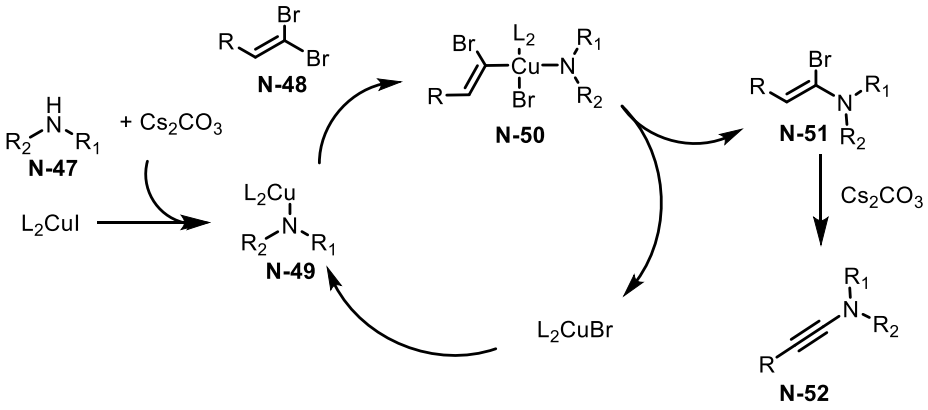

Scheme 73 Plausible reaction mechanism for the copper-mediated formation of ynamides from dibromo alkenes.

2.3.1.4 Deprotection Attempts of Sulfonamide Derivatives

Given the fact that a direct coupling of the *L*-isoleucine amides **N-42** and **N-43** to either substrate **N-30** or **N-34** was not feasible, we pursued the further elaboration with ynamides **N-36** – **N-38**. Thus, we embarked on the tosyl deprotection of **N-36** (Scheme 74) to give ynamine **N-53**, which was envisioned to be coupled to *L*-isoleucine.

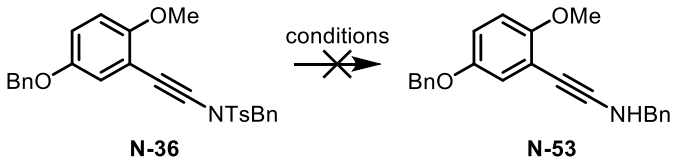

Scheme 74 Attempted tosyl removal from ynamide **N-36**.

As shown in Table 15, a series of conditions to remove the tosyl protecting group were investigated, but these efforts remained unsuccessful. Substrate **N-36** either showed very low reactivity or was prone to decomposition under harsh conditions. The use of RedAl at ambient or elevated reaction temperatures led to cleavage of the amide moiety to give the terminal alkyne (entry **5**, **6**). Both, magnesium- and samarium iodide-mediated deprotection attempts did not affect the starting material (entry **1** - **4**). Aqueous HBr either brominated the alkyne or gave a complex reaction mixture at higher temperatures (entry **7**, **8**). Finally, an attempt to remove the tosyl group with sodium naphthalene anion radicals at -78 °C (entry **9** - **11**) was also unsuccessful.

Table 15 Screening of tosyl removal conditions for **N-36**.

Entry	Conditions	Temp. [°C]	Equiv[a]	Time [h]	Observation[b]
1	Mg, MeOH:THF	23	10	> 72	no conversion
2	Mg, MeOH:THF	45	20	16	no conversion
3	SmI_2, pyrrolidine, H_2O, THF	23	10	> 72	no conversion
4	SmI_2, pyrrolidine, H_2O, THF	45	10	16	no conversion
5	RedAl, toluene	120	20	16	terminal alkyne detected, SM fully consumed
6	RedAl, toluene	23	20	1	terminal alkyne detected, SM fully consumed
7	HBr (aq.)	80	80	2	bromination of alkyne
8	HBr (aq.), phenol	80	80	1	complex reaction mixture
9	Na/naphthalene	-78	2	0.1	recovered SM
10	Na/naphthalene	-78	20	0.1	recovered SM
11	Na/naphthalene	-78	excess	0.1	decomposition

[a] The given equivalents refer to the actual active reagent. [b] Observations are based on findings made by TLC and TLC-MS analysis. Alkyne from entry **6** or **7** was isolated and analysed by obtained spectral data. SM: starting material.

Being unable to remove the tosyl group from **N-36**, conditions were screened for PMB-removal from **N-38** (Scheme 75).

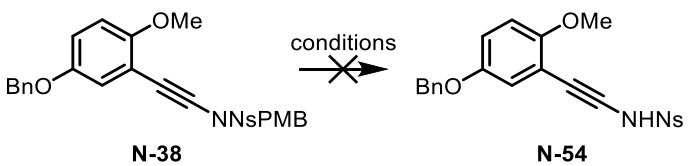

N-38 **N-54**

Scheme 75 PMB-ether cleavage attempts on ynamide motif **N-38**.

As shown in Table 16, standard oxidizing conditions such as DDQ or CAN gave complex reaction mixtures. Likewise, treating **N-38** gave none of the desired secondary sulfonamide **N-54**.

Table 16 Screening of PMB removal conditions for **N-38**.

Entry	Conditions	Temp. [°C]	Equiv	Time [h]	Observation[a]
1	DDQ	23	3	6	complex mixture
2	CAN	23	2.6	4	complex mixture
3	CAN	0	2.6	6	complex mixture
4	TFA	0	0.6	5	no conversion
5	TFA	0 - 23	0.6	4	complex mixture

[a] Observations are based on findings made by TLC and TLC-MS analysis.

As an alternative to PMB-removal, the cleavage of the nosyl protecting group in **N-38** was also investigated, which would have delivered the secondary amine **N-55** (Scheme 76).

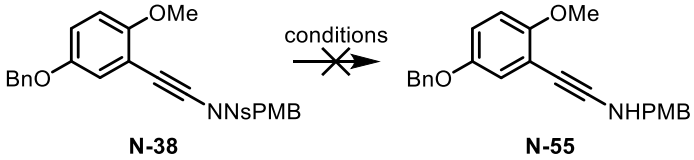

N-38 **N-55**

Scheme 76 Nosyl group removal attempts on ynamide motif **N-38**.

However, treatment of **N-38** with thiophenol/*p*-methoxythiophenol in the presence of K_2CO_3 gave none of the desired product (Table 17).[256]

Table 17 Screening of nosyl removal conditions for **N-38**.

Entry	Conditions	Temp. [°C]	Equiv[a]	Time [h]	Observation[b]
1	K_2CO_3, TolSH	23	6	5	no conversion of SM
2	K_2CO_3, TolSH	60	6	8	complex mixture
3	K_2CO_3, *p*-methoxythiophenol	23	6	16	complex mixture

[a] Equivalents of K_2CO_3. [b] Based on TLC and TLC-MS analysis. SM: starting material.

In light of the failed attempts to generate a secondary propargylic amine from a sulfonamide protected precursor, *N*-benzyl sulfonamide **N-36** was selectively reduced to enamide **N-56** using *Lindlar*'s catalyst (Scheme 77) and the latter was subjected to various debenzylation conditions (Table 18).

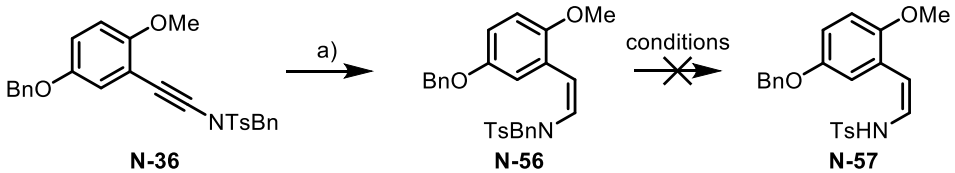

N-36 **N-56** **N-57**

Scheme 77 Attempted benzyl ether cleavage from enamide **N-56**. Reagents and conditions: a) *Lindlar*, H_2, EtOAc, 70%.

As shown in Table 18, an excess of DDQ (entry **1**) as well as *Birch* conditions (entry **6**) led to a complex mixture of various products that did not include the desired **N-57**. More defined results were obtained with BBr_3 at low temperatures. Two products were formed in the reaction, which, however could not be characterised. We were not able to modify the reaction conditions such that the desired product could be obtained (entry **2** - **5**). Transfer hydrogenation was ineffective (entry **7**) and after addition of a catalytic amount of acid (entry **8**), we isolated the compound with the reduced olefin and debenzylation of the phenolic hydroxy group. The same results were obtained for acidified *Lindlar* catalyst under hydrogen atmosphere. We further examined a recently published protocol[257] using a combination of palladium acetate and sodium hydride, which left the starting material unaffected (entry **10**, **11**).

Table 18 Screening of benzyl removal conditions for **N-56**.

Entry	Conditions	Temp. [°C]	Equiv	Time [h]	Observation[a]
1	DDQ, CH_2Cl_2	23	10	18	complex mixture
2	BBr_3 (1 M in CH_2Cl_2)	0	7	< 1	full decomposition
3	BBr_3 (1 M in CH_2Cl_2)	-78	3	< 1	complex mixture
4	BBr_3 (1 M in CH_2Cl_2)	-78	7	< 1	complex mixture
5	BBr_3 (1 M in CH_2Cl_2)	-95	7	< 1	complex mixture
6	Na, NH_3	-78	2	< 1	complex mixture
7	Pd/C, cyclohexane	23	10 mol %	5	no reaction
8	Pd/C, cyclohexane, formic acid	23	10 mol %	18	monodebenzylation, olefin reduction[b]
9	*Lindlar* cat., HCl, H_2[c]	23	10 mol %	18	monodebenzylation, olefin reduction[b]
10	$Pd(OAc)_2$, NaH	23	0.05 / 1.5	6	no reaction
11	$Pd(OAc)_2$, NaH	60	0.05 / 1.5	12	no reaction

[a] Based on TLC and TLC-MS analysis. [b] Confirmed by crude proton NMR spectrum. [c] Balloon pressure.

In light of the above deprotection issues, we decided to direct our attention to a different strategy, accessing the enamide moiety present in nummularine H (**N-1**) by other means (*vide infra*).

2.3.2 Late Stage Dehydration Approach

Since our intention to access the enamide functionality via a copper catalysed amidation reaction failed, we revised our overall plan and elaborated a new strategy to synthesise nummularine H (**N-1**).

2.3.2.1 Retrosynthetic Considerations

The revised retrosynthesis of **N-1** is outlined in Scheme 78. As for the first generation strategy, the attachment of the dipeptide side chain was to be performed at the very end of the synthesis. The enamide moiety was planned to be installed by dehydration of a secondary alcohol or via selenide formation and subsequent elimination. Macrocycle **N-58** was still to be formed by an intramolecular *Mitsunobu* reaction of the linear precursor **N-59**. The latter was to be obtained by an amide bond formation between **N-60** and hydroxyproline **N-28**. Finally, the coupling between protected isoleucine **N-62** and the primary amine **N-61** was envisioned to furnish intermediate **N-60**.

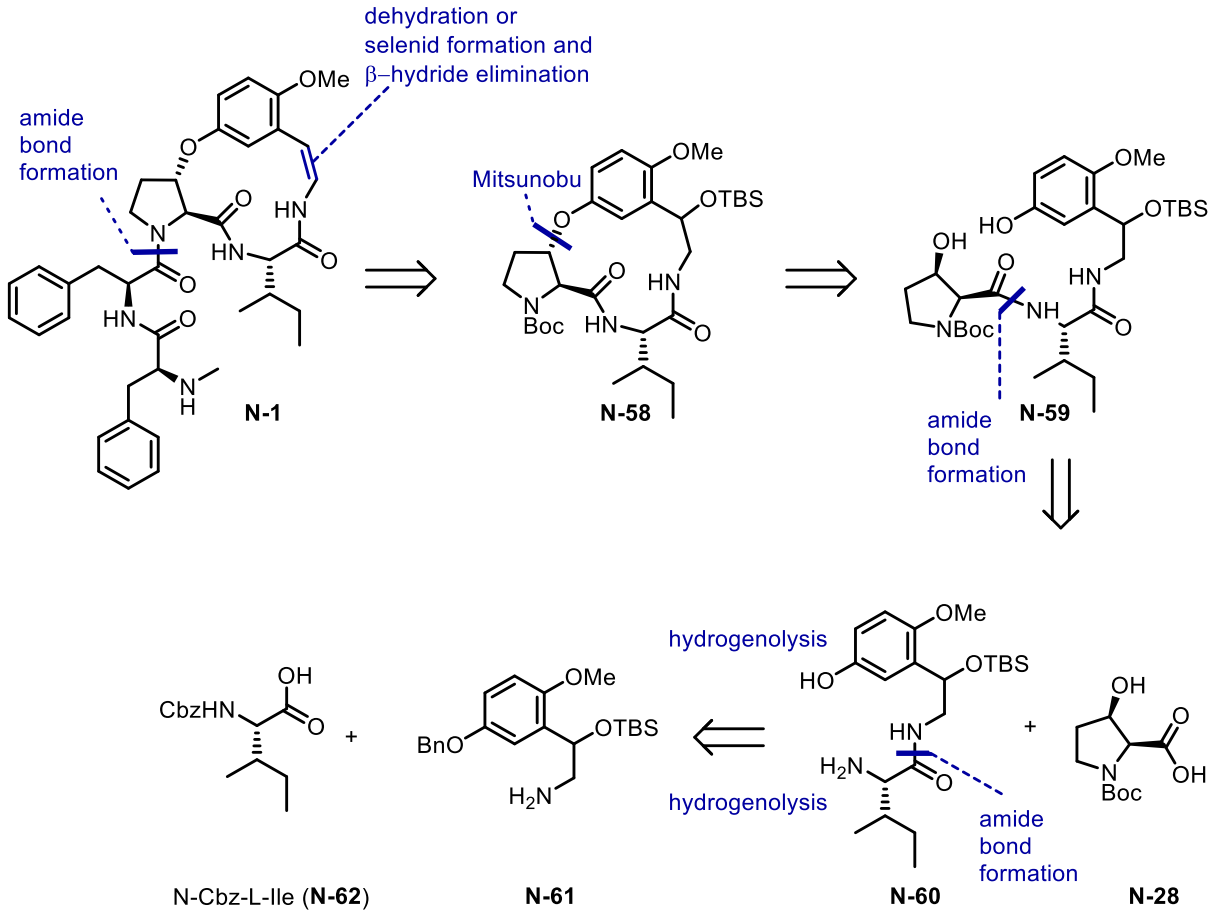

Scheme 78 Second generation retrosynthesis of **N-1**.

Intermediate **N-61** was believed to be accessible through a *Henry* reaction and subsequent nitro reduction departing from aldehyde **N-33 (**Scheme 79). Evidently, the generation of a racemic mixture would be inconsequential due to the loss of stereoinformation at a later stage.

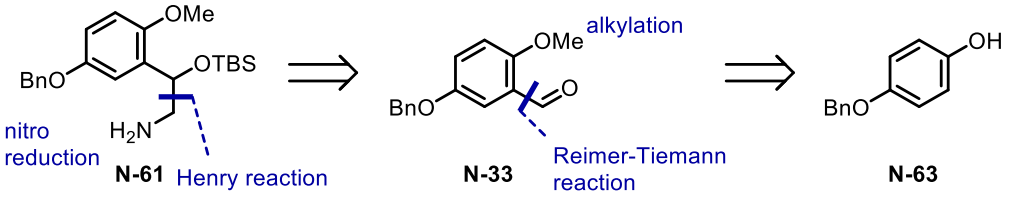

Scheme 79 Retrosynthesis of β-aminoalcohol **N-61**.

*2.3.2.2 Synthesis of Linear Precursor **N-59***

As shown in Scheme 80, the synthesis of **N-61** departed from monoprotected hydroquinone **N-64** which underwent a *Reimer-Tiemann* reaction[258] to provide aromatic aldehyde **N-65**. Unfortunately, conversion of **N-64** was incomplete and starting material was recovered in significant amounts. Efforts to optimize the reaction (longer reaction times, larger amounts of chloroform/H_2O or dropwise addition of alkaline chloroform mixture) were ineffective. The sequence was continued with the alkylation of the free hydroxy group to give **N-33** in almost quantitative yield. The aldehyde in **N-33** was successfully transformed into a β-nitro alcohol by dropwise addition of a mixture of nitromethane and sodium methoxide. After an aqueous workup, the intermediate free alcohol was directly TBS-protected to give the desired product **N-66** in 59% yield over two steps. Catalytic hydrogenation using *Lindlar*'s catalyst to reduce the nitro moiety in **N-66** resulted in the formation of a complex product mixture. In contrast, the use of palladium on charcoal combined with ammonium formate,[259] left the starting material completely unaffected. Not surprisingly, the combination of palladium on charcoal and hydrogen led to the removal of the benzylether moiety concomitant with nitro reduction. The aliphatic nitro group could eventually be reduced selectively with sodium borohydride in the presence of a nickel salt, as first reported by *Brown,*[260] to give the free amine **N-61** in 74% yield. The catalyst system forms a colloidal black suspension, which has been described to have comparable catalytic activity as *Raney* nickel and readily reduces aliphatic nitro compounds.[261]

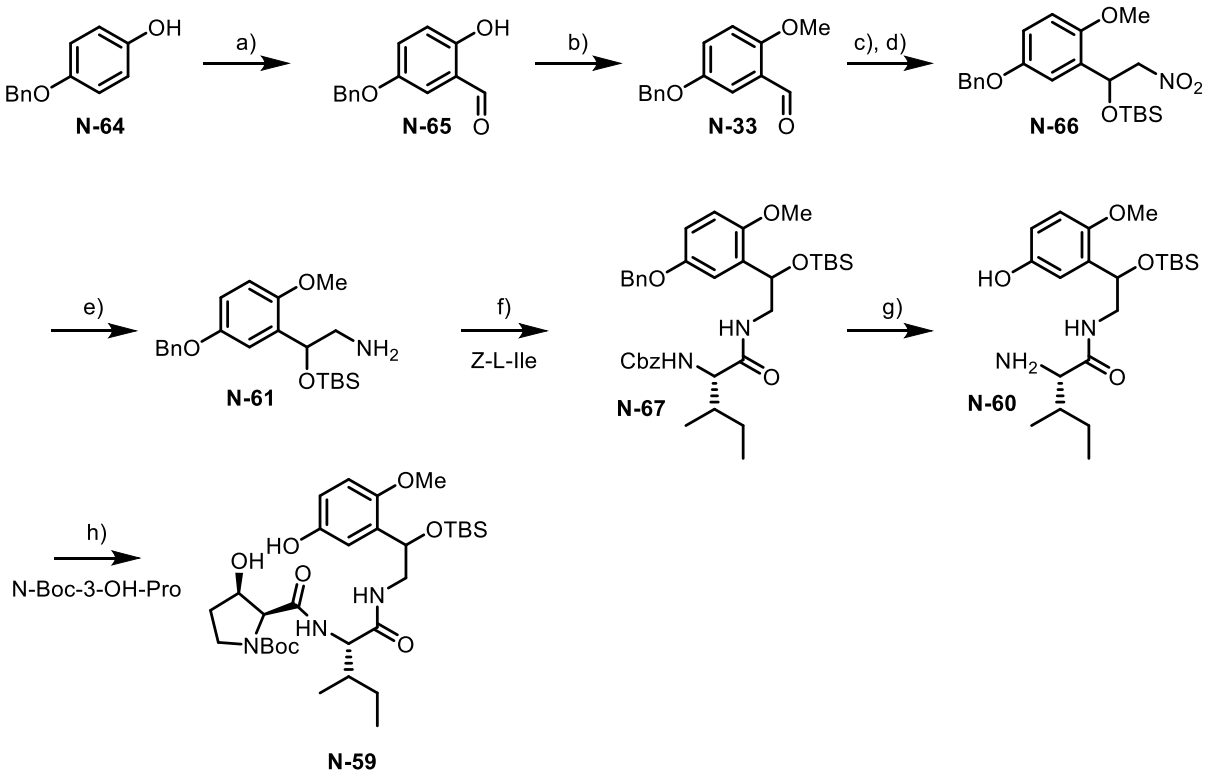

Scheme 80 Reagents and conditions: a) NaOH, $CHCl_3$, H_2O, 70 °C, 4 h, 21% and 49% back recovered SM; b) MeI, K_2CO_3, DMF, 23 °C, 16 h, 98%; c) NaOMe (25 wt%), $MeNO_2$, MeOH, 23 °C, 16 h; d) TBSCl, imidazole, DMF, 23 °C, 16 h; 59% over two steps; e) $NiCl_2 \cdot 6H_2O$, $NaBH_4$, MeOH, THF, 0 °C, 50 min, 74%; f) DCC, HOBt, NMM, CH_2Cl_2, 0 – 23 °C, 16 h, 90%; g) Pd/C, H_2, EtOH, 23 °C, 2 h, 77%; h) EDC, HOBt, DMAP, CH_2Cl_2, 23 °C, 16 h, 87%.

With the primary amine **N-61** in hand, we turned our attention towards the elongation of the peptide bridge. Coupling of **N-61** with Cbz-protected *L*-isoleucine proceeded smoothly employing a DCC/HOBt protocol in dichloromethane to furnish intermediate **N-67** in excellent 90% yield. Simultaneous benzyl ether- and Cbz-removal was accomplished by catalytic hydrogenation over palladium on charcoal to give the desired product **N-60** within 2 h in 77% yield. Coupling of the β-hydroxy proline was first examined under the same DCC/HOBt conditions that had provided **N-67** in high yield, but only traces of the desired product were formed. The use of HCTU and NMM, surprisingly, only led to the formation of desilylated starting material. Desilylation may have been caused by the hexafluorophospate counter ion present in the HCTU coupling reagent. Finally, the desired linear precursor **N-59** could be successfully prepared in excellent yield (87%) by using a combination of EDC/HOBt and catalytic DMAP.

With diol **N-59** in hand, the stage was set for the crucial macrocyclization under *Mitsunobu* conditions. Under standard *Mitsunobu* conditions (Scheme 81), **N-59** was completely consumed within 15 min to give another product with the desired mass (according to TLC- and LC-MS). However, upon isolation and spectroscopic characterization, this material was established to be the elimination product **N-68** rather than the desired macrocycle **N-58**.

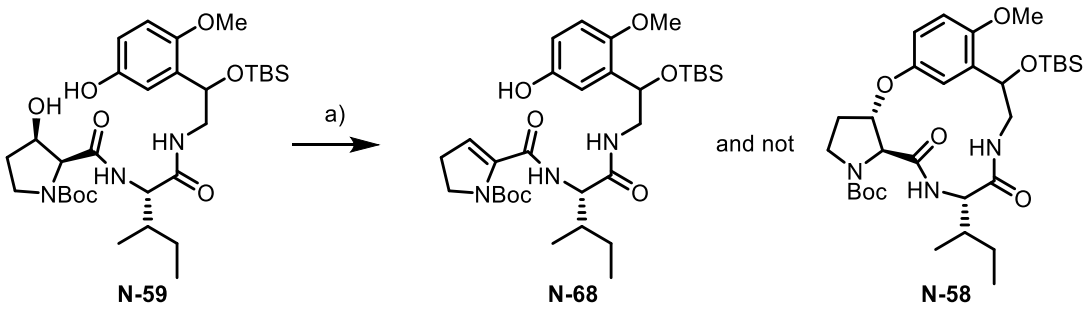

Scheme 81 Failed *Mitsunobu* macrocyclization. Reagents and conditions: a) DEAD, PPh_3, THF, 23 °C, 15 min, 88% of **N-68**.

Different conditions were then screened with the most commonly used azodicarboxylates DIAD, DEAD or ADDP in combination with PPh_3 or P(*n*Bu)$_3$ (Table 19). Optionally, pyridine was also added to these systems in order to suppress the formation of elimination product **N-68** as it was suggested in literature.[262] However, under no conditions was the macrocyclic core structure **N-58** obtained.

Table 19 Screening experiments for *Mitsunobu* conditions to obtain the macrocycle **N-58**.[a]

Entry	Azodicarboxylate	Phosphine	Pyridine	Observation
1	DEAD	PPh_3	+	no reaction
2	DEAD	PPh_3	-	elimination
3	DIAD	PPh_3	+	no reaction
4	DIAD	PPh_3	-	no reaction
5	ADDP	PPh_3	+	no reaction
6	ADDP	PPh_3	-	no reaction
7	DEAD	P(*n*Bu)$_3$	-	no reaction
8	DIAD	P(*n*Bu)$_3$	-	no reaction
9	ADDP	P(*n*Bu)$_3$	-	no reaction

[a:] All reactions were carried out in dry THF at 23 °C on a 5 mg scale.

Additional experiments were then carried out at 80 °C (Table 20) but to our disappointment, elimination product **N-68** remained the only isolable product.

Table 20 Screening experiments for *Mitsunobu* conditions to obtain the macrocycle **N-58** at 80 °C.[a]

Entry	Azodicarboxylate	Phosphine	Pyridine (cat.)	Observation
1	DEAD	PPh_3	+	elimination
2	DEAD	PPh_3	-	elimination
3	DIAD	PPh_3	+	elimination
4	DIAD	PPh_3	-	elimination
5	DEAD	P(*n*Bu)$_3$	-	elimination
6	DIAD	P(*n*Bu)$_3$	-	elimination

[a:] All reactions were carried out in a sealed microwave tube at 80 °C on a 5 mg scale.

The above experiments led to the conclusion that the macrocyclization of **N-59** through a *Mitsunobu* reaction seemed not to be feasible and, therefore, this strategy was abandoned.

2.3.2.3 Synthesis of Linear Aryl Fluoride Precursors

A possible alternative to the failed *Mitsunobu* strategy for the construction of the crucial ether bond in macrocycle **N-59** would be the nucleophilic displacement of a leaving group on the aromatic ring by the hydroxy group on the proline ring. In principle, such an approach is precedented by others.[263,264] *Carreira* and co-workers used KHMDS in THF/toluene at 65 °C to affect ring closure of tertiary alcohol **N-69** and substituted aryl fluoride **N-70** in their synthesis of a THC variant (Scheme 82).[264]

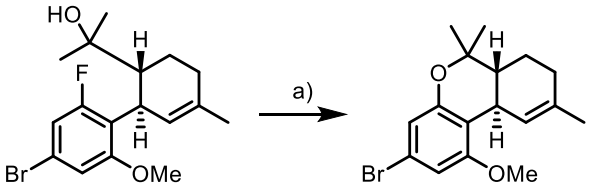

N-69 **N-70**

Scheme 82 *Carreira's* cyclization in the total synthesis of 3-Br-THC. Reagents and conditions: a) KHMDS, THF-PhMe, 65 °C, 90%.

The synthesis of the requisite cyclization precursor **N-76** started with aldehyde **N-71** and proceeded analogously to the synthesis of **N-59** (Scheme 80). Nitromethane readily attacked the aldehyde moiety in **N-71** under basic conditions and subsequent TBS protection of the ensuing alcohol gave nitro intermediate **N-72** in 21% overall yield (based on **N-71**). Reduction of the nitro group was achieved with sodium borohydride and nickel-(II)-chloride to give the primary amine **N-73**. Amide bond formation between **N-73** and *Z*-L-Ile was achieved with DCC/HOBt. The *Z*-protecting group of **N-74** was removed by means of catalytic hydrogenation over palladium to give **N-75** in over 95% yield. The 3-hydroxy proline acid was coupled with EDC/HOBt and a catalytic amount of DMAP to give the linear intermediate **N-76**. The use of *N*-Boc-protected *cis*-hydroxy proline instead of the *trans*

derivative was due to time reasons and the availability of the *cis*-derivative. Compound **N-76** was considered to be a reasonable model substrate for initial macrocyclization attempts.

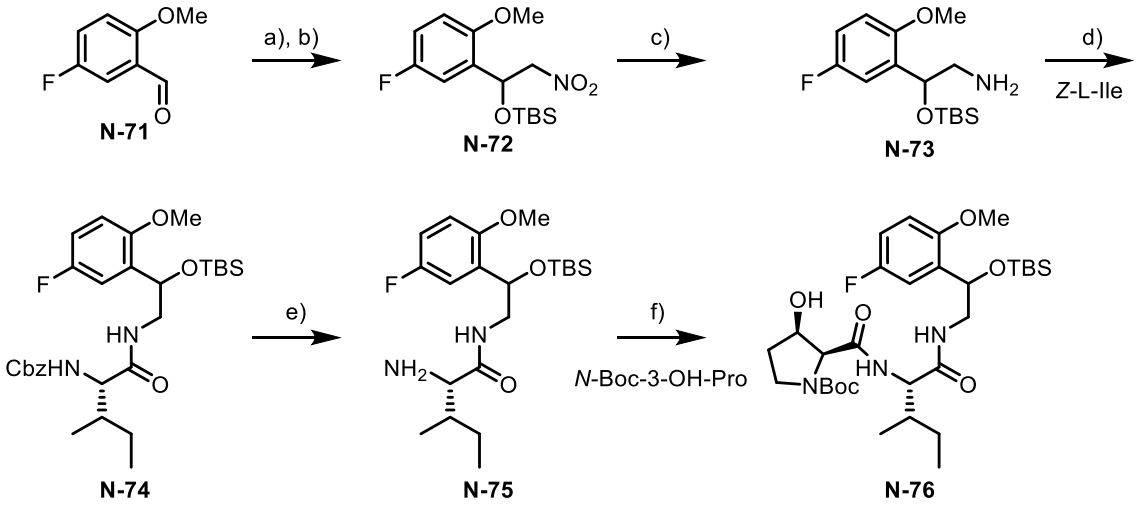

Scheme 83 Reagents and conditions: a) NaOMe (25 wt%), $MeNO_2$, MeOH, 23 °C, 16 h; b) TBSCl, imidazole, DMF, 23 °C, 16 h; 21% over two steps; c) $NiCl_2 \cdot 6H_2O$, $NaBH_4$, MeOH, THF, 0 °C, 50 min, 70%; d) DCC, HOBt, NMM, CH_2Cl_2, 0 – 23 °C, 16 h, 93%; e) Pd/C, H_2, EtOH, 23 °C, 2 h, quant.; f) EDC, HOBt, DMAP, CH_2Cl_2, 23 °C, 16 h, 98%.

With compound **N-76** in hand, we were keen to see whether a base-mediated cyclization might be successful. Disappointingly, treatment of **N-76** with TBAF or with KHMDS, LiHMDS, NaH at various temperatures only led to loss of the TBS-protecting group or to the formation of complex product mixtures as soon as the reaction temperature was raised.

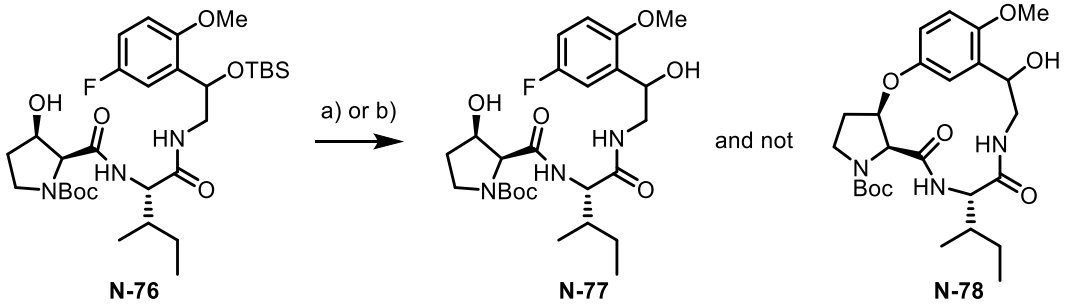

Scheme 84 Base-mediated ring closing attempts. Reagents and conditions: a) TBAF, DMF, 23 °C for 2 h, then 20 h at 70 °C, then 20 h at 100 °C. b) KHMDS (0.5 M in THF), THF, 65 °C 20 h, then 20 h at 100 °C; c) LiHMDS, THF, 65 °C 20 h; d) NaH 60 wt% on mineral oil, THF, 60 °C, 16 h.

As another option envisioned that the silylation of the free hydroxy group in **N-76** followed by treatment with a catalytic amount of cesium fluoride would lead to the formation of an alkoxide that would then displace the fluoride ion from the aromatic ring, thus effecting the macrocycle to close. Additional free fluoride anions would be generated and continue to liberate new alkoxide. We were able to synthesise intermediate **N-79** (based on TLC-MS, LC-MS) but upon purification by FC, the compound was lost in several attempts.

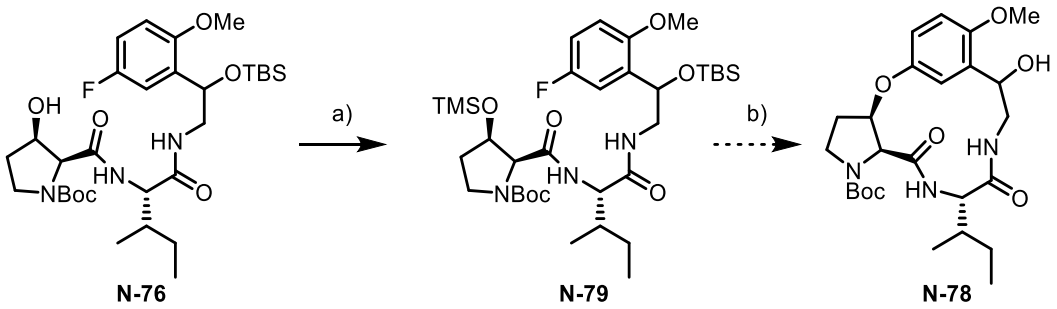

Scheme 85 Reagents and conditions: a) TMSCl, imidazole, CH_2Cl_2, 23 °C, 18 h; b) cat. CsF, THF, rt.

Further efforts using *N*-Boc-protected *trans*-hydroxy proline for the coupling reaction with **N-75** led to the synthesis of **N-76b** in excellent yield of 97% (Scheme 86).

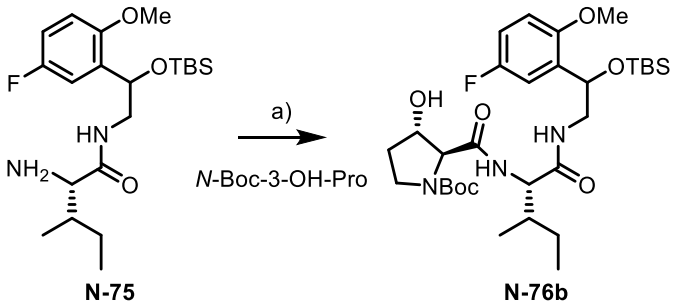

Scheme 86 Reagents and conditions: a) EDC, HOBt, DMAP, CH_2Cl_2, 23 °C, 16 h, 97%.

Compound **N-76b** was submitted to base-mediated macrocyclization conditions using KHMDS (Scheme 87). As in previous studies with substrate **N-76** (Scheme 84) the macrocycle was not obtained but only TBS-removal was observed.

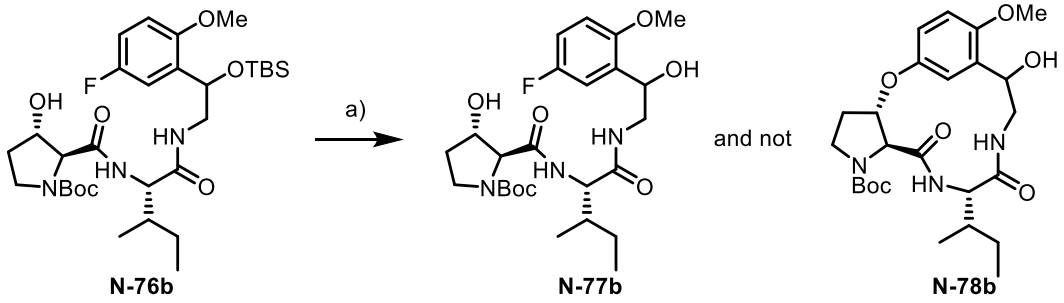

Scheme 87 Reagents and conditions: a) KHMDS (0.5 M in toluene), THF, rt, 8 h, then 8 h at 65 °C, then 12 h at 100 °C. Reaction was carried out on a 10 mg scale.

Additionally, **N-76b** was treated with TMSCl and in a subsequent step with potassium fluoride to furnish the desired macrocycle (Scheme 88). This time, no purification by FC was performed and the intermediate silylated **N-76b** was directly treated with potassium fluoride after an aqueous work-up. Unfortunately, and analogous to previous studies with **N-76** (Scheme 85) the desired macrocycle was not formed.

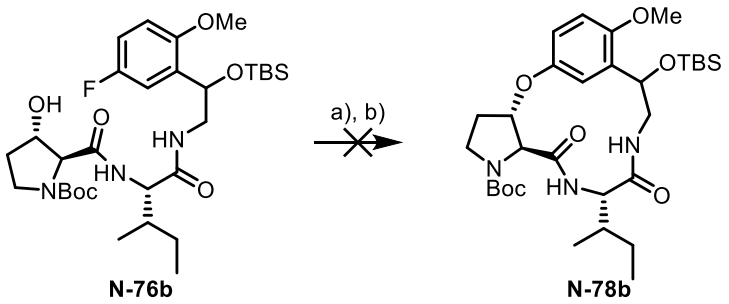

Scheme 88 Reagents and conditions: a) TMSCl, imidazole, CH_2Cl_2, 23 °C, 18 h, crude quant.; b) KF, CH_2Cl_2, rt.

Based on these findings we discontinued the described approach.

2.4 Conclusion and Outlook

In the course of this project the linear dipeptide derivatives **N-59** and **N-76** were synthesised as potential intermediates for the total synthesis of the natural product nummularine H (**N-1**). Phenol **N-59** was elaborated from 4-(benzyloxy)phenol (**N-64**) in 8 consecutive steps and 11% overall yield. Aryl fluoride **N-76** was synthesised starting from aldehyde **N-71** in 6 steps and 13% overall yield. The exclusive formation of the elimination product **N-68** from **N-59** under *Mitsunobu* conditions indicate that this strategy has no potential for future studies. To our disappointment, a base-mediated macrocyclization of substrate **N-76**/**N-76b** was unfeasible too.

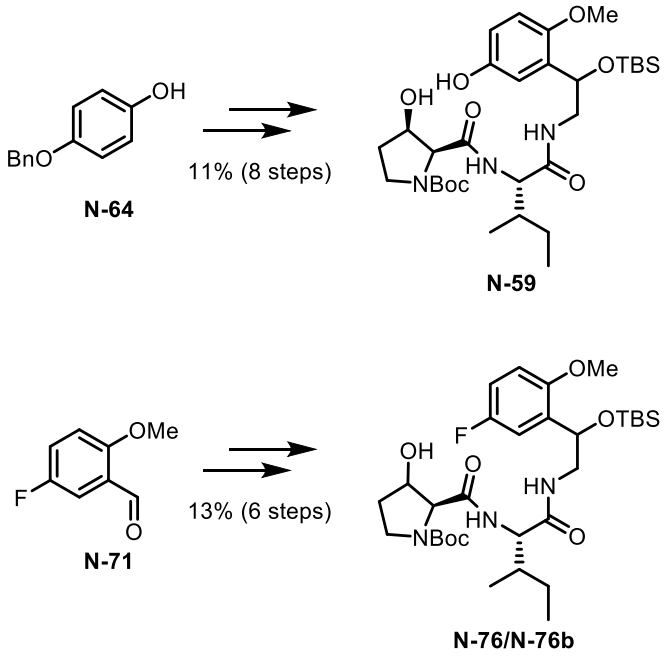

An alternative synthesis of nummularine H (**N-1**) could be envisioned through a selective protection of the phenol moiety in **N-59** according to a protocol reported by *Sefkov*,[265] which involves the use of a trityl-protecting group (Scheme 89).

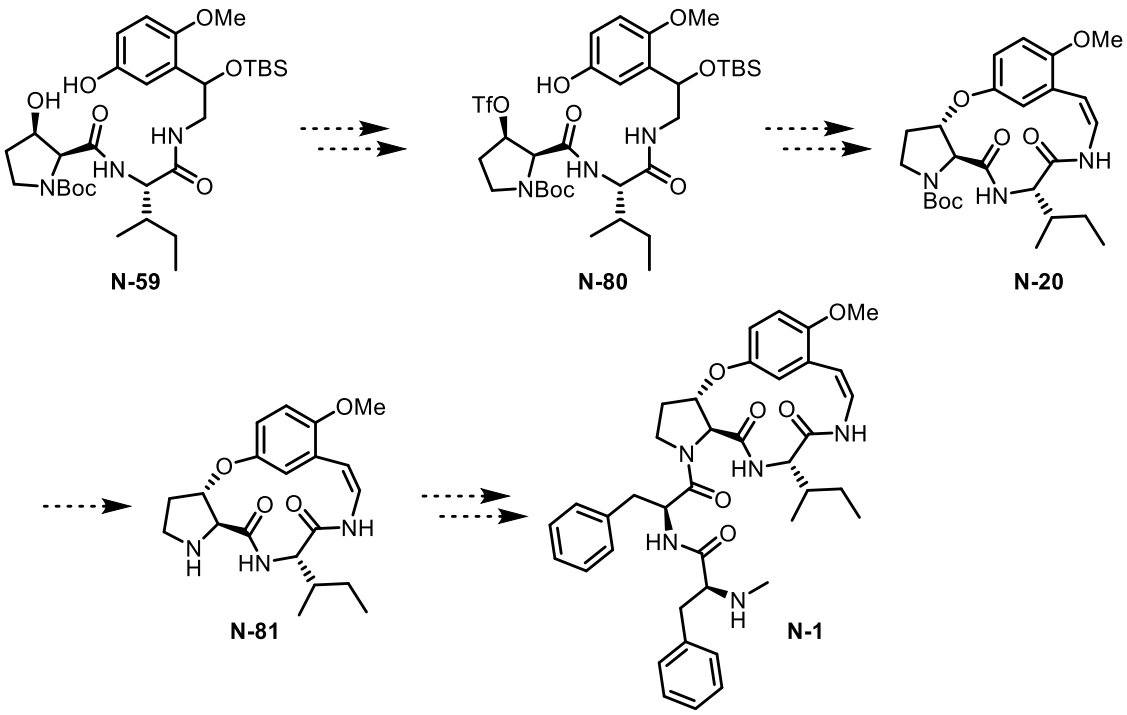

Scheme 89 Alternative synthesis of **N-1**.

This would allow the installation of a leaving group at the 3-position of the proline moiety. The macrocycle could then be formed through treatment with base (*e.g.* BEMP, *Hanessian*[266]) after deprotection of the phenolic hydroxy group. It would remain to be seen if conditions could be identified where elimination to **N-68** would be less prevalent than under *Mitsunobu* conditions. After TBS-deprotection of the benzylic hydroxy group, the enamide moiety in the eastern part should be obtained by treatment with the *Burgess* reagent[267,268]. Boc-removal would be performed according to the protocol described by *Evano*[248] and the installation of the peptide side chain would be accomplished using commonly used coupling reagents.

3 Experimental

3.1 General Methods

All non-aqueous reactions were performed under an argon atmosphere using flame-dried glassware and standard syringe/septa techniques. CH_2Cl_2, THF and Et_2O used for reactions were distilled under argon prior to use (CH_2Cl_2 from CaH_2, THF and Et_2O from Na/benzophenone). All other absolute solvents were purchased as anhydrous grade from Fluka or Acros (puriss.; dried over molecular sieves; H_2O <0.005%) and used without further purification unless otherwise stated. Solvents for extractions, flash column chromatography (FC) and thin layer chromatography (TLC) were purchased as commercial grade; hexane, Et_2O and EtOAc were distilled prior to use. All other commercially available reagents were used without further purification unless otherwise stated. Reactions were magnetically stirred and monitored by TLC performed on Merck TLC aluminum sheets (silica gel 60 F254). Spots were visualized with UV light (λ = 254 nm) or through staining with $KMnO_4/K_2CO_3$ and in rare cases $Ce_2(SO_4)_3$/phosphomolybdic acid/H_2SO_4 (CPS) or vanillin/H_2SO_4/EtOH. Chromatographic purification of products (FC) was performed using Fluka silicagel 60 or Silicycle Silia Flash® P60 for preparative column chromatography (particle size 40-63 µm) unless otherwise stated. For automated tirations a setup from Metrohm was used: A combination of Titrando 801 and 836 coupled to a Dosimo 800 unit was operated with a touch control system.

^{1}H- and ^{13}C-NMR spectra were recorded in $CDCl_3$, CD_3OD or C_6D_6, DMSO-d_6, TFA-d on a Bruker AV-400 400 MHz or on a Bruker AV-500 500 MHz spectrometer at room temperature. Chemical shifts (δ) are reported in ppm and are referenced to chloroform (δ 7.26 ppm for ^{1}H, δ 77.16 ppm for ^{13}C), MeOH (δ 3.31 ppm for ^{1}H, δ 49.00 ppm for ^{13}C) or benzene (δ 7.16 ppm for ^{1}H, δ 128.06 ppm for ^{13}C). All ^{13}C-NMR spectra were measured with complete proton decoupling. Data for NMR spectra are reported as follows: s = singlet, d = doublet, t = triplet, q = quartet, m = multiplet, br = broad signal, *J* = coupling constant in Hz.

Melting points were obtained in open capillary tubes using a Büchi melting point apparatus B-540 and are uncorrected.

Infrared spectra (IR) were recorded on a Jasco FT/IR-6200 instrument. Resonance frequencies are given as wavenumbers in cm^{-1}.

Optical rotations were measured on a Jasco P-1020 polarimeter or on an Anton-Paar MCP 300 at the sodium D line with a 10 or 100 mm path length cell and are reported as follows: (concentration (g/100 mL), and solvent).

High resolution mass spectra (HRMS) were recorded on one of the following devices by the ETH Zürich MS service: Waters' AutoSpec Ultima (EI), Bruker's maXis (ESI) or Bruker's solariX (MALDI) AutoSpec Ultima spectrometer (EI), respectively.

X-Ray diffraction analysis was performed on a Bruker D8 Apexll or on a Nonius/Bruker Kappa Apexll diffractometer, respectively, at ETH Zürich Small Molecule Crystallography Center.

3.2 Preparations and Analytical Data

3.2.1 Amicetin (A-1)

A-62 (S)-3-hydroxy-1-methoxy-1-oxopropan-2-aminium chloride

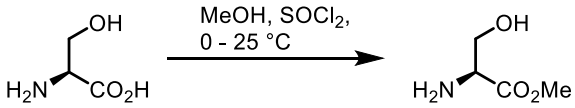

Assay: To a cooled suspension of **A-61** (15.0 g, 142.7 mmol, 1.0 equiv) in MeOH (100 mL), was slowly added $SOCl_2$ (11.8 mL, 162.7 mmol, 1.14 equiv.) using a syringe pump at a rate of 0.2 mL/min. After complete addition of $SOCl_2$ the reaction was allowed to reach room temperature and was stirred for 20 h. The reaction mixture was then concentrated under reduced pressure. In order to remove excess HCl the white crystalline residue was azeotropically purified with MeOH (3 x 25 mL) followed by hexane (3 x 25 mL). To give the title compound as a white crystalline solid (22.1 g, 142.7 mmol, 98%).

Analytics: **^{1}H NMR** (400 MHz, DMSO) δ 8.62 (s, 3H), 5.63 (s, 1H), 4.08 (s, 1H), 3.82 (d, *J* = 3.3 Hz, 2H), 3.73 (s, 3H). **$[\alpha]^{23}_D$** +3.46 (c = 2.89, MeOH).

Lit.: **$[\alpha]^{23}_D$** +4.6 (c = 2.89, MeOH)

Compound literature known

C02LL020-1-crude
pnmr_1H_16 DMSO /v pkanmr 2

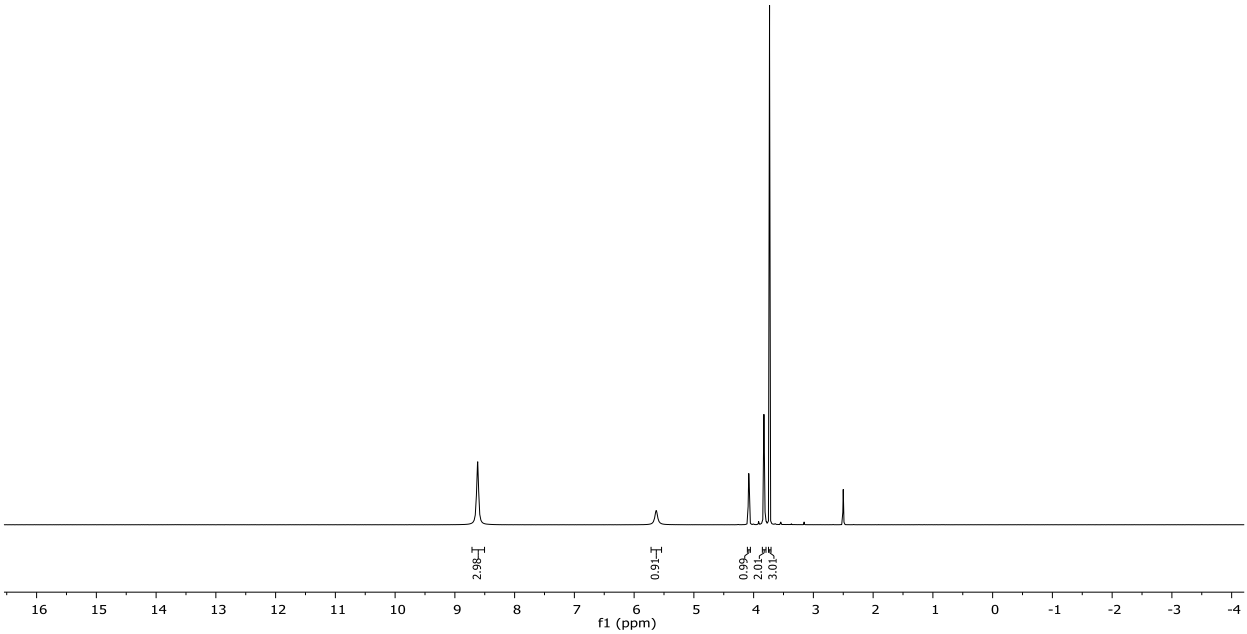

A-64 (2R,4S)-3-tert-butyl 4-methyl 2-(tert-butyl)oxazolidine-3,4-dicarboxylate

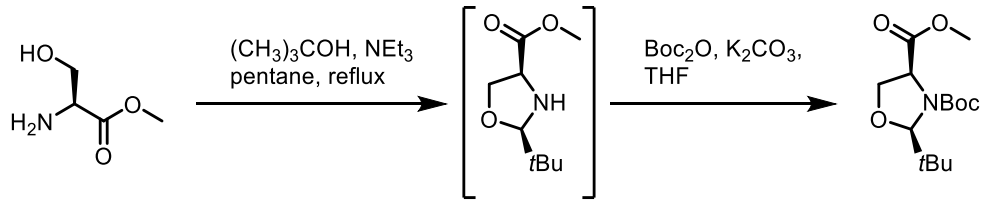

Assay: A-62 (2.0 g, 12.86 mmol, 1.0 equiv), NEt_3 (1.96 mL, 14.14 mmol, 1.1 equiv) and pivalaldehyde (1.68 mL, 15.42 mmol, 1.2 equiv) were suspended in pentane and the reaction mixture was refluxed under Dean-Stark conditions for 3.5 h. The reaction mixture was allowed to reach room temperature and the remaining solids were filtered off and washed with pentane (3 x 5 mL). The filtrate was concentrated under reduced pressure to a volume of about 7 mL to provide a concentrated solution of the intermediate N-unprotected oxazolidine. THF (10 mL) and Boc_2O (3.08 g, 14.14 mmol, 1.1 equiv) were charged and the reaction was stirred over night at room temperature. A 20% w/w aqueous solution of potassium carbonate was added and the resulting biphasic mixture was stirred for another 2 h. Et_2O (15 mL) was added and the phases were separated. The aqueous phase was extracted twice with Et_2O (15 mL). The combined organic phases where then washed with sat. aqueous $NaHCO_3$ and dried over $MgSO_4$. The solvent was evaporated under reduced pressure and the yellowish oil was purified by FC (EtOAc:hexane, 1:4) to give the title compound as a colorless oil (2.26 g, 7.86 mmol, 61%).

Analytics: $\mathbf{R_f}$ = 0.19 (EtOAc:hexane, 1:4). **^{1}H NMR** (400 MHz, Chloroform-*d*) δ 5.03 (s, 1H), 4.70 (s, 1H), 4.28 (dd, *J* = 8.5, 5.8 Hz, 1H), 4.14 (t, *J* = 8.4 Hz, 1H), 3.75 (s, 3H), 1.47 (s, 9H), 0.94 (s, 9H). **^{13}C NMR** (101 MHz, $CDCl_3$) δ 171.18, 146.90, 97.76, 85.33, 68.48, 59.85, 52.46, 37.91, 28.38 (3C), 25.93 (3C). **$[\alpha]^{20}_D$** = -27 (c = 0.3, MeOH).

Lit.: **$[\alpha]^{20}_D$** = -30 (c = 0.3, MeOH).

Compound literature known

C03LL022-1-fr2-12dry
pnmr_1H_16 CDCl3 /v pkanmr 60

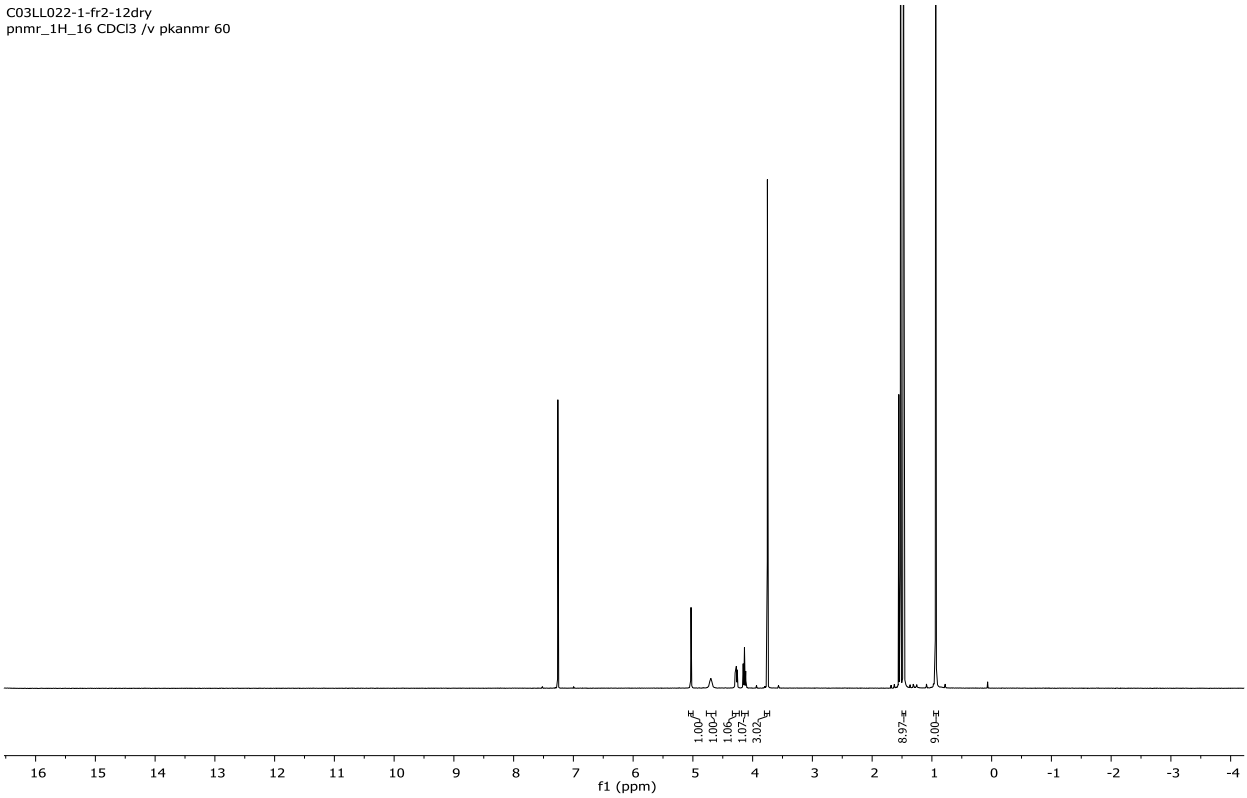

C03LL022-1-fr2-12dry
pnmr_13C_1024 CDCl3 /v pkanmr 60

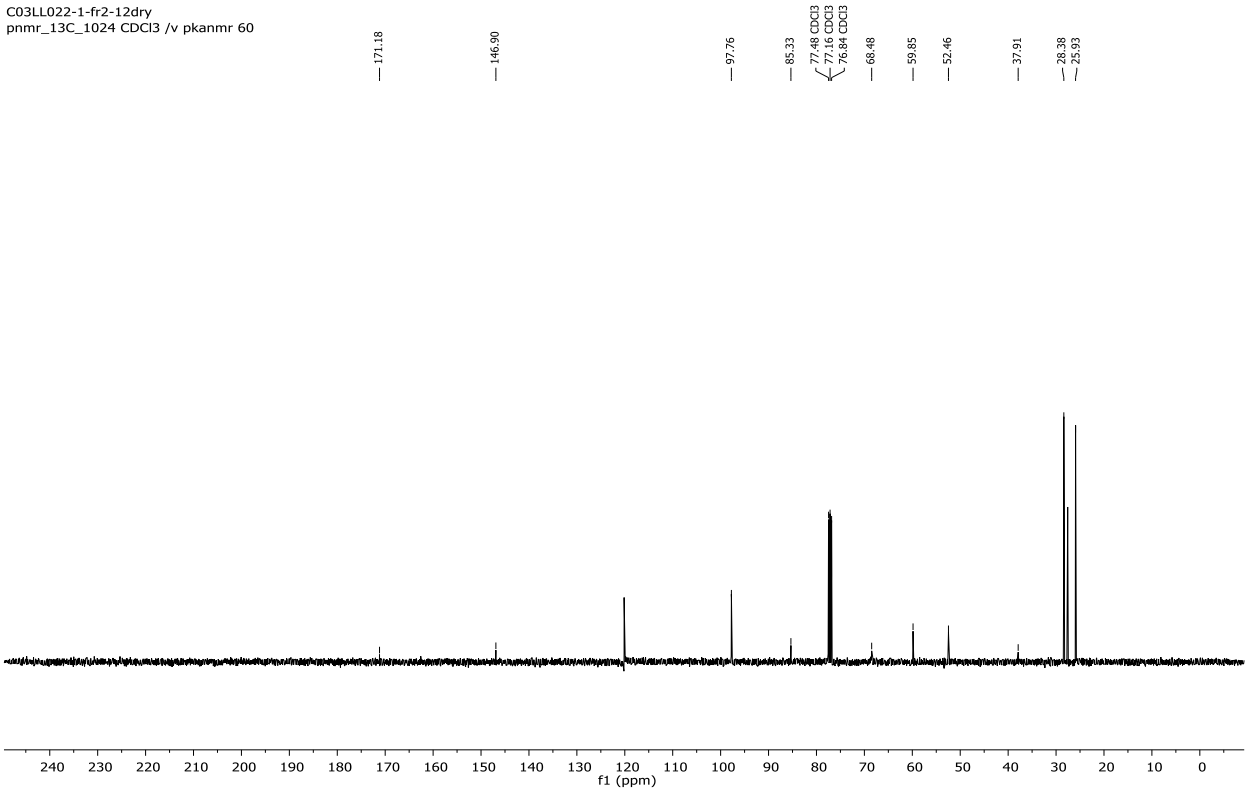

A-65 (2R,4S)-3-tert-butyl 4-methyl 2-(tert-butyl)-4-methyloxazolidine-3,4-dicarboxylate

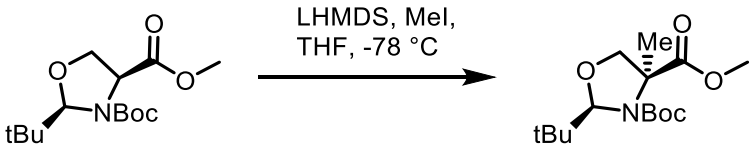

Assay: A 100 mL two neck round bottom flask was charged with dry THF (1.0 mL) and cooled to -78 °C. LHMDS (1 M in THF, 1.25 mL, 1.2 equiv) was freshly prepared and added to the reaction mixture. Oxazolidine **A-64** (0.3 g, 1.05 mmol, 1.0 equiv) was dissolved in dry THF (4 mL) and added dropwise to the reaction mixture as such that the internal temperature was kept at -78 °C. The reaction was stirred for 30 min. at -78 °C where upon iodomethane (0.20 mL, 3.24 mmol, 3.1 equiv) was added dropwise. The reaction mixture was stirred for 6 h at -78 °C. The reaction mixture was then poured onto a saturated solution of NH_4Cl (15 mL) and EtOAc (50 mL). The aqueous phase was extracted twice with EtOAc (30 mL) and the combined organic phases where then washed with brine (30 mL) and dried over $MgSO_4$. The crude yellow oil was purified by FC (EtOAc:hexane, 1:10) giving the title compound as a colorless oil (0.219 g, 0.73 mmol, 70 %).

Analytics: $\mathbf{R_f}$ = 0.15 (EtOAc:hexane, 1:10). **^{1}H NMR** (400 MHz, $CDCl_3$) δ 5.10 (s, 1H, s, 1H), 4.24 (dd, *J* = 8.1, 0.8 Hz), 3.81 (d, *J* = 8.1 Hz, 1H), 3.76 (s, 3H), 1.63 (d, *J* = 0.7 Hz, 3H), 1.44 (s, 9H), 1.00 (s, 9H). **^{13}C NMR** (101 MHz, $CDCl_3$) δ 172.70, 97.21, 77.24, 52.56, 39.41, 28.30, 26.62, 21.41. Quarternary C's were not detected. **$[\alpha]^{20}_D$** = -4.5 (c = 0.4, $CHCl_3$).

Compound literature known

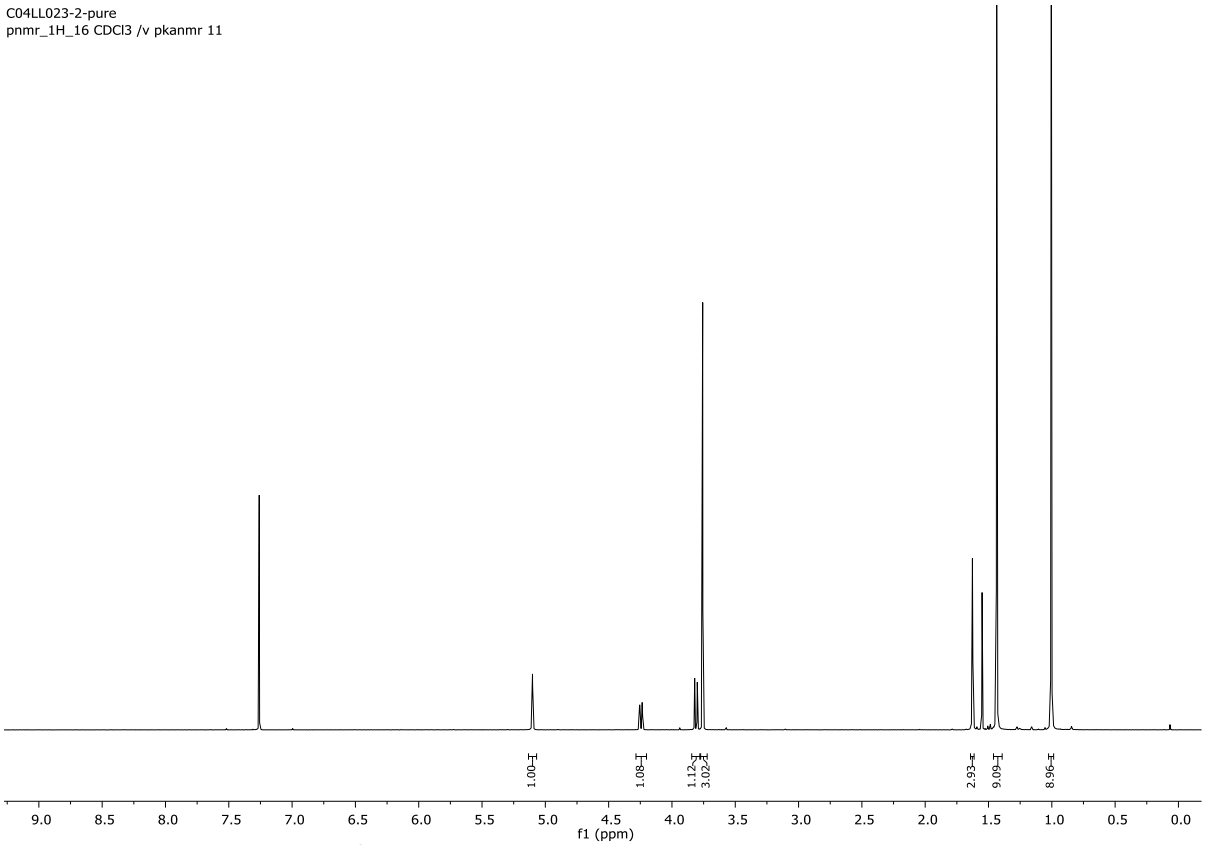
C04LL023-2-pure
pnmr_1H_16 CDCl3 /v pkanmr 11
1.00
1.08
1.12
3.02
2.93
9.09
8.96
f1 (ppm)

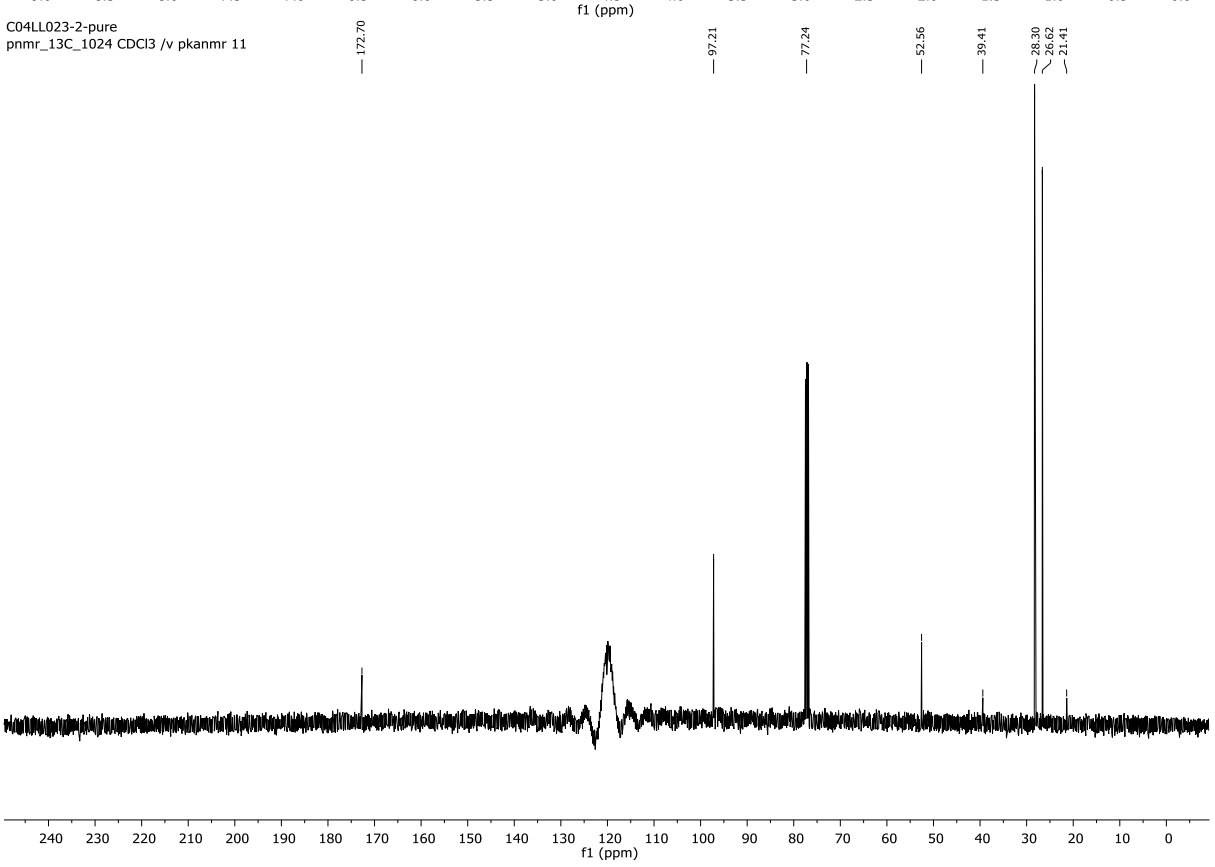
C04LL023-2-pure
pnmr_13C_1024 CDCl3 /v pkanmr 11
172.70
97.21
77.24
52.56
39.41
28.30
26.62
21.41
f1 (ppm)

A-44 (2R,4S)-3-(tert-butoxycarbonyl)-2-(tert-butyl)-4-methyloxazolidine-4-carboxylic acid

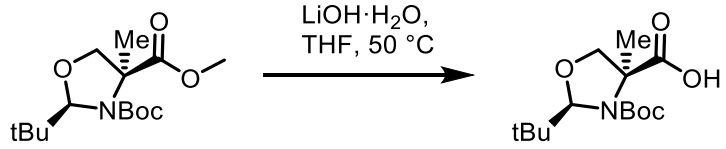

Assay: The alkylated oxazolidine **A-65** (1.4 g, 4.88 mmol, 1.0 equiv) was dissolved in THF (30 mL) and $LiOH \cdot H_2O$ (2.05 g, 48.75 mmol, 10.0 equiv) was added. Distilled H_2O (8 mL) was given to the reaction mixture and the solution was stirred for 48 h at 50 °C. The reaction mixture was then poured onto a mixture of H_2O (35 mL) and Et_2O (70 mL). The aqueous phase was then separated and acidified to a pH of 3 with 1M HCl and subsequently extracted with EtOAc (3 x 30 mL). The combined organic phases where dried over $MgSO_4$ and concentrated under reduced pressure. The crude yellow oil was purified by FC (EtOAc:hexane, 1:1) giving only impure fractions. The impurity was washed away with hexane and crystalline white solid was filtered off. Since the product is only little soluble in hexane, the filtrate was concentrated under reduced pressure and the washing with hexane was repeated several times to give the desired title compound (1.04 g, 3.64 mmol, 75 %).

Analytics: $\mathbf{R_f}$ = 0.18 (EtOAc:hexane, 1:1). **^{1}H NMR** (400 MHz, $CDCl_3$) δ 5.15 (s, 1H), 4.68 (d, *J* = 9.3 Hz, 1H), 3.91 (d, *J* = 9.3 Hz, 1H), 1.70 (s, 3H), 1.52 (s, 9H), 0.93 (s, 9H). **^{13}C NMR** (101 MHz, $CDCl_3$) δ 173.02, 157.31, 97.56, 84.50, 76.31, 66.66, 38.76, 28.07 (3C), 26.30 (3C), 21.80. **HRMS (ESI)**: 310.1622 $[M+Na^+]^+$; calculated for $[C_{14}H_{25}NNaO_5]$: 310.1625.

Remarks: ^{13}C NMR had to change the pulse delay from 2 to 6 in order to detect quarternary carbons.

Compound literature known

C24LL024-2-pure
pnmr_1H_16 CDCl3 /v pkanmr 10

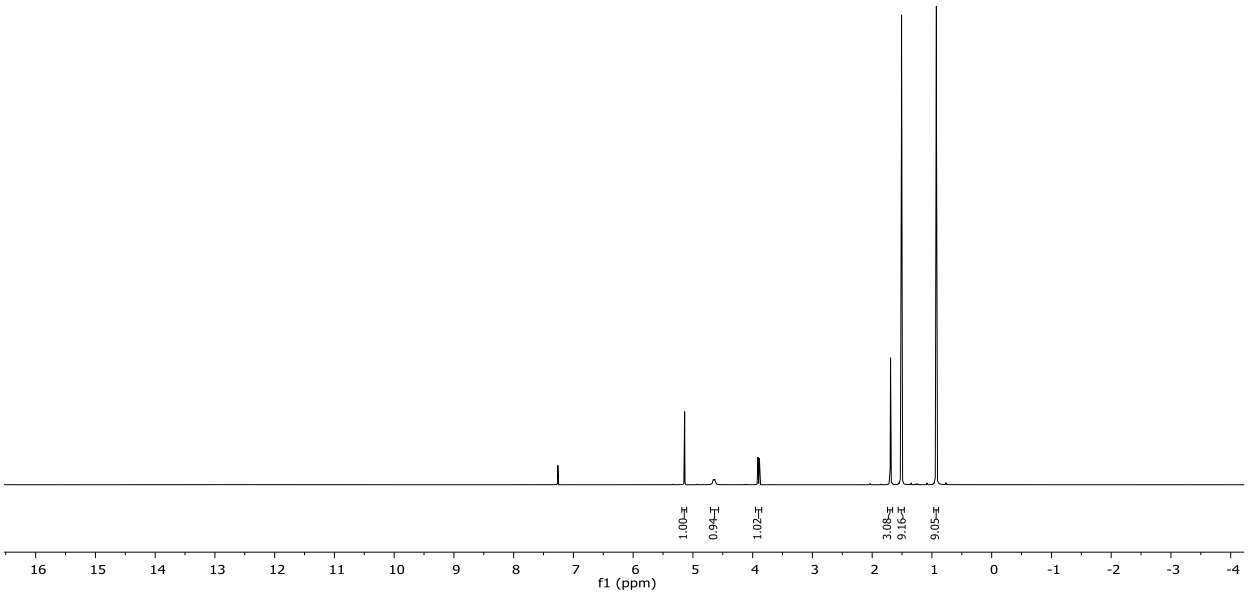

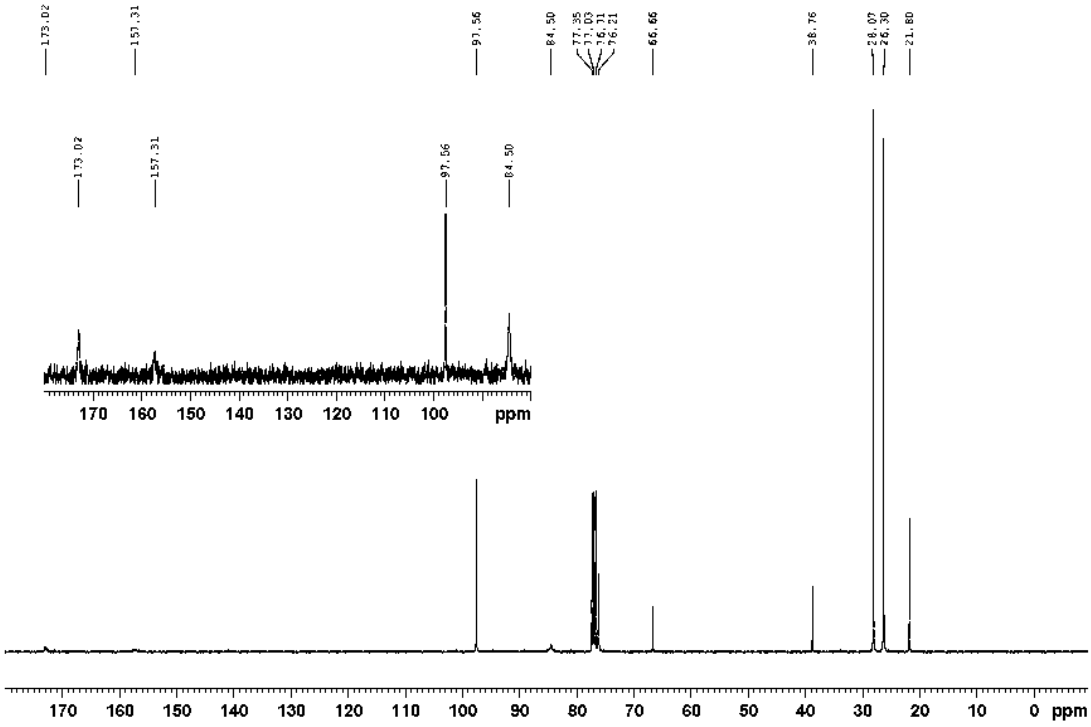

A-55 (2R,4S)-tert-butyl 2-(tert-butyl)-4-carbamoyl-4-methyloxazolidine-3-carboxylate

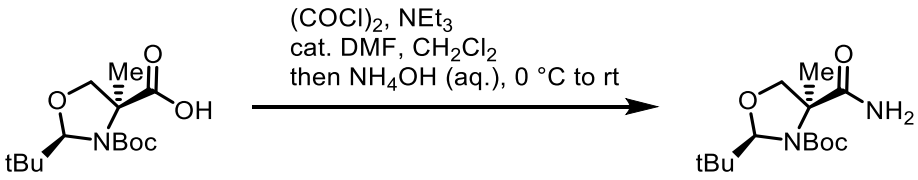

Assay: The acid oxazolidine **A-44** (0.1 g, 0.35 mmol, 1.0 equiv) was dissolved in dichloromethane (3.0 mL) and cooled down to 0 °C, NEt_3 (0.24 mL, 1.74 mmol, 5.0 equiv) was then added dropwise. Three drops of DMF (via 1 mL syringe) were then added to the reaction mixture. Subsequently, oxalyl chloride (0.09 mL, 1.04 mmol, 3.0 equiv) was added dropwise. The solution turned yellowish. A syringe needle was installed in order to have a gas outlet. The reaction was then allowed to warm to room temperature and was stirred for another 3 h. Concentrated NH_4OH solution (0.7 mL) was slowly added to the reaction mixture and was stirred for another 3 h at room temperature. The reaction was then quenched with aqueous saturated NH_4Cl (2 mL) and extracted with EtOAc (3 x 2 mL). The combined organic layers were washed with brine, dried over $MgSO_4$ and concentrated under reduced pressure. The crude product was then purified by FC (EtOAc:hexane, 2:3) to give the title compound (49.3 mg, 0.17 mmol, 49%).

Analytics: $\mathbf{R_f}$ = 0.31 (EtOAc:hexane, 2:3). **^{1}H NMR** (400 MHz, $CDCl_3$) δ 5.42 (s, 1H), 5.18 (s, 1H), 4.61 (d, *J* = 8.6 Hz, 1H), 3.79 (d, *J* = 8.9 Hz, 1H), 1.67 (s, 3H), 1.50 (s, 9H), 0.94 (s, 9H). **^{13}C NMR** (101 MHz, $CDCl_3$) δ 176.08, 155.34, 98.10, 82.30, 76.84, 67.48, 38.51, 28.31 (3 C), 26.36 (3 C), 22.32. **HRMS (MALDI)**: 287.1964 $[M+NH_4]^+$; calculated for $[C_{14}H_{27}N_2O_4]$: 287.1965. **$[\alpha]^{20}_D$** = -98.50 (c = 0.4, $CHCl_3$).

Compound literature known

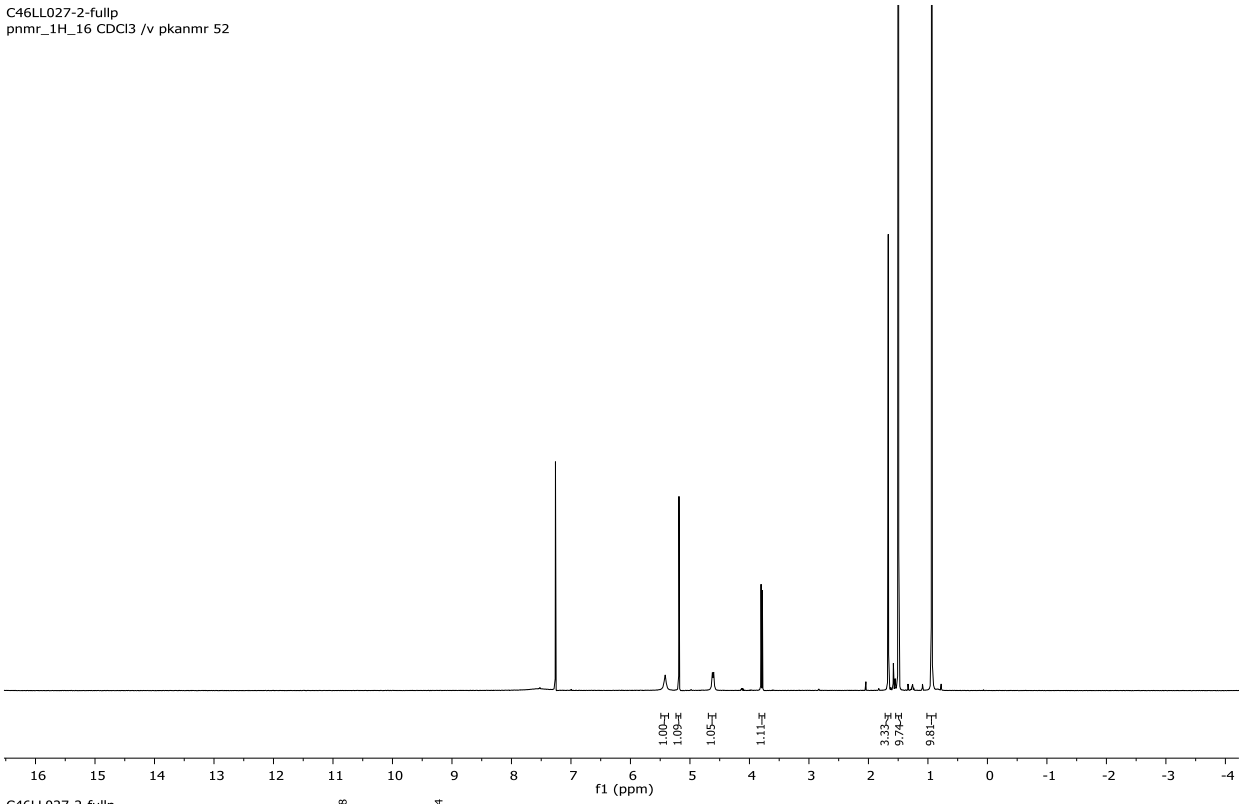
C46LL027-2-fullp
pnmr_1H_16 CDCl3 /v pkanmr 52
1.00
1.09
1.05
1.11
3.33
9.74
9.81
f1 (ppm)

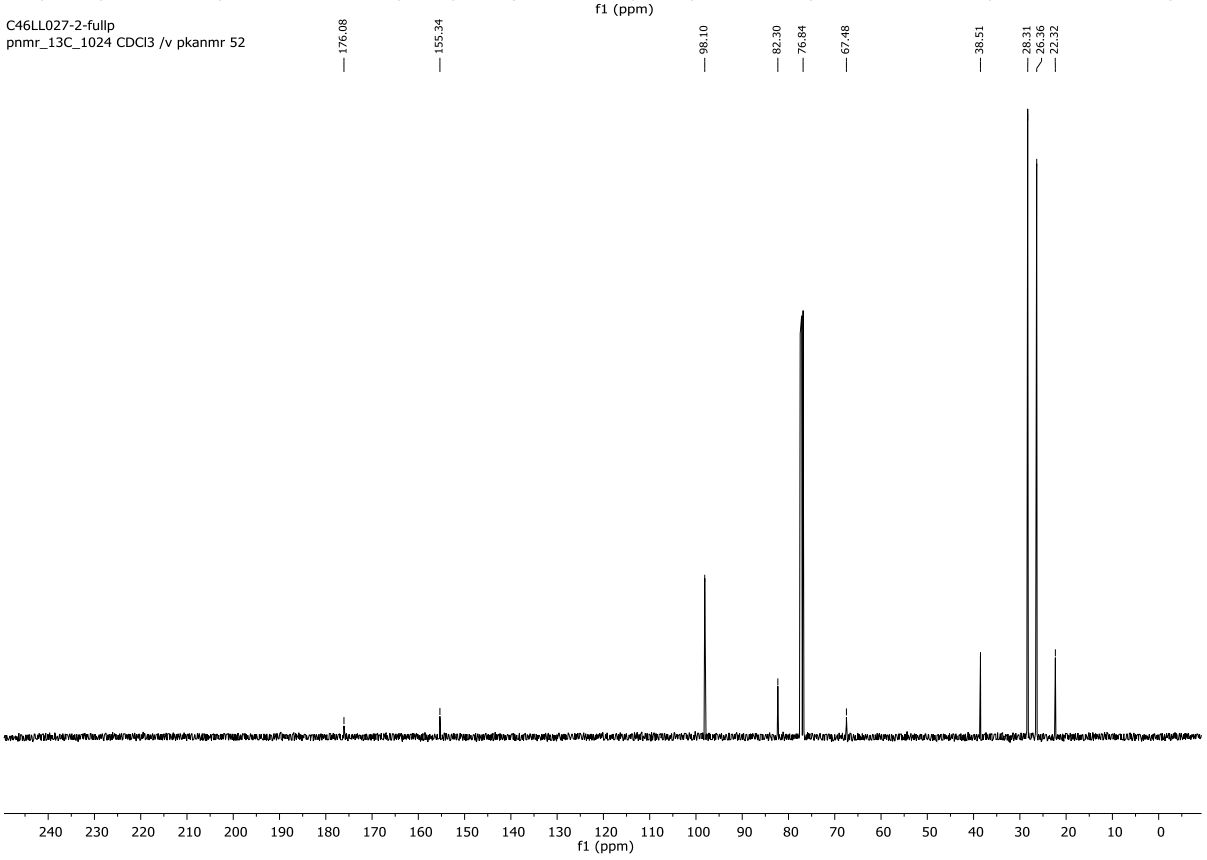
C46LL027-2-fullp
pnmr_13C_1024 CDCl3 /v pkanmr 52
176.08
155.34
98.10
82.30
76.84
67.48
38.51
28.31
26.36
22.32
f1 (ppm)

A-70 4-bromo-2-(methylthio)pyrimidine

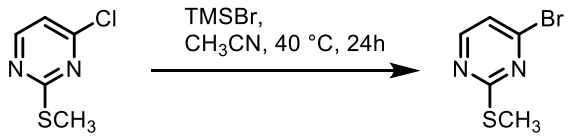

Assay: To a stirring solution of **A-69** (0.72 mL, 6.23 mmol, 1.0 equiv) in CH_3CN (60 mL) was added trimethylsilyl bromide (11.18 mL, 84.67 mmol, 13.6 equiv). The mixture was stirred at 40 °C for 23 h. The reaction was then quenched with a saturated solution of $NaHCO_3$ (80 mL) and was extracted with EtOAc (3 x 20 mL). The organic layer was washed with brine, dried over $MgSO_4$ and concentrated under reduced pressure. The crude orange oil was then purified by FC (EtOAc:hexane, 1:10) to give the title compound (1.25 g, 6.09 mmol, 97 %).

Analytics: $\mathbf{R_f}$ = 0.26 (1:10, EtOAc:hexane). **^{1}H NMR** (400 MHz, $CDCl_3$) δ 8.25 (d, *J* = 5.2 Hz, 1H), 7.15 (d, *J* = 5.2 Hz, 1H), 2.56 (s, 3H).

Compound literature known

C05LL028-1-pure
pnmr_1H_16 CDCl3 /v pkanmr 15

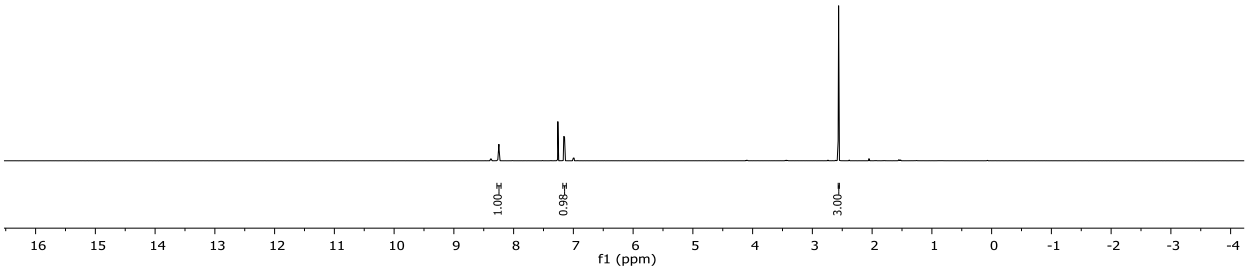

A-70 4-bromo-2-(methylsulfonyl)pyrimidine

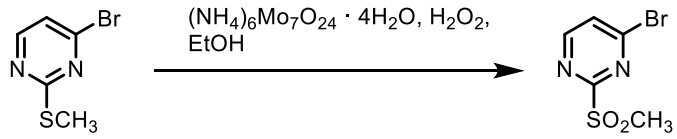

Assay: Ammonium molybdate tetrahydrate (92.2 mg, 7.5 µmol, 0.03 equiv) was added to a 30% solution of H_2O_2 (0.576 ml, 6.22 mmol, 3.0 equiv) and cooled to 0 °C, subsequently it was dropwise added to a (precooled) solution of **A-69** (0.51 g, 2.49 mmol, 1.0 equiv) in ethanol (10 mL) at 0 °C. The reaction was stirred for 24 h. The solvent was then evaporated under reduced pressure and the remaining crude was taken up in CH_2Cl_2 and H_2O. The two layers were separated and the aqueous phase was twice extracted with CH_2Cl_2 (3 x 5). The combined organic phases where washed with $Na_2S_2O_3$ (10 ml) and dried over $MgSO_4$ and the solvent was evaporated under reduced pressure to give the title compound as a white solid (563 mg, 2.37 mmol, 95 %) pure enough without further purification.

Analytics: $\mathbf{R_f}$ = 0.23 (1:1, EtOAc:hexane). **^{1}H NMR** (400 MHz, $CDCl_3$) δ 8.69 (d, *J* = 5.2 Hz, 1H), 7.76 (d, *J* = 5.2 Hz, 1H), 3.38 (s, 3H).

Compound literature known

C05LL028-1-pure.1.fid
pnmr_1H_16 CDCl3 /v pkanmr 15

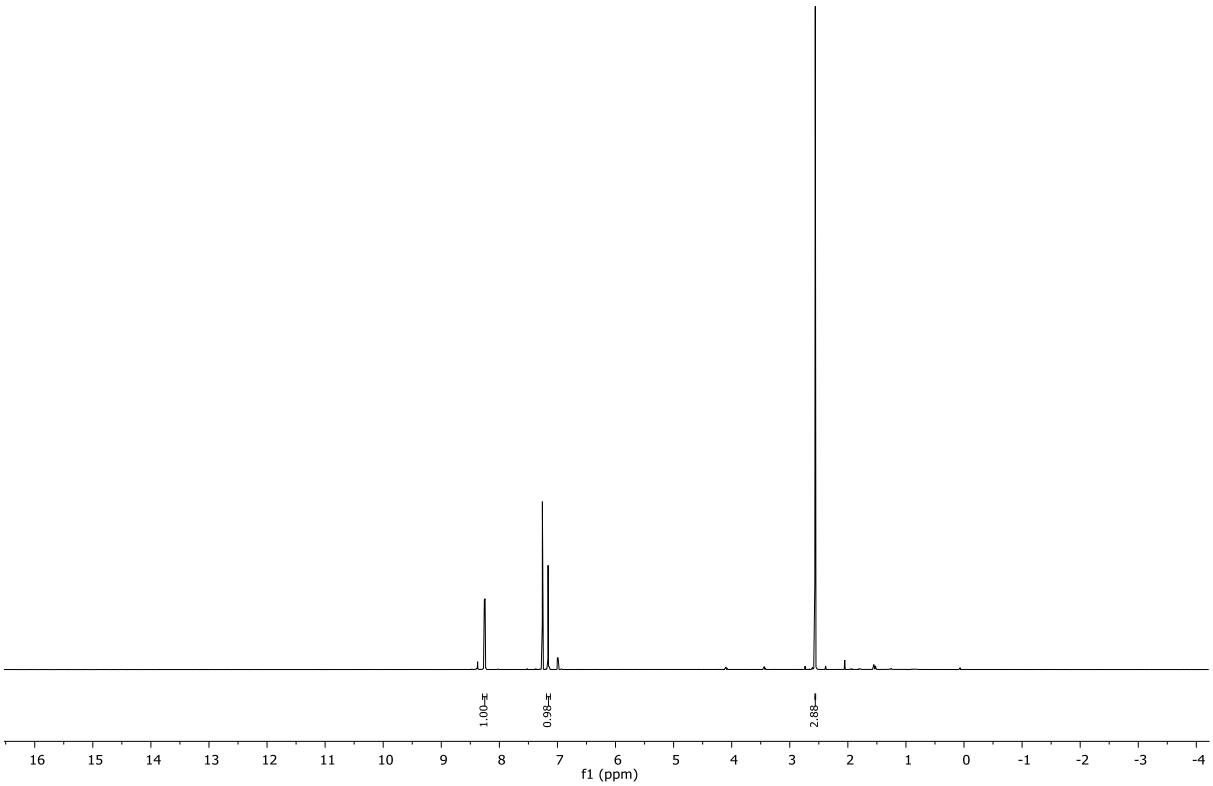

A-71 2-(allyloxy)-4-bromopyrimidine

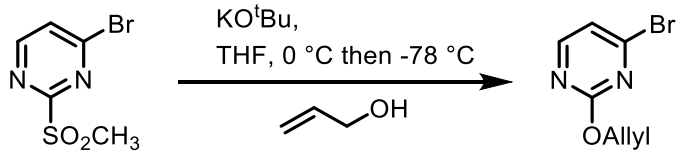

Assay: Allyl alcohol (0.21 mL, 3.02 mmol, 1.10 equiv) was dissolved in THF (15 mL) and cooled to 0 °C, then KO*t*Bu (0.37 g, 3.29 mmol, 1.20 equiv) was slowly added. The reaction mixture was stirred for 15 min. The potassium salt of allyl alcohol was subsequently added dropwise to a stirring solution of **A-70** (0.65 g, 2.74 mmol, 1.0 equiv) in THF (30 mL) at – 78 °C. The reaction mixture was kept at -78 °C for 3.5 h. It was then diluted with diethyl ether (15 mL) and was washed with H_2O (20 mL) and brine (10 mL). The combined organic phases where dried over $MgSO_4$ and the solvent was evaporated under reduced pressure. The crude was purified by FC (EtOAc:hexane, 1:3) giving the title compound (0.51 g, 2.39 mmol, 87 %).

Analytics: $\mathbf{R_f}$ = 0.28 (EtOAc:hexane, 1:3). **^{1}H NMR** (400 MHz, $CDCl_3$) δ 8.27 (d, *J* = 5.1 Hz, 1H), 7.14 (d, *J* = 5.1 Hz, 1H), 6.07 (ddt, *J* = 17.2, 10.5, 5.6 Hz, 1H), 5.44 (dq, *J* = 17.2, 1.5 Hz, 1H), 5.29 (dq, *J* = 10.5, 1.3 Hz, 1H), 4.90 (dt, *J* = 5.6, 1.4 Hz, 2H). **^{13}C NMR** (101 MHz, $CDCl_3$) δ 164.45, 159.47, 153.92, 132.10, 119.17, 118.64, 68.99.

Compound literature known

C06LL035-1-afterFC
pnmr_1H_16 CDCl3 /v pkanmr 28

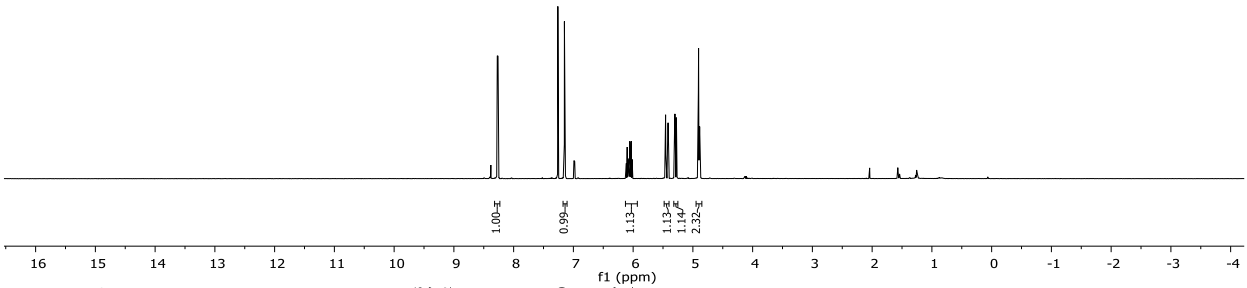

C06LL035-1-afterFC
pnmr_13C_1024 CDCl3 /v pkanmr 28

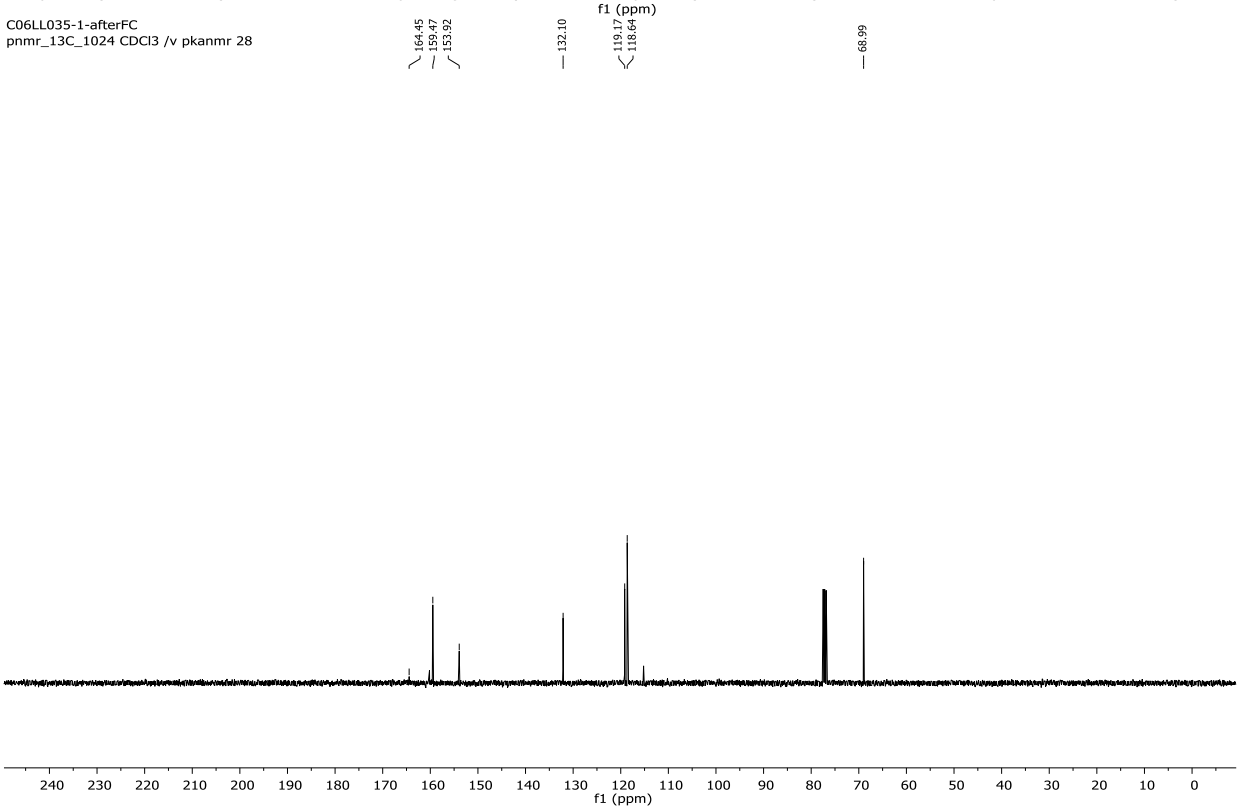

A-72 N-(2-(allyloxy)pyrimidin-4-yl)-4-iodobenzamide

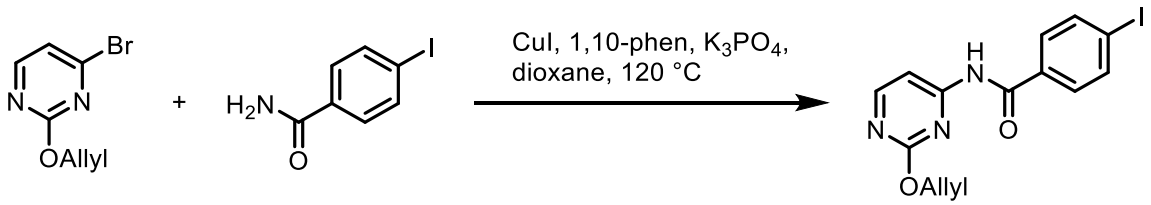

Assay: A flame dried microwave tube was charged with CuI (26.6 mg, 0.14 mmol, 0.15 equiv), 1,10-phen (33.5 mg, 0.19 mmol, 0.2 equiv), K_3PO_4 (415 mg, 1.95 mmol, 2.1 equiv) and 4-iodobenzamide (252.7 mg, 1.02 mmol, 1.1 equiv) under constant argon flow. Meanwhile, **A-71** (200 mg, 0.93 mmol, 1.0 equiv) was stepwise dissolved in dioxane (total 10 mL) and added to the reaction mixture. The microwave vial was then sealed and stirred for 19 h at 120 °C. The reaction mixture turned from grey to deep black while heating. The reaction was then allowed to reach room temperature and diluted with EtOAc (10 mL). The reaction mixture was filtered over Celite and washed with EtOAc (10 mL). The filtrate was concentrated under reduced pressure to give a white solid with brown impurities. The crude was then purified by FC (EtOAc:hexane, 1:9) to give the title compound (239.07 mg, 0.627 mmol, 67%) and re-isolated **A-71** (45 mg, 0.21 mmol, 23%).

Analytics: $\mathbf{R_f}$ = 0.13 (EtOAc:hexane, 1:5). **^{1}H NMR** (400 MHz, $CDCl_3$) δ 8.52 (s, 1H), 8.47 (d, *J* = 5.6 Hz, 1H), 7.93 (d, *J* = 5.6 Hz, 1H), 7.87 (d, *J* = 8.5 Hz, 2H), 7.61 (d, *J* = 8.5 Hz, 2H), 6.07 (ddd, *J* = 22.6, 10.7, 5.5 Hz, 1H), 5.41 (dd, *J* = 17.2, 1.4 Hz, 1H), 5.27 (dd, *J* = 10.5, 1.1 Hz, 1H), 4.87 (d, *J* = 5.4 Hz, 2H). **^{13}C NMR** (101 MHz, $CDCl_3$) δ 165.26, 164.41, 160.80, 159.03, 138.31 (2 C), 132.65, 132.52, 128.75 (2 C), 117.94, 104.18, 100.42, 68.12.

Compound literature known

C19-LL-054-1-full
pnmr_1H_16 CDCl3 /v pkanmr 19

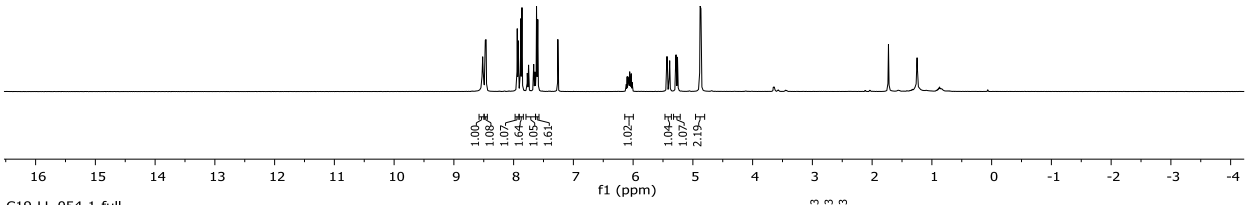

C19-LL-054-1-full
pnmr_13C_1024 CDCl3 /v pkanmr 19

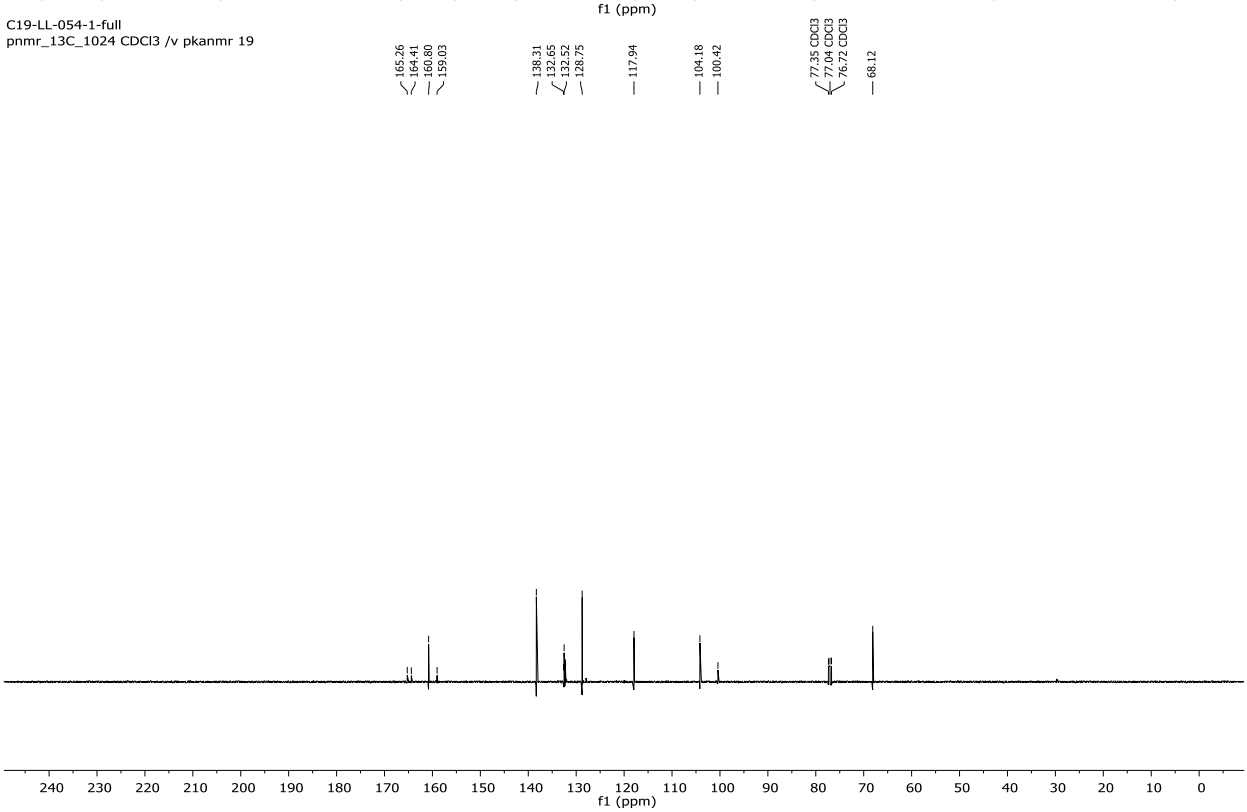

A-74 4-bromo-2-((4-methoxybenzyl)oxy)pyrimidine

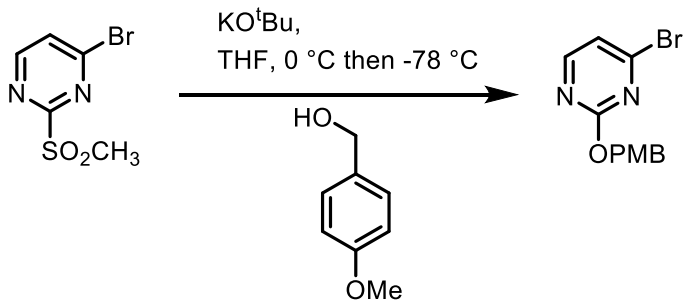

Assay: Anis alcohol (0.058 mL, 0.46 mmol, 1.10 equiv) was dissolved in THF (2 mL) and cooled to 0 °C, then KO^tBu (56.8 mg, 0.51 mmol, 1.20 equiv) was added slowly. The reaction mixture was stirred for 15 min at 0 °C. The potassium salt of the anis alcohol was subsequently added dropwise to a stirring solution of **A-70** (0.1 g, 0.42 mmol, 1.0 equiv) in THF (4.5 mL) at - 78 °C. The reaction mixture was kept at -78 °C for 6 h. It was then diluted with diethyl ether (5 mL) and was washed with H_2O (10 mL) and brine (10 mL). The combined organic phases where dried over $MgSO_4$ and the solvent was evaporated under reduced pressure. The crude was purified by FC (EtOAc:hexane, 1:3) giving the title compound (119 g, 0.40 mmol, 96%) as a crystalline white solid.

Analytics: $\mathbf{R_f}$ = 0.35 (EtOAc:hexane, 1:3). **^{1}H NMR** (400 MHz, $CDCl_3$) δ 8.27 (d, *J* = 5.1 Hz, 1H), 7.42 (d, *J* = 8.8 Hz, 2H), 7.14 (d, *J* = 5.1 Hz, 1H), 6.89 (d, *J* = 8.7 Hz, 2H), 5.37 (s, 2H), 3.81 (s, 3H). **^{13}C NMR** (101 MHz, $CDCl_3$) δ 164.57, 159.82, 159.48, 153.87, 130.32 (2 C), 127.94, 119.13, 113.98 (2 C), 69.87, 55.43. **HRMS** (EI): 293.9999 [M^+]; calculated for $[C_{12}H_{11}BrN_2O_2]^+$: 294.0004. **IR** [ATR]: υ = 3113.0 w, 3013.7 w, 2957.3 w, 2936.1 w, 2838.2 w, 1678.73 w 1612.2 m, 1570.7 s, 1527.8 s, 1511.9 s, 1441.5 s, 1416.9 s, 1359.6 s, 1321.5 s, 1302 s, 1249.7 s, 1202.4 s, 1154.2 s, 1113.7 m, 1090.1 m, 1030.3 s, 1011.0 s, 906.9 s, 809.5 s, 533.2 s.

C24LL062-1-full
pnmr_1H_16 CDCl3 /v pkanmr 51

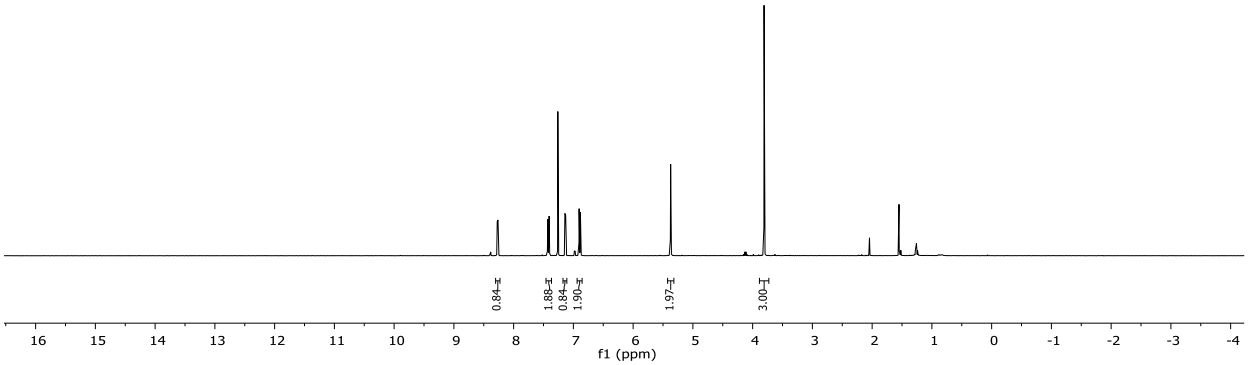

C24LL062-1-full
pnmr_13C_1024 CDCl3 /v pkanmr 51

164.57
159.82
159.48
153.87
130.32
127.94
119.13
113.98
69.87
55.43

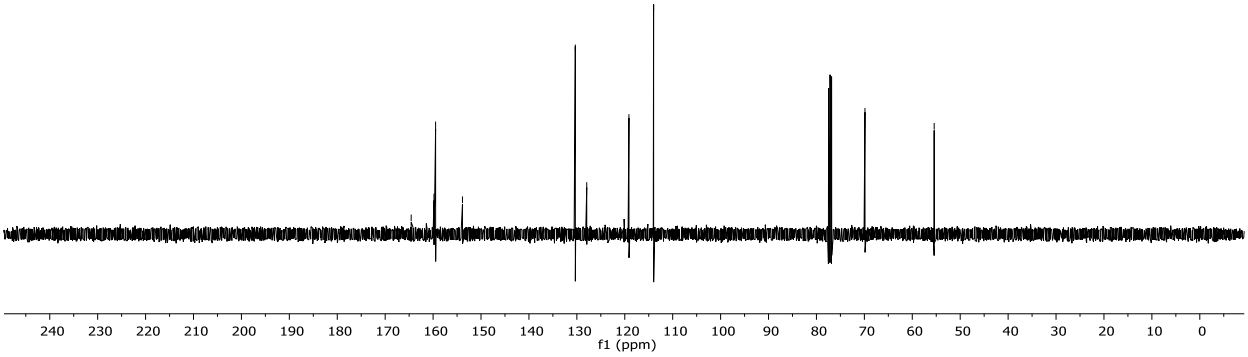

A-75 4-iodo-N-(2-((4-methoxybenzyl)oxy)pyrimidin-4-yl)benzamide

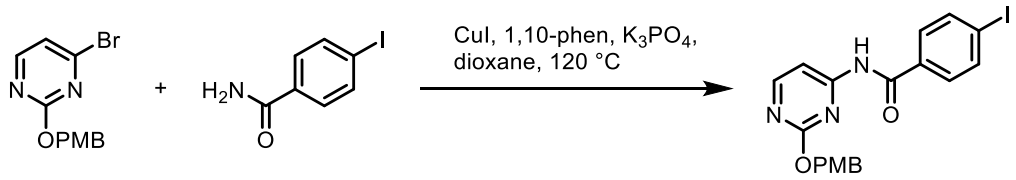

Assay: A flame dried round bottom flask was charged with CuI (484 mg, 2.54 mmol, 0.15 equiv), 1,10-phen (0.61 mg, 3.39 mmol, 0.2 equiv), K_3PO_4 (7.55 mg, 35.58 mmol, 2.1 equiv) and 4-iodobenzamide (4.81 g, 19.48 mmol, 1.15 equiv) under constant argon flow. Meanwhile, compound **A-74** (5 g, 16.94 mmol, 1.0 equiv) was stepwise dissolved in dioxane (160 mL) and added to the reaction mixture. The reaction mixture was then stirred for 48 h at 120 °C. The reaction mixture turned from grey to deep red-orange while heating and was monitored by TLC analysis. The reaction seemed to halt at some point and did not proceed over time. It was then allowed to reach room temperature and was diluted with EtOAc (50 mL). The reaction mixture was filtered over Celite and washed with EtOAc (30 mL). The filtrate was then concentrated under reduced pressure and purified by FC (EtOAc:hexane, 1:5) to give the title compound (5.26 g, 11.412 mmol, 67%).

Analytics: $\mathbf{R_f}$ = 0.26 (EtOAc:hexane, 1:3). **^{1}H NMR** (400 MHz, Chloroform-*d*) δ 8.49 (s, 2H), 7.93 (d, *J* = 5.0 Hz, 1H), 7.86 (d, *J* = 8.4 Hz, 2H), 7.59 (d, *J* = 8.5 Hz, 2H), 7.39 (d, *J* = 8.5 Hz, 2H), 6.89 (d, *J* = 8.6 Hz, 2H), 5.35 (s, 2H), 3.80 (s, 3H).**^{13}C NMR** (101 MHz, $CDCl_3$) δ 165.36, 164.66, 160.85, 159.67, 159.13, 138.41 (2 C), 132.77, 129.90 (2 C), 128.85 (2 C), 128.46, 113.98 (2 C), 104.35, 100.52, 69.11, 55.41. **HRMS (ESI)**: 462.0297 $[M+H]^+$; calculated for $[C_{12}H_{12}BrN_2O_2]$: 462.0309. **IR** [ATR, neat]: ν = 2949.59 w, 1690.3 s, 1587.13 s, 1509.99 s, 1458.88 w, 1435.74 w, 1395.25 m, 1355.71 s, 1288.22 s, 1249.65 s, 1175.4 s, 1110.8 m, 830.205 m cm^{-1}. **m.p.**: 147 °C.

C49LL065-full
pnmr_1H_16 CDCl3 /v pkanmr 59

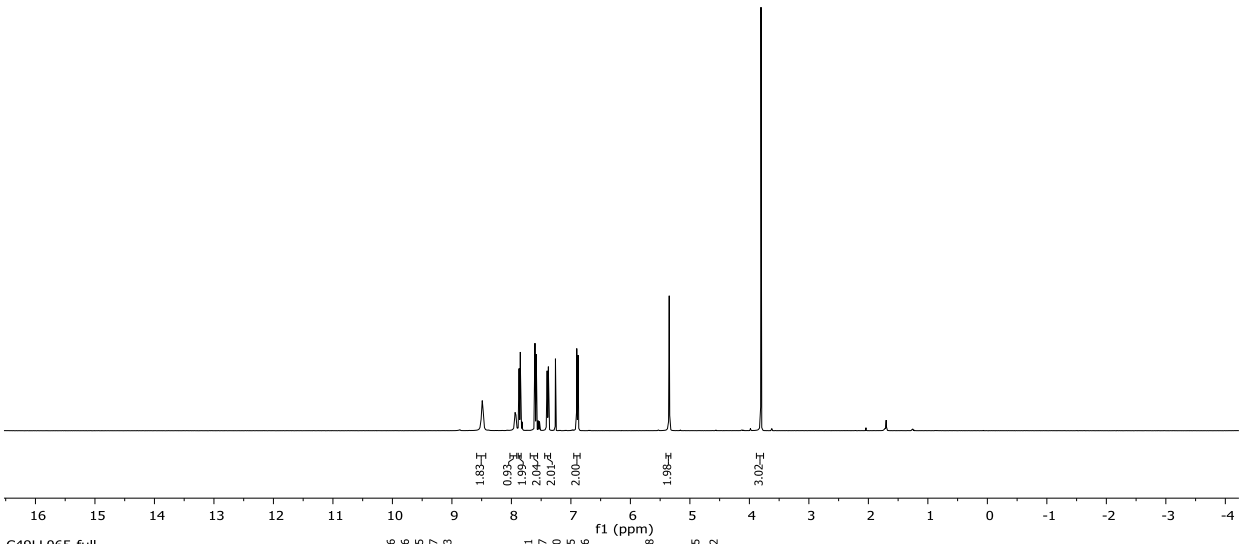

C49LL065-full
pnmr_13C_256 CDCl3 /v pkanmr 59

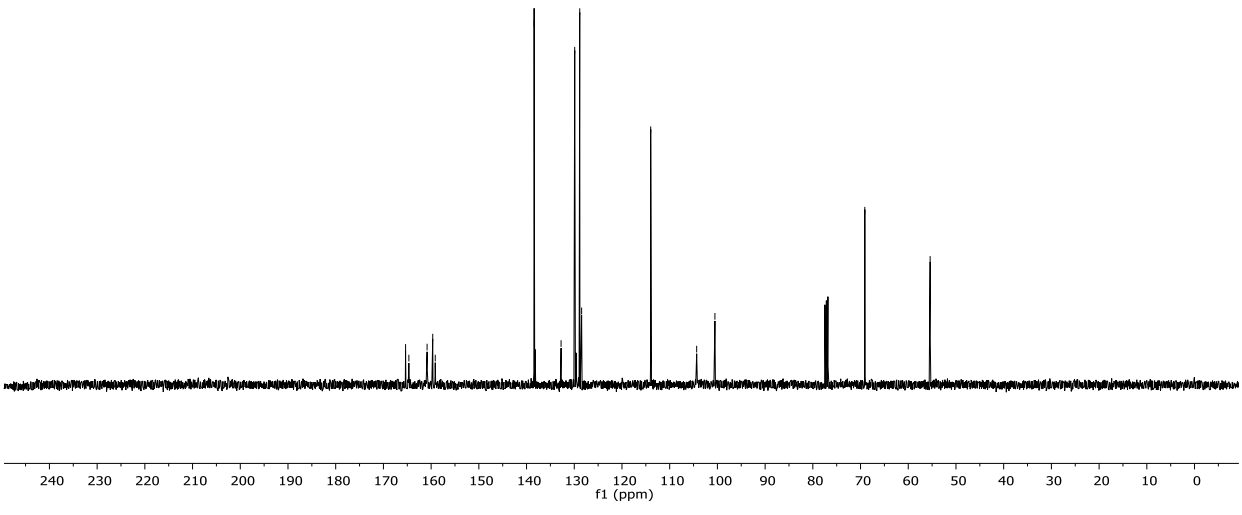

A-73 4-iodo-N-(2-oxo-1,2-dihydropyrimidin-4-yl)benzamide

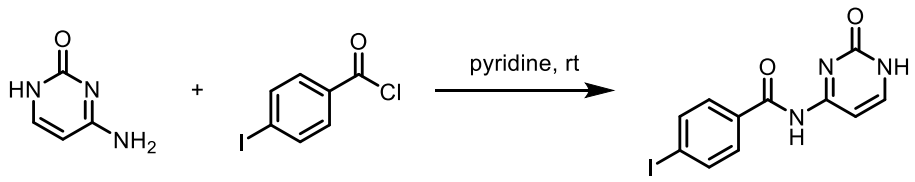

Assay: 4-Iodobenzoylchloride (180 mg, 0.68 mmol, 1.0 equiv) in pyridine (2 mL) was added dropwise over 30 min to a stirred suspension of cytosine (50 g, 10 mmol, 14.7 equiv) in pyridine (2.5 mL), and stirring was continued at room temperature for another 4 h. The reaction mixture turned blurry over the time, and a white precipitate was formed. The reaction was quenched by adding a small amount of MeOH. The solid was filtered, washed with EtOH and dried *in vacuo* to give the title compound as a white solid (98.3 mg, 0.288 mmol, 64%).

Analytics: **^{1}H NMR** (400 MHz, TFA-d) δ 8.46 (d, *J* = 7.2 Hz, 1H), 8.06 (d, *J* = 8.3 Hz, 2H), 7.78 (d, *J* = 8.3 Hz, 2H), 6.98 (d, *J* = 7.1 Hz, 1H). **^{13}C NMR** (101 MHz, TFA-d) δ 172.23, 162.59, 154.99, 149.26, 141.44 (2 C), 131.32 (2 C), 130.21, 106.57, 98.55. **HRMS (MALDI)**: 363.9553 [M+Na]; calculated for [$C_{11}H_8IN_3NaO_2$]: 363.9553. **IR** [ATR, neat]: ν = 3215.23 w, 3146.77 w, 3077.35 w, 1699.46 s, 1622.32 m, 11585.68 m, 1507.58 m, 1462.26 s, 1297.38 m, 1264.59 s, 1186.49 m, 1093.92 m, 805.62 m, 741.98 cm^{-1}. **m.p.**: 365°C.

C50LLTFA
pnmr_1H_16 CDCl3 /v pkanmr 46

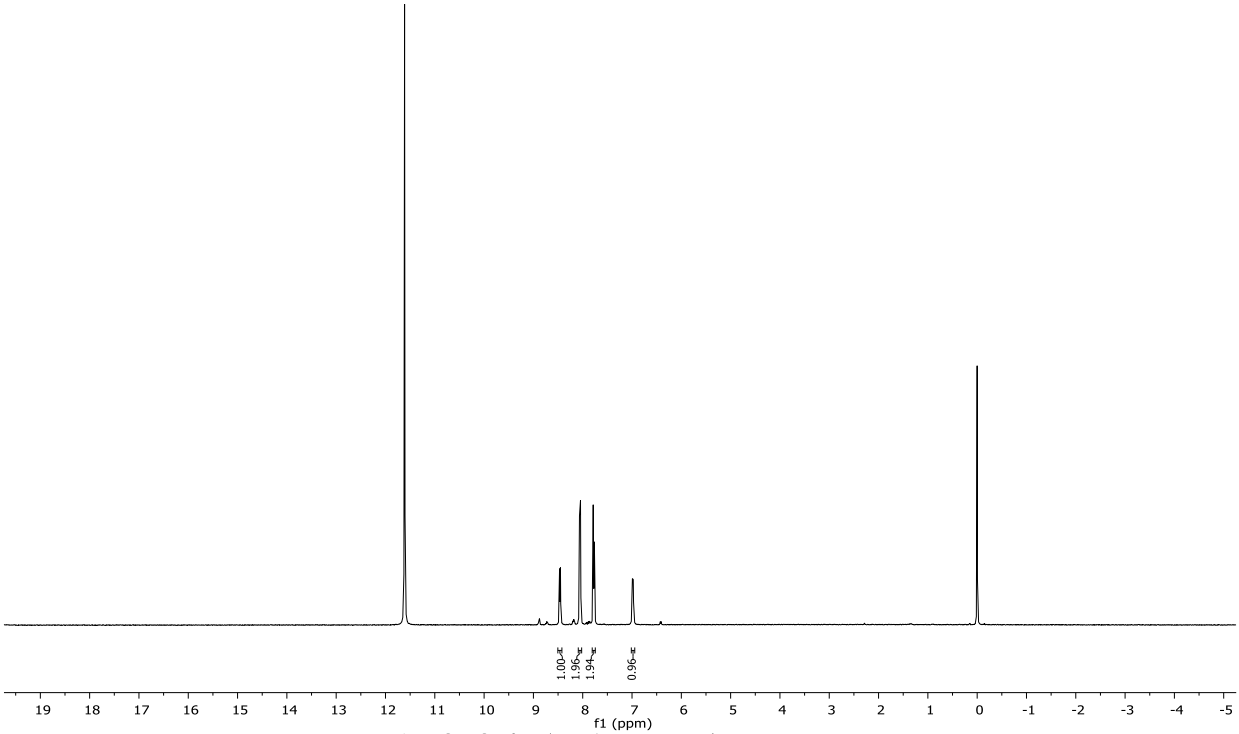

C50LLTFA
pnmr_13C_1024 CDCl3 /v sernmr 46

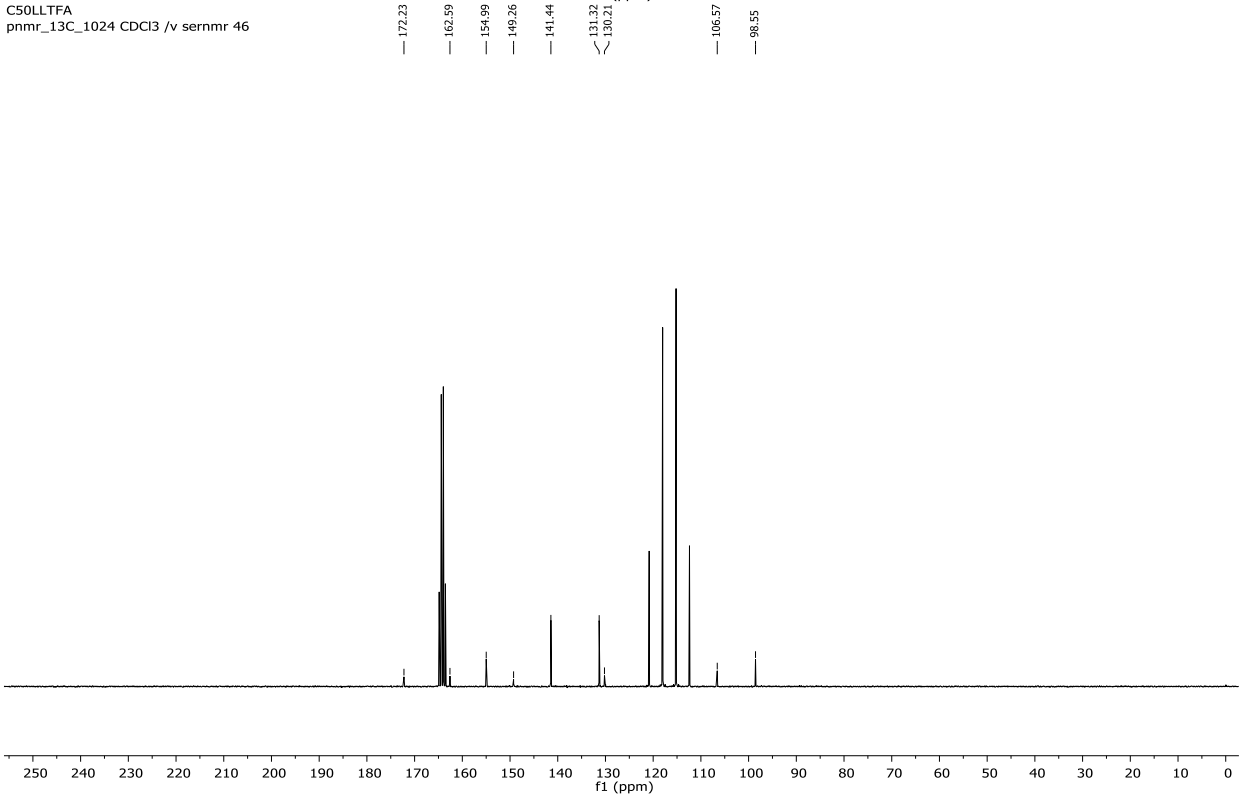

A77 4-iodo-N-(2-oxo-1-(trimethylsilyl)-1,2-dihydropyrimidin-4-yl)benzamide

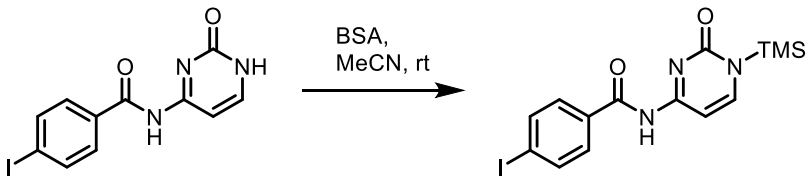

Assay: In a flame dried Schlenk tube, **A-73** (40 mg, 0.1 mmol, 1.0 equiv) was suspended in MeCN (1.1 mL) and N,O-bis(trimethylsilyl)acetamid (0.057 mL, 0.24 mmol, 2.0 equiv) was added dropwise at room temperature. Within 5 min, the white milky suspension turned into a clear transparent solution. The reaction mixture was stirred for another 25 min at room temperature. The acetonitrile was then evaporated via distillation apparatus at 10 mbar at ambient temperature. From the remaining crude was then taken an NMR sample. Product formation was observed. Thus, all the remaining impurities were removed by distillation at 120 °C and 35 mbar. Product formation was not quantitatively determined.

Analytics: **^{1}H NMR** (400 MHz, $CDCl_3$) δ 8.53 (s, 1H), 8.41 (d, *J* = 5.6 Hz, 1H), 7.90 (d, *J* = 5.6 Hz, 1H), 7.86 (d, *J* = 8.6 Hz, 2H), 7.58 (d, *J* = 8.6 Hz, 2H), 0.37 (s, 9H).**^{13}C NMR** (101 MHz, $CDCl_3$) δ 165.34, 163.22, 161.01, 159.27, 138.42 (2 C), 132.86, 128.84 (2 C), 104.13, 100.46, 0.29 (3 C).

Remarks: Further analytical data could not be obtained due to instability of the compound.

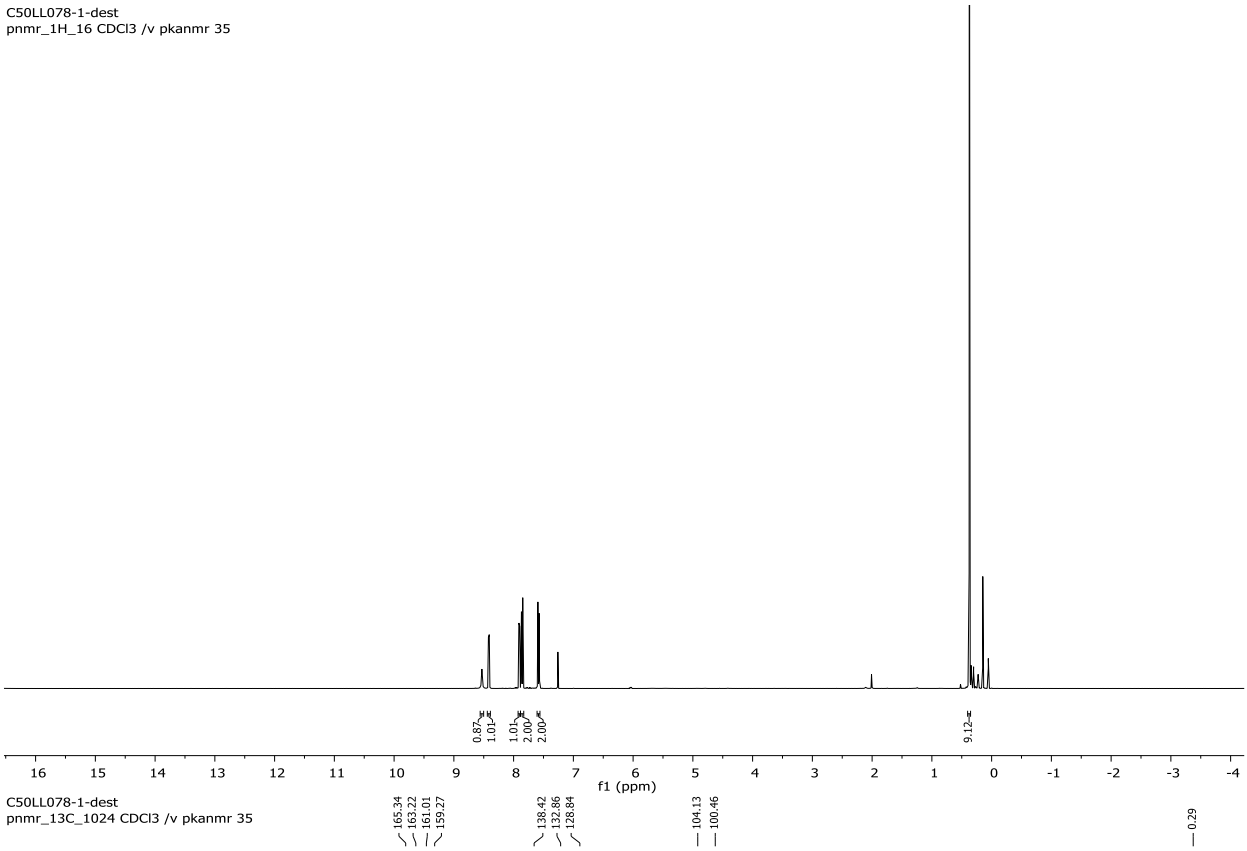
C50LL078-1-dest
pnmr_1H_16 CDCl3 /v pkanmr 35
0.87
1.01
1.01
2.00
2.00
9.12
16 15 14 13 12 11 10 9 8 7 6 5 4 3 2 1 0 -1 -2 -3 -4
f1 (ppm)

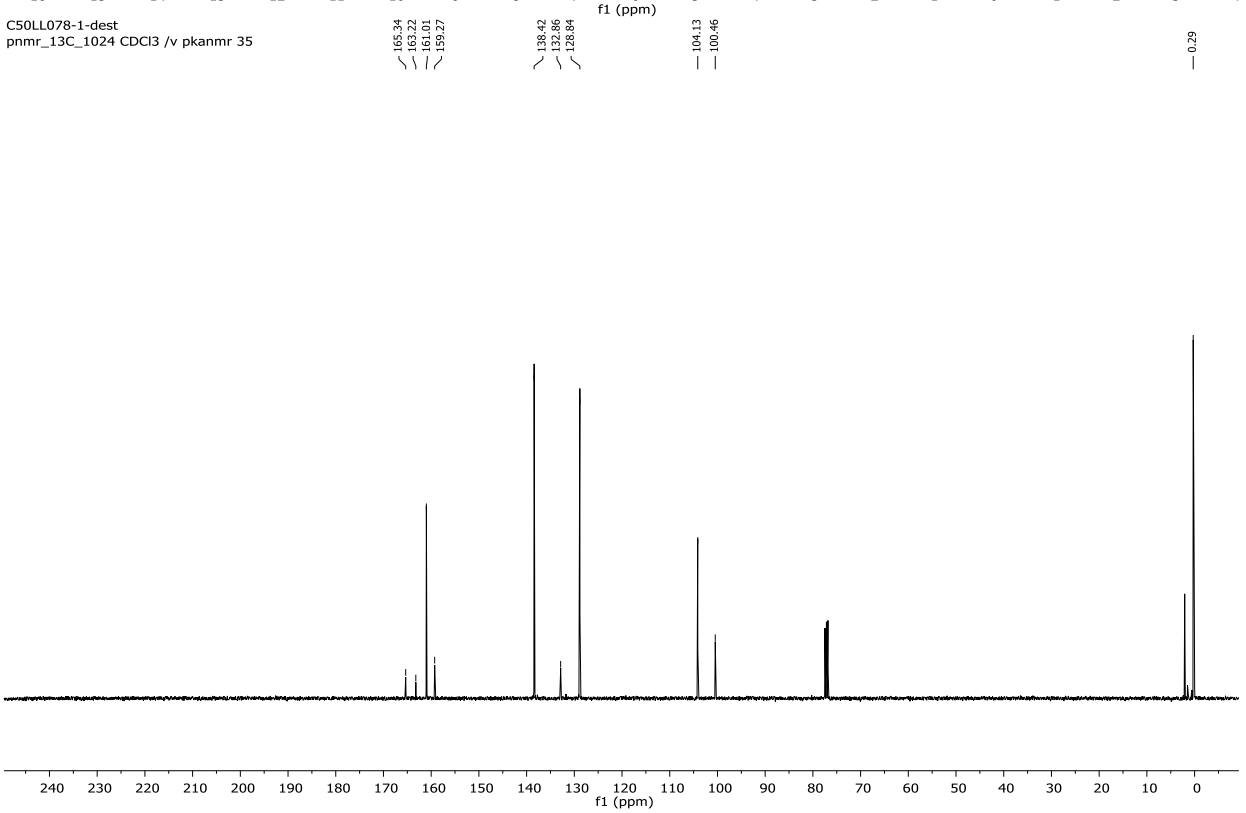
C50LL078-1-dest
pnmr_13C_1024 CDCl3 /v pkanmr 35
165.34
163.22
161.01
159.27
138.42
132.86
128.84
104.13
100.46
0.29
240 230 220 210 200 190 180 170 160 150 140 130 120 110 100 90 80 70 60 50 40 30 20 10 0
f1 (ppm)

A-78 (2R,4S)-tert-butyl 2-(tert-butyl)-4-((4-((2-((4-methoxybenzyl)oxy)pyrimidin-4-yl)carbamoyl)phenyl)carbamoyl)-4-methyloxazolidine-3-carboxylate

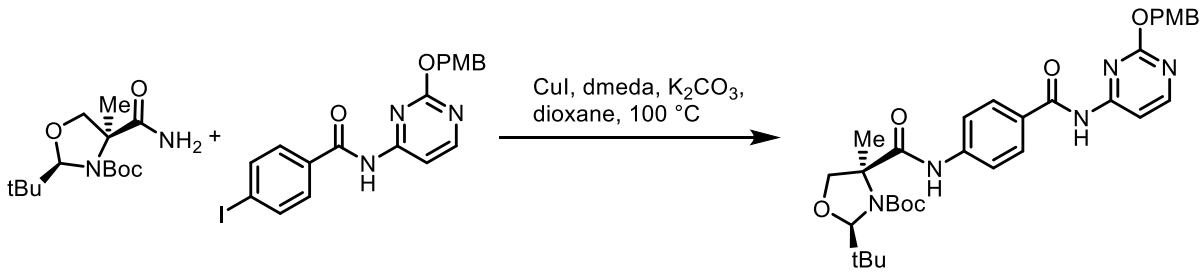

Assay: A flame dried round bottom flask was charged with CuI (21 mg, 0.11 mmol, 0.2 equiv), anhydrous K_2CO_3 (0.30 mg, 2.16 mmol, 2.0 equiv), **A-75** (0.5 g, 1.08 mmol, 1.0 equiv) and **A-55** (325 mg, 1.13 mmol, 1.05 equiv), finally N,N'-dimethylethylenediamine (23 µl, 0.22 mmol, 0.2 equiv) was added and the tube walls were washed with dioxane (4 mL). The flask was then quickly sealed with a rubber septum and the reaction mixture was stirred at 100 °C for 60 h. The reaction mixture was then allowed to reach ambient temperature and filtered over Celite (prewashed with EtOAc). It was concentrated under reduced pressure and purified as such by FC (EtOAc:hexane, 1:5) to give the title compound contaminated with starting material (**A-55**, which is not UV active) thus another purification by FC (EtOAc:toluene, 2:3) gave the title compound (402 mg, 0.65 mmol, 60%).

Analytics: $\mathbf{R_f}$ = 0.21 (EtOAc:hexane, 1:3). **^{1}H NMR** (400 MHz, $CDCl_3$) δ 10.36 (s, 1H), 8.47 (d, *J* = 5.6 Hz, 1H), 8.44 (s, 1H), 7.96 (d, *J* = 5.6 Hz, 1H), 7.88 (d, *J* = 8.7 Hz, 2H), 7.70 (d, *J* = 8.7 Hz, 2H), 7.41 (d, *J* = 8.6 Hz, 2H), 6.90 (d, *J* = 8.6 Hz, 2H), 5.37 (s, 2H), 5.21 (s, 1H), 4.82 (d, *J* = 8.8 Hz, 1H), 3.82 (d, *J* = 7.3 Hz, 4H), 1.73 (s, 3H), 1.54 (s, 9H), 0.92 (s, 9H). **^{13}C NMR** (101 MHz, Chloroform-*d*) δ 171.86, 165.23, 164.62, 160.58, 159.57, 159.37, 155.98, 142.62, 129.84 (2 C), 128.70 (2 C), 128.51, 128.30, 119.42 (2 C), 113.90 (2 C), 104.23, 98.03, 83.07, 76.08, 68.96, 68.12, 55.33, 38.26, 28.21 (3 C), 26.20 (3 C), 22.15. **HRMS (MALDI)**: 642.2897 $[M+Na]^+$; calculated for $[C_{33}H_{41}N_5NaO_7]$: 642.2898. **$[\alpha]^{20}_D$** = -91.20 (c = 1, $CHCl_3$). **IR** [ATR, neat]: ν = 2949.59 w, 1690.3 s, 1587.13 s, 1509.99 s, 1458.88 w, 1435.74 w, 1395.25 m, 1355.71 s, 1288.22 s, 1249.65 s, 1175.4 s, 1110.8 m, 830.205 m cm^{-1}. **m.p.:** 75°C.

C49LL067-d-full
pnmr_1H_16 CDCl3 /v pkanmr 58

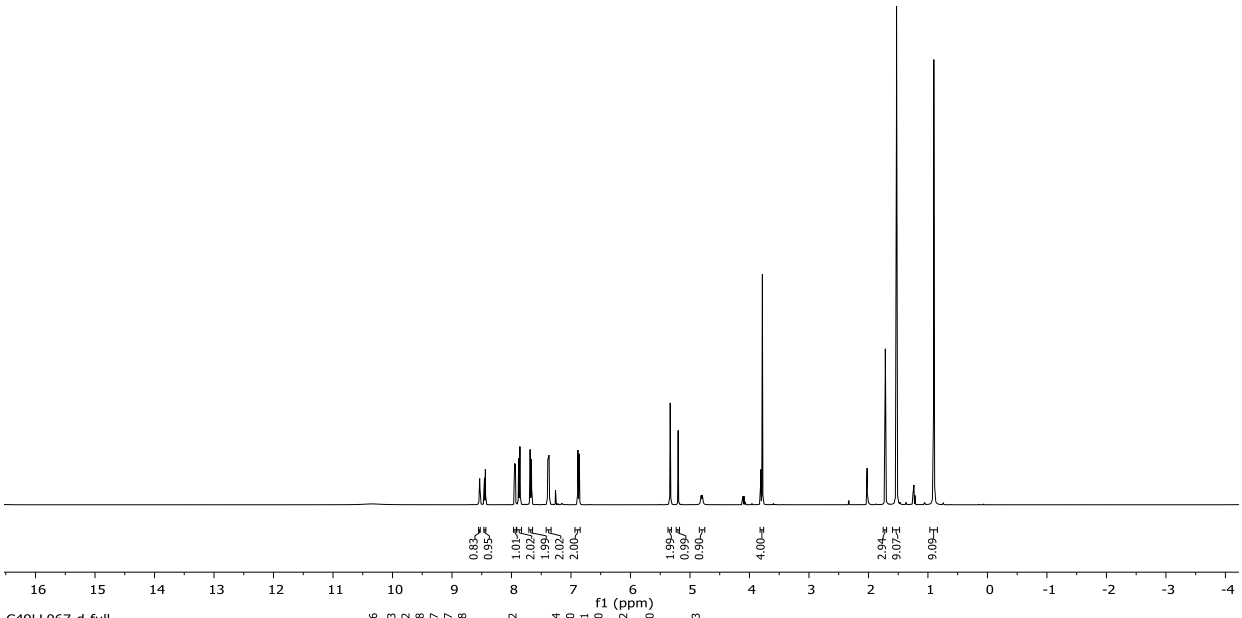

C49LL067-d-full
pnmr_13C_1024 CDCl3 /v pkanmr 58

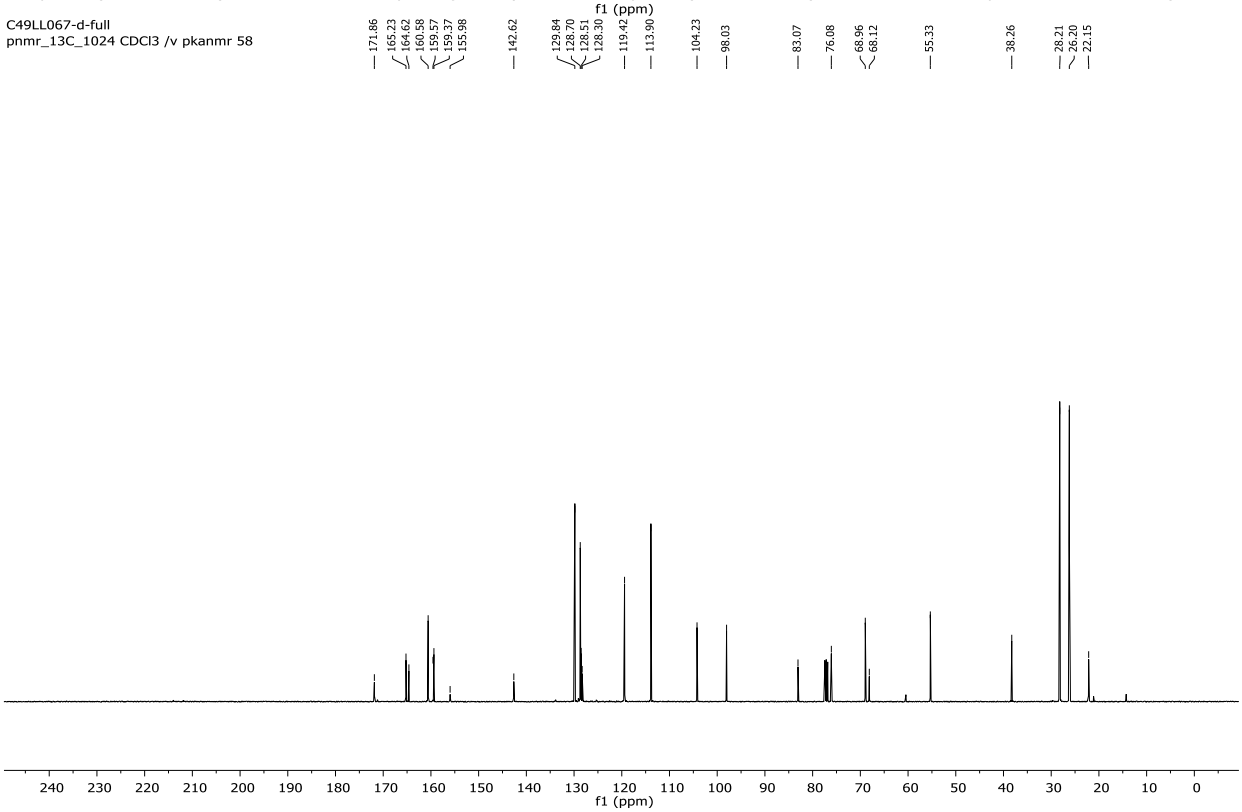

A-53 (2R,4S)-tert-butyl 2-(tert-butyl)-4-methyl-4-((4-((2-oxo-1,2-dihydropyrimidin-4-yl)carbamoyl)phenyl)carbamoyl)oxazolidine-3-carboxylate

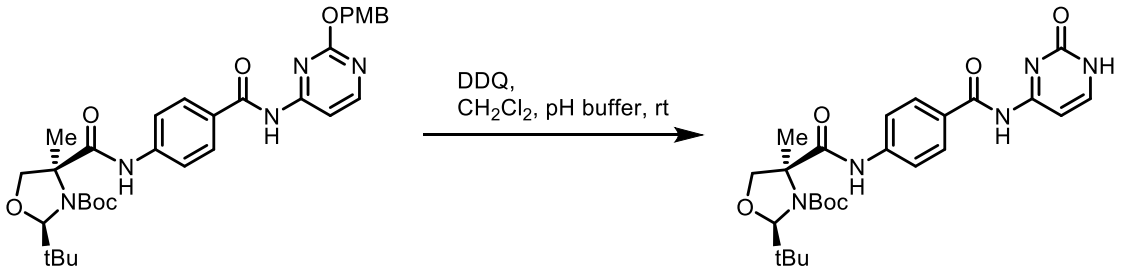

Assay: To a stirring solution of **A-78** (50 mg, 0.081 mmol, 1.0 equiv) in CH_2Cl_2 (0.8 mL) and pH 7 buffer (0.08 mL), was added DDQ (55 mg, 0.24 mmol, 3.0 equiv) at ambient temperature. The reaction mixture was stirred as such for 72 h. It was then quenched by the addition of saturated aqueous $NaHCO_3$ and the sluggish crude was directly filtered over a Nutsch filter. The brownish precipitate was then washed with saturated aqueous $NaHCO_3$ and H_2O. The brown crude was then taken up in EtOH and recrystallized from MeOH and Hexane and dried *in vacuo* to give the title compound (39 mg, 0.078 mmol, 96%).

Analytics: No $\mathbf{R_f}$ can be given. ^{1}**H NMR** (500 MHz, DMSO-d_6) δ 11.52 (s, 1H), 9.57 (s, 1H), 8.04 (d, *J* = 8.6 Hz, 2H), 7.87 (d, *J* = 6.8 Hz, 1H), 7.66 (d, *J* = 8.4 Hz, 2H), 6.86 (s, 1H), 5.07 (s, 1H), 4.41 (d, *J* = 8.6 Hz, 1H), 3.85 (d, *J* = 8.6 Hz, 1H), 1.64 (s, 3H), 1.44 (s, 9H), 0.91 (s, 9H).^{13}**C NMR** (126 MHz, DMSO-d_6) δ 170.95, 163.98, 156.86, 154.86, 141.82, 129.98 (2 C), 119.71 (2 C), 97.31, 96.45, 81.83, 76.37, 68.08, 38.55, 28.19 (3 C), 26.45 (3 C), 21.62. **HRMS (MALDI)**: 500.2505 $[M+H]^+$; calculated for $[C_{25}H_{34}N_5O_6]$: 500.2504. $\mathbf{[\alpha]^{20}_D}$ = -49.00 (c = 0.2, DMSO). **IR** [ATR, neat]: ν = 3673.25 w, 2974.66 s, 2904.27 s, 236093 s, 2337.78 s, 1685.48 m, 1605.93 m, 1453.58 m, 1396.69 m, 1248.68 m, 1052.46 s, 893.84 w cm^{-1}.

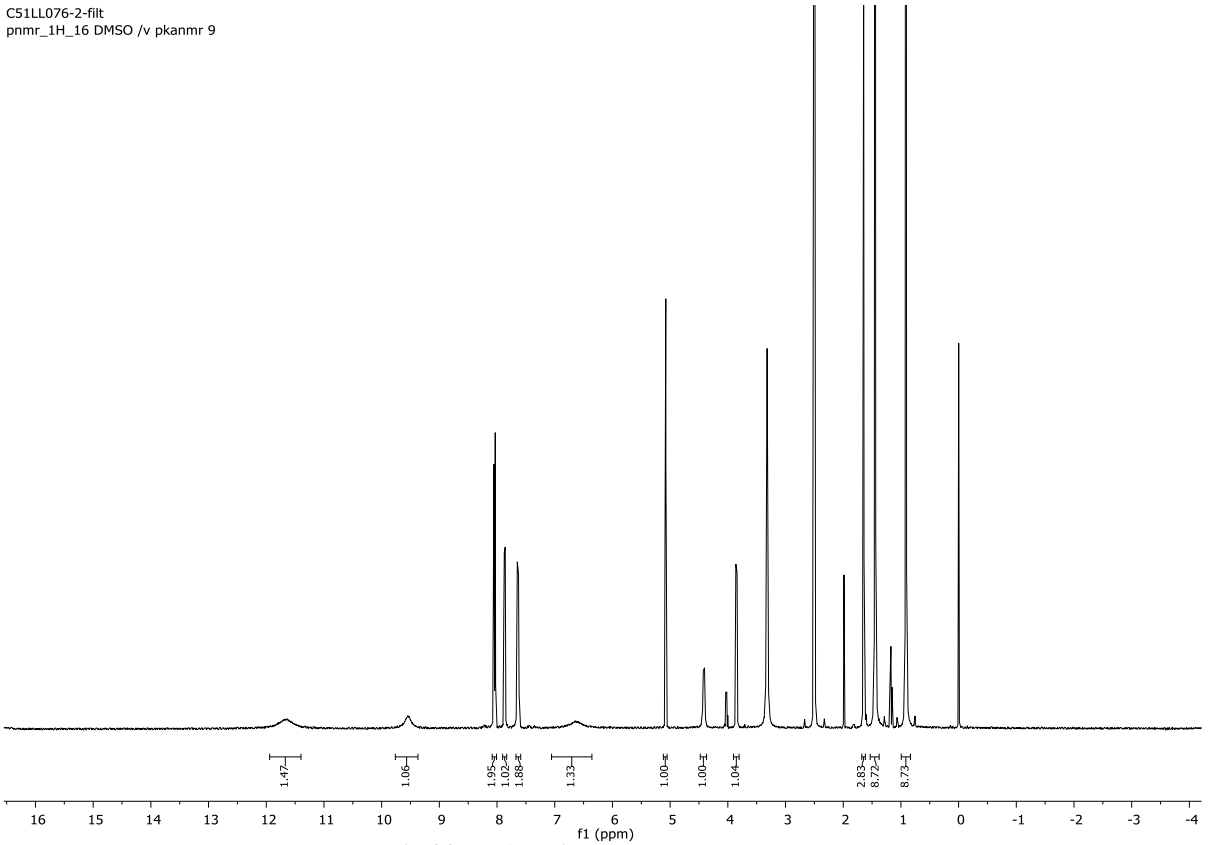
C51LL076-2-filt
pnmr_1H_16 DMSO /v pkanmr 9
1.47
1.06
1.95
1.02
1.88
1.33
1.00
1.00
1.04
2.83
8.72
8.73
f1 (ppm)

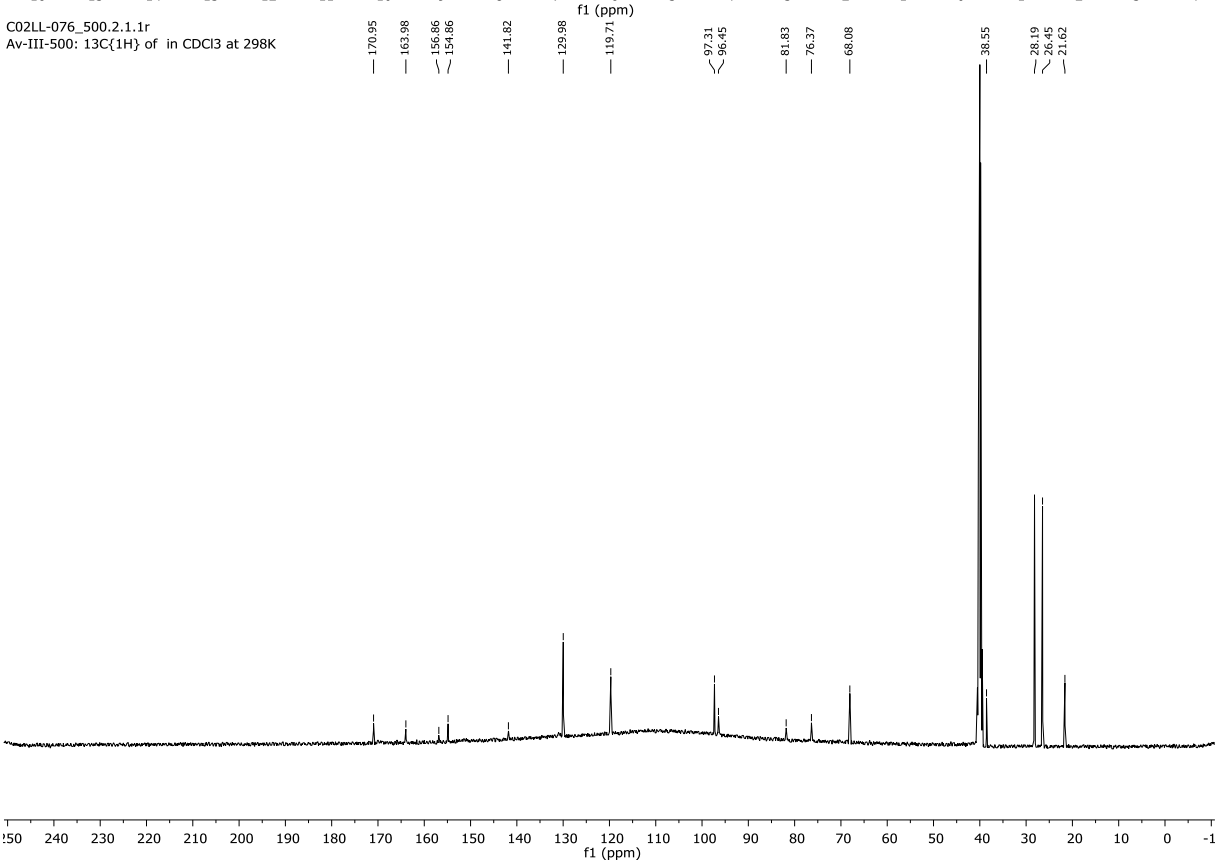
C02LL-076_500.2.1.1r
Av-III-500: 13C{1H} of in CDCl3 at 298K
170.95
163.98
156.86
154.86
141.82
129.98
119.71
97.31
96.45
81.83
76.37
68.08
38.55
28.19
26.45
21.62
f1 (ppm)

A-85 (R)-ethyl 2-((tert-butyldimethylsilyl)oxy)propanoate

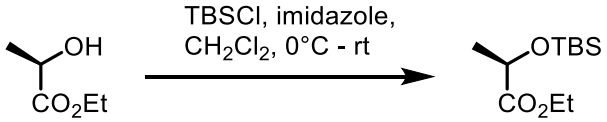

Assay: A-84 (4.0 g, 33.86 mmol, 1.0 equiv) was dissolved in CH_2Cl_2 (170 mL), imidazole (4.61 g, 67.72 mmol, 2.0 equiv) was added and the reaction mixture was cooled to 0 °C. Under vigorous stirring, TBSCl (4.64 g, 44.02 mmol, 1.3 equiv) was added and the reaction mixture was allowed to reach room temperature. After 16 h starting material was fully consumed. The reaction mixture was filtered into a separatory funnel. The remaining white solids, were washed with dichloromethane. The organic phase was washed with 1M HCl (60 mL), sat. aqueous $NaHCO_3$ (60 mL), brine (60 mL) and dried over $MgSO_4$. The solvent was evaporated under reduced pressure. The crude yellow oil was purified by FC (EtOAc:hexane, 1:10) to yield the title compound as a colourless oil (7.55 g, 32.49 mmol, 96%).

Analytics: $\mathbf{R_f}$ = 0.63 (EtOAc:hexane, 1:10). **^{1}H NMR** (400 MHz, $CDCl_3$) δ 4.31 (q, *J* = 6.7 Hz, 1H), 4.25 – 4.08 (m, 2H), 1.39 (d, *J* = 6.8 Hz, 3H), 1.28 (t, *J* = 7.2 Hz, 3H), 0.90 (s, 9H), 0.10 (s, 3H), 0.07 (s, 3H). **^{13}C NMR** (101 MHz, $CDCl_3$) δ 174.28, 68.62, 60.88, 25.87 (3 C), 21.46, 18.47, 14.34, -4.79, -5.12.

Compound literature known

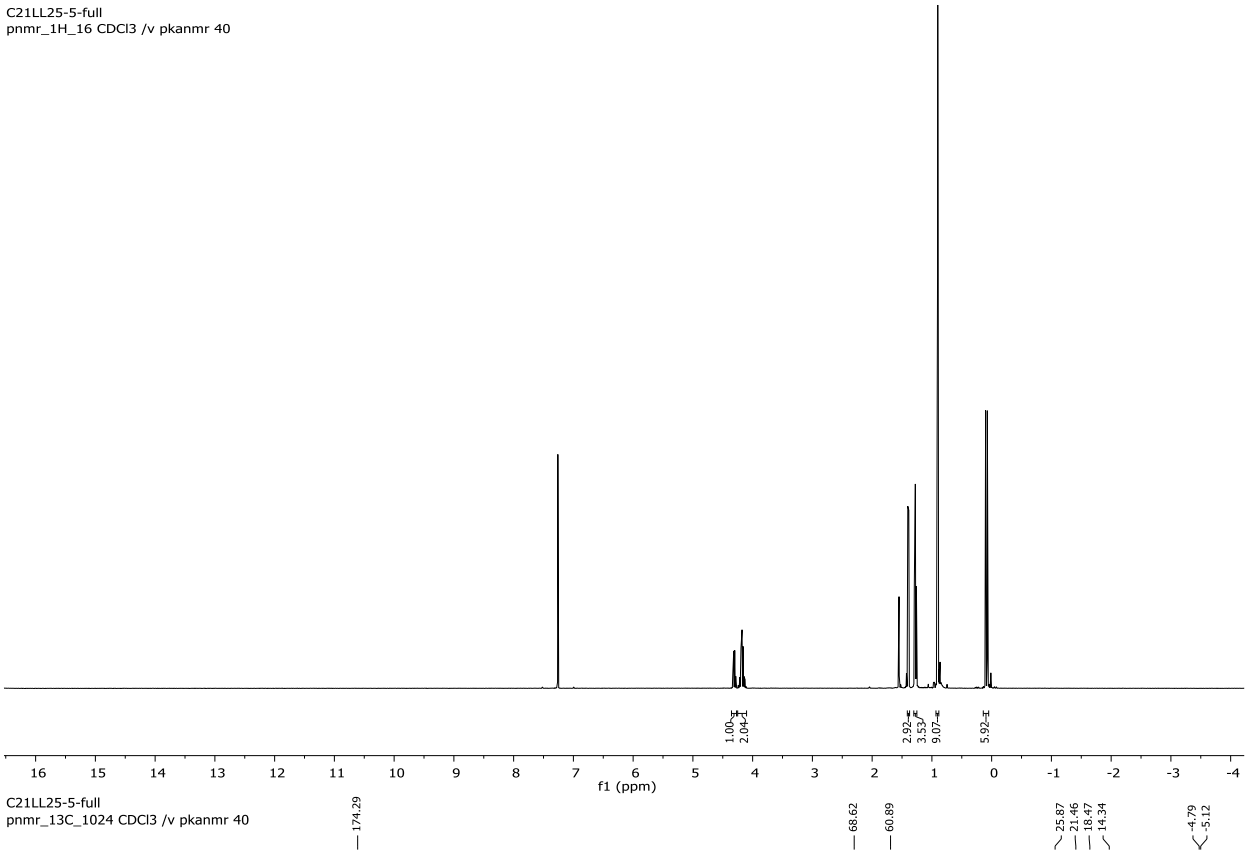
C21LL25-5-full
pnmr_1H_16 CDCl3 /v pkanmr 40
1.00
2.04
2.92
3.53
9.07
5.92
16 15 14 13 12 11 10 9 8 7 6 5 4 3 2 1 0 -1 -2 -3 -4
f1 (ppm)

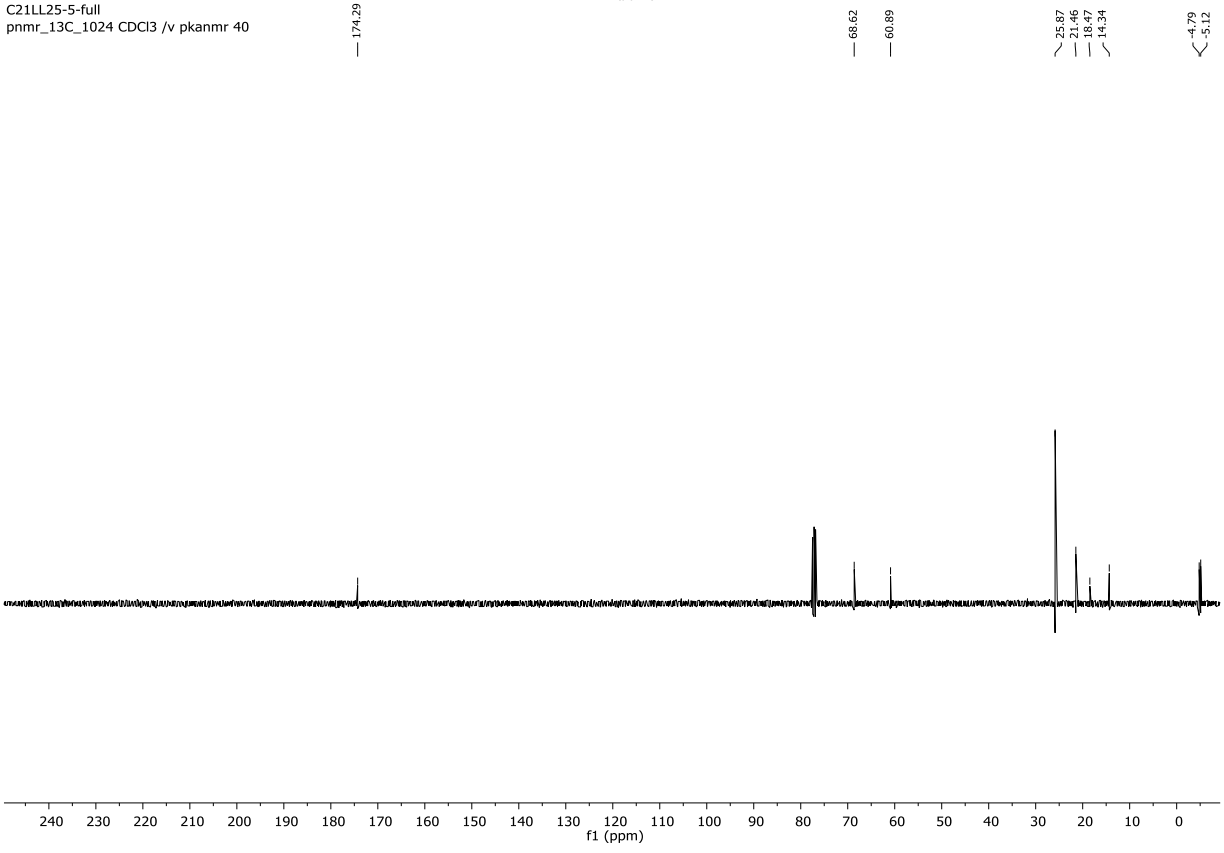
C21LL25-5-full
pnmr_13C_1024 CDCl3 /v pkanmr 40
174.29
68.62
60.89
25.87
21.46
18.47
14.34
-4.79
-5.12
240 230 220 210 200 190 180 170 160 150 140 130 120 110 100 90 80 70 60 50 40 30 20 10 0
f1 (ppm)

A-86 (3S,4R)-4-((tert-butyldimethylsilyl)oxy)pent-1-en-3-ol

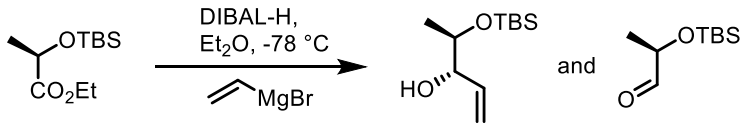

Assay: A-85 (10.70 g, 46.02 mmol, 1.0 equiv) which was co-evaporated in benzene (3 x 5 mL) was dissolved in diethyl ether (260 mL) and cooled to - 90 °C (in an EtOAc/liquid nitrogen bath). DIBALH (1 M in CH_2Cl_2, 63.05 mL, 1.37 equiv) was then dropwise added via syringe pump (0.6 mL/min with a Hamilton glass pipette 25 mL) while the reaction mixture was kept at around – 85 °C. Briefly after complete DIBALH addition, the starting material was fully consumed (TLC analysis confirmed; EtOAc:hexane, 1:10). MeOH (10 mL) was then added in order to quench the reaction, followed by the addition of saturated potassium tartrate (250 mL) and the reaction mixture was allowed to reach room temperature. The biphasic mixture was stirred for 90 min. The two phases were then separated and the aqueous phase was extracted with diethyl ether (3 x 25 mL). The combined organic phases were dried over $MgSO_4$ and the solvent was evaporated under reduced pressure. The clear oil was purified by FC (diethyl ether:hexane, 1:10) to give the aldehyde in reasonable purity (no epimerisation took place. Confirmed by α_D).

The clear oil was then dissolved in diethyether (260 mL) and again cooled to – 90 °C. Dropwise addition of the Grignard reagent (1M in THF, 92.04 mL, 2.0 equiv) was conducted (1.1 mL/min with a Hamilton glass pipette 25 mL. Attention; Grignard can freeze!). After full addition, the reaction mixture was allowed to stir for another 45 min. The reaction mixture was quenched by the addition of MeOH (10 mL) and aqueous sat. $NaHCO_3$ (150 mL) and stirred as such for 45 min (After quenching, a sluggish, viscous phase starts to form which dissolves over time -> nicely separable phases). The two layers were then separated and the aqueous layer was extracted with diethyl ether (3 x 50 mL). The combined organic phases were dried over $MgSO_4$ and the solvent was evaporated under reduced pressure. The crude oil was purified by FC (diethyl ether:hexane 1:10) to give the title compound **6** (5.76 g, 26.6 mmol, 59%, dr: 3.7:1) and reisolated aldehyde (1.681 g, 8.925 mmol, 19%).

Analytics: $\mathbf{R_f}$ = 0.27 (EtOAc:hexane, 1:10). **^{1}H NMR** (400 MHz, $CDCl_3$) δ 5.88 – 5.69 (m, 1H), 5.29 (dt, 1H), 5.20 (dt, 1H), 4.07 – 4.00 (m, 1H), 3.86 (qd, *J* = 6.3, 3.6 Hz, 1H), 2.27 (d, *J* = 4.2 Hz, 1H), 1.08 (d, *J* = 6.3 Hz, 3H), 0.90 (s, 9H), 0.09 (s, 6H). **^{13}C NMR** (101 MHz, $CDCl_3$) δ 136.68, 116.66, 76.68, 71.43, 25.94 (3 C), 18.20, 17.72, -4.28, -4.71. **$[\alpha]^{20}_D$** = 10.1 (c = 1, $CHCl_3$) for the aldehyde. **IR** [ATR, neat]: ν = 2955.37 w, 2929.34 w, 2884.99 w, 2857.99 w, 1473.35 w, 1463.71 w, 1254.47 m, 1147.44 w, 1093.44 m, 1047.16 m, 979.66 m, 833.10 s, 774.28 s cm^{-1}.

Compound literature known

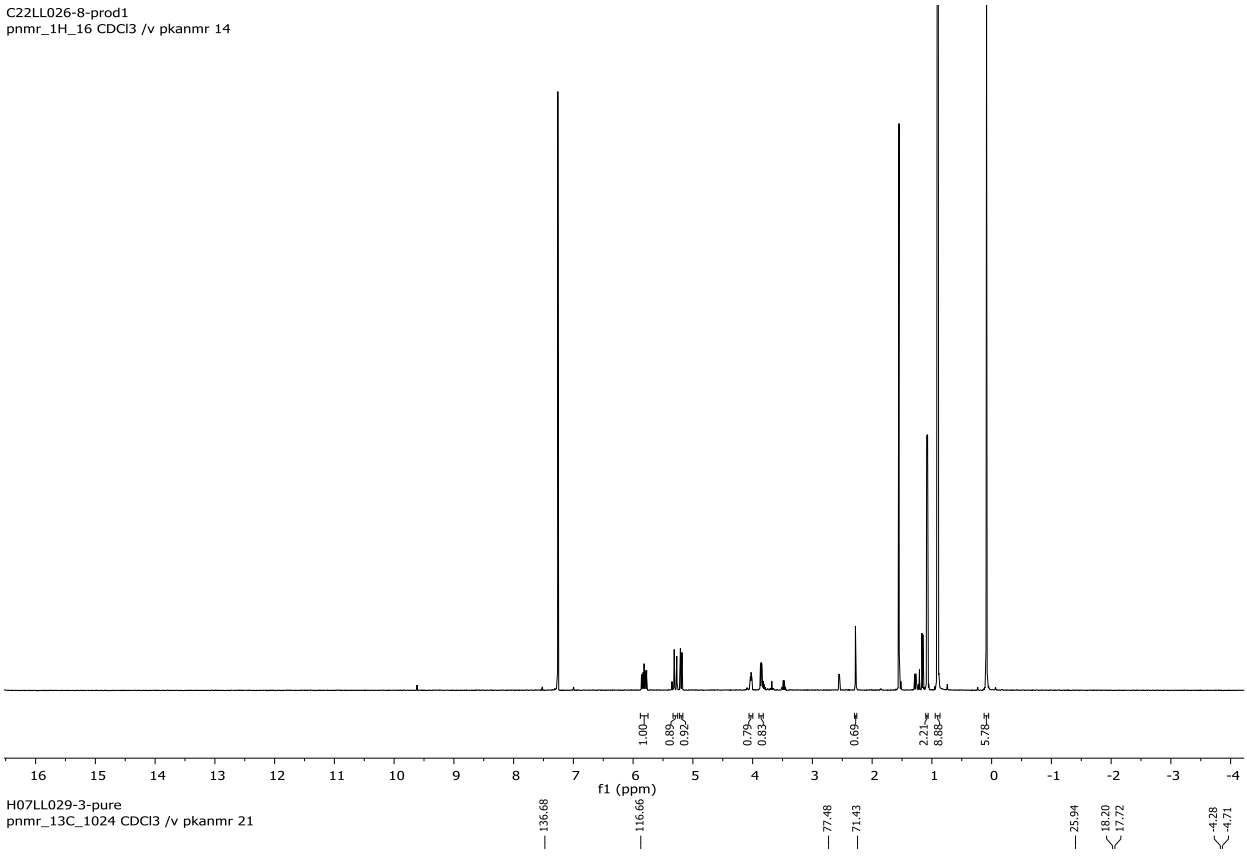
C22LL026-8-prod1
pnmr_1H_16 CDCl3 /v pkanmr 14
1.00
0.89
0.92
0.79
0.83
0.69
2.21
8.88
5.78
f1 (ppm)

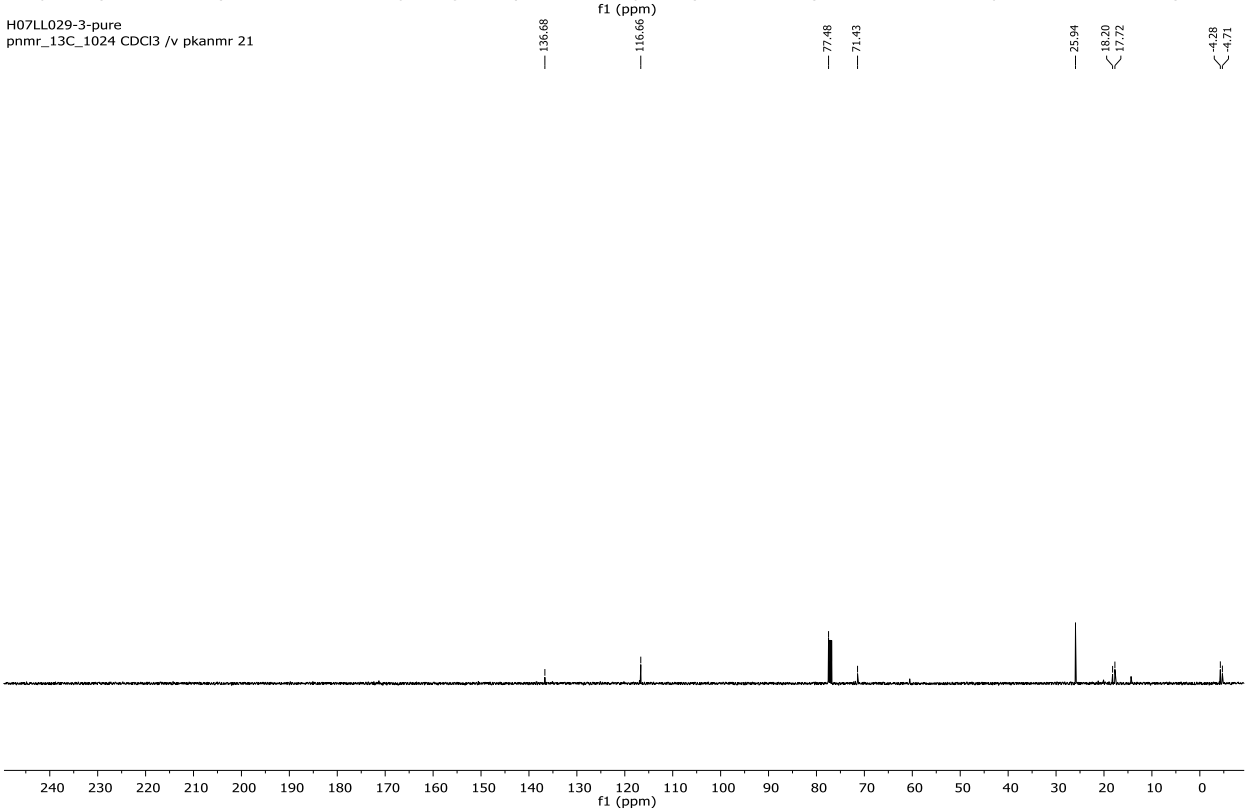
H07LL029-3-pure
pnmr_13C_1024 CDCl3 /v pkanmr 21
136.68
116.66
77.48
71.43
25.94
18.20
17.72
-4.28
-4.71
f1 (ppm)

A-87 (1R,2S)-tert-Butyl-[2-(2-methoxy-ethoxymethoxy)-1-methyl-but-3-enyloxy]dimethylsilane

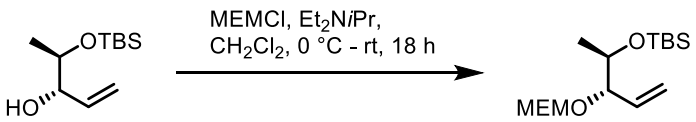

Assay: Crude **A-86** (440 mg, 2.03 mmol, 1.0 equiv) was dissolved in dichloromethane (5 mL) and DIPEA (1.36 mL, 7.79 mmol, 3.8 equiv) was added. The reaction mixture was cooled to 0 °C and MEM-chloride (0.58 mL, 5.08 mmol, 2.5 equiv) was added. After full addition, the reaction mixture was allowed to warm to ambient temperature and was stirred for 18 h. The dark yellow solution was diluted with H_2O and CH_2Cl_2 and saturated aqueous $NaHCO_3$ was added. The two phases were separated and the aqueous phase was washed with CH_2Cl_2 (2 x 5 mL). The yellow oil was purified by FC (EtOAc:hexane, 1:5) to give the title compound (410.5 mg, 1.35 mmol, 66%).

Analytics: $\mathbf{R_f}$ = 0.29 (EtOAc:hexane, 1:5). **^{1}H NMR** (400 MHz, Chloroform-*d*) δ 5.83 – 5.59 (m, 1H), 5.33 – 5.10 (m, 2H), 4.73 (dd, *J* = 32.7, 6.8 Hz, 2H), 3.90 – 3.84 (m, 1H), 3.83 – 3.72 (m, 2H), 3.67 – 3.59 (m, 1H), 3.57 – 3.50 (m, 2H), 3.39 (s, 3H), 1.14 (d, *J* = 6.2 Hz, 3H), 0.87 (s, 9H), 0.05 (d, *J* = 4.3 Hz, 6H). **^{13}C NMR** (101 MHz, $CDCl_3$) δ 135.62, 118.99, 93.15, 81.86, 71.92, 70.84, 67.03, 59.17, 26.00 (3 C), 19.82, 18.29, -4.43, -4.48.

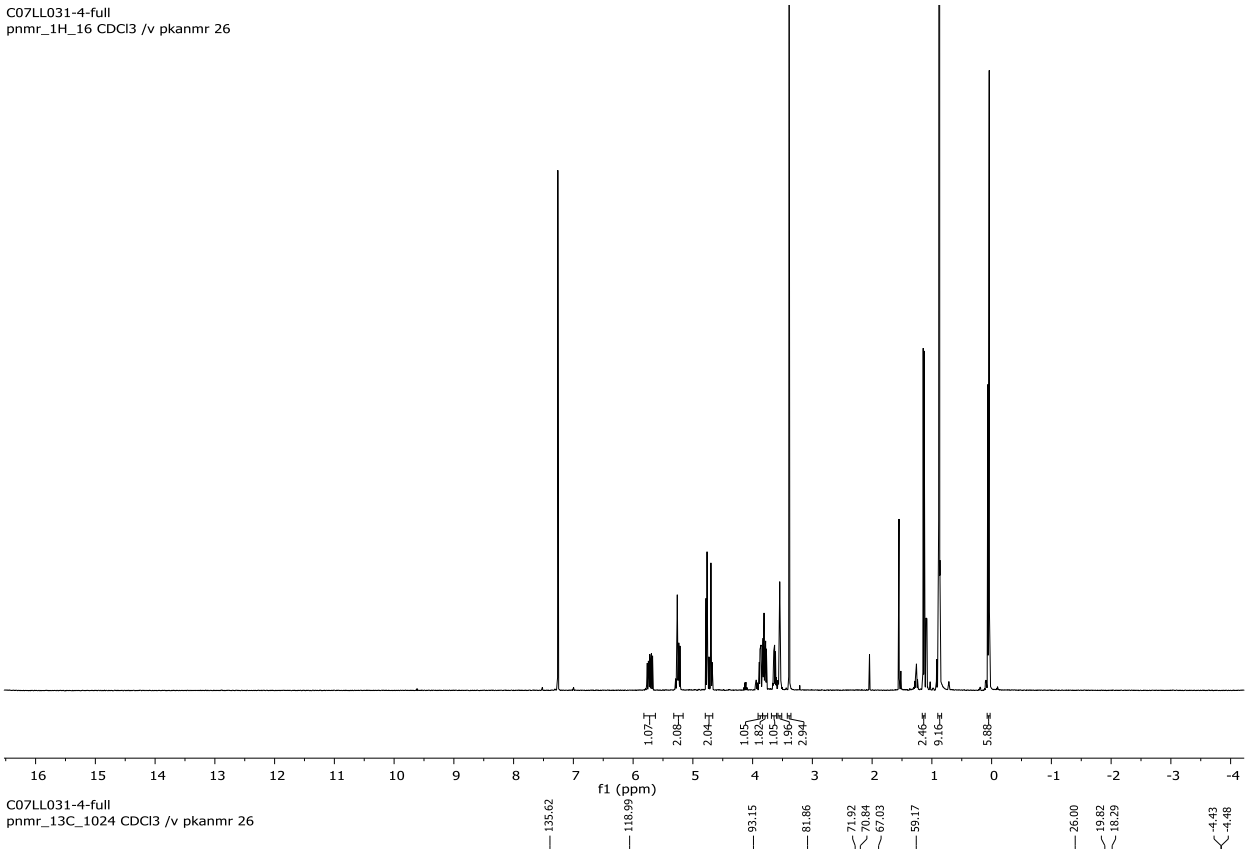
C07LL031-4-full
pnmr_1H_16 CDCl3 /v pkanmr 26
1.07
2.08
2.04
1.05
1.82
1.05
1.96
2.94
2.46
9.16
5.88
f1 (ppm)
C07LL031-4-full
pnmr_13C_1024 CDCl3 /v pkanmr 26
135.62
118.99
93.15
81.86
71.92
70.84
67.03
59.17
26.00
19.82
18.29
-4.43
-4.48
f1 (ppm)

A-88 (2R,3S)-3-((2-methoxyethoxy)methoxy)pent-4-en-2-ol

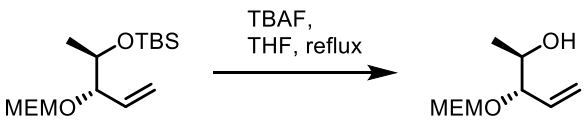

Assay: A-87 (390 mg, 1.80 mmol, 1.0 equiv) was dissolved in THF (14 mL) and TBAF (1 M in THF, 3.60 mL, 2.0 equiv) was added to the reaction mixture and the solution was heated up to 60 °C. After 50 min at elevated temperature the reaction mixture was allowed to reach room temperature. The reaction mixture was poured onto a biphasic EtOAc / H_2O mixture. The two layers were separated and the aqueous phase was twice extracted with EtOAc (10 mL). The combined organic phases where dried over $MgSO_4$ and the solvent was evaporated under reduced pressure. The crude oil was purified by FC (EtOAc:hexane, 1:1) giving the title compound (259.1 mg, 1.36 mmol, 76 %) in only reasonable purity.

Analytics: $\mathbf{R_f}$ = 0.13 (EtOAc:hexane, 1:1). **^{1}H NMR** (400 MHz, $CDCl_3$) δ 5.69 (ddd, *J* = 17.1, 10.7, 7.6 Hz, 1H), 5.22 (dddd, *J* = 17.1, 11.4, 1.8, 1.0 Hz, 2H), 4.87 – 4.56 (m, 2H), 3.91 (dd, *J* = 7.6, 3.7 Hz, 1H), 3.83 – 3.70 (m, 2H), 3.68 – 3.50 (m, 2H), 3.48 (t, 2H), 3.30 (s, 3H), 2.87 (s, 1H), 1.06 (d, *J* = 6.5 Hz, 3H). **^{13}C NMR** (101 MHz, Chloroform-*d*) δ 135.44, 135.07, 118.95, 116.62, 93.19, 79.67, 76.98, 71.91, 70.36, 67.04, 59.16, 15.77.

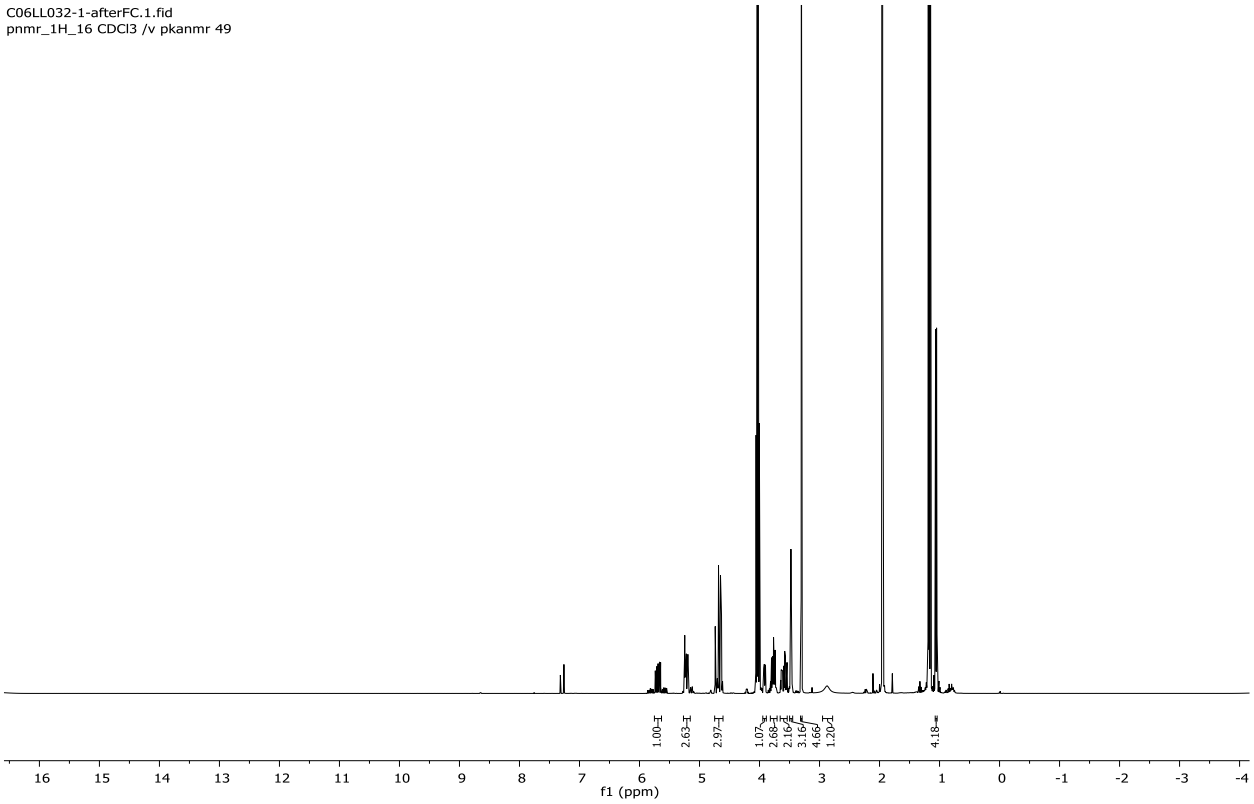
C06LL032-1-afterFC.1.fid
pnmr_1H_16 CDCl3 /v pkanmr 49
1.00
2.63
2.97
1.07
2.68
2.16
3.16
4.66
1.20
4.18
f1 (ppm)

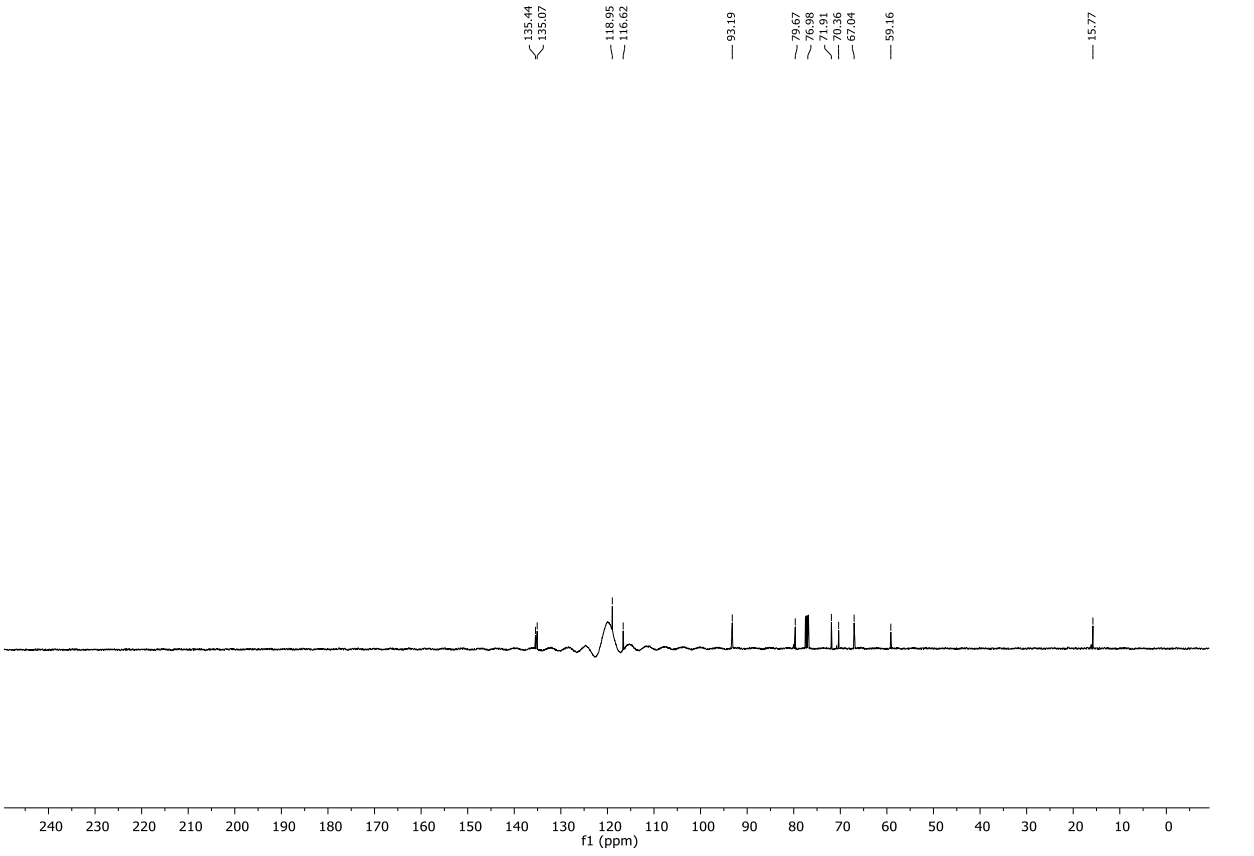
135.44
135.07
118.95
116.62
93.19
79.67
76.98
71.91
70.36
67.04
59.16
15.77
f1 (ppm)

A-89 (8S,9R)-9-methyl-8-vinyl-2,5,7,10-tetraoxatridec-12-ene

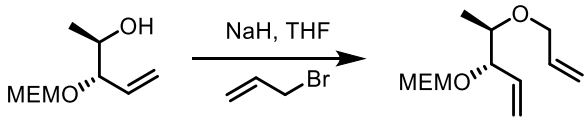

Assay: To a solution of **A-88** (20 mg, 0.11 mmol, 1.0 equiv) in THF (1.5 mL), was given NaH 60 wt % in mineral oil (8.4 mg, 0.21 mmol, 2.0 equiv) and the reaction mixture was refluxed at 67 °C. After 30 min. allyl bromide (0.03 mL, 0.21 mmol, 2.0 equiv) was added and the reaction mixture was stirred for another 60 min. at 67 °C. After full consumption of starting material, the reaction mixture was allowed to reach room temperature. The reaction mixture was poured onto a mixture of H_2O (5 mL) and EtOAc (5 mL). The aqueous phase was then separated and extracted with EtOAc (3 x 5 mL). The combined organic phases where dried over $MgSO_4$ and concentrated under reduced pressure. The crude yellow oil was purified by FC (EtOAc:hexane, 1:5) to give the title compound (16 mg, 0.07 mmol, 66 %).

Analytics: $\mathbf{R_f}$ = 0.36 (1:5, EtOAc:hexaneane). **^{1}H NMR** (400 MHz, Chloroform-*d*) δ 5.91 (ddt, *J* = 17.2, 10.9, 5.5 Hz, 1H), 5.82 – 5.70 (m, 1H), 5.33 – 5.22 (m, 3H), 5.14 (dd, *J* = 10.4, 1.7 Hz, 1H), 4.78 (d, *J* = 6.9 Hz, 1H), 4.72 (d, *J* = 6.9 Hz, 1H), 4.11 – 4.08 (m, 1H), 4.06 (dt, *J* = 5.5, 1.5 Hz, 2H), 3.87 – 3.77 (m, 1H), 3.70 – 3.59 (m, 1H), 3.58 – 3.51 (m, 3H), 3.39 (s, 3H), 1.15 (d, *J* = 6.4 Hz, 3H). **^{13}C NMR** (101 MHz, $CDCl_3$) δ 135.44, 135.07, 118.95, 116.62, 93.19, 79.67, 76.98, 71.91, 70.36, 67.04, 59.16, 15.77.

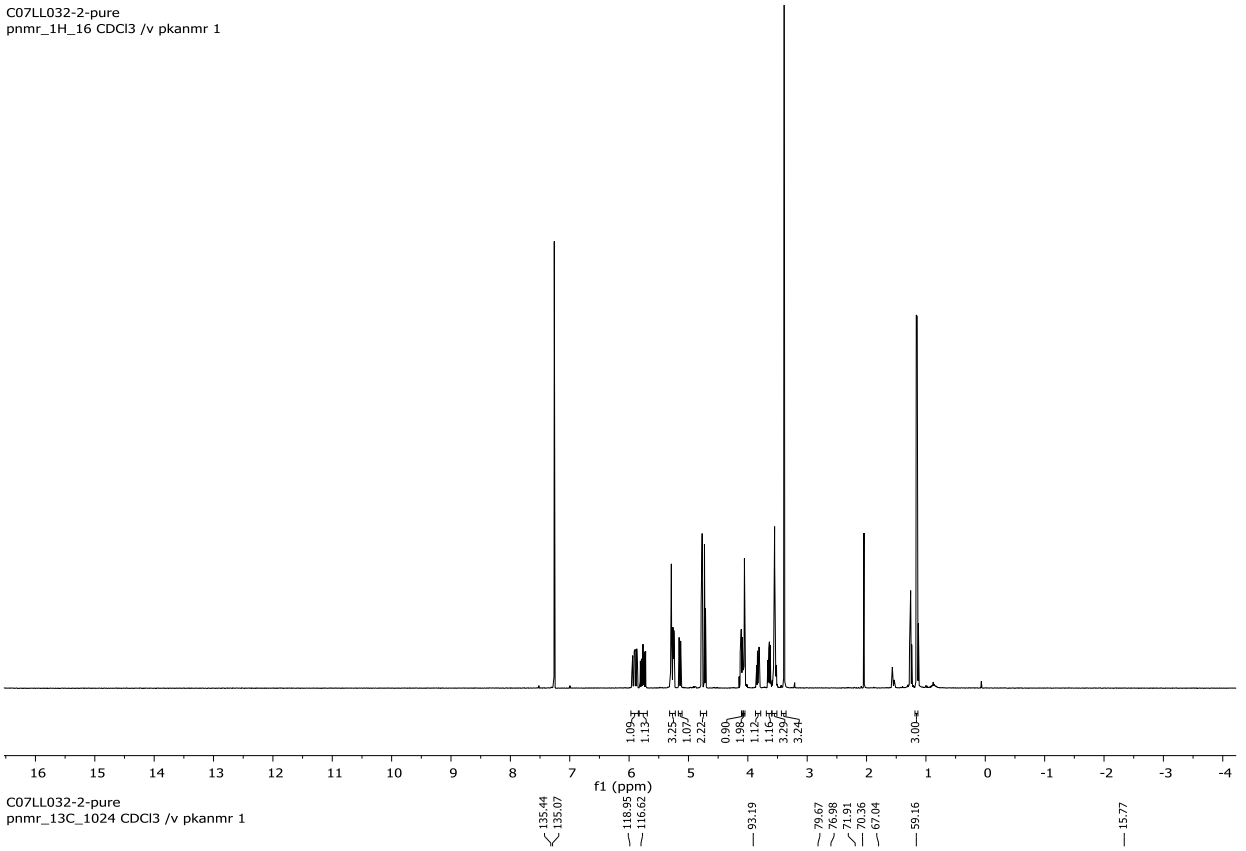
C07LL032-2-pure
pnmr_1H_16 CDCl3 /v pkanmr 1
1.09
1.13
3.25
1.07
2.22
0.90
1.98
1.12
1.16
3.29
3.24
3.00
16 15 14 13 12 11 10 9 8 7 6 5 4 3 2 1 0 -1 -2 -3 -4
f1 (ppm)

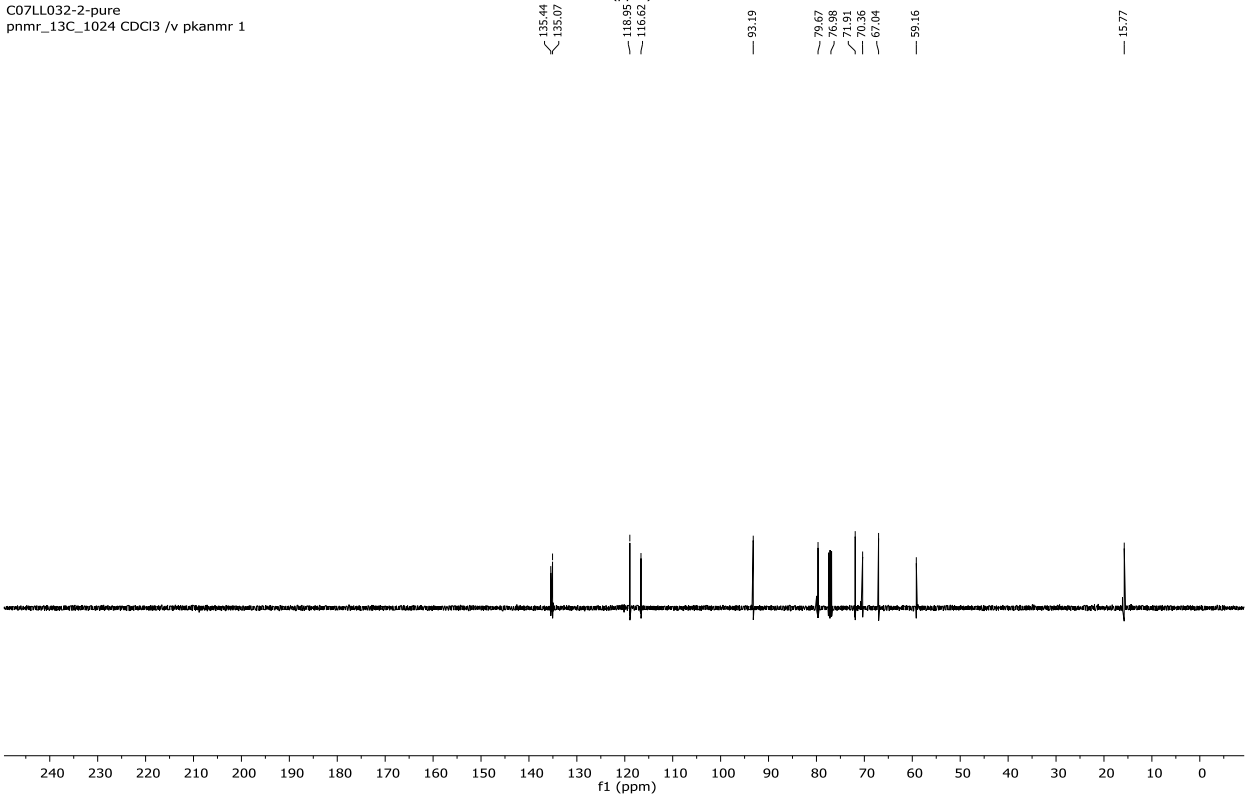
C07LL032-2-pure
pnmr_13C_1024 CDCl3 /v pkanmr 1
135.44
135.07
118.95
116.62
93.19
79.67
76.98
71.91
70.36
67.04
59.16
15.77
240 230 220 210 200 190 180 170 160 150 140 130 120 110 100 90 80 70 60 50 40 30 20 10 0
f1 (ppm)

A-90 (2R,3S)-3-((2-methoxyethoxy)methoxy)-2-methyl-3,4-dihydro-2H-pyran

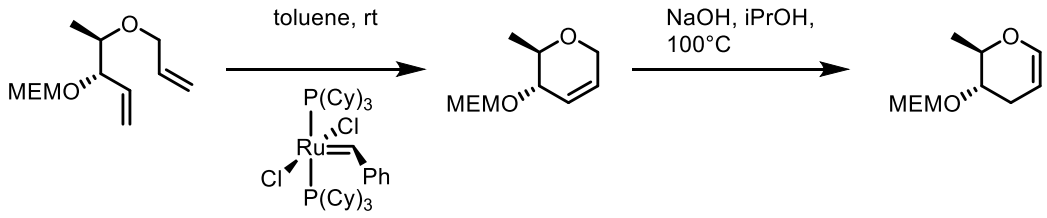

Assay: In the glove box, Grubbs first Generation catalyst (7.8 mg, 9.5 µmol, 5 mol %) was given into a flame dried schlenk tube. Meanwhile, toluene was freeze pumped and set under argon atmosphere. **A-89** (45.5 mg, 0.20 mmol, 1.0 equiv) was then dissolved in toluene (1.0 mL) and given to the ruthenium catalyst. The reaction mixture was stirred for 24 h at ambient temperature. TLC analysis showed full consumption of starting material. Then, isopropanol (0.19 mL) and NaOH (pellets, 5.6 mg) were added to the reaction mixture and the temperature was raised to 100 °C. The reaction mixture was stirred for 1.5 h. The intermediate RCM product was fully consumed and the solution was washed with H_2O. The aqueous phase was then separated and extracted with EtOAc (3 x 5 mL). The combined organic phases where dried over $MgSO_4$. All the volatiles were evaporated under reduced pressure and the residue was purified by FC (EtOAc:hexane, 1:3) to give the title compound (26 mg, 0.129 mmol, 65%).

Analytics: $\mathbf{R_f}$ = 0.48 (EtOAc:hexane 1:1). **^{1}H NMR** (400 MHz, $CDCl_3$) δ 6.29 (dt, *J* = 6.0, 1.9 Hz, 1H), 4.85 (d, *J* = 7.1 Hz, 1H), 4.78 (d, *J* = 7.1 Hz, 1H), 4.62 (ddd, *J* = 6.0, 4.3, 3.3 Hz, 1H), 3.89 (p, *J* = 6.5 Hz, 1H), 3.76 – 3.68 (m, 2H), 3.59 – 3.51 (m, 3H), 3.39 (s, 3H), 2.42 – 2.30 (m, 1H), 2.09 – 1.98 (m, 1H), 1.30 (d, *J* = 6.4 Hz, 3H). **^{13}C NMR** (101 MHz, $CDCl_3$) δ 142.74, 97.58, 94.26, 73.39, 73.36, 71.85, 67.18, 59.20, 25.99, 17.64.

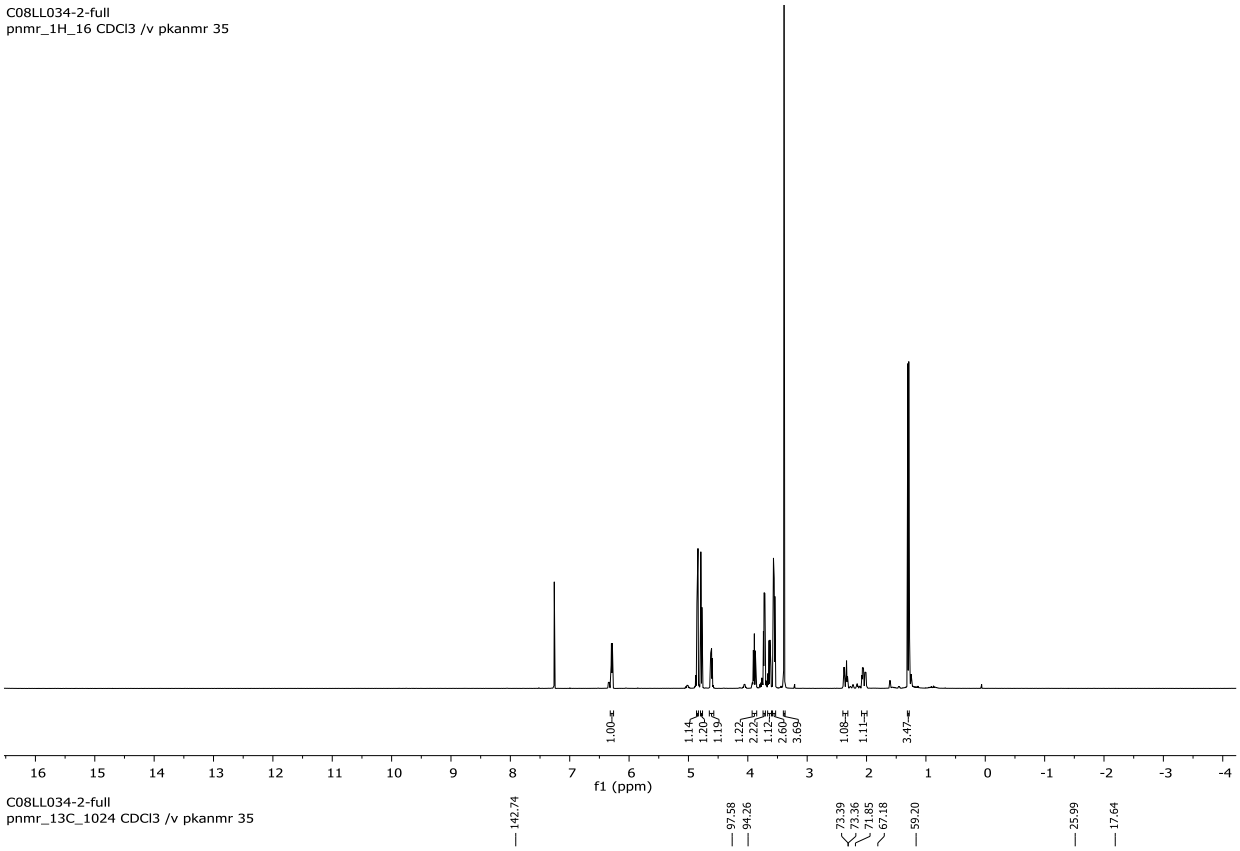
C08LL034-2-full
pnmr_1H_16 CDCl3 /v pkanmr 35
1.00
1.14
1.20
1.19
1.22
2.22
1.12
2.60
3.69
1.08
1.11
3.47
f1 (ppm)

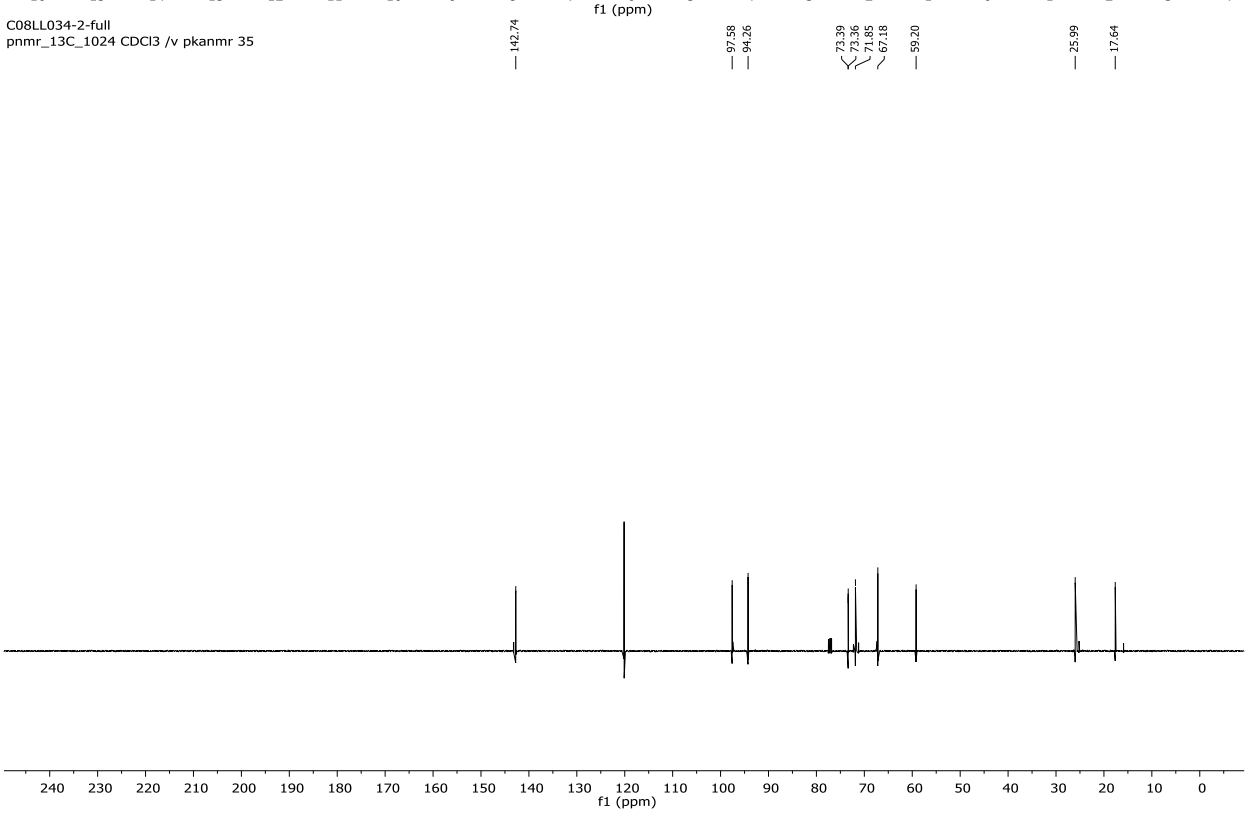
C08LL034-2-full
pnmr_13C_1024 CDCl3 /v pkanmr 35
142.74
97.58
94.26
73.39
73.36
71.85
67.18
59.20
25.99
17.64
f1 (ppm)

A-91 (2R,3S)-6-methoxy-3-((2-methoxyethoxy)methoxy)-2-methyltetrahydro-2H-pyran

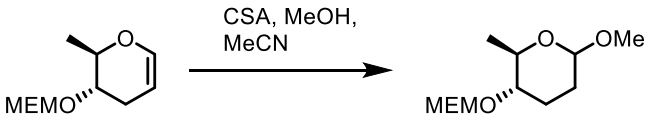

Assay: Glycal **A-90** (30 mg, 0.15 mmol, 1.0 equiv) was dissolved in MeCN (0.8 mL) and MeOH (0.17 mL). CSA (5.2 mg, 22.2 µmol, 0.15 equiv) was then added and the reaction mixture was stirred for 3 h at ambient temperature. After full consumption of starting material, EtOAc (2 mL) and saturated aqueous $NaHCO_3$ (1 mL) was added and the biphasic mixture was poured into a separatory funnel. The aqueous phase was then separated and extracted with EtOAc (3 x 3 mL). The combined organic phases where dried over $MgSO_4$. The crude oil was purified by FC (EtOAc:hexane, 1:2) giving the title compound (25.5 mg, 0.11 mmol, 73%).

Analytics: $\mathbf{R_f}$ = 0.31 (EtOAc:hexane, 1:1). **^{1}H NMR** (400 MHz, $CDCl_3$) δ 4.82 (dd, *J* = 8.9, 7.0 Hz, 1H), 4.71 (dd, *J* = 7.0, 2.2 Hz, 1H), 4.61 (d, *J* = 1.8 Hz, 1H), 3.73 – 3.69 (m, 2H), 3.66 (m, 1H), 3.56 (m, 2H), 3.39 (s, 3H), 3.34 (s, 3H), 3.29 – 3.21 (m, 1H), 2.01 – 1.65 (m, 4H), 1.23 (d, *J* = 6.2 Hz, 3H). **^{13}C NMR** (101 MHz, $CDCl_3$) δ 97.47, 94.12, 77.22, 71.88, 67.74, 67.11, 59.20, 54.54, 29.34, 24.74, 18.35. **HRMS** (ESI): 252.1805 $[M+NH_4^+]^+$; calculated for $[C_{11}H_{26}NO_5]$: 252.1806.

C10LL042-1-full
pnmr_1H_16 CDCl3 /v pkanmr 21

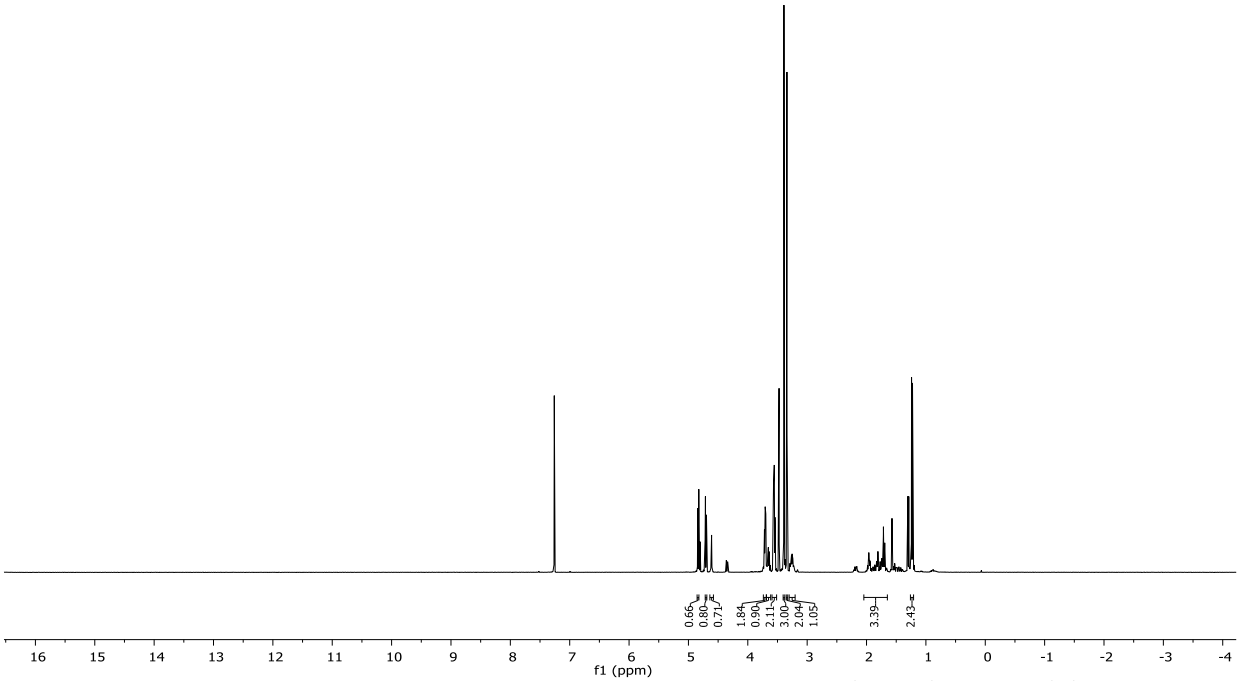

C10LL042-1-full
pnmr_13C_1024 CDCl3 /v pkanmr 21

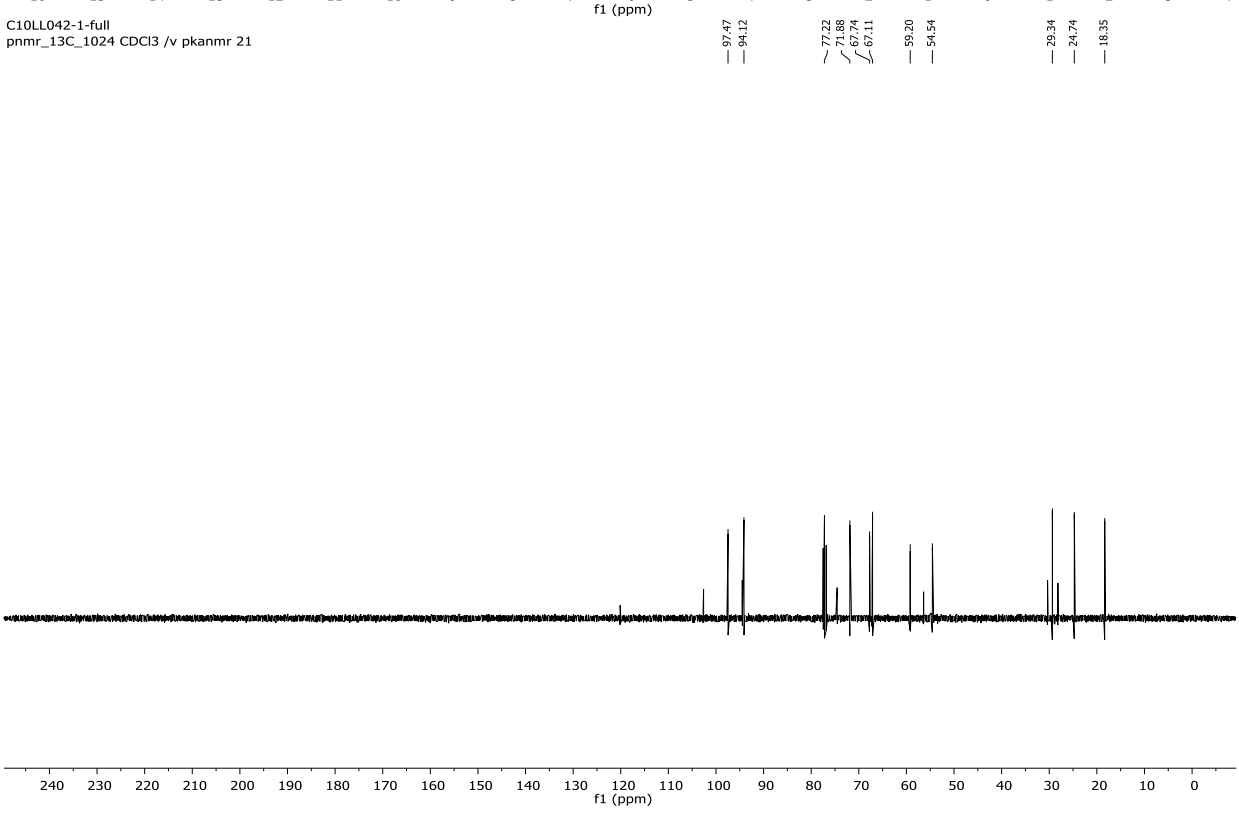

A-99 (((2R,3S)-3-(benzyloxy)pent-4-en-2-yl)oxy)(tert-butyl)dimethylsilane

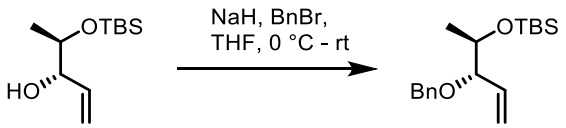

Assay: Allylic alcohol **A-86** (20 mg, 0.092 mmol, 1.0 equiv) was dissolved in THF (0.6 mL) and NaH (60% in mineral oil, 5.5 mg, 0.14 mmol, 1.5 equiv) was added and the reaction mixture was stirred at ambient temperature for 1 h. Then BnBr (13 µl, 0.11 mmol, 1.2 equiv) was added and the reaction mixture was stirred for 4 h. The reaction was quenched with MeOH (until the effervescence ceased) and additional NH_4Cl (3 mL) was added. The biphasic mixture was then poured into a separatory funnel and was separated. The aqueous phase was extracted with EtOAc (3 x 3 mL). The combined organic phases were washed with brine, dried over $MgSO_4$ and concentrated under reduced pressure. Purification by FC (CH_2Cl_2:MeOH, 98:2) gave the title compound (25 mg, 0.081 mmol, 88%).

Analytics: $\mathbf{R_f}$ = 0.28 (EtOAc:hexane 1:49 (trans)) $\mathbf{R_f}$ = 0.21 (EtOAc:hexane 1:49 (cis)). **^{1}H NMR** (400 MHz, $CDCl_3$) δ 7.35 – 7.31 (m, 5H), 5.86 – 5.73 (m, 1H), 5.32 – 5.21 (m, 2H), 4.62 (d, *J* = 12.0 Hz, 2H), 4.41 (d, *J* = 12.0 Hz, 1H), 3.88 – 3.76 (m, 1H), 3.56 (ddd, *J* = 7.6, 5.3, 0.7 Hz, 1H), 1.18 (d, *J* = 6.2 Hz, 3H), 0.87 (d, *J* = 0.8 Hz, 9H), 0.04 (d, *J* = 5.0 Hz, 6H). **^{13}C NMR** (101 MHz, $CDCl_3$) δ 138.96, 136.61, 128.39 (2 C), 127.86 (2 C), 127.48, 118.76, 85.35, 71.05, 70.65, 26.01 (3 C), 20.33, 18.28, -4.36, -4.43. **HRMS** (ESI): 329.1912 $[M+Na]^+$; calculated for $[C_{18}H_{30}NaO_2Si]$: 329.1907. **$[\alpha]^{20}_D$** = +20.43 (c = 3.04, $CHCl_3$). **IR** [ATR, neat]: ν = 2955.37 w, 2929.34 w, 2857.99 w, 1252.54 m, 1130.08 w, 1078.98 m, 1024.98 m, 833.10 s, 774.28 s cm^{-1}.

Compound literature known

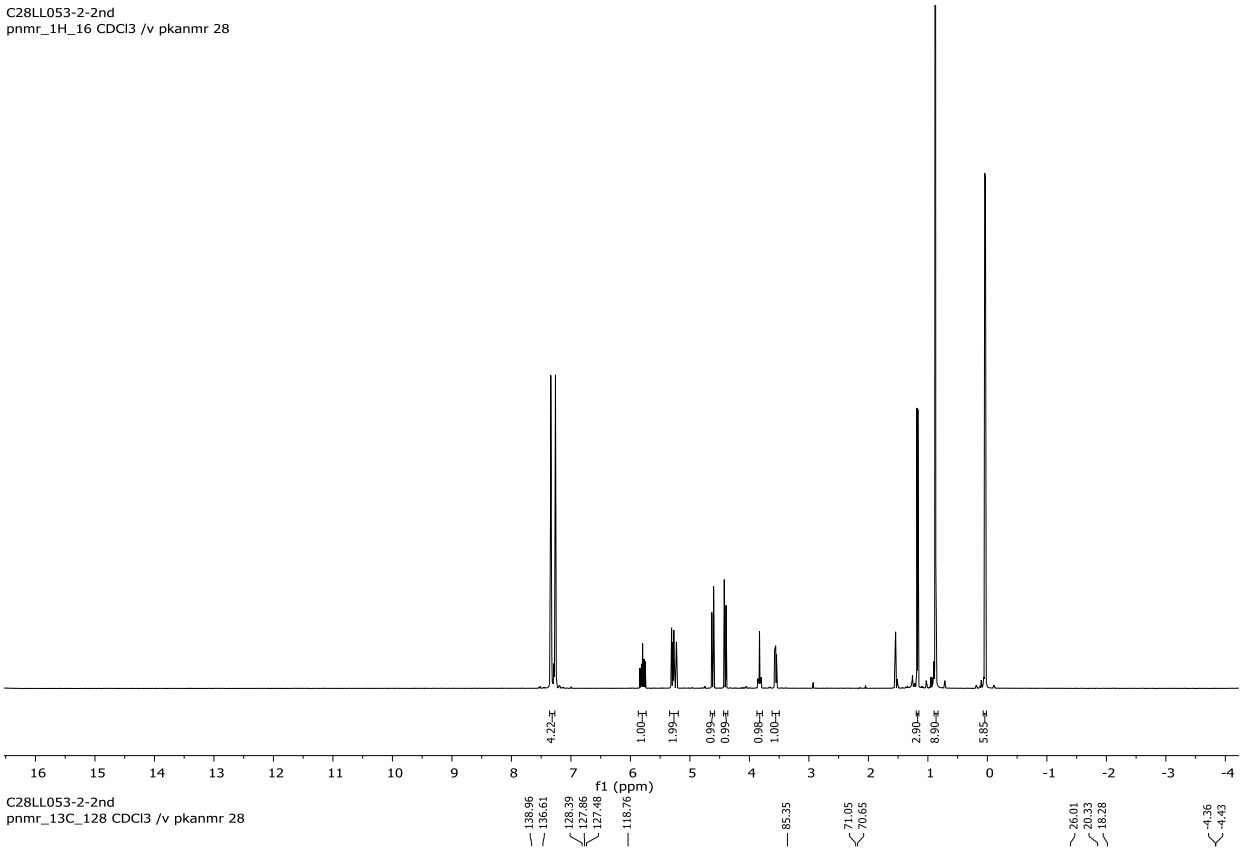
C28LL053-2-2nd
pnmr_1H_16 CDCl3 /v pkanmr 28
4.22
1.00
1.99
0.99
0.99
0.98
1.00
2.90
8.90
5.85
f1 (ppm)

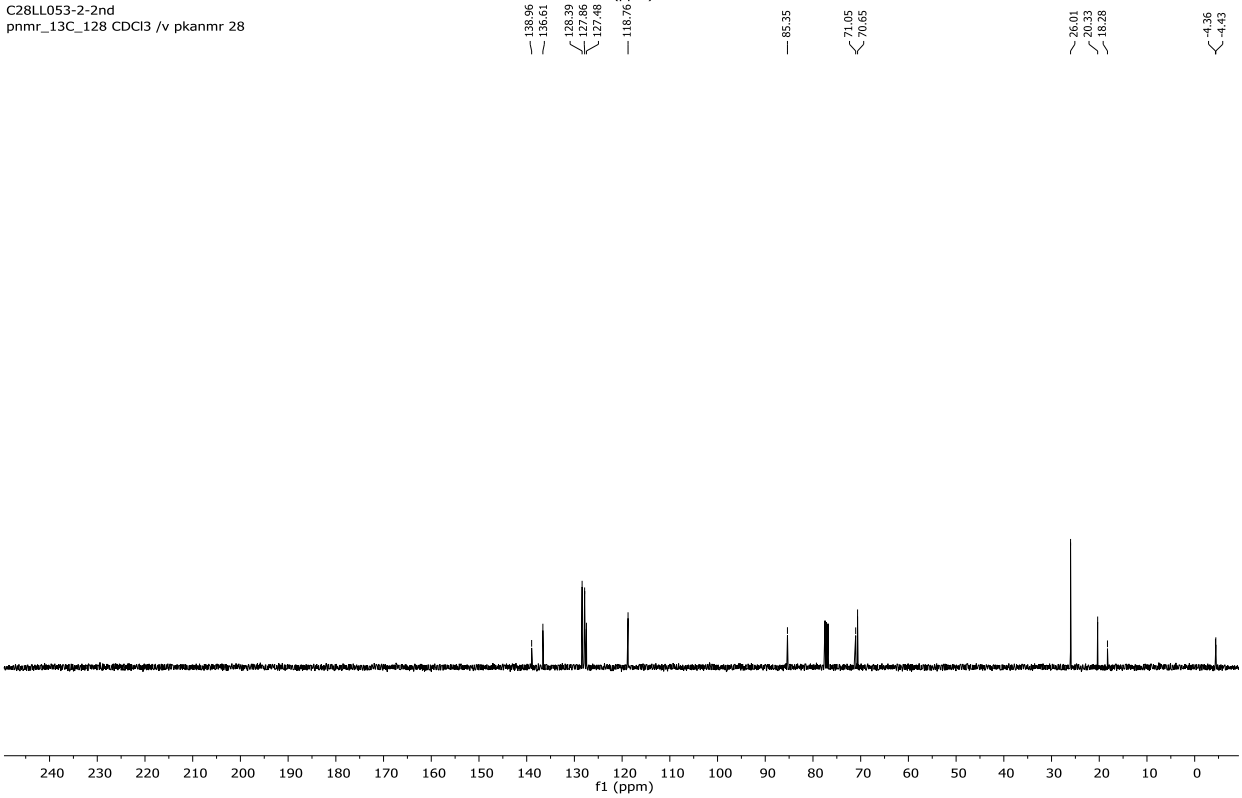
C28LL053-2-2nd
pnmr_13C_128 CDCl3 /v pkanmr 28
138.96
136.61
128.39
127.86
127.48
118.76
85.35
71.05
70.65
26.01
20.33
18.28
-4.36
-4.43
f1 (ppm)

A-100 (2R,3S)-3-(benzyloxy)pent-4-en-2-ol

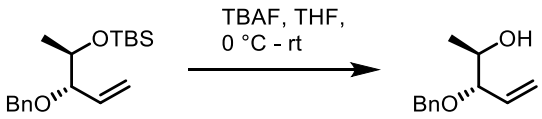

Assay: TBAF (1 M in THF, 1.67 mL, 2.0 equiv) was added to a cooled solution of **A-99** (0.26 g, 0.84 mmol, 1.0 equiv) in THF (2 mL) at 0 °C. After full addition, the reaction mixture was allowed to reach room temperature and was stirred at ambient temperature for 16 h. It was then quenched by the addition of H_2O (4 mL). The biphasic mixture was transferred to a separatory funnel and the phases were separated. The aqueous phase was extracted wit EtOAc (3 x 5 mL). Combined organic phases were dried over $MgSO_4$ and concentrated under reduced pressure. The crude was purified by FC (EtOAc:hexane, 1:5) to give the title compound (154.2 mg, 0.80 mmol, 96%).

Analytics: $\mathbf{R_f}$ = 0.15 (EtOAc:hexane, 13:87). **^{1}H NMR** (400 MHz, $CDCl_3$) δ 7.38 – 7.27 (m, 5H), 5.83 (ddd, *J* = 17.3, 10.4, 8.1 Hz, 1H), 5.36 (dddd, *J* = 40.9, 17.3, 1.8, 0.8 Hz, 2H), 4.52 (dd, *J* = 102.1, 11.9 Hz, 2H), 3.90 (s, 1H), 3.69 (ddd, *J* = 8.1, 2.7, 2.0 Hz, 1H), 1.15 (d, *J* = 6.5 Hz, 3H). **^{13}C NMR** (101 MHz, $CDCl_3$) δ 138.31, 134.56, 128.42 (2 C), 127.77 (2 C), 127.66, 120.38, 84.31, 70.30, 69.32, 17.94. **HRMS** (ESI): 215.1047 $[M+Na]^+$; calculated for $[C_{12}H_{16}NaO_2]$: 215.1043. **$[\alpha]^{25}_D$** = +44.27 (c = 3.3, $CHCl_3$). **IR** [ATR, neat]: ν = 3446.17 w, 2977.55 w, 2869.56 w, 1451.17 w, 11391.39 w, 1302.68 w, 1257.36 w, 1065.48 s, 1023.05 m, 996.05 m, 928.56 m, 736.67 s, 698.11 s cm^{-1}.

Compound literature known

C29LL059-2-3rdpure
pnmr_1H_16 CDCl3 /v pkanmr 29

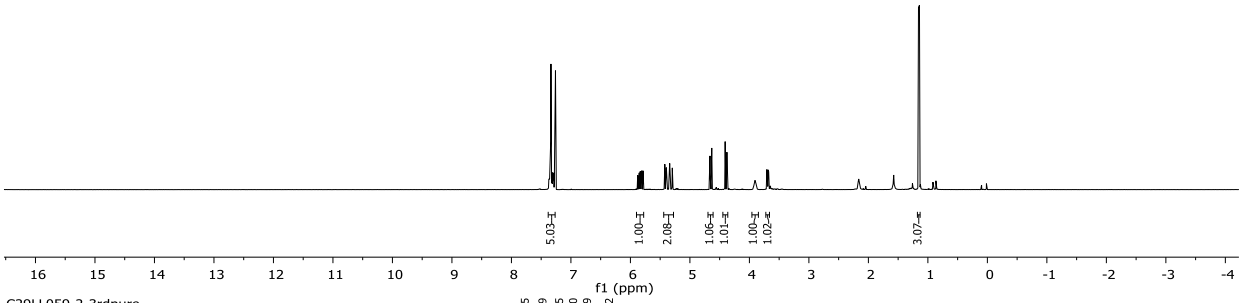

C29LL059-2-3rdpure
pnmr_13C_128 CDCl3 /v pkanmr 29

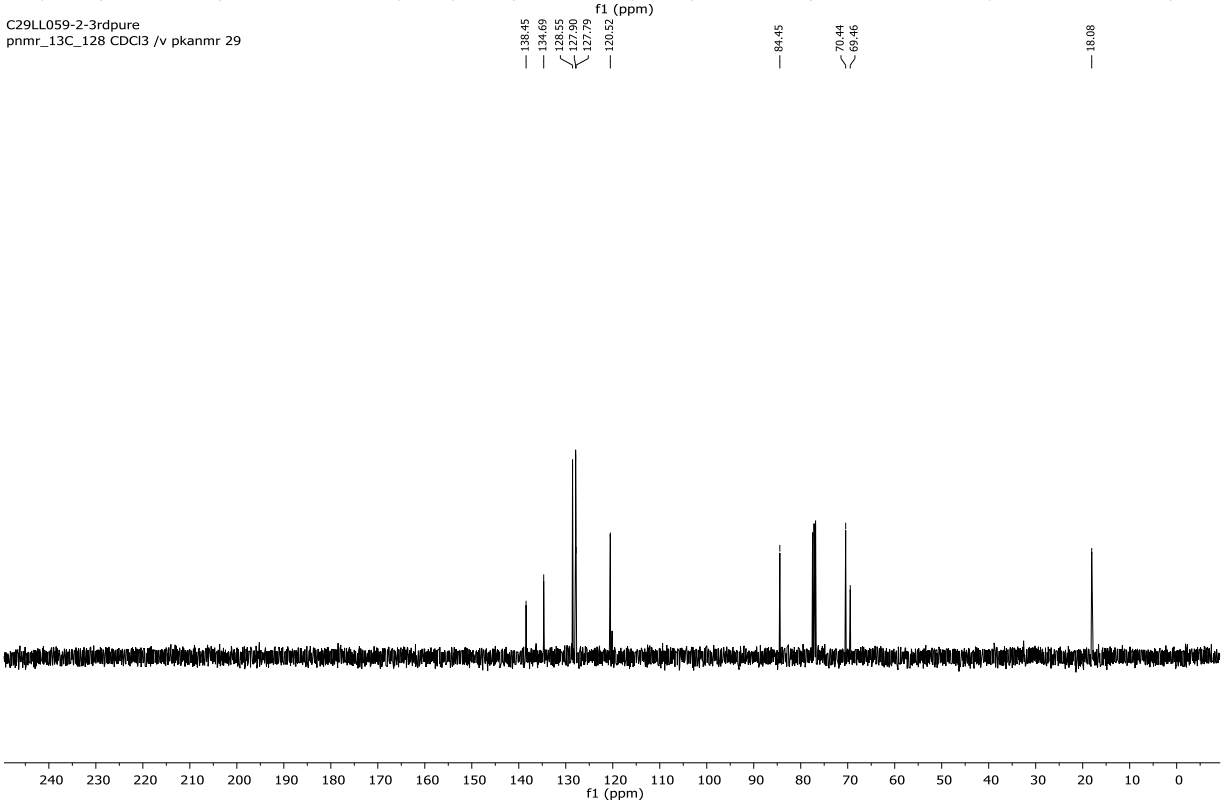

A-101 ((((3S,4R)-4-(allyloxy)pent-1-en-3-yl)oxy)methyl)benzene

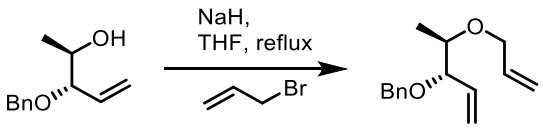

Assay: To a stirring solution of **A-100** (2.3 g, 11.96 mmol, 1.0 equiv) dissolved in THF (150 mL), was added NaH (60 wt % in mineral oil, 0.96 g, 23.93 mmol, 2.0 equiv) at room temperature. After full addition, the reaction mixture was heated up to 40 °C and stirred for 30 min. Allyl bromide (3.45 mL, 23.93 mmol, 2.0 equiv) was then added and the reaction mixture was stirred at 40 °C for 15 min. It was then allowed to cool to room temperature and was stirred overnight. The reaction was quenched by the addition of a few drops MeOH and was then poured onto a mixture of H_2O (15 mL) and EtOAc (15 mL). The aqueous phase was extracted wit EtOAc (3 x 20 mL). Combined organic phases were dried over $MgSO_4$ and concentrated under reduced pressure. The crude was purified by FC (EtOAc:hexane, 1:5) to give the title compound (2.16 g, 9.28 mmol, 76%).

Analytics: $\mathbf{R_f}$ = 0.54 (EtOAc:hexane, 1:10). **^{1}H NMR** (400 MHz, $CDCl_3$) δ 7.37 - 7.26 (m, 5H), 5.99 - 5.79 (m, 2H), 5.40 - 5.08 (m, 4H), 4.65 (d, *J* = 12.2 Hz, 1H), 4.43 (d, *J* = 12.2 Hz, 1H), 4.06 (ddd, *J* = 5.5, 3.1, 1.6 Hz, 2H), 3.74 (ddt, *J* = 7.5, 4.4, 0.8 Hz, 1H), 3.57 (qd, *J* = 6.4, 4.4 Hz, 1H), 1.18 (d, *J* = 6.4 Hz, 3H). **^{13}C NMR** (101 MHz, $CDCl_3$) δ 138.85, 135.93, 135.53, 128.41 (2 C), 127.78 (2 C), 127.52, 118.89, 116.58, 83.37, 77.25, 70.56 (2 C), 16.33. **HRMS (EI)**: 174.1040 $[M\text{-}C_3H_6O]^+$; calculated for $[C_{12}H_{14}O]$: 174.1045. **$[\alpha]^{20}_D$** = +37.50 (c = 1, $CHCl_3$). **IR** [ATR, neat]: ν = 3114.47 w, 3011.78 w, 2931.75 w, 2836.77 w, 1681.14 w, 1613.16 w, 1569.77 s, 1513.85 s, 1442.49 s, 1356.68 s, 1320.52 m, 1303.16 m, 1247.24 s, 1174.92 m, 1008.59 s, 759.816 m, 534.667 m cm^{-1}.

C34LL060-FC
pnmr_1H_16 CDCl3 /v pkanmr 36

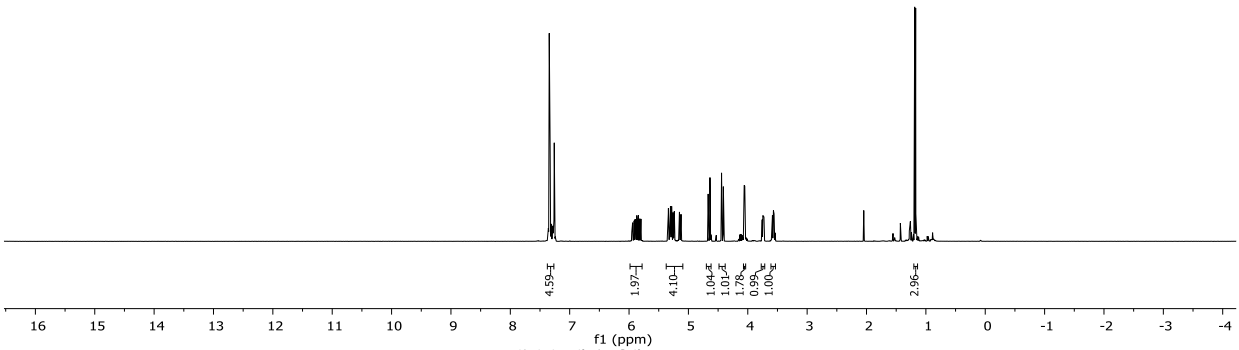

C34LL060-FC
pnmr_13C_128 CDCl3 /v pkanmr 36

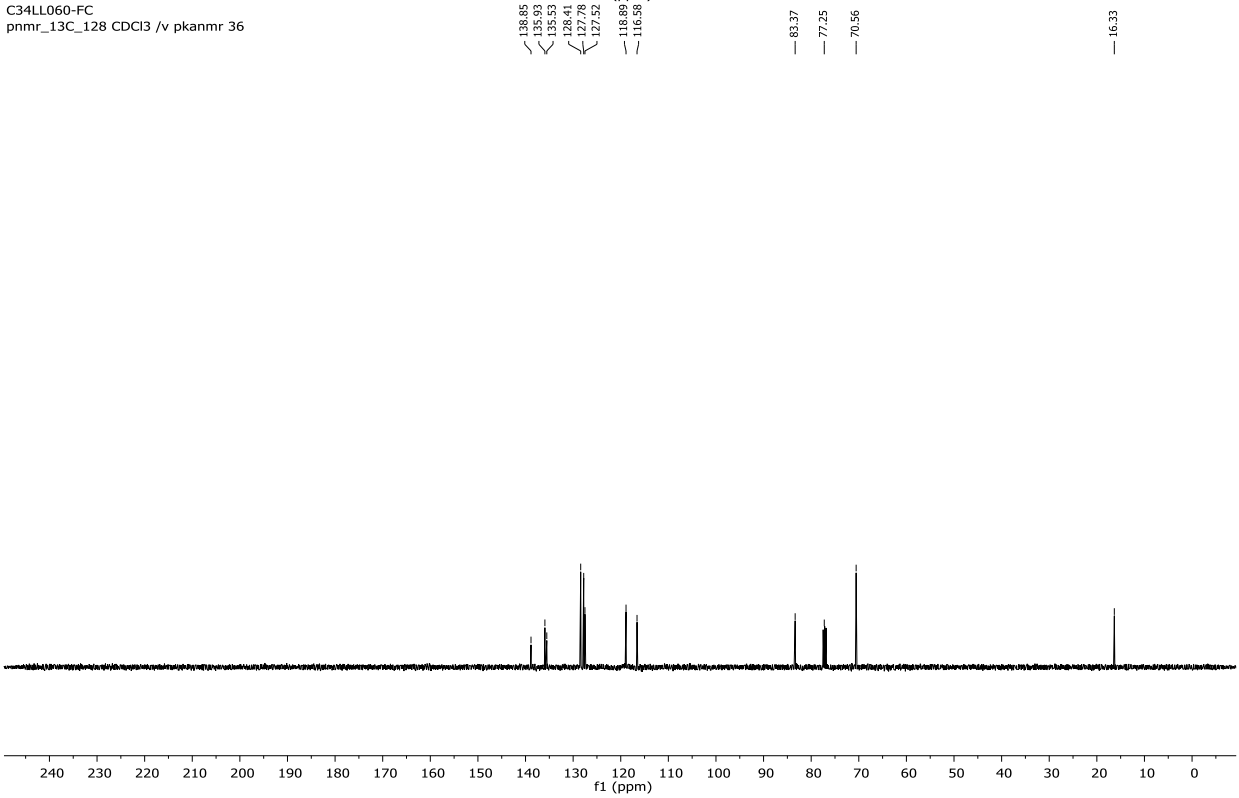

A-102 (2R,3S)-3-(benzyloxy)-2-methyl-3,4-dihydro-2H-pyran

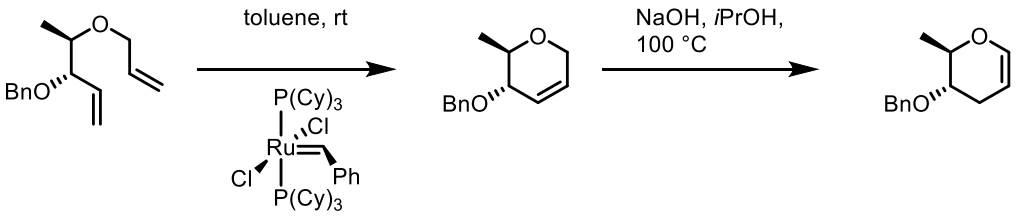

Assay: In the glove box, Grubbs first generation catalyst (351 mg, 0.45 mmol, 5 mol %) was given into a flame dried Schlenk tube. Meanwhile, toluene was freeze pumped (3 times) and set under argon atmosphere. **A-101** (1.98 mg, 8.54 mmol, 1.0 equiv) was then dissolved in toluene (44 mL) and given to the ruthenium catalyst. The reaction mixture was stirred for 22 h at ambient temperature. Starting material was fully consumed. Then isopropanol (9 mL) and NaOH (239 mg, 5.98 mmol, 0.7 equiv) were added and the reaction was stirred add 110 °C for 40 min. Important to carefully monitor the reaction, since the fully reduced pyran starts to arise as soon the intermediate RCM product is formed. The reaction mixture was filtered over a pad of Celite (washed with EtOAc) and a short plug of silica. The resulting solution was concentrated under reduced pressure. The crude brown oil was then purified by FC (hexane -> EtOAc:hexane, 1:10) to give the title compound (1.44 g, 7.05 mmol, 83%).

Analytics: $\mathbf{R_f}$ = 0.55 (EtOAc:hexane, 1:10). **^{1}H NMR** (400 MHz, $CDCl_3$) δ 7.38 – 7.27 (m, 5H), 6.30 (dt, *J* = 6.0, 2.0 Hz, 1H), 4.68 (d, *J* = 11.8 Hz, 1H), 4.64 (ddd, *J* = 6.0, 4.8, 2.8 Hz, 1H), 4.56 (d, *J* = 11.8 Hz, 1H), 3.87 (dq, *J* = 12.7, 6.3 Hz, 1H), 3.41 (td, *J* = 7.9, 5.6 Hz, 1H), 2.43 – 2.33 (m, 1H), 2.07 (ddt, *J* = 16.6, 7.9, 2.5 Hz, 1H), 1.35 (d, *J* = 6.3 Hz, 3H). **^{13}C NMR** (101 MHz, $CDCl_3$) δ 143.06, 138.48, 128.55 (2 C), 127.86 (2 C), 127.83, 97.76, 75.42, 73.83, 71.10, 26.32, 17.88. **HRMS (EI)**: 204.1145 $[M^+]^+$; calculated for $[C_{13}H_{16}O_2]$: 204.1150. **$[\alpha]^{20}_D$** = +112.20 (c = 1, $CHCl_3$). **IR** [ATR, neat]: ν = 3062.89 w, 2975.14 w, 2873.9 w, 1652.21 m, 1451.65 w, 1237.59 s, 1091.03 s, 1061.14 s, 884.684 w, 732.335 s, 696.658 s, 612.77 w, 443.065 m, cm^{-1}.

C39LL069-1-pQ
pnmr_1H_16 CDCl3 /v pkanmr 20

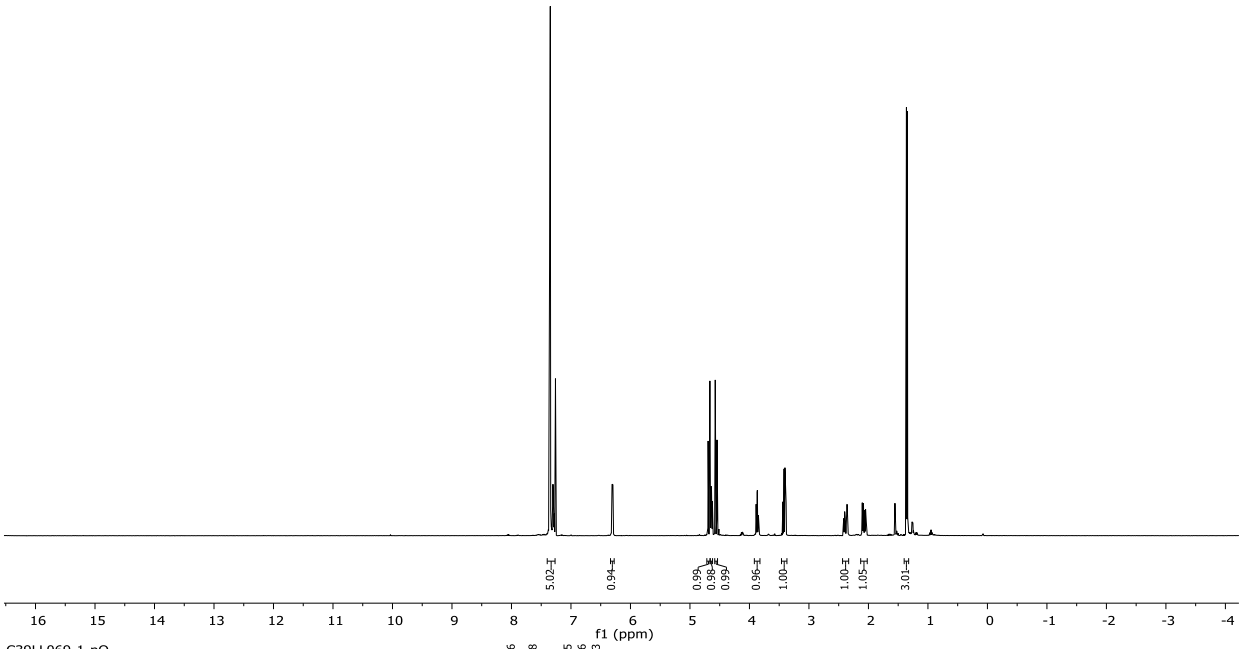

C39LL069-1-pQ
pnmr_13C_1024 CDCl3 /v pkanmr 20

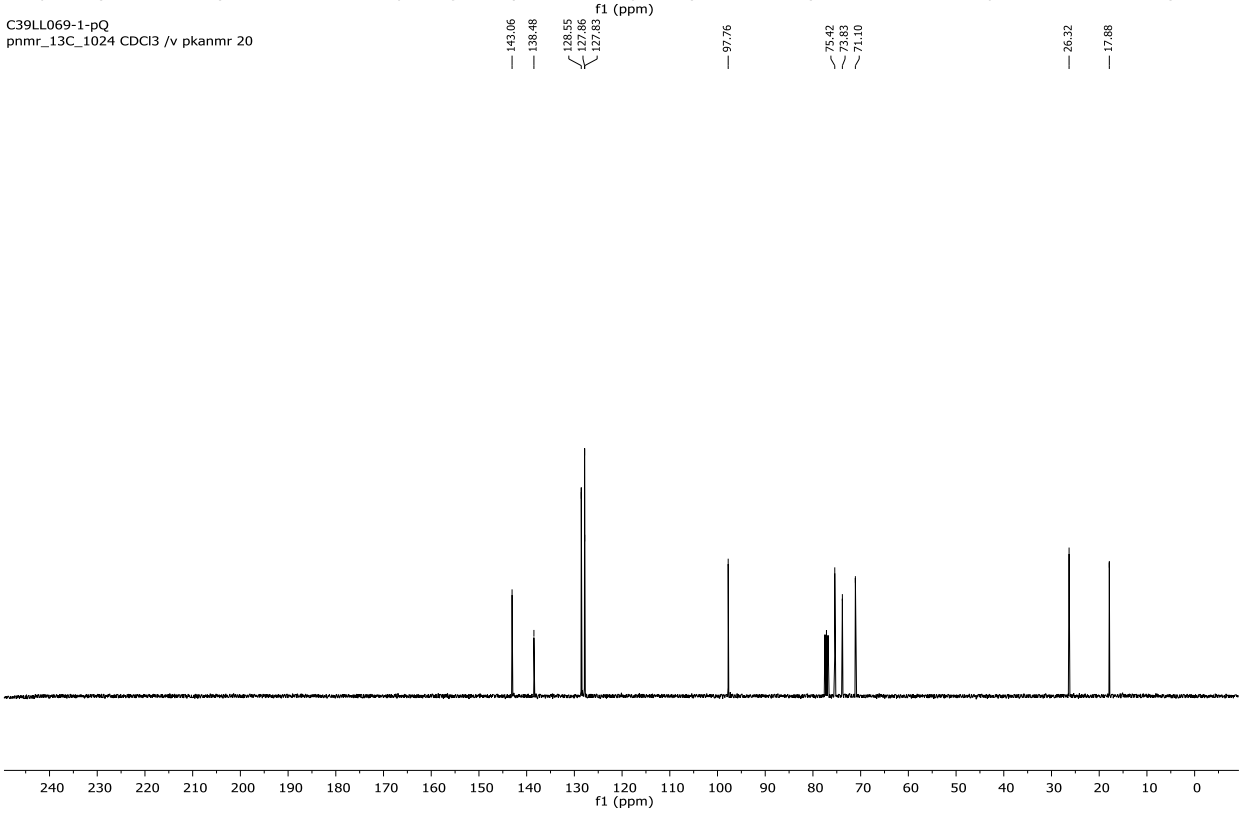

A-103 (2R,3S)-3-(benzyloxy)-6-methoxy-2-methyltetrahydro-2H-pyran

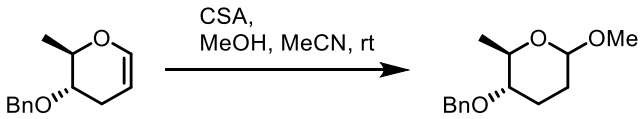

Assay: Glycal **A-102** (200 mg, 0.98 mmol, 1.0 equiv) was dissolved in MeCN (5.4 mL) and MeOH (1.2 mL). CSA (34.1 mg, 0.15 mmol, 0.15 equiv) was then added and the reaction mixture was stirred for 1 h at ambient temperature. After full consumption of starting material, EtOAc (2 mL) and saturated aqueous $NaHCO_3$ (10 mL) was added and the biphasic mixture was poured into a separatory funnel. The aqueous phase was then separated and extracted with EtOAc (3 x 2 mL). The combined organic phases where dried over $MgSO_4$. The crude oil was purified by FC (EtOAc:hexane, 1:5) giving the title compound (201.5 mg, 0.85 mmol, 87%) as a diastereomeric mixture (dr = 1:2.6).

Analytics: $\mathbf{R_f}$ = 0.18 (EtOAc:hexane, 1:10) resp. $\mathbf{R_f}$ = 0.21 (EtOAc:hexane, 1:10). **^{1}H NMR** (400 MHz, $CDCl_3$) δ 7.37 – 7.26 (m), 4.68 – 4.61 (m), 4.48 (d, *J* = 11.7 Hz), 4.37 (dd, *J* = 8.9, 2.1 Hz), 3.72 (dq, *J* = 9.2, 6.2 Hz), 3.48 (s), 3.46 – 3.39 (m), 3.34 (s), 3.14 – 3.02 (m), 2.25 – 2.16 (m), 2.00 (ddd, *J* = 7.3, 5.6, 3.4 Hz), 1.94 – 1.63 (m), 1.60 – 1.42 (m), 1.33 (d, *J* = 6.2 Hz), 1.27 (d, *J* = 6.2 Hz). **^{13}C NMR** (101 MHz, $CDCl_3$) δ 138.75, 138.53, 128.54, 128.49, 127.87, 127.83, 127.80, 127.71, 102.63, 97.45, 78.98, 78.66, 74.70, 71.44, 70.77, 67.91, 56.39, 54.48, 30.45, 29.40, 27.55, 24.02, 18.58, 18.46. **HRMS (ESI)**: 252.1806 $[M+NH_4]^+$; calculated for $[C_{12}H_{16}BrN_3O_2]$: 252.1805. **IR** [ATR, neat]: ν = 2932.23 w, 2890.77 w, 1453.10 w, 1367.28 w, 1212.04 w, 1126.22 m, 1072.23 m, 1054.87 s, 1019.19 m, 980.63 m, 735.71 m, 697.14 m cm^{-1}.

Remarks: For the ^{1}H NMR & ^{13}C NMR all the signals, for both the compounds are given. No integrals are specified.

C45LL074-2-full
pnmr_1H_16 CDCl3 /v pkanmr 34

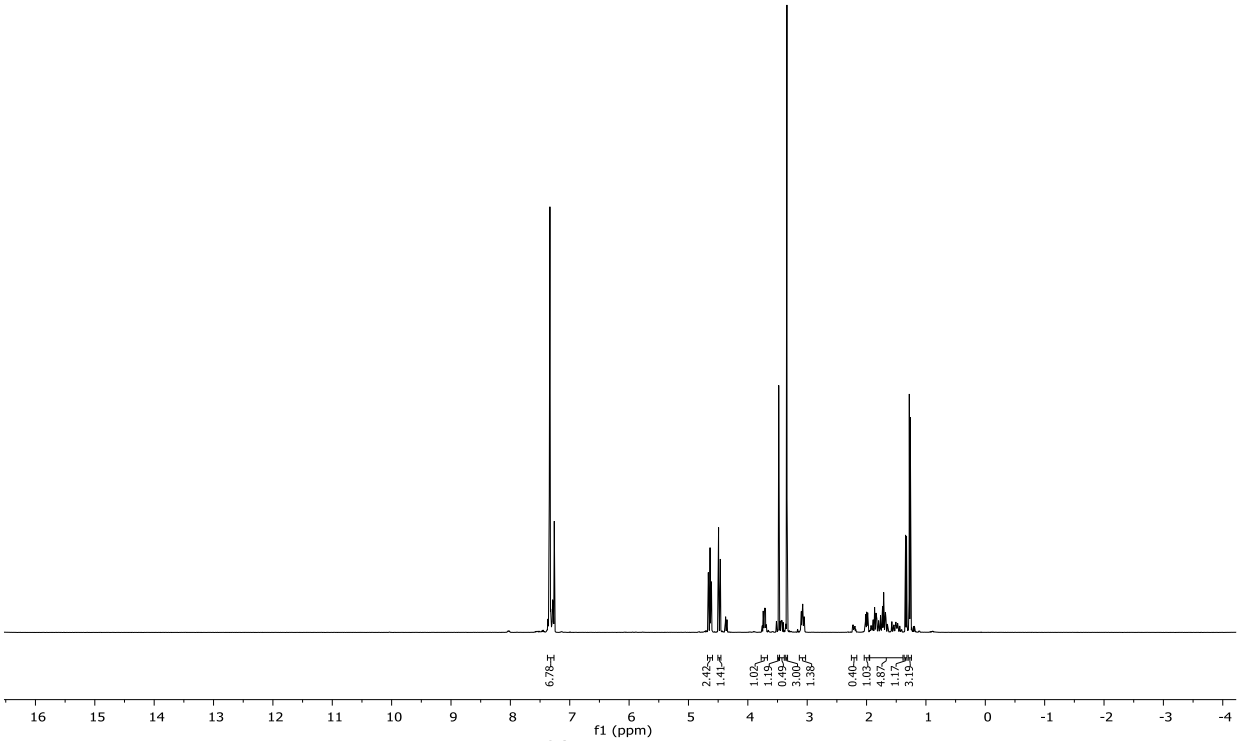

C45LL074-2-full
pnmr_13C_1024 CDCl3 /v pkanmr 34

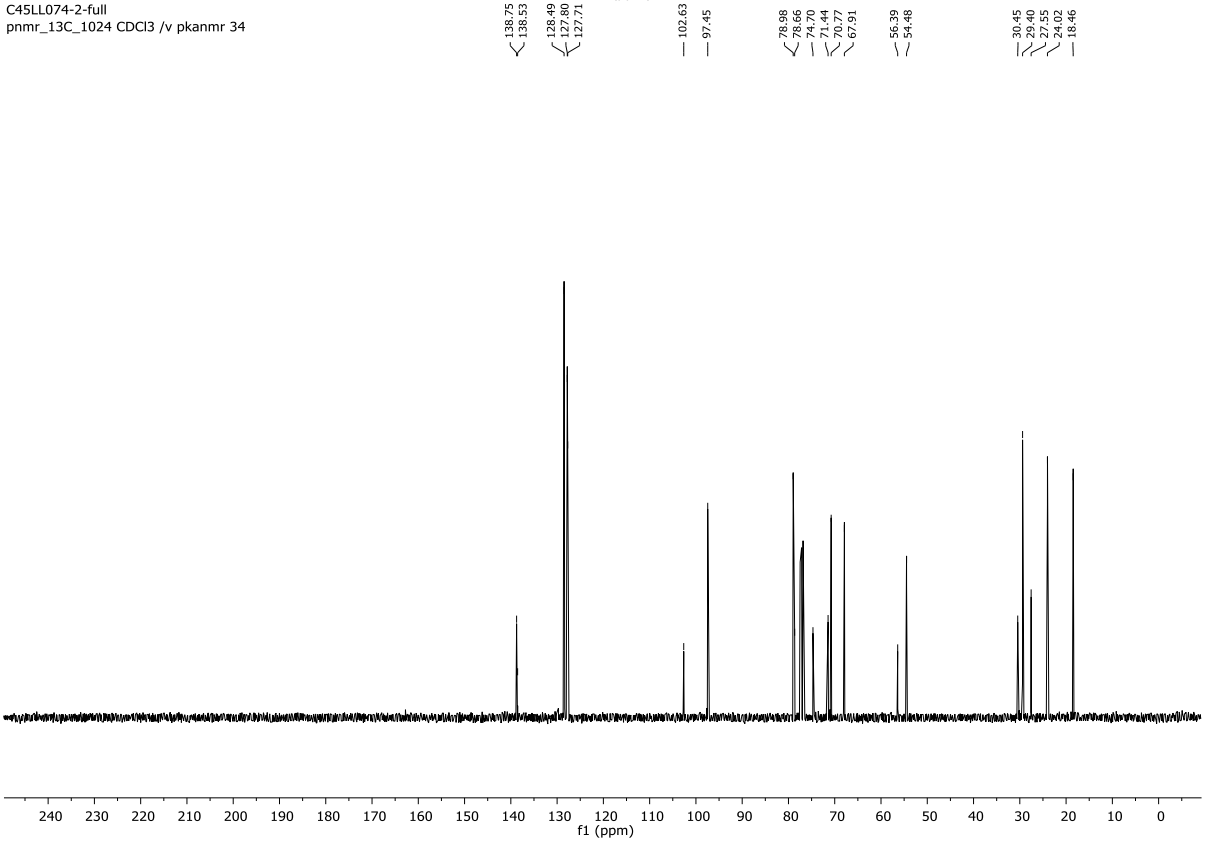

A-79 (2R,3S)-6-methoxy-2-methyltetrahydro-2H-pyran-3-ol

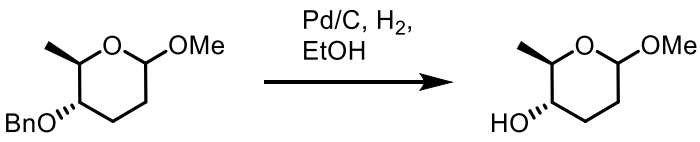

Assay: A-103 (100 mg, 0.42 mmol, 1.0 equiv) was dissolved in EtOH (4 mL), Pd/C (10 wt %, 45 mg, 0.042 mmol, 10 mol %) was then added and the reaction mixture was set under H_2 atmosphere (balloon). After 1.5 hours at ambient temperature, starting material was fully consumed. The reaction mixture was filtered over a pad of Celite, which was washed with EtOH. The crude sticky syrup was purified by FC (EtOAc:hexane, 1:3) to give the title compound as an anomeric mixture (55 mg, 0.38 mmol, 89%).

Analytics: $\mathbf{R_f}$ = 0.35 (EtOAc:hexane, 1:1) resp. $\mathbf{R_f}$ = 0.41 (EtOAc:hexane, 1:1). **^{1}H NMR** (400 MHz, Chloroform-*d*) δ 4.69 – 4.54 (m, 1H), 3.56 (dq, *J* = 9.2, 6.2 Hz, 1H), 3.34 (s, 3H), 3.31 – 3.19 (m, 2H), 1.90 – 1.44 (m, 4H), 1.26 (d, *J* = 6.2 Hz, 3H). **^{13}C NMR** (101 MHz, Chloroform-*d*) δ 102.65, 97.43, 75.87, 72.20, 71.71, 69.40, 56.42, 54.56, 31.12, 30.69, 29.67, 27.73, 18.18, 18.03. **HRMS (EI)**: 115.0755 [M-CH_3O]$^+$; calculated for [$C_6H_{11}O_2$]: 115.0754. **IR** [ATR, neat]: ν = 3413.39 w, 2929.34 w, 1454.06 w, 1367.28 w, 1126.22 m, 1051.98 s, 980.63 m cm-1.

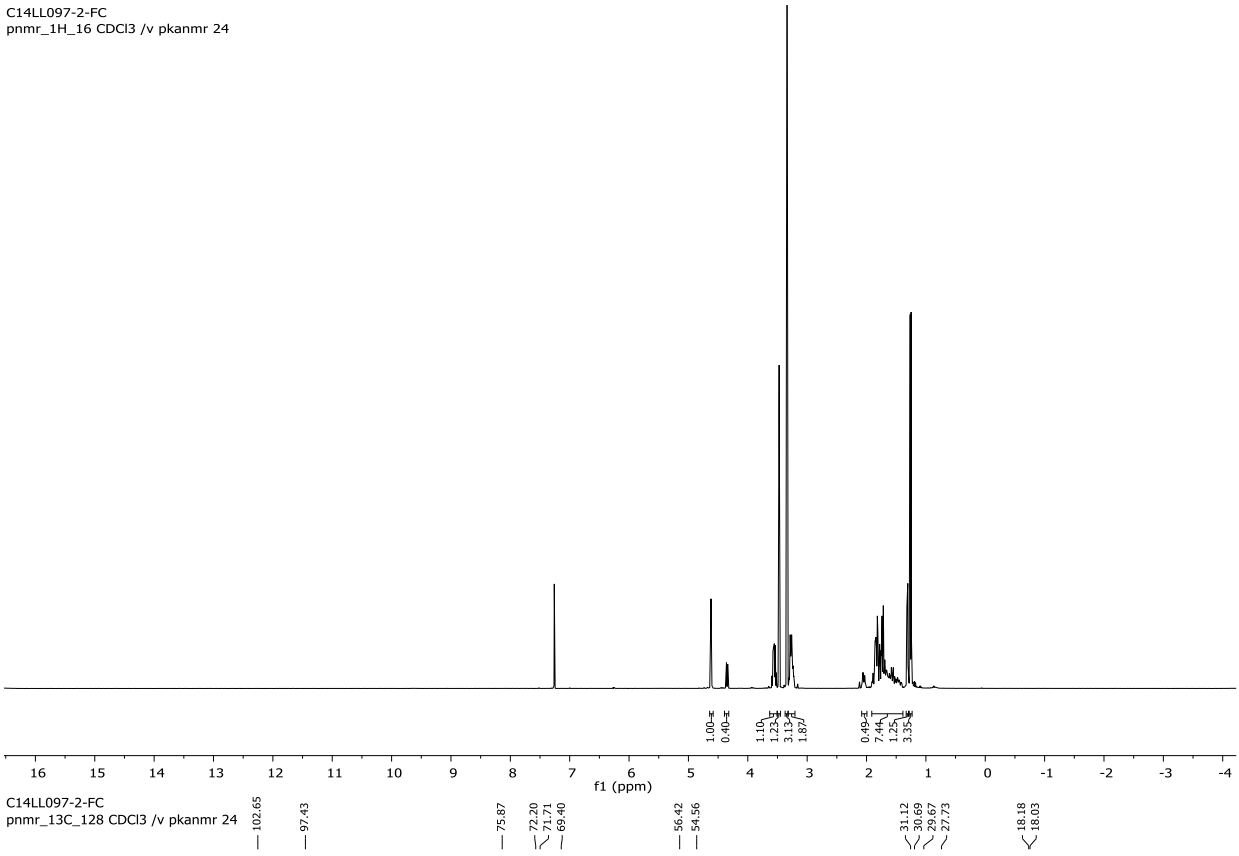
C14LL097-2-FC
pnmr_1H_16 CDCl3 /v pkanmr 24
1.00
0.40
1.10
1.23
3.13
1.87
0.49
7.44
1.25
3.35
16 15 14 13 12 11 10 9 8 7 6 5 4 3 2 1 0 -1 -2 -3 -4
f1 (ppm)
C14LL097-2-FC
pnmr_13C_128 CDCl3 /v pkanmr 24
102.65
97.43
75.87
72.20
71.71
69.40
56.42
54.56
31.12
30.69
29.67
27.73
18.18
18.03
130 125 120 115 110 105 100 95 90 85 80 75 70 65 60 55 50 45 40 35 30 25 20 15 10 5 0
f1 (ppm)

A-109 N-(1-((5S,6R)-5-hydroxy-6-methyltetrahydro-2H-pyran-2-yl)-2-oxo-1,2-dihydropyrimidin-4-yl)benzamide

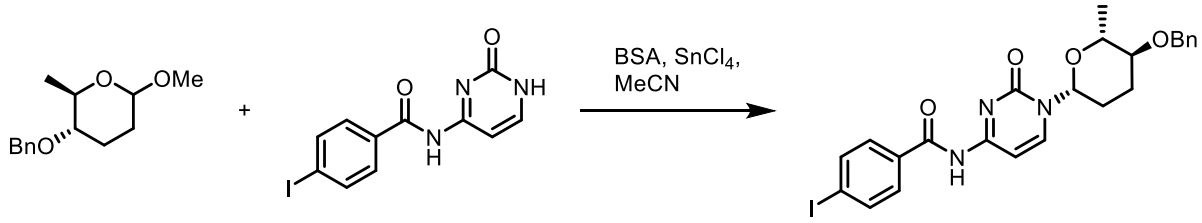

Assay: Pyrimidine base **A-73** (29 mg, 0.085 mmol, 1.0 equiv) was dried in a 5 mL round bottom flask over night at high vacuum (10^{-3} mbar). It was then suspended in dry MeCN (0.6 mL) and N,O-bis(trimethylsilyl)acetamid (0.042 mL, 0.17 mmol, 2.0 equiv) was added at room temperature. The white suspension slowly turned into a homogeneous clear solution. After 30 min of stirring, pyranose **A-103** (20.1 mg, 0.085 mmol, 1.0 equiv) dissolved in MeCN (0.3 mL) was added, followed by dropwise addition of $SnCl_4$ (0.025 mL, 0.21 mmol, 2.5 equiv) in MeCN (0.4 mL), which was prepared as a stock solution. The reaction mixture was stirred for 50 min at ambient temperature and monitored via LC-MS. After 50 min the reaction was completed. The solvent was evaporated under reduced pressure and the oily yellow crude was taken up in EtOAc, transferred to a separatory funnel and mixed with saturated aqueous $NaHCO_3$ (4 mL). The two phases were separated and the aqueous phase was extracted with EtOAc (3 x 4 mL), combined organic phases were dried over $MgSO_4$ and concentrated under reduced pressure. Purification by FC (EtOAc:hexane 3:1) gave the title compound (24.7 mg, 0.045 mmol, 53%) presenting exclusively β-anomeric linkage.

Analytics: $\mathbf{R_f}$ = 0.37 (EtOAc:hexane, 3:1). **^{1}H NMR** (400 MHz, Chloroform-*d*) δ 8.72 (s, 1H), 7.83 (d, *J* = 7.5 Hz, 1H), 7.79 (d, *J* = 8.5 Hz, 2H), 7.56 (d, *J* = 8.1 Hz, 2H), 7.33 – 7.21 (m, 6H), 5.67 (dd, *J* = 10.3, 1.6 Hz, 1H), 4.60 (d, *J* = 11.6 Hz, 1H), 4.43 (d, *J* = 11.6 Hz, 1H), 3.60 (dq, *J* = 8.8, 6.1 Hz, 1H), 3.12 – 3.00 (m, 1H), 2.32 – 2.18 (m, 2H), 1.70 – 1.51 (m, 1H), 1.42 – 1.33 (m, 1H), 1.29 (d, *J* = 6.1 Hz, 3H). **^{13}C NMR** (101 MHz, Chloroform-*d*) δ 161.83, 138.44 (2 C), 138.12, 129.26, 128.63 (2 C), 128.02 (2 C), 127.94 (2 C), 101.01, 83.38, 77.99, 77.67, 71.35, 30.92, 27.94, 18.60. **HRMS (MALDI)**: 568.0704 $[M+Na]^+$; calculated for $[C_{24}H_{24}IN_3NaO_4]$: 568.0703. **HRMS (ESI)**: 546.0876 $[M+H]^+$; calculated for $[C_{24}H_{25}IN_3O4]$: 546.0884. **$[\alpha]^{20}_D$** = +114.5 (c = 0.2, $CHCl_3$). **IR** [ATR, neat]: ν = 3730.14 w, 2924.04 w, 1669.57 m, 1555.79 w, 1484.44 m, 1300.75 w, 1259.29 w, 1106.94 w, 1008.11 w, 670.14 w cm^{-1}.

C10LL080-5-fc
pnmr_1H_16 CDCl3 /v pkanmr 32

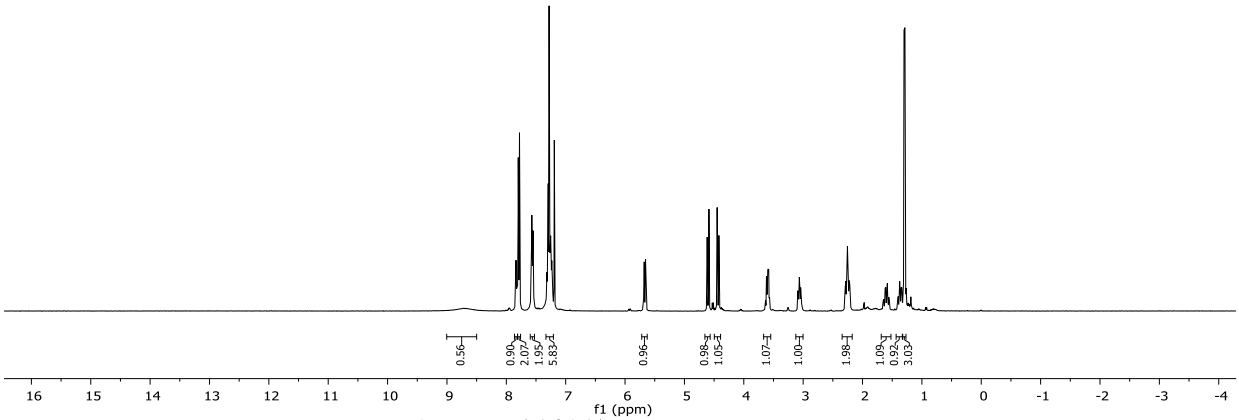

C09LL080-3-recryst.4.1.1r
pnmr_13C_1024 CDCl3 /v pkanmr 24

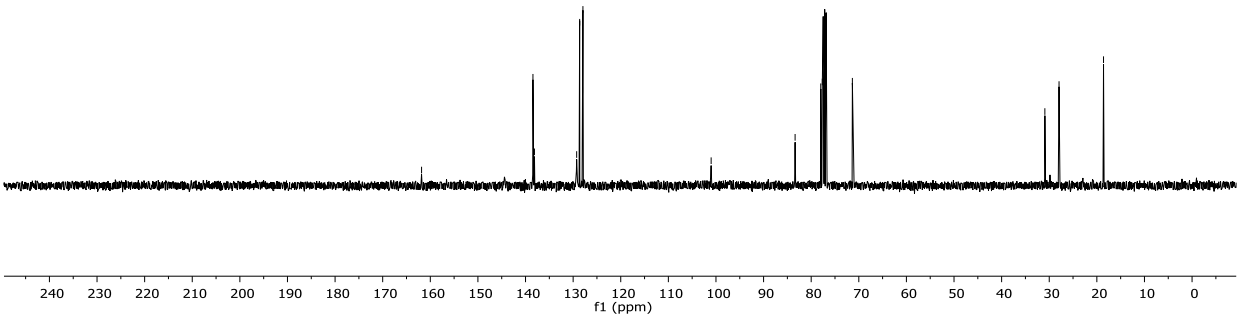

A-110 (2R,4S)-tert-butyl 4-((4-((1-((2R,5S,6R)-5-(benzyloxy)-6-methyltetrahydro-2H-pyran-2-yl)-2-oxo-1,2-dihydropyrimidin-4-yl)carbamoyl)phenyl)carbamoyl)-2-(tert-butyl)-4-methyloxazolidine-3-carboxylate

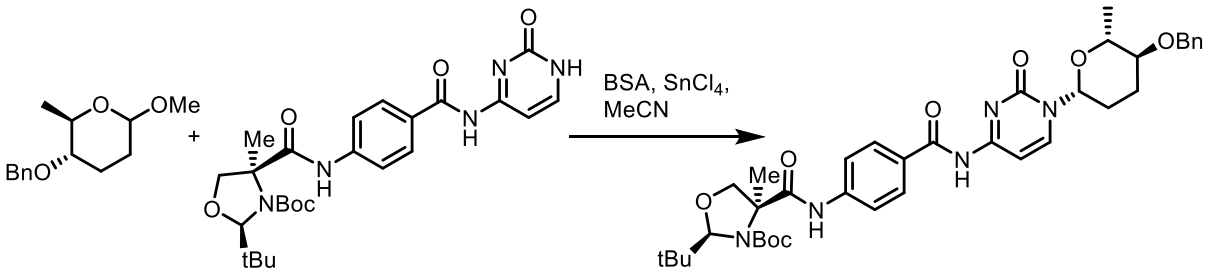

Assay: A-53 (153.3 mg, 0.31 mmol, 1.45 equiv) was dried in a 10 mL round bottom flask over night under high vaccum (10^{-3} mbar). It was then suspended in dry MeCN (1.5 mL) and N,O-bis(trimethylsilyl)acetamid (0.10 mL, 0.42 mmol, 2.0 equiv) was added at room temperature. After 30 min of stirring, **A-103** (50.0 mg, 0.21 mmol, 1.0 equiv) dissolved in MeCN (1.1 mL) was added, followed by dropwise addition of freshly distilled (over P_2O_5) $SnCl_4$ (0.037 mL, 0.317 mmol, 1.5 equiv) in MeCN (1 mL), which was prepared as a stock solution. The reaction mixture was stirred for 150 min at ambient temperature and meanwhile monitored via LC-MS. The reaction mixture was then dropwise given into a stirring solution of saturated aqueous $NaHCO_3$ (4 mL) and the aqueous phase was extracted with EtOAc (3 x 4 mL), combined organic phases were dried over $MgSO_4$ and concentrated under reduced pressure. Purification by FC (EtOAc:hexane 3:1 -> EtOAc) gave the title compound (106.7 mg, 0.15 mmol, 72%) as a white/yellowish foam.

Analytics: $\mathbf{R_f}$ = 0.19 (EtOAc:hexane, 3:1). **^{1}H NMR** (400 MHz, Chloroform-*d*) δ 10.39 (s, 1H), 8.69 (s, 1H), 7.91 – 7.86 (m, 3H), 7.69 (d, *J* = 8.7 Hz, 2H), 7.53 (s, 1H), 7.40 – 7.29 (m, 5H), 5.76 (dd, *J* = 10.3, 1.6 Hz, 1H), 5.21 (s, 1H), 4.81 (d, *J* = 8.8 Hz, 1H), 4.67 (d, *J* = 11.6 Hz, 1H), 4.50 (d, *J* = 11.6 Hz, 1H), 3.81 (d, *J* = 9.0 Hz, 1H), 3.73 – 3.61 (m, 1H), 3.21 – 3.08 (m, 1H), 2.43 – 2.24 (m, 2H), 1.72 (s, 3H), 1.70 – 1.61 (m, 1H), 1.54 (s, 9H), 1.49 – 1.40 (m, 1H), 1.36 (d, *J* = 6.1 Hz, 3H), 0.91 (s, 9H).**^{13}C NMR** (101 MHz, $CDCl_3$) δ 171.93, 162.13, 156.06, 154.51, 144.40, 143.01, 138.40, 138.13, 129.05, 128.61 (2 C), 127.99 (2 C), 127.93 (2 C), 119.49 (2 C), 98.11, 96.88, 83.36, 83.16, 77.93, 77.71, 77.36, 76.15, 71.32, 68.18, 38.33, 30.94, 28.28 (3 C), 27.95, 26.25 (3 C), 22.22, 18.59. **HRMS (ESI)**: 726.3467 $[M+Na]^+$; calculated for $[C_{38}H_{49}N_5NaO_8]$: 726.3473. **$[\alpha]^{20}_D$** = -06.00 (c = 0.5, $CHCl_3$). **IR** [ATR, neat]: ν = 2971.77 w, 2931.75 w, 1694.16 m, 1666.2 m, 1666.2 m, 1597.73 m, 1484.44 s, 1361.98 m, 1307.5 m, 1249.16 s, 1164.31 m, 1103.57 m, 784.40 w cm^{-1}. **m.p.** = 110°C.

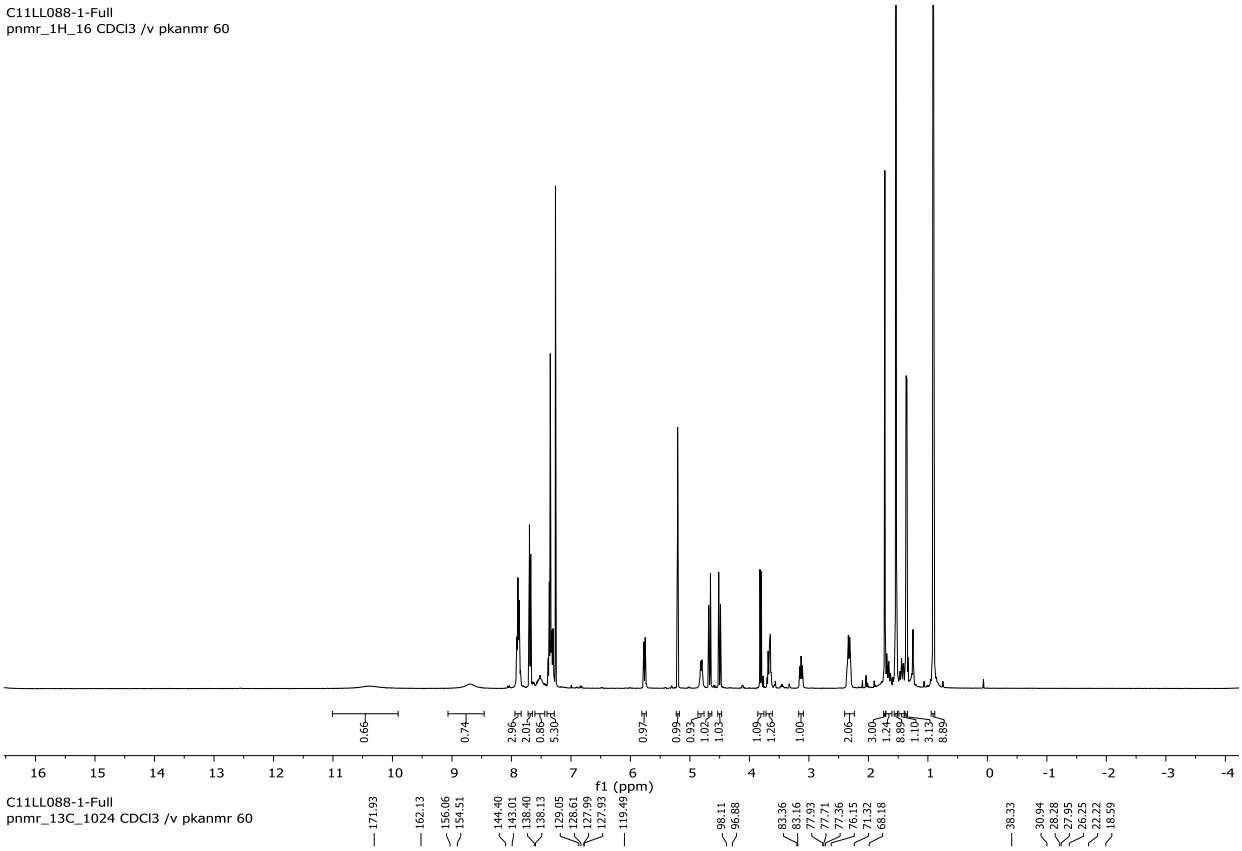
C11LL088-1-Full
pnmr_1H_16 CDCl3 /v pkanmr 60
0.66
0.74
2.96
2.01
0.86
5.30
0.97
0.99
0.93
1.02
1.03
1.09
1.26
1.00
2.06
3.00
1.24
8.89
1.10
3.13
8.89
16 15 14 13 12 11 10 9 8 7 6 5 4 3 2 1 0 -1 -2 -3 -4
f1 (ppm)

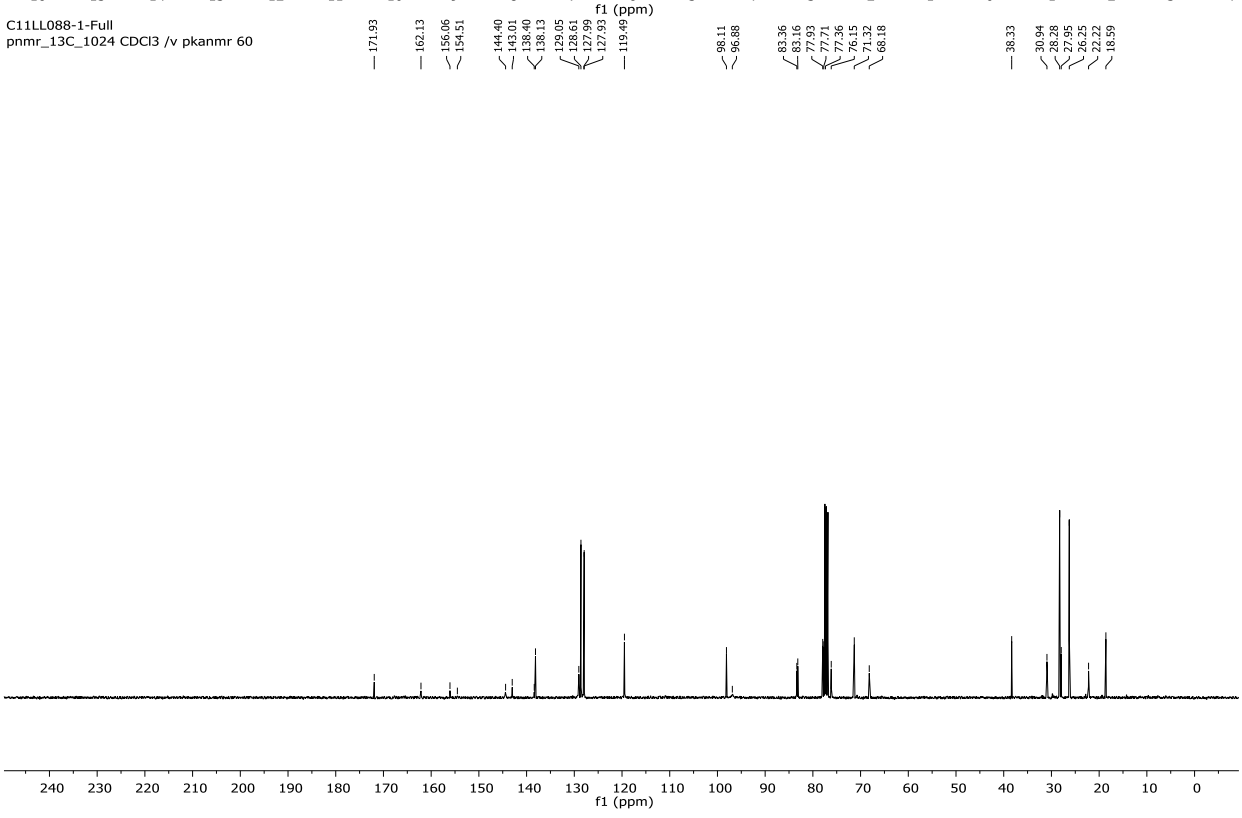
C11LL088-1-Full
pnmr_13C_1024 CDCl3 /v pkanmr 60
171.93
162.13
156.06
154.51
144.40
143.01
138.40
138.13
129.05
128.61
127.99
127.93
119.49
98.11
96.88
83.36
83.16
77.93
77.71
77.36
76.15
71.32
68.18
38.33
30.94
28.28
27.95
26.25
22.22
18.59
240 230 220 210 200 190 180 170 160 150 140 130 120 110 100 90 80 70 60 50 40 30 20 10 0
f1 (ppm)

A-116 tert-butyl(((2R,3S)-6-methoxy-2-methyltetrahydro-2H-pyran-3-yl)oxy)dimethylsilane

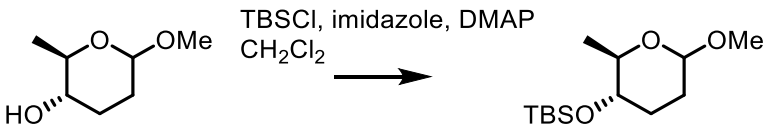

Assay: A-79 (31.0 mg, 0.21 mmol) was dissolved in CH_2Cl_2 (1.2 mL), imidazole (28.9 mg, 0.42 mmol, 2.0 equiv), DMAP (1.3 mg, 0.01 mmol, 0.05 equiv) was added and the reaction mixture was cooled to 0 °C. Under vigorous stirring, TBSCl (0.042 mg, 0.28 mmol, 1.30 equiv) was added and the reaction mixture was allowed to reach room temperature. After 1 h no full consumption of starting material was observed (via TLC, EtOAc:Hex 1:1), thus the reaction was heated up to 40 °C for 5 h. The reaction temperature was then lowered to 24 °C and the mixture was stirred over night. The reaction was quenched with saturated aqueous $NaHCO_3$ (5 mL) and the remaining white solids, were washed with EtOAc (2 mL). The organic phase was again washed with H_2O (2 mL) and the aqueous phase was then extracted with EtOAc (3 x 2 mL) and dried over $MgSO_4$. The solvent was evaporated under reduced pressure. The crude oil was purified by FC (EtOAc:hexane, 1:10) giving the desired target molecule (49.2 mg, 0.19 mmol, 89%) as a clear oil.

Analytics: $\mathbf{R_f}$ = 0.56, EtOAc:hexane (1:10). **^{1}H NMR** (400 MHz, Chloroform-*d*) δ 4.62 – 4.58 (m), 4.34 (dd, *J* = 9.0, 2.1 Hz), 3.58 (dq, *J* = 9.0, 6.2 Hz), 3.47 (s), 3.34 (s), 3.30 – 3.19 (m), 1.98 – 1.66 (m), 1.25 (d, *J* = 5.9 Hz), 1.19 (d, *J* = 6.2 Hz), 0.88 (s, 13H), 0.06 (s), 0.06 (s). **^{13}C NMR** (101 MHz, Chloroform-*d*) δ 102.72, 97.51, 76.28, 72.93, 72.48, 69.53, 56.37, 54.47, 31.77, 30.83, 29.86, 29.69, 28.32, 25.93, 25.86, 18.58, 18.49, 18.11, -2.79, -3.89, -3.99, -4.57, -4.60. **HRMS (ESI)**: 283.1705 $[M+Na]^+$; calculated for $[C_{13}H_{28}NaO_3Si]$: 283.1700. **IR** [ATR, neat]: ν = 2953.45 m, 2931.27 m, 2892.7 m, 2857.02 m, 1467.56 m, 1254.47 m, 1128.15 s, 1057.76 s, 916.022 m, 835.991 s, 774.28 s, 670.143 m cm^{-1}.

Remarks: No integrals are given for the ^{1}H due to overlap of signals (anomeric mixture).

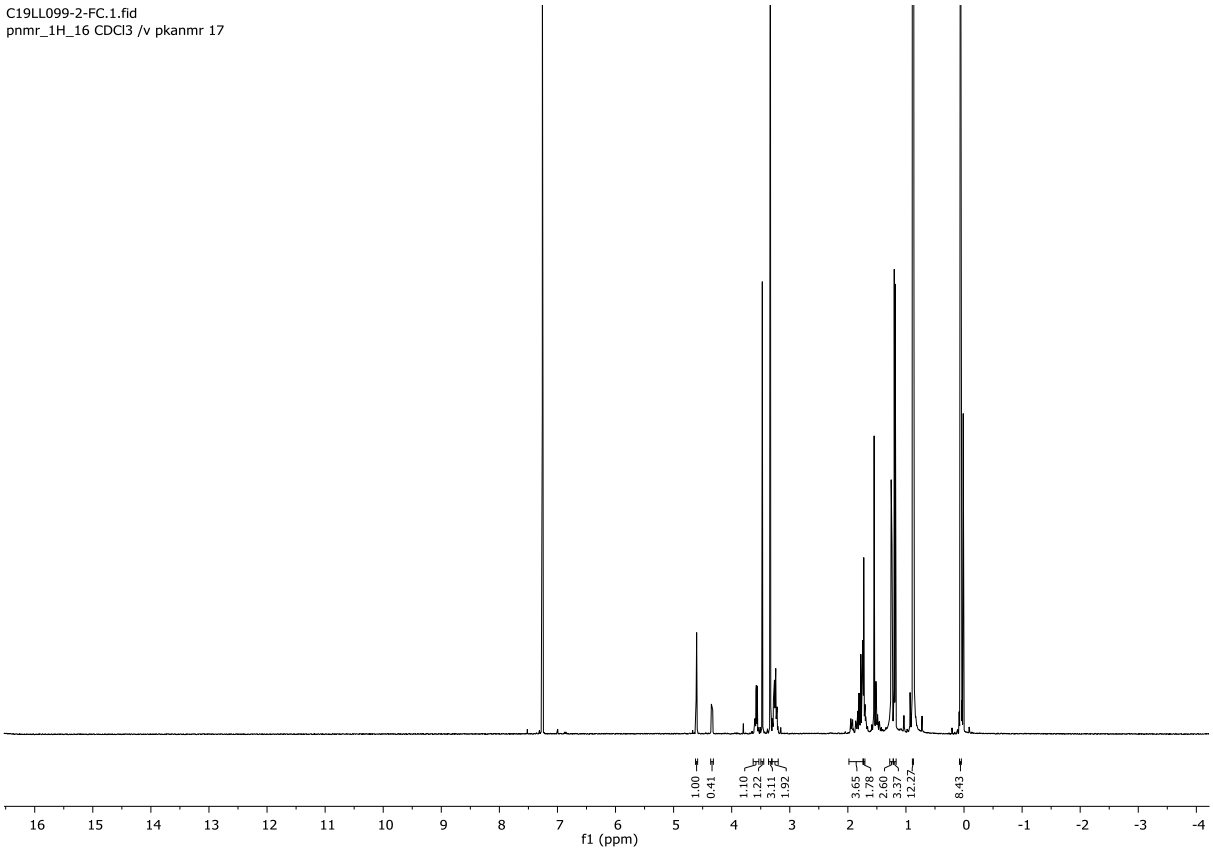
C19LL099-2-FC.1.fid
pnmr_1H_16 CDCl3 /v pkanmr 17
1.00
0.41
1.10
1.22
3.11
1.92
3.65
1.78
2.60
3.37
12.27
8.43
f1 (ppm)

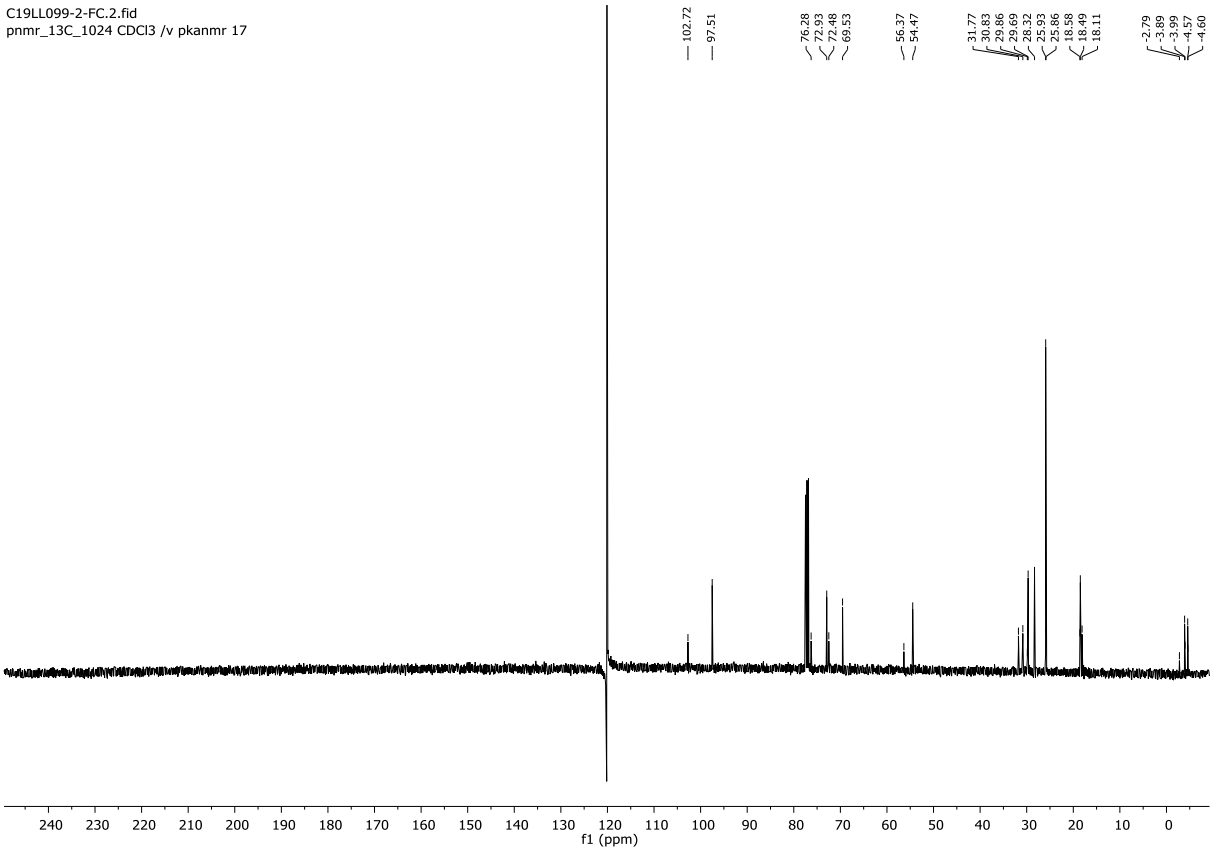
C19LL099-2-FC.2.fid
pnmr_13C_1024 CDCl3 /v pkanmr 17
102.72
97.51
76.28
72.93
72.48
69.53
56.37
54.47
31.77
30.83
29.86
29.69
28.32
25.93
25.86
18.58
18.49
18.11
-2.79
-3.89
-3.99
-4.57
-4.60
f1 (ppm)

A-115 (2R,3S)-6-methoxy-2-methyltetrahydro-2H-pyran-3-yl acetate

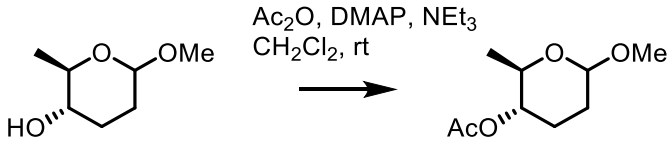

Assay: To a solution of alcohol **A-79** (50 mg, 0.34 mmol, 1.0 equiv) in CH_2Cl_2 (3.2 mL) was added NEt_3 (104 µL, 0.75 mmol, 2.2 equiv), Ac_2O (71 µL, 0.75 mmol, 2.2 equiv) and a catalytic amount of DMAP. The reaction was monitored via TLC and was found to be completed after 2 h. The reaction was then quenched with saturated aqueous NH_4Cl solution (2 mL). The phases were separated and the aqueous phase was extracted with EtOAc (3 x 2 mL). Combined organic phases were dried over $MgSO_4$ and concentrated under reduced pressure. The crude oil was purified by FC (ether:pentane, 1:5) to give the acylated product (54.6 mg, 0.29 mmol, 85%).

Analytics: $\mathbf{R_f}$ = 0.39, EtOAc:hexane 1:5 resp. $\mathbf{R_f}$ = 0.49, EtOAc:hexane 1:5. ^{1}H NMR (400 MHz, Chloroform-*d*) δ 4.64 (d, *J* = 1.9 Hz), 4.53 – 4.34 (m), 3.83 – 3.72 (m), 3.48 (s), 3.35 (s), 2.21 – 2.12 (m), 2.05 (s), 1.97 – 1.84 (m), 1.84 – 1.73 (m), 1.23 (d, *J* = 6.3 Hz), 1.16 (d, *J* = 6.3 Hz).

C35LL133-2-prodQ.1.fid
BBFO_1H_16 CDCl3 /v pkanmr 42

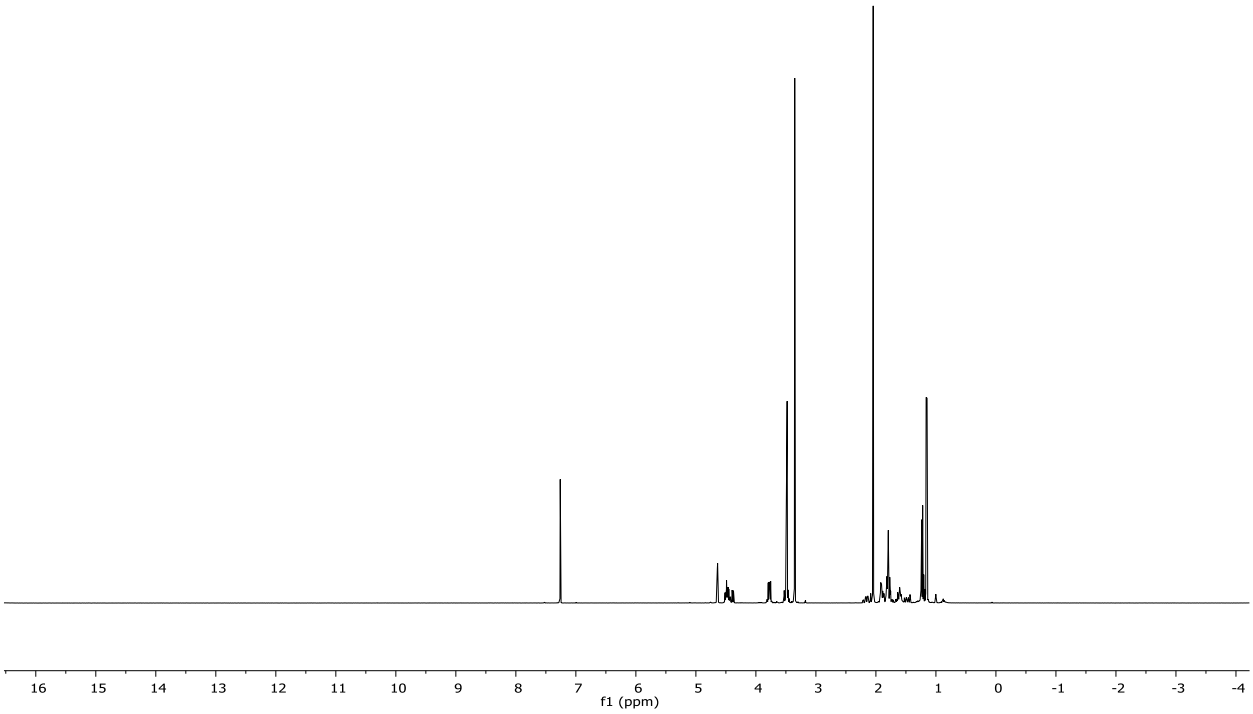

A-118 (2R,4S)-tert-butyl 2-(tert-butyl)-4-methyl-4-((4-((1-((2R,5S,6R)-6-methyl-5-((trimethylsilyl)oxy)tetrahydro-2H-pyran-2-yl)-2-oxo-1,2-dihydropyrimidin-4-yl)carbamoyl)phenyl)carbamoyl)oxazolidine-3-carboxylate

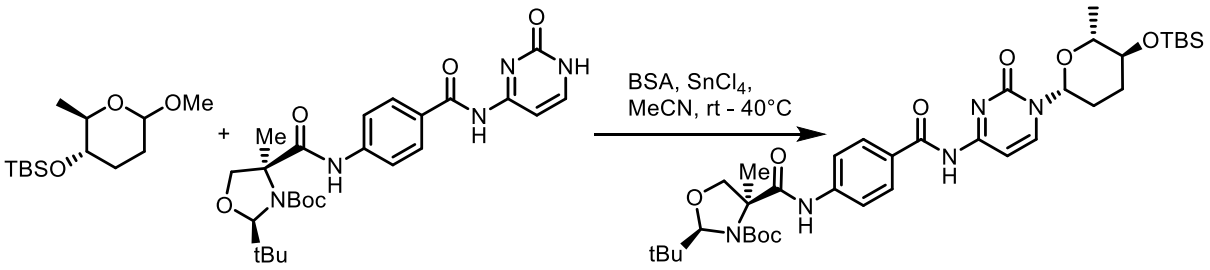

Assay: A-53 (27.2 mg, 0.054 mmol, 1.2 equiv) was dried in a flame dried 5 mL round bottom flask over night at high vaccum (10^{-3} mbar). It was then suspended in MeCN (0.3 mL) and N,O-bis(trimethylsilyl)acetamid (0.022 mL, 0.091 mmol, 2.0 equiv) was added at room temperature which instantly turns the brown suspension into a homogeneous dark brown solution. After 30 min of stirring, **A-116** (11.8 mg, 0.045 mmol, 1.0 equiv), which was azeotropically dried with benzene (3 x 1 mL), dissolved in MeCN (0.4 mL) was added, followed by freshly distilled $SnCl_4$ (8 µl, 0.068 mmol, 1.5 equiv) in MeCN (0.25 mL), which was prepared as a stock solution. The reaction mixture was stirred for 16 h at ambient temperature and meanwhile monitored via LC-MS. At that point, starting material was still existing and therefore the reaction mixture was heated to 40°C for additional 2 h. It was then allowed to reach ambient temperature and was quenched with saturated aqueous $NaHCO_3$ (few drops). H_2O (1 mL) was added. The layers were separated and the aqueous phase was extracted with EtOAc (5 x 2 mL). The organic layers were combined, dried over $MgSO_4$ and concentrated under reduced pressure The brown crude was purified by FC (EtOAc:hexane, 1:1) to give the title compound as a yellowish powder (10 mg, 0.014 mmol, 30%).

Analytics: $\mathbf{R_f}$ = 0.35 (EtOAc:hexane, 1:1). **^{1}H NMR** (400 MHz, $CDCl_3$) δ 10.36 (s, 1H), 8.85 (s, 1H), 7.96 – 7.85 (m, 3H), 7.69 (d, *J* = 8.7 Hz, 2H), 7.53 (d, *J* = 5.4 Hz, 1H), 5.75 (d, *J* = 10.3 Hz, 1H), 5.21 (s, 1H), 4.81 (d, *J* = 8.6 Hz, 1H), 3.81 (d, *J* = 9.0 Hz, 1H), 3.53 (tt, *J* = 12.2, 6.1 Hz, 1H), 3.31 (td, *J* = 10.5, 4.6 Hz, 1H), 2.28 (d, *J* = 12.2 Hz, 1H), 2.14 – 1.99 (m, 1H), 1.73 (s, 3H), 1.74 – 1.62 (m, 1H), 1.54 (s, 9H), 1.55 – 1.42 (m, 1H), 1.29 (d, *J* = 6.1 Hz, 3H), 0.91 (s, 9H), 0.89 (s, 9H), 0.09 (d, *J* = 2.4 Hz, 6H). **^{13}C NMR** (101 MHz, Chloroform-*d*) δ 171.94, 162.20, 144.56, 143.00, 129.11 (2 C), 119.49 (2 C), 98.12, 83.41, 83.17, 79.48, 76.17, 72.00, 68.20, 38.35, 32.02, 31.27, 29.84, 28.29 (3 C), 26.27 (3 C), 25.87 (3 C), 22.23, 18.60, 18.08, -3.93, -4.59.

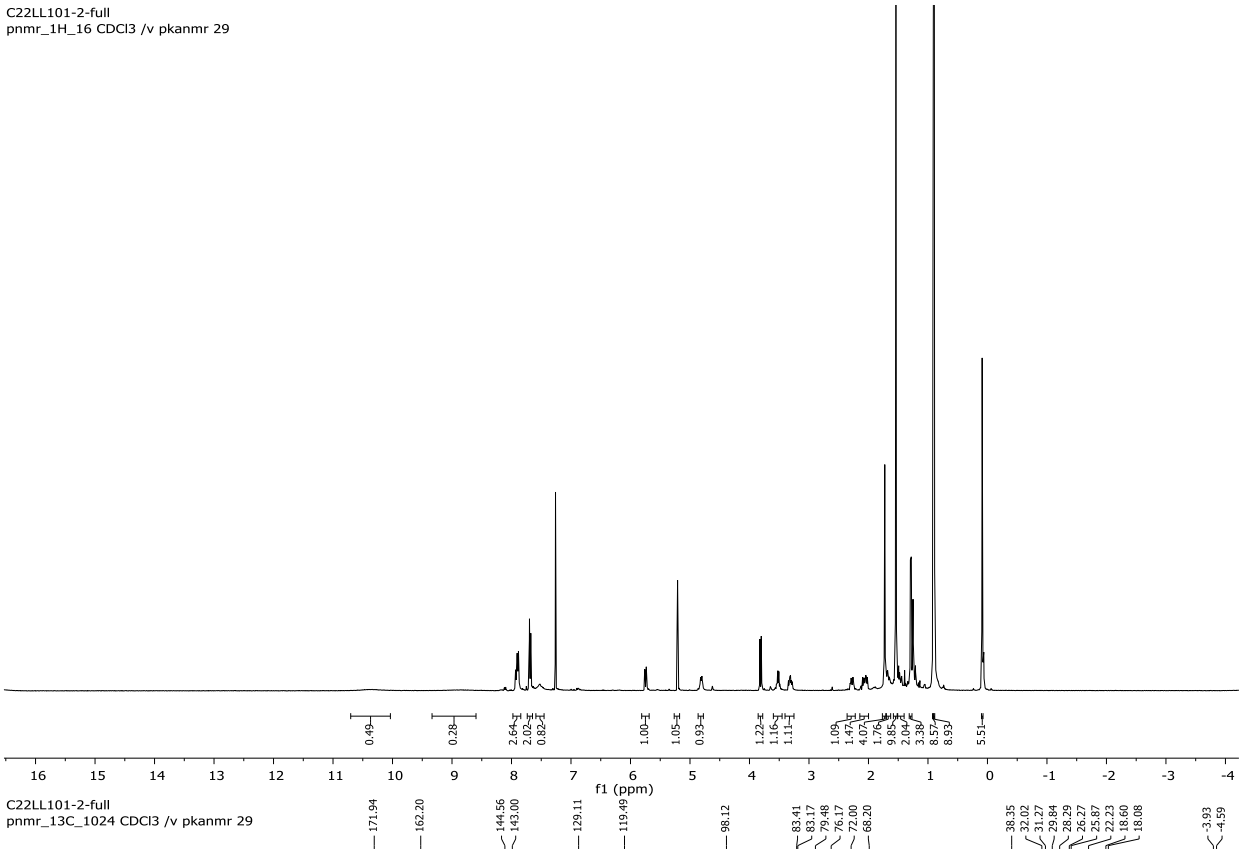
C22LL101-2-full
pnmr_1H_16 CDCl3 /v pkanmr 29
0.49
0.28
2.64
2.02
0.82
1.00
1.05
0.93
1.22
1.16
1.11
1.09
1.47
4.07
1.76
9.85
2.04
3.38
8.57
8.93
5.51
f1 (ppm)
C22LL101-2-full
pnmr_13C_1024 CDCl3 /v pkanmr 29
171.94
162.20
144.56
143.00
129.11
119.49
98.12
83.41
83.17
79.48
76.17
72.00
68.20
38.35
32.02
31.27
29.84
28.29
26.27
25.87
22.23
18.60
18.08
-3.93
-4.59
f1 (ppm)

A-60 (2R,4S)-tert-butyl 2-(tert-butyl)-4-((4-((1-((2R,5S,6R)-5-hydroxy-6-methyltetrahydro-2H-pyran-2-yl)-2-oxo-1,2-dihydropyrimidin-4-yl)carbamoyl)phenyl)carbamoyl)-4-methyloxazolidine-3-carboxylate

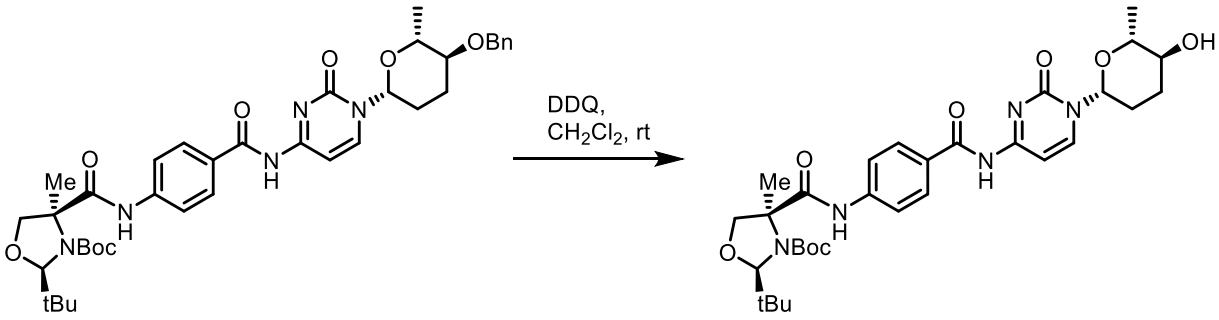

Assay: To a solution of benzyl protected **A-110** (14.5 mg, 20.6 µmol, 1.0 equiv) in CH_2Cl_2 (0.2 mL) was added pH 7 phosphate buffer (0.5 M, 20 µL) and DDQ (23.4 mg, 103 µmol, 5.0 equiv). The reaction mixture was stirred at ambient temperature and monitored via LC-MS. After 27 h the reaction did not proceed any longer and starting material was still existing, thus another 5.0 equiv of DDQ was added. Again, another 5.0 equiv of DDQ was added after 44 h and additional phosphate buffer (0.5 M, 20 µL). After 66 h starting material was fully consumed. The crude was then directly applied to a flash column (EtOAc –> EtOAc:MeOH 5%) without evaporating solvents or working the reaction up. The fractions containing the product were then collected and extracted with pH 7 buffer to give the title compound as a yellow powder (8.6 mg, 0.014 mmol, 68%).

Analytics: $\mathbf{R_f}$ = 0.24 (EtOAc:MeOH (5%)). **^{1}H NMR** (400 MHz, Chloroform-*d*) δ 10.36 (s, 1H), 9.25 (s, 1H), 7.91 (d, *J* = 7.9 Hz, 3H), 7.68 (d, *J* = 8.7 Hz, 2H), 7.53 (s, 1H), 5.76 (dd, *J* = 10.4, 1.9 Hz, 1H), 5.20 (s, 1H), 4.80 (d, *J* = 8.8 Hz, 1H), 3.81 (d, *J* = 9.0 Hz, 1H), 3.65 (s, 1H), 3.55 (dq, *J* = 9.0, 6.1 Hz, 1H), 3.40 – 3.28 (m, 1H), 2.29 (d, *J* = 12.3 Hz, 1H), 2.24 – 2.16 (m, 1H), 1.72 (s, 3H), 1.72 – 1.66 (m, 1H), 1.53 (s, 9H), 1.50 (m, 1H), 1.37 (d, *J* = 6.1 Hz, 3H), 0.91 (s, 9H). **^{13}C NMR** (101 MHz, $CDCl_3$) δ 171.96, 162.39, 156.05, 154.58, 144.43, 142.95, 129.20 (2 C), 128.10, 119.47 (2 C), 98.11, 97.04, 83.38, 83.17, 79.20, 76.15, 71.27, 68.19, 38.33, 31.58, 31.21, 28.27 (3 C), 26.26 (3 C), 22.22, 18.26. **HRMS (ESI)**: 636.2996 $[M+Na]^+$; calculated for $[C_{31}H_{43}N_5NaO_8]$: 636.3004. **$[\alpha]^{20}_D$** = -35.53 (c = 0.076, MeOH). **IR** [ATR, neat]: ν = 3387.35 w, 2971.77 w, 2930.3 w, 1693.19 m, 1657.52 m, 1597.73 m, 1483.96 s, 1305.57 m, 1248.68 s, 1162.87 s, 1051.98 s, 852.383 w, 784.886 m cm^{-1}. **m.p.**: 155 °C.

Remarks: second proton spectrum shows that upon prolonged drying (remove residual EtOAc) the compound starts to decompose.

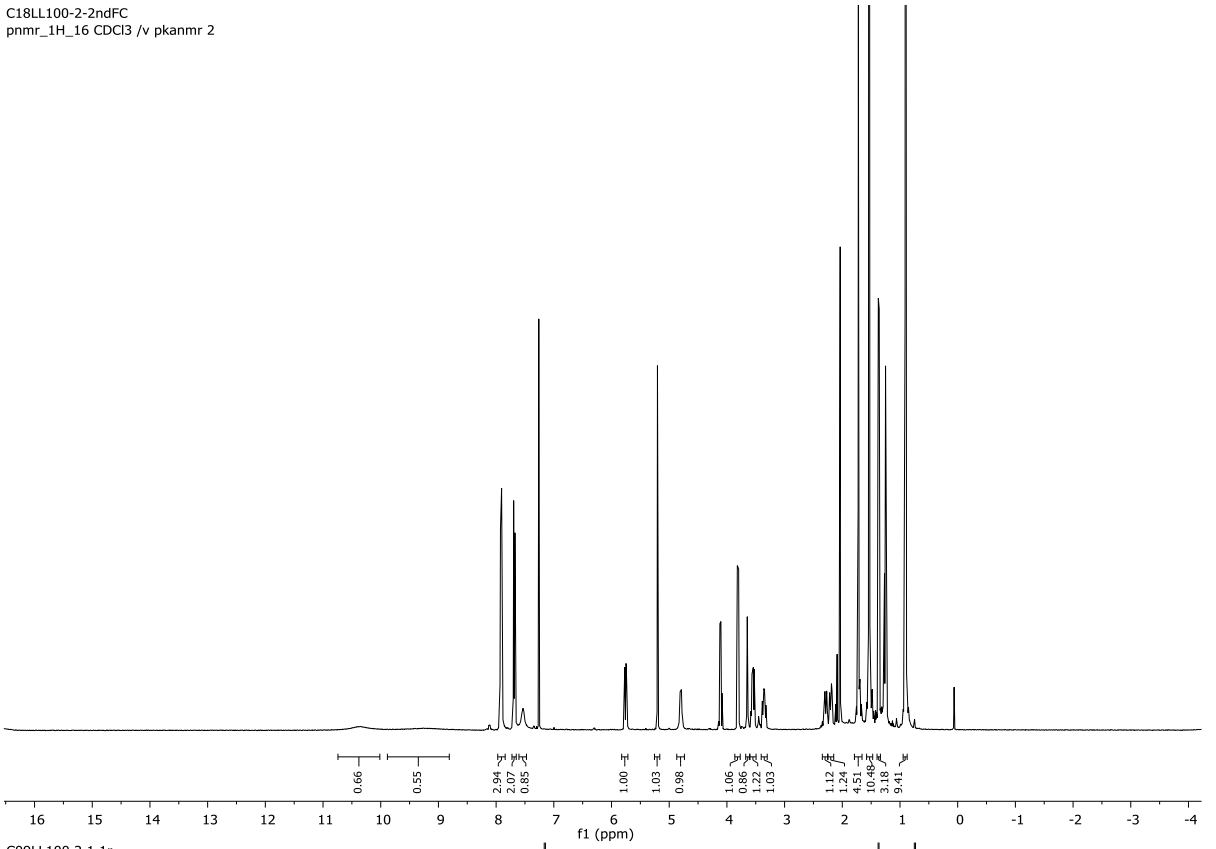
C18LL100-2-2ndFC
pnmr_1H_16 CDCl3 /v pkanmr 2
0.66
0.55
2.94
2.07
0.85
1.00
1.03
0.98
1.06
0.86
1.22
1.03
1.12
1.24
4.51
10.48
3.18
9.41
f1 (ppm)

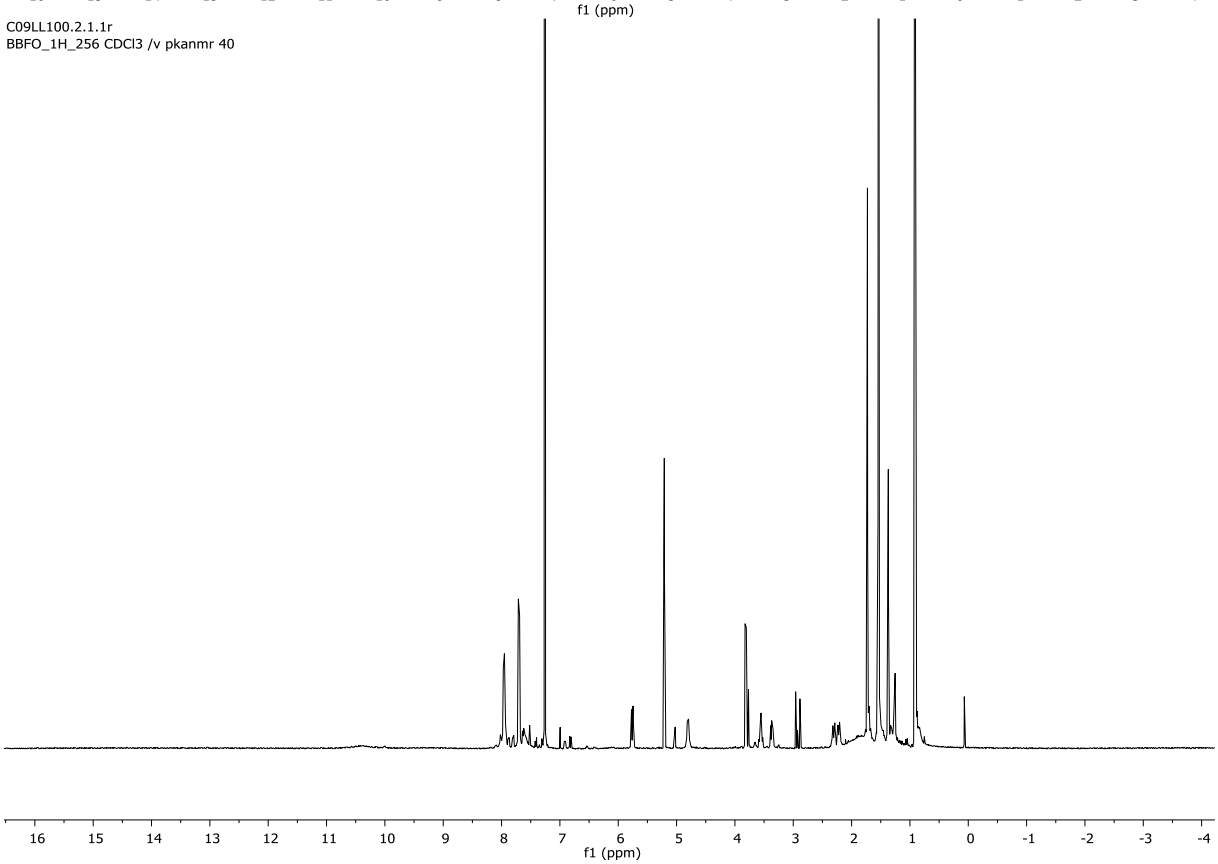
C09LL100.2.1.1r
BBFO_1H_256 CDCl3 /v pkanmr 40
f1 (ppm)

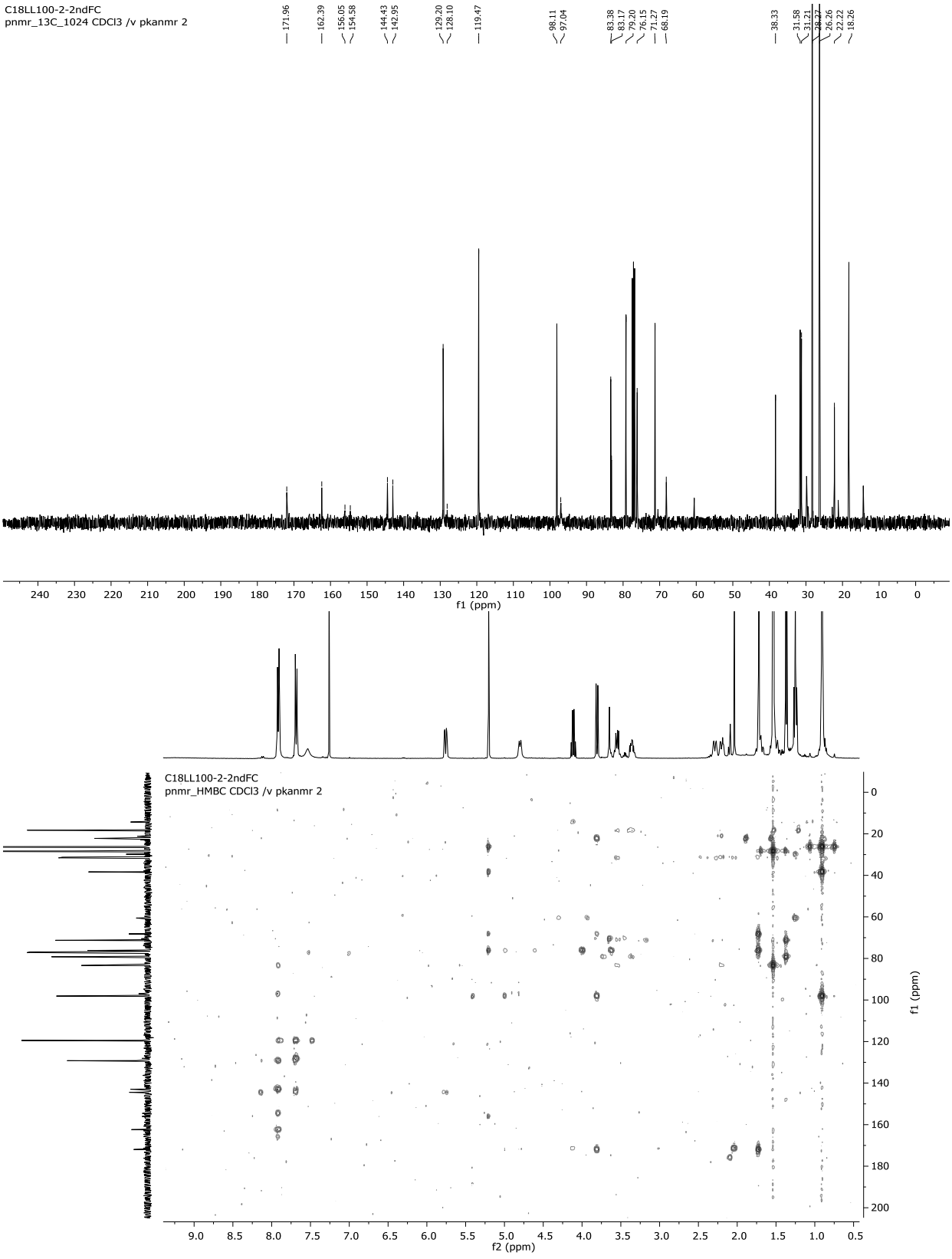
C18LL100-2-2ndFC
pnmr_13C_1024 CDCl3 /v pkanmr 2
171.96
162.39
156.05
154.58
144.43
142.95
129.20
128.10
119.47
98.11
97.04
83.38
83.17
79.20
76.15
71.27
68.19
38.33
31.58
31.21
28.27
26.26
22.22
18.26
f1 (ppm)
C18LL100-2-2ndFC
pnmr_HMBC CDCl3 /v pkanmr 2
f2 (ppm)
f1 (ppm)

A-60 tert-butyl(2R,4S)-2-(tert-butyl)-4-((4-((1-((2R,5S,6R)-5-hydroxy-6-methyltetrahydro-2H-pyran-2-yl)-2-oxo-1,2-dihydropyrimidin-4-yl)carbamoyl)phenyl)carbamoyl)-4-methyloxazolidine-3-carboxylate

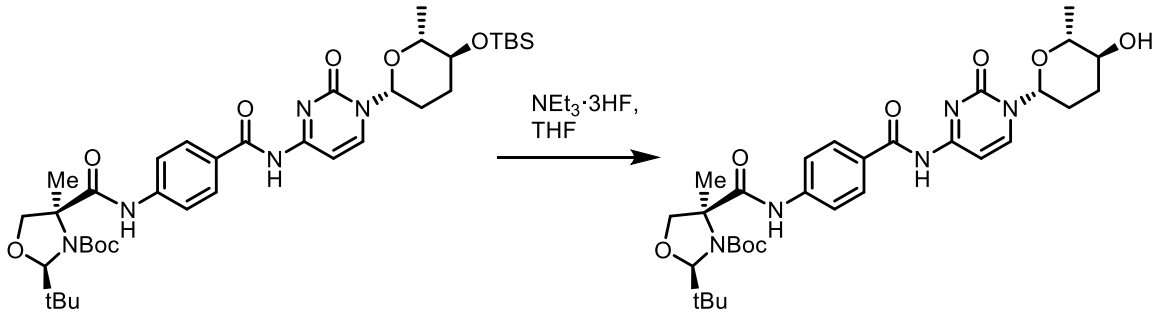

Assay: To a stirring solution of **A-118** (7.5 mg, 0.01 mmol, 1.0 equiv) in THF (1.0 mL) was added $NEt_3 \cdot HF$ (17 µL, 0.1 mmol, 10.0 equiv) at 0 °C. The reaction was allowed to reach ambient temperature and was stirred for 9 h whereas no conversion of starting material was observed. Thus another aliquot of $NEt_3 \cdot HF$ (100 µL) was added and the reaction was allowed to stir over the weekend at ambient temperature. TLC analysis indicated decomposition of starting material. The reaction mixture was quenched with saturated aqueous $NaHCO_3$ (1 mL). The aqueous phase was extracted with EtOAc (3 x 2 mL). The combined organic phases were dried over $MgSO_4$. Purification by FC (EtOAc) gave a very small amount of product (roughly 1 mg) and several side products.

Analytics: $\mathbf{R_f}$ = 0.28 (EtOAc:hexane, 1:1).

A-60 tert-butyl(2R,4S)-2-(tert-butyl)-4-((4-((1-((2R,5S,6R)-5-hydroxy-6-methyltetrahydro-2H-pyran-2-yl)-2-oxo-1,2-dihydropyrimidin-4-yl)carbamoyl)phenyl)carbamoyl)-4-methyloxazolidine-3-carboxylate

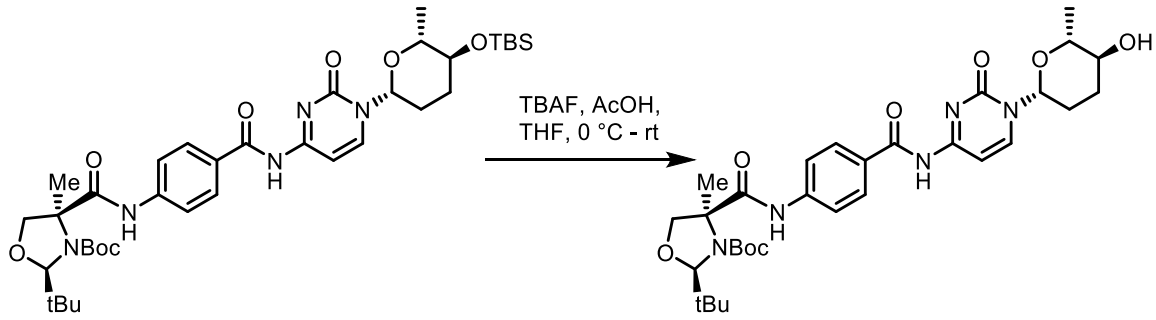

Assay: To a solution of TBS protected pyranol (11 mg, 15.1 µmol, 1.0 equiv) in THF (0.6 ml) at ambient temperature was added TBAF (16.6 µl/1M in THF, 16.6 µmol, 1.1 equiv) followed by AcOH (0.2 µl, 3.0 µmol, 0.2 equiv). After 8 h at room temperature very little product formation was observed by TLC (EtOAc:MeOH (5%)). Thus, the reaction was stirred over night. Still a lot of starting material was present – thus, another 1.1 equiv of TBAF in THF was added. The reaction temperature was then raised to 40°C and the reaction mixture was stirred as such for 4 h. Starting material was fully consumed. The reaction was then diluted with EtOAc (2 ml) and quenched with saturated aqueous $NHCl_4$ (2 ml). The two phases were separated and the aqueous phase was twice extracted with EtOAc (5 ml). The combined organic phases where dried over Mg_2SO_4 and the solvent was evaporated under reduced pressure. The crude oil was purified by FC (EtOAc:MeOH 5%) giving LL109-5 was a white solid (6.2 mg, 0.101 mmol, 67%).

A-121 (2R,3R,4S,5R,6S)-2-(hydroxymethyl)-6-(phenylthio)tetrahydro-2H-pyran-3,4,5-triol

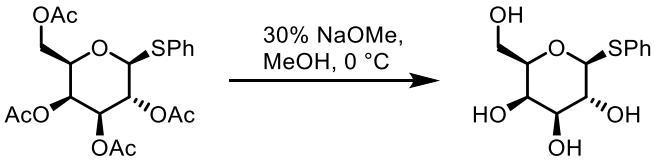

Assay: A-120 (4.9 g, 11.12 mmol, 1.0 equiv) was dissolved in MeOH (73.5 mL) and cooled to 0 °C. NaOMe (30 wt % in MeOH, 7.6 mL, 33.37 mmol, 3.0 equiv) was then added and the reaction mixture was stirred for 20 min. TLC analysis confirmed full conversion of starting material. In order to neutralize the reaction mixture, Amberlyst 15 was added (approximate). After stirring for additional 5 min, the reaction mixture was filtered over cotton wool and the filtrate was concentrated under reduced pressure. Co-evaporation with toluene gave the title compound as a white powder in quantitative yield.

Analytics: **^{1}H NMR** (400 MHz, MeOD) δ 7.57 – 7.53 (m, 2H), 7.31 – 7.19 (m, 3H), 4.59 (d, *J* = 9.7 Hz, 1H), 3.91 (d, *J* = 3.2 Hz, 1H), 3.74 (qd, *J* = 11.5, 6.0 Hz, 2H), 3.61 (t, *J* = 9.4 Hz, 1H), 3.58 – 3.54 (m, 1H), 3.50 (dd, *J* = 9.2, 3.3 Hz, 1H). **^{13}C NMR** (101 MHz, MeOD) δ 136.13, 132.09 (2 C), 129.85 (2 C), 127.98, 90.33, 80.61, 76.43, 71.08, 70.50, 62.64.

Compound literature known

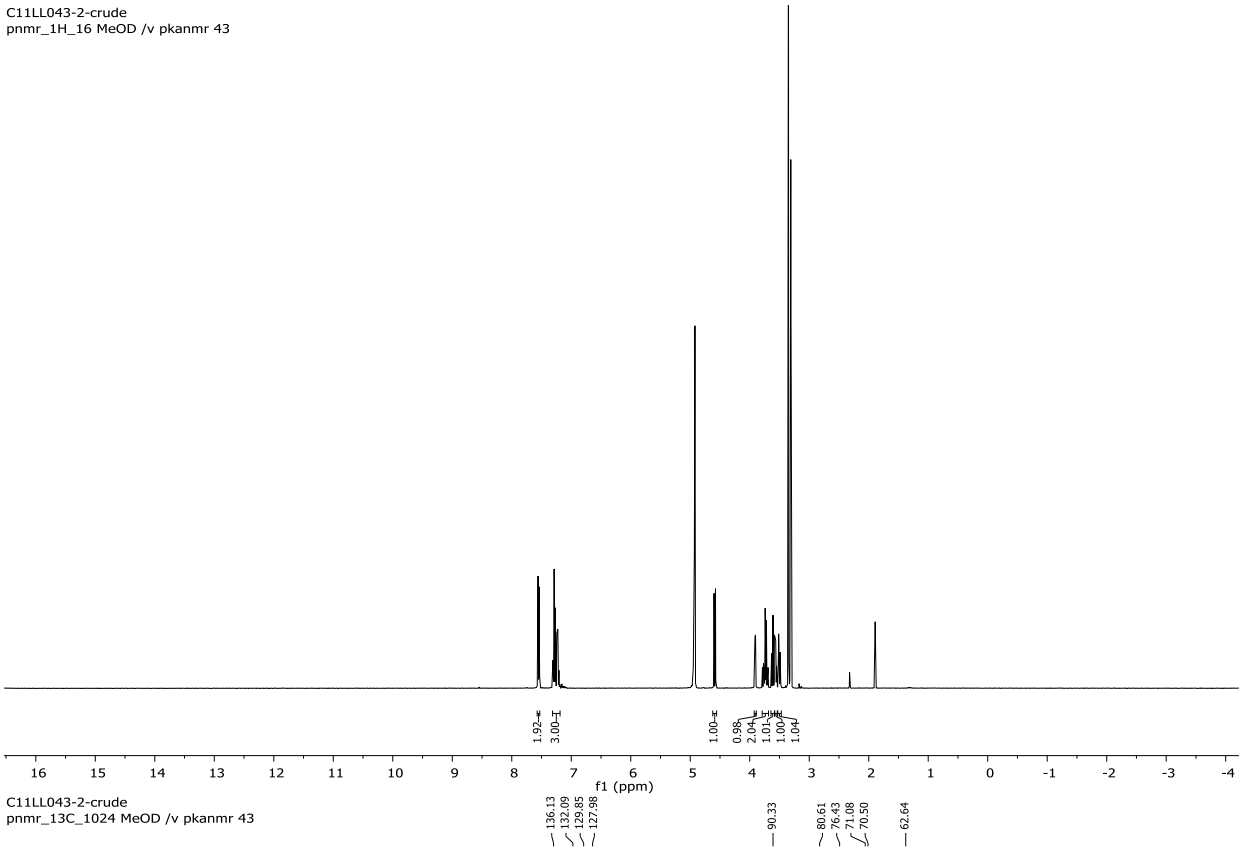
C11LL043-2-crude
pnmr_1H_16 MeOD /v pkanmr 43
1.92
3.00
1.00
0.98
2.04
1.01
1.00
1.04
f1 (ppm)

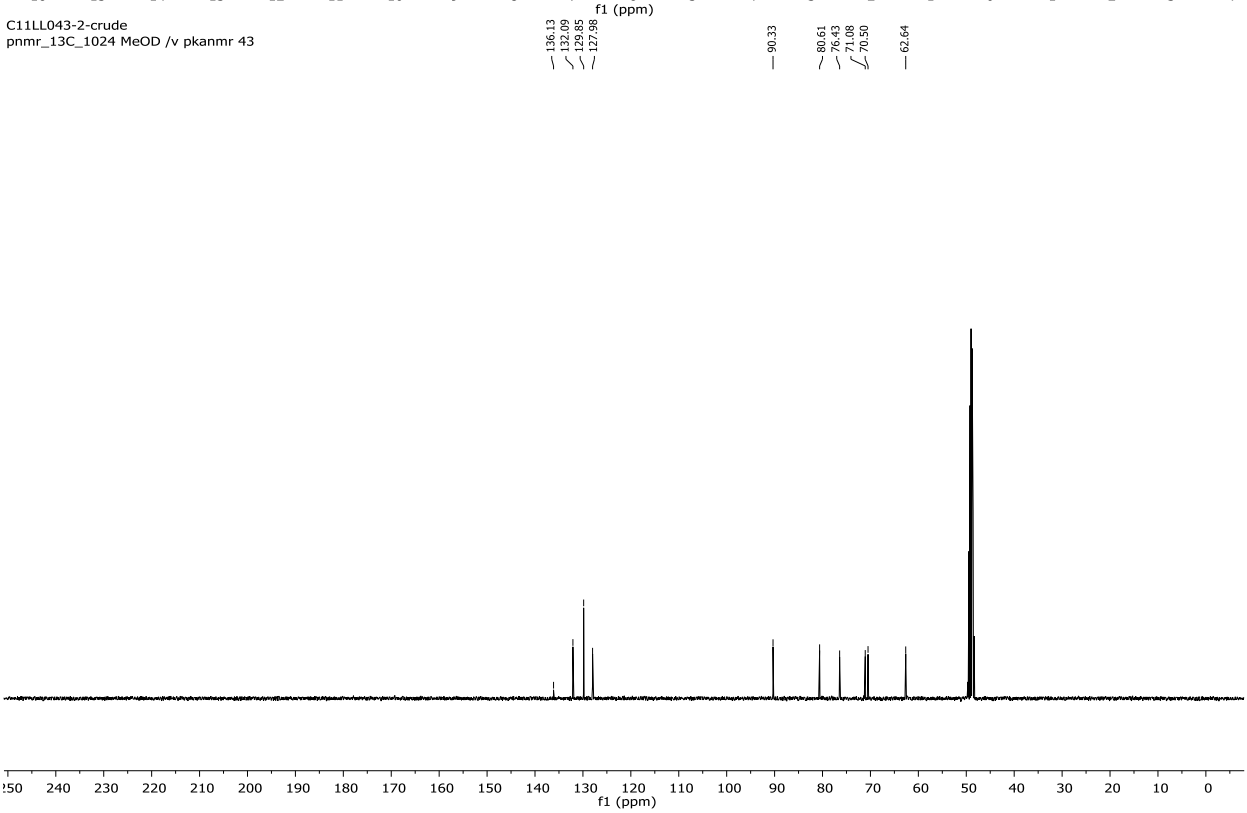
C11LL043-2-crude
pnmr_13C_1024 MeOD /v pkanmr 43
136.13
132.09
129.85
127.98
90.33
80.61
76.43
71.08
70.50
62.64
f1 (ppm)

A-122 (2S,4aR,6S,7R,8R,8aR)-2-phenyl-6-(phenylthio)hexahydropyrano[3,2-d][1,3]dioxine-7,8-diol

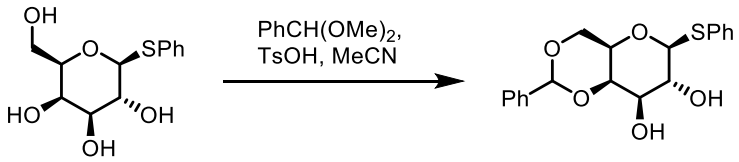

Assay: A-121 (8.1 g, 29.74 mmol, 1.0 equiv) was suspended in MeCN (75 ml) and α,α-dimethoxytoluene (5.8 ml, 38.67 mmol, 1.3 equiv), pTsOH (85 mg, 0.45 mmol, 0.02 equiv) were then added. Upon addition of the acid, the starting material is getting completely dissolved. The product is built within 2 h and precipitates as a white solid, which can then be filtered off. Both, the *p*TsOH and α,α-dimethoxytoluene were removed by washing with hexane and very little MeOH. Pure product was obtained as a white solid (10.02g, 27.8 mmol, 93%).

Analytics: $\mathbf{R_f}$ = 0.23, EtOAc. **^{1}H NMR** (400 MHz, $CDCl_3$) δ 7.69 (dd, *J* = 8.0, 1.6 Hz, 2H), 7.42 – 7.27 (m, 8H), 5.52 (s, 1H), 4.51 (d, *J* = 9.2 Hz, 1H), 4.39 (dd, *J* = 12.5, 1.5 Hz, 1H), 4.23 (d, *J* = 1.9 Hz, 1H), 4.04 (dd, *J* = 12.5, 1.8 Hz, 1H), 3.75 – 3.64 (m, 2H), 3.57 (d, *J* = 1.2 Hz, 1H), 2.52 (dd, *J* = 11.2, 4.9 Hz, 1H). **^{13}C NMR** (101 MHz, $CDCl_3$) δ 137.70, 133.92, 129.52, 129.11, 128.39, 126.66, 101.58, 87.15, 75.47, 73.97, 70.24, 69.44, 68.99.

Compound literature known

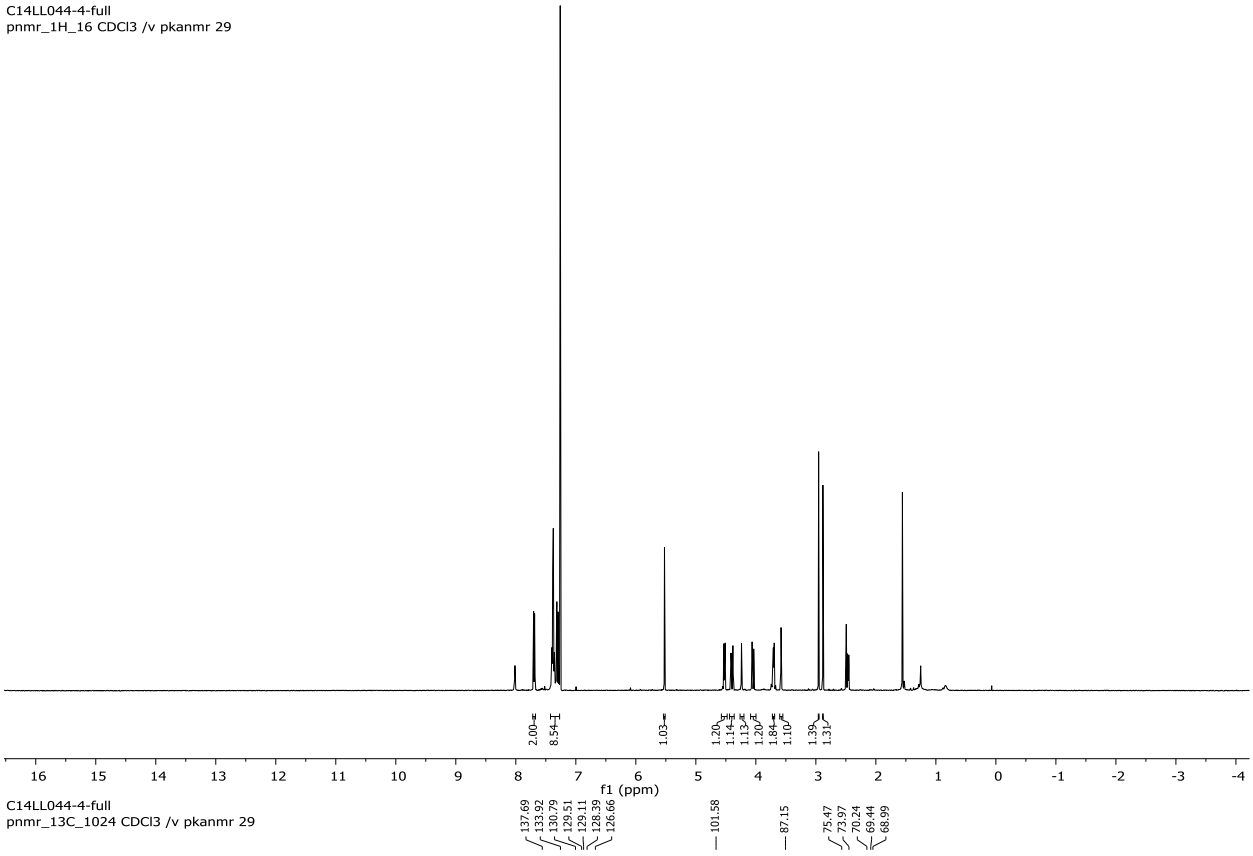
C14LL044-4-full
pnmr_1H_16 CDCl3 /v pkanmr 29
2.00
8.54
1.03
1.20
1.14
1.13
1.20
1.84
1.10
1.39
1.31
f1 (ppm)

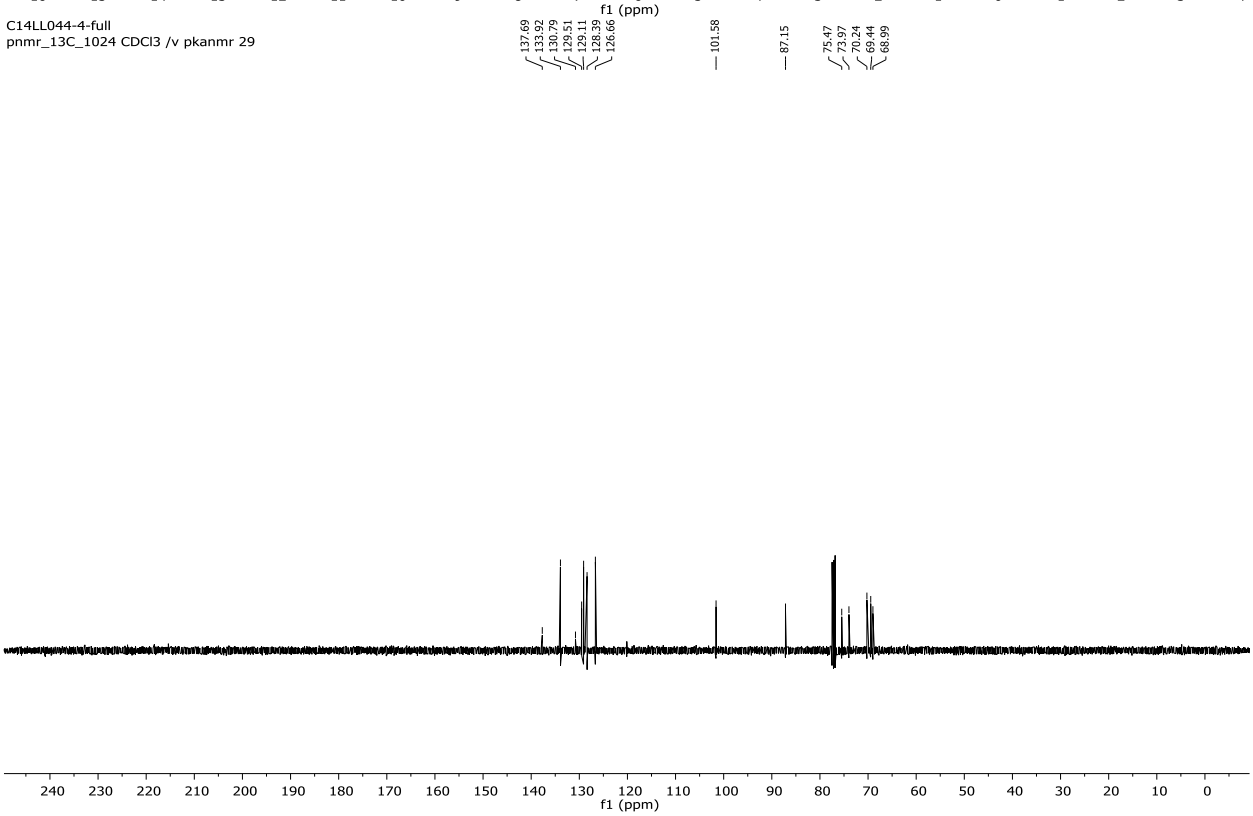
C14LL044-4-full
pnmr_13C_1024 CDCl3 /v pkanmr 29
137.69
133.92
130.79
129.51
129.11
128.39
126.66
101.58
87.15
75.47
73.97
70.24
69.44
68.99
f1 (ppm)

A-123 (2S,4aR,6S,7R,8S,8aS)-7,8-bis(benzyloxy)-2-phenyl-6-(phenylthio)hexahydropyrano[3,2-d][1,3]dioxine

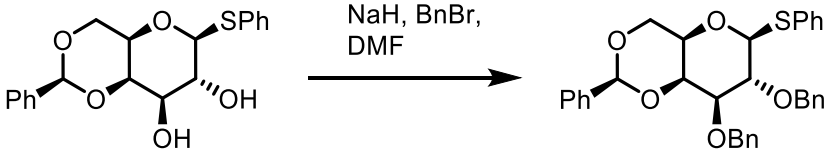

Assay: In a flame dried round bottom flask **A-122** (630 mg, 1.75 mmol, 1.0 equiv) was dissolved in DMF (17 mL). NaH (60% in mineral oil, 210 mg, 5.24 mmol, 3.0 equiv) was added and the reaction mixture was stirred for 1 h at ambient temperature before BnBr (0.52 mL, 4.37 mmol, 2.5 equiv) was given to the reaction mixture. The reaction mixture was stirred over night and then quenched by the addition of MeOH. Saturated aqueous NH_4Cl was added in order to neutralize the reaction. The biphasic mixture was poured into a separatory funnel and the two phases were separated. The aqueous phase was washed with $CHCl_3$ (3 x 10 mL). The combined organic phases were dried over $MgSO_4$ and concentrated under reduced pressure. The pale crystalline crude was purified by FC (EtOAc:hexane 3:1 -> 1:1 -> pure EtOAc) to give the title compound (703.3 mg, 1.3 mmol, 75%).

Analytics: $\mathbf{R_f}$ = 0.42, (EtOAc:hexane, 1:1). **^{1}H NMR** (400 MHz, $CDCl_3$) δ 7.71 (m, 2H), 7.53 (m, 2H), 7.44 – 7.27 (m, 13H), 7.24 – 7.15 (m, 3H), 5.49 (s, 1H), 4.71 (dd, *J* = 7.0, 2.5 Hz, 4H), 4.62 (d, *J* = 9.6 Hz, 1H), 4.38 (dd, *J* = 12.3, 1.5 Hz, 1H), 4.16 (d, *J* = 2.8 Hz, 1H), 3.99 (dd, *J* = 12.3, 1.6 Hz, 1H), 3.90 (t, *J* = 9.4 Hz, 1H), 3.63 (dd, *J* = 9.2, 3.4 Hz, 1H), 3.43 (d, *J* = 0.9 Hz, 1H). **^{13}C NMR** (101 MHz, $CDCl_3$) δ 138.65, 138.28, 138.04, 132.93 (2 C), 132.89, 129.21, 129.02 (2 C), 128.56 (2 C), 128.50 (2 C), 128.36 (2 C), 128.32 (2 C), 127.97 (2 C), 127.86, 127.61, 126.76 (2 C), 101.52, 86.70, 81.55, 75.62, 75.54, 73.88, 72.02 (2 C), 70.02, 69.59.

Compound literature known

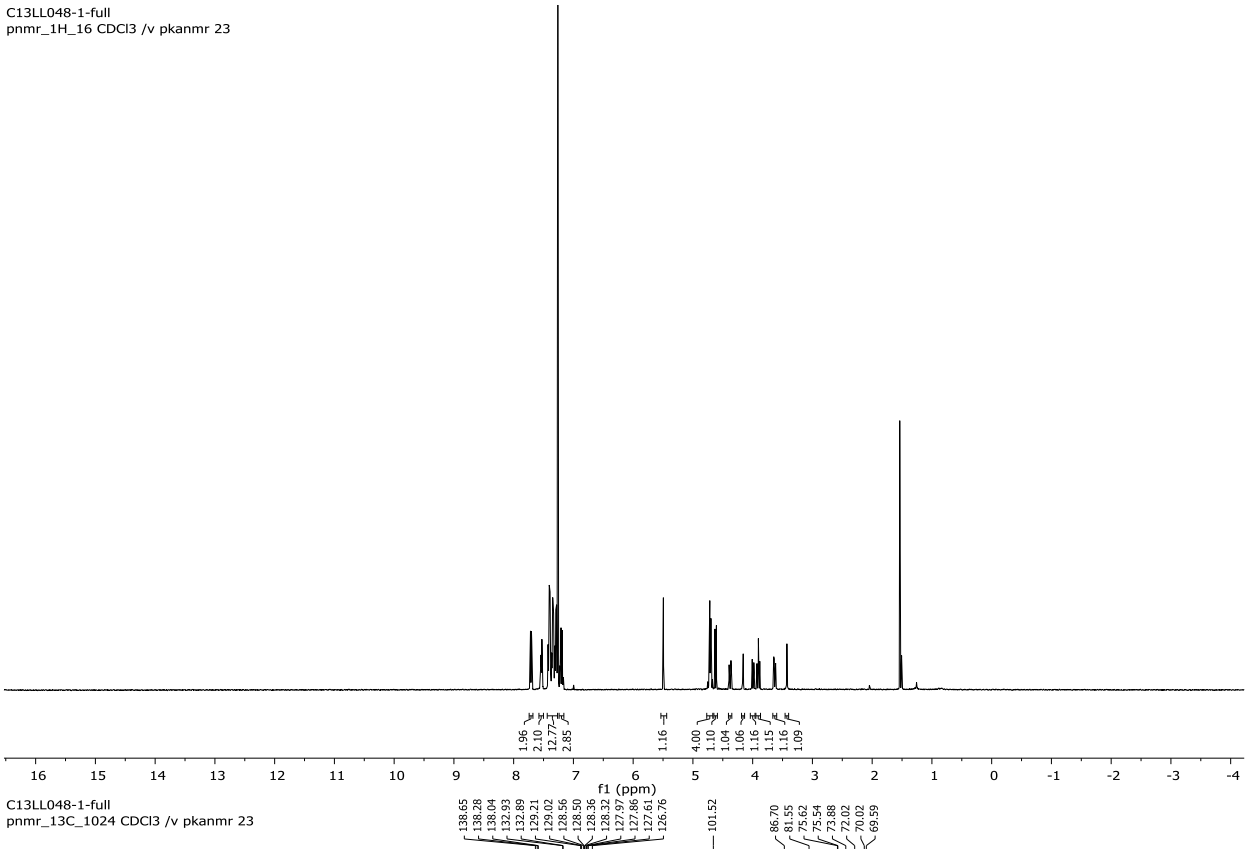
C13LL048-1-full
pnmr_1H_16 CDCl3 /v pkanmr 23
1.96
2.10
12.77
2.85
1.16
4.00
1.10
1.04
1.06
1.16
1.15
1.16
1.09
f1 (ppm)
C13LL048-1-full
pnmr_13C_1024 CDCl3 /v pkanmr 23
138.65
138.28
138.04
132.93
132.89
129.21
129.02
128.56
128.50
128.36
128.32
127.97
127.86
127.61
126.76
101.52
86.70
81.55
75.62
75.54
73.88
72.02
70.02
69.59
f1 (ppm)

A-124 (2R,3S,4S,5R,6S)-4,5-bis(benzyloxy)-2-(hydroxymethyl)-6-(phenylthio)tetrahydro-2H-pyran-3-ol

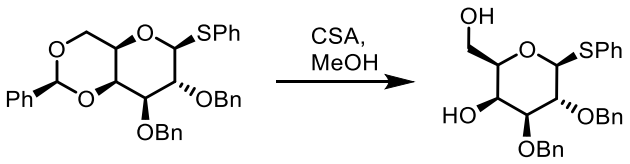

Assay: A-123 (2.87 g, 5.31 mmol, 1.0 equiv) was suspended in MeOH (50 mL) and CSA (0.62 g, 2.66 mmol, 0.5 equiv) was added. The reaction was stirred at ambient temperature 60 h. Complete consumption of starting material was observed by TLC, (EtOAc:hexane, 1:1). The reaction was quenched with saturated aqueous $NaHCO_3$ and the biphasic mixture was poured into a separatory funnel. The aqueous phase was extracted with EtOAc (3 x 15 mL). The combined organic layers were dried over $MgSO_4$ and concentrated under reduced pressure. Purification by FC (EtOAc:hexane, 1:1) gave the title compound (2.07 g, 4.57 mmol, 86%).

Analytics: $\mathbf{R_f}$ = 0.22, (EtOAc:hexane, 1:1). **^{1}H NMR** (400 MHz, $CDCl_3$) δ 7.58 – 7.52 (m, 2H), 7.45 – 7.27 (m, 13H), 4.84 (d, *J* = 10.3 Hz, 1H), 4.75 (d, *J* = 10.3 Hz, 1H), 4.71 (s, 2H), 4.65 (d, *J* = 9.8 Hz, 1H), 4.05 (s, 1H), 4.01 – 3.92 (m, 1H), 3.80 – 3.70 (m, 2H), 3.59 (dd, *J* = 8.9, 3.3 Hz, 1H), 3.50 (dd, *J* = 6.3, 4.6 Hz, 1H), 2.59 (s, 1H), 2.13 – 2.00 (m, 1H). **^{13}C NMR** (101 MHz, $CDCl_3$) δ 138.23, 137.64, 133.77, 132.00 (2 C), 129.12 (2 C), 128.76 (2 C), 128.55 (2 C), 128.41 (2 C), 128.28, 128.07 (2 C), 128.02, 127.66, 87.73, 82.55, 78.15, 75.93, 72.49 (2 C), 67.56, 62.97.

Compound literature known

C16LL051-1-full
pnmr_1H_16 CDCl3 /v pkanmr 33

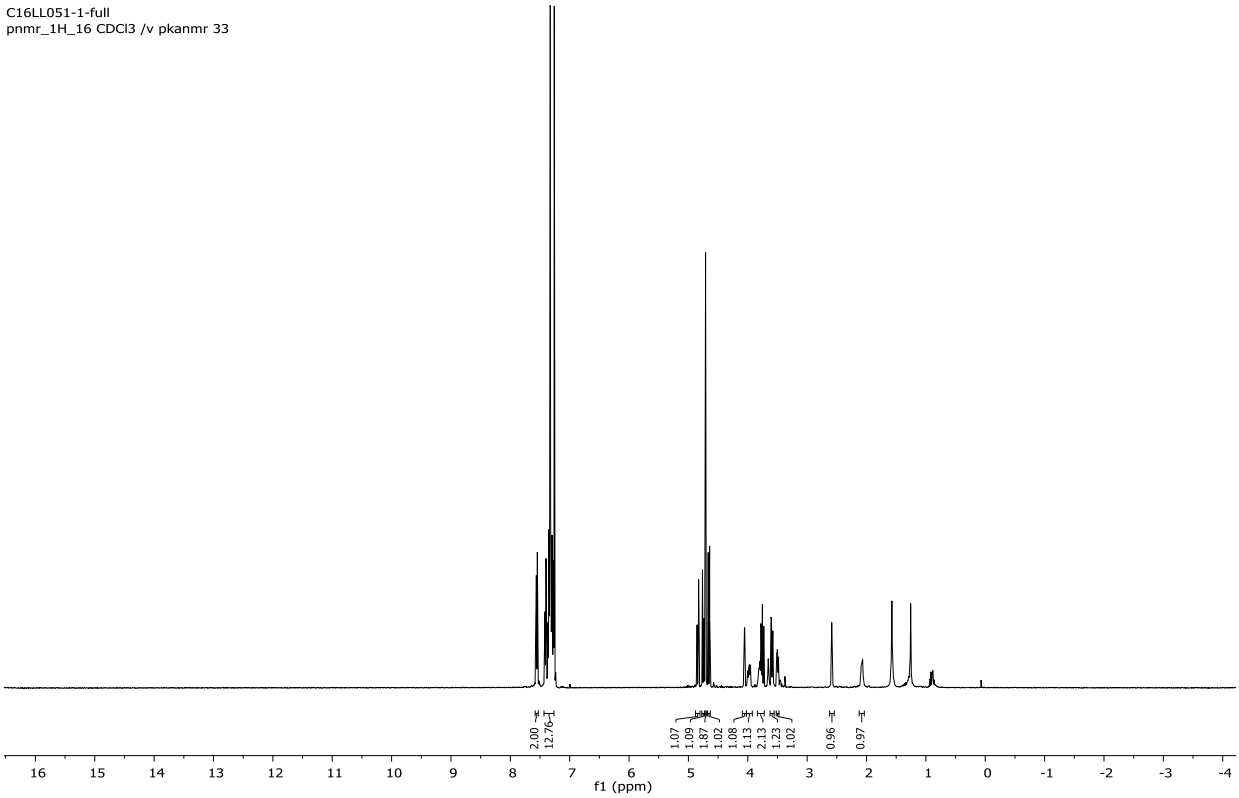

C16LL051-1-full
pnmr_13C_1024 CDCl3 /v pkanmr 33

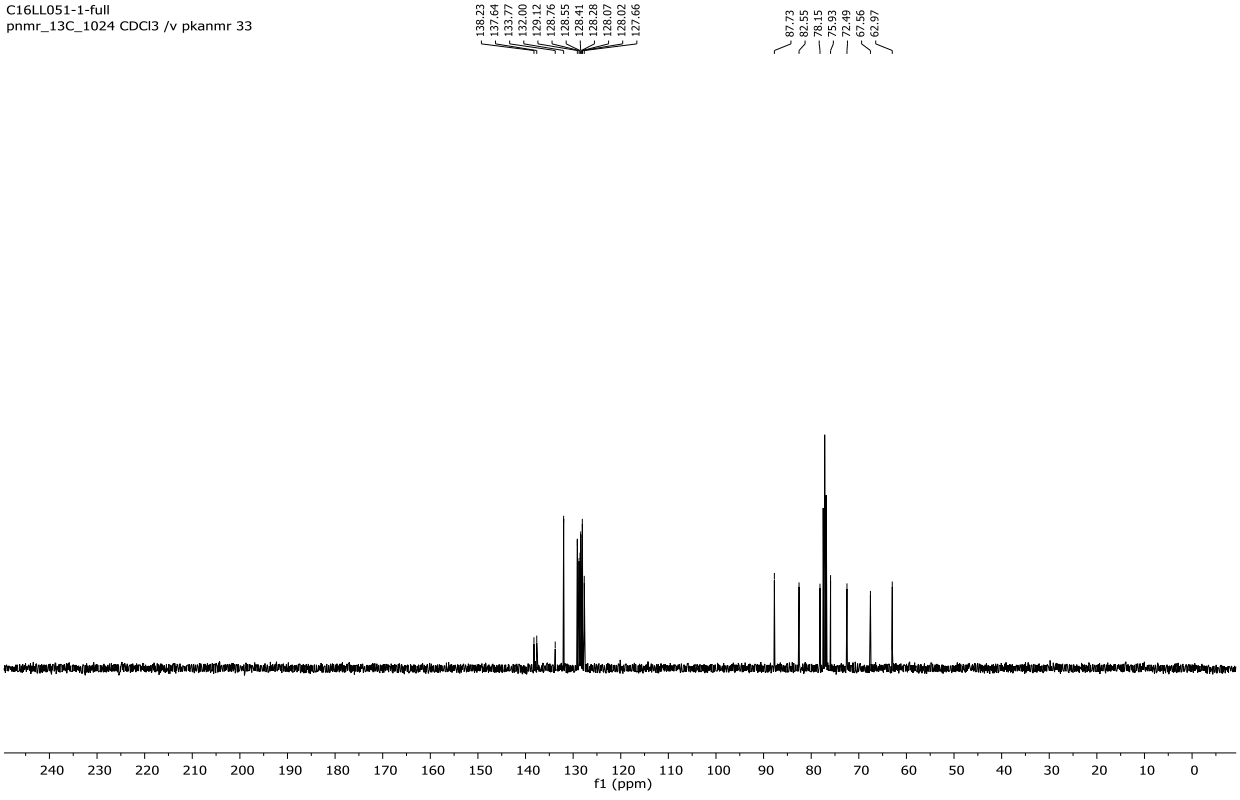

A-125 (2R,3R,4S,5R,6S)-4,5-bis(benzyloxy)-3-hydroxy-6-(phenylthio)tetrahydro-2H-pyran-2-yl 4-methylbenzenesulfonate

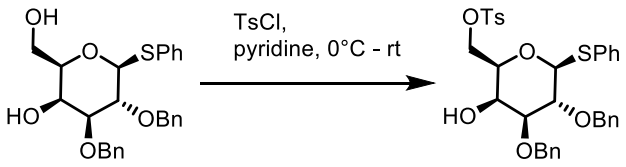

Assay: A-124 (2.36 g, 5.21 mmol, 1.0 equiv) was dissolved in pyridine (50 mL) and tosyl chloride (1.49 g, 7.81 mmol, 1.5 equiv) was added at 0 °C. The reaction mixture was then allowed to warm to room temperature and continued to stir over night. It was then quenched with H_2O (70 mL) and extracted with $CHCl_3$ (3 x 50 mL). The combined organic phases were then again washed with H_2O (70 mL), dried over $MgSO_4$ and concentrated under reduced pressure. The clear, viscous liquid was purified by FC (EtOAc:hexane, 1:2) to give the title compound (2.79 g, 4.60 mmol, 88%).

Analytics: $\mathbf{R_f}$ = 0.33, (EtOAc:Hexane 1:2). **^{1}H NMR** (400 MHz, $CDCl_3$) δ 7.73 (d, *J* = 8.3 Hz, 2H), 7.46 (m, 2H), 7.36 – 7.17 (m, 15H), 4.75 (d, *J* = 10.4 Hz, 1H), 4.66 (d, *J* = 10.4 Hz, 1H), 4.60 (s, 2H), 4.52 (d, *J* = 9.8 Hz, 1H), 4.26 – 4.14 (m, 2H), 3.93 (d, *J* = 2.4 Hz, 1H), 3.69 – 3.58 (m, 2H), 3.50 (dd, *J* = 8.9, 3.2 Hz, 1H), 2.33 (s, 3H). **^{13}C NMR** (101 MHz, $CDCl_3$) δ 145.09, 138.13, 137.49, 133.70, 132.61, 131.77 (2 C), 130.02 (2 C), 129.01 (2 C), 128.68 (2 C), 128.47 (2 C), 128.30 (2 C), 128.22, 128.09 (2 C), 128.01 (2 C), 127.95, 127.56, 87.54, 82.07, 76.74, 75.77, 75.40, 72.46 (2 C), 68.67, 66.23, 21.71.

Compound literature known

C18LL052-2-pure
pnmr_1H_16 CDCl3 /v pkanmr 17

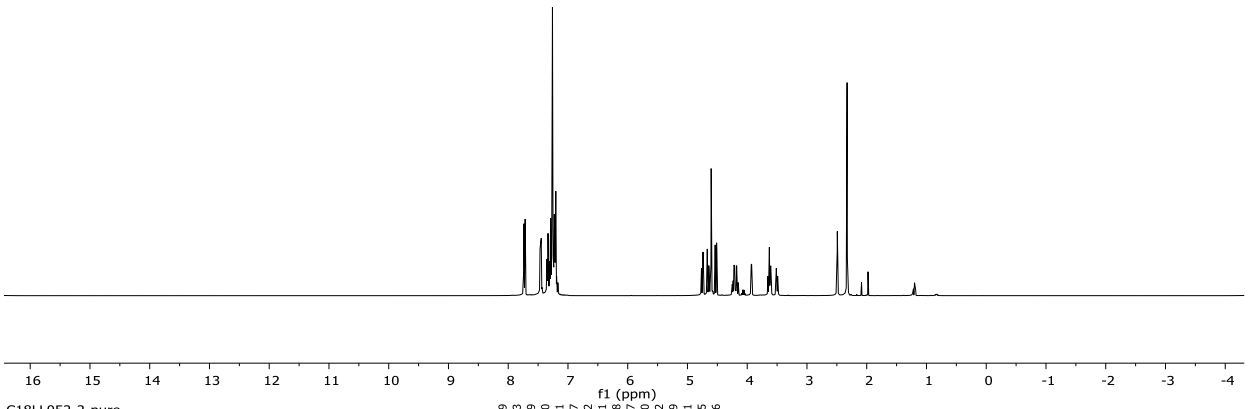

C18LL052-2-pure
pnmr_13C_128 CDCl3 /v pkanmr 17

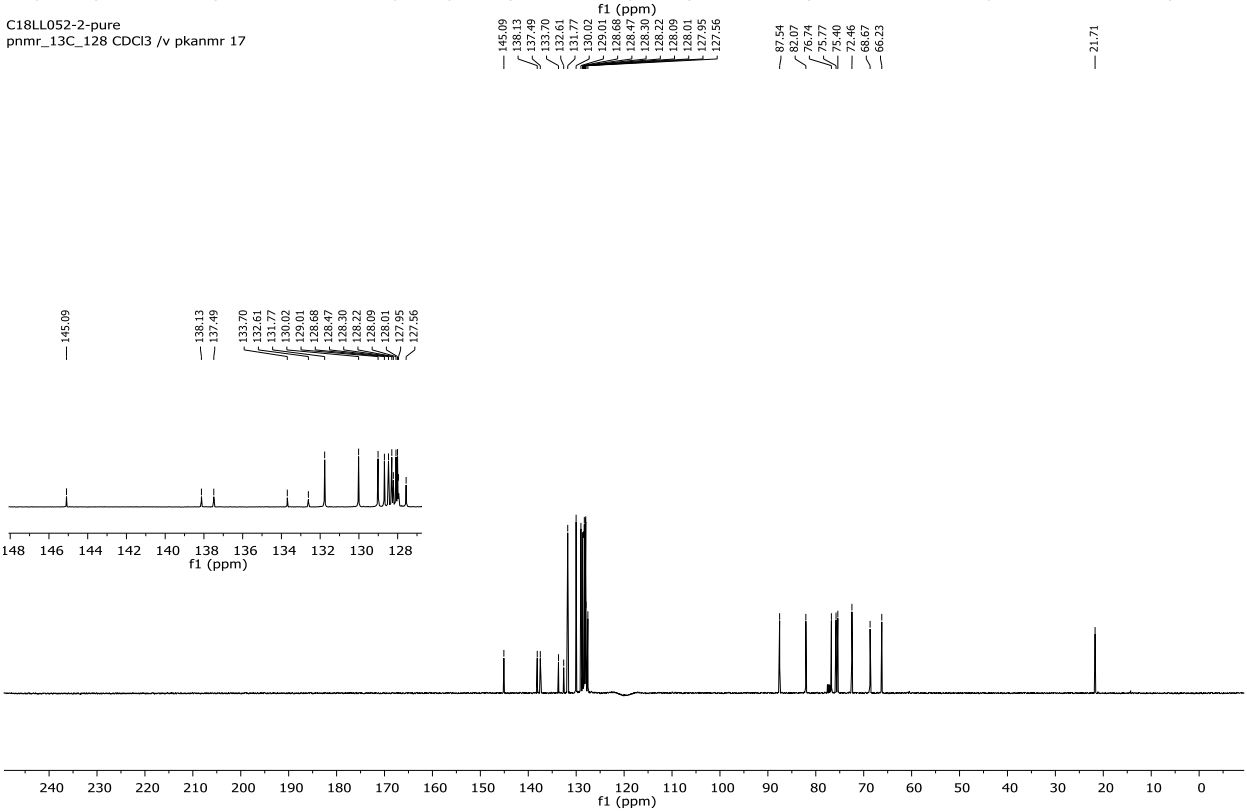

A-126 (2R,3S,4S,5R,6S)-4,5-bis(benzyloxy)-2-methyl-6-(phenylthio)tetrahydro-2H-pyran-3-ol

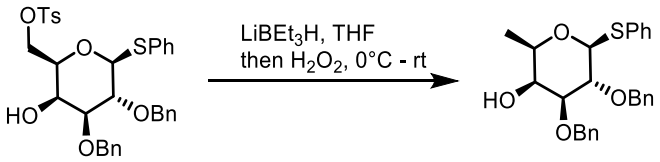

Assay: A-125 (7.20 g, 11.86 mmol, 1.0 equiv) was dissolved in THF (28 mL) and super hydride (1 M in THF, 35.58 mL, 3.0 equiv) was then added via syringe pump (25 mL Hamilton, 0.8 mL/min) at ambient temperature. An effervescence was observed when adding the first few drops of superhydride. After full addition the clear solution was stirred for 2.5 h at 24 °C, the reaction mixture was then cooled to 0 °C and MeOH (about 10 mL, until the effervescence has ceased) followed by H_2O_2 30% (24.22 mL, added via syringe pump; 25 mL Hamilton, 0.8 mL/min) was added cautiously. After stirring for 10 min, the reaction mixture was stirred at 40°C for 30 min in order to quench the excess H_2O_2. The mixture was then extracted with CH_2Cl_2 (3 x 30 mL). The combined organic phases were then dried over $MgSO_4$ and concentrated under reduced pressure. The vicious oil was purified by FC (EtOAc:hexane, 1:4 -> 1:3 -> 1:2) to give the title compound as a clear oil (3.94 g, 9.01 mmol, 76%)

Analytics: $\mathbf{R_f}$ = 0.39 (EtOAc:hexane, 1:2). **^{1}H NMR** (400 MHz, Chloroform-*d*) δ 7.54 – 7.48 (m, 2H), 7.36 – 7.32 (m, 2H), 7.30 – 7.20 (m, 11H), 4.76 (d, *J* = 10.3 Hz, 1H), 4.67 (d, *J* = 10.4 Hz, 1H), 4.64 (d, *J* = 1.7 Hz, 2H), 4.53 (d, *J* = 9.7 Hz, 1H), 3.78 – 3.72 (m, 1H), 3.62 (t, *J* = 9.3 Hz, 1H), 3.55 – 3.47 (m, 2H), 2.20 (d, *J* = 3.1 Hz, 1H), 1.30 (d, *J* = 6.5 Hz, 3H).**^{13}C NMR** (101 MHz, Chloroform-*d*) δ 138.37, 137.82, 134.10, 132.10 (2 C), 128.99 (2 C), 128.70 (2 C), 128.52 (2 C), 128.41 (2 C), 128.17, 128.04 (2 C), 127.95, 127.51, 87.68, 83.03, 76.98, 75.85, 74.35, 72.31, 69.54, 16.91.

Compound literature known

C09LL057-3-solid.1.fid
pnmr_1H_16 CDCl3 /v pkanmr 51

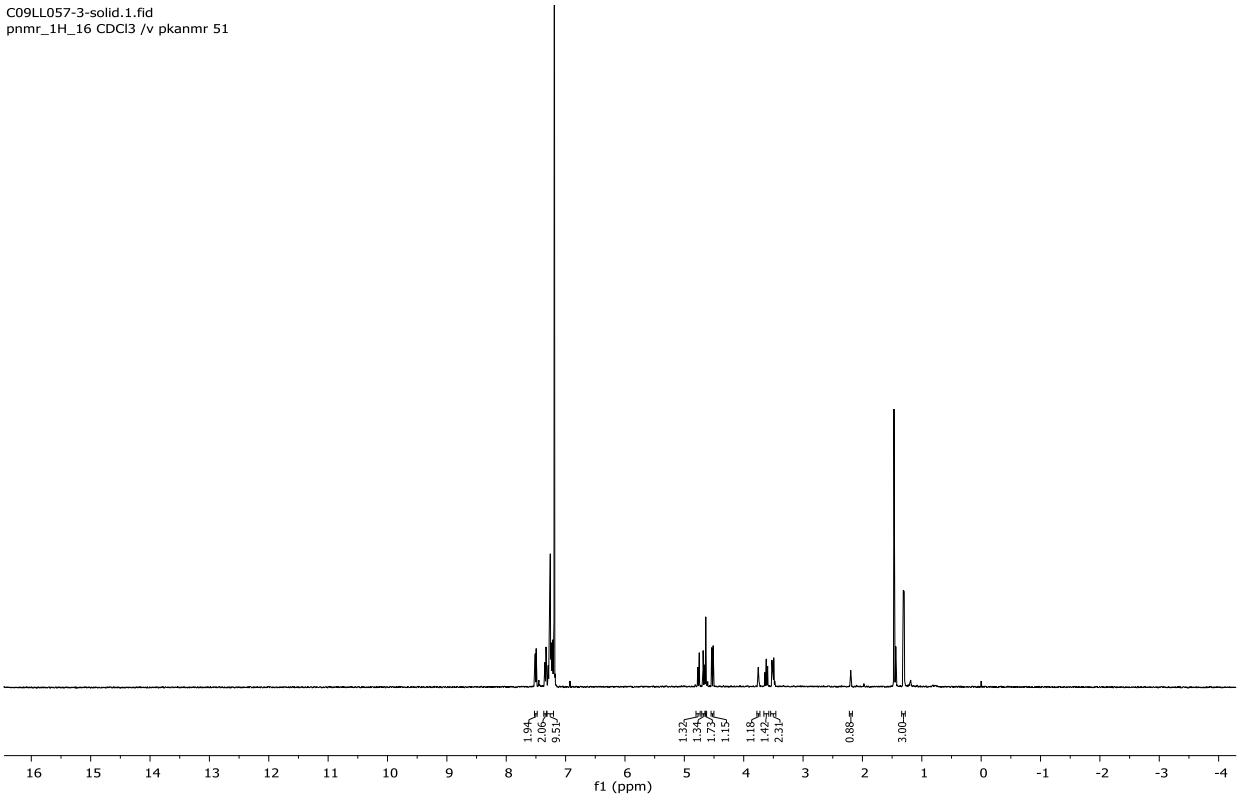

C06LL057-4-FC.2.1.1r
pnmr_13C_256 CDCl3 /v pkanmr 22

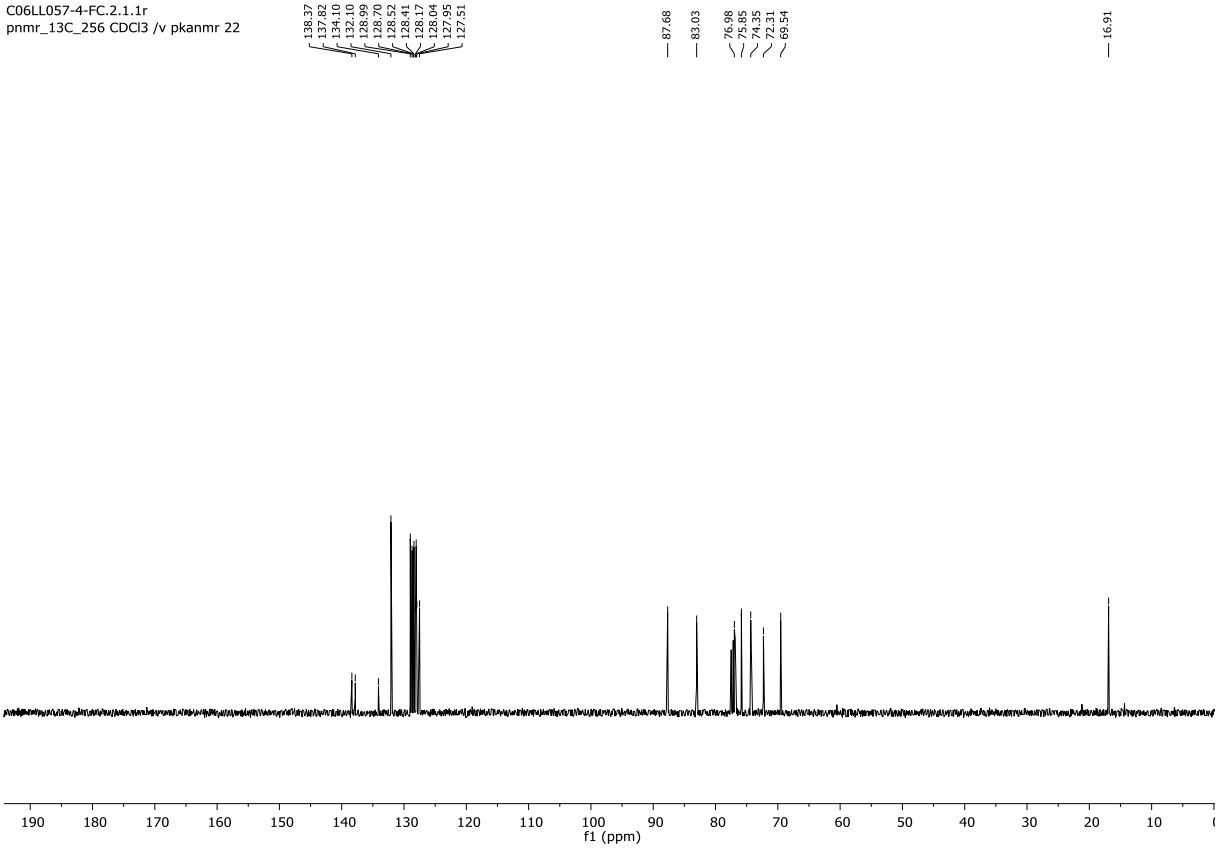

A-127 (2R,3S,4R,5R,6S)-4,5-bis(benzyloxy)-2-methyl-6-(phenylthio)tetrahydro-2H-pyran-3-yl methanesulfonate

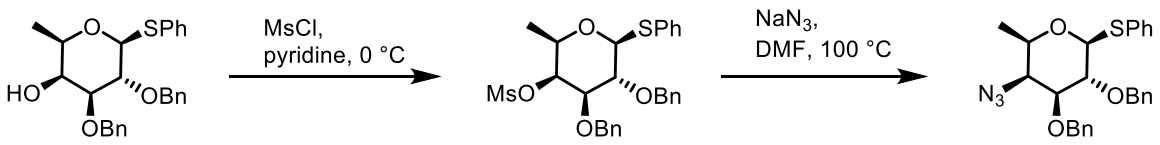

Assay: In a flame dried round bottom flask, **A-26** (495 mg, 1.13 mmol, 1.0 equiv) was dissolved in dry pyridine (6.3 mL) and the reaction mixture was cooled to 0 °C. MsCl (0.26 mL, 3.4 mmol, 3.0 equiv) was then added dropwise and the reaction mixture was stirred for 3 h at 0 °C. The reaction was then quenched with H_2O (15 mL) and the majority of pyridine was then evaporated under reduced pressure. The aqueous phase was extracted with diethyl ether (3 x 8 mL). The combined organic phases were then washed with 0.5 M $CuSO_4$ (3 x 8 mL), H_2O (2 x 4 mL), brine (2 x 8 mL) and dried over $MgSO_4$ and concentrated under reduced pressure. Crucial that all copper is removed - NaN_3 forms highly explosive azides with metals such as Cu.

The crude mesylate was dissolved in DMF (6 mL), NaN_3 (368.6 mg, 5.67 mmol, 5.0 equiv) was added and the reaction mixture was heated to 100 °C for 30 h. The reaction was then cooled to ambient temperature and diluted with diethyl ether, transferred to a separatory funnel and mixed with saturated aqueous $NaHCO_3$ (6 mL). The two phases were separated and the aqueous phase was extracted with diethyl ether (3 x 6 mL). Combined organic phases were dried over $MgSO_4$ and concentrated under reduced pressure. The crude was then purified by FC (EtOAc:hexane 1:20) to give the desired title compound (334 mg, 0.72 mmol, 64%).

Analytics: $\mathbf{R_f}$ = 0.39 (EtOAc:hexane, 1:10). **^{1}H NMR** (400 MHz, $CDCl_3$) δ 7.48 – 7.43 (m, 2H), 7.35 – 7.20 (m, 13H), 4.86 (d, *J* = 10.3 Hz, 1H), 4.79 (q, *J* = 10.6 Hz, 2H), 4.65 (d, *J* = 10.3 Hz, 1H), 4.55 (d, *J* = 9.4 Hz, 1H), 3.44 (dt, *J* = 19.6, 8.7 Hz, 2H), 3.24 – 3.07 (m, 2H), 1.32 (d, *J* = 6.0 Hz, 3H). **^{13}C NMR** (101 MHz, $CDCl_3$) δ 137.98, 137.78, 132.22, 129.12, 128.64, 128.36, 128.29, 128.14, 127.86, 87.76, 84.91, 81.10, 75.95, 75.60, 74.99, 67.91, 18.91. **HRMS (ESI)**: 484.1662 $[M+Na]^+$; calculated for $[C_{26}H_{27}N_3NaO_3S]$: 484.1665. **$[\alpha]^{20}_D$** = +80.90 (c = 1.0, $CHCl_3$). **IR** [ATR, neat]: ν = 2868.59 w, 2105.88 s, 1453.10 w, 1356.68 w, 1128.15 m, 1091.51 m, 1068.37 m, 742.46 m, 696.18 m cm^{-1}.

Compound literature known

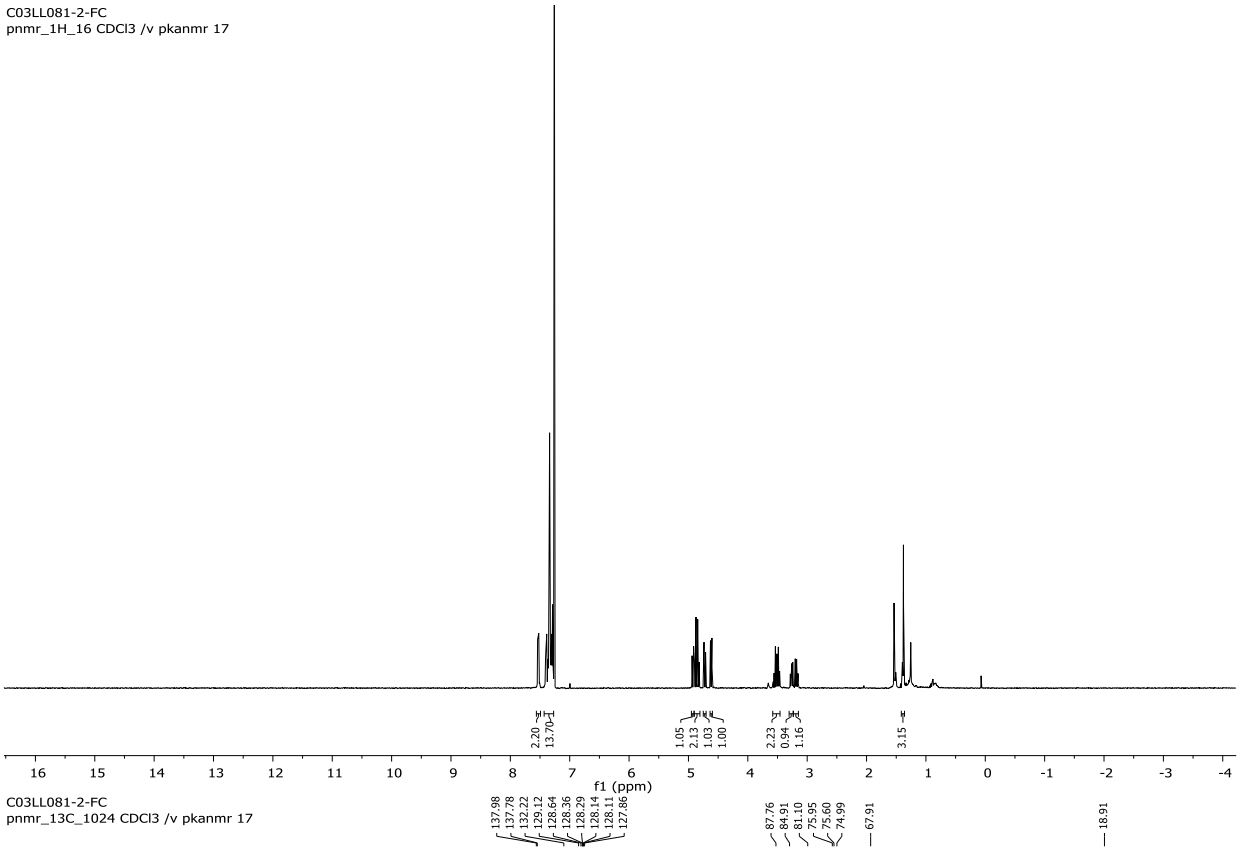
C03LL081-2-FC
pnmr_1H_16 CDCl3 /v pkanmr 17
2.20
13.70
1.05
2.13
1.03
1.00
2.23
0.94
1.16
3.15
f1 (ppm)

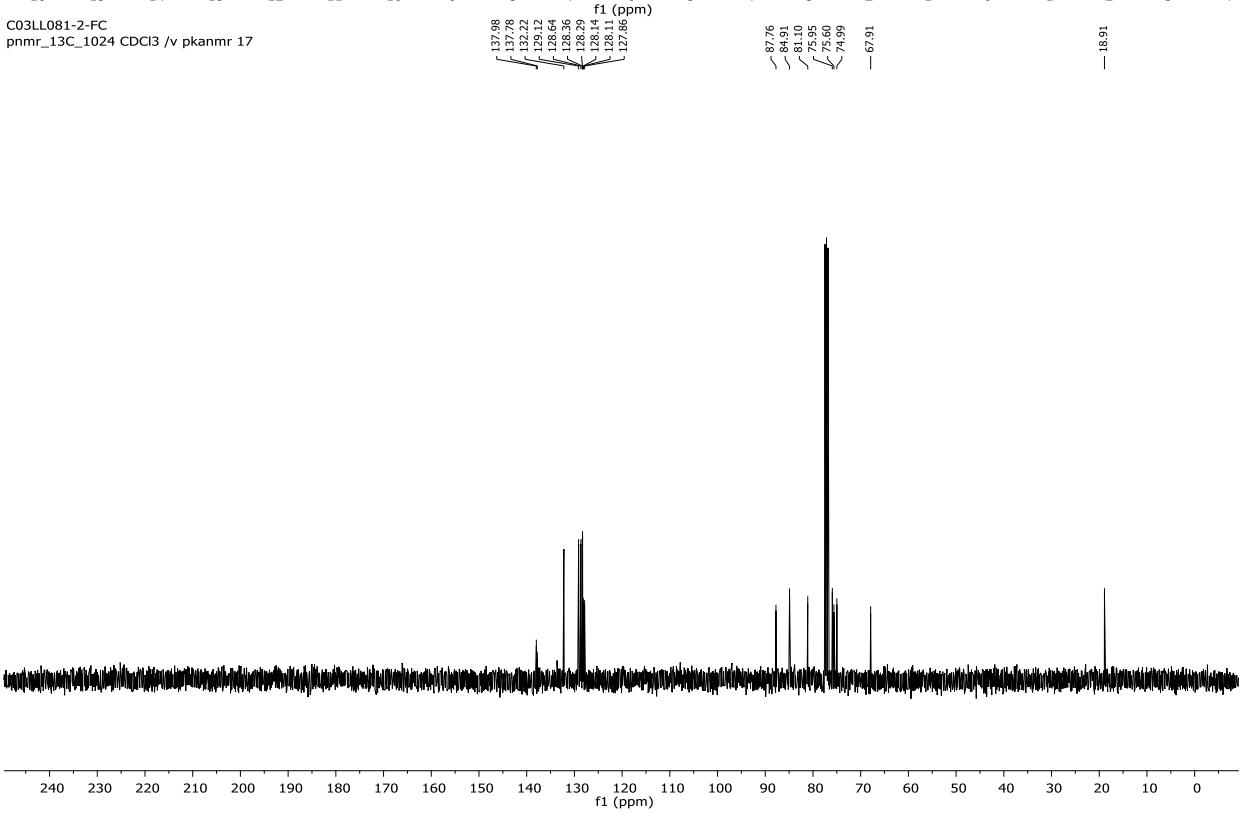
C03LL081-2-FC
pnmr_13C_1024 CDCl3 /v pkanmr 17
137.98
137.78
132.22
129.12
128.64
128.36
128.29
128.14
128.11
127.86
87.76
84.91
81.10
75.95
75.60
74.99
67.91
18.91
f1 (ppm)

A-128 (2R,3R,4S,5R,6S)-4,5-bis(benzyloxy)-N,N,2-trimethyl-6-(phenylthio)tetrahydro-2H-pyran-3-amine

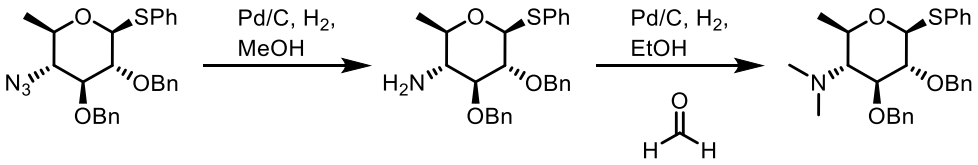

Assay: To a stirring solution of **A-127** (206 mg, 0.45 mmol, 1.0 equiv) in dry MeOH (4.4 mL), was added Pd/C (10 wt %, 47.5 mg, 10 mol %) and the reaction mixture was set under H_2 atmosphere (balloon). After stirring for 3.5 h at 23 °C starting material was fully consumed. The crude was then filtrated over a pad of Celite which was washed with MeOH. Proton NMR and LC-MS confirmed the full reduction of the azide. No debenzylation was observed. The crude was then dried under reduced pressure and subsequently dissolved in EtOH (4.4 mL). To the stirring solution was then added Pd/C (10 wt %, 47.5 mg, 10 mol %) and the reaction mixture was set under H_2 atmosphere (balloon). Formaldehyde 37% in water (83 µl, 1.12 mmol, 2.5 equiv) was added and the reaction mixture was stirred at ambient temperature for 24 h. The crude was then filtrated over a pad of Celite which was washed with EtOAc. Purification by FC (EtOAc:hexane 1:5) gave the title compound (183.5 mg, 0.40 mmol, 89%).

Analytics: $\mathbf{R_f}$ = 0.59 (EtOAc:hexane, 1:3). **^{1}H NMR** (400 MHz, Chloroform-*d*) δ 7.51 – 7.43 (m, 2H), 7.33 – 7.19 (m, 13H), 4.86 (d, *J* = 10.2 Hz, 1H), 4.84 (d, *J* = 10.8 Hz, 1H), 4.75 (d, *J* = 10.8 Hz, 1H), 4.62 (d, *J* = 10.2 Hz, 1H), 4.52 (d, *J* = 9.9 Hz, 1H), 3.66 (dd, *J* = 10.0, 8.4 Hz, 1H), 3.43 (dd, *J* = 9.9, 8.4 Hz, 1H), 3.36 (dd, *J* = 9.9, 6.1 Hz, 1H), 2.38 (s, 6H), 2.41 – 2.32 (m, 1H), 1.26 (d, *J* = 6.1 Hz, 3H).**^{13}C NMR** (101 MHz, $CDCl_3$) δ 138.88, 138.31, 134.49, 131.78 (2 C), 129.00 (2 C), 128.57 (2 C), 128.50 (2 C), 128.35 (2 C), 127.95, 127.93 (2 C), 127.68, 127.42, 87.64, 82.73, 81.83, 75.36, 74.97, 74.33, 70.08, 42.05 (2 C), 19.70. **HRMS (ESI)**: 464.2247 $[M+H]^+$; calculated for $[C_{28}H_{34}NO_3S]$: 464.2254. **$[\alpha]^{20}_D$** = +39.00 (c = 1.0, $CHCl_3$). **IR** [ATR, neat]: ν = 3671.32 m, 2984.3 s, 2904.27 m, 1406.33 m, 1246.27 m, 1070.3 s, 894.33 w cm^{-1}.

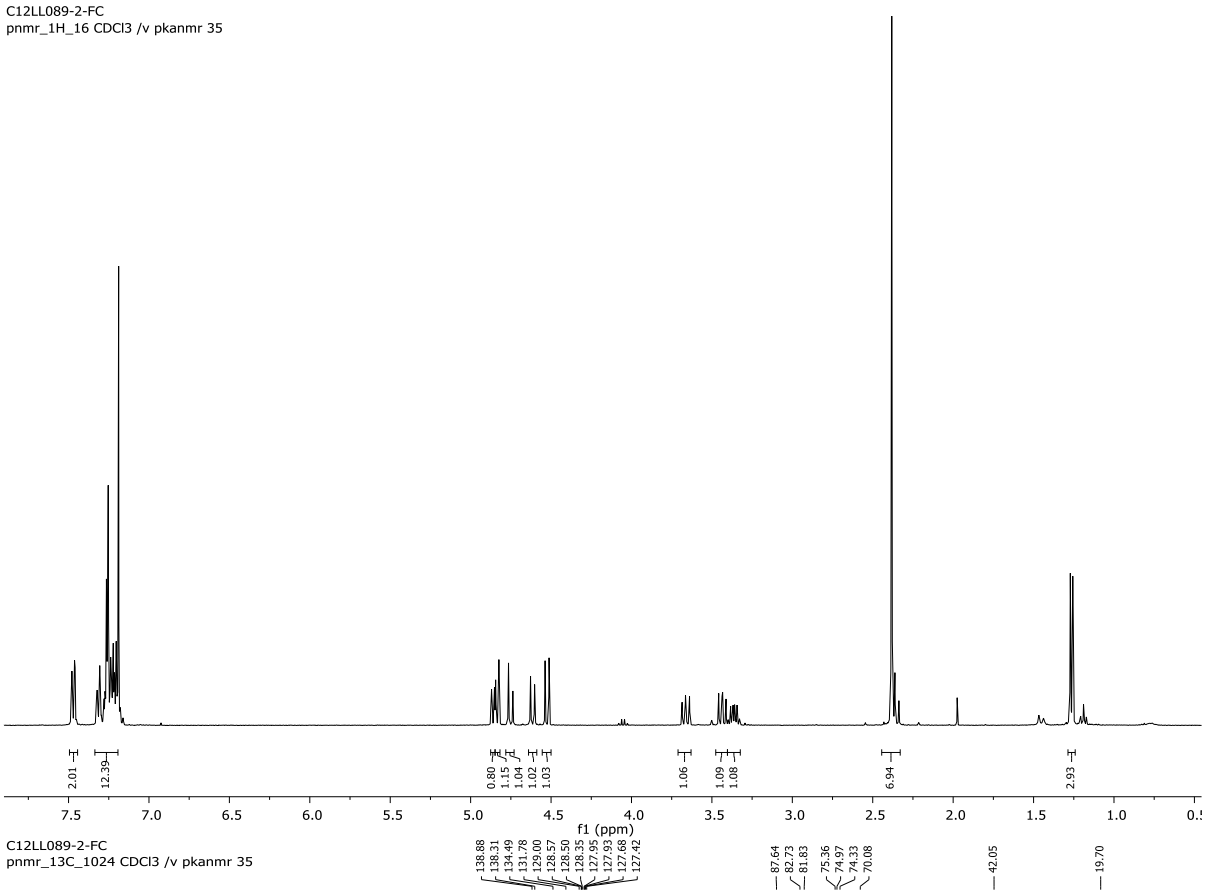
C12LL089-2-FC
pnmr_1H_16 CDCl3 /v pkanmr 35
2.01
12.39
0.80
1.15
1.04
1.02
1.03
1.06
1.09
1.08
6.94
2.93
f1 (ppm)

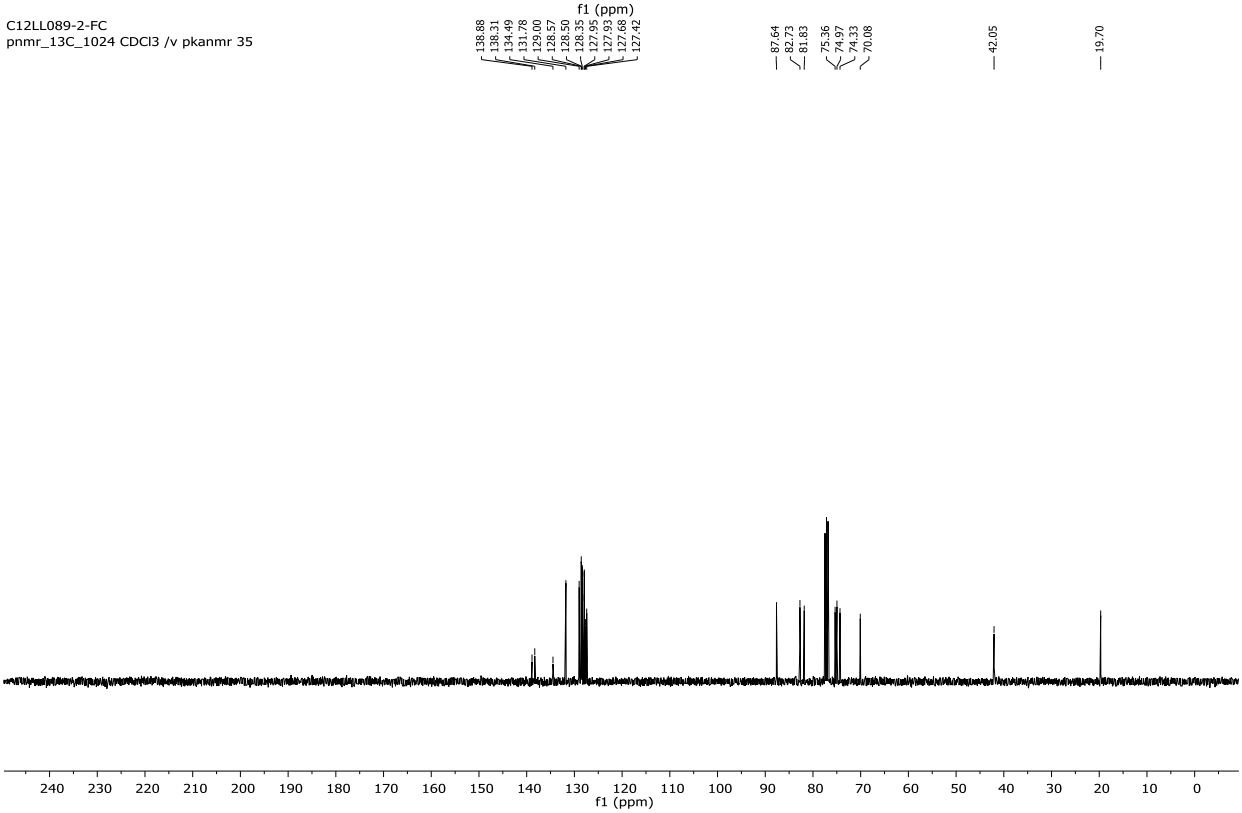
C12LL089-2-FC
pnmr_13C_1024 CDCl3 /v pkanmr 35
138.88
138.31
134.49
131.78
129.00
128.57
128.50
128.35
127.95
127.93
127.68
127.42
87.64
82.73
81.83
75.36
74.97
74.33
70.08
42.05
19.70
f1 (ppm)

A-129 (2R,3R,4S,5R)-4,5-bis(benzyloxy)-6-fluoro-N,N,2-trimethyltetrahydro-2H-pyran-3-amine

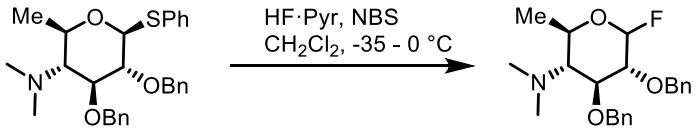

Assay: A-128 (166 mg, 0.36 mmol, 1.0 equiv) was dissolved in CH_2Cl_2 (5.0 mL) and cooled to -35 °C (in an acetonitrile/dry ice bath). HF·pyrdidine (70% HF, 0.37 mL), followed by N-bromosuccinimide (69 mg, 0.39 mmol, 1.08 equiv) were then added. The reaction mixture was slowly allowed to warm to 0 °C over 1 h. An aliquot of the reaction mixture was taken and quenched with saturated aqueous $NaHCO_3$ in order to run a TLC, which showed full conversion. The reaction mixture was then diluted with EtOAc (5 mL) and carefully quenched with saturated aqueous $NaHCO_3$ (8 mL) at 0 °C. The aqueous phase was extracted with EtOAc (3 x 5 mL). Combined organic layers were washed with saturated aqueous $NaHCO_3$ (4 mL), dried over $MgSO_4$ and concentrated under reduced pressure. The crude deep yellow oil was then purified by FC (EtOAc:hexane 1:10) to give an anomeric mixture of glycosyl fluoride (111 mg, 0.30 mmol, 83%) as a colourless sticky syrup.

Analytics: $\mathbf{R_f}$ = 0.18 (EtOAc:hexane, 1:10). **^{1}H NMR** (400 MHz, Chloroform-*d*) δ 7.32 – 7.20 (m, 10H), 5.40 (dd, *J* = 53.6, 2.6 Hz, 1H), 4.90 (d, *J* = 10.8 Hz, 1H), 4.74 (d, *J* = 10.8 Hz, 1H), 3.97 (t, *J* = 9.6 Hz, 1H), 3.84 (dq, *J* = 10.2, 6.2 Hz, 1H), 3.48 (ddd, *J* = 25.7, 9.2, 2.6 Hz, 1H), 2.39 (s, 6H), 2.30 (t, *J* = 10.2 Hz, 1H), 1.20 (d, *J* = 6.2 Hz, 3H). **^{13}C NMR** (101 MHz, Chloroform-*d*) δ 138.88, 137.89, 128.87, 128.72, 128.69, 128.52, 128.49, 128.16, 128.09, 127.79, 127.70, 125.82, 124.40, 81.79, 81.54, 76.35, 75.07, 74.38, 73.40, 69.41, 68.88, 68.83, 42.37, 29.85, 19.22, 19.08. **HRMS (ESI)**: 374.2126 $[M+H]^+$; calculated for $[C_{22}H_{29}FNO_3]$: 374.2126. **IR** [ATR, neat]: ν = 2968.87 w, 2926.45 w, 29868.59 w, 1452.14 m, 1368.25 m, 1164.79 s, 1107.90 s, 1044.26 s, 836.96 w, 739.57 s cm^{-1}.

Compound literature known

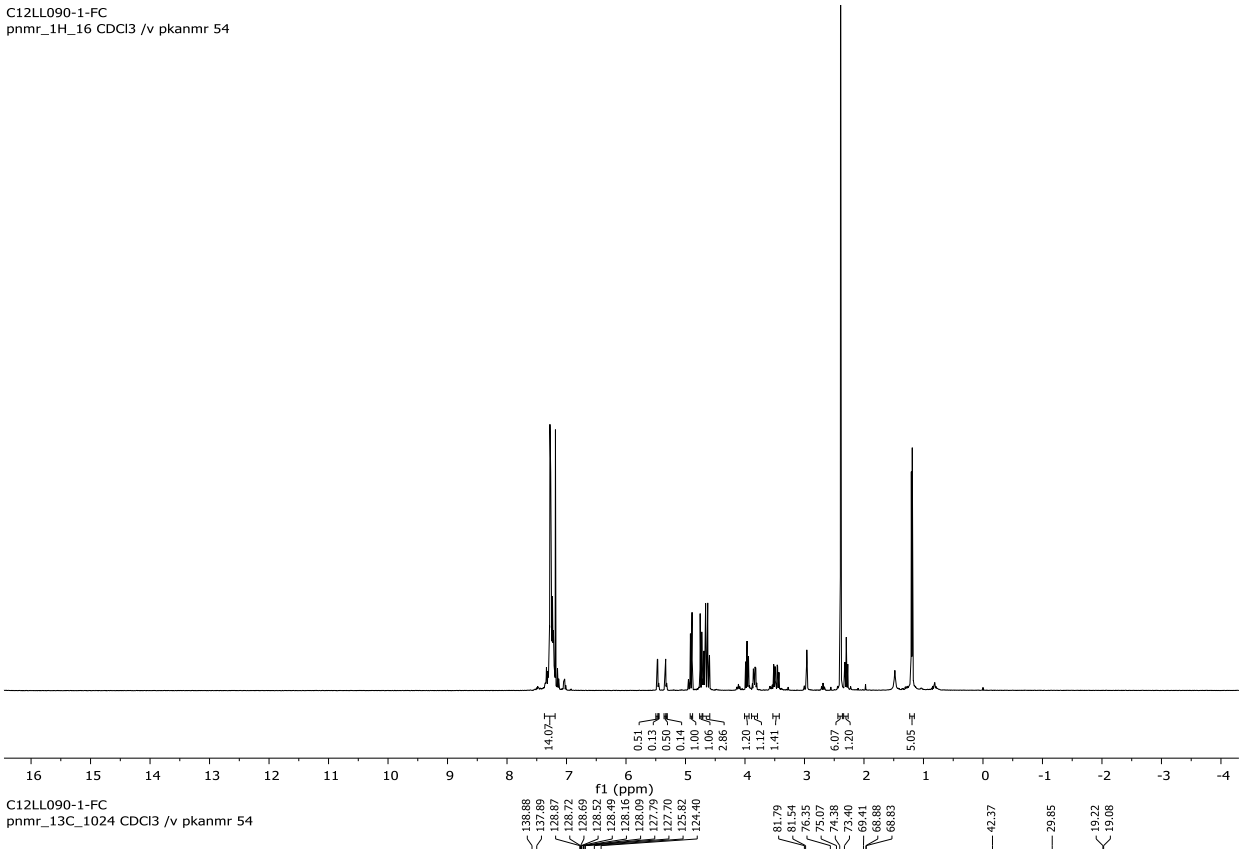
C12LL090-1-FC
pnmr_1H_16 CDCl3 /v pkanmr 54
14.07
0.51
0.13
0.50
0.14
1.00
1.06
2.86
1.20
1.12
1.41
6.07
1.20
5.05
f1 (ppm)

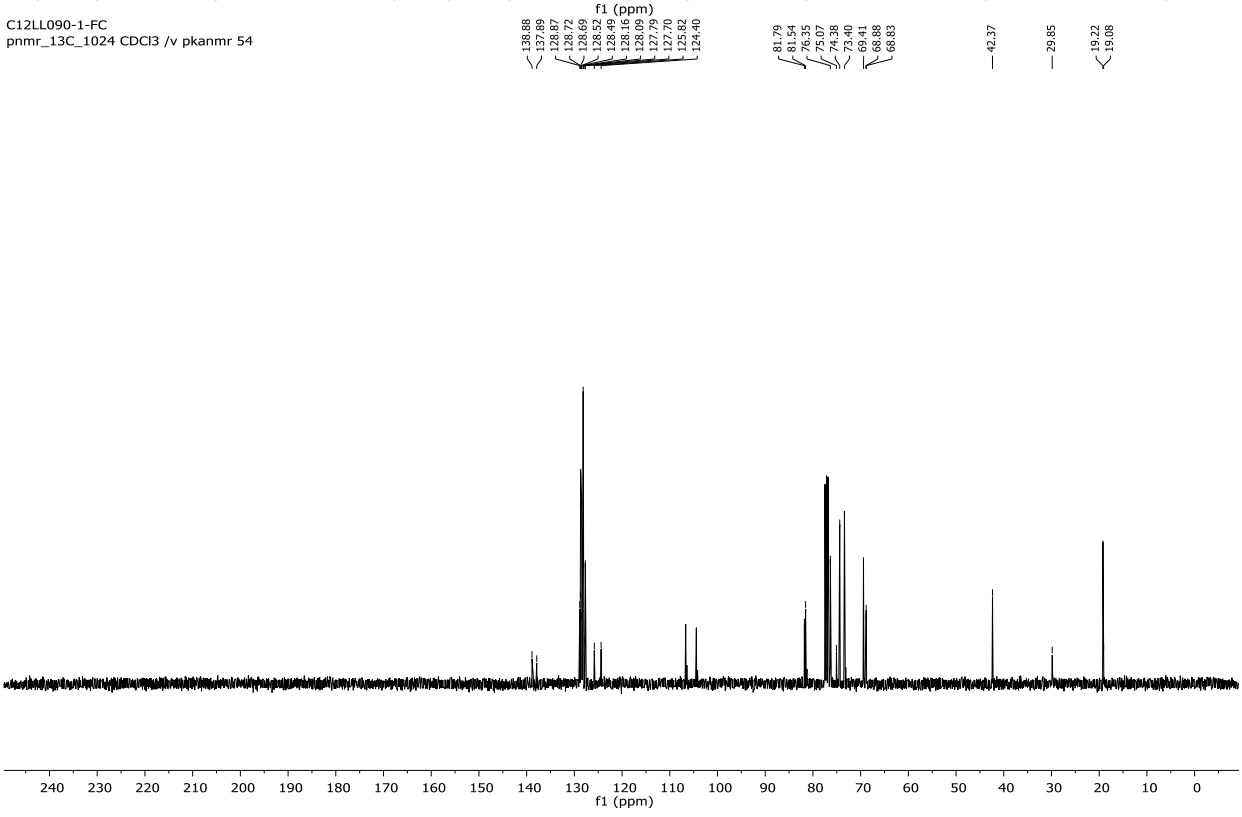
C12LL090-1-FC
pnmr_13C_1024 CDCl3 /v pkanmr 54
138.88
137.89
128.87
128.72
128.69
128.52
128.49
128.16
128.09
127.79
127.70
125.82
124.40
81.79
81.54
76.35
75.07
74.38
73.40
69.41
68.88
68.83
42.37
29.85
19.22
19.08
f1 (ppm)

A-130 (3R,4S,5S,6R)-5-(dimethylamino)-2-fluoro-6-methyltetrahydro-2H-pyran-3,4-diol

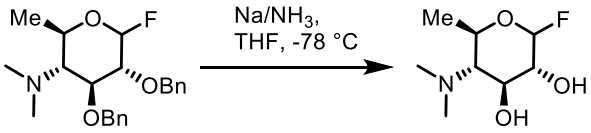

Assay: In a flame dried 50 mL Schlenk tube, gaseous ammonia was condensed at -78 °C (roughly 6.5 mL). **A-129** (107 mg, 0.29 mmol, 1.0 equiv) dissolved in THF (6.5 mL) was added to the ammonia followed by solid Na (13.2 mg, 0.57 mmol, 2.0 equiv). The sodium was quickly washed with hexane and roughly weighted. Solid sodium pieces (about 3 x 3 mg) were then subsequently added until the reaction mixture turned completely blue, which took about 60 min. The deep blue reaction mixture was stirred for 10 min and then quenched with saturated aqueous NH_4Cl (25 mL). The biphasic mixture was poured into a separatory funnel. The aqueous phase was then separated and extracted with EtOAc (6 x 10 mL). Combined organic phases were dried over $MgSO_4$ and concentrated under reduced pressure. No purification by flash column was performed. The crude was used as such for the following step. Based on crude mass and purity of the proton NMR, the reaction was high yielding.

Analytics: $\mathbf{R_f}$ = 0.3 (EtOAc). ^{1}**H NMR** (400 MHz, Chloroform-*d*) δ 5.56 (dd, *J* = 53.6, 2.7 Hz, 1H), 4.09 – 3.99 (m, 1H), 3.76 (t, *J* = 9.7 Hz, 1H), 3.61 (ddd, *J* = 24.5, 9.4, 2.9 Hz, 1H), 2.46 (s, 6H), 2.21 (t, *J* = 10.1 Hz, 1H), 1.30 (d, *J* = 6.3 Hz, 3H). **HRMS (ESI)**: 194.1188 $[M+H]^+$; calculated for $[C_8H_{17}FNO_3]$: 194.1187.

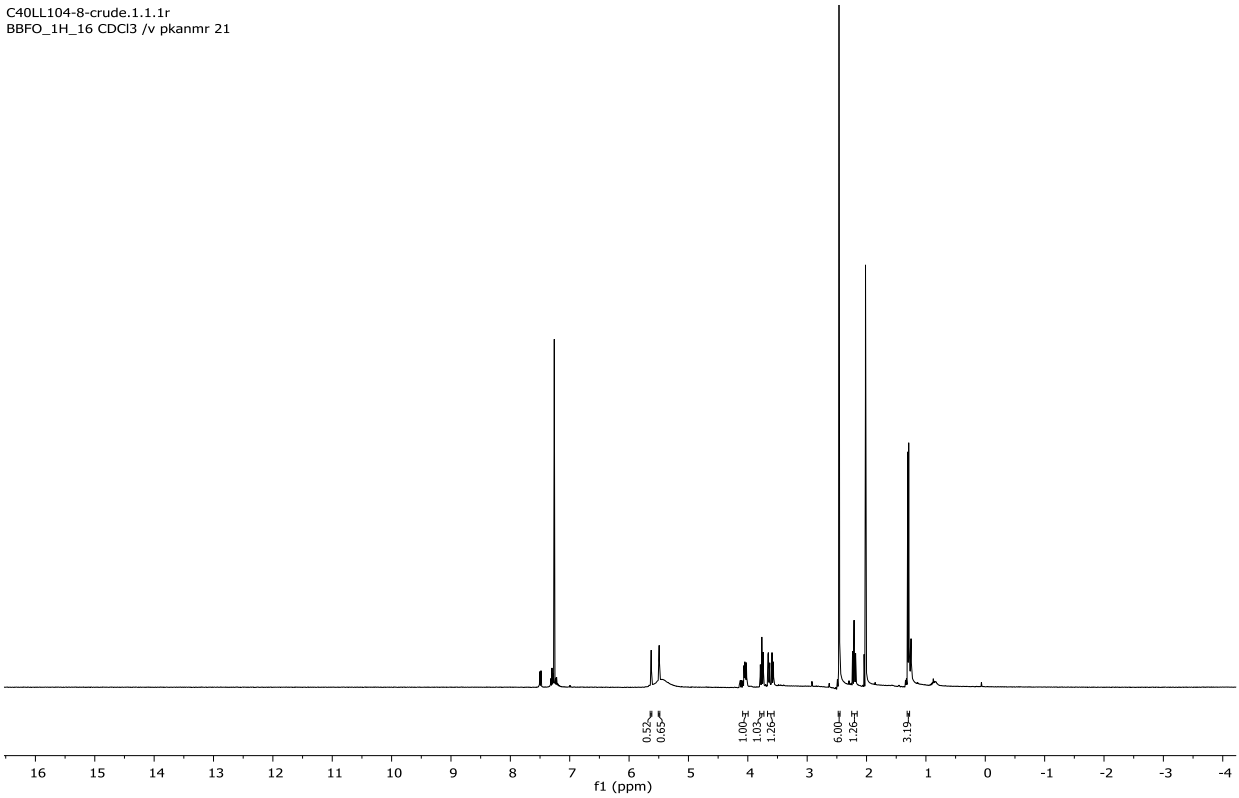
C40LL104-8-crude.1.1.1r
BBFO_1H_16 CDCl3 /v pkanmr 21
0.52
0.65
1.00
1.03
1.26
6.00
1.26
3.19
16 15 14 13 12 11 10 9 8 7 6 5 4 3 2 1 0 -1 -2 -3 -4
f1 (ppm)

A-137 (3R,4S,5R,6R)-5-(dimethylamino)-2-fluoro-6-methyltetrahydro-2H-pyran-3,4-diyl diacetate

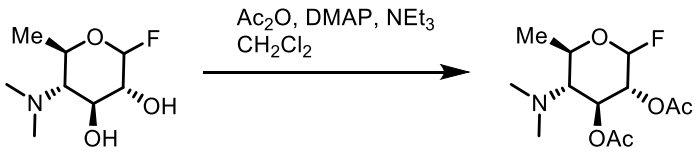

Assay: To a solution of crude diol **A-130** (12.8 mg, 66.2 µmol, 1.0 equiv) in CH_2Cl_2 (750 µl) was added NEt_3 (29 µl, 212 µmol, 3.2 equiv), Ac_2O (21 µl, 219 µmol, 3.3 equiv) and a catalytic amount of DMAP. The reaction was monitored via TLC analysis and was found to be completed after 2 h. The reaction was then quenched with saturated aqueous NH_4Cl solution (2 mL). The phases were separated and the aqueous phase was extracted with EtOAc (3 x 2 mL). Combined organic phases were dried over $MgSO_4$ and concentrated under reduced pressure. The crude oil was purified by FC (EtOAc:hexane, 1:5) to give the desired title compund (13.3 mg, 48 µmol, 72%).

Analytics: $\mathbf{R_f}$ = 0.21 (EtOAc:hexane, 1:5). **^{1}H NMR** (400 MHz, Chloroform-*d*) δ 5.60 (dd, *J* = 53.7, 2.8 Hz, 1H), 5.54 (t, *J* = 10.1 Hz, 1H), 4.02 (dq, *J* = 10.1, 6.2 Hz, 1H), 2.52 (t, *J* = 10.4 Hz, 1H), 2.38 (s, 6H), 2.08 (s, 3H), 2.04 (s, 3H), 1.31 (d, *J* = 6.2 Hz, 3H).

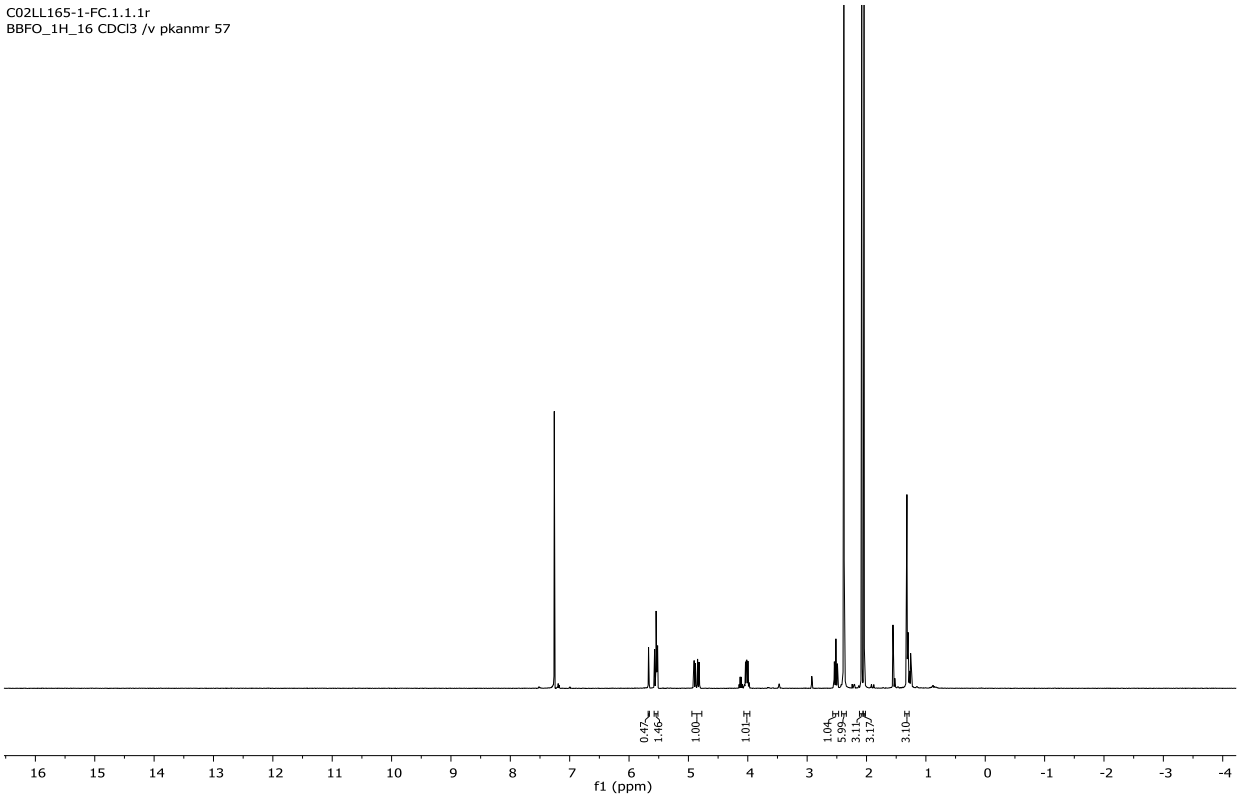
C02LL165-1-FC.1.1.1r
BBFO_1H_16 CDCl3 /v pkanmr 57
0.47
1.46
1.00
1.01
1.04
5.99
3.11
3.17
3.10
16 15 14 13 12 11 10 9 8 7 6 5 4 3 2 1 0 -1 -2 -3 -4
f1 (ppm)

A-138 (2R,3R,4S,5R,6R)-6-fluoro-N,N,2-trimethyl-4,5-bis((triethylsilyl)oxy)tetrahydro-2H-pyran-3-amine

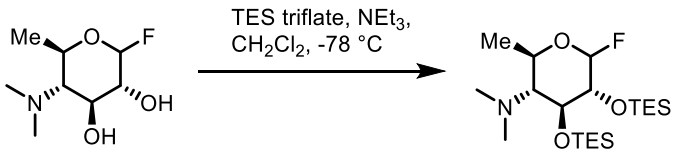

Assay: Crude **A-130** (10 mg, 0.052 mmol, 1.0 equiv) was dissolved in CH_2Cl_2 (2.1 mL) and cooled to -78 °C. NEt_3 (36 µl, 0.26 mmol, 5.0 equiv) was then added followed by dropwise addition of TES triflate (26 µl, 0.11 mmol, 2.2 equiv). The reaction was monitored via TLC whereas full consumption of starting material was confirmed after 10 min at -78 °C. The reaction mixture was then quenched with saturated aqueous $NaHCO_3$ (2.1 mL) and the two layers were separated. The aqueous layer was extracted with CH_2Cl_2 (3 x 2 mL). The combined organic phases were dried over $MgSO_4$ and concentrated under reduced pressure to give a slight yellowish crude. Purification by FC (pure pentane -> EtOAc:hexane, 1:10) gave the desired title compound (22.1 mg, 0.052 mmol, 67%).

Analytics: **^{1}H NMR** (400 MHz, Chloroform-*d*) δ 5.41 (dd, *J* = 53.5, 2.7 Hz, 1H), 4.00 (dq, *J* = 10.5, 6.2 Hz, 1H), 3.79 (t, *J* = 9.1 Hz, 1H), 3.52 (ddd, *J* = 25.4, 8.5, 2.8 Hz, 1H), 2.40 (s, 6H), 2.18 (t, *J* = 9.9 Hz 1H), 1.24 (d, *J* = 6.2 Hz, 3H), 0.97 (td, *J* = 7.9, 5.9 Hz, 18H), 0.70 – 0.57 (m, 12H). **^{13}C NMR** (101 MHz, Chloroform-*d*) δ 107.58 (d, *J* = 225.8 Hz), 75.42 – 74.98 (d, *J* = 24.3 Hz), 71.15, 71.07, 67.64, 41.68, 20.27 (2C), 7.23, 6.97 (3C), 5.46 (3C), 5.30 (3C). **HRMS (ESI)**: 422.2921 $[M+H]^+$; calculated for $[C_{20}H_{45}FNO_3Si_2]$: 422.2917. **$[\alpha]^{20}_D$** = +40.67 (c = 0.75, $CHCl_3$) for α-anomer. **$[\alpha]^{20}_D$** = +2.11 (c = 0.76, $CHCl_3$) for β-anomer. **IR** [ATR, neat]: ν = 2954.41 w, 2877.27 w, 1458.89 w, 1415.49 w, 1238.08 w, 1140.69 s, 1115.62 s, 1041.37 s, 1017.27 s, 850.45 s, 737.64 s cm^{-1}.

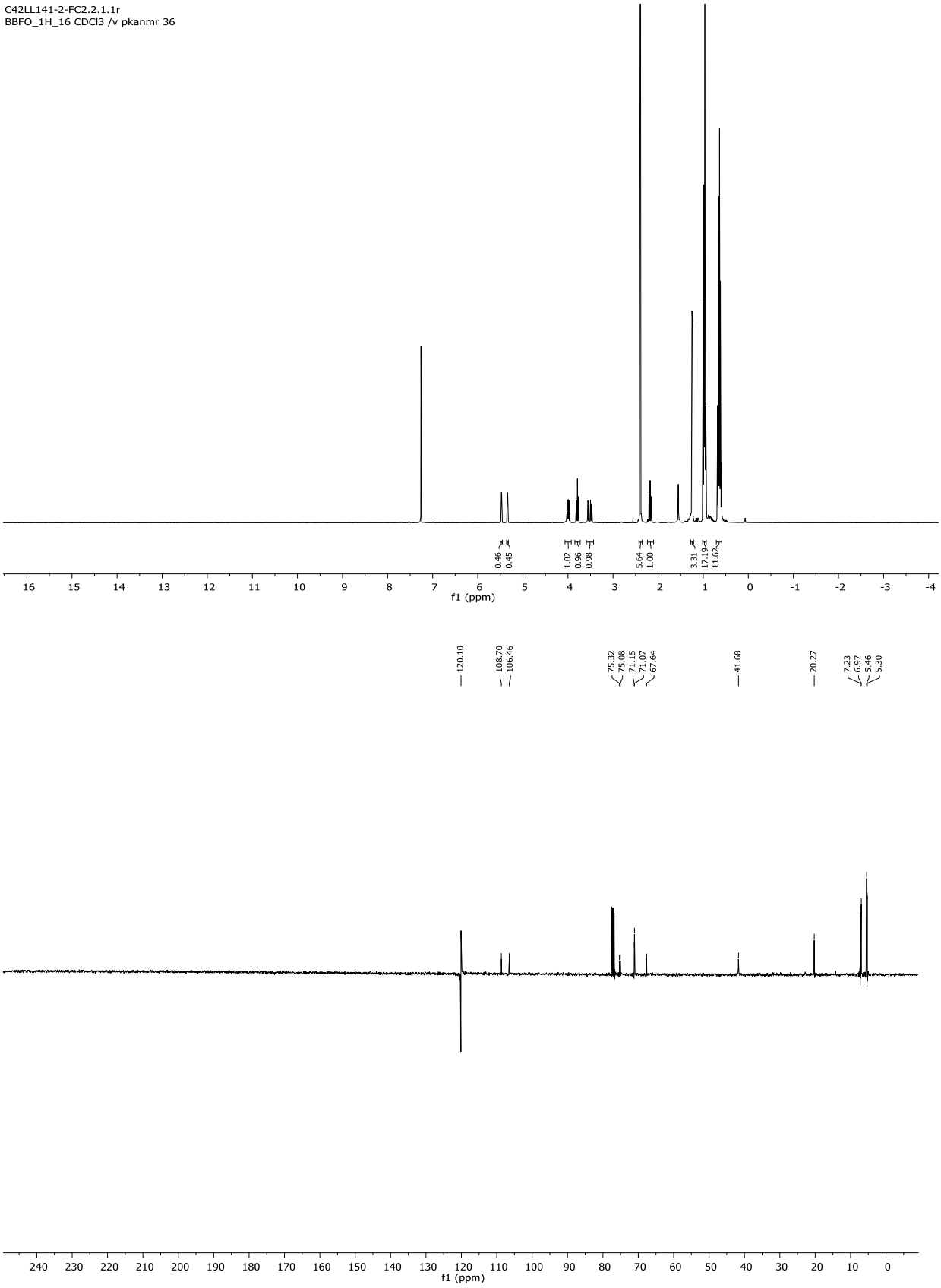
C42LL141-2-FC2.2.1.1r
BBFO_1H_16 CDCl3 /v pkanmr 36
0.46
0.45
1.02
0.96
0.98
5.64
1.00
3.31
17.19
11.62
f1 (ppm)
120.10
108.70
106.46
75.32
75.08
71.15
71.07
67.64
41.68
20.27
7.23
6.97
5.46
5.30
f1 (ppm)

A-139 (3aR,6R,7R,7aS)-2,2-di-tert-butyl-4-fluoro-N,N,6-trimethyltetrahydro-4H-[1,3,2]dioxasilolo[4,5-c]pyran-7-amine

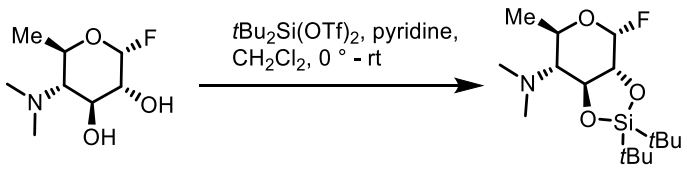

Assay: To a cooled solution of **A-130** (28.5 mg, 0.15 mmol, 1.0 equiv) in CH_2Cl_2 (1.3 mL) at 0 °C was added pyridine (60 µl, 0.74 mmol, 5.0 equiv) and DTBS ditriflate (72 µl, 0.22 mmol, 1.5 equiv). The reaction mixture was stirred at 0 °C for 30 min. The reaction mixture was then diluted with MeOH (1 mL) and quenched with saturated aqueous $NaHCO_3$ (2.5 mL) and diluted with CH_2Cl_2 (2 mL). The phases were separated and the aqueous phase was extracted with CH_2Cl_2 (3 x 3 mL), combined organic phases were dried over $MgSO_4$ and concentrated under reduced pressure. Compound smears on TLC and obtained fractions after column purification do not look cleaner as the crude. Thus, the crude was used as such in the following reactions. Calculated yield based on the crude: 45 mg, 0.135 mmol, 92%.

Analytics: **^{1}H NMR** (400 MHz, Chloroform-*d*) δ 5.76 (dd, *J* = 57.0, 2.1 Hz, 1H), 4.25 (t, *J* = 10.3 Hz, 1H), 3.87 (dq, *J* = 9.7, 6.2 Hz, 1H), 3.61 (ddd, *J* = 24.7, 10.0, 2.2 Hz, 1H), 2.48 (s, 6H), 2.38 (t, *J* = 9.5 Hz, 1H), 1.32 (d, *J* = 6.3 Hz, 3H), 1.09 (s, 9H), 1.06 (s, 9H). **HRMS (ESI)**: 334.2211 $[M+H]^+$; calculated for $[C_{16}H_{33}FNO_3Si]$: 334.2208. **IR** [ATR, neat]: ν = 2934.16 m, 2859.92 m, 1475.28 m, 1365.35 w, 1084.76 s, 910.24 m, 861.06 m, 837.92 s, 825.38 s, 758.85 s, 654.72 s cm^{-1}.

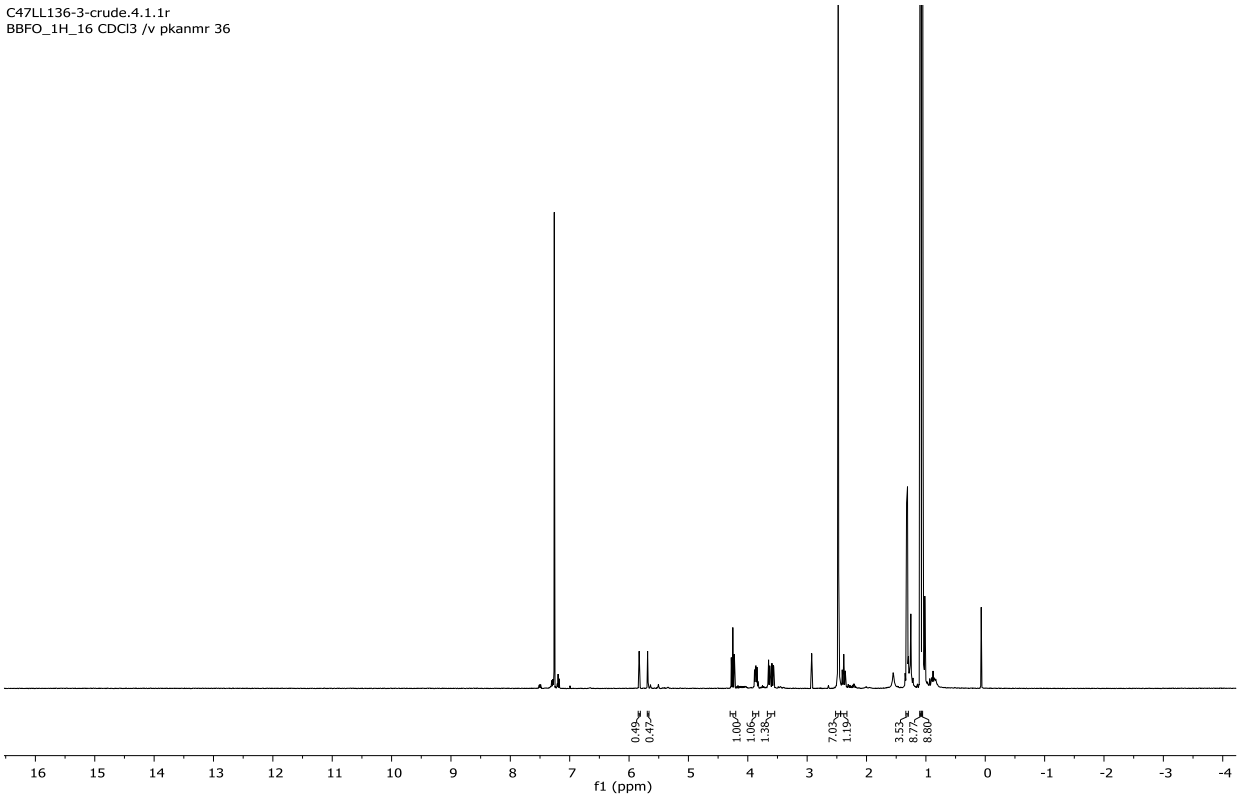
C47LL136-3-crude.4.1.1r
BBFO_1H_16 CDCl3 /v pkanmr 36
0.49
0.47
1.00
1.06
1.38
7.03
1.19
3.53
8.77
8.80
16 15 14 13 12 11 10 9 8 7 6 5 4 3 2 1 0 -1 -2 -3 -4
f1 (ppm)

A-140 (2R,4S)-tert-butyl 4-((4-((1-((2R,5S,6R)-5-(((3R,4S,5R,6R)-3,4-bis(benzyloxy)-5-(dimethylamino)-6-methyltetrahydro-2H-pyran-2-yl)oxy)-6-methyltetrahydro-2H-pyran-2-yl)-2-oxo-1,2-dihydropyrimidin-4-yl)carbamoyl)phenyl)carbamoyl)-2-(tert-butyl)-4-methyloxazolidine-3-carboxylate

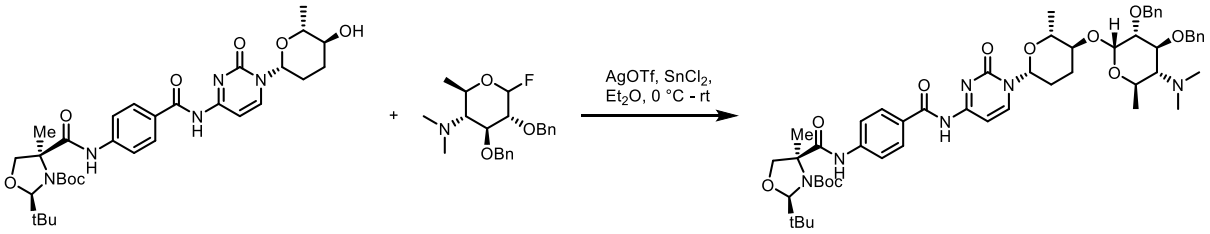

Assay: In a flame dried round bottom flask, **A60** (12 mg, 0.02 mmol, 1.0 equiv) was azeotropically dried with benzene (3 x 1 mL). It was then transferred into the glovebox where activated 4 Å molecular sieves (30.3 mg), AgOTf (12.6 mg, 0.049 mmol, 2.5 equiv) and $SnCl_2$ (9.3 mg, 0.049 mmol, 2.5 equiv) was added. The mixture was then suspended in Et_2O (0.8 mL) and cooled to 0 °C. The reaction mixture was stirred as such for 5 min, before glycosyl fluoride **A-129** (8.4 mg, 0.023 mmol, 1.15 equiv) in Et_2O (0.5 mL) was dropwise added. The reaction mixture was then allowed to reach ambient temperature and was stirred for 96 h. The reaction mixture was then filtered over cotton wool and rinsed with EtOAc. The organic phase was washed with water (3 x 2 mL), dried over $MgSO_4$ and concentrated under reduced pressure. The brown crude was purified by FC (EtOAc:hexane, 3:1) to give the putative complete amicetin skeleton (impure, roughly 5%) and reisolated starting material (only traces).

Analytics: $\mathbf{R_f}$ = 0.63 (EtOAc:hexane 3:1).

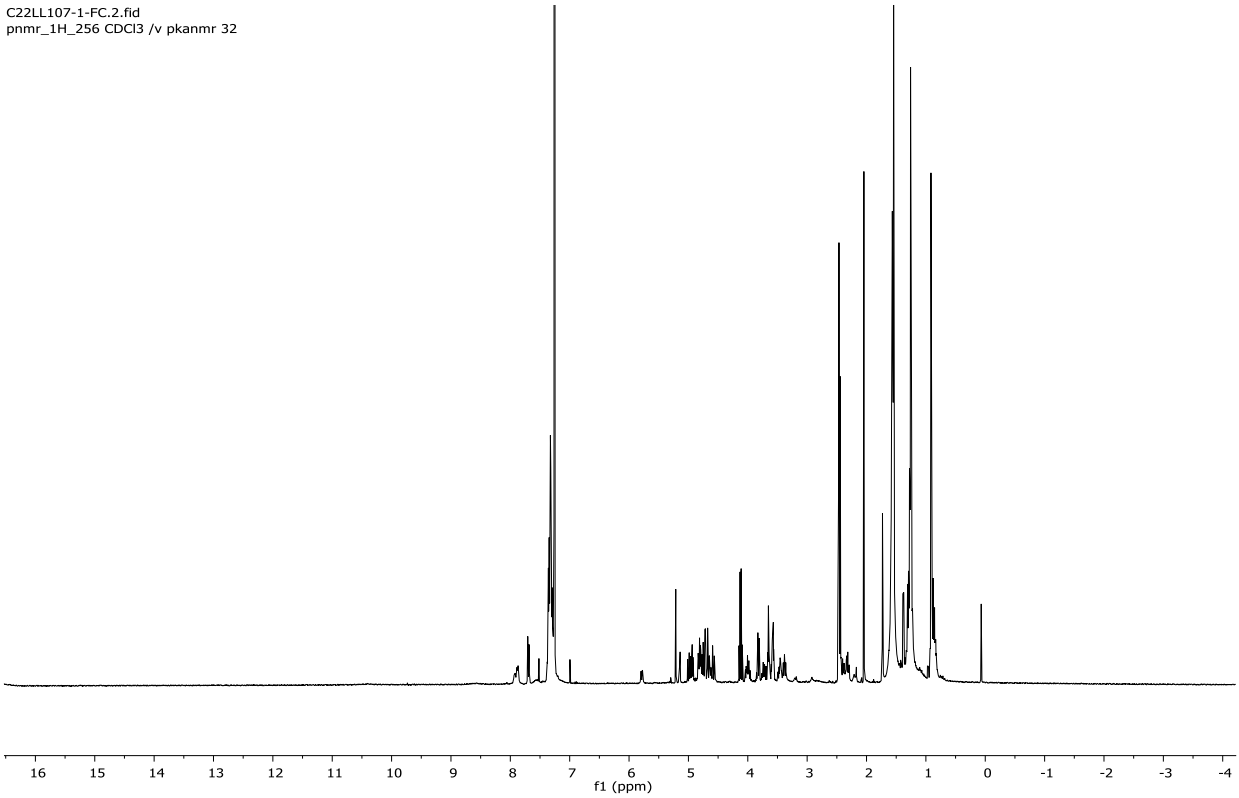
C22LL107-1-FC.2.fid
pnmr_1H_256 CDCl3 /v pkanmr 32
16 15 14 13 12 11 10 9 8 7 6 5 4 3 2 1 0 -1 -2 -3 -4
f1 (ppm)

A-151 2-(Hex-1-yn-1-yl)benzoic acid

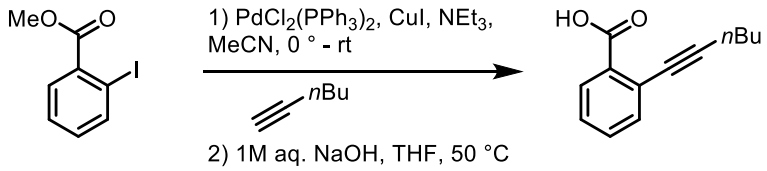

Assay: In a flame dried Schlenk tube was given $PdCl_2(PPh_3)_2$ (21.4 mg, 30.5 µmol, 0.02 equiv), CuI (11.6 mg, 61.1 µmol, 0.05 equiv) and **A-150** (0.4 g, 1.53 mmol, 1.0 equiv). The Schlenk tube was evacuated and backfilled with argon (3 times) before it was rinsed with degassed MeCN (3.0 mL). NEt_3 (1.69 mL, 12.22 mmol, 1.0 equiv) was added before dropwise addition of 1-hexyne (263 µl, 2.29 mmol, 1.5 equiv) at ambient temperature. Upon the addition of the alkyne, the reaction mixture turned from orange to deep black. The reaction was allowed to stir over night at ambient temperature. TLC (EtOAc:hexane, 1:10) analysis showed full conversion of starting material. The reaction mixture was quenched with saturated aqueous NH_4Cl (5 mL) and the aqueous phase was extracted with EtOAc (3 x 5 mL). The combined organic phases were then dried over $MgSO_4$ and concentrated under reduced pressure. Purification by FC (hexane -> EtOAc:hexane, 1:10) gave the desired product as a yellow oil. The oily substance was then transferred to a pear shaped 25 mL flask and diluted with THF (5 mL). 1 M NaOH aqueous solution (5 mL) was added and the reaction was stirred at 50 °C over 12 h. Starting material was fully consumed whereupon the reaction mixture was cooled to 0 °C and acidified with concentrated HCl. The biphasic mixture was then diluted with CH_2Cl_2 (10 mL) and the organic phase was separated. The aqueous phase was extracted with CH_2Cl_2 (3 x 6 mL). Combined organic phases were dried over $MgSO_4$ and concentrated under reduced pressure. Purification by a short FC (EtOAc:hexane, 1:5 -> 1:3 -> 1:1) gave the target compound as an orange oil (not quantified).

Analytics: **^{1}H NMR** (400 MHz, Chloroform-*d*) δ 8.25 (ddt, *J* = 7.9, 1.3, 0.7 Hz, 1H), 7.72 – 7.61 (m, 1H), 7.45 (ddd, *J* = 8.2, 7.4, 1.2 Hz, 1H), 7.35 (dt, *J* = 7.9, 0.9 Hz, 1H), 6.25 (d, *J* = 0.9 Hz, 1H), 2.59 – 2.48 (m, 2H), 1.75 – 1.63 (m, 2H), 1.41 (h, *J* = 7.3 Hz, 2H), 0.95 (t, *J* = 7.4 Hz, 3H).

Compound literature known

C29LL208-2-FCacid.1.1.1r
BBFO_1H_16 CDCl3 /y pkanmr 29

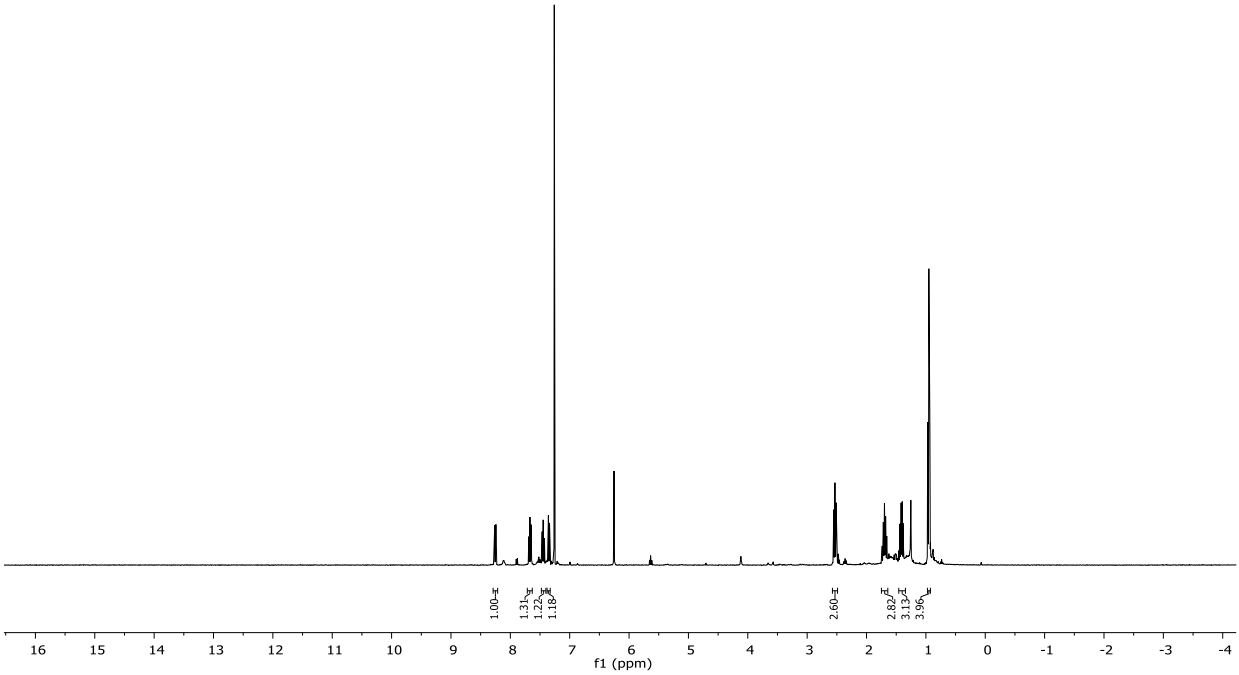

A-162 (2R,3R,4S,5R,6S)-2-((benzoyloxy)methyl)-6-(2,2,2-trichloro-1-iminoethoxy)tetrahydro-2H-pyran-3,4,5-triyl tribenzoate

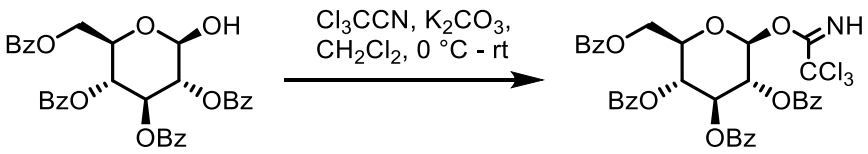

Assay: Tetra-O-benzoylated glucopyranose (100 mg, 0.17 mmol, 1.0 equiv), was dissolved in CH_2Cl_2 (1.9 mL), cooled to 0 °C and trichloroacetonitrile (0.17 mL, 1.68 mmol, 10.0 equiv) was added followed by anhydrous K_2CO_3 (115.8 mg, 0.84 mmol, 5.0 equiv). The reaction mixture was stirred for 16 h after which TLC (EtOAc:hexane, 1:1) indicated full consumption of starting material. The reaction mixture was then filtered over a pad of Celite, concentrated under reduced pressure and applied on a short FC (Alox, EtOAc:hexane, 1:1) to give the title compound (54.8 mg, 0.074 mmol, 44%) which was immediately used in the following reaction.

Analytics: **^{1}H NMR** (400 MHz, Chloroform-*d*) δ 8.63 (s, 1H), 8.13 – 7.81 (m, 8H), 7.61 – 7.28 (m, 12H), 6.84 (d, *J* = 3.7 Hz, 1H), 6.27 (t, *J* = 10.0 Hz, 1H), 5.81 (t, *J* = 9.9 Hz, 1H), 5.62 (dd, *J* = 10.2, 3.7 Hz, 1H), 4.64 (d, *J* = 11.2 Hz, 2H), 4.54 – 4.40 (m, 1H).

Compound literature known

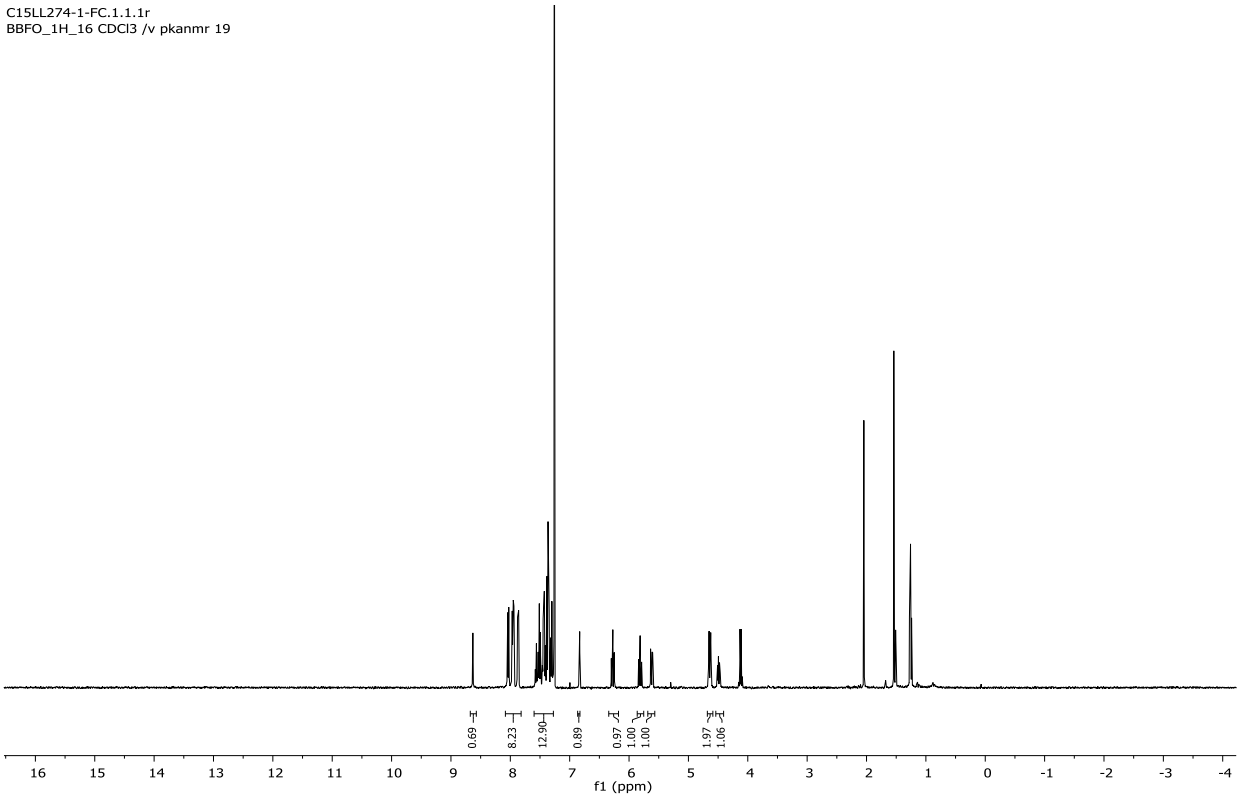
C15LL274-1-FC.1.1.1r
BBFO_1H_16 CDCl3 /v pkanmr 19
0.69
8.23
12.90
0.89
0.97
1.00
1.00
1.97
1.06
16 15 14 13 12 11 10 9 8 7 6 5 4 3 2 1 0 -1 -2 -3 -4
f1 (ppm)

A-168 (2R,3R,4S,5R)-6-(benzyloxy)-N,N,2-trimethyl-4,5-bis((triethylsilyl)oxy)tetrahydro-2H-pyran-3-amine

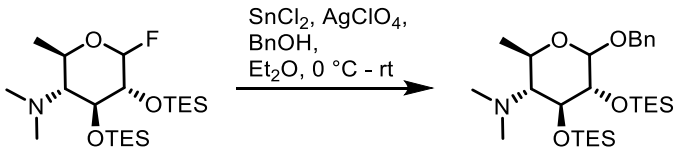

Assay: In the glove box, $SnCl_2$ (46.8 mg, 0.25 mmol, 1.3 equiv) and $AgClO_4$ (51.1 mg, 0.25 mmol, 1.3 equiv) were given into a flame dried 10 mL round bottom flask. After exporting the flask, activated molecular sieves were added and the solids were suspended in Et_2O (1.5 mL) and cooled to 0 °C. Following addition of benzyl alcohol (196 µl, 1.90 mmol, 10.0 equiv) and **A-138** (80 mg, 0.19 mmol, 1.0 equiv) in Et_2O (0.4 mL). The reaction was monitored by TLC and showed no product formation after 4 h at ambient temperature. Thus, the reaction was allowed to stir over night at ambient temperature whereas full consumption of starting material was observed. The reaction mixture was diluted in Et_2O (2 mL) and quenched with saturated aqueous $NaHCO_3$ solution (2 mL) and then filtered over cotton wool. The two phases were separated and the aqueous phase was extracted with with Et_2O (3 x 3 mL). The combined organic phases were dried over $MgSO_4$ and concentrated under reduced pressure. Purification by FC (EtOAc:hexane, 1:10) gave the desired target molecule (77.8 mg, 0.15 mmol, 80%) as an anomeric mixture (1:1).

Analytics: $\mathbf{R_f}$ = 0.36 (EtOAc:hexane 1:10). **^{1}H NMR** (400 MHz, Chloroform-*d*) δ 7.44 – 7.27 (m, 10H_{ab}), 4.88 (d, *J* = 11.5 Hz, 1H_a), 4.71 (d, *J* = 3.5 Hz, 1H_a), 4.67 (d, *J* = 12.3 Hz, 1H_b), 4.50 (d, *J* = 11.5 Hz, 1H_a), 4.49 (d, *J* = 12.3 Hz, 1H_b), 4.16 (d, *J* = 7.4 Hz, 1H_b), 3.84 (t, *J* = 9.0 Hz, 1$H_{a/b}$), 3.79 (dd, *J* = 10.3, 6.2 Hz, 1$H_{a/b}$), 3.53 (dd, *J* = 8.7, 3.6 Hz, 1$H_{a/b}$), 3.49 – 3.38 (m, 2H_{ab}), 2.37 (s, 6$H_{a/b}$), 2.36 (s, 6$H_{a/b}$), 2.19 (t, *J* = 9.5 Hz, 1H_a), 2.10 (t, *J* = 9.7 Hz, 1H_a), 1.27 (d, *J* = 6.3 Hz, 3H_a), 1.15 (d, *J* = 6.3 Hz, 3H_b), 1.01 – 0.83 (m, 36H_{ab}), 0.66 – 0.52 (m, 24H_{ab}). **^{13}C NMR** (101 MHz, Chloroform-*d*) δ 138.17, 137.71, 128.35, 128.27, 127.86, 127.61, 102.18, 98.75, 75.53, 75.44, 72.18, 71.84, 71.62, 70.73, 69.54, 69.15, 64.96, 41.63, 20.77, 20.48, 7.34, 7.17, 7.09, 5.52, 5.31. **HRMS (ESI)**: 510.3430 $[M+H]^+$; calculated for $[C_{27}H_{52}NO_4Si_2]$: 510.3429. **$[\alpha]^{20}_D$** = +17.10 (c = 1.0, $CHCl_3$). **IR** [ATR, neat]: ν = 2953.45 m, 2912.95 m, 2877.27 m, 1457.92 w, 1237.11 w, 1134.90 m, 1095.37 s, 1066.44 m, 1040.41 m, 1009.55 m, 812.85 w, 732.82 s cm^{-1}.

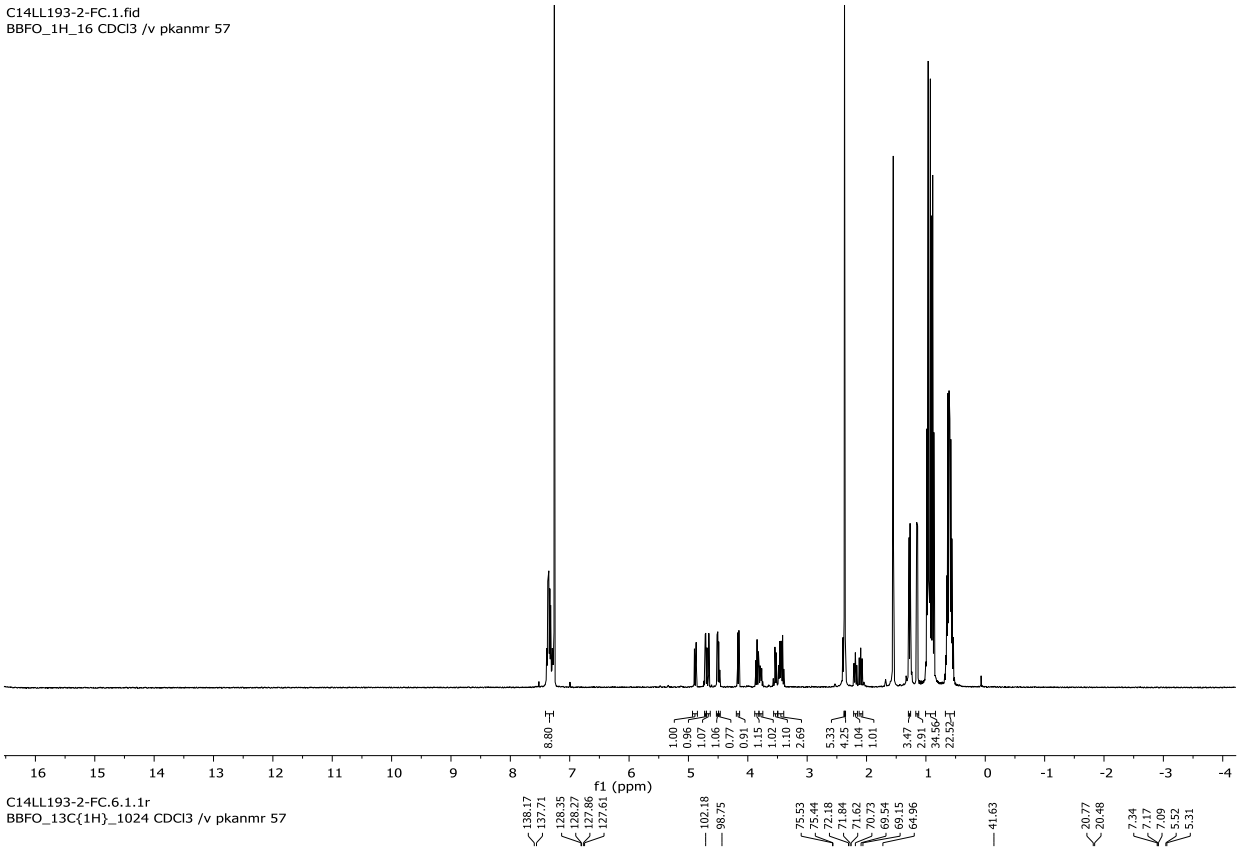
C14LL193-2-FC.1.fid
BBFO_1H_16 CDCl3 /v pkanmr 57
8.80
1.00
0.96
1.07
1.06
0.77
0.91
1.15
1.02
1.10
2.69
5.33
4.25
1.04
1.01
3.47
2.91
34.56
22.52
f1 (ppm)
C14LL193-2-FC.6.1.1r
BBFO_13C{1H}_1024 CDCl3 /v pkanmr 57
138.17
137.71
128.35
128.27
127.86
127.61
102.18
98.75
75.53
75.44
72.18
71.84
71.62
70.73
69.54
69.15
64.96
41.63
20.77
20.48
7.34
7.17
7.09
5.52
5.31
f1 (ppm)

A-175 (3R,4S,5R,6R)-5-azido-3,4-bis(benzyloxy)-6-methyltetrahydro-2H-pyran-2-ol

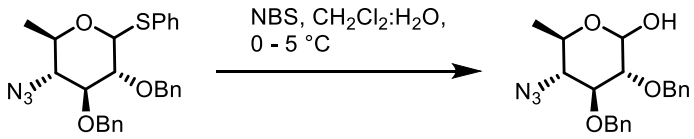

Assay: A-127 (580 mg, 1.26 mmol, 1.0 equiv) was dissolved in CH_2Cl_2 (10.35 mL) and H_2O (1.15 mL) and cooled to 0 °C. NBS (268.4 mg, 1.51 mmol, 1.2 equiv) was then added in one portion. The reaction mixture stayed clear. After stirring for 3 h at 0 °C, TLC analysis showed still existing starting material. The reaction was therefore allowed to slowly warm up. Meanwhile the reaction mixture turned yellow. After stirring for 5 h the reaction mixture started to turn orange/red. After 5.5 h the reaction was quenched with saturated aqueous $NaHCO_3$ (10 mL) and diluted with CH_2Cl_2 (6 mL). The two layers were separated and the aqueous phase was extracted with CH_2Cl_2 (3 x 7 mL). The combined organic phases were dried over $MgSO_4$ and concentrated under reduced pressure to give a brown crude. The crude was then purified by FC (EtOAc:hexane, 1:3) to give the pure title compound as an anomeric mixture (272.6 mg, 0.74 mmol, 59%).

Analytics: $\mathbf{R_f}$ = 0.52 (EtOAc:toluene, 1:3). **^{1}H NMR** (400 MHz, Chloroform-*d*) δ 7.46 – 7.29 (m, 10H), 5.14 (t, *J* = 3.0 Hz, 1H), 4.93 (d, *J* = 10.5 Hz, 1H), 4.84 (d, *J* = 13.0 Hz, 1H), 4.77 (d, *J* = 11.5 Hz, 1H), 4.68 (d, *J* = 11.8 Hz, 1H), 3.82 (t, *J* = 9.4 Hz, 1H), 3.56 (dd, *J* = 9.4, 3.5 Hz, 1H), 3.38 (dd, *J* = 9.1, 7.7 Hz, 1H), 3.09 (t, *J* = 9.9 Hz, 1H), 1.28 (d, *J* = 6.2 Hz, 3H). **^{13}C NMR** (101 MHz, Chloroform-*d*) δ 138.24, 138.04, 137.90, 137.69, 97.36, 91.27, 83.38, 82.81, 80.25, 79.67, 75.85, 74.98, 73.41, 70.84, 68.03, 67.78, 66.38, 18.64, 18.56. **HRMS (ESI)**: 392.1583 $[M+Na]^+$; calculated for $[C_{20}H_{23}N_3NaO_4]$: 392.1581. **$[\alpha]^{20}_D$** = + 102.6 (c = 0.5, $CHCl_3$). **IR** [ATR, neat]: ν = 3382.53 m, 2921.63 w, 2108.78 s, 1355.71 w, 1268.93 m, 1103.08 m, 1071.26 s, 1025.94 s, 746.32 m, 695.21 m cm^{-1}. **m.p.** = 86°C.

C46LL148-2-2ndFC.1.fid
BBFO_1H_16 CDCl3 /v pkanmr 9

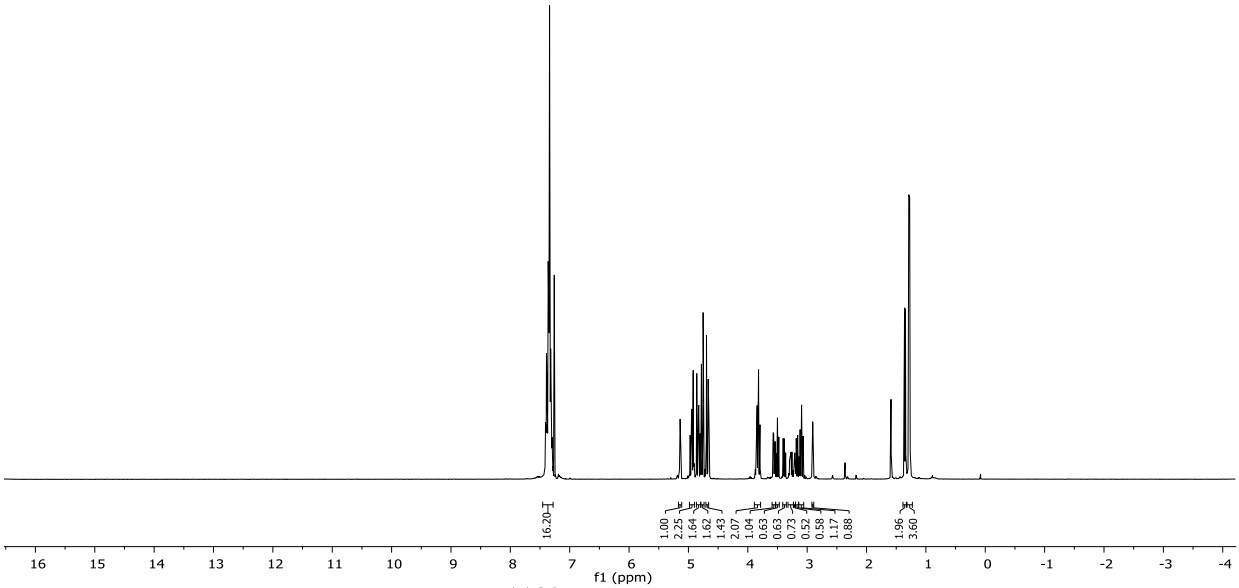

C46LL148-2-2ndFC.5.1.1r
BBFO_13C{1H}_256 CDCl3 /v pkanmr 9

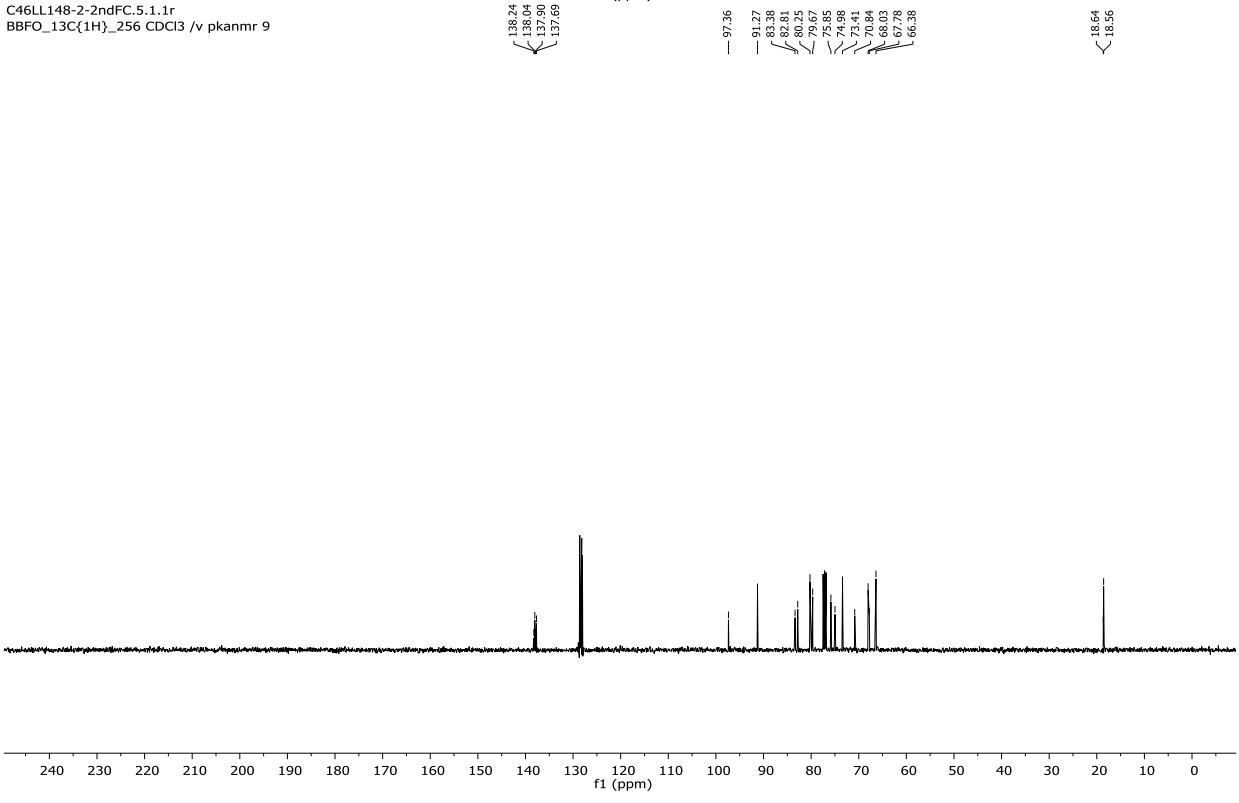

A-148 (3R,4S,5R,6R)-5-azido-3,4-bis(benzyloxy)-6-methyltetrahydro-2H-pyran-2-yl 2,2,2-trichloroacetimidate

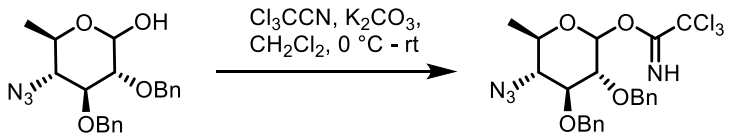

Assay: A-175 (9.3 mg, 25.2 µmol, 1.0 equiv), was dissolved in CH_2Cl_2 (140 µL), and trichloroacetonitrile (25 µL, 25.2 µmol) was added followed by anhydrous K_2CO_3 (17.4 mg, 12.6 µmol). The reaction mixture was stirred for 9 h after which TLC (EtOAc:hexane, 1:3) indicated full consumption of starting material. The reaction mixture was then filtered over a pad of Celite which was washed with EtOAc. The filtrate was then concentrated under reduced pressure and the crude was purified by FC (basic Alox, EtOAc:hexane, 1:3) to give the title compound (9 mg, 18 µmol, 70%) as an anomeric mixture of α:β (1:4).

Analytics: $\mathbf{R_f}$ = 0.56 (EtOAc:hexane, 1:3). **^{1}H NMR** (400 MHz, Chloroform-*d*) δ 8.71 (s, 1H), 7.37 – 7.28 (m, 10H), 5.76 (d, *J* = 8.1 Hz, 1H), 4.96 (d, *J* = 10.8 Hz, 1H), 4.91 (d, *J* = 10.7 Hz, 1H), 4.82 (d, *J* = 10.7 Hz, 1H), 4.75 (d, *J* = 10.9 Hz, 1H),, 3.77 – 3.68 (m, 1H), 3.60 (t, *J* = 9.2 Hz, 1H), 3.42 (dq, *J* = 10.0, 6.1 Hz, 1H), 3.22 (t, *J* = 9.7 Hz, 1H), 1.38 (d, *J* = 6.1 Hz, 3H). **^{13}C NMR** (101 MHz, Chloroform-*d*) δ 161.27, 137.88, 137.77, 128.58 (4C), 128.36 (2C), 128.07 (2C), 128.04 (2C), 98.12, 90.96, 82.86, 81.24, 75.83, 75.12, 71.71, 67.52, 18.56. **HRMS (ESI)**: 535.0680 $[M+Na]^+$; calculated for $[C_{22}H_{23}Cl_3N_4NaO_4]$: 535.0677. **$[\alpha]^{20}_D$** = + 99.0 (c = 0.5, $CHCl_3$). **IR** [ATR, neat]: ν = 2107.81 s, 1674.87 m, 1282.43 s, 1094.4 s, 1054.87 s, 1029.8 s, 834.06 w, 796.46 s, 736.67 s, 698.11 s, 647.96 s cm^{-1}.

C46LL150-1-FC.1.fid
BBFO_1H_16 CDCl3 /v pkanmr 4

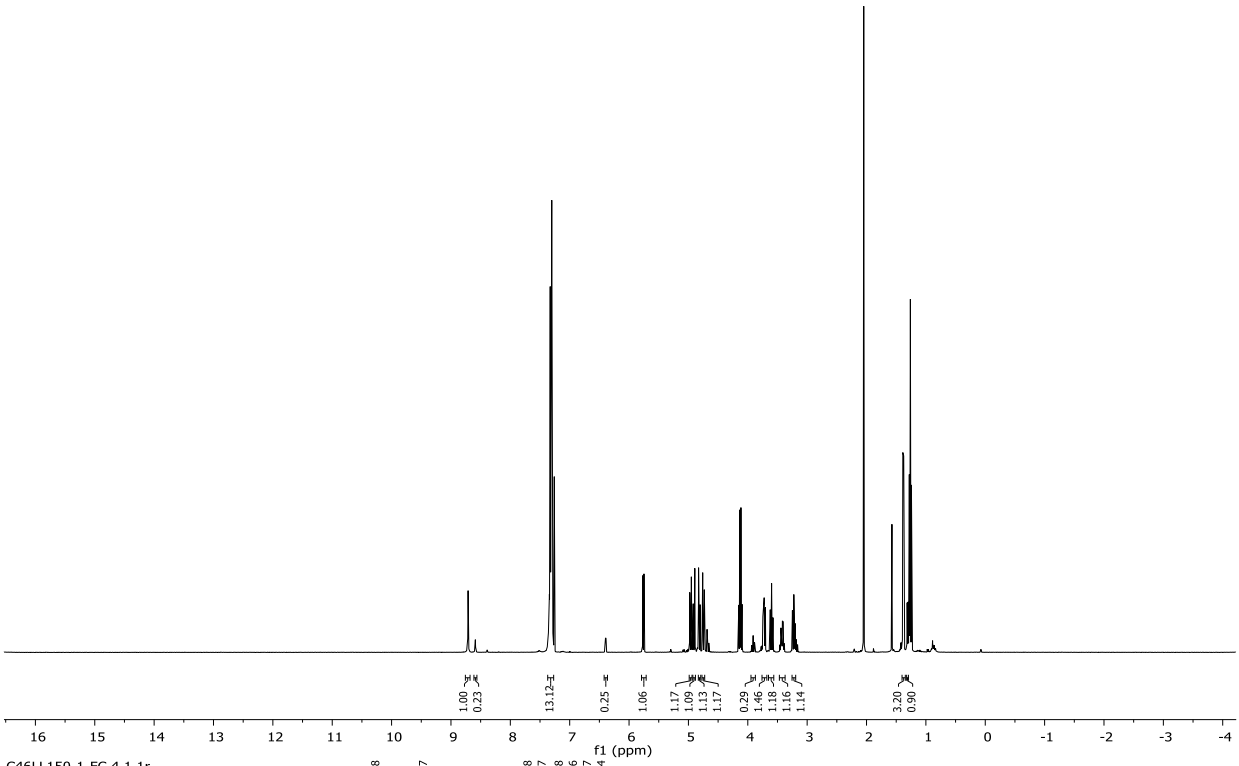

C46LL150-1-FC.4.1.1r
BBFO_13C{1H}_256 CDCl3 /v pkanmr 4

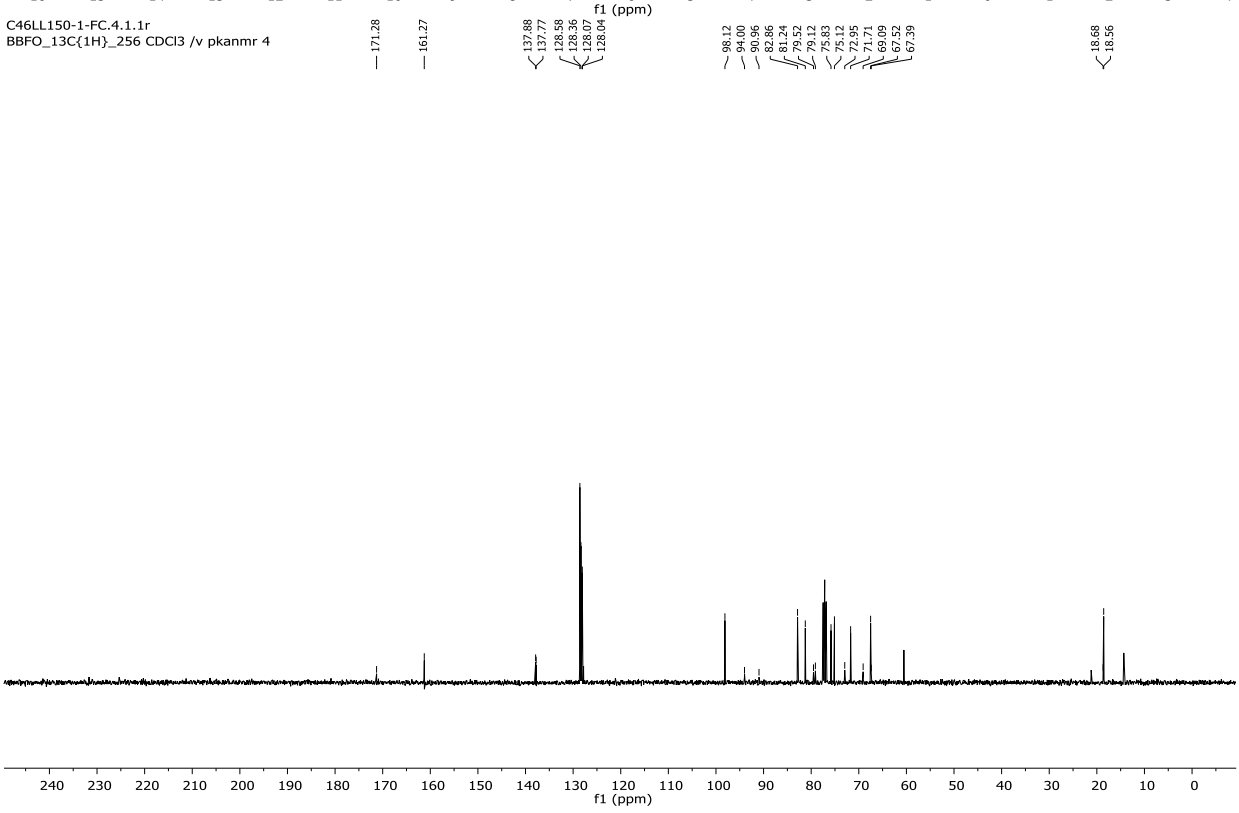

A-179 (2R,3S,4S,5R)-2-(acetoxymethyl)-6-((4-methoxybenzyl)oxy)tetrahydro-2H-pyran-3,4,5-triyl triacetate

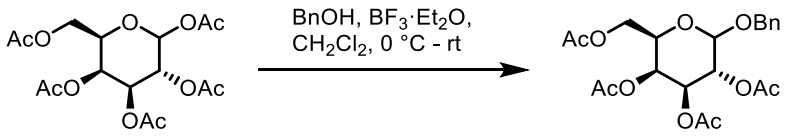

Assay: To a solution of **A-178** (50 g, 128.1 mmol, 1.0 equiv) and benzyl alcohol (29.0 mL, 279.24 mmol, 2.18 equiv) in CH_2Cl_2 (1.0 L) at 0 °C was added $BF_3{\cdot}Et_2O$ (20.55 mL, 166.5 mmol, 1.3 equiv) dropwise (with a syringe pump at a flow rate of 0.7 mL/min), whereas the reaction mixture turned brightly pink. The reaction mixture was stirred at ambient temperature for 24 h and after that cooled again to 0 °C. The reaction was carefully quenched with NEt_3 (23.08 mL) and subsequently diluted with H_2O (250 mL). After the addition of NEt_3, the reaction turned into an amber solution. The biphasic mixture was separated and the organic layer was washed with H_2O (2 x 250 mL) before being dried over $MgSO_4$ and concentrated under reduced pressure. The crude compound was used as such in the following reaction without any further purification. Crude appears as an amber coloured, sticky syrup.

Compound literature known

C29LL210-2-crude.1.1.1r
BBFO_1H_16 CDCl3 /y pkanmr 47

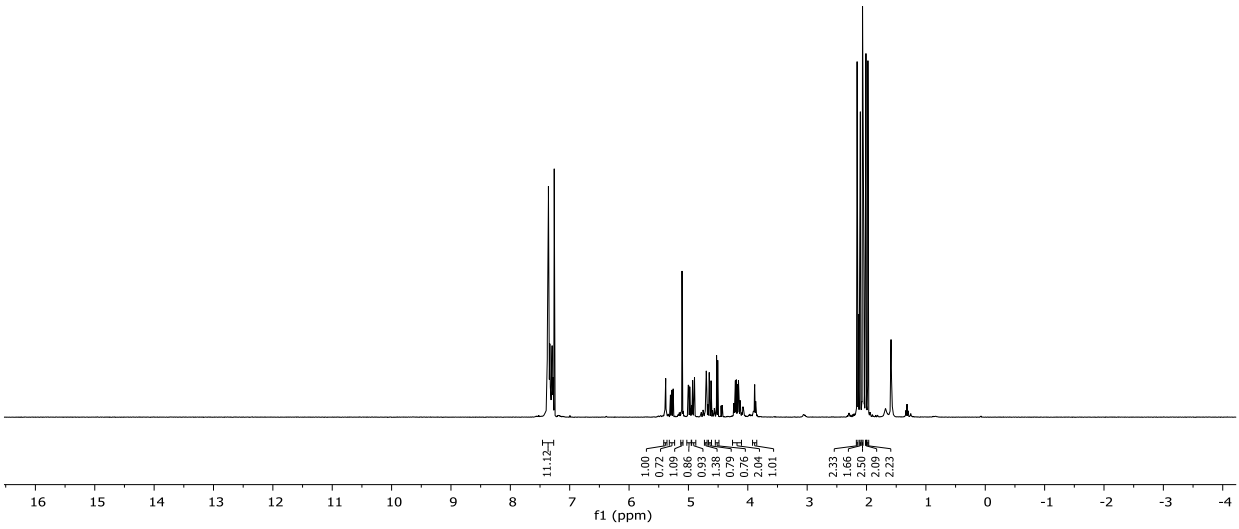

A-180 (2R,3R,4S,5R,6R)-2-(benzyloxy)-6-(hydroxymethyl)tetrahydro-2H-pyran-3,4,5-triol

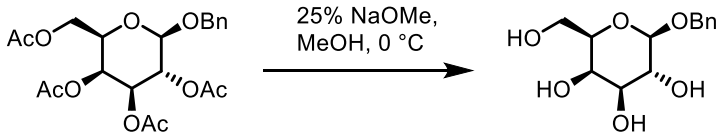

Assay: Crude intermediate of **A-179** (55 g, 125.45 mmol, 1.0 equiv) was dissolved in MeOH (800 mL) and cooled to 0 °C. NaOMe (30 wt % in MeOH, 31.5 mL, 137.99 mmol, 1.1 equiv) was then slowly added over a dropping funnel and the reaction mixture was stirred for 2 h allowing to slowly warm to ambient temperature. TLC analysis confirmed full consumption of starting material. In order to neutralize the reaction mixture, Amberlyst 15 hydrogen form was added. After stirring for additional 5 min, the reaction mixture was filtered over cotton wool and the filtrate was concentrated under reduced pressure giving a yellowish sticky syrup which was purified by FC (MeOH:CH_2Cl_2, 1:8 -> 1:5) to give the desired product as a white solid (23 g, 85.1 mmol, 66% over two steps).

Analytics: $\mathbf{R_f}$ = 0.43 (MeOH:CH_2Cl_2, 1:5). **^{1}H NMR** (400 MHz, Methanol-d_4) δ 7.46 – 7.42 (m, 2H), 7.37 – 7.25 (m, 3H), 4.95 (d, *J* = 11.8 Hz, 1H), 4.68 (d, *J* = 11.7 Hz, 1H), 4.33 (d, *J* = 7.7 Hz, 1H), 3.85 (dd, *J* = 3.5, 1.1 Hz, 1H), 3.78 (qd, *J* = 11.3, 6.0 Hz, 2H), 3.60 (dd, *J* = 9.7, 7.7 Hz, 1H), 3.52 (ddd, *J* = 6.7, 5.3, 1.2 Hz, 1H), 3.47 (dd, *J* = 9.7, 3.4 Hz, 1H). **^{13}C NMR** (101 MHz, Chloroform-*d*) δ 139.20, 129.26 (2 C), 129.20 (2 C), 128.64, 103.93, 76.77, 75.02, 72.59, 71.67, 70.36, 62.58.

Compound literature known

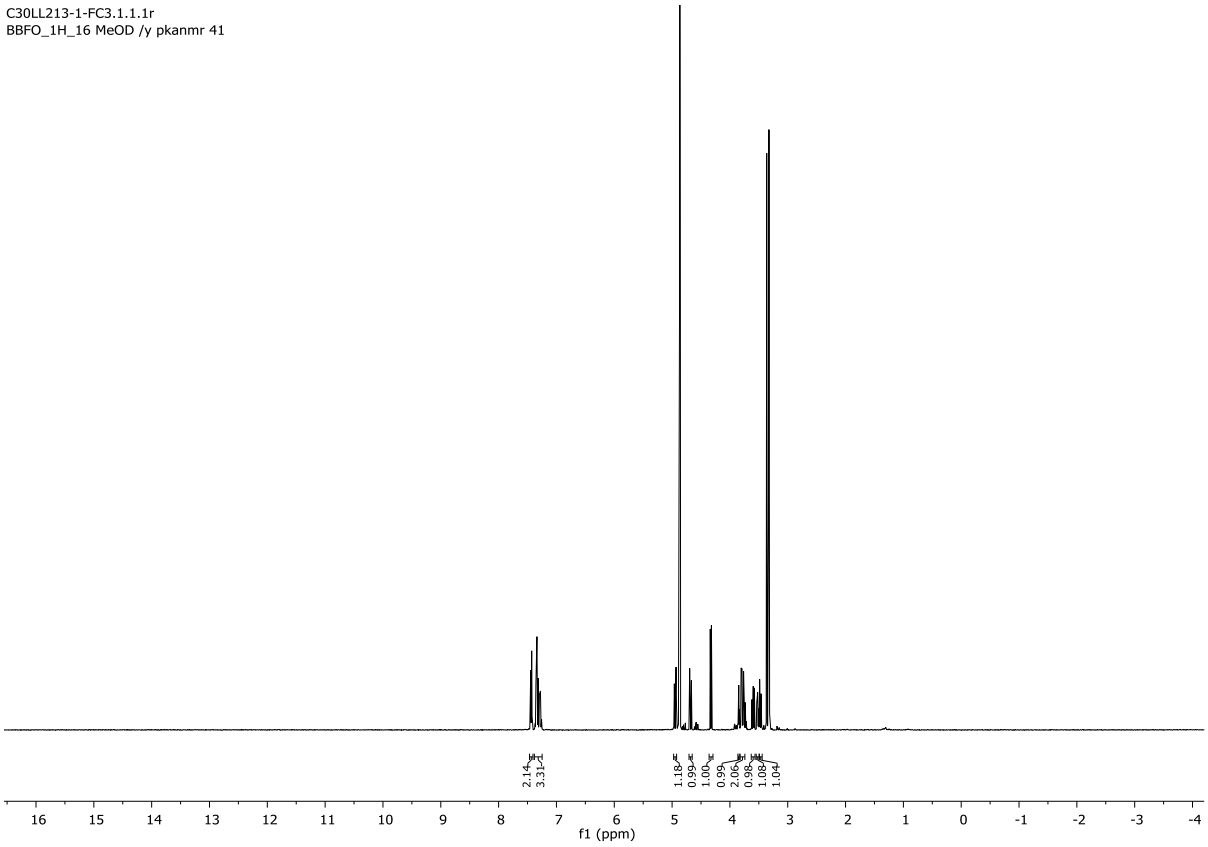
C30LL213-1-FC3.1.1.1r
BBFO_1H_16 MeOD /y pkanmr 41
2.14
3.31
1.18
0.99
1.00
0.99
2.06
0.98
1.08
1.04
f1 (ppm)

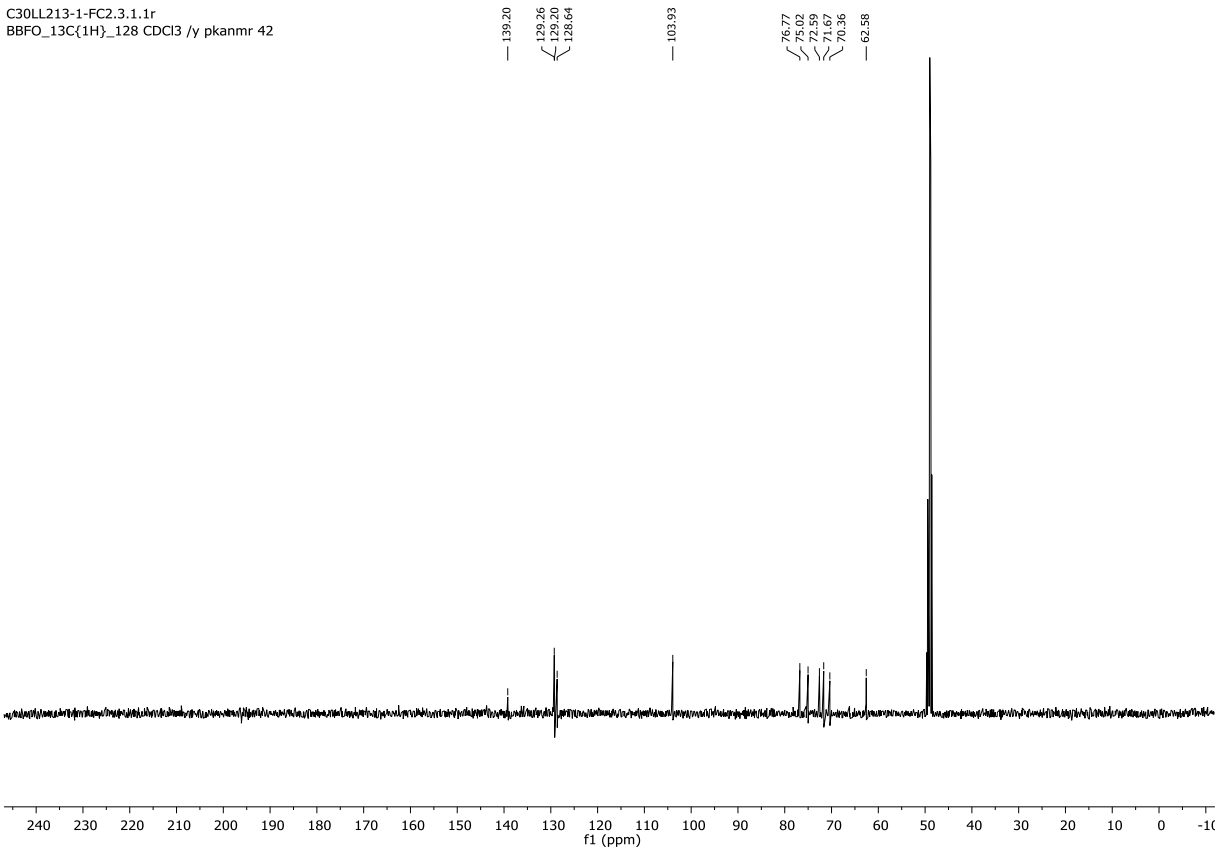
C30LL213-1-FC2.3.1.1r
BBFO_13C{1H}_128 CDCl3 /y pkanmr 42
139.20
129.26
129.20
128.64
103.93
76.77
75.02
72.59
71.67
70.36
62.58
f1 (ppm)

A-180 (2S,3S,4aR,5R,7R,8S,8aS)-5-(benzyloxy)-7-(hydroxymethyl)-2,3-dimethoxy-2,3-dimethylhexahydro-5H-pyrano[3,4-b][1,4]dioxin-8-ol

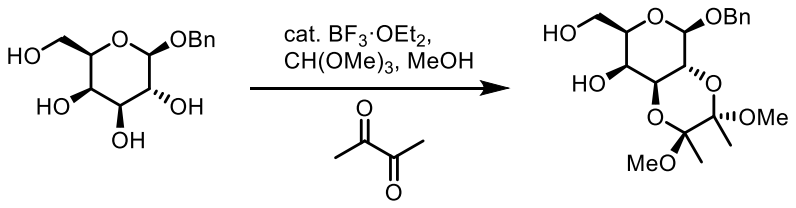

Assay: To a solution of **A-179** (22.5 g, 83.25 mmol, 1.0 equiv), butane-2,3-dione (8.99 mL, 102.39 mmol, 1.23 equiv) and trimethylorthoformate (36.43 mL, 333 mmol, 4.0 equiv) in MeOH (450 mL) was added $BF_3{\cdot}OEt_2$ (1.03 mL, 8.32 mmol, 0.1 equiv) at ambient temperature. The reaction mixture slowly turned from bright yellow to orange/red. The reaction mixture was stirred as such for 3 d and was then carefully quenched by the addition of NEt_3 (6 mL). The mixture was directly concentrated under reduced pressure. Purification by FC (EtOAc:hexane, 3:1) gave the title compound as a white solid (23.98 g, 62.38 mmol, 75%).

Analytics: $\mathbf{R_f}$ = 0.51 (EtOAc:hexane, 3:1). $^{\mathbf{1}}$**H NMR** (400 MHz, Chloroform-*d*) δ 7.41 – 7.27 (m, 5H), 4.91 (d, *J* = 12.3 Hz, 1H), 4.72 (d, *J* = 12.4 Hz, 1H), 4.61 (d, *J* = 7.9 Hz, 1H), 4.04 – 3.94 (m, 1H), 3.97 – 3.89 (m, 2H), 3.81 (dd, *J* = 11.7, 4.7 Hz, 1H), 3.73 (dd, *J* = 10.3, 3.1 Hz, 1H), 3.61 – 3.53 (m, 1H), 3.29 (s, 3H), 3.25 (s, 3H), 1.33 (s, 3H), 1.32 (s, 3H). $^{\mathbf{13}}$**C NMR** (101 MHz, Chloroform-*d*) δ 137.87, 128.25 (2C), 127.53, 127.42 (2C), 100.71, 100.29, 99.79, 75.04, 71.08, 70.25, 68.16, 66.91, 62.46, 48.07, 47.92, 17.73, 17.59.

C31LL214-2-FC.2.1.1r
BBFO_1H_16 CDCl3 /y pkanmr 22

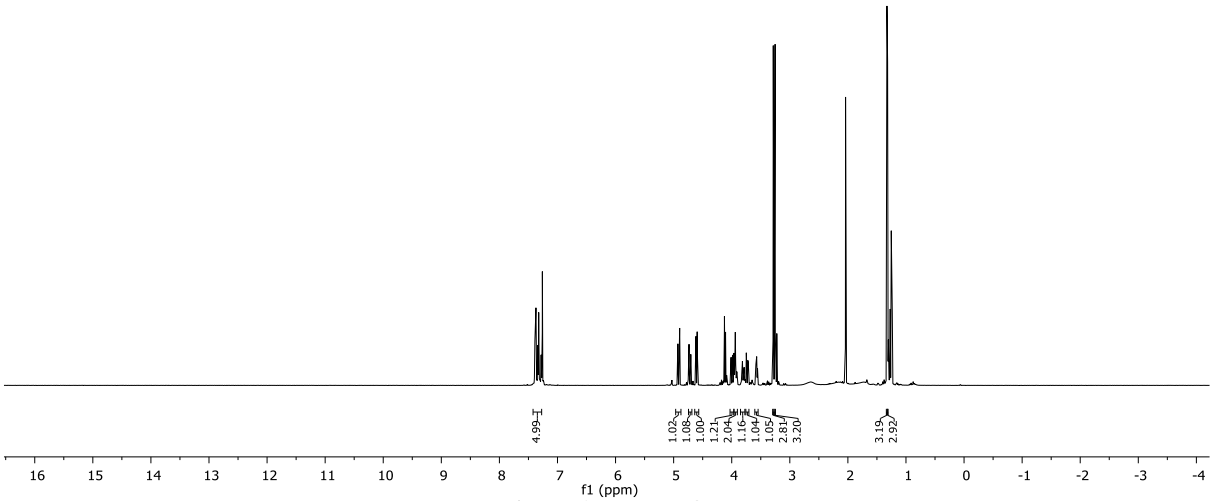

C31LL214-2-FC.7.1.1r
BBFO_13C{1H}_1024 CDCl3 /y pkanmr 22

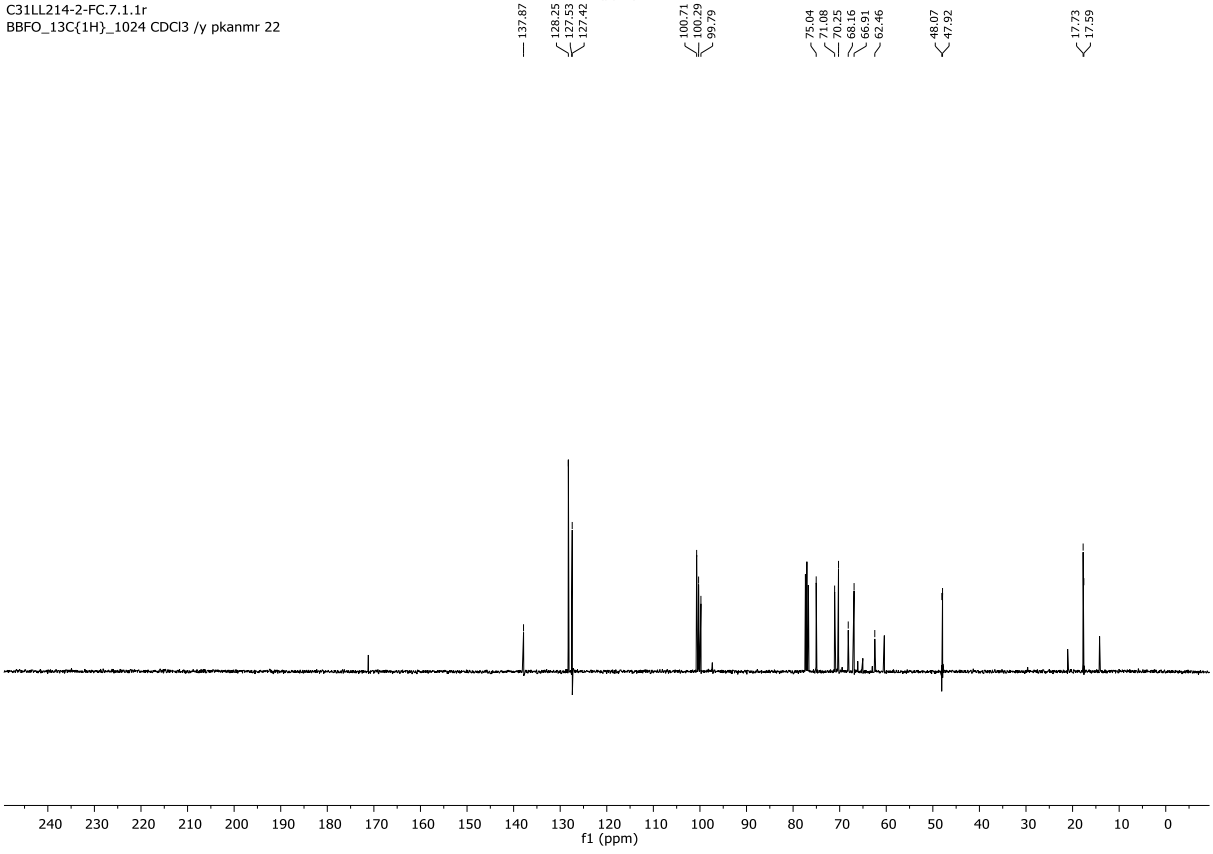

A-193 ((2S,3S,4aR,5R,7R,8S,8aS)-5-(benzyloxy)-8-hydroxy-2,3-dimethoxy-2,3-dimethylhexahydro-5H-pyrano[3,4-b][1,4]dioxin-7-yl)methyl 4-methylbenzenesulfonate

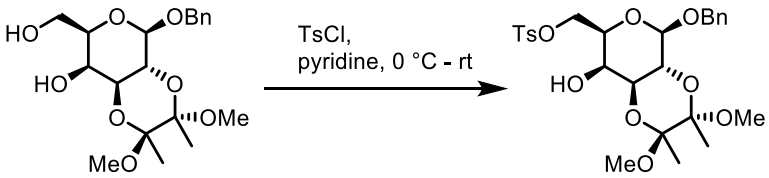

Assay: A-180 (11.55 g, 30.04 mmol, 1.0 equiv) was dissolved in pyridine (200 mL) and freshly purified p-toluenesulfonyl chloride (7.45 g, 39.06 mmol, 1.3 equiv) was added portionwise at 0 °C. The reaction mixture was then allowed to warm to ambient temperature and continued to stir for 18 h. It was then quenched with H_2O (200 mL) and extracted with $CHCl_2$ (3 x 80 mL). The combined organic phases were then dried over $MgSO_4$ and concentrated under reduced pressure. The reddish viscous liquid was filtered over a short plug of silica (EtOAc:hexane, 1:1). The white, fluffy solid was then taken up in as little CH_2Cl_2 as possible and washed with HCl (1 M, 60 mL) (to remove residual pyridine). The organic phase was again dried over $MgSO_4$ and concentrated under reduced pressure to give the title compound as a white foam (14.15 g, 26.26 mmol, 87%) which was directly used as such in in the following reaction. Compound can be purified by FC if needed.

Analytics: No full characterization due to instability. $\mathbf{R_f}$ = 0.5 (EtOAc:hexane, 1:1). **^{1}H NMR** (400 MHz, Chloroform-*d*) δ 7.80 (d, *J* = 8.4 Hz, 2H), 7.43 – 7.28 (m, 7H), 4.86 (d, *J* = 12.2 Hz, 1H), 4.61 (d, *J* = 12.2 Hz, 1H), 4.53 (d, *J* = 8.0 Hz, 1H), 4.28 (dd, *J* = 10.3, 5.7 Hz, 1H), 4.19 (dd, *J* = 10.3, 6.8 Hz, 1H), 3.94 – 3.88 (m, 2H), 3.79 (dd, *J* = 6.9, 5.6 Hz, 1H), 3.70 (dd, *J* = 10.4, 3.0 Hz, 1H), 3.25 (d, *J* = 1.2 Hz, 6H), 2.43 (s, 3H), 2.20 (dd, *J* = 2.7, 1.3 Hz, 1H), 1.30 (d, *J* = 4.2 Hz, 6H). **HRMS (ESI)**: 556.2215 $[M+NH_4]^+$; calculated for $[C_{26}H_{38}NO_{10}S]$: 556.221. **IR** [ATR, neat]: ν = 3445.21 w, 2944.77 w, 1455.99 w, 1374.03 w, 1115.62 s, 1037.73 s, 733.78 s, 698.11 m cm^{-1}.

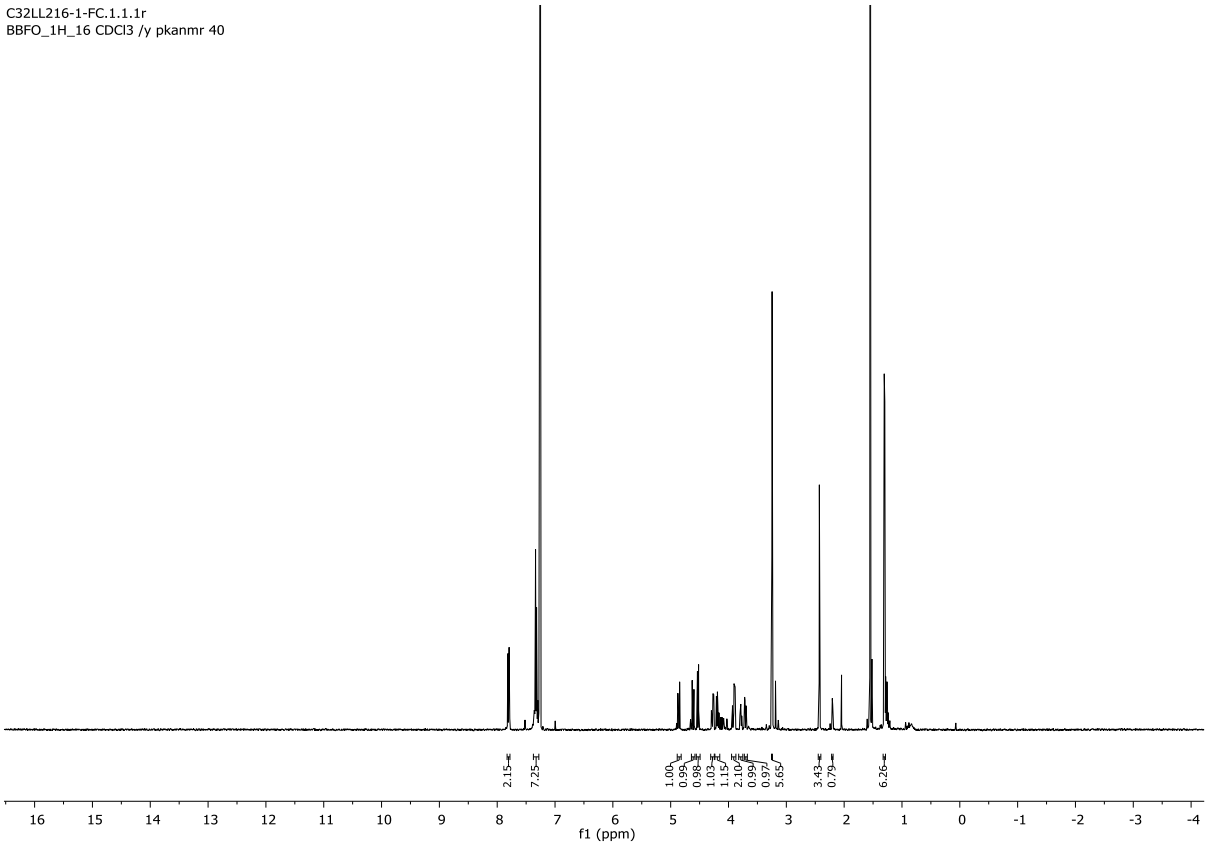
C32LL216-1-FC.1.1.1r
BBFO_1H_16 CDCl3 /y pkanmr 40
2.15
7.25
1.00
0.99
0.98
1.07
1.15
2.10
0.99
0.97
5.65
3.43
0.79
6.26
16 15 14 13 12 11 10 9 8 7 6 5 4 3 2 1 0 -1 -2 -3 -4
f1 (ppm)

A-181 (2S,3S,4aR,5R,7R,8S,8aS)-5-(benzyloxy)-2,3-dimethoxy-2,3,7-trimethylhexahydro-5H-pyrano[3,4-b][1,4]dioxin-8-ol

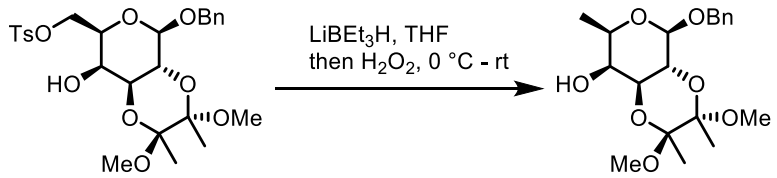

Assay: Tosylate **A-193** (14.14 g, 26.25 mmol, 1.0 equiv) was dissolved in THF (65 mL) and super hydride (1M in THF, 78.76 mL, 3.0 equiv) was then added dropwise (carefully via syringe pump, flow rate 1.1 mL/min) at ambient temperature. An effervescence was observed when adding the first few drops of superhydride. After full addition, the clear solution was stirred for 14 h at 24 °C. The reaction mixture was then cooled to 0 °C and the excess of super hydride was quenched by the addition of MeOH (about 10 mL) followed by carefull addition of hydrogen peroxide (21 mL). After stirring for 10 min, the reaction mixture was stirred at 40 °C for 30 min in order to quench the excess H_2O_2. To the mixture was then added saturated aqueous $NaHCO_3$ (100 mL) and CH_2Cl_2 (100 mL). The aqueous phase was extracted with CH_2Cl_2 (2 x 100 mL). The combined organic phases were then dried over $MgSO_4$ and concentrated under reduced pressure. The vicious oil was purified by FC (EtOAc:hexane; 1:1) to give the title compound as a clear sticky foam (8.87 g, 24.08 mmol, 92%).

Analytics: $\mathbf{R_f}$ = 0.43 (EtOAc:hexane, 1:1). **^{1}H NMR** (400 MHz, Chloroform-*d*) δ 7.42 – 7.22 (m, 5H), 4.94 (d, *J* = 12.2 Hz, 1H), 4.66 (d, *J* = 12.3 Hz, 1H), 4.55 (d, *J* = 8.0 Hz, 1H), 3.94 (dd, *J* = 10.3, 8.0 Hz, 1H), 3.73 (dd, *J* = 10.3, 3.0 Hz, 1H), 3.70 – 3.62 (m, 2H), 3.28 (s, 3H), 3.25 (s, 3H), 2.21 (s, 1H), 1.36 (d, *J* = 6.5 Hz, 3H), 1.33 (s, 3H), 1.31 (s, 3H). **^{13}C NMR** (101 MHz, Chloroform-*d*) δ 137.98, 128.17 (2 C), 127.34 (3 C), 100.27, 100.17, 99.72, 71.22, 70.67, 70.45, 70.12, 66.87, 48.01, 47.86, 17.76, 17.63, 16.36. **HRMS (ESI)**: 386.2176 $[M+NH_4]^+$; calculated for $[C_{19}H_{32}NO_7]$: 386.2173. **$[\alpha]^{20}_D$** = -123.0 (c = 0.5, $CHCl_3$). **IR** [ATR, neat]: ν = 1455.03 w, 1373.07 w, 1115.62 s, 1076.08 m, 1034.62 s, 921.87 m, 731.85 m cm^{-1}.

C39LL218-1-repurif.1.fid
BBFO_1H_16 CDCl3 /y pkanmr 28

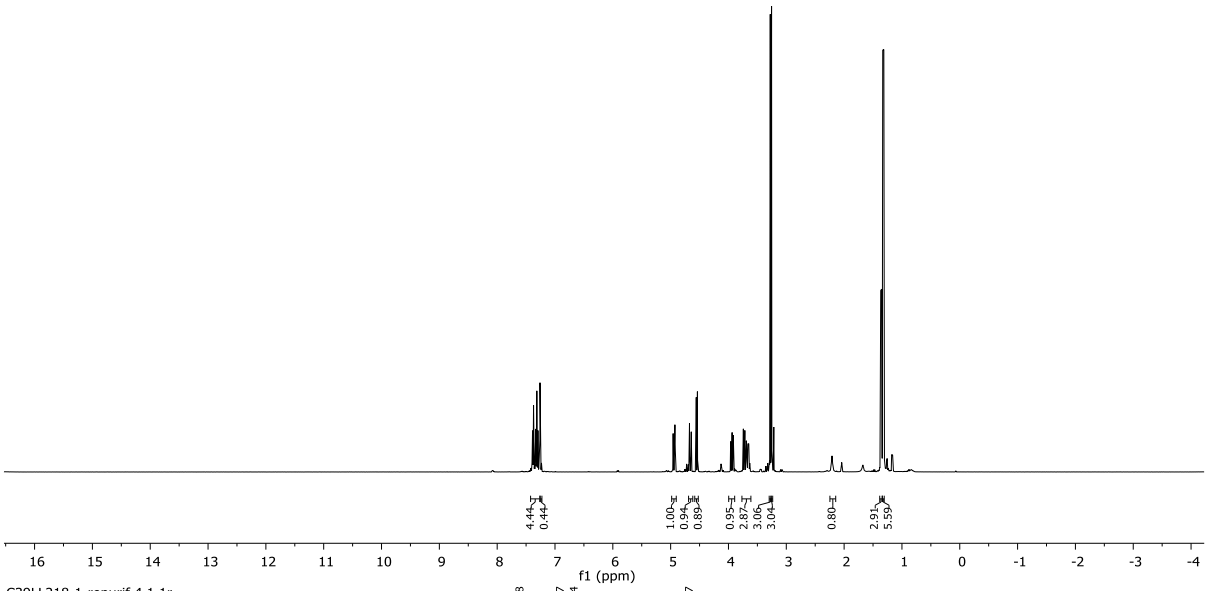

C39LL218-1-repurif.4.1.1r
BBFO_13C{1H}_256 CDCl3 /y pkanmr 28

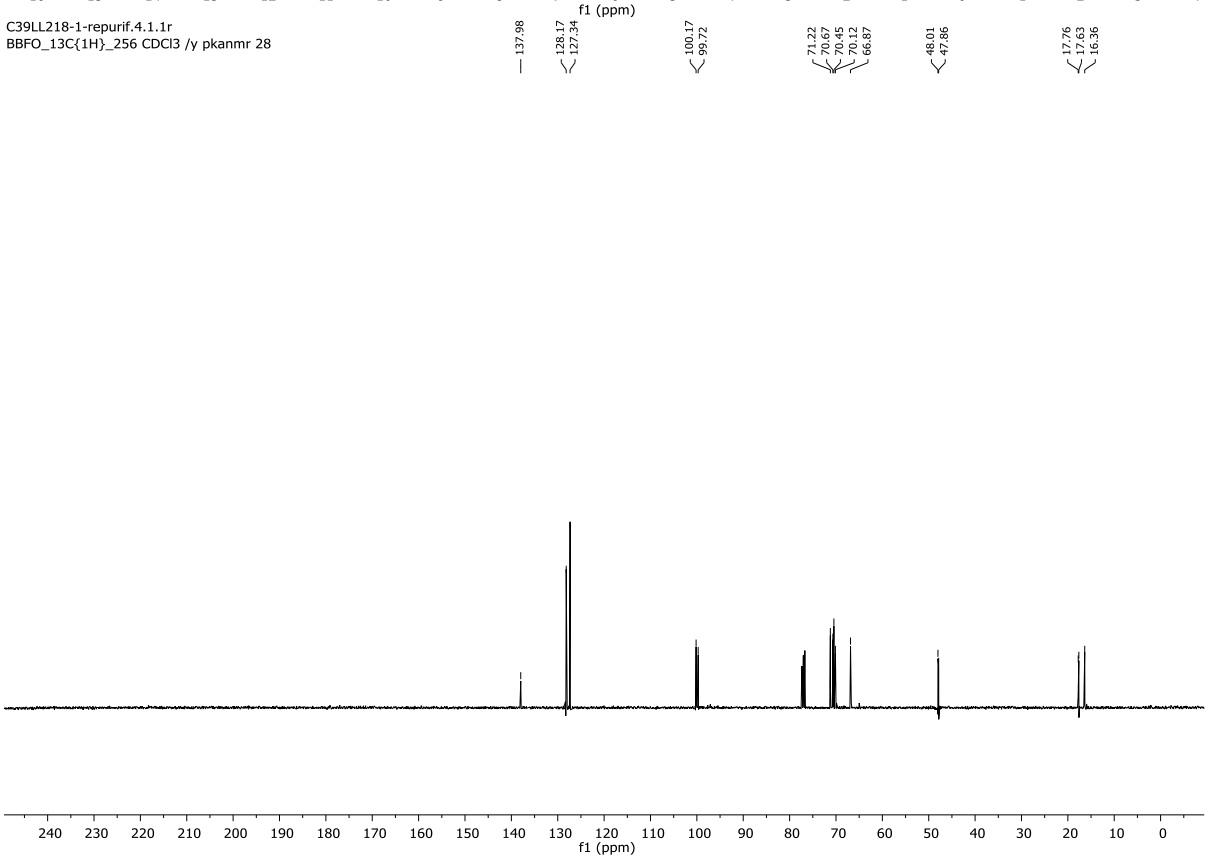

A-182 (2R,3R,4S,5R,6S)-3-azido-4,5-bis((4-methoxybenzyl)oxy)-2-methyl-6-(phenylthio)tetrahydro-2H-pyran

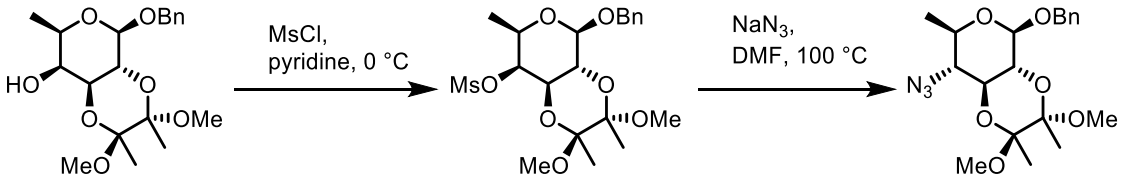

Assay: In a flame dried round bottom flask (250 mL), **A-181** (8.87 g, 24.08 mmol, 1.0 equiv) was dissolved in pyridine (150 mL) and the reaction mixture was cooled to 0 °C. MsCl (5.59 mL, 72.23 mmol, 3.0 equiv) was then added dropwise and the reaction was stirred at 0 °C for 5 h. The reaction was then quenched by the addition of water (150 mL) and extracted with diethyl ether (3 x 60 mL). The combined organic phases were dried to complete dryness (remove pyridine) under reduced pressure. The sticky yellowish syrup was taken up in diethyl ether (100 mL) and washed with HCl 1 M (100 mL), H_2O (100 mL) and was dried over $MgSO_4$. The crude mixture was then transformed into a round bottom flask (1 L) and taken up in DMF (300 mL), then NaN_3 (7.83 g, 120.38 mmol, 5.0 equiv) was added and the reaction was heated to 100 °C and stirred for 64 h. A substantial amount of starting material was still present, thus another portion of NaN_3 (5.0 equiv) was added and the reaction was continued to stir for another 24 h. The reaction was then allowed to cool to ambient temperature, was filtered over cotton wool and the filtrate was mixed with saturated aqueous $NaHCO_3$ (100 mL). The two phases were transferred to a separatory funnel and the aqueous phase was extracted with diethyl ether (3 x 100 mL), dried over $MgSO_4$ and concentrated under reduced pressure. The crude was then purified by FC (EtOAc:hexane 1:10 -> 1:5) to give the title compound (7.15 g, 18.17 mmol, 75%) as a white solid.

Analytics: $\mathbf{R_f}$ = 0.68 (EtOAc:hexane, 1:1) for mesylate. $\mathbf{R_f}$ = 0.38 (EtOAc:hexane, 1:10) for title compound. **^{1}H NMR** (400 MHz, Chloroform-*d*) δ 7.40 – 7.27 (m, 5H), 4.90 (d, *J* = 12.2 Hz, 1H), 4.65 (d, *J* = 12.2 Hz, 1H), 4.54 (d, *J* = 7.9 Hz, 1H), 3.81 – 3.75 (m, 1H), 3.64 (dd, *J* = 10.0, 7.9 Hz, 1H), 3.34 (s, 3H), 3.30 (s, 3H), 3.28 – 3.24 (m, 2H), 1.35 (s, 3H), 1.36 – 1.34 (m, 3H), 1.33 (s, 3H). **^{13}C NMR** (101 MHz, Chloroform-*d*) δ 137.58, 128.26 (2 C), 127.57, 127.39 (2 C), 100.02 (2 C), 99.70, 72.07, 71.41, 70.87, 69.85, 64.02, 48.01 (2 C), 18.29 (2 C), 17.61. **$[\alpha]^{20}_D$** = -76.4 (c = 0.5, $CHCl_3$). **HRMS (ESI)**: 416.1781 $[M+Na]^+$; calculated for $[C_{19}H_{27}N_3NaO_6]$: 416.1792. **IR** [ATR, neat]: ν = 2107.81 s, 1455.99 w, 1371.14 w, 1264.11 w, 1138.76 s, 1081.87 m, 1043.3 s, 889.02 m, 740.53 m, 698.11 m cm^{-1}. **m.p.**: 85–87 °C.

C35LL220-1-2ndBatchdry.1.fid
BBFO_1H_16 CDCl3 /y pkanmr 35

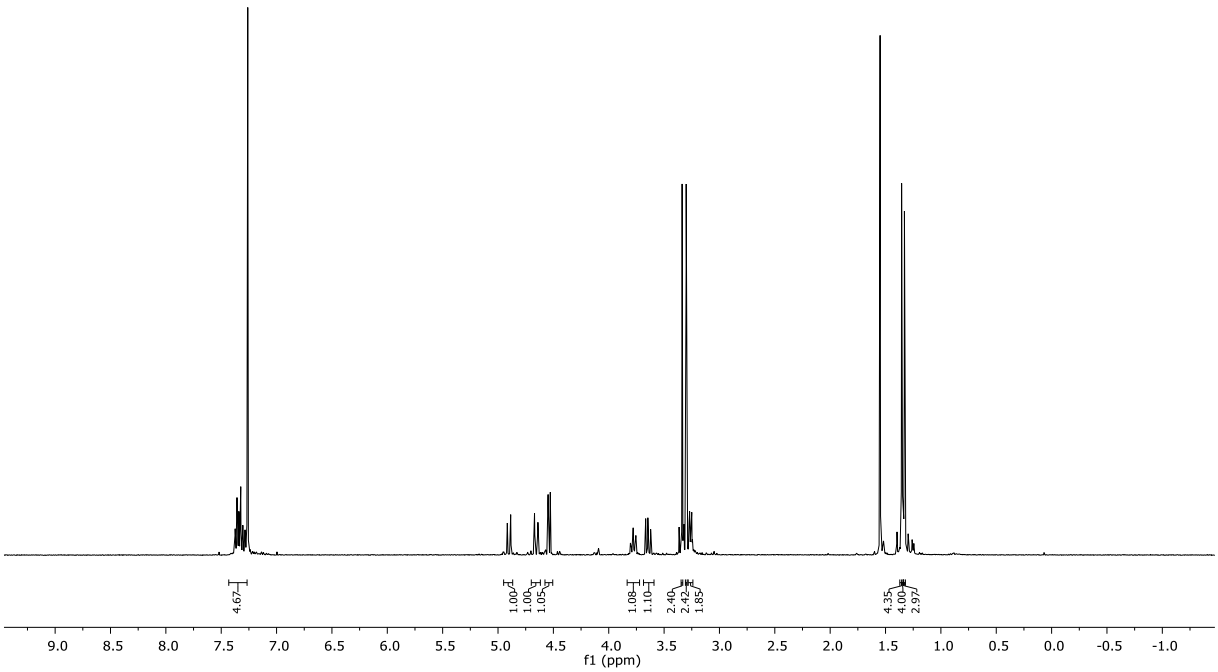

C35LL220-1-2ndBatchdry.2.fid
BBFO_13C{1H}_1024 CDCl3 /y pkanmr 35

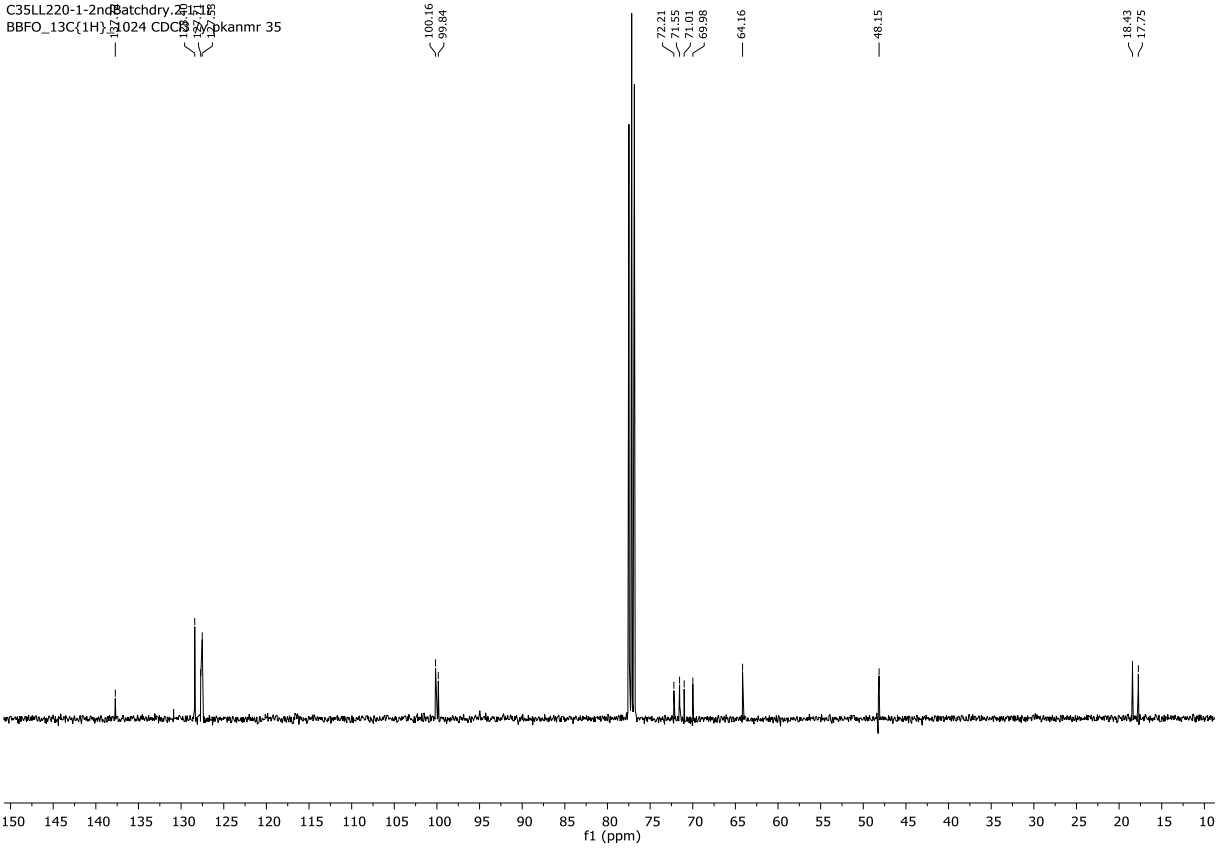

A-153 (2S,3S,4aR,5R,7R,8R,8aS)-8-azido-2,3-dimethoxy-2,3,7-trimethylhexahydro-5H-pyrano[3,4-b][1,4]dioxin-5-ol

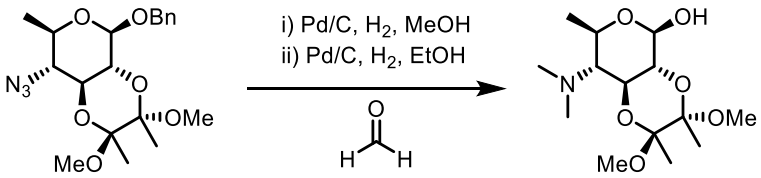

Assay: To **A-182** (3.16 g, 8.03 mmol, 1.0 equiv), dissolved in MeOH (80.0 mL), was added Pd/C (10 wt %, 855 mg, 28 µmol, 0.1 equiv) in one portion and the reaction vessel was subsequently set under H_2-atmosphere (balloon pressure). The reaction mixture was stirred as such for 21 h. The reaction mixture was then filtered over Celite and washed with MeOH. The filtrate was concentrated under reduced pressure and subsequently dissolved in EtOH (80.0 mL). Formaldehyde (37% in H_2O, 1.5 mL, 2.5 equiv) was then added to the reaction mixture followed by Pd/C (10 wt %, 855 mg, 28 µmol, 0.1 equiv) and the reaction vessel was subsequently set under H_2-atmosphere (balloon pressure). It was stirred at ambient temperature for 48 h. Again, the crude was filtrated over a pad of Celite and the filtrate was concentrated under reduced pressure. Purification by FC (EtOAc:hexane, 1:3 -> 1:1) gave the target compound as a white powder (2.016 g, 6.3 mmol, 82%).

Analytics: $\mathbf{R_f}$ = 0.20 (EtOAc:hexane, 1:1). **^{1}H NMR** (400 MHz, Chloroform-*d*) δ 5.13 (d, *J* = 3.3 Hz, $1H_a$), 4.68 (d, *J* = 7.6 Hz, $1H_b$), 4.44 (t, *J* = 10.1 Hz, $1H_a$), 4.10 (t, *J* = 10.1 Hz, $1H_b$), 4.00 (dq, *J* = 10.0, 6.2 Hz, $1H_a$), 3.76 (dd, *J* = 10.0, 3.5 Hz, $1H_a$), 3.56 – 3.42 (m, $2H_b$), 3.39 (s, $3H_b$), 3.38 (s, $3H_a$), 3.30 (s, $3H_b$), 3.26 (s, $3H_a$), 2.89 (s, $1H_b$), 2.72 (s, $1H_a$). 2.48 (s, $3H_a$), 2.46 (s, $3H_a$), 2.43 – 2.36 (m, $1H_a$, $1H_b$), 1.33 – 1.29 (m, $6H_a$, $9H_b$), 1.25 (d, *J* = 6.2 Hz, $3H_a$). **^{13}C NMR** (101 MHz, Chloroform-*d*) δ 99.95, 99.57, 94.12, 91.39, 72.44, 71.44, 70.31, 67.98, 67.51, 67.08, 66.99, 64.66, 49.37, 49.17, 47.91, 42.11, 41.88, 18.87, 18.19, 18.07, 17.82. **$[\alpha]^{20}_D$** = -54.9 (c = 0.38, $CHCl_3$). **HRMS (ESI)**: 306.1914 $[M+H]^+$; calculated for $[C_{14}H_{28}NO_6]$: 306.1911. **IR** [ATR, neat]: ν = 3421.1 w, 2929.34 m, 1456.96 m, 1375.0 s, 1135.87 w, 1037.52 w, 883.24 w, 844.67 cm^{-1}. **m.p.**: 161 °C.

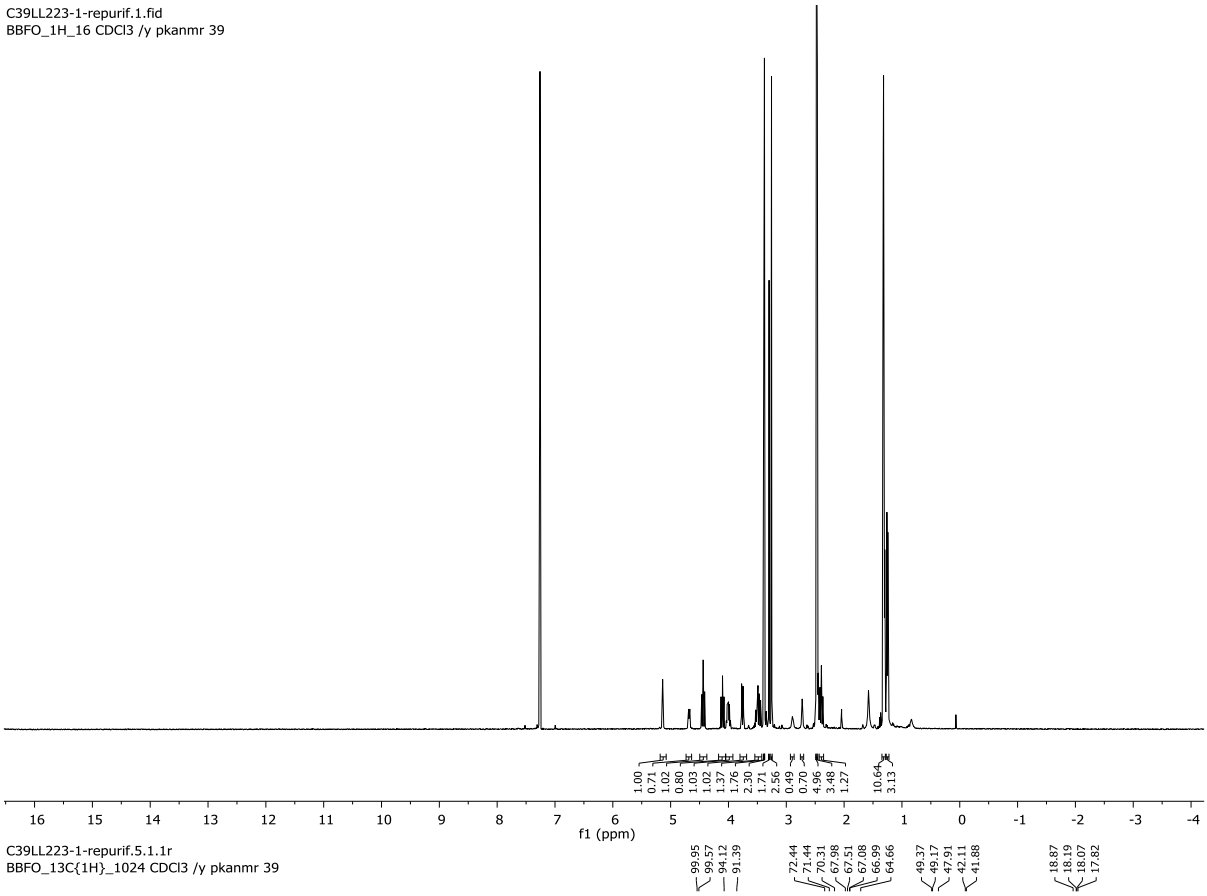
C39LL223-1-repurif.1.fid
BBFO_1H_16 CDCl3 /y pkanmr 39
1.00
0.71
1.02
0.80
1.03
1.02
1.37
1.76
2.30
1.71
2.56
0.49
0.70
4.96
3.48
1.27
10.64
3.13
16 15 14 13 12 11 10 9 8 7 6 5 4 3 2 1 0 -1 -2 -3 -4
f1 (ppm)

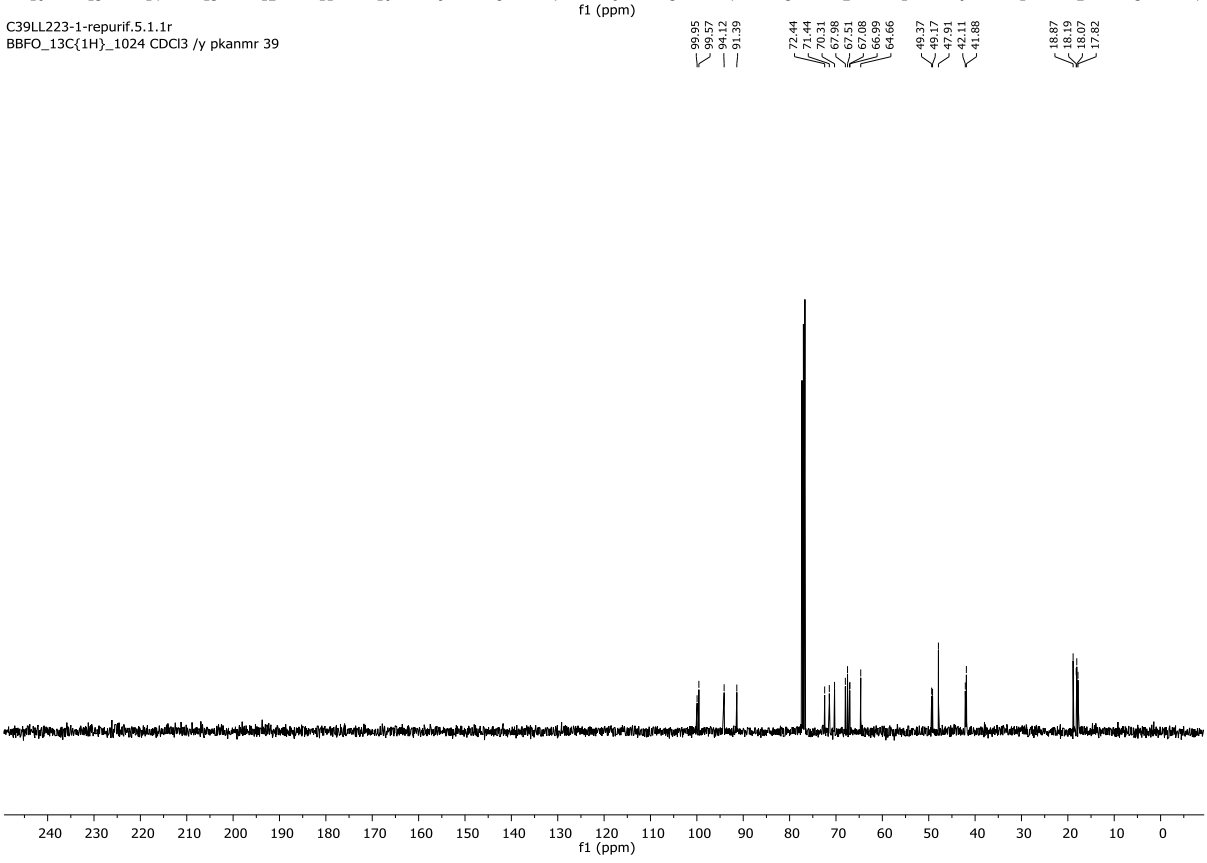
C39LL223-1-repurif.5.1.1r
BBFO_13C{1H}_1024 CDCl3 /y pkanmr 39
99.95
99.57
94.12
91.39
72.44
71.44
70.31
67.98
67.51
67.08
66.99
64.66
49.37
49.17
47.91
42.11
41.88
18.87
18.19
18.07
17.82
240 230 220 210 200 190 180 170 160 150 140 130 120 110 100 90 80 70 60 50 40 30 20 10 0
f1 (ppm)

A-149 (2S,3S,4aR,7R,8R,8aS)-8-(dimethylamino)-2,3-dimethoxy-2,3,7-trimethylhexahydro-5H-pyrano[3,4-b][1,4]dioxin-5-yl 2,2,2-trichloroacetimidate

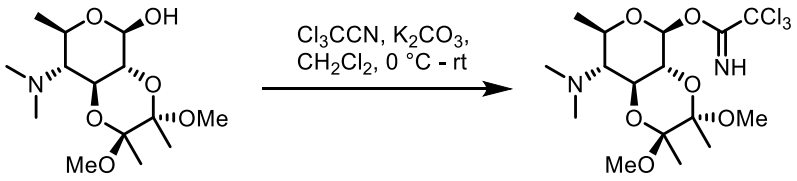

Assay: A-153(67.0 mg, 0.22 mmol, 1.0 equiv), was dissolved in CH_2Cl_2 (2.0 mL), cooled to 0 °C and trichloroacetonitrile (0.22 mL, 2.19 mmol, 10.0 equiv) was added followed by anhydrous K_2CO_3 (152 mg, 1.09 mmol, 5.0 equiv). The reaction mixture was allowed to slowly warm to ambient temperature and was stirred for 13 h. The reaction mixture was then filtrated over a pad of Celite and the filtrate was concentrated. The yellowish oil was then directly applied on a FC (Alox, EtOAc:hexane, 1:3) to give the title compound as a clear sticky syrup and an anomeric mixture of 1:1 (35 mg, 0.078 mmol, 35%). The compound was then directly used as such in the following reactions.

Analytics: $\mathbf{R_f}$ = 0.52 resp. 0.61 (EtOAc:hexane, 1:3) on Alox. **^{1}H NMR** (400 MHz, Chloroform-*d*) δ 8.56 (s, $1H_a$), 8.52 (s, $1H_b$), 6.18 (d, *J* = 3.1 Hz, $1H_a$), 5.78 (d, *J* = 8.2 Hz, $1H_b$), 4.56 (t, *J* = 10.2 Hz, $1H_a$), 4.18 (t, *J* = 10.1 Hz, $1H_b$), 3.94 (dq, *J* = 10.0, 6.2 Hz, $1H_a$), 3.90 – 3.79 (m, $2H_{ab}$), 3.72 (dq, *J* = 8.7, 6.3 Hz, $1H_b$), 3.39 (s, $3H_a$), 3.35 (s, $3H_a$), 3.29 (s, $3H_b$), 3.26 (s, $3H_b$), 2.54 (m, $1H_a$), 2.51 (m, $1H_b$). 2.48 (s, $6H_a$), 2.46 (s, $6H_b$), 1.36 (d, *J* = 6.3 Hz, $3H_a$), 1.33 (s, $3H_a$), 1.30 – 1.22 (m, $3H_a$, $9H_b$). **^{13}C NMR** (101 MHz, Chloroform-*d*) δ 161.39, 161.08, 99.76, 99.64, 99.49, 96.11, 94.81, 91.57, 91.11, 72.53, 69.93, 69.30, 67.37, 67.23, 66.95, 64.46, 49.25, 49.08, 47.94, 47.78, 42.11, 41.75, 19.55, 19.12, 18.14, 17.99, 17.76, 17.60. **HRMS (ESI)**: 449.1004 $[M+H]^+$; calculated for $[C_{16}H_{28}Cl_3N_2O_6]$: 449.1007. **IR** [ATR, neat]: ν = 2933.2 w, 1673.91 m, 1374.03 m, 1288.22 s, 1134.9 s, 1111.76 s, 1036.55 s, 795.493 m cm^{-1}.

Remarks: third spectrum represents β-anomer. Purity suffers from extensive purification.

C09LL225.1.1.1r
BBFO_1H_16 CDCl3 /v pkanmr 34

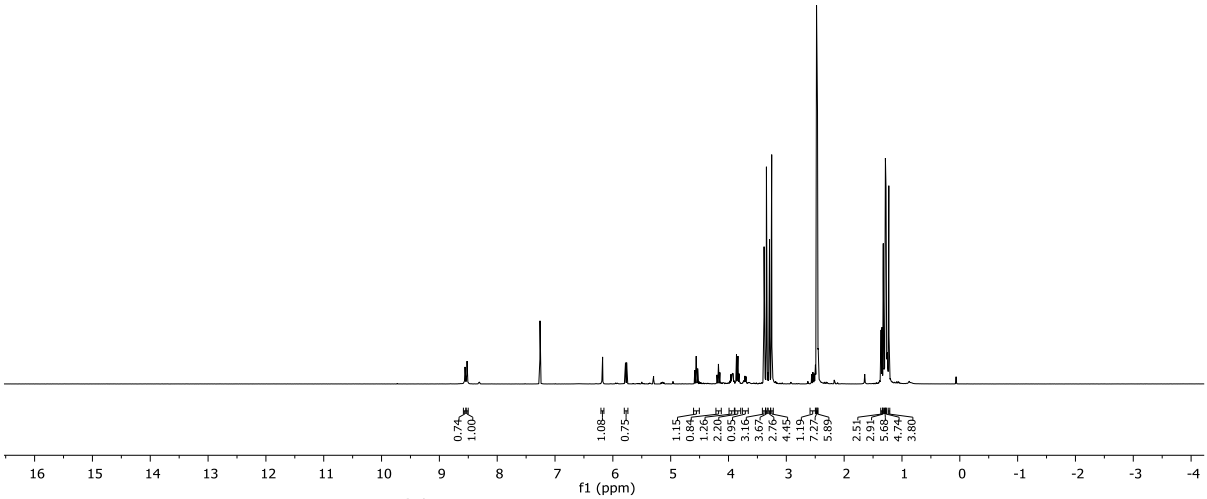

C09LL225.4.1.1r
BBFO_13C{1H}_1024 CDCl3 /v pkanmr 34

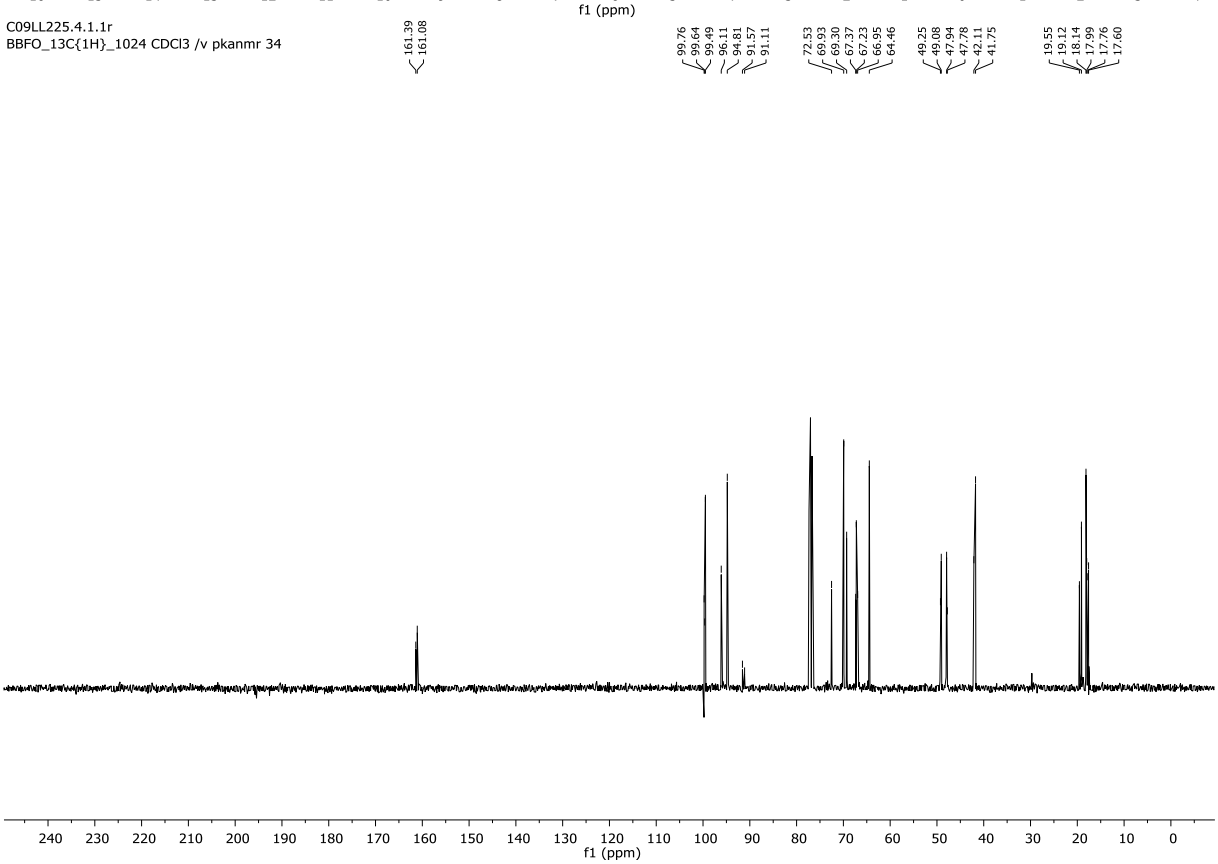

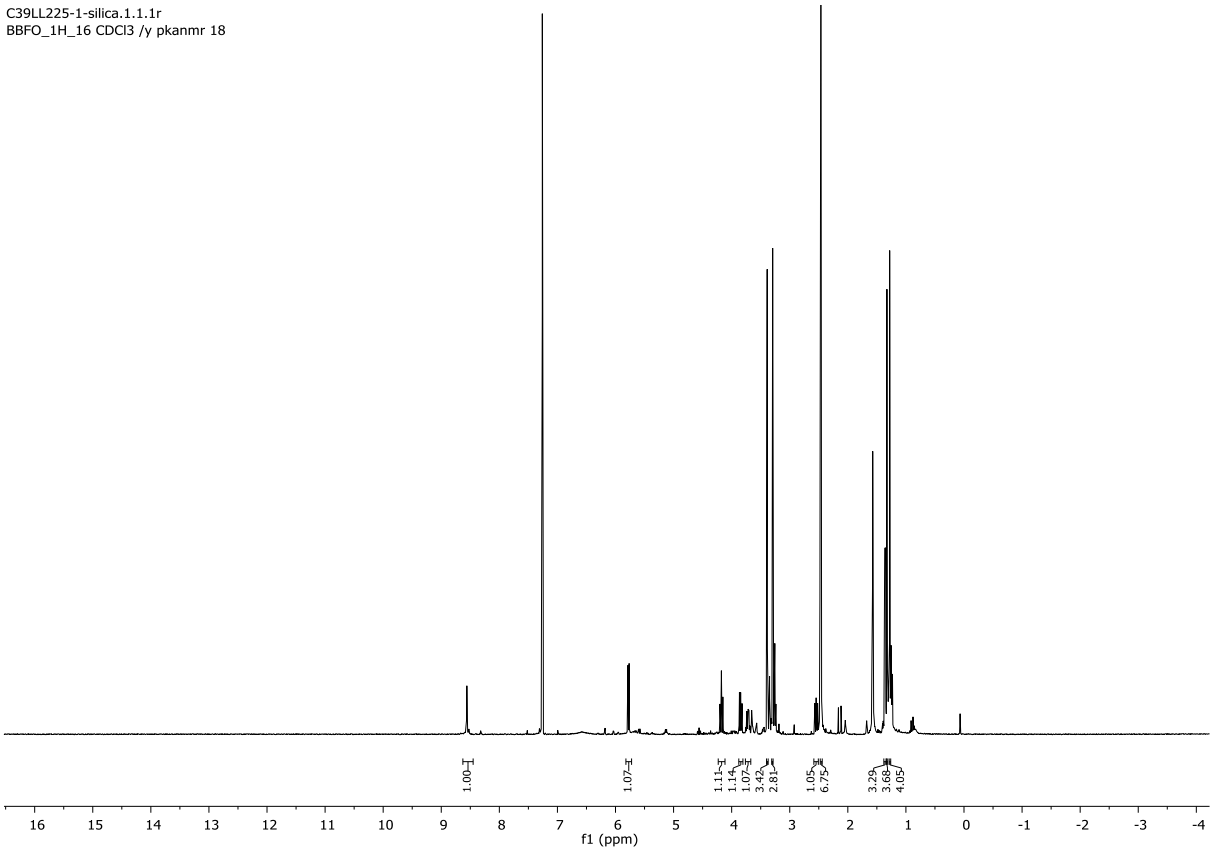
C39LL225-1-silica.1.1.1r
BBFO_1H_16 CDCl3 /y pkanmr 18
1.00
1.07
1.11
1.14
1.07
3.42
2.81
1.05
6.75
3.29
3.68
4.05
16 15 14 13 12 11 10 9 8 7 6 5 4 3 2 1 0 -1 -2 -3 -4
f1 (ppm)

A-184 (2S,3S,4aR,5R,7R,8R,8aR)-5-hydroxy-2,3-dimethoxy-2,3,7-trimethylhexahydro-5H-pyrano[3,4-b][1,4]dioxin-8-yl methanesulfonate

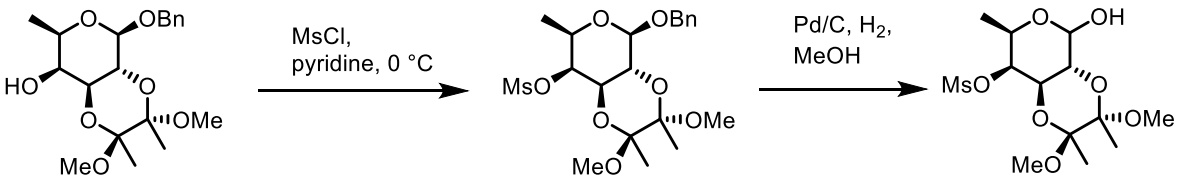

Assay: In a flame dried round bottom flask (5 mL) **A-181** (8.9 g, 24.16 mmol, 1.0 equiv) was dissolved in pyridine (240 mL) and the reaction mixture was cooled to 0 °C. MsCl (8.3 mL, 72.47 mmol, 3.0 equiv) was then added dropwise and the reaction was stirred at 0 °C for 6 h. The reaction was then quenched by the addition of water (120 mL) and extracted with diethyl ether (3 x 80 mL). The combined organic phases were dried over $MgSO_4$ and concentrated under reduced pressure. The crude mesylate was then dissolved in MeOH (240 mL) and Pd/C (10 wt %, 2.57 g, 10 mol %) was added and the reaction mixture was set under H_2 atmosphere (balloon). After stirring for 14 h, starting material was fully consumed. The reaction mixture was then filtered over Celite, which was previously washed with MeOH and the filtrate was concentrated under diminished pressure. Purification by FC (EtOAc:hexane, 1:1) gave the target compound (7 g, 19.6 mmol, 81%) as an anomeric mixture.

Analytics: $\mathbf{R_f}$ = 0.26 (EtOAc:hexane, 1:1). **^{1}H NMR** (400 MHz, Chloroform-*d*) δ 5.28 (t, *J* = 3.3 Hz, 1H), 4.82 – 4.73 (m, 2H), 4.70 (dd, *J* = 2.9, 1.1 Hz, 1H), 4.40 – 4.30 (m, 1H), 4.26 (dd, *J* = 10.7, 2.9 Hz, 1H), 4.11 – 4.07 (m, 1H), 3.90 – 3.82 (m, 2H), 3.76 (dd, *J* = 10.5, 7.7 Hz, 1H), 3.29 (s, 3H), 3.28 (s, 3H), 3.28 (s, 3H), 3.25 (s, 3H), 3.19 (s, 6H), 2.92 (d, *J* = 6.4 Hz, 1H), 2.81 (dd, *J* = 2.8, 0.8 Hz, 1H), 1.37 (d, *J* = 6.4 Hz, 3H), 1.32 (s, 9H), 1.29 (d, *J* = 6.9 Hz, 6H). **^{13}C NMR** (101 MHz, Chloroform-*d*) δ 100.20, 100.11, 99.76, 94.93, 91.61, 81.30, 80.12, 70.41, 68.69, 68.21, 66.09, 65.12, 64.55, 48.33, 48.26, 48.16, 39.16, 17.68, 17.60, 17.48, 16.69, 16.54. **HRMS (ESI)**: 379.1028 $[M+Na]^+$; calculated for $[C_{13}H_{24}NaO_9S]$: 379.1033. **IR** [ATR, neat]: ν = 3466.42 w, 2990.09 w, 1350.89 m, 1271.82 m, 1169.61 m, 1113.69 s, 1037.52 s, 921.81 s cm^{-1}.

Remarks: Multiplett report (for ^{1}H) accounts for both anomeric compounds.

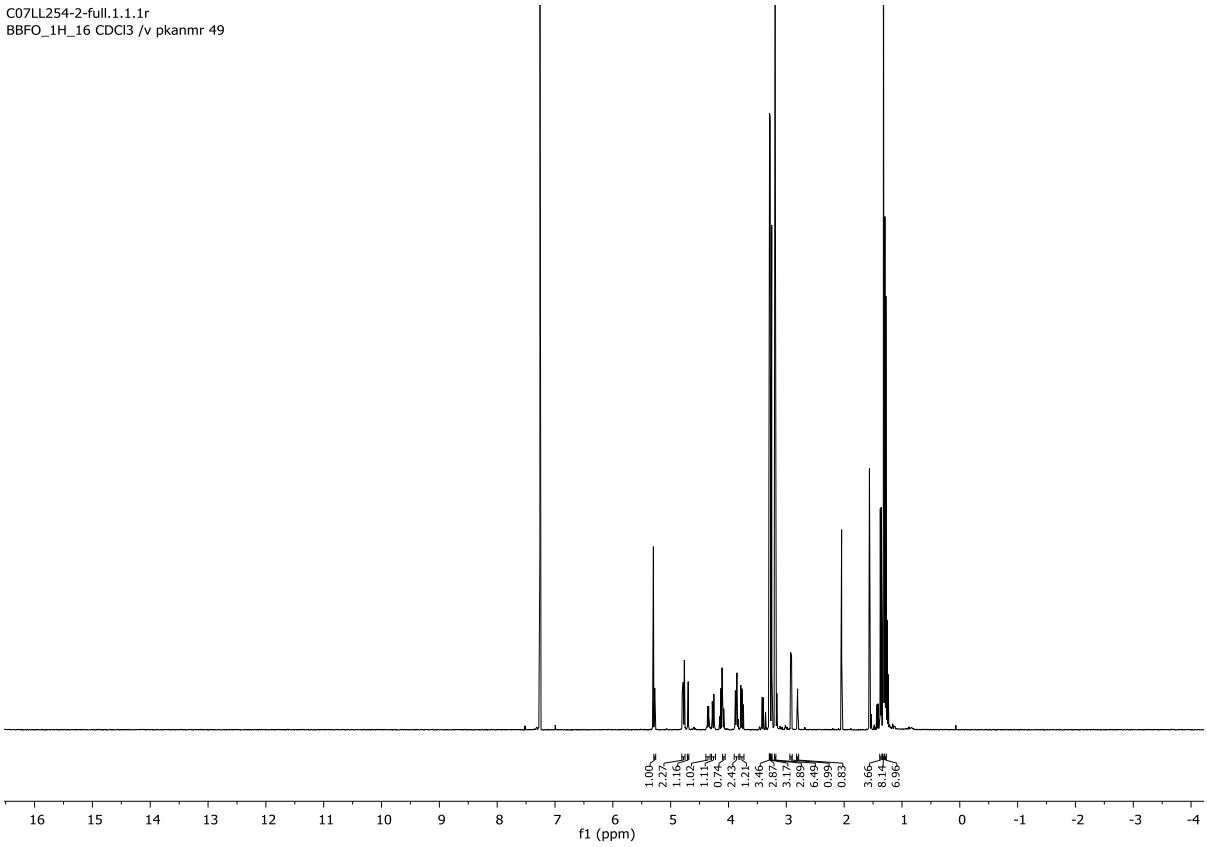
C07LL254-2-full.1.1.1r
BBFO_1H_16 CDCl3 /v pkanmr 49
1.00
2.27
1.16
1.02
1.11
0.74
2.43
1.21
3.46
2.87
3.17
2.89
6.49
0.99
0.83
3.66
8.14
6.96
16 15 14 13 12 11 10 9 8 7 6 5 4 3 2 1 0 -1 -2 -3 -4
f1 (ppm)

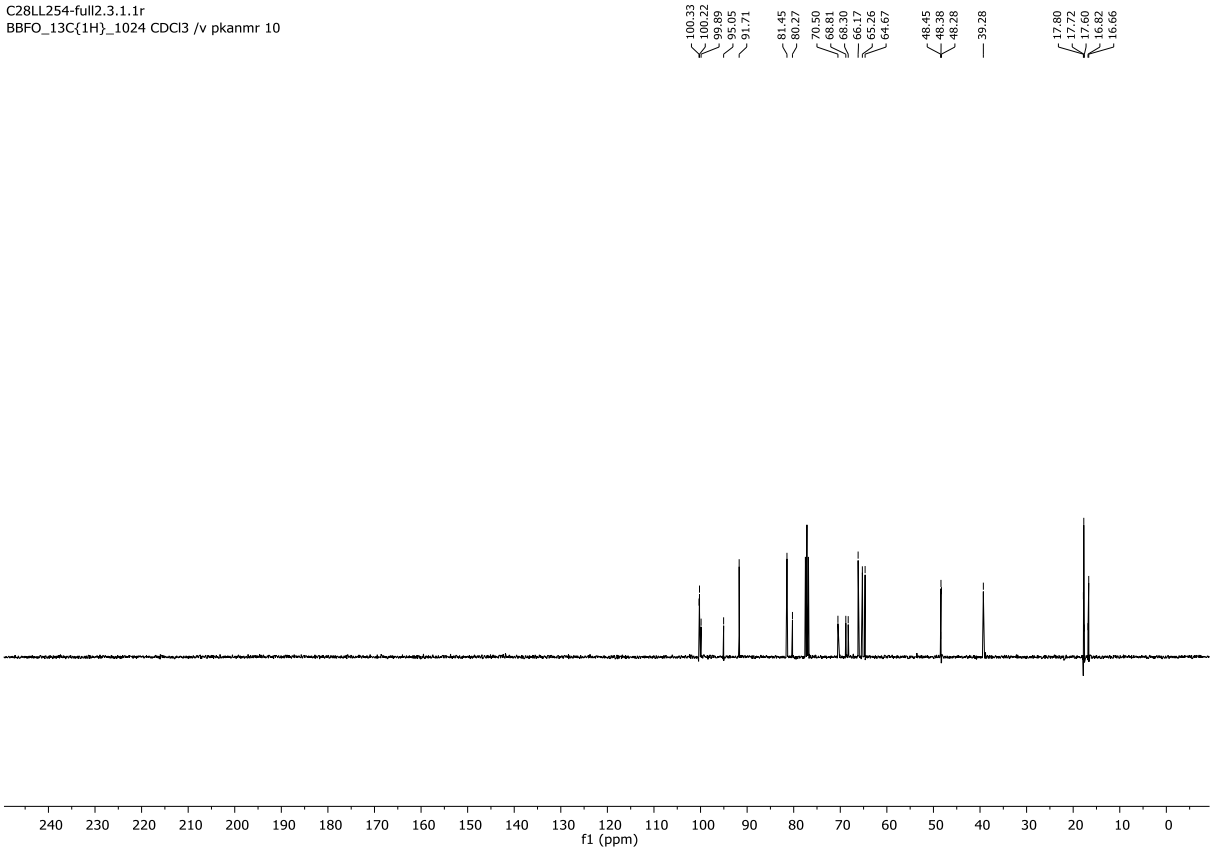
C28LL254-full2.3.1.1r
BBFO_13C{1H}_1024 CDCl3 /v pkanmr 10
100.33
100.22
99.89
95.05
91.71
81.45
80.27
70.50
68.81
68.30
66.17
65.26
64.67
48.45
48.38
48.28
39.28
17.80
17.72
17.60
16.82
16.66
240 230 220 210 200 190 180 170 160 150 140 130 120 110 100 90 80 70 60 50 40 30 20 10 0
f1 (ppm)

A-185 (2S,3S,4aR,5R,7R,8R,8aS)-8-azido-2,3-dimethoxy-2,3,7-trimethylhexahydro-5H-pyrano[3,4-b][1,4]dioxin-5-ol

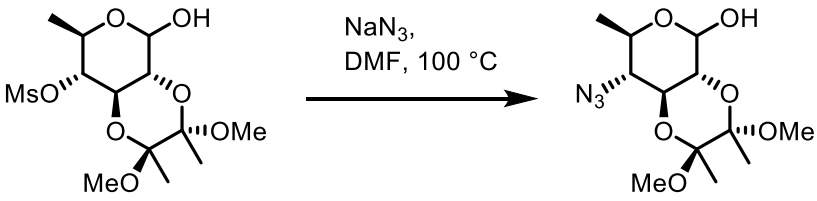

Assay: To **A-184** (7 g, 19.64 mmol, 1.0 equiv) in DMF (200 mL) was added NaN_3 (12.77 g, 196.41 mmol, 10.0 equiv) and the suspension was heated to 100 °C over 3 days. It was then allowed to cool to ambient temperature, was filtered over cotton wool and washed with Et_2O. To the yellowish organic layer was added saturated aqueous $NaHCO_3$ (80 mL). The phases were separated followed by the extraction of the aqueous layer with Et_2O (3 x 50 mL). Combined organic phases were dried over $MgSO_4$ and concentrated under reduced pressure. The yellowish oil was then purified by FC (EtOAc:hexane, 1:1) to give the title compound as a white solid (4.55 g, 15 mmol, 76%).

Analytics: $\mathbf{R_f}$ = 0.51 (EtOAc:hexane, 1:1). **^{1}H NMR** (400 MHz, Chloroform-*d*) δ 5.13 (t, *J* = 3.3 Hz, $1H_a$), 4.69 (dd, *J* = 7.9, 5.5 Hz, $1H_b$), 4.08 (t, *J* = 10.1 Hz, $1H_a$), 3.82 – 3.75 (m, $1H_a$), 3.74 – 3.69 (m, $2H_{ab}$), 3.43 (dd, *J* = 10.0, 7.9 Hz, $1H_b$), 3.28 (s, $6H_a$), 3.32 – 3.25 (m, $1H_b$), 3.24 (s, $3H_b$), 3.21 (s, $3H_b$), 3.25 – 3.16 (m, $1H_b$), 3.19 – 3.13 (m, $1H_a$), 2.88 (d, *J* = 5.6 Hz, $1H_b$), 2.71 (dd, *J* = 2.8, 0.8 Hz, $1H_a$), 1.30 – 1.26 (m, $15H_{ab}$), 1.22 (d, *J* = 6.2 Hz, $3H_a$). **^{13}C NMR** (101 MHz, Chloroform-*d*) δ 100.19, 100.03, 99.79, 94.40, 91.30, 71.74, 71.07, 68.85, 67.93, 67.20, 64.51, 63.93, 48.10, 18.26, 17.75, 17.53. **HRMS (ESI)**: 326.1322 $[M+Na]^+$; calculated for $[C_{12}H_{21}N_3NaO_6]$: 326.1323. **IR** [ATR, neat]: ν = 3443.28 w, 2944.77 w, 1375.96 w, 1265.07 w, 1132.97 s, 1035.59 s, 885.17 s cm^{-1}.

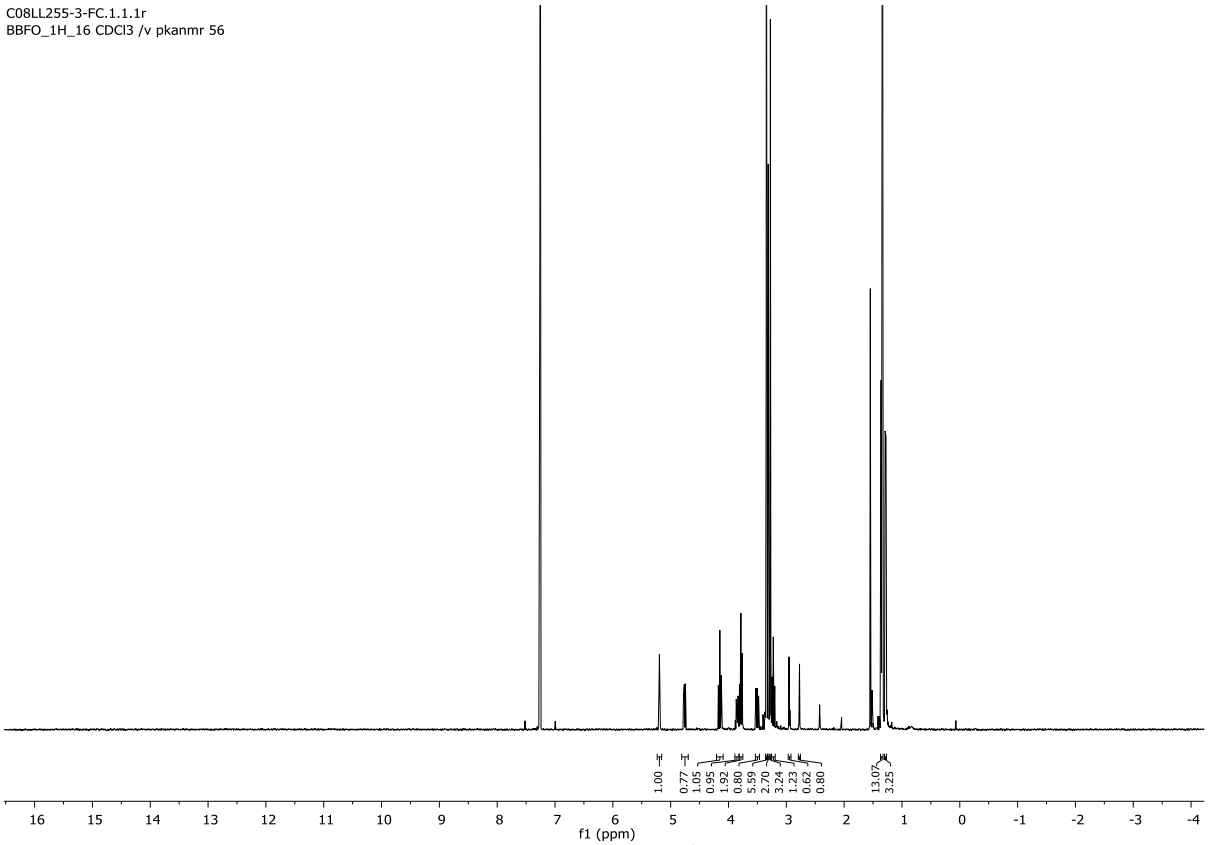
C08LL255-3-FC.1.1.1r
BBFO_1H_16 CDCl3 /v pkanmr 56
1.00
0.77
1.05
0.95
1.92
0.80
5.59
2.70
3.24
1.23
0.62
0.80
13.07
3.25
f1 (ppm)

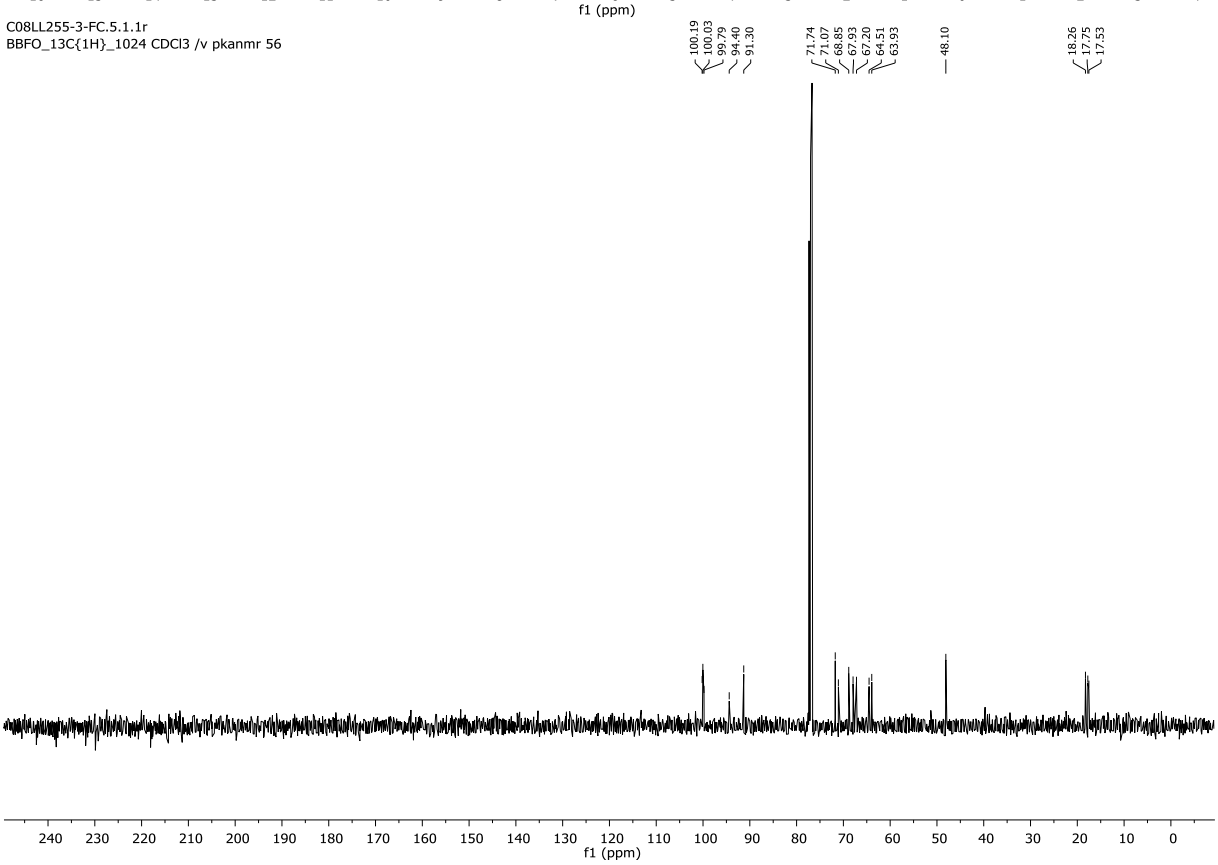
C08LL255-3-FC.5.1.1r
BBFO_13C{1H}_1024 CDCl3 /v pkanmr 56
100.19
100.03
99.79
94.40
91.30
71.74
71.07
68.85
67.93
67.20
64.51
63.93
48.10
18.26
17.75
17.53
f1 (ppm)

A-186 (2S,3S,4aR,5R,7R,8R,8aS)-5-(allyloxy)-8-azido-2,3-dimethoxy-2,3,7-trimethylhexahydro-5H-pyrano[3,4-b][1,4]dioxine

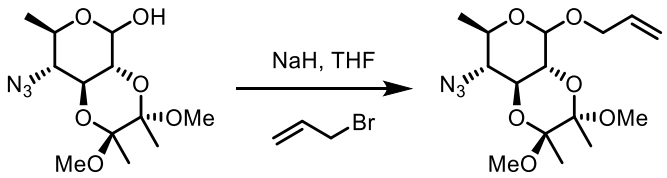

Assay: To an anomeric mixture of **A-185** (2.19 g, 7.22 mol, 1.0 equiv) dissolved in THF (120 mL) was added NaH (60% in mineral oil, 577.6 mg, 14.44 mmol, 2.0 equiv) and the greyish reaction mixture was stirred at ambient temperature for 30 min. Allyl bromide (2.08 mL, 14.44 mmol, 2.0 equiv) was then added and the reaction mixture was heated to 50 °C. After stirring for 13 h at elevated temperature, the reaction was carefully quenched by the addition of H_2O (100 mL) and diluted with EtOAc (100 mL). The two phases were separated and the aqueous phase was extracted with EtOAc (3 x 60 mL). The combined organic phases were dried over $MgSO_4$ and the crude was purified by FC (EtOAc:hexane, 1:5) to give the target compound as an anomeric mixture (1.57 g, 4.57 mmol, 70%).

Analytics: $\mathbf{R_f}$ = 0.45, resp. 0.53 (EtOAc:hexane 1:5). **^{1}H NMR** (400 MHz, Chloroform-*d*) δ 6.00 – 5.79 (m, $2H_{ab}$), 5.37 – 5.26 (m, $2H_a$), 5.25 – 5.12 (m, $2H_b$), 4.83 (d, *J* = 3.6 Hz, $1H_a$), 4.47 (d, *J* = 7.9 Hz, $1H_b$), 4.33 (ddt, *J* = 13.1, 5.1, 1.6 Hz, $1H_b$), 4.23 – 4.06 (m, $4H_{ab}$), 3.83 – 3.74 (m, $2H_{ab}$), 3.68 – 3.53 (m, $2H_{ab}$), 3.34 (s, $3H_a$), 3.34 (s, $3H_a$), 3.29 (s, $3H_b$), 3.26 (s, $3H_b$), 3.27 – 3.17 (m, $2H_{ab}$), 1.37 – 1.29 (m, $15H_{ab}$), 1.26 (d, *J* = 6.2 Hz, $3H_a$). **^{13}C NMR** (101 MHz, Chloroform-*d*) δ 133.96, 117.95, 117.04, 100.07, 99.86, 99.65, 99.44, 95.59, 72.09, 71.33, 69.98, 69.77, 68.61, 68.46, 68.36, 66.75, 64.82, 64.03, 48.08, 48.00, 18.28, 18.14, 17.78, 17.61, 17.55.

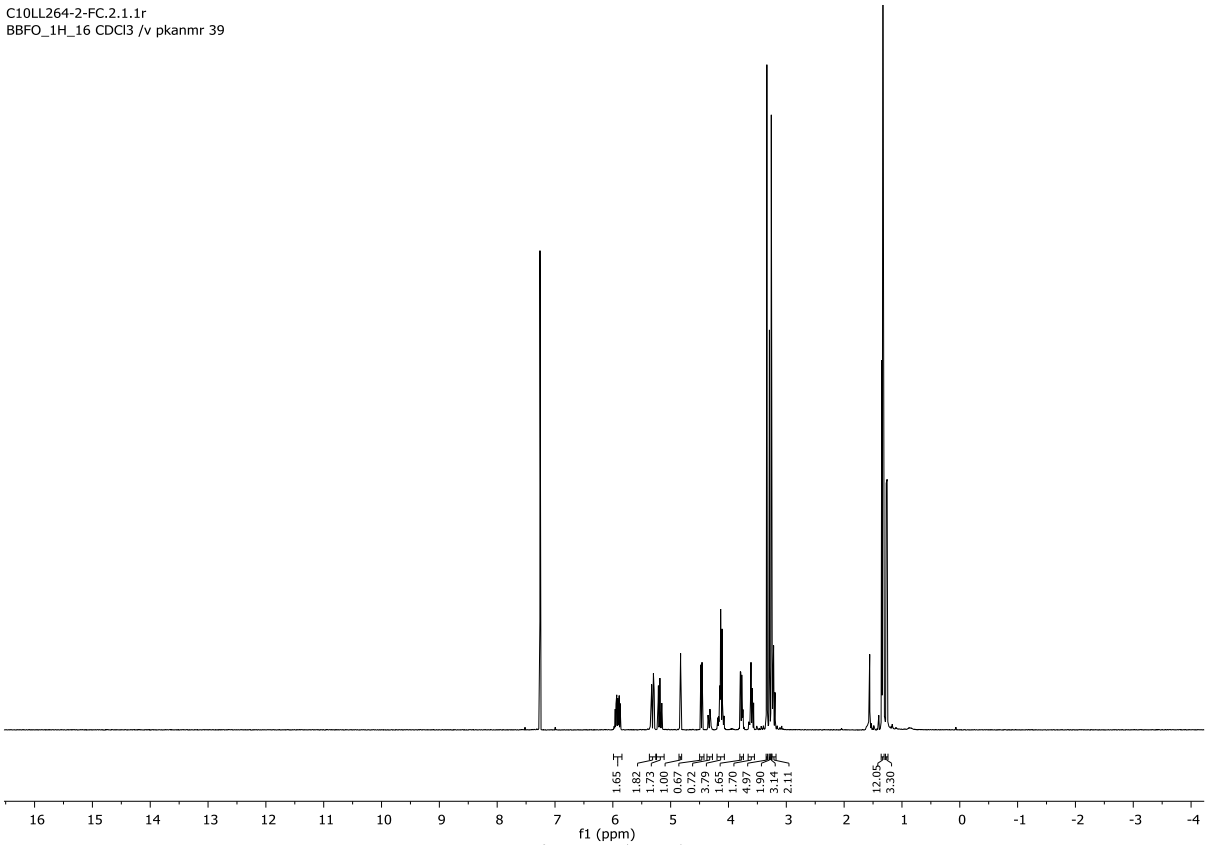
C10LL264-2-FC.2.1.1r
BBFO_1H_16 CDCl3 /v pkanmr 39
1.65
1.82
1.73
1.00
0.67
0.72
3.79
1.65
1.70
4.97
1.90
3.14
2.11
12.05
3.30
f1 (ppm)

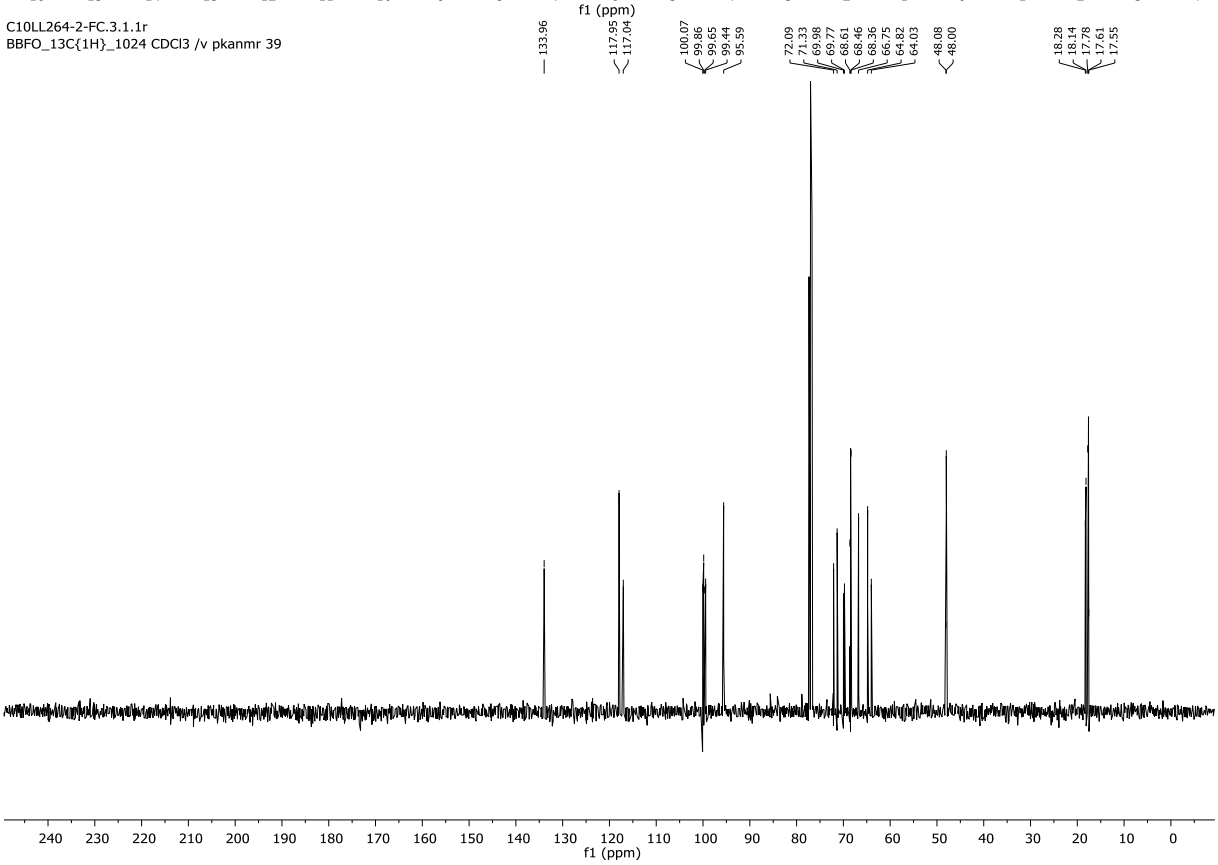
C10LL264-2-FC.3.1.1r
BBFO_13C{1H}_1024 CDCl3 /v pkanmr 39
133.96
117.95
117.04
100.07
99.86
99.65
99.44
95.59
72.09
71.33
69.98
69.77
68.61
68.46
68.36
66.75
64.82
64.03
48.08
48.00
18.28
18.14
17.78
17.61
17.55
f1 (ppm)

A-187 (2R,3R,4S,5S,6R)-2-(allyloxy)-5-azido-6-methyltetrahydro-2H-pyran-3,4-diol

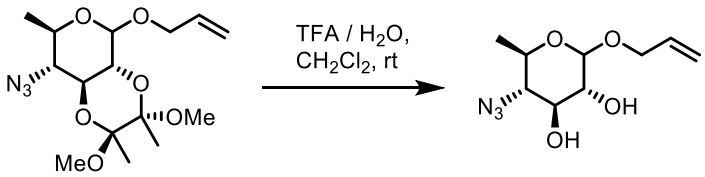

Assay: To **A-186** (93.0 mg, 0.27 mmol, 1.0 equiv) in CH_2Cl_2 (10.0 mL) was added dropwise a mixture of TFA:H_2O (10:1, 0.8 mL, 35.0 equiv of TFA) and the mixture was stirred at ambient temperature for 18 h. The reaction was then carefully quenched by the addition of saturated aqueous $NaHCO_3$ (3 mL) and diluted with CH_2Cl_2 (2 mL). The phases were separated and the aqueous phase was then extracted with CH_2Cl_2 (6 x 8 mL). The combined organic phases were then dried over $MgSO_4$ and concentrated under reduced pressure. Purification by FC (EtOAc:hexane, 1:1) gave the target compound as a slightly yellowish syrup (47.3 mg, 0.21 mmol, 76%).

Analytics: $\mathbf{R_f}$ = 0.32 resp. 0.41 (EtOAc:hexane, 1:5). **^{1}H NMR** (400 MHz, Chloroform-*d*) δ 6.01 – 5.81 (m, $2H_{ab}$), 5.32 (dq, *J* = 17.2, 1.5 Hz, $1H_b$), 5.30 (dq, *J* = 17.2, 1.6 Hz, $1H_a$), 5.23 (dq, *J* = 10.4, 1.2 Hz, $2H_{ab}$), 4.88 (d, *J* = 4.0 Hz, $1H_a$), 4.37 (ddt, *J* = 12.5, 5.3, 1.4 Hz, $1H_b$), 4.26 (d, *J* = 7.7 Hz, $1H_b$), 4.20 (ddt, *J* = 12.8, 5.3, 1.5 Hz, $1H_a$), 4.10 (ddt, *J* = 12.6, 6.6, 1.3 Hz, $1H_b$), 4.02 (ddt, *J* = 12.9, 6.3, 1.3 Hz, $1H_a$), 3.77 (td, *J* = 9.4, 2.4 Hz, $1H_a$), 3.67 – 3.57 (m, $2H_{ab}$), 3.53 (ddd, *J* = 10.4, 9.4, 4.0 Hz, $1H_a$), 3.43 (ddd, *J* = 9.3, 7.8, 2.4 Hz, $1H_b$), 3.30 (dq, *J* = 9.8, 6.1 Hz, $1H_b$), 3.11 (t, *J* = 9.6 Hz, $1H_b$), 3.05 (t, *J* = 9.8 Hz, $1H_a$), 2.69 (s, $1H_b$), 2.63 (s, $1H_a$), 2.47 (s, $1H_b$), 2.03 (dd, *J* = 10.4, 1.5 Hz, $1H_a$), 1.37 (d, *J* = 6.1 Hz, $3H_b$), 1.31 (d, *J* = 6.3 Hz, $3H_a$). **^{13}C NMR** (101 MHz, Chloroform-*d*) δ 133.52, 133.32, 118.29, 118.17, 101.10, 97.02, 75.33, 74.28, 73.77, 72.74, 70.94, 68.71, 67.53, 66.49, 18.33, 18.18. **HRMS (ESI)**: 252.0958 $[M+Na]^+$; calculated for $[C_9H_{15}N_3NaO_4]$: 252.0955.

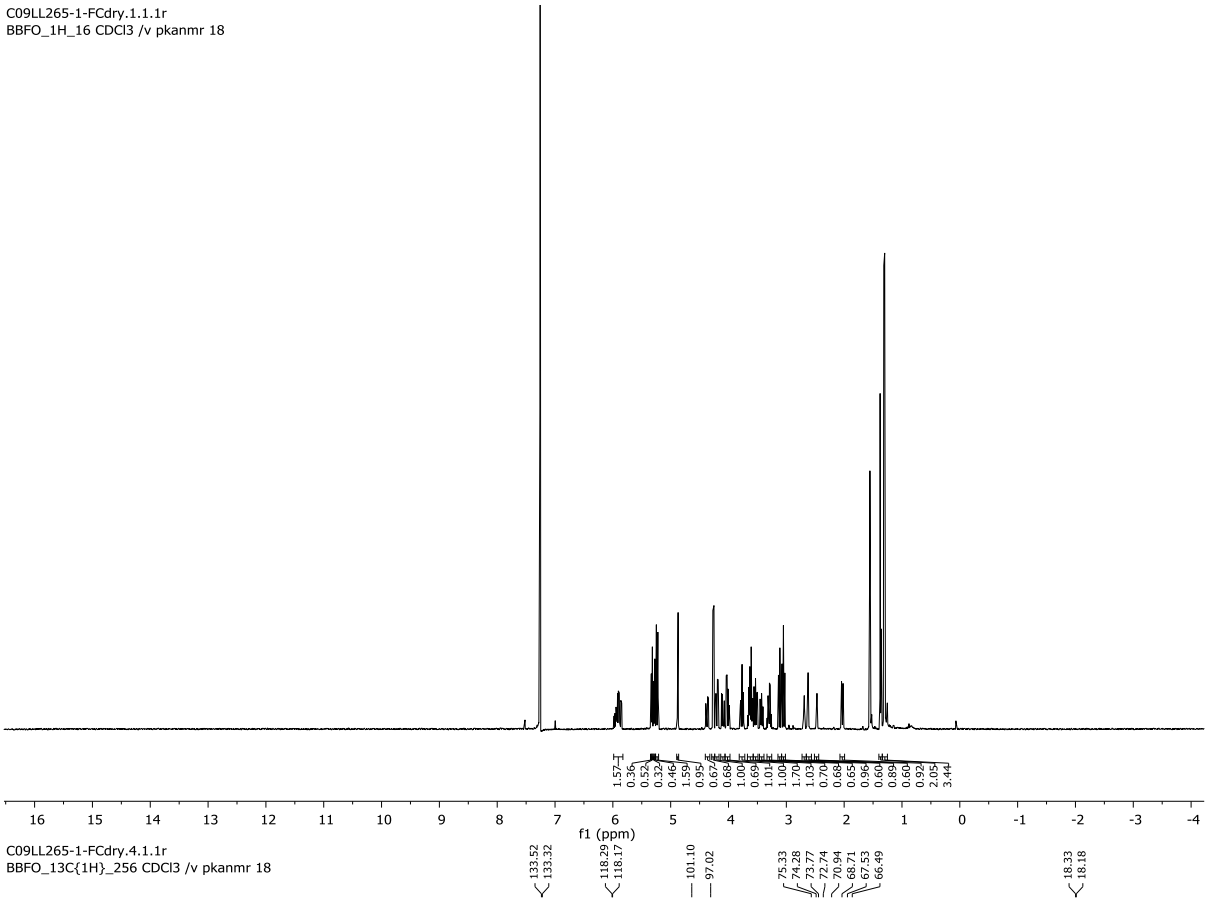
C09LL265-1-FCdry.1.1.1r
BBFO_1H_16 CDCl3 /v pkanmr 18
1.57
0.36
0.52
0.32
0.46
1.59
0.95
0.67
0.68
1.00
0.69
1.01
1.00
1.70
1.03
0.70
0.68
0.65
0.96
0.89
0.60
0.92
2.05
3.44
16 15 14 13 12 11 10 9 8 7 6 5 4 3 2 1 0 -1 -2 -3 -4
f1 (ppm)

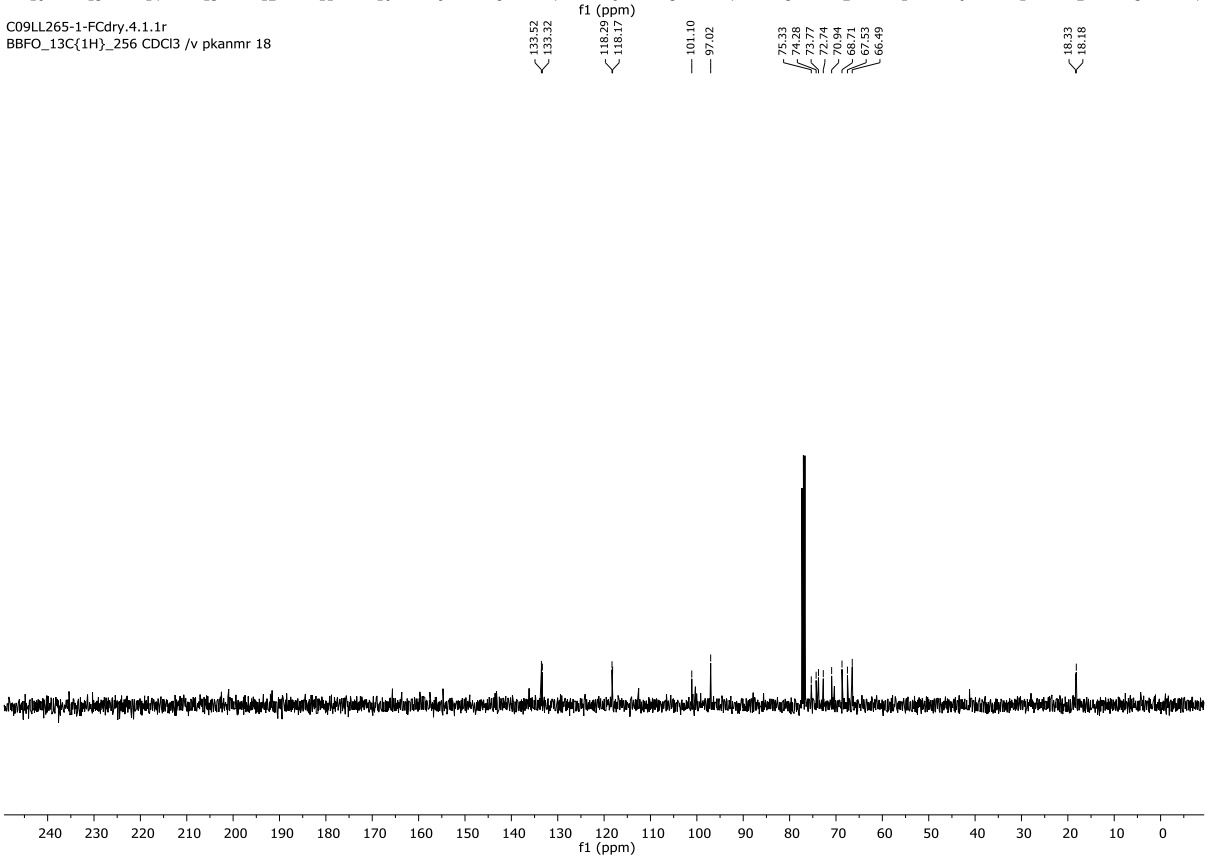
C09LL265-1-FCdry.4.1.1r
BBFO_13C{1H}_256 CDCl3 /v pkanmr 18
133.52
133.32
118.29
118.17
101.10
97.02
75.33
74.28
73.77
72.24
70.94
68.71
67.53
66.49
18.33
18.18
240 230 220 210 200 190 180 170 160 150 140 130 120 110 100 90 80 70 60 50 40 30 20 10 0
f1 (ppm)

A-188 (3R,4S,5R,6R)-2-(allyloxy)-5-azido-3,4-bis((4-methoxybenzyl)oxy)-6-methyltetrahydro-2H-pyran

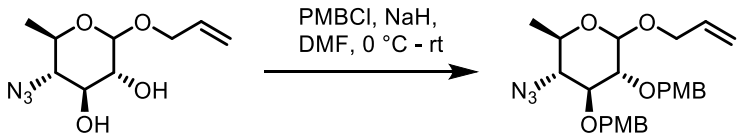

Assay: To **A-187** (26 mg, 0.11 mmol, 1.0 equiv) dissolved in DMF (1.0 mL) was added NaH (60% in mineral oil, 18.6 mg, 0.47 mmol, 4.1 equiv) and PMBCl (34.0 µl, 0.25 mmol, 2.2 equiv) at ambient temperature. The brown solution was stirred as such over night. The reaction was then cooled to 0 °C and carefully quenched with MeOH until the effervescent had ceased. Saturated aqueous NH_4Cl solution (4 mL) was added and the reaction mixture was stirred as such for 10 min. The biphasic mixture was separated and the aqueous layer was extracted with CH_2Cl_2 (3 x 4 mL). Combined organic phases were dried over $MgSO_4$ and concentrated under reduced pressure. The crude was purified by FC (EtOAc:hexane, 1:5) to give the title compound as an anomeric mixture (51 mg, 0.108 mmol, 96%).

Analytics: $\mathbf{R_f}$ = 0.38 (EtOAc:hexane 1:5). **^{1}H NMR** (400 MHz, Chloroform-*d*) δ 7.40 – 7.19 (m), 6.94 – 6.79 (m), 6.02 – 5.84 (m), 5.34 (dq, *J* = 17.2, 1.7 Hz), 5.31 (dq, *J* = 17.2, 1.6 Hz), 4.89 (d, *J* = 10.6 Hz), 5.22 (ddq, *J* = 10.5, 2.9, 1.3 Hz), 4.88 (d, *J* = 10.1 Hz), 4.84 (d, *J* = 10.2 Hz), 4.73 (d, *J* = 10.5 Hz), 4.70 – 4.67 (m), 4.65 (d, *J* = 10.8 Hz), 4.57 (d, *J* = 11.7 Hz), 4.46 (s), 4.38 (ddd, *J* = 6.4, 3.6, 1.6 Hz), 4.21 – 4.08 (m), 4.00 – 3.93 (m), 3.87 – 3.76 (m), 3.58 (dq, *J* = 10.0, 6.2 Hz), 3.49 (dd, *J* = 9.6, 3.6 Hz), 3.46 – 3.41 (m), 3.23 – 3.15 (m), 3.15 – 3.09 (m), 3.09 – 3.00 (m), 1.33 (d, *J* = 5.9 Hz), 1.24 (d, *J* = 6.3 Hz). **^{13}C NMR** (101 MHz, Chloroform-*d*) δ 159.59, 159.49, 134.01, 133.84, 130.63, 130.50, 130.23, 130.16, 130.09, 130.01, 129.83, 129.56, 118.40, 117.64, 114.01, 113.97, 102.61, 95.69, 82.49, 82.14, 79.78, 79.67, 75.49, 75.37, 74.71, 72.89, 71.61, 70.58, 70.50, 68.45, 68.20, 67.79, 66.17, 55.42, 18.61, 18.53. **HRMS (ESI)**: 492.2107 $[M+Na]^+$; calculated for $[C_{25}H_{31}N_3NaO_6]$: 492.2105. **IR** [ATR, neat]: ν = 2909.09 w, 1613.16 m, 1512.88 s, 1456.96 w, 1355.71 w, 1245.79 w, 1073.19 s, 1032.69 s, 927.59 w, 819.60 m cm^{-1}.

Remarks: proton integrals are not indicated due to complex anomeric mixture and overlapping of signals.

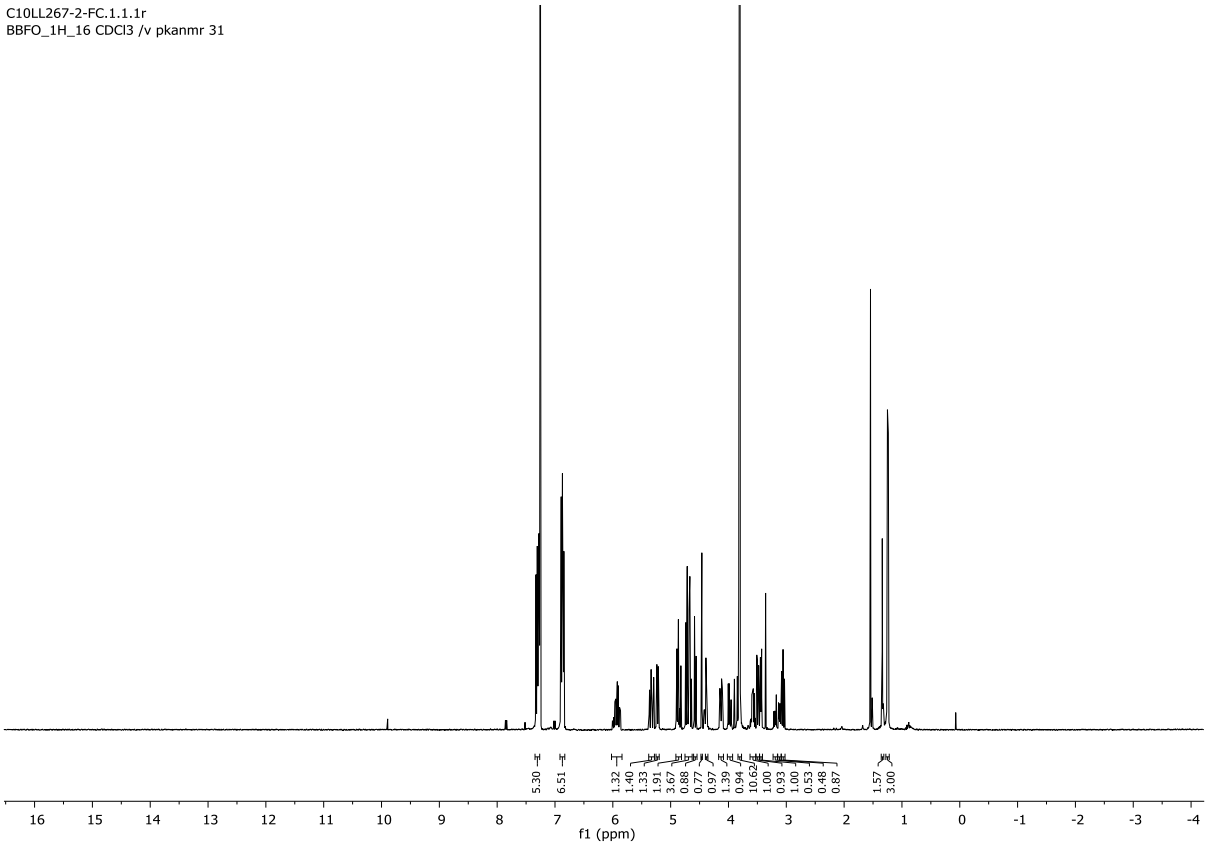
C10LL267-2-FC.1.1.1r
BBFO_1H_16 CDCl3 /v pkanmr 31
5.30
6.51
1.32
1.40
1.33
1.91
3.67
0.88
0.77
0.97
1.39
0.94
10.62
1.00
1.00
0.53
0.48
0.87
1.57
3.00
f1 (ppm)

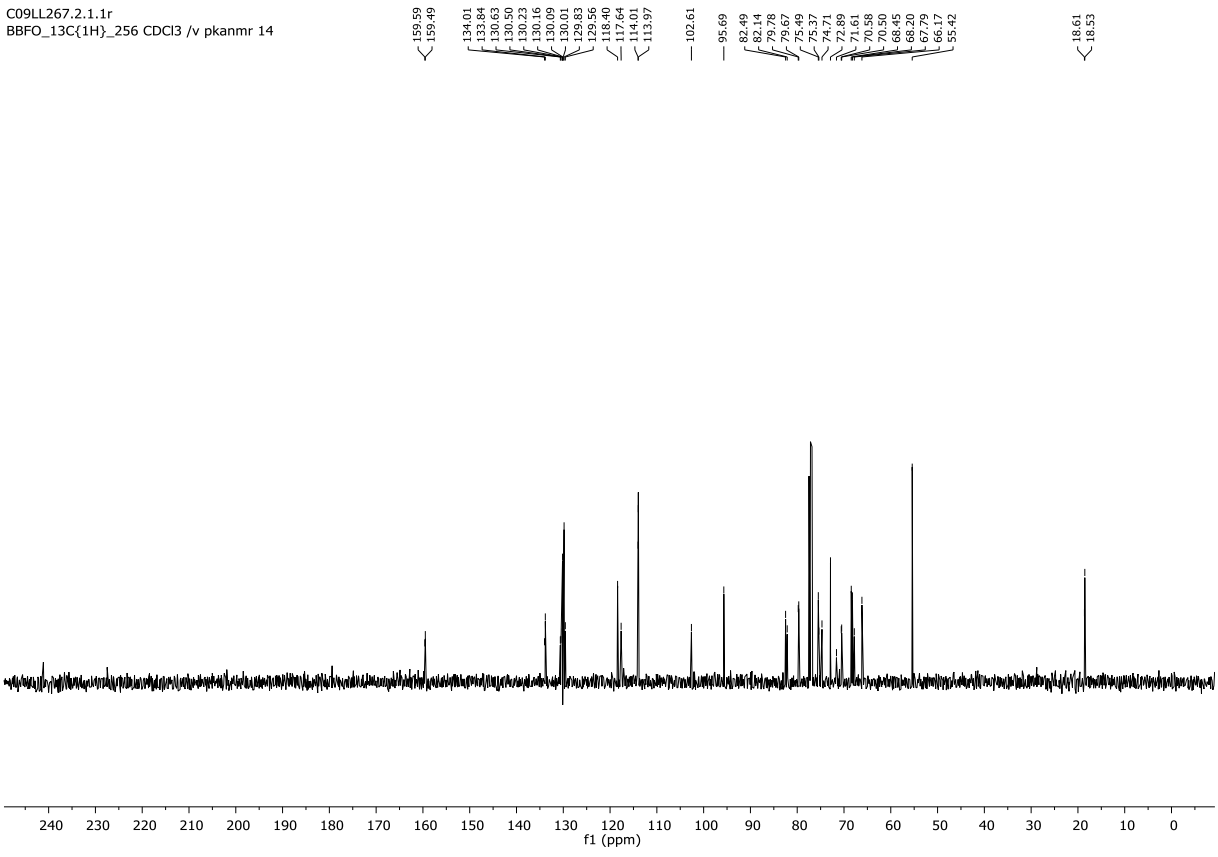
C09LL267.2.1.1r
BBFO_13C{1H}_256 CDCl3 /v pkanmr 14
159.59
159.49
134.01
133.84
130.63
130.50
130.23
130.16
130.09
130.01
129.83
129.56
118.40
117.64
114.01
113.97
102.61
95.69
82.49
82.14
79.78
79.67
75.49
75.37
74.71
72.89
71.61
70.58
70.50
68.45
68.20
67.79
66.17
55.42
18.61
18.53
f1 (ppm)

A-189 (3R,4S,5R,6R)-5-azido-3,4-bis((4-methoxybenzyl)oxy)-6-methyltetrahydro-2H-pyran-2-ol

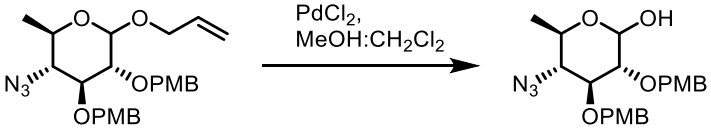

Assay: To a solution of **A-188** in MeOH:CH_2Cl_2 (1:1, 1.0 mL) was added $PdCl_2$ (10.0 mg, 21.3 µmol, 0.3 equiv) and the reaction was stirred at ambient temperature for 5 h. The colour changed from rusty red to black. Starting material was fully consumed, the mixture was filtered over a pad of Celite and concentrated under reduced pressure. Purification by FC (EtOAc:hexane, 1:3 -> 1:1) gave the target compound as an anomeric mixture. Product was not quantified.

Analytics: R_f = 0.18 (EtOAc:hexane 1:3). **^{1}H NMR** (400 MHz, Chloroform-*d*) δ 7.36 – 7.22 (m), 6.93 – 6.84 (m), 4.90 – 4.81 (m), 4.79 – 4.68 (m), 4.66 – 4.57 (m), 3.81 (d, *J* = 2.2 Hz), 3.56 – 3.40 (m), 3.38 – 3.29 (m), 3.28 – 3.02 (m), 2.94 – 2.87 (m), 1.33 (d, *J* = 6.1 Hz), 1.26 (d, *J* = 6.2 Hz). **^{13}C NMR** (101 MHz, Chloroform-*d*) δ 159.70, 159.53, 130.43, 130.28, 130.16, 130.10, 129.95, 129.84, 114.13, 114.06, 113.98, 97.36, 91.34, 83.07, 82.48, 79.92, 79.33, 75.47, 75.40, 74.63, 73.07, 70.81, 67.98, 67.78, 66.33, 55.41, 18.64, 18.56. **HRMS (ESI)**: 452.1798 $[M+Na]^+$; calculated for $[C_{22}H_{27}N_3NaO_6]$: 452.1792. **IR** [ATR, neat]: ν = 2911.98 w, 2104.92 s, 1612.2 m, 1512.88 w, 1245.79 s, 1173.47 w, 1031.73 s, 819.60 s cm^{-1}.

Remarks: proton integrals are not indicated due to complex anomeric mixture and overlapping of signals.

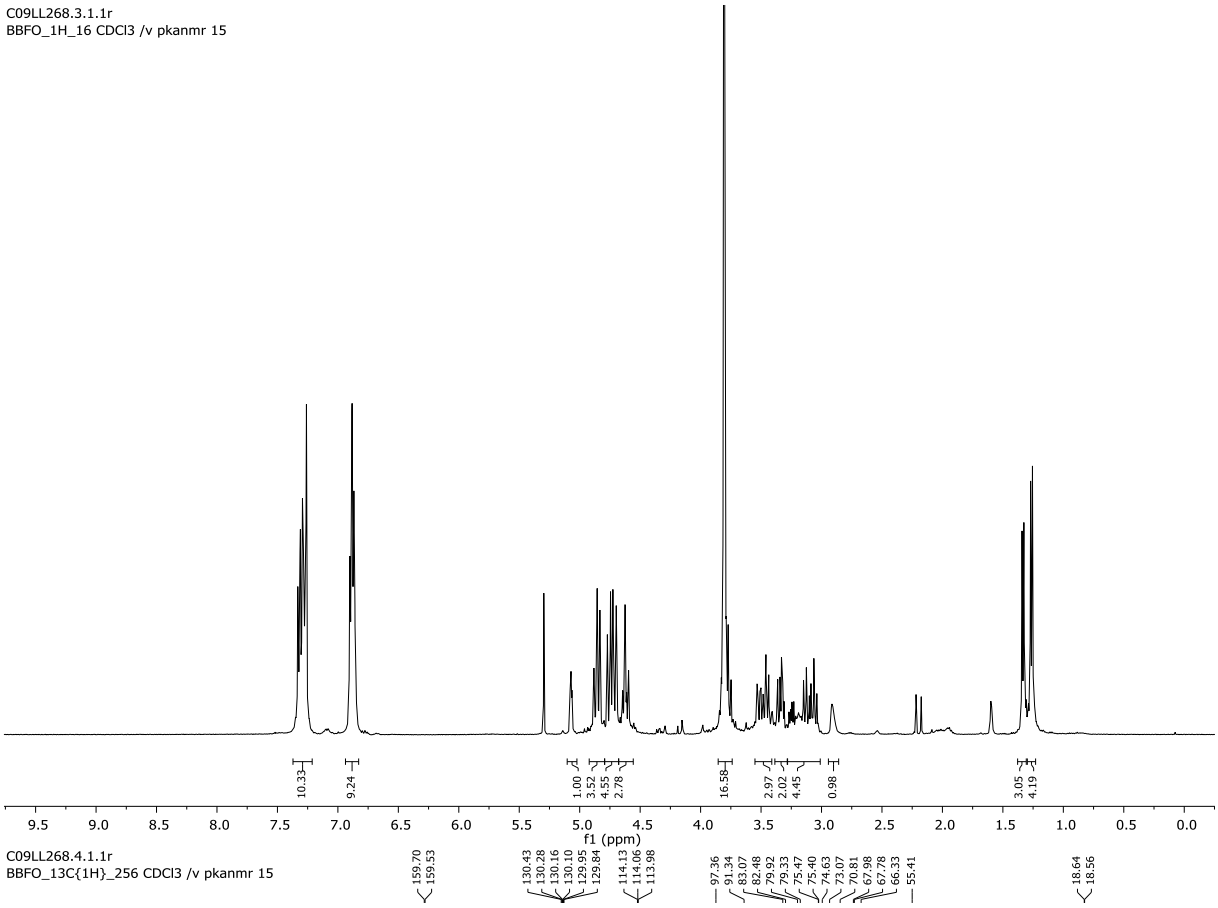
C09LL268.3.1.1r
BBFO_1H_16 CDCl3 /v pkanmr 15
10.33
9.24
1.00
3.52
4.55
2.78
16.58
2.97
2.02
4.45
0.98
3.05
4.19
f1 (ppm)
C09LL268.4.1.1r
BBFO_13C{1H}_256 CDCl3 /v pkanmr 15
159.70
159.53
130.43
130.28
130.16
130.10
129.95
129.84
114.13
114.06
113.98
97.36
91.34
83.07
82.48
79.92
79.33
75.47
75.40
74.63
73.07
70.81
67.98
67.78
66.33
55.41
18.64
18.56
f1 (ppm)

A-38 (2S,3R,4S,5R,6R)-5-azido-3,4-bis((4-methoxybenzyl)oxy)-6-methyltetrahydro-2H-pyran-2-yl 2,2,2-trichloroacetimidate

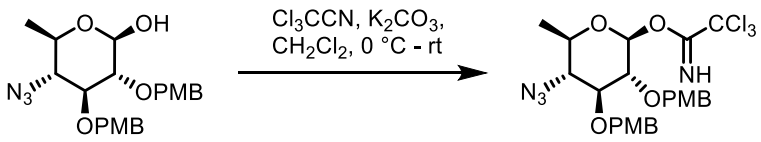

Assay: A-189 (53.0 mg, 0.12 mmol, 1.0 equiv), was dissolved in CH_2Cl_2 (1.2 mL), cooled to 0 °C and trichloroacetonitrile (0.12 mL, 1.23 mmol, 10.0 equiv) was added followed by anhydrous K_2CO_3 (85.3 mg, 0.62 mmol, 5.0 equiv). The reaction mixture was allowed to slowly warm to ambient temperature and was stirred for 23 h. The reaction mixture was then filtered over a pad of Celite and the filtrate was concentrated. The brown oil was then directly filtrated over a short pad of Alox (EtOAc:hexane, 1:3) to give the title compound as a clear sticky syrup and an anomeric mixture of 1:1 (35 mg, 0.078 mmol, 35%). The compound was directly used as such in the following reaction.

Analytics:

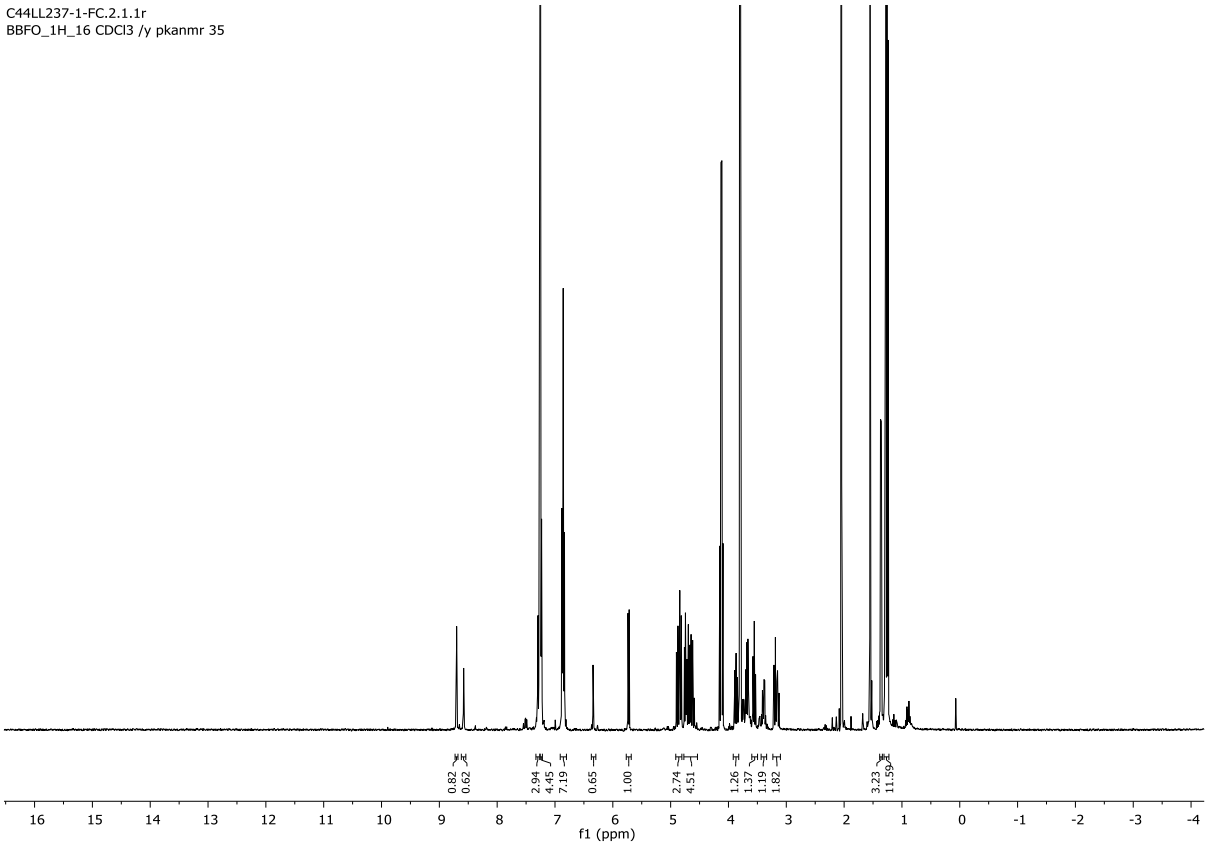
C44LL237-1-FC.2.1.1r
BBFO_1H_16 CDCl3 /y pkanmr 35
0.82
0.62
2.94
4.45
7.19
0.65
1.00
2.74
4.51
1.26
1.37
1.19
1.82
3.23
11.59
16 15 14 13 12 11 10 9 8 7 6 5 4 3 2 1 0 -1 -2 -3 -4
f1 (ppm)

A-172 (2R,3R,4S,5R)-3-azido-4,5-bis(benzyloxy)-6-(((2R,3S)-6-methoxy-2-methyltetrahydro-2H-pyran-3-yl)oxy)-2-methyltetrahydro-2H-pyran

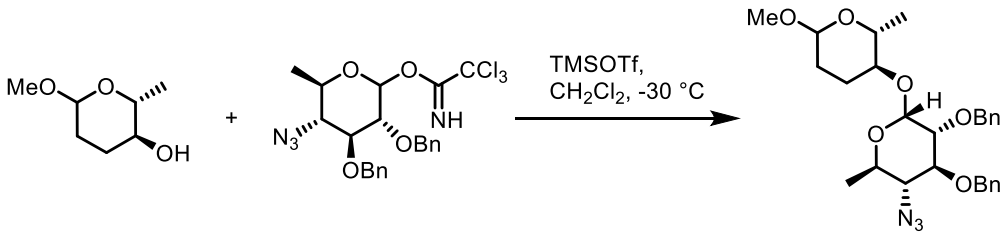

Assay: In a flame dried 5 mL pear shaped flask, **A-79** (18.7 mg, 128.2 µmol, 1.08 equiv) was azeotropically dried with benzene (3 x 2 mL) over 6 h. **A-148** (61 mg, 118.7 µmol, 1.0 equiv) was dried under high vacuum over night. Molecular sieves were dried under high vacuum ($3*10^{-3}$ mbar) at 250 °C over 20 min. **A-148** was then dissolved in dry CH_2Cl_2 (2.1 mL) and given to the acceptor. The activated molecular sieves (32 mg) was added as quickly as possible. The mixture was then stirred for an additional hour to thoroughly desiccate the two carbohydrates. Meanwhile, a stock solution of TMSOTf (0.1 M in CH_2Cl_2) was prepared. After the before mentioned 60 min, the suspension was cooled to -78 °C and TMSOTf (356 µl, 0.1 M in CH_2Cl_2) was carefully added to the reaction mixture. The reaction was monitored via TLC analysis. Full consumption was observed after 50 min. The reaction was then quenched with dry NEt_3 (0.5 mL) and diluted with CH_2Cl_2 (2 mL) and saturated aqueous $NaHCO_3$ (2 mL). The two phases were separated and the aqueous phase was extracted with CH_2Cl_2 (3 x 3 mL). The combined organic phases were dried over $MgSO_4$ and the solvents were evaporated under reduced pressure. The yellowish crude was then purified by FC (EtOAc:hexane, 1:3) to give the target disaccharide (mainly α glycosidic bond, 4:1) (53.9 mg, 0.11 mmol, 91%).

Analytics: $\mathbf{R_f}$ = 0.44 resp. 0.52 (EtOAc:hexane, 1:3). **^{1}H NMR** (400 MHz, Chloroform-*d*) δ 7.43 – 7.28 (m, 10H), 4.95 (d, *J* = 10.5 Hz, 1H), 4.88 (d, *J* = 3.7 Hz, 1H), 4.81 (d, *J* = 10.5 Hz, 1H), 4.74 (d, *J* = 11.9 Hz, 1H), 4.66 – 4.60 (m, 2H), 3.86 (dd, *J* = 9.4, 6.2 Hz, 1H), 3.79 (t, *J* = 9.5 Hz, 1H), 3.60 (dt, *J* = 10.3, 6.2 Hz, 1H), 3.54 (dd, *J* = 9.6, 3.7 Hz, 1H), 3.35 (s, 3H), 3.32 – 3.22 (m, 1H), 3.08 (t, *J* = 9.8 Hz, 1H), 1.96 – 1.80 (m, 2H), 1.72 (ddd, *J* = 12.7, 9.1, 4.8 Hz, 2H), 1.26 (dd, *J* = 6.2, 4.4 Hz, 6H). **^{13}C NMR** (101 MHz, Chloroform-*d*) δ 138.19, 137.90, 128.69 (2C), 128.57 (2C), 128.46 (2C), 128.36 (2C), 128.22, 128.00, 97.34, 92.40, 79.89 (2C), 75.87, 74.87, 73.41, 68.13, 67.11, 66.54, 54.43, 29.26, 22.79, 18.86, 18.49. **$[\alpha]^{20}_D$** = + 145.2 (c = 0.5, $CHCl_3$). **HRMS (ESI)**: 515.2869 $[M+NH_4]^+$; calculated for $[C_{27}H_{39}N_4NaO_6]$: 515.2864. **IR** [ATR, neat]: ν = 2932.23 w, 2107.81 s, 1453.1 w, 1365.35 w, 1269.89 w, 1074.16 m, 1052.94 s, 740.53 w, 698.10 w cm^{-1}.

C51LL154-2-FC.1.1.1r
BBFO_1H_16 CDCl3 /v pkanmr 59

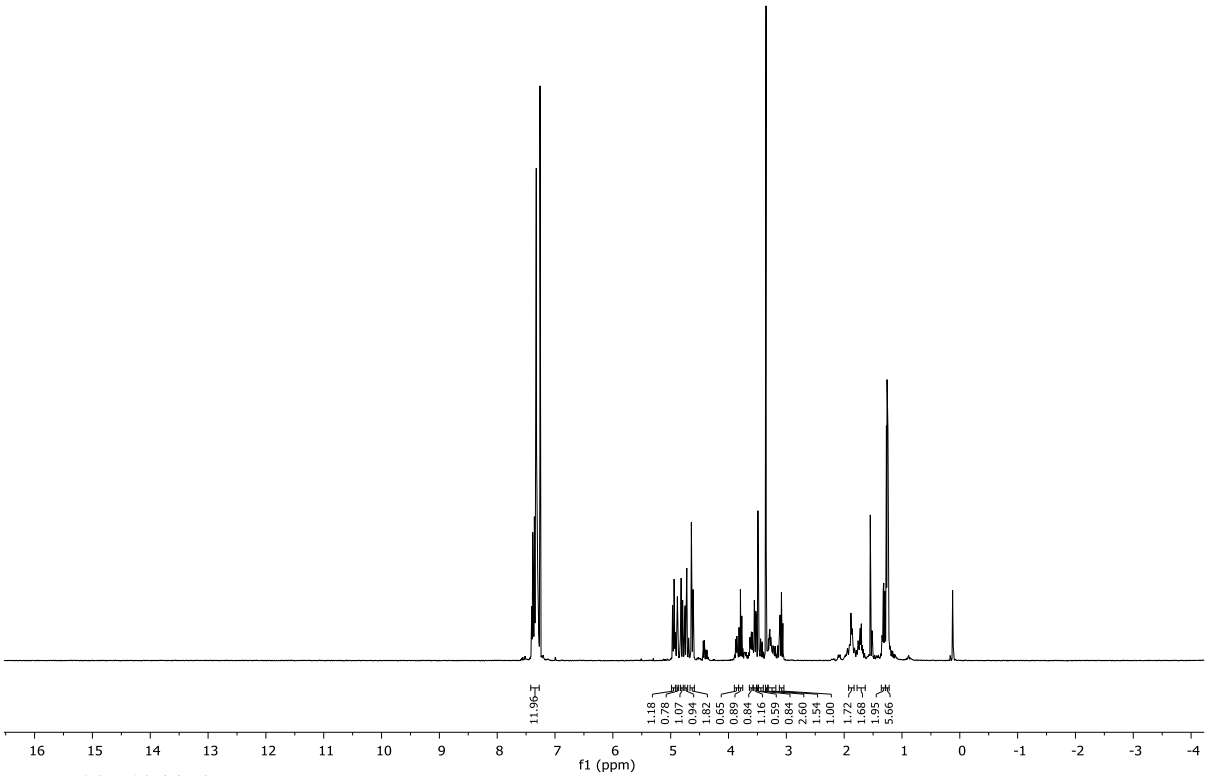

C51LL154-2-FC.2.13.1r
BBFO_13C{1H}_256 CDCl3 /v pkanmr 59

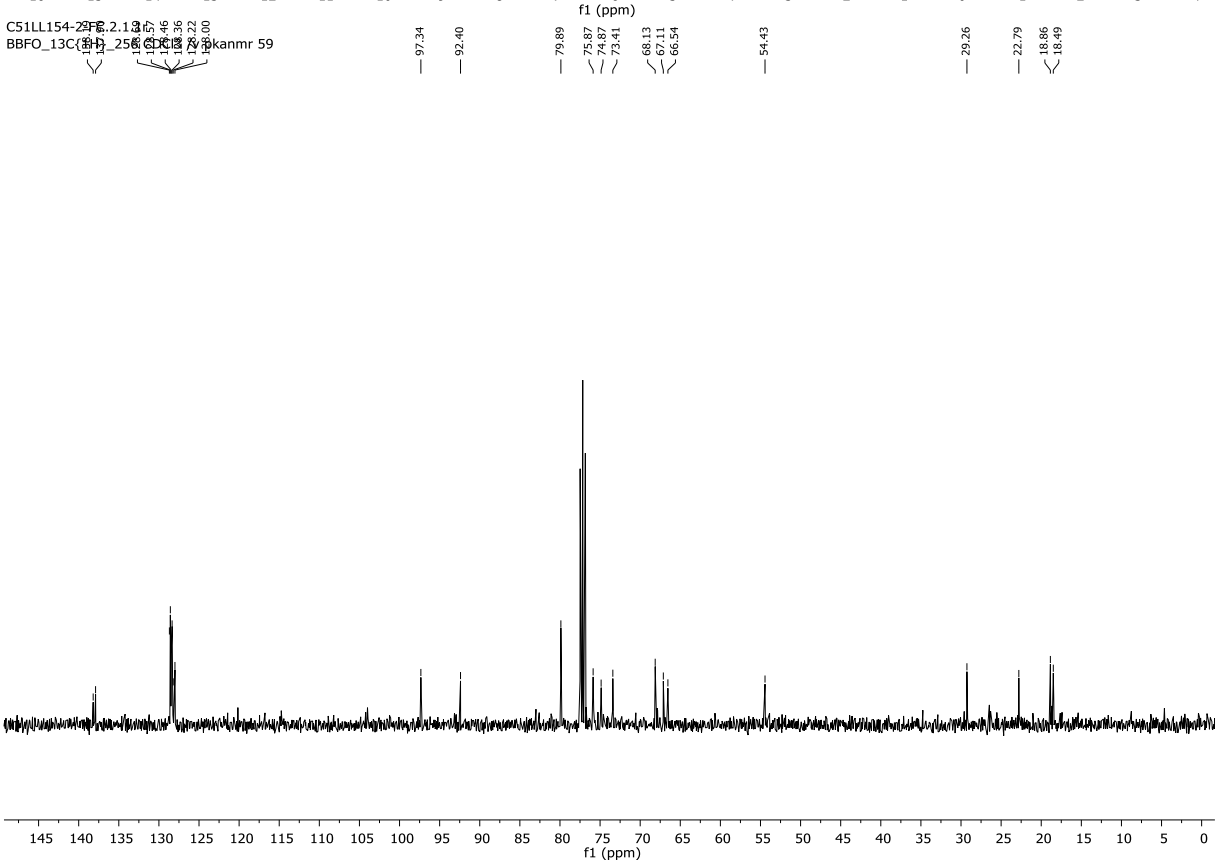

A-171 (2R,3R,4S,5R,6R)-4,5-bis(benzyloxy)-6-(((2R,3S)-6-methoxy-2-methyltetrahydro-2H-pyran-3-yl)oxy)-N,N,2-trimethyltetrahydro-2H-pyran-3-amine

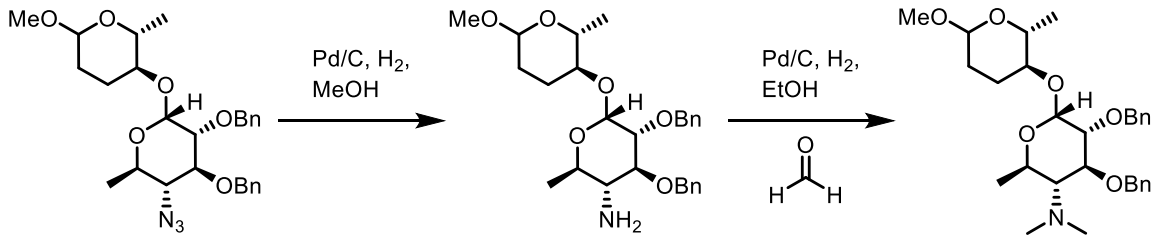

Assay: To **A-172** (53 mg, 106.5 µmol, 1.0 equiv) in dry MeOH (1.0 mL), was added Pd/C (10 wt %, 11.3 mg, 10 mol %) and the reaction mixture was set under H_2 atmosphere (balloon). The reaction was monitored via TLC, starting material was fully consumed after 4 h at ambient temperature. The crude was then filtrated over a pad of Celite which was washed with MeOH. Solvents were evaporated and the crude was taken up in dry EtOH (1.0 mL). To the stirring solution was then added Pd/C (10 wt %, 11.3 mg, 10 mol %) and the reaction mixture was set under H_2 atmosphere. Formaldehyde 37% in water (20 µl, 266.3 µmol, 2.5 equiv) was added and the reaction mixture was stirred at ambient temperature for 16 h. TLC analysis showed full consumption of starting material. The crude was then again filtrated over a pad of Celite which was washed with EtOAc. Solvents were evaporated and the crude was purified by FC (EtOAc:hexane, 1:3) to give disaccharide (39.1 mg, 7.8 µmol, 73%) in reasonable purity.

Analytics: $\mathbf{R_f}$ = 0.42 (EtOAc:hexane, 1:3). **^{1}H NMR** (400 MHz, Chloroform-*d*) δ 7.40 – 7.27 (m, 10H), 5.00 (d, *J* = 10.7 Hz, 1H), 4.87 (d, *J* = 3.7 Hz, 1H), 4.77 (d, *J* = 10.9 Hz, 1H), 4.70 (d, *J* = 11.7 Hz, 1H), 4.65 (s, 1H), 4.60 (d, *J* = 11.7 Hz, 1H), 4.03 (t, *J* = 9.6 Hz, 1H), 3.89 (dq, *J* = 9.2, 6.1 Hz, 1H), 3.80 – 3.70 (m, 1H), 3.56 (dd, *J* = 9.4, 3.5 Hz, 1H), 3.35 (s, 3H), 3.33 (t, *J* = 1.6 Hz, 1H), 2.46 (s, 6H), 2.31 (t, *J* = 10.1 Hz, 1H), 1.95 – 1.81 (m, 2H), 1.77 – 1.66 (m, 2H), 1.28 (d, *J* = 6.3 Hz, 3H), 1.22 (d, *J* = 6.3 Hz, 3H).**^{13}C NMR** (101 MHz, Chloroform-*d*) δ 139.23, 138.19, 128.63 (3C), 128.46 (3C), 128.05 (2C), 127.56 (2C), 97.41, 91.87, 81.93, 76.54, 74.21, 74.04, 73.30, 70.29, 67.24, 66.27, 54.38, 42.54 (2C), 29.30, 22.67, 19.24, 18.89. **$[\alpha]^{20}_D$** = + 127.4 (c = 0.5, $CHCl_3$). **HRMS (ESI)**: 500.3008 $[M+H]^+$; calculated for $[C_{29}H_{42}NO_6]$: 500.3007. **IR** [ATR, neat]: ν = 2929.34 w, 1452.13 w, 1367.28 w, 1128.15 m, 1047.16 s, 983.52 w, 736.67 w, 698.11 w cm^{-1}.

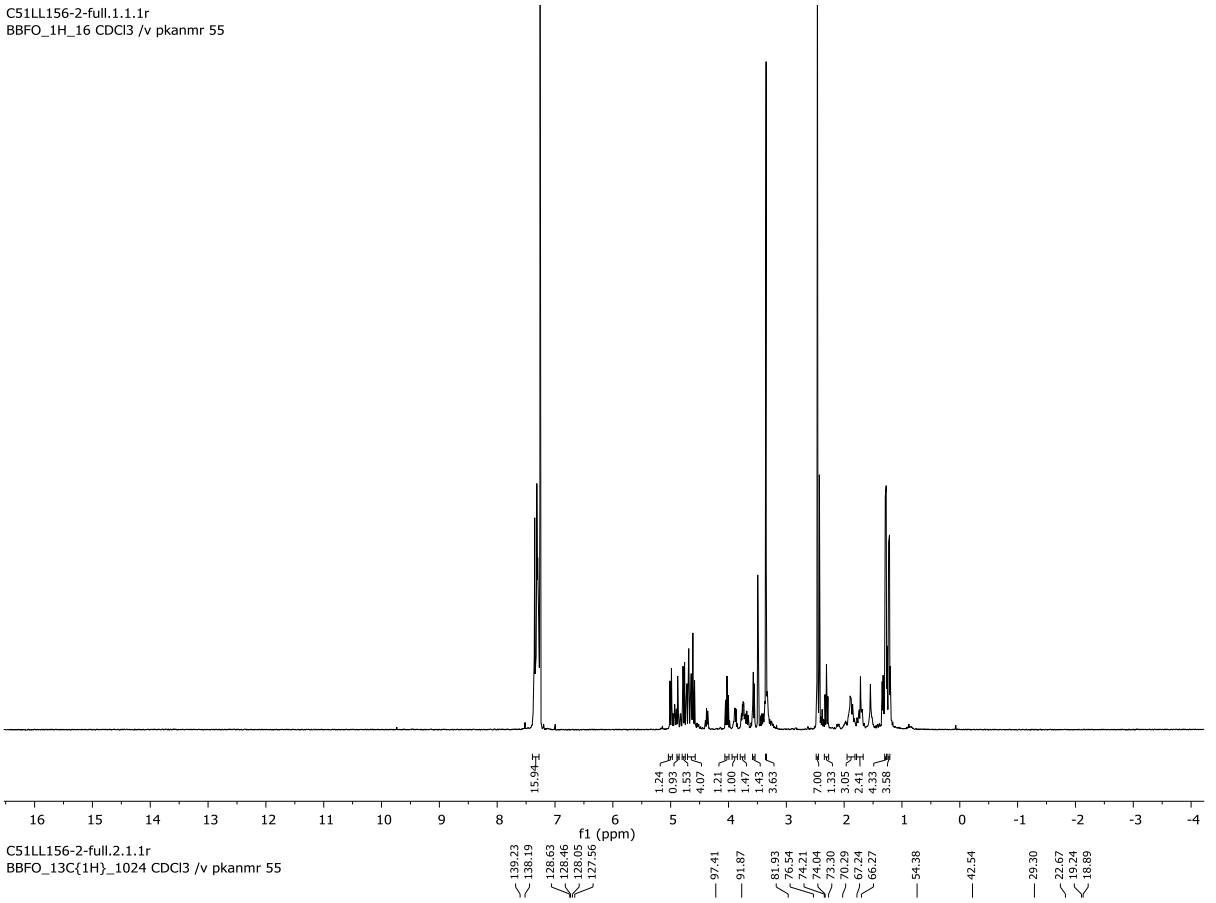
C51LL156-2-full.1.1.1r
BBFO_1H_16 CDCl3 /v pkanmr 55
15.94
1.24
0.93
1.53
4.07
1.21
1.00
1.47
1.43
3.63
7.00
1.33
3.05
2.41
4.33
3.58
f1 (ppm)
C51LL156-2-full.2.1.1r
BBFO_13C{1H}_1024 CDCl3 /v pkanmr 55
139.23
138.19
128.63
128.46
128.05
127.56
97.41
91.87
81.93
76.54
74.21
74.04
73.30
70.29
67.24
66.27
54.38
42.54
29.30
22.67
19.24
18.89
f1 (ppm)

A-190 (2R,3R,4S,5S,6R)-5-(dimethylamino)-2-(((2R,3S)-6-methoxy-2-methyltetrahydro-2H-pyran-3-yl)oxy)-6-methyltetrahydro-2H-pyran-3,4-diol

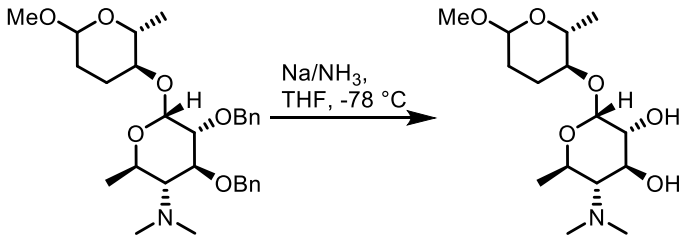

Assay: In a flame dried 10 mL Schlenk tube, gaseous ammonia was condensed at -78 °C (roughly 250 µL). **A-171** (3 mg, 6 µmol, 1.0 equiv) dissolved in THF (250 µl) was added to the ammonia followed by solid Na (3.0 µg, 12.0 µmol, 2.0 equiv). The sodium was quickly washed with hexane and roughly weighted. The reaction mixture turned deeply blue within 5 min. The deep blue reaction mixture was then quenched after 60 s with saturated aqueous NH_4Cl (2 mL). The aqueous phase was then separated and extracted with EtOAc (4 x 1.5 mL). Combined organic phases were dried over $MgSO_4$ and concentrated under reduced pressure. The title compound was obtained as a crude and not further purified (3 mg).

Analytics: $\mathbf{R_f}$ = 0.27 (EtOAc). **^{1}H NMR** (400 MHz, Chloroform-*d*) δ 4.96 (d, *J* = 4.0 Hz, 1H), 4.63 (d, *J* = 2.0 Hz, 1H), 3.86 (dq, *J* = 9.8, 6.2 Hz, 1H), 3.73 (dt, *J* = 9.4, 6.2 Hz, 1H), 3.69 – 3.62 (m, 1H), 3.59 – 3.51 (m, 1H), 3.34 (s, 3H), 3.36 – 3.28 (m, 1H), 2.45 (s, 6H), 2.14 (t, *J* = 10.0 Hz, 1H), 1.92 – 1.55 (m, 4H), 1.31 (s, 3H), 1.29 (s, 3H). **^{13}C NMR** (101 MHz, Chloroform-*d*) δ 96.31, 92.96, 73.73, 72.27, 69.27, 68.38, 66.06, 64.44, 53.43, 40.24 (2 C), 28.67, 27.95, 18.50, 17.51.

C49LL158-1-crude.1.fid
BBFO_1H_16 CDCl3 /v pkanmr 11

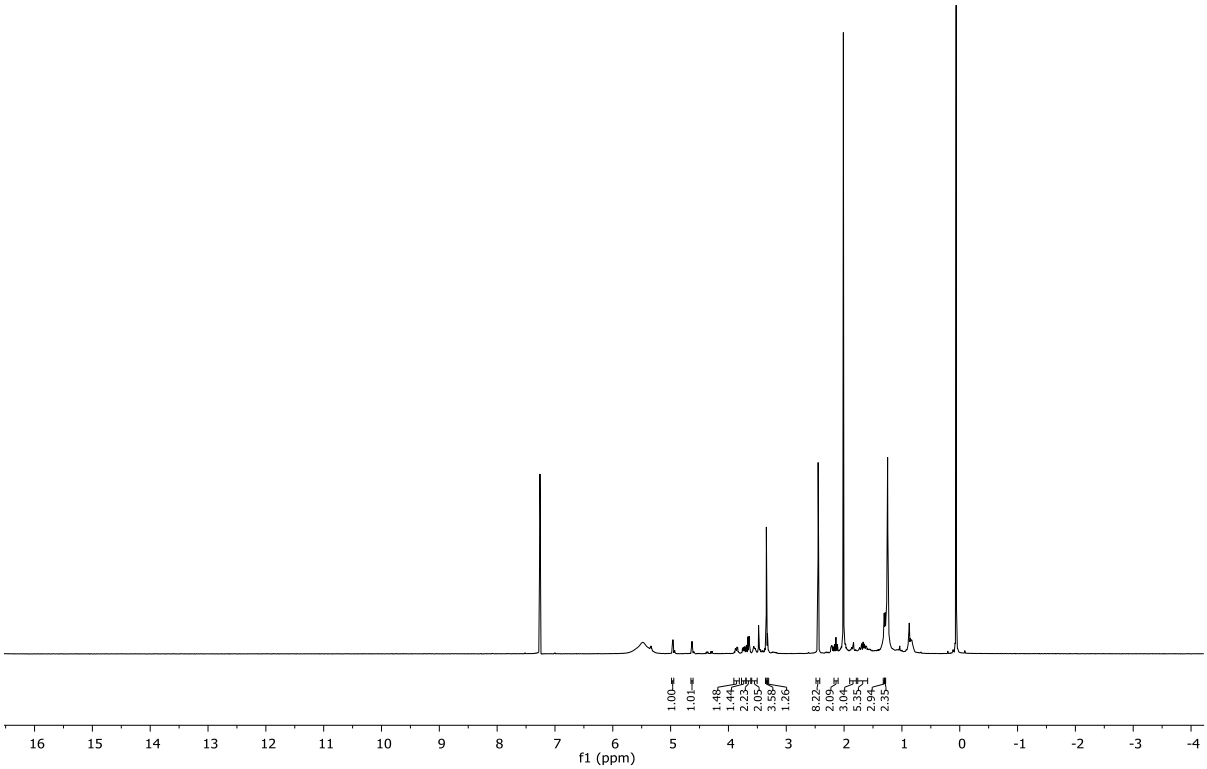

C49LL158-1-crude.4.fid
BBFO_13C{1H}_1024 CDCl3 /v pkanmr 11

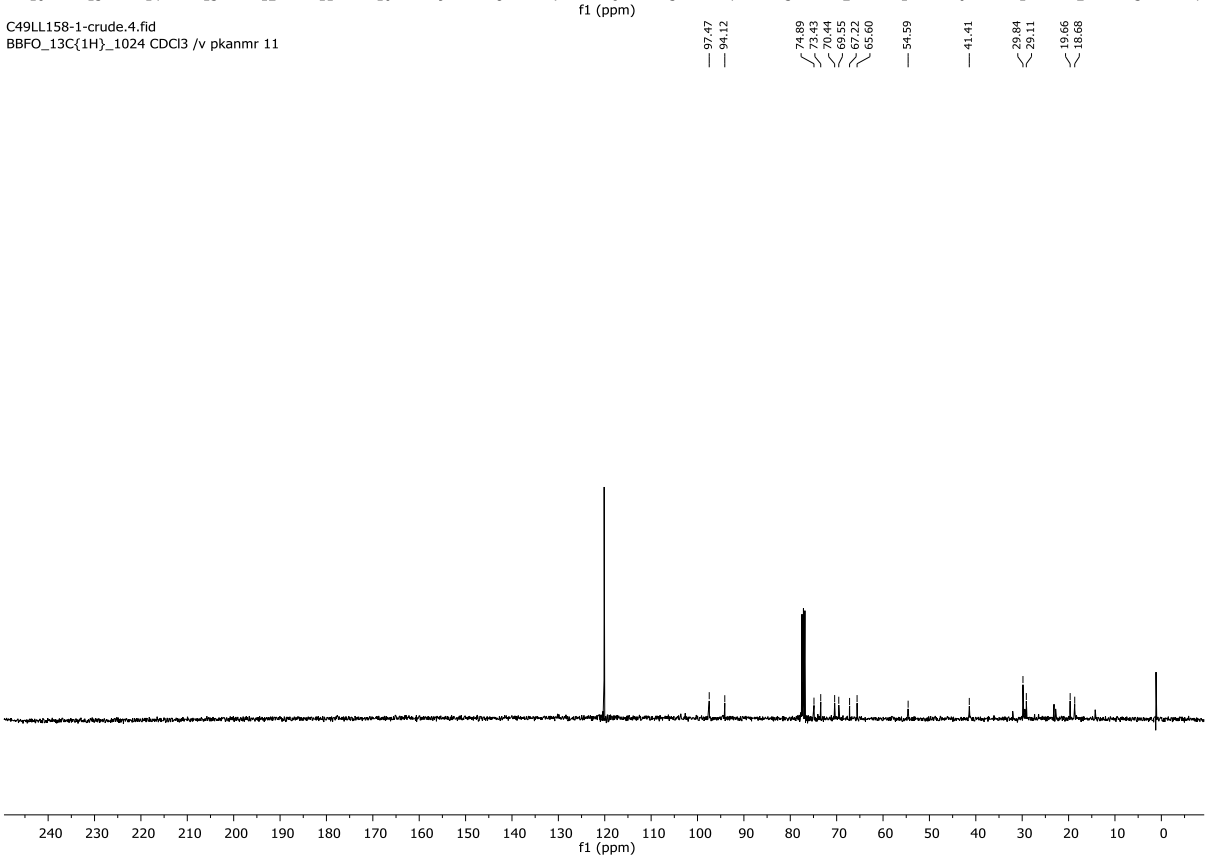

A-166 (2R,3R,4S,5R,6R)-6-fluoro-N,N,2-trimethyl-4,5-bis((triethylsilyl)oxy)tetrahydro-2H-pyran-3-amine

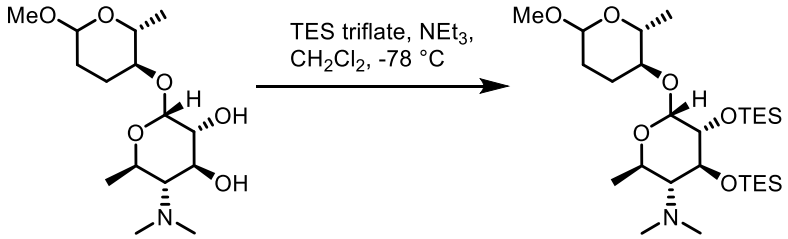

Assay: The crude **A-190** (9.5 mg, 30 µmol, 1.0 equiv) was dissolved in CH_2Cl_2 (1.25 mL) and cooled to -78 °C. NEt_3 (21 µl, 0.15 mmol, 5.0 equiv) was then added followed by dropwise addition of TES triflate (15 µl, 65.4 µmol, 2.2 equiv). The reaction was monitored via TLC whereas full consumption of starting material was confirmed after 15 min at -78 °C. The reaction was then quenched with saturated aqueous $NaHCO_3$ (3.0 mL) and the two layers were separated. The aqueous layer was extracted with CH_2Cl_2 (3 x 3 mL). The combined organic phases were dried over $MgSO_4$ and concentrated under reduced pressure to give a slight yellowish crude. MS analysis confirmed product formation. Purification by FC (EtOAc:hexane, 1:10) gave the target compound (10.0 mg, 18 µmmol, 61% calculated from crude of **A-190**).

Analytics: $\mathbf{R_f}$ = 0.32 (EtOAc:hexane 1:10). **^{1}H NMR** (400 MHz, Chloroform-*d*) δ 4.81 (d, *J* = 3.5 Hz, 1H), 4.63 (m, 1H), 3.86 (dq, *J* = 10.4, 6.2 Hz, 1H), 3.79 – 3.70 (m, 2H), 3.50 (dd, *J* = 8.7, 3.5 Hz, 1H), 3.35 (s, 3H), 3.31 – 3.20 (m, 1H), 2.38 (s, 6H), 2.09 (t, *J* = 10.0 Hz, 1H), 2.02 – 1.94 (m, 1H), 1.91 – 1.81 (m, 1H), 1.74 – 1.62 (m, 2H), 1.25 (d, *J* = 6.4 Hz, 3H), 1.19 (d, *J* = 6.2 Hz, 3H), 0.96 (td, *J* = 7.9, 3.8 Hz, 18H), 0.72 – 0.44 (m, 12H). **^{13}C NMR** (101 MHz, Chloroform-*d*) δ 97.42, 94.24, 74.99, 73.90, 72.09, 70.99, 67.54, 64.95, 54.41, 41.54 (2C), 29.18, 22.49, 20.35, 18.51, 7.12, 5.31. **HRMS (ESI)**: 548.3801 $[M+H]^+$; calculated for $[C_{27}H_{58}NO_6Si_2]$: 548.3797.

C01LL160-1-FC.1.1.1r
BBFO_1H_16 CDCl3 /v pkanmr 6

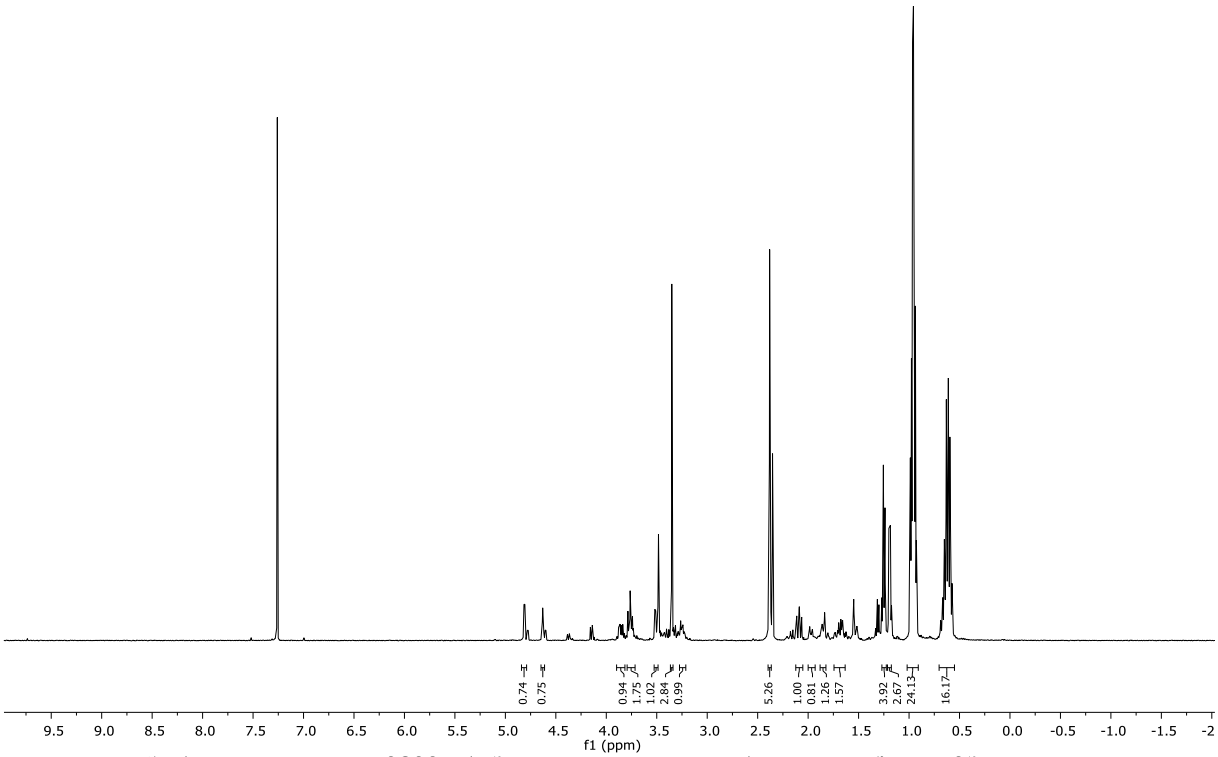

C01LL160-1-FC.4.1.1r
BBFO_13C{1H}_256 CDCl3 /v pkanmr 6

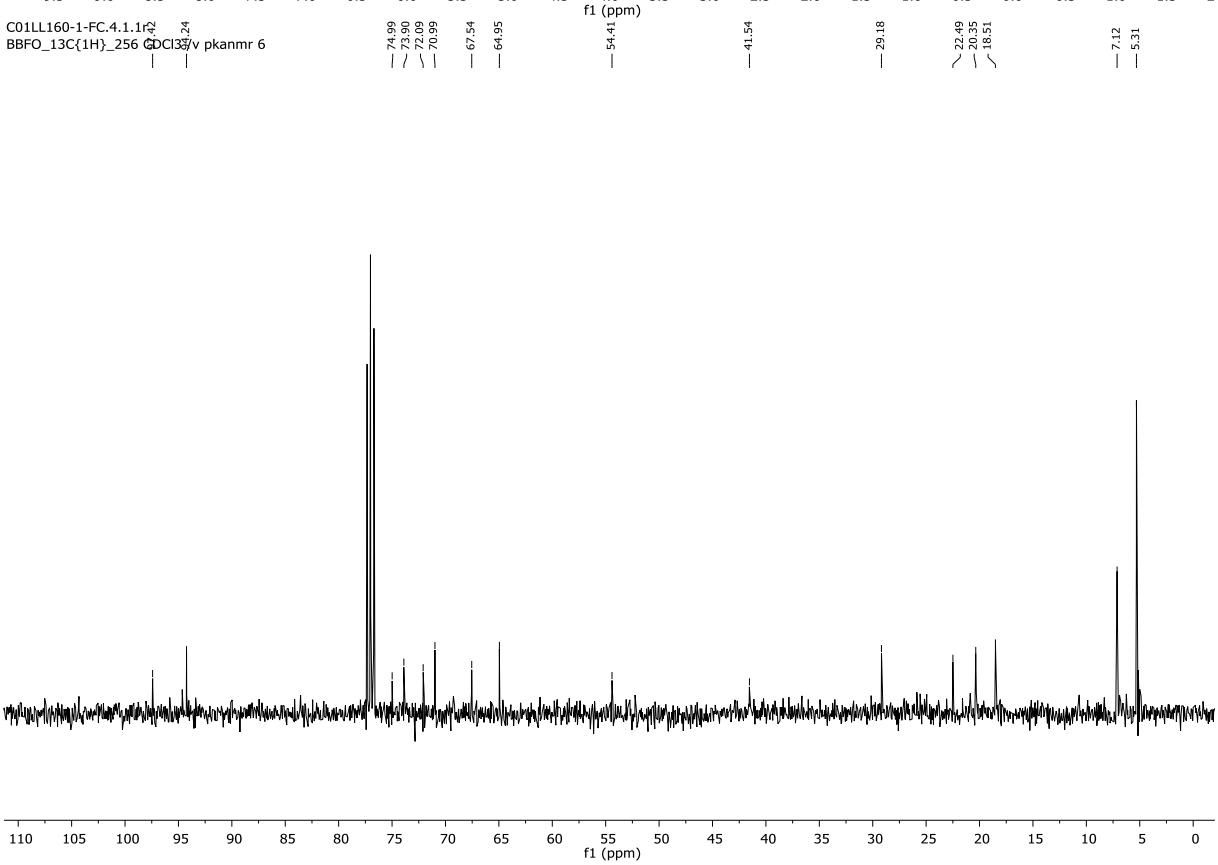

A-191 (2R,3S)-6-methoxy-2-methyltetrahydro-2H-pyran-3-yl acetate

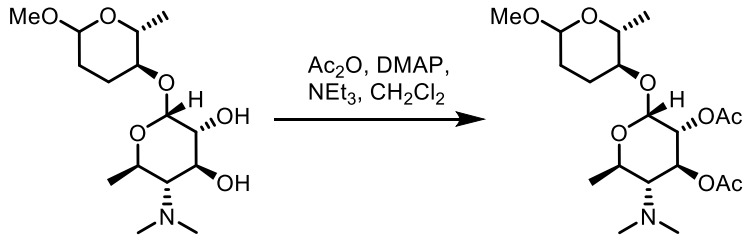

Assay: To a solution of crude **A-190** (18.3 mg, 57.3 µmol, 1.0 equiv) in CH_2Cl_2 (600 µL) was added NEt_3 (25 µL, 183.3 µmol, 3.2 equiv), Ac_2O (18.0 µL, 189.1 µmol, 3.3 equiv) and a catalytic amount of DMAP. The reaction was monitored via TLC and was found to be completed after 2 h 45 min. The reaction was then quenched with saturated aqueous NH_4Cl solution (2 mL). The phases were separated and the aqueous phase was extracted with EtOAc (3 x 2 mL). Combined organic phases were dried over $MgSO_4$ and concentrated under reduced pressure. The crude oil was purified by FC (EtOAc:hexane, 1:3) to give the desired title compound (15.9 mg, 0.039 mmol, 69%).

Analytics: $\mathbf{R_f}$ = 0.27 (EtOAc:hexane 1:3). **^{1}H NMR** (400 MHz, Chloroform-*d*) δ 5.50 (t, *J* = 10.1 Hz, 1H), 5.08 (d, *J* = 3.9 Hz, 1H), 4.74 (dd, *J* = 10.0, 3.9 Hz, 1H), 4.62 (d, *J* = 3.0 Hz, 1H), 3.89 (dq, *J* = 10.1, 6.1 Hz, 1H), 3.78 (dq, *J* = 9.2, 6.2 Hz, 1H), 3.35 (s, 3H), 3.30 – 3.23 (m, 1H), 2.42 (t, *J* = 10.2 Hz, 1H), 2.36 (s, 6H), 2.03 (s, 3H), 2.02 (s, 3H), 1.90 – 1.78 (m, 2H), 1.71 – 1.48 (m, 2H), 1.26 (dd, *J* = 6.2, 4.5 Hz, 6H). **^{13}C NMR** (101 MHz, Chloroform-*d*) δ 170.78, 170.02, 97.41, 91.87, 75.61, 72.97, 68.98, 68.21, 67.09, 65.96, 54.56, 41.65 (2C), 29.16, 23.08, 21.50, 20.94, 18.95, 18.75. **$[\alpha]^{20}_D$** = + 149.2 (c = 0.5, $CHCl_3$). **HRMS (ESI)**: 404.2278 $[M+H]^+$; calculated for $[C_{19}H_{34}NO_8]$: 404.2279. **IR** [ATR, neat]: ν = 2932.23 w, 1748.15 s, 1452.14 w, 1369.21 w, 1226.5 m, 1127.19 w, 1054.87 s, 982.554 w cm^{-1}.

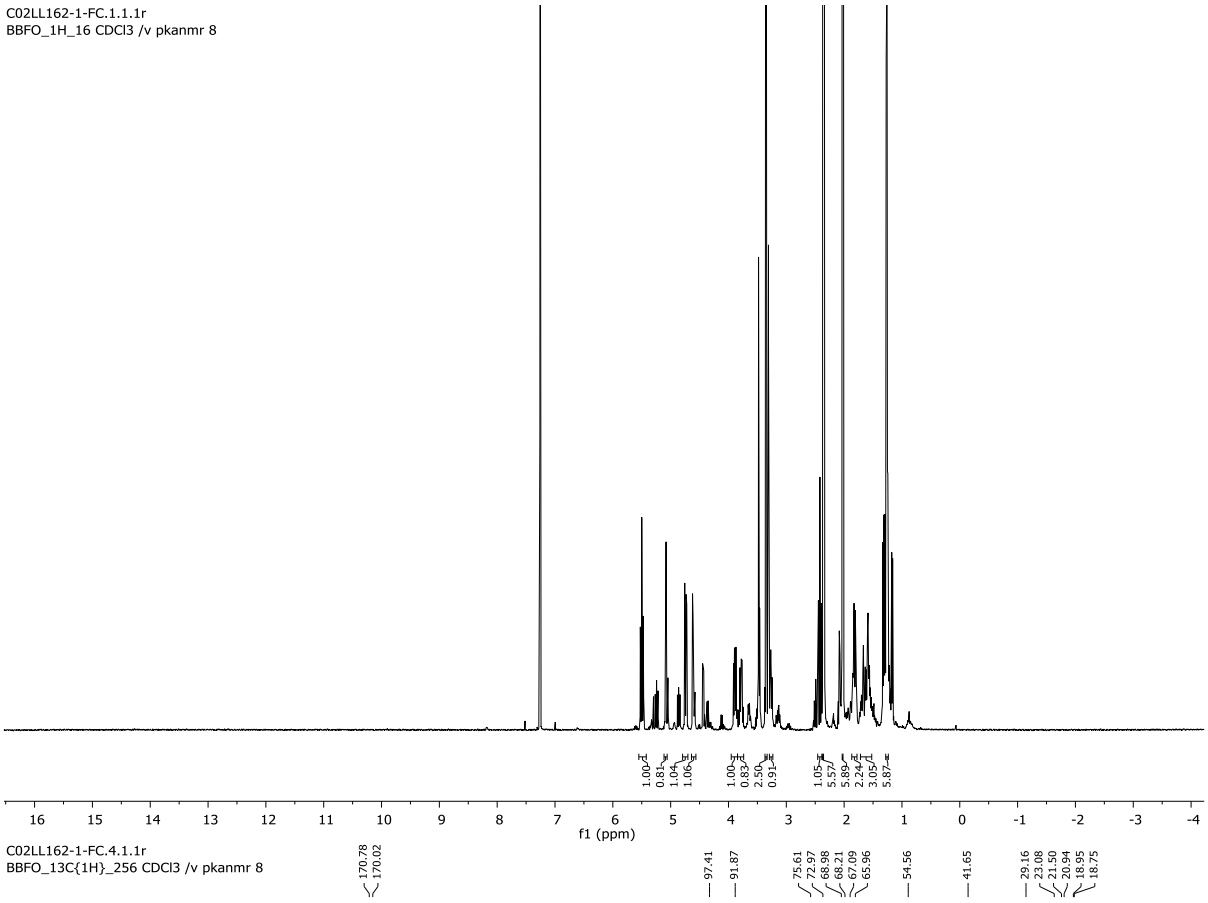
C02LL162-1-FC.1.1.1r
BBFO_1H_16 CDCl3 /v pkanmr 8
1.00
0.81
1.04
1.06
1.00
0.83
2.50
0.91
1.05
5.57
5.89
2.24
3.05
5.87
16 15 14 13 12 11 10 9 8 7 6 5 4 3 2 1 0 -1 -2 -3 -4
f1 (ppm)
C02LL162-1-FC.4.1.1r
BBFO_13C{1H}_256 CDCl3 /v pkanmr 8
170.78
170.02
97.41
91.87
75.61
72.97
68.98
68.21
67.09
65.96
54.56
41.65
29.16
23.08
21.50
20.94
18.95
18.75
240 230 220 210 200 190 180 170 160 150 140 130 120 110 100 90 80 70 60 50 40 30 20 10 0
f1 (ppm)

A-173 (2R,3R,4S,5R,6R)-3-azido-6-(((2R,3S)-6-methoxy-2-methyltetrahydro-2H-pyran-3-yl)oxy)-4,5-bis((4-methoxybenzyl)oxy)-2-methyltetrahydro-2H-pyran

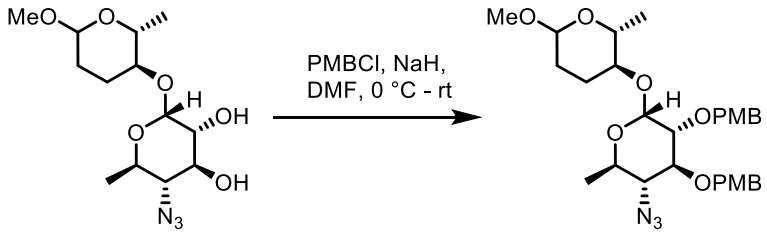

Assay: To **A-190** (28.0 mg, 0.88 mmol, 1.0 equiv) dissolved in DMF (0.8 mL) was added NaH (60% in mineral oil, 16.2 mg, 0.41 mmol, 4.6 equiv) and PMBCl (26.0 µL, 0.19 mmol, 2.2 equiv) at ambient temperature. The yellow/brown solution was stirred as such over night. The reaction was then cooled to 0 °C and carefully quenched with MeOH until the effervescent had ceased. Saturated aqueous NH_4Cl solution (4 mL) was added and the reaction mixture was stirred as such for 10 min. The biphasic mixture was separated and the aqueous layer was extracted with CH_2Cl_2 (3 x 4 mL). Combined organic layers were combined, dried over $MgSO_4$ and concentrated under reduced pressure. The crude was purified by FC (EtOAc:hexane, 1:3) to give the title compound as a slight yellowish oil (32.8 mg, 0.059 mmol, 67%).

Analytics: $\mathbf{R_f}$ = 0.43 (EtOAc:hexane, 1:3). **^{1}H NMR** (400 MHz, Chloroform-*d*) δ 7.36 – 7.24 (m, 4H), 6.87 (dd, *J* = 11.3, 8.6 Hz, 4H), 4.87 (d, *J* = 10.0 Hz, 1H), 4.82 (d, *J* = 3.7 Hz, 1H), 4.72 (d, *J* = 10.1 Hz, 1H), 4.69 (d, *J* = 11.6 Hz, 1H), 4.65 – 4.63 (m, 1H), 4.56 (d, *J* = 11.6 Hz, 1H), 3.89 – 3.83 (m, 1H), 3.81 (s, 3H), 3.80 (s, 3H), 3.79 – 3.75 (m, 1H), 3.58 (dq, *J* = 9.8, 6.2 Hz, 1H), 3.50 (dd, *J* = 9.6, 3.6 Hz, 1H), 3.35 (s, 3H), 3.31 – 3.23 (m, 1H)., 3.06 (t, *J* = 9.8 Hz, 1H), 1.87 (d, m, 2H), 1.76 – 1.64 (m, 1H), 1.36 – 1.27 (m, 1H), 1.25 (d, *J* = 2.2 Hz, 3H), 1.24 (d, *J* = 2.2 Hz, 3H).

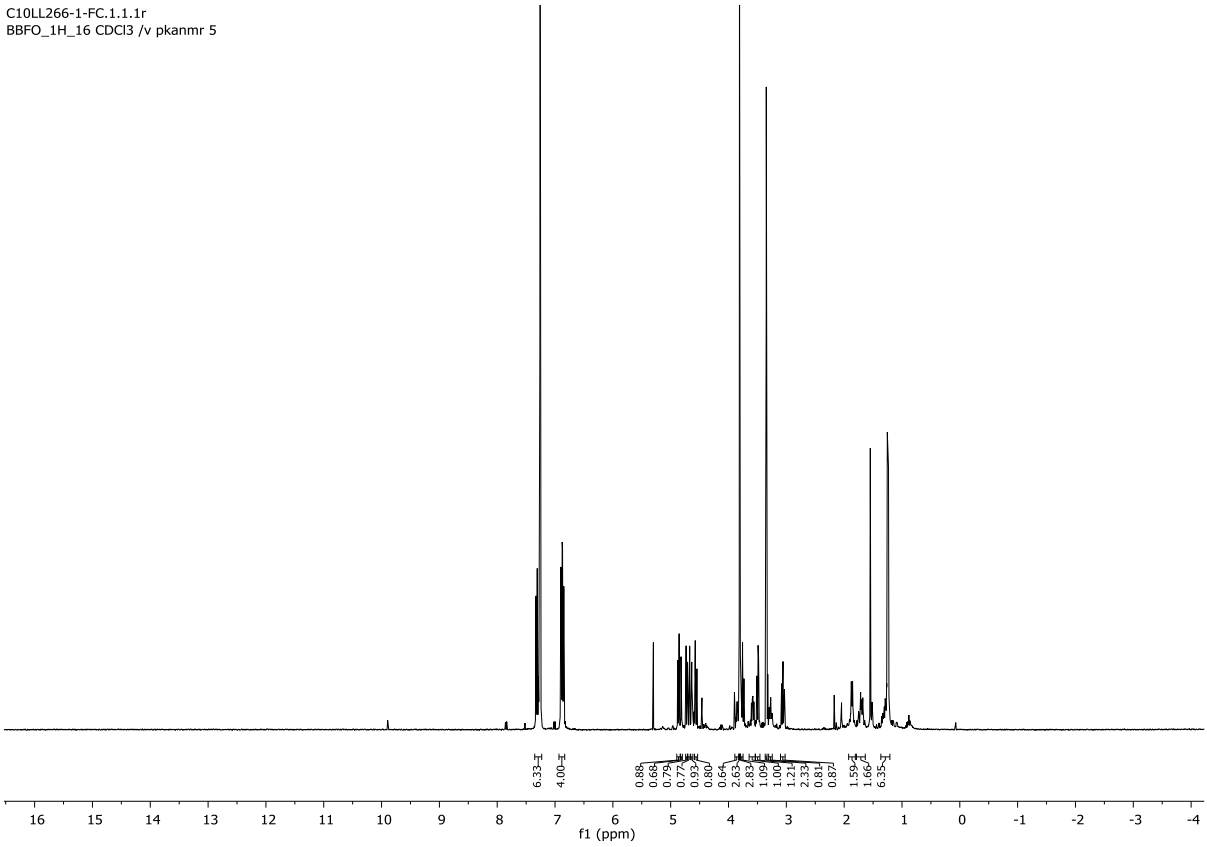
C10LL266-1-FC.1.1.1r
BBFO_1H_16 CDCl3 /v pkanmr 5
6.33
4.00
0.88
0.68
0.79
0.77
0.93
0.80
0.64
2.63
2.83
1.09
1.00
1.21
2.33
0.81
0.87
1.59
1.66
6.35
16 15 14 13 12 11 10 9 8 7 6 5 4 3 2 1 0 -1 -2 -3 -4
f1 (ppm)

A-192 (3aR,6R,7R,7aS)-2,2-di-tert-butyl-4-fluoro-N,N,6-trimethyltetrahydro-4H-[1,3,2]dioxasilolo[4,5-c]pyran-7-amine

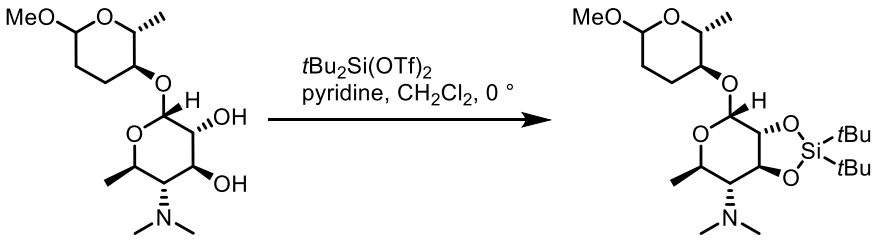

Assay: To a cooled solution of crude **A-190** (3.0 mg, 15.5 µmol, 1.0) in CH_2Cl_2 (1.3 µL) at 0 °C was added pyridine (6 µL, 77.6 µmol, 5.0 equiv) and DTBS ditriflate (8.0 µl, 23.3 µmol, 1.5 equiv). The reaction mixture was stirred at 0 °C for 40 min. TLC analysis showed full consumption of starting material. The reaction mixture was then diluted with MeOH (0.2 mL) and quenched with saturated aqueous $NaHCO_3$ (1.0 mL) and diluted with EtOAc (2 mL). The phases were separated and the aqueous phase was extracted with EtOAc (3 x 2 mL), combined organic phases were dried over $MgSO_4$ and concentrated under reduced pressure. A short pipette FC (EtOAc:hexane, 1:3) gave very little of the expected product. Yield not determined. No pure spectrum was obtained.

Analytics: $\mathbf{R_f}$ = 0.34 (EtOAc:hexane1:3). **HRMS (ESI)**: 460.3088 $[M+H]^+$; calculated for $[C_{23}H_{46}NO_6Si]$: 460.3089.

A-194 (2S,3S,4aR,5R,7R,8R,8aS)-5-(benzyloxy)-2,3-dimethoxy-2,3,7-trimethylhexahydro-5H-pyrano[3,4-b][1,4]dioxin-8-yl acetate

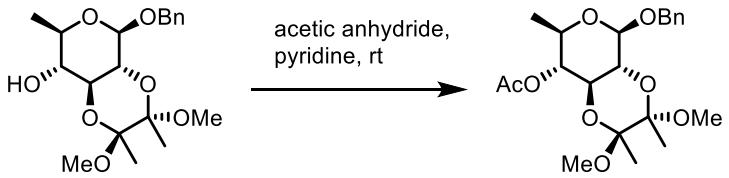

Assay: A-181 (90 mg, 0.244 mmol, 1.0 equiv) was dissolved in pyridine (2.6 mL) and acetic anhydride (624 µL, 2.44 mmol, 10.0 equiv) was then added at 0 °C and the reaction was allowed to warm to ambient temperature. After stirring for 84 h the reaction mixture was directly concentrated under diminished pressure. The yellowish oil was then taken up in CH_2Cl_2 (5 mL) and washed with saturated aq. $NHCl_4$ solution (6 mL). The phases were separated and the organic phase was dried over $MgSO_4$ and concentrated under reduced pressure. The crude was used as such in the following reaction.

A-195 (2S,3S,4aR,7R,8R,8aS)-5-hydroxy-2,3-dimethoxy-2,3,7-trimethylhexahydro-5H-pyrano[3,4-b][1,4]dioxin-8-yl acetate

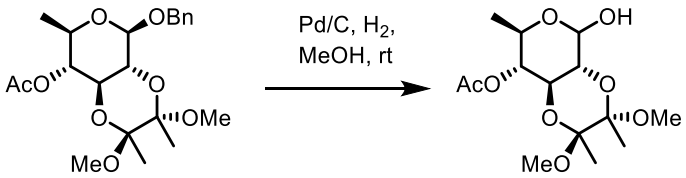

Assay: Crude **A-194** (330.0 mg, 0.80 mmol, 1.0 equiv) was dissolved in MeOH (8 mL) and Pd/C (10 wt%, 85.6 mg, 80.4 µmol, 0.1 equiv) was added in one portion and the reaction vessel was subsequently set under H_2-atmosphere (balloon pressure). The reaction mixture was stirred as such for 24 h. It was then filtered over a pad of Celite and the organic phase concentrated under diminished pressure. Purification of the yellow crude oil by FC (EtOAc:hexane, 1:1) gave a 1:1 anomeric mixture of the free hydroxyl-pyranose (140.4 mg, 0.43 mmol, 54% over two steps).

Analytics: $\mathbf{R_f}$ = 0.27, EtOAc:hexane (1:1). **^{1}H NMR** (400 MHz, Chloroform-*d*) δ 5.28 (t, *J* = 3.2 Hz, 1H), 5.20 (dd, *J* = 3.2, 1.3 Hz, 1H), 5.14 (dd, *J* = 3.1, 1.2 Hz, 1H), 4.79 (dd, *J* = 7.4, 5.7 Hz, 1H), 4.38 – 4.30 (m, 1H), 4.19 (dd, *J* = 10.6, 3.3 Hz, 1H), 4.15 – 4.11 (m, 1H), 4.09 (dd, *J* = 10.4, 3.7 Hz, 1H), 3.86 – 3.75 (m, 3H), 3.29 (s, 3H), 3.25 – 3.24 (m, 6H), 2.99 (d, *J* = 5.8 Hz, 1H), 2.82 (d, *J* = 2.5 Hz, 1H), 2.18 (s, 3H), 2.17 (s, 3H), 1.31 (s, 3H), 1.30 (s, 3H), 1.25 (s, 3H), 1.23 (s, 3H), 1.19 (d, *J* = 6.4 Hz, 3H), 1.14 (d, *J* = 6.6 Hz, 3H). **^{13}C NMR** (101 MHz, Chloroform-*d*) δ 170.98, 100.30, 100.15, 99.90, 95.19, 91.96, 71.40, 70.80, 70.65, 68.72, 68.59, 66.38, 65.67, 64.44, 48.21, 48.13, 48.05, 21.07, 17.87, 17.79, 17.67, 16.54, 16.39. **HRMS (ESI)**: 343.1366 $[M+Na]^+$; calculated for $[C_{14}H_{24}NaO_8]$: 343.1363. **IR** [ATR, neat]: ν = 3441.35 w, 2991.05 w, 2950.55 w, 1742.37 m, 1375.00 m, 1234.22 m, 1114.65 s, 1031.73 s, 967.13 w, 935.31 w, 883.24 w, 821.53 w, 734.75 w, 629.64 w cm^{-1}.

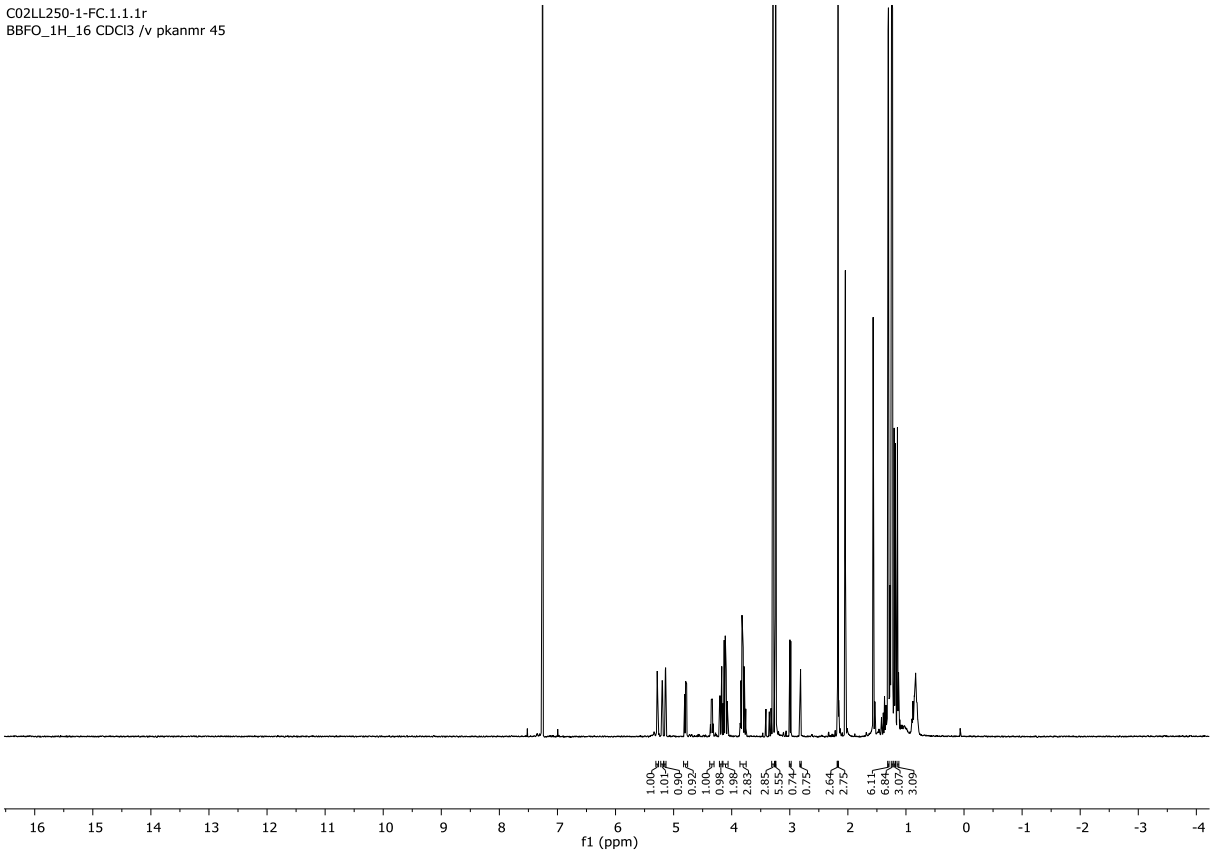
C02LL250-1-FC.1.1.1r
BBFO_1H_16 CDCl3 /v pkanmr 45
1.00
1.01
0.90
0.92
1.00
0.98
1.98
2.83
2.85
5.55
0.74
0.75
2.64
2.75
6.11
6.84
3.07
3.09
16 15 14 13 12 11 10 9 8 7 6 5 4 3 2 1 0 -1 -2 -3 -4
f1 (ppm)

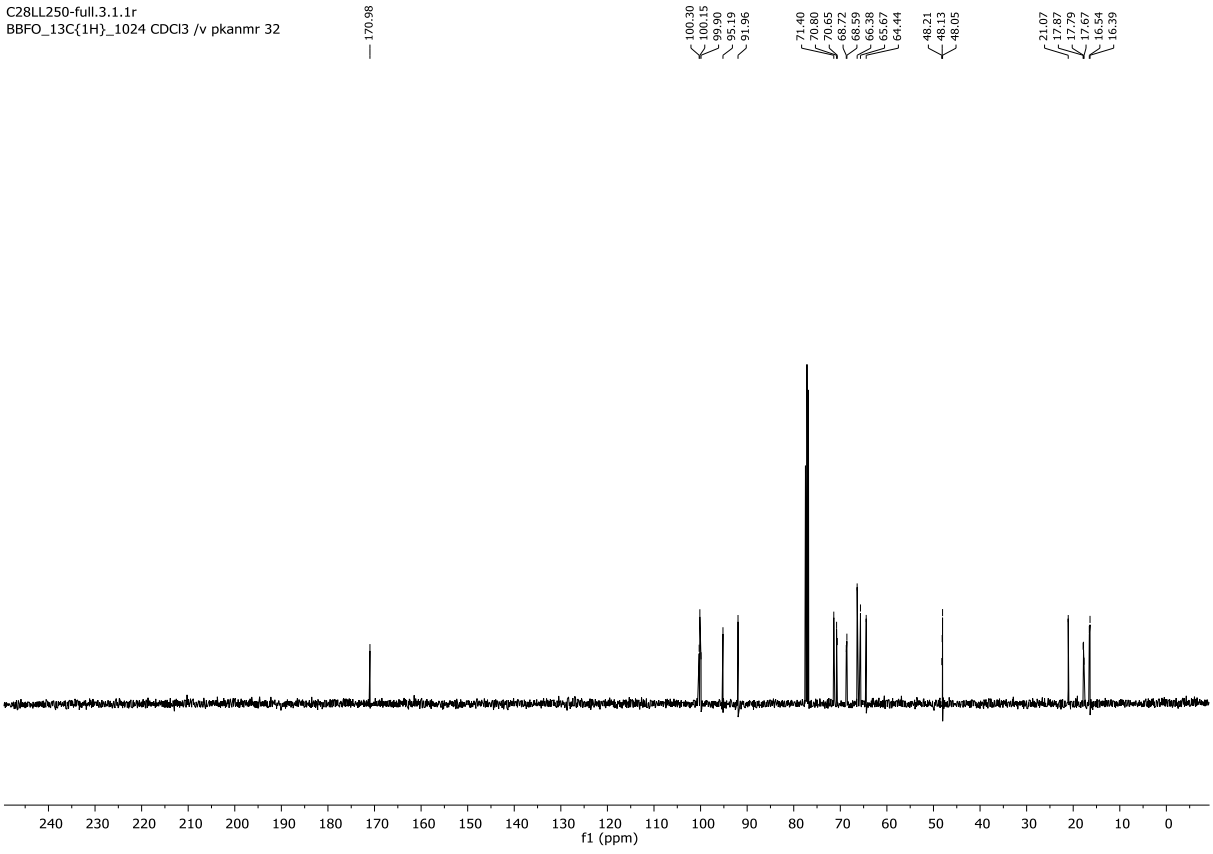
C28LL250-full.3.1.1r
BBFO_13C{1H}_1024 CDCl3 /v pkanmr 32
170.98
100.30
100.15
99.90
95.19
91.96
71.40
70.80
70.65
68.72
68.59
66.38
65.67
64.44
48.21
48.13
48.05
21.07
17.87
17.79
17.67
16.54
16.39
240 230 220 210 200 190 180 170 160 150 140 130 120 110 100 90 80 70 60 50 40 30 20 10 0
f1 (ppm)

A-146 (2S,3S,4aR,7R,8R,8aS)-2,3-dimethoxy-2,3,7-trimethyl-5-(2,2,2-trichloro-1-iminoethoxy)hexahydro-5H-pyrano[3,4-b][1,4]dioxin-8-yl acetate

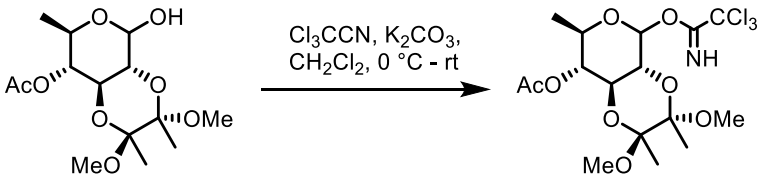

Assay: A-195 (47.3 mg, 147.7 µmol, 1.0 equiv), was dissolved in CH_2Cl_2 (1.5 mL), cooled to 0 °C and trichloroacetonitrile (148.0 µL, 1.477 mmol, 10.0 equiv) was added followed by anhydrous K_2CO_3 (102.0 mg, 738.3 µmol, 5.0 equiv). The reaction mixture was stirred for 6 h. Starting material was fully consumed and the crude suspension was then filtered over a pad of Celite. The filtrate was concentrated under reduced pressure and applied to a FC (Alox, EtOAc:Hex, 1:3) to give the desired trichloroacetimidate (64 mg, 0.138 mmol, 93%) as a mixture of α-&β-anomers (almost 1:1).

Analytics: $\mathbf{R_f}$ = 0.16, 0.38 respectively for both anomers (EtOAc:hexane, 1:3). **^{1}H NMR** (400 MHz, Chloroform-*d*) δ 8.61 (s, 1H), 8.56 (s, 1H), 6.36 (d, *J* = 3.3 Hz, 1H), 5.82 (d, *J* = 8.3 Hz, 1H), 5.26 (dd, *J* = 3.4, 1.4 Hz, 1H), 5.18 (dd, *J* = 3.4, 1.2 Hz, 1H), 4.34 – 4.26 (m, 2H), 4.22 (dd, *J* = 10.6, 3.3 Hz, 1H), 4.14 – 4.04 (m, 1H), 4.00 – 3.89 (m, 2H), 3.28 (s, 3H), 3.25 (s, 3H), 3.25 (s, 3H), 3.21 (s, 3H), 2.20 (s, 3H), 2.18 (s, 3H), 1.26 (s, 3H), 1.25 (s, 3H), 1.23 (d, *J* = 6.4 Hz, 3H), 1.22 (s, 3H), 1.21 (s, 3H), 1.16 (d, *J* = 6.5 Hz, 3H). **^{13}C NMR** (101 MHz, Chloroform-*d*) δ 171.01, 170.88, 161.58, 161.29, 100.27, 100.12, 100.04, 99.87, 96.56, 95.11, 71.69, 70.99, 70.24, 69.27, 68.62, 66.33, 64.67, 64.56, 48.23, 48.09, 47.99, 47.91, 21.11, 21.02, 17.83, 17.75, 17.61, 16.42, 16.35. **HRMS (ESI)**: 486.0460 $[M+Na]^+$; calculated for $[C_{16}H_{24}Cl_3NNaO_8]$: 486.0460. **IR** [ATR, neat]: ν = 2991.05 w, 2951.52 w, 1745.26 s, 1675.84 m, 1374.03 m, 1294.97 m, 1234.22 s, 1137.80 s, 1113.69 s, 1035.59 s, 965.20 w, 933.34 m, 883.24 w, 835.03 w, 979.42 m, 645.07 w cm^{-1}.

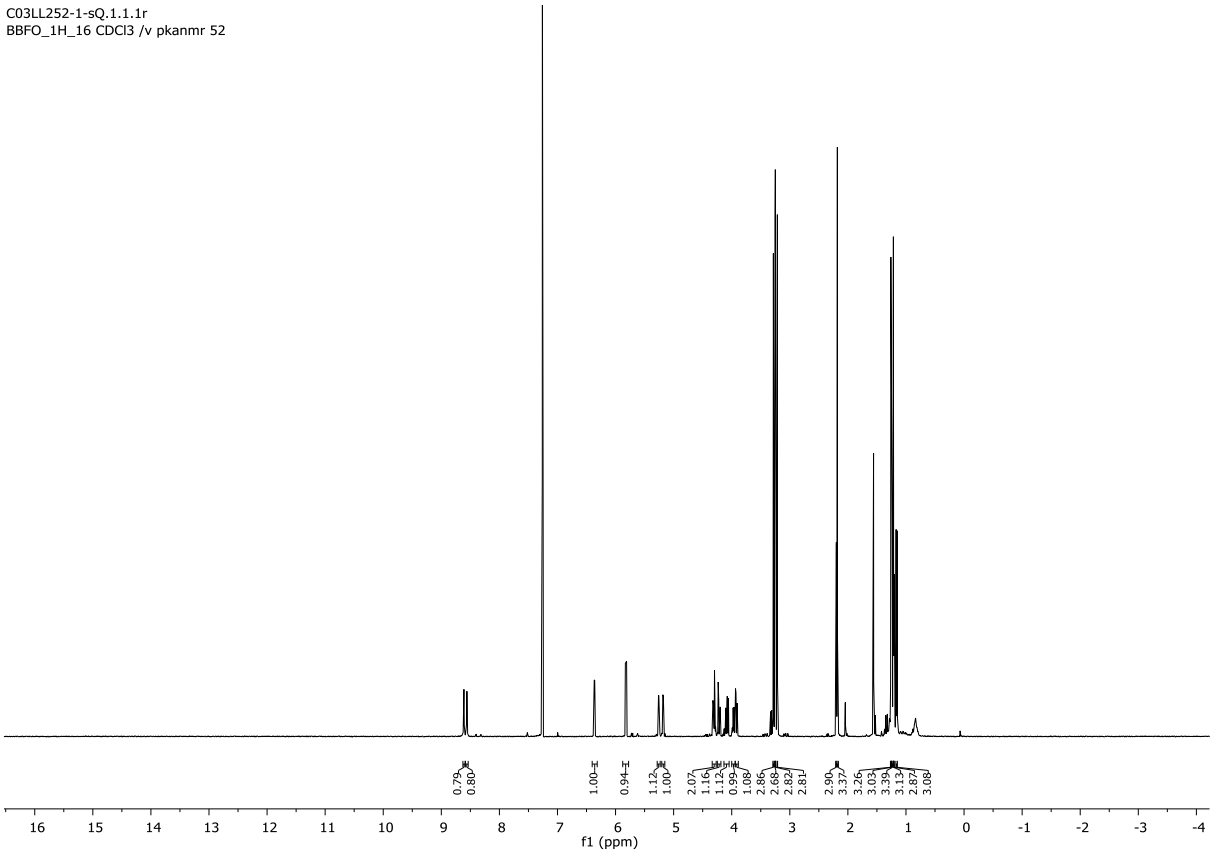
C03LL252-1-sQ.1.1.1r
BBFO_1H_16 CDCl3 /v pkanmr 52
0.79
0.80
1.00
0.94
1.12
1.00
2.07
1.16
1.12
0.99
1.08
2.86
2.68
2.82
2.81
2.90
3.37
3.26
3.03
3.39
3.13
2.87
3.08
16 15 14 13 12 11 10 9 8 7 6 5 4 3 2 1 0 -1 -2 -3 -4
f1 (ppm)

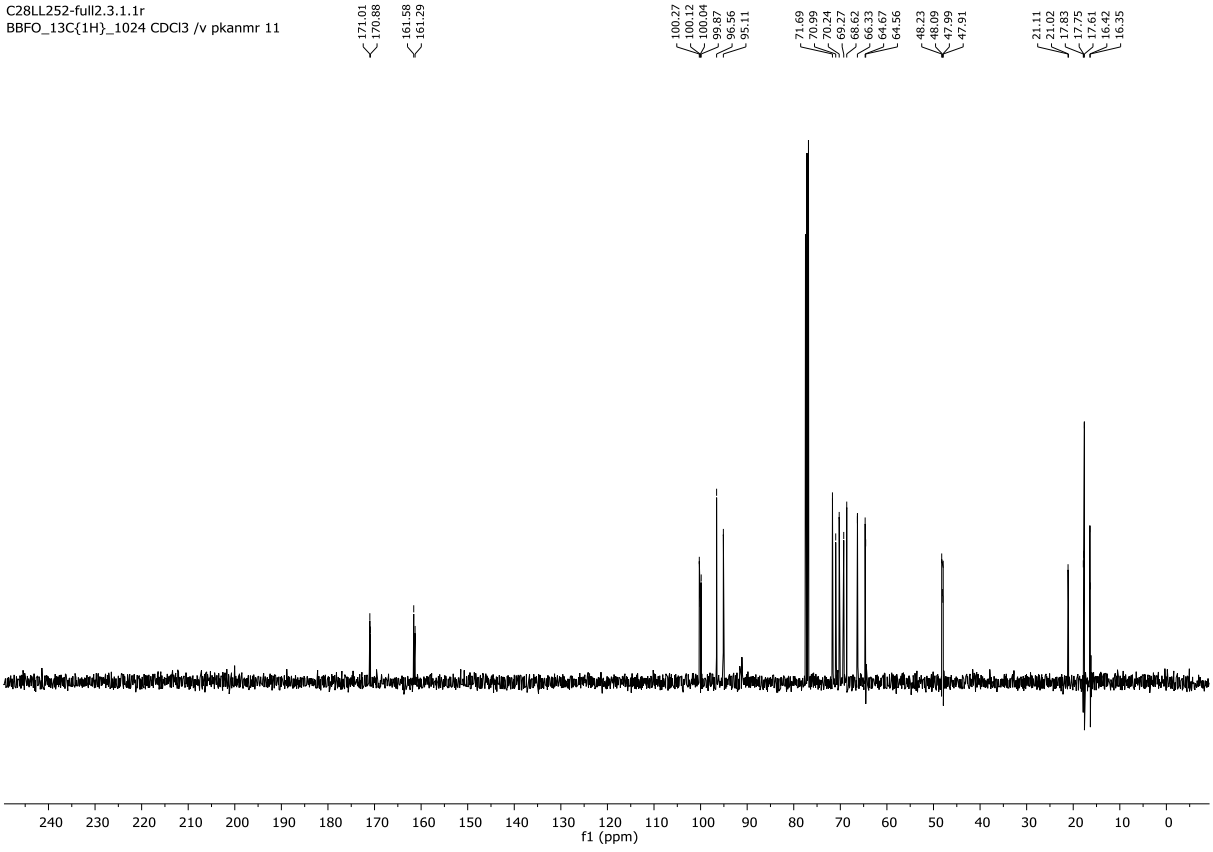
C28LL252-full2.3.1.1r
BBFO_13C{1H}_1024 CDCl3 /v pkanmr 11
171.01
170.88
161.58
161.29
100.27
100.12
100.04
99.87
96.56
95.11
71.69
70.99
70.24
69.27
68.62
66.33
64.67
64.56
48.23
48.09
47.99
47.91
21.11
21.02
17.83
17.75
17.61
16.42
16.35
240 230 220 210 200 190 180 170 160 150 140 130 120 110 100 90 80 70 60 50 40 30 20 10 0
f1 (ppm)

A-196 (2R,3R,4aR,5R,7R,8R,8aS)-2,3-dimethoxy-5-(((2R,3S)-6-methoxy-2-methyltetrahydro-2H-pyran-3-yl)oxy)-2,3,7-trimethylhexahydro-5H-pyrano[3,4-b][1,4]dioxin-8-yl acetate

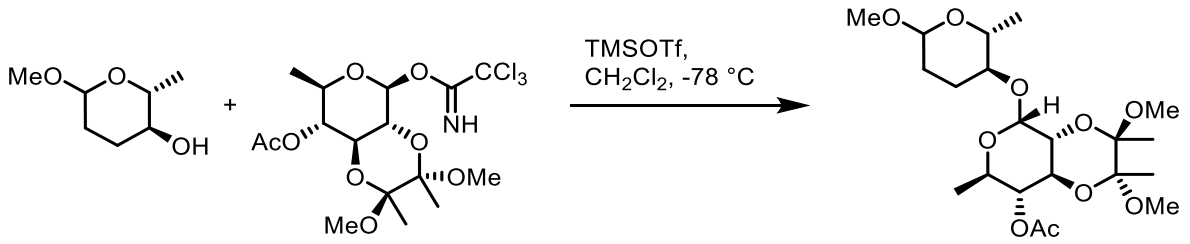

Assay: In a flame dried 5 ml pear shaped flask, **A-79** (22.8 mg, 49.1 µmol, 1.0 equiv) and **A-146** (7.2 mg, 49.1 µmol, 1.0 equiv) were azeotropically dried with benzene (3 x 3 mL) over 2 h. Molecular sieves were dried under high vacuum (3 * 10^{-3} mbar) at 250 °C over 40 min. The dried sugars were then dissolved in CH_2Cl_2 (1.05 mL) and the activated molecular sieves were added as quickly as possible. The mixture was then stirred for an additional hour to thoroughly desiccate the two carbohydrates. Meanwhile, a stock solution of TMSOTf (266 µL of TMSOTf in CH_2Cl_2 (5 mL)) was prepared. After the before mentioned 60 min, the suspension was cooled to –78 °C and TMSOTf stock solution (53.0 µL) was carefully added to the reaction mixture. The reaction was monitored via TLC analysis. After 2 h at -78 °C starting material was fully consumed. The product mass was clearly detected on TLC-MS. The reaction was quenched by addition of NEt_3 (few drops) and saturated aqueous $NaHCO_3$ (3 mL) solution. The aqueous phase was extracted with CH_2Cl_2 (3 x 3 mL). Combined organic phases were dried over $MgSO_4$. Purification by FC (EtOAc:hexane, 1:3) gave a slightly yellow sticky syrup (13.7 mg, 0.031 mmol, 62%, impure).

Analytics: $\mathbf{R_f}$ = 0.31 (EtOAc:hexane, 1:3). **^{1}H NMR** (400 MHz, Chloroform-*d*) δ 5.16 – 5.14 (m, 1H), 5.11 – 5.08 (m, 1H), 4.98 – 4.96 (m, 1H), 4.63 – 4.56 (m, 1H), 4.50 (dd, *J* = 4.5, 3.3 Hz, 1H), 4.06 – 4.04 (m, 1H), 3.81 – 3.78 (m, 2H), 3.46 (d, *J* = 4.1 Hz, 1H), 3.33 (s, 3H), 3.31 (s, 3H), 3.24 – 3.22 (m, 6H), 3.22 (s, 3H), 3.20 (s, 3H), 2.14 (s, 6H), 1.26 (s, 3H), 1.24 (s, 12H), 1.23 – 1.21 (m, 6H), 1.14 (d, *J* = 6.5 Hz, 3H), 1.11 (d, *J* = 6.6 Hz, 3H). **^{13}C NMR** (101 MHz, Chloroform-*d*) δ 171.31, 102.34, 100.42, 100.15, 99.96, 99.91, 99.74, 97.46, 97.39, 93.93, 82.41, 75.92, 71.44, 70.52, 70.24, 68.85, 67.67, 67.36, 67.04, 66.19, 65.08, 64.79, 56.39, 54.44, 48.13, 47.99, 47.86, 29.45, 29.28, 26.26, 22.90, 21.16, 21.12, 20.99, 18.63, 17.97, 17.83, 17.79, 17.61, 16.66, 16.24, 14.30. **HRMS (ESI)**: 471.2203 $[M+Na]^+$; calculated for $[C_{21}H_{36}NaO_{10}]$: 471.2201.

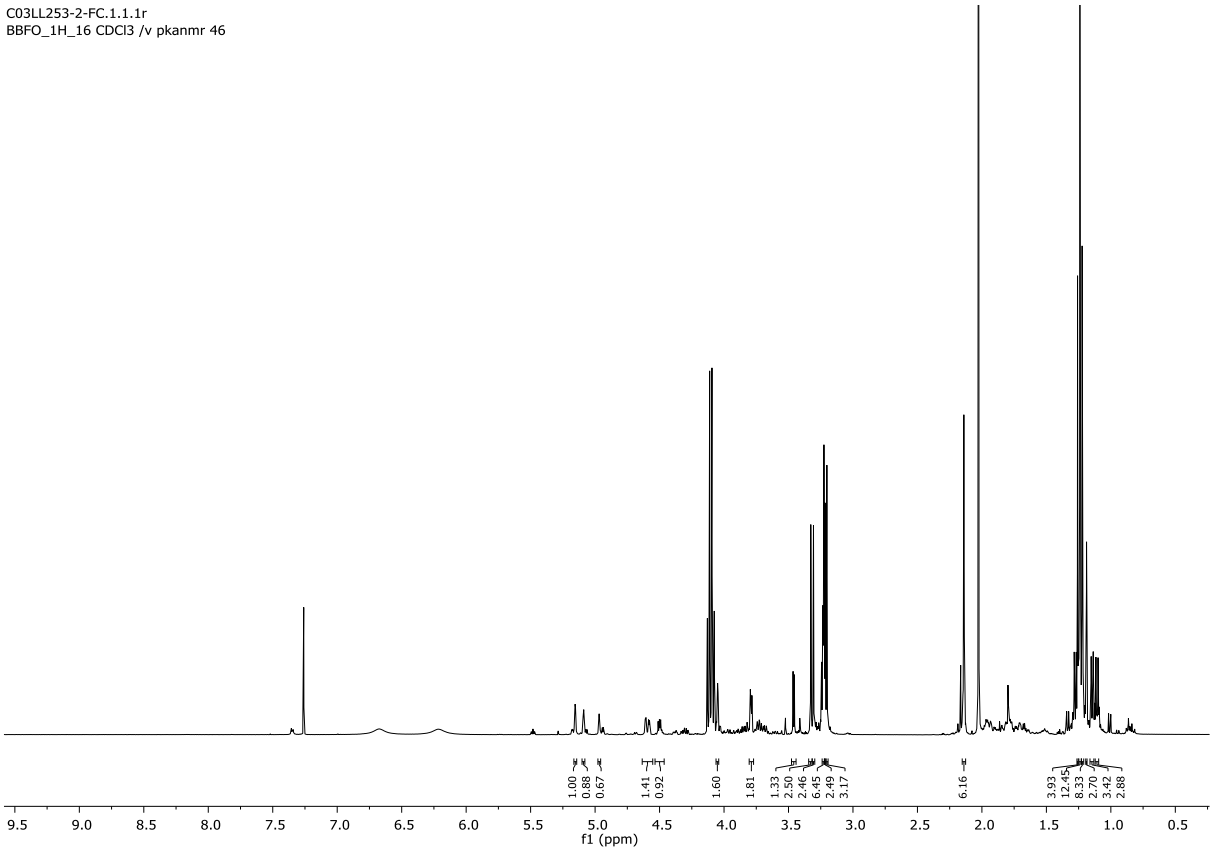
C03LL253-2-FC.1.1.1r
BBFO_1H_16 CDCl3 /v pkanmr 46
1.00
0.88
0.67
1.41
0.92
1.60
1.81
1.33
2.50
2.46
6.45
2.49
3.17
6.16
3.93
12.45
8.33
2.70
3.42
2.88
f1 (ppm)

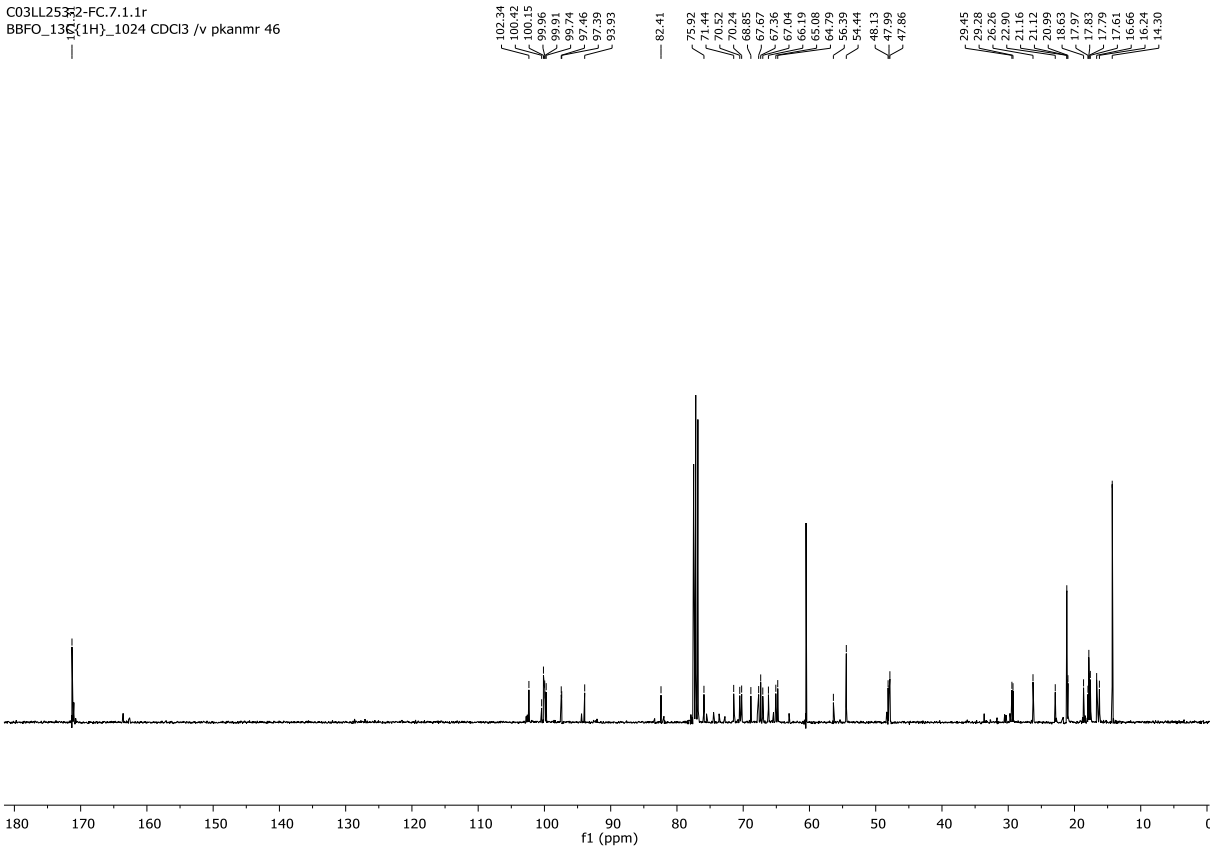
C03LL253-2-FC.7.1.1r
BBFO_13C{1H}_1024 CDCl3 /v pkanmr 46
102.34
100.42
100.15
99.96
99.91
99.74
97.46
97.39
93.93
82.41
75.92
71.44
70.52
70.24
68.85
67.67
67.36
67.04
66.19
65.08
64.79
56.39
54.44
48.13
47.99
47.86
29.45
29.28
26.26
22.90
21.16
21.12
20.99
19.63
18.07
17.83
17.79
17.61
16.66
16.24
14.30
f1 (ppm)

A-197 (2S,3S,4aR,5S,7R,8R,8aS)-8-(dimethylamino)-2,3-dimethoxy-2,3,7-trimethylhexahydro-5H-pyrano[3,4-b][1,4]dioxin-5-yl (Z)-2,2,2-trifluoro-N-phenylacetimidate

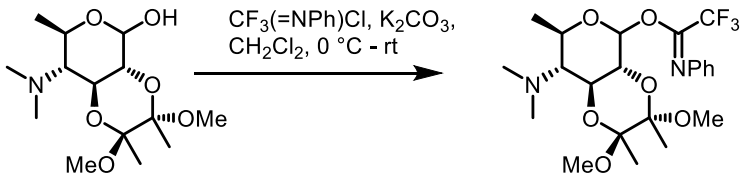

Assay: To **A-153** dissolved in CH_2Cl_2 (2.0 mL) was given, at 0 °C, trifluoroacetimidoyl chloride (70.0 µL, 0.439 mmol, 2.0 equiv.) and potassium carbonate (60.6 mg, 0.439 mmol, 2.0 equiv). The reaction mixture was allowed to reach ambient temperature and was stirred for 16 h. Only little starting material was consumed, therefore another portion of trifluoroacetimidoyl chloride (4.0 equiv) was added and stirring was continued. After another 24 h, staring material still present but less. Potential product observed on TLC-MS. Another portion of trifluoroacetimidoyl chloride (4.0 equiv) was added and stirring was continued for again 24 h. Little starting material was detected, nevertheless the reaction mixture was filtered over a pad of Celite. The filtrate was concentrated under reduced pressure and the brown cure was purified by FC (EtOAc:Hex, 1:10) to give a brown sticky syrup (53.1 mg, 0.111 mmol, 51%). The glycosyl donor was directly used as such in the following reaction.

Analytics: full characterisation could not be done due to the reactivity of the compound.

A-200 (2R,3R,4aR,5R,7R,8R,8aS)-8-azido-2,3-dimethoxy-5-(((2R,3S)-6-methoxy-2-methyltetrahydro-2H-pyran-3-yl)oxy)-2,3,7-trimethylhexahydro-5H-pyrano[3,4-b][1,4]dioxine

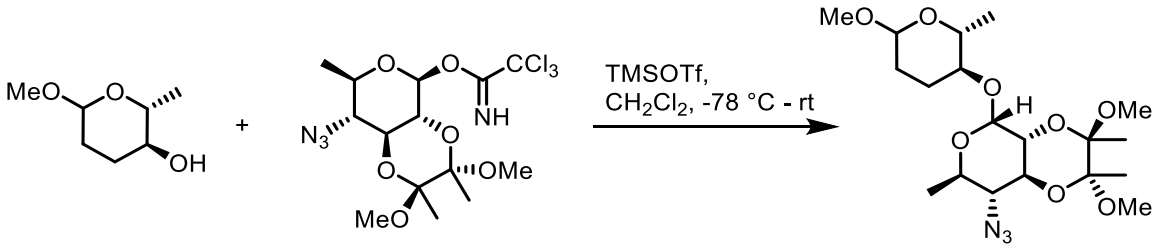

Assay: In a flame dried 5 ml pear shaped flask, **A-79** (55.3 mg, 378.3 µmol, 1.0 equiv) and **A-199** (223.5 mg, 499.3 µmol, 1.0 equiv) was azeotropically dried with benzene (3 x 3 mL) over 2 h. Molecular sieves were dried under high vacuum (3 * 10^{-3} mbar) at 250 °C over 40 min. The dried sugars were then dissolved in CH_2Cl_2 (3.8 mL) and the activated molecular sieves was added as quickly as possible. The mixture was then stirred for an additional hour to thoroughly desiccate the two carbohydrates. Meanwhile, a stock solution of TMSOTf (210 µL of TMSOTf in 2 mL CH_2Cl_2) was prepared. After the before mentioned 60 min, the suspension was cooled to –78 °C and TMSOTf stock solution (221 µL) was carefully added to the reaction mixture. The reaction was monitored via TLC analysis. After 2 h at -78 °C, the reaction was quenched with dry NEt_3 (few drops) and the mixture was filtered over Celite. The filtrate was concentrated under reduced pressure.

The clear crude oil was then purified by FC (EtOAc:Hex, 1:3) to give impure product (157 mg, 0.364 mmol, 96%)

Analytics: $\mathbf{R_f}$ = 0.36 (EtOAc:hexane, 1:3). **^{1}H NMR** (400 MHz, Chloroform-*d*) δ 4.90 (d, *J* = 3.6 Hz, 1H), 4.62 (d, *J* = 3.0 Hz, 1H), 4.07 – 4.00 (m, 1H), 3.88 – 3.81 (m, 1H), 3.74 (ddd, *J* = 10.2, 3.6, 1.7 Hz, 2H), 3.34 (s, 6H), 3.33 (s, 3H), 3.25 (s, 3H), 1.98 – 1.90 (m, 2H), 1.88 – 1.80 (m, 2H), 1.76 – 1.65 (m, 2H), 1.32 (s, 6H), 1.29 (s, 6H), 1.27 (s, 3H), 1.26 (s, 3H). **^{13}C NMR** (101 MHz, Chloroform-*d*) δ 100.02, 97.48, 93.37, 75.88, 68.46, 67.27, 67.04, 64.91, 48.07, 29.29, 22.92, 18.73, 18.35, 17.94, 17.72. **HRMS (ESI)**: 454.2164 $[M+Na]^+$; calculated for $[C_{19}H_{33}N_3NaO_8]$: 454.2160.

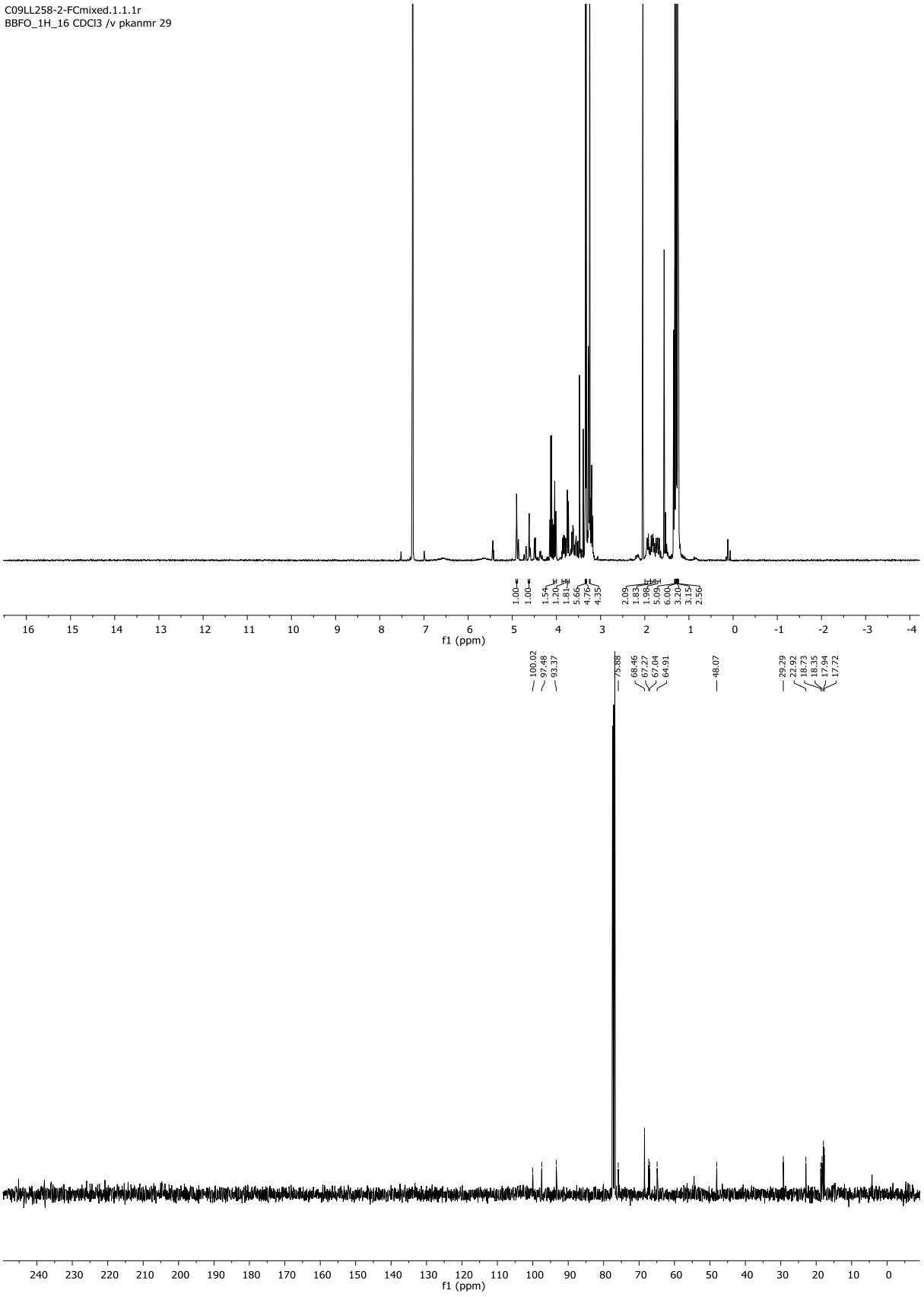
C09LL258-2-FCmixed.1.1.1r
BBFO_1H_16 CDCl3 /v pkanmr 29
1.00
1.00
1.54
1.20
1.81
5.66
4.76
4.35
2.09
1.83
1.98
5.09
6.00
3.20
3.15
2.56
f1 (ppm)
100.02
97.48
93.37
75.88
68.46
67.27
67.04
64.91
48.07
29.29
22.92
18.73
18.35
17.94
17.72
f1 (ppm)

A-198 (2R,3R,4aR,5R,7R,8R,8aS)-2,3-dimethoxy-5-(((2R,3S)-6-methoxy-2-methyltetrahydro-2H-pyran-3-yl)oxy)-N,N,2,3,7-pentamethylhexahydro-5H-pyrano[3,4-b][1,4]dioxin-8-amine

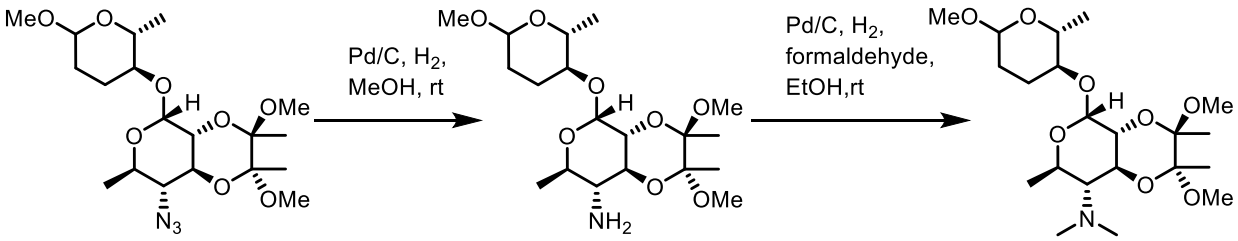

Assay: To disaccharide LL258 (1.3 mg, 3.0 µmol, 1.0 equiv) in dry MeOH (130 µL), was added Pd/C (10 wt %, 0.3 mg, 10 mol%) and the reaction mixture was set under H_2 atmosphere (balloon). The reaction was monitored via TLC analysis, starting material was fully consumed after 30 min at ambient temperature. The crude was then filtrated over a pad of Celite which was washed with MeOH. Solvents were evaporated and the crude was taken up in dry EtOH (130 µL). To the stirring solution was then added Pd/C (10 wt %, 0.3 mg, 10 mol%) and the reaction mixture was set under H_2 atmosphere. Formaldehyde 37% in water (1 µL, 7.5 µmol, 2.5 equiv) was added and the reaction mixture was stirred at ambient temperature for 2 h. TLC analysis showed full consumption of starting material. The crude was then again filtrated over a pad of Celite which was washed with EtOAc. Solvents were evaporated and the crude was purified by FC (EtOAc:hexane, 1:3) to give only traces of disaccharide.

Analytics: $\mathbf{R_f}$ = 0.42 (EtOAc:hexane, 1:3). **HRMS (ESI)**: 434.2753 $[M+H]^+$; calculated for $[C_{21}H_{40}NO_8]$: 434.2748.

A-203 tert-butyl (2R,4S)-2-(tert-butyl)-4-((4-((1-((2R,5S,6R)-5-(((2R,3R,4S,5R,6R)-5-(dimethylamino)-3,4-bis((4-methoxybenzyl)oxy)-6-methyltetrahydro-2H-pyran-2-yl)oxy)-6-methyltetrahydro-2H-pyran-2-yl)-2-oxo-1,2-dihydropyrimidin-4-yl)carbamoyl)phenyl)carbamoyl)-4-methyloxazolidine-3-carboxylate

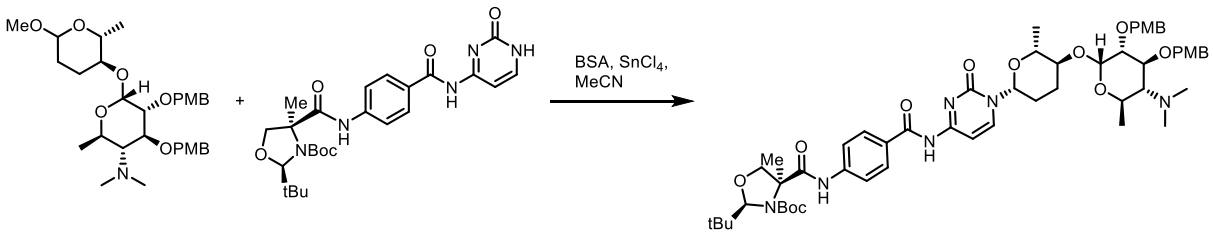

Assay: A-53 (3.3 mg, 10.5 µmol, 1.3 equiv) was dried in a flame dried pear shaped 5 mL flask over night under high vaccum (1 x 10^{-3} mbar). It was then suspended in MeCN (70 µL) and N,O-bis(trimethylsilyl)acetamid (4 µL, 16.1 µmol, 2.0 equiv) was added at room temperature. After 40 min of stirring, **A-173** (4.5 mg, 8.0 µmol, 1.0 equiv) dissolved in MeCN (70 µL) was added, followed by dropwise addition of $SnCl_4$ (prior distilled over P_2O_5 at 115 °C and atmospheric pressure) (1.4 µL, 12.1 µmol, 1.5 equiv) in MeCN (40 µL), which was prepared as a stock solution. The reaction mixture was stirred at ambient temperature and meanwhile monitored via LC-MS and TLC. The reaction mixture was directly filtered over a short pad of Alox and concentrated under reduced pressure. A short FC (EtOAc:hexane, 3:1) gave traces of the target compound (impure) along with reisolated **A-173**.

Analytics: R_f = 0.21 (EtOAc:hexane, 3:1).

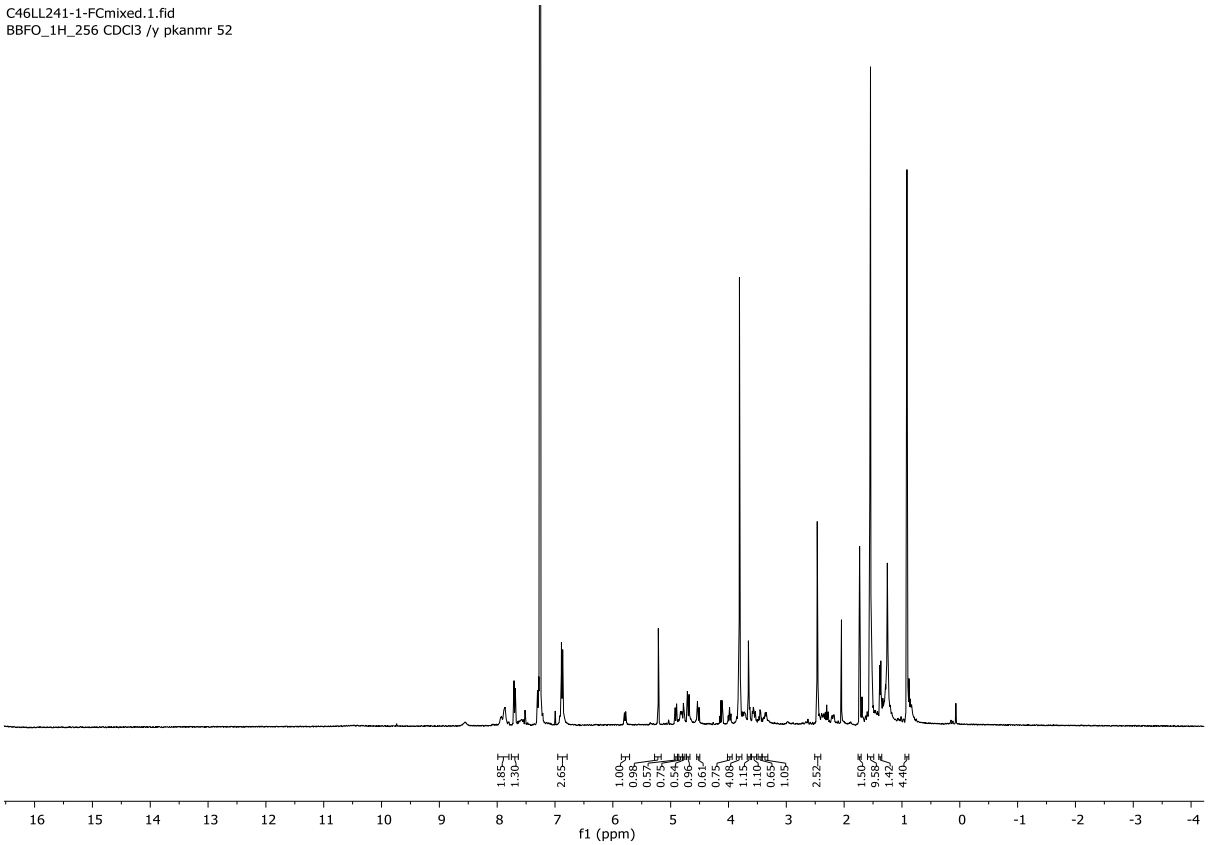
C46LL241-1-FCmixed.1.fid
BBFO_1H_256 CDCl3 /y pkanmr 52
1.85
1.30
2.65
1.00
0.98
0.57
0.75
0.54
0.96
0.61
0.75
4.08
1.15
1.10
0.69
1.05
2.52
1.50
9.58
1.42
4.40
16 15 14 13 12 11 10 9 8 7 6 5 4 3 2 1 0 -1 -2 -3 -4
f1 (ppm)

A-201 (2R,4S)-tert-butyl 4-((4-((1-((2R,5S,6R)-5-(benzyloxy)-6-methyltetrahydro-2H-pyran-2-yl)-2-oxo-1,2-dihydropyrimidin-4-yl)carbamoyl)phenyl)carbamoyl)-2-(tert-butyl)-4-methyloxazolidine-3-carboxylate

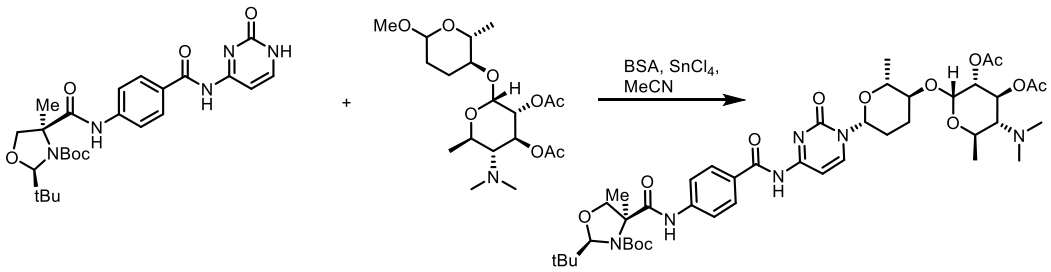

Assay: A-53 (6.4 mg, 12.8 µmol, 1.2 equiv) was dried in a flame dried microwave vial (0.2 – 0.5 mL vial) over night under high vaccum ($1*10^{-3}$ mbar). It was then suspended in MeCN (70 µL) and N,O-bis(trimethylsilyl)acetamid (5 µL, 21.3 µmol, 2.0 equiv) was added at room temperature. After 40 min of stirring, **A-191** (4.3 mg, 10.7 µmol, 1.0 equiv) dissolved in MeCN (70 µL) was added, followed by dropwise addition of freshly distilled $SnCl_4$ (1.6 µL, 13.7 µmol, 1.5 equiv) in MeCN (40 µL), which was prepared as a stock solution. The reaction mixture was stirred for 4.5 h at ambient temperature and meanwhile monitored via LC-MS and TLC. At some point, the reaction did no longer proceed. It was then decided to quench the reaction mixture with pH 7 buffer. The phases were separated and the aqueous phase was extracted with EtOAc (3 x 2 mL), combined organic phases were dried over $MgSO_4$ and concentrated under reduced pressure. A short pipette FC (EtOAc:hexane, 3:1) gave the target compound (impure) and reisolated **A-191** in quantities below 1 mg.

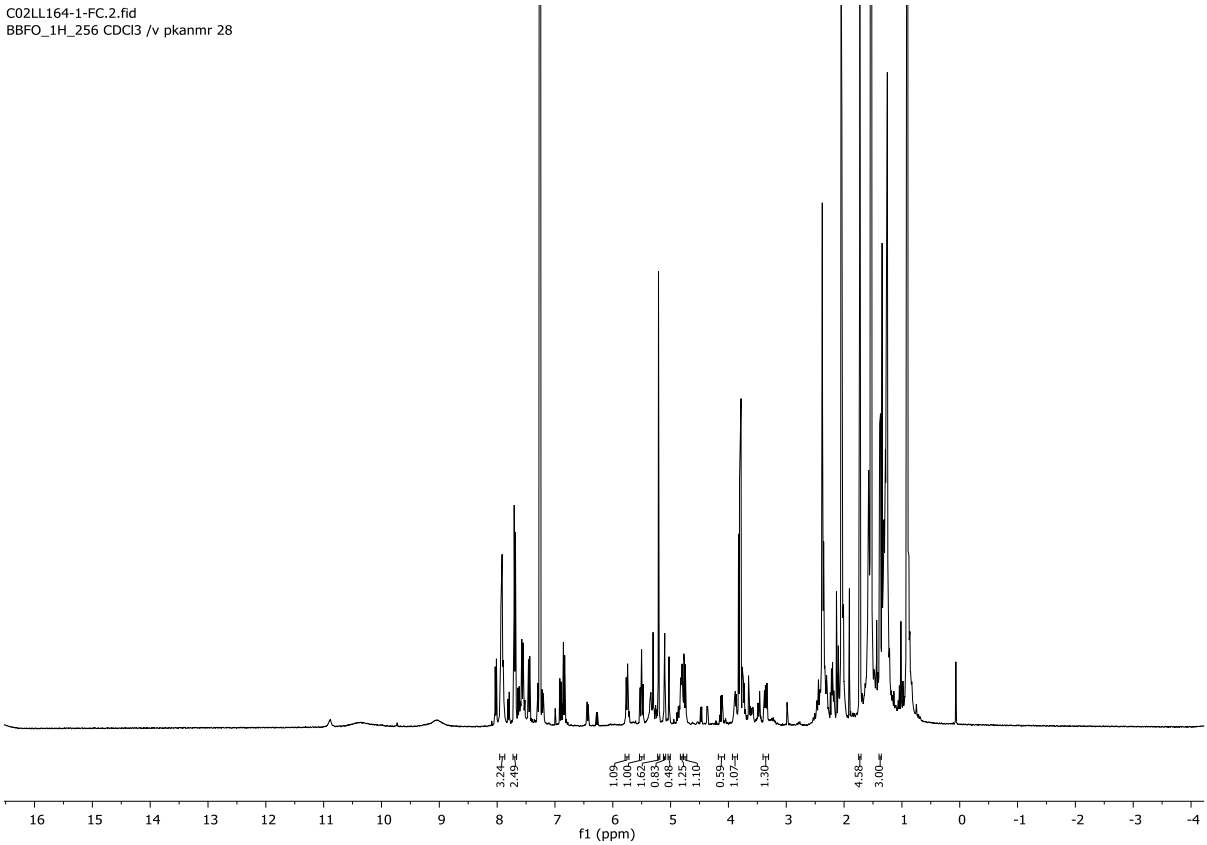
C02LL164-1-FC.2.fid
BBFO_1H_256 CDCl3 /v pkanmr 28
3.24
2.49
1.09
1.00
1.62
0.93
0.48
1.25
1.10
0.59
1.07
1.30
4.58
3.00
16 15 14 13 12 11 10 9 8 7 6 5 4 3 2 1 0 -1 -2 -3 -4
f1 (ppm)

A-208 tert-butyl (2R,4S)-2-(tert-butyl)-4-((4-((1-((2R,5S,6R)-5-((dimethylglycyl)oxy)-6-methyltetrahydro-2H-pyran-2-yl)-2-oxo-1,2-dihydropyrimidin-4-yl)carbamoyl)phenyl)carbamoyl)-4-methyloxazolidine-3-carboxylate

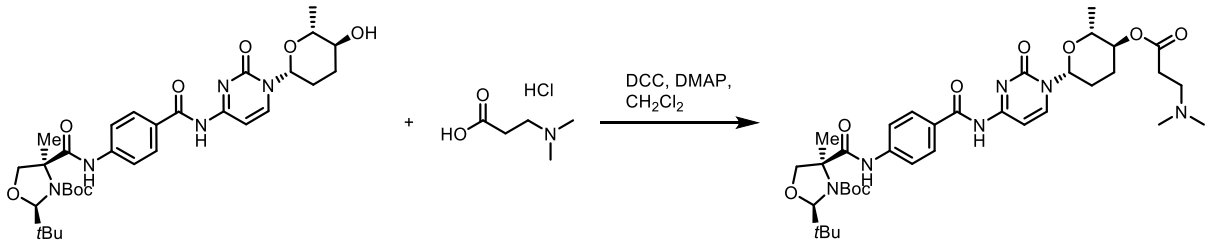

Assay: To pyranose **A-60** (20 mg, 32.6 µmol, 1.0 equiv) dissolved in DMF (0.3 mL) was added **A-206** (7.5 mg, 48.9 µmol, 1.5 equiv), DCC (10.1 mg, 48.9 µmol, 1.5 equiv) and DMAP (6.0 mg, 48.9 µmol, 1.5 equiv) at ambient temperature. The reaction mixture was stirred as such for 6 h whereas full consumption of starting material was observed. The crude was filtered over cotton wool and concentrated under reduced pressure. The brown crude was then taken up in very little MeOH and absorbed in as little silica as possible. Purification by FC ($CHCl_3$:MeOH:H_2O, 85:13:2) gave clean product (7.4 mg, 0.01 mmol, 32%).

Analytics: $\mathbf{R_f}$ = 0.56 ($CHCl_3$:MeOH:H_2O, 85:13:2). **^{1}H NMR** (400 MHz, Chloroform-*d*) δ 7.84 (dd, *J* = 8.1, 3.2 Hz, 3H), 7.63 (d, *J* = 8.8 Hz, 2H), 7.48 (s, 1H), 5.74 (dd, *J* = 10.4, 2.1 Hz, 1H), 5.14 (s, 1H), 4.74 (d, *J* = 9.1 Hz, 1H), 4.51 (ddd, *J* = 10.9, 9.5, 4.5 Hz, 1H), 3.75 (d, *J* = 9.0 Hz, 1H), 3.67 (dq, *J* = 9.6, 6.1 Hz, 1H), 2.57 (t, *J* = 7.2 Hz, 2H), 2.44 (t, *J* = 7.1 Hz, 2H), 2.24 (m, 2H), 2.19 (s, 6H), 1.66 (s, 3H), 1.67 – 1.57 (m, 1H), 1.58 – 1.47 (m, 1H), 1.47 (s, 9H), 1.21 (d, *J* = 6.1 Hz, 3H), 0.84 (s, 9H). **^{13}C NMR** (101 MHz, Chloroform-*d*) δ 171.81, 171.65, 162.22, 159.21, 155.93, 144.18, 142.90, 129.00 (2C), 119.37 (2C), 97.99, 83.11, 83.04, 77.24, 76.52, 76.04, 72.00, 68.07, 54.67, 45.17 (2C), 38.21, 33.03, 30.62, 28.16 (3C), 27.98, 26.13 (2C), 22.10, 18.01. **HRMS (ESI)**: 713.3859 $[M+H]^+$; calculated for $[C_{36}H_{53}N_6O_9]$: 713.3869. **$[\alpha]^{20}_D$** = -24.39 (c = 0.41, MeOH). **IR** [ATR, neat]: ν = 2928.38 w, 1671.02 s, 1598.7 m, 1544.7 m, 1483.95 s, 1366.32 m, 1248.68 s, 1165.76 m, 1095.37 m, 783.92 s cm^{-1}.

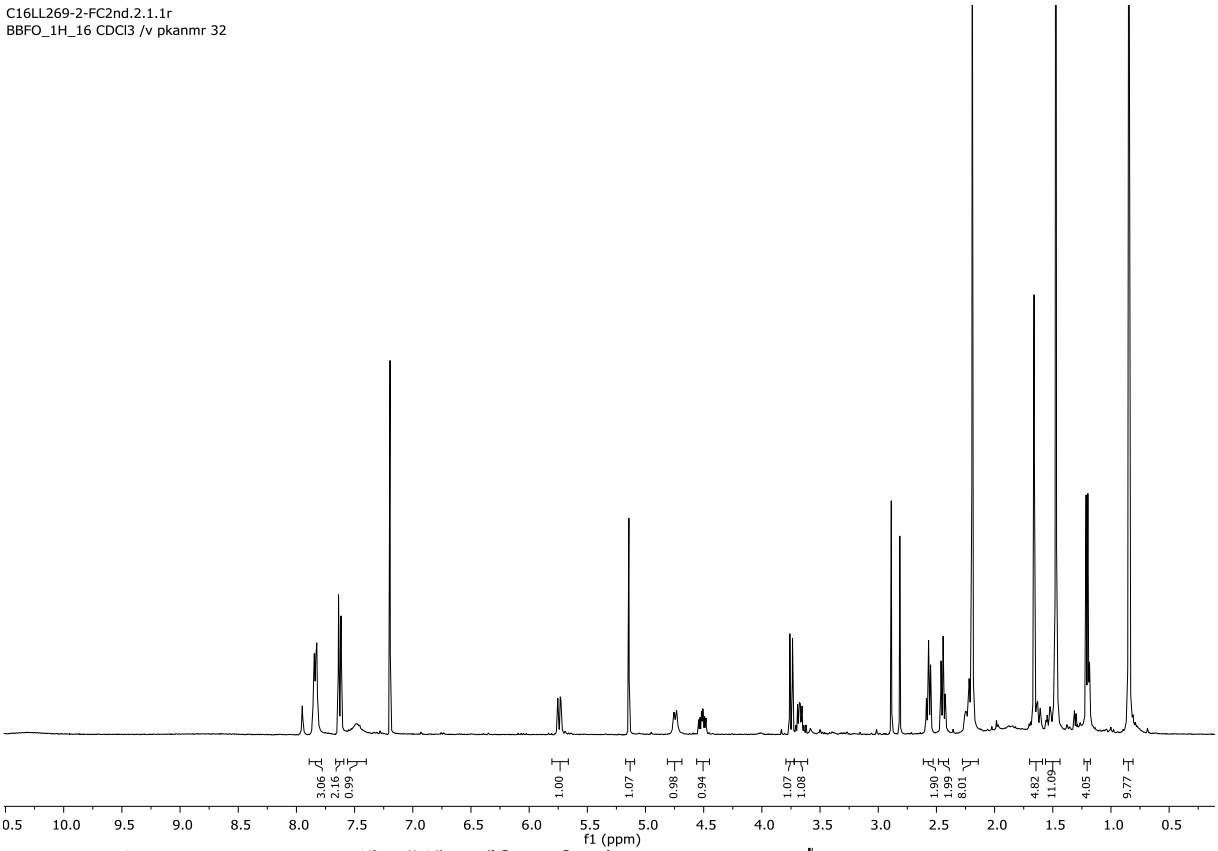
C16LL269-2-FC2nd.2.1.1r
BBFO_1H_16 CDCl3 /v pkanmr 32
3.06
2.16
0.99
1.00
1.07
0.98
0.94
1.07
1.08
1.90
1.99
8.01
4.82
11.09
4.05
9.77
f1 (ppm)

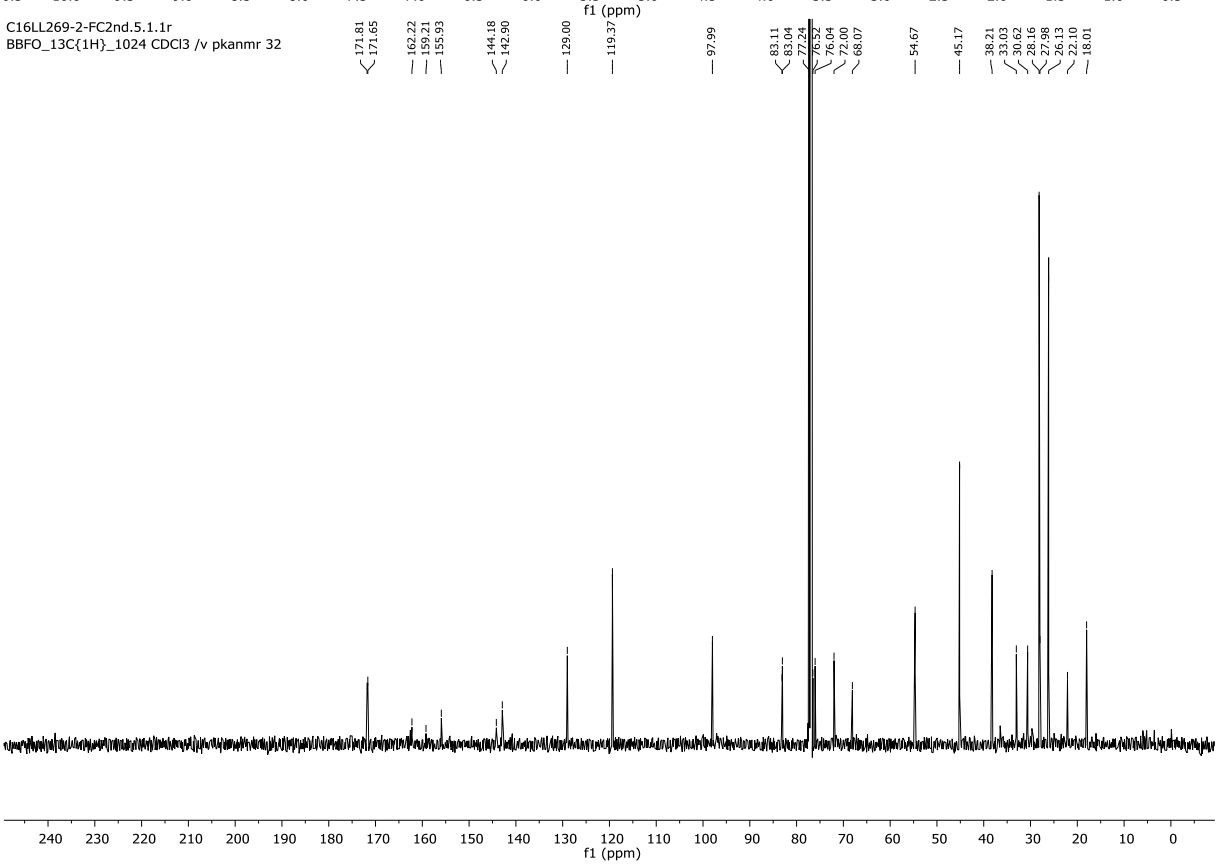
C16LL269-2-FC2nd.5.1.1r
BBFO_13C{1H}_1024 CDCl3 /v pkanmr 32
171.81
171.65
162.22
159.21
155.93
144.18
142.90
129.00
119.37
97.99
83.11
83.04
77.24
76.52
76.04
72.00
68.07
54.67
45.17
38.21
33.03
30.62
28.16
27.98
26.13
22.10
18.01
f1 (ppm)

A-209 tert-butyl (2R,4S)-2-(tert-butyl)-4-((4-((1-((2R,5S,6R)-5-((4-(dimethylamino)butanoyl)oxy)-6-methyltetrahydro-2H-pyran-2-yl)-2-oxo-1,2-dihydropyrimidin-4-yl)carbamoyl)phenyl)carbamoyl)-4-methyloxazolidine-3-carboxylate

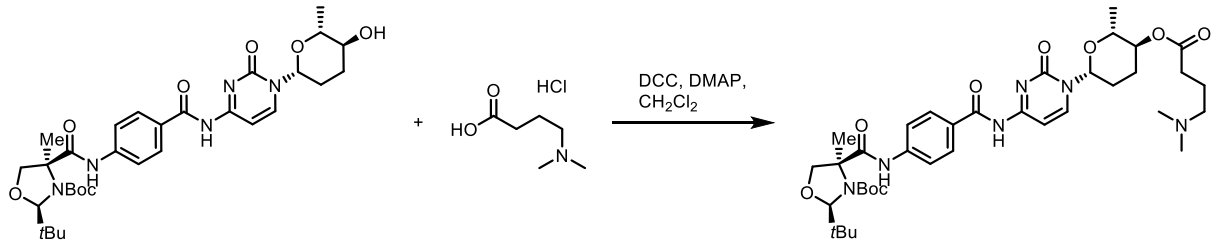

Assay: To **A-60** (13.2 mg, 21.5 µmol, 1.0 equiv) dissolved in DMF (0.3 mL) was added **A-207** (5.4 mg, 32.3 µmol, 1.5 equiv), DCC (6.7 mg, 32.3 µmol, 1.5 equiv) and DMAP (3.9 mg, 32.3 µmol, 1.5 equiv) at ambient temperature. The reaction mixture was stirred as such for 18 h. The crude was filtered over cotton wool and concentrated under reduced pressure. The brown crude was then purified by FC ($CHCl_3$:MeOH:H_2O, 85:13:2) to give the desired product (10 mg, 0.013 mmol, 64%).

Analytics: $\mathbf{R_f}$ = 0.47 ($CHCl_3$:MeOH:H_2O, 85:13:2). **^{1}H NMR** (400 MHz, Chloroform-*d*) δ 7.93 – 7.81 (m, 3H), 7.69 (d, *J* = 8.8 Hz, 2H), 7.56 – 7.50 (m, 1H), 5.81 (dd, *J* = 10.4, 2.2 Hz, 1H), 5.21 (s, 1H), 4.81 (d, *J* = 9.0 Hz, 1H), 4.60 – 4.49 (m, 1H), 3.81 (d, *J* = 9.0 Hz, 1H), 3.74 (dq, *J* = 9.6, 6.1 Hz, 1H), 2.37 (t, *J* = 7.4 Hz, 2H), 2.33 – 2.27 (m, 4H), 2.23 (s, 6H), 1.86 – 1.76 (m, 2H), 1.72 (s, 3H), 1.70 – 1.66 (m, 1H), 1.54 (s, 9H), 1.53 – 1.52 (m, 1H), 1.25 (s, 3H), 0.91 (s, 9H). **^{13}C NMR** (101 MHz, Chloroform-*d*) δ 172.76, 171.82, 162.15, 155.93, 144.16, 142.90, 128.95 (2C), 119.38 (2C), 118.84, 97.99, 83.12, 83.04, 76.48, 76.04, 71.96, 68.07, 58.67, 45.31 (2C), 38.21, 32.18, 30.62, 28.16 (3C), 27.98, 26.13 (3C), 22.83, 22.10, 18.06. **HRMS (ESI)**: 727.4021 $[M+H]^+$; calculated for $[C_{37}H_{55}N_6O_9]$: 727.4025. **$[\alpha]^{20}_D$** = -25.56 (c = 0.133, MeOH) **IR** [ATR, neat]: ν = 2925.48 m, 2855.09 m, 1697.05 s, 1669.09 s, 1597.73 m, 1483.95 s, 1376.92 m, 1247.72 s, 1162.87 m, 1093.44 m, 785.85 s cm^{-1}.

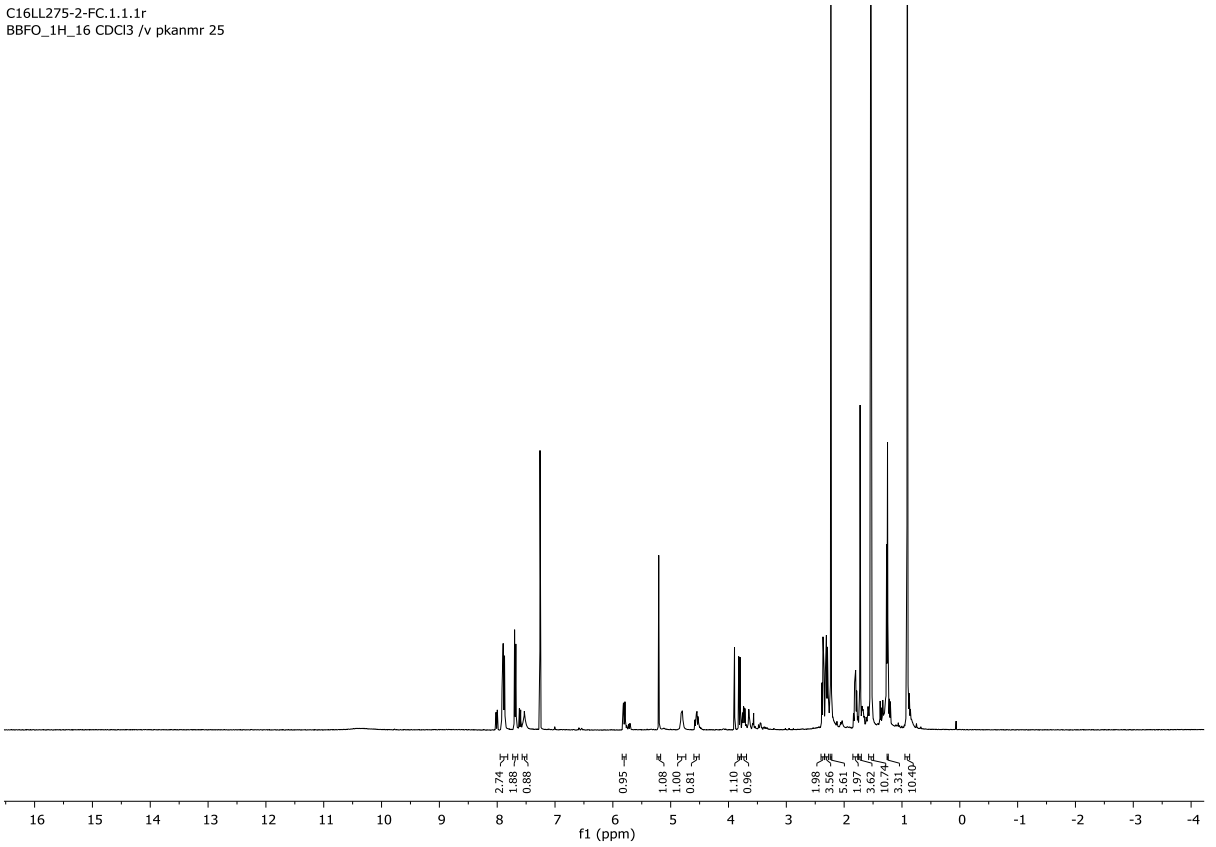
C16LL275-2-FC.1.1.1r
BBFO_1H_16 CDCl3 /v pkanmr 25
2.74
1.88
0.88
0.95
1.08
1.00
0.81
1.10
0.96
1.98
3.56
5.61
1.97
3.62
10.74
3.31
10.40
f1 (ppm)

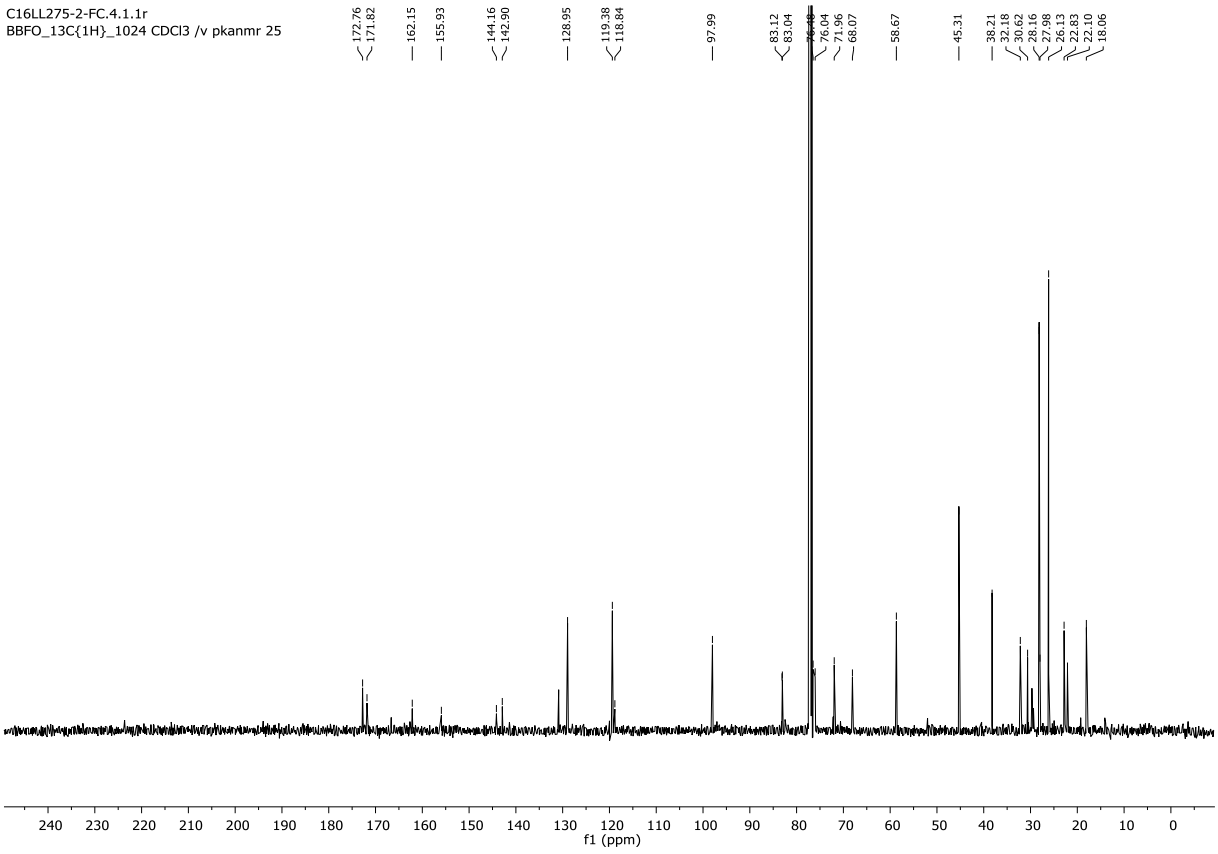
C16LL275-2-FC.4.1.1r
BBFO_13C{1H}_1024 CDCl3 /v pkanmr 25
172.76
171.82
162.15
155.93
144.16
142.90
128.95
119.38
118.84
97.99
83.12
83.04
76.04
71.96
68.07
58.67
45.31
38.21
32.18
30.62
28.16
27.98
26.13
22.83
22.10
18.06
f1 (ppm)

A-214 4-((S)-2-amino-3-hydroxy-2-methylpropanamido)-N-(1-((2R,5S,6R)-5-hydroxy-6-methyltetrahydro-2H-pyran-2-yl)-2-oxo-1,2-dihydropyrimidin-4-yl)benzamide

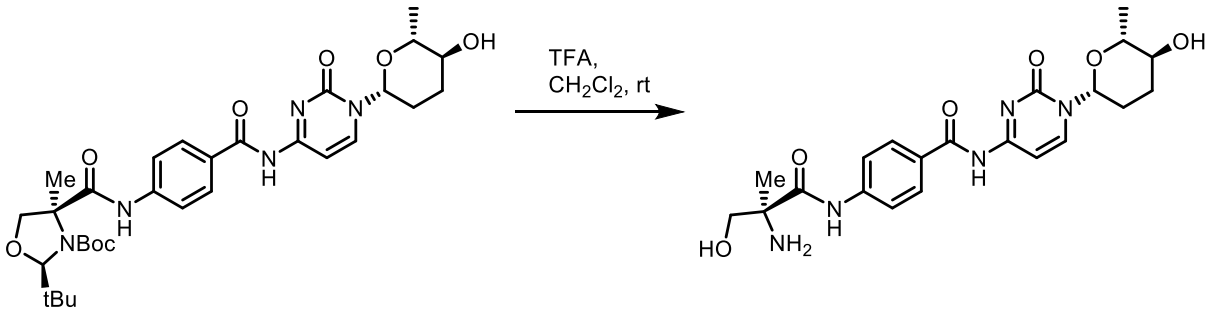

Assay: A-60 (4.0 mg, 6.5 µmol, 1.0 equiv.) was dissolved in CH_2Cl_2 (400 µL) and TFA (37.0 µL, 482.3 µmol, 74.0 equiv) was added in one portion at room temperature. The reaction mixture was stirred for 7 h and meanwhile monitored via TLC. Deuterated DMSO was then added and the dichloromethane was evaporated under diminished pressure. Crude NMR was measured (see C21LL176-3-DMSO). The reddish solution was then again dried to complete dryness.

Analytics: $\mathbf{R_f}$ = 0.51, EtOAc:MeOH (5%) for oxazolidine opened compound (TLC-MS: 658 m/z). **^{1}H NMR** (400 MHz, Methanol-d_4) δ 8.21 (d, *J* = 7.6 Hz, 1H), 8.01 (d, *J* = 8.6 Hz, 2H), 7.84 (d, *J* = 8.8 Hz, 2H), 7.56 (d, *J* = 7.6 Hz, 1H), 5.79 – 5.65 (m, 1H), 4.09 (d, *J* = 11.8 Hz, 1H), 3.82 (d, *J* = 11.8 Hz, 1H), 3.55 – 3.49 (m, 1H), 3.30 – 3.25 (m, 1H), 2.20 – 2.10 (m, 2H), 1.74 – 1.66 (m, 2H), 1.65 (s, 3H), 1.35 (d, *J* = 6.2 Hz, 3H). **HRMS (MALDI/ESI)**: 468.1863 $[M+Na]^+$; calculated for $[C_{21}H_{27}N_5NaO_6]$: 468.1854

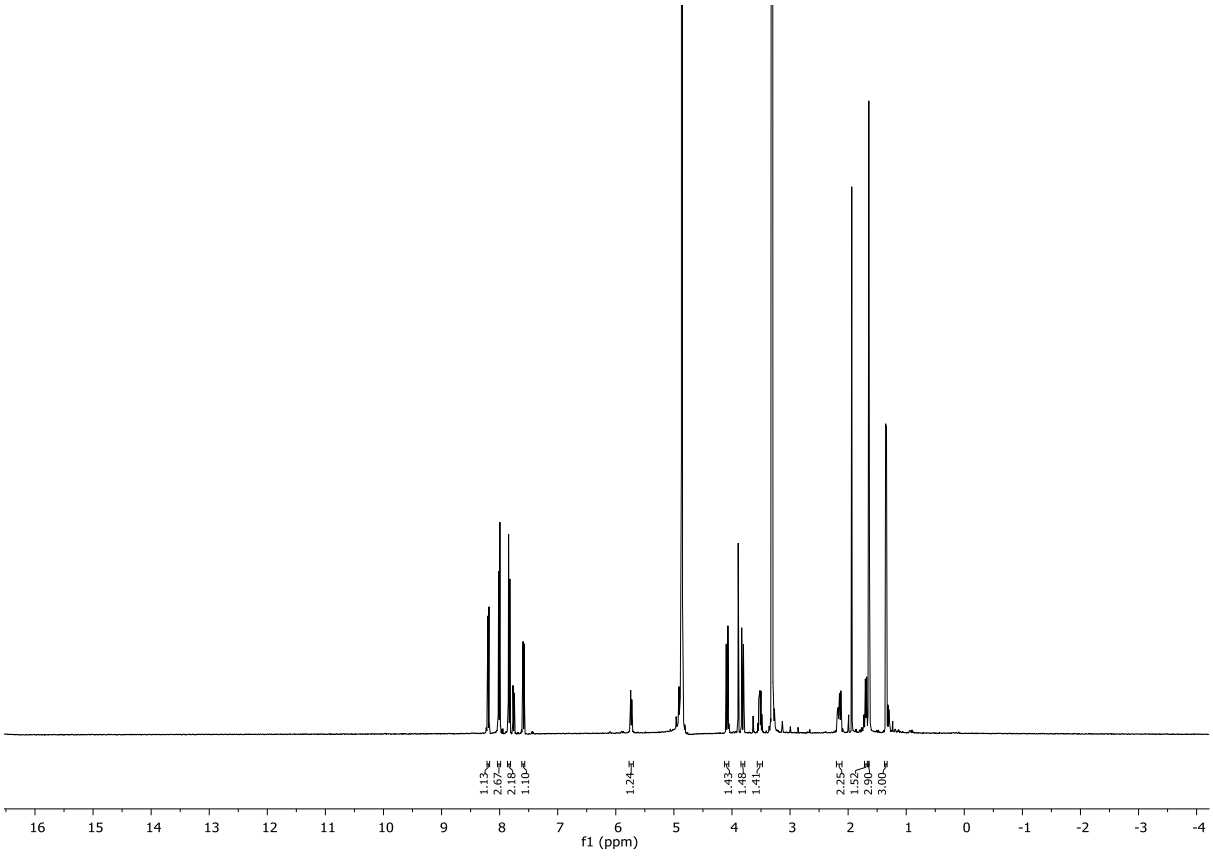
1.13
2.67
2.18
1.10
1.24
1.43
1.48
1.41
2.25
1.52
2.90
3.00
16 15 14 13 12 11 10 9 8 7 6 5 4 3 2 1 0 -1 -2 -3 -4
f1 (ppm)

A-215 (2R,3S,6R)-6-(4-(4-((S)-2-amino-3-hydroxy-2-methylpropanamido)benzamido)-2-oxopyrimidin-1(2H)-yl)-2-methyltetrahydro-2H-pyran-3-yl 3-(dimethylamino)propanoate

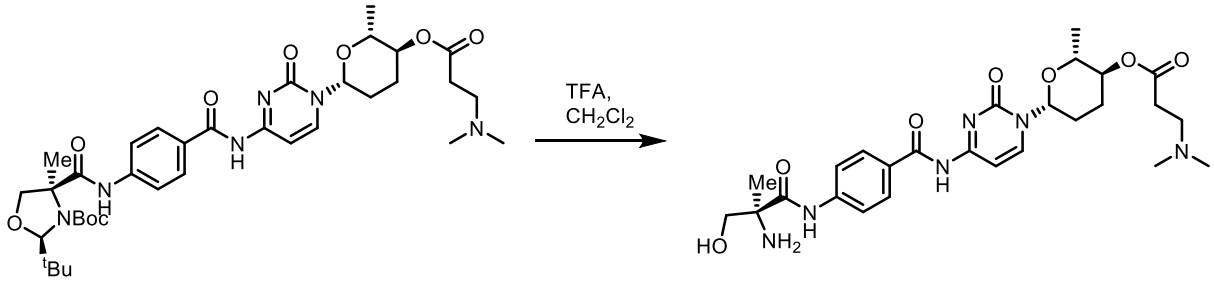

Assay: To a solution of **A-208** (4.0 mg, 5.6 µmol, 1.0 equiv.) in CH_2Cl_2 (0.4 mL) was given TFA (32 µL, 0.42 mmol, 74.0 equiv) in one portion at room temperature. The reaction mixture was stirred for 4.5 h and meanwhile monitored via TLC. The reaction mixture was then directly concentrated under diminished pressure to obtain a crude sticky oil. Purification by HPLC (RP-semiPrep 2 min isocratic 5/95 followed by 5/95 to 90/10 ACN/H_2O) gave the title compound as a white powder (2.63 mg, 4.8 µmol, 86%).

Analytics: **^{1}H NMR** (500 MHz, Methanol-d_4) δ 8.18 (dd, *J* = 7.5, 2.6 Hz, 1H), 8.00 – 7.93 (m, 2H), 7.79 (dd, *J* = 8.8, 3.6 Hz, 2H), 7.56 (d, *J* = 7.5 Hz, 1H), 5.79 (dd, *J* = 7.1, 2.9 Hz, 1H), 4.63 (td, *J* = 9.9, 3.3 Hz, 1H), 4.17 (d, *J* = 11.9 Hz, 1H), 3.89 (d, *J* = 12.3 Hz, 1H), 3.80 (ddd, *J* = 9.8, 6.2, 4.0 Hz, 1H), 3.46 (t, *J* = 7.0 Hz, 2H), 2.97 – 2.88 (m, 8H), 2.32 – 2.28 (m, 1H), 2.22 – 2.12 (m, 1H), 1.78 (td, *J* = 9.7, 9.2, 4.7 Hz, 2H), 1.68 (s, 3H), 1.27 (dd, *J* = 6.2, 1.6 Hz, 3H). **^{13}C NMR** (126 MHz, Methanol-d_4) δ 171.07, 170.38, 168.13, 164.66, 157.10, 146.37, 143.63, 130.26 (2 C), 130.10 (2 C), 121.32, 98.84, 84.44, 77.34, 74.42, 65.53, 63.60, 54.19, 43.74 (2 C), 30.80, 30.07, 28.79, 18.84, 18.35. **$[\alpha]^{20}_D$** = +34.24 (c = 0.146, MeOH). **IR** [ATR, neat]: ν = 1674.87 s, 1635.34 m, 1481.06 m, 1243.86 w, 1201.43 m, 1133.94 w, 1016.3 s, 669.18 m cm^{-1}. **HRMS** was not found.

C37LL-281_500.1.1.1r
Av500: proton of
Temp: 298K
Solv: CDCl3

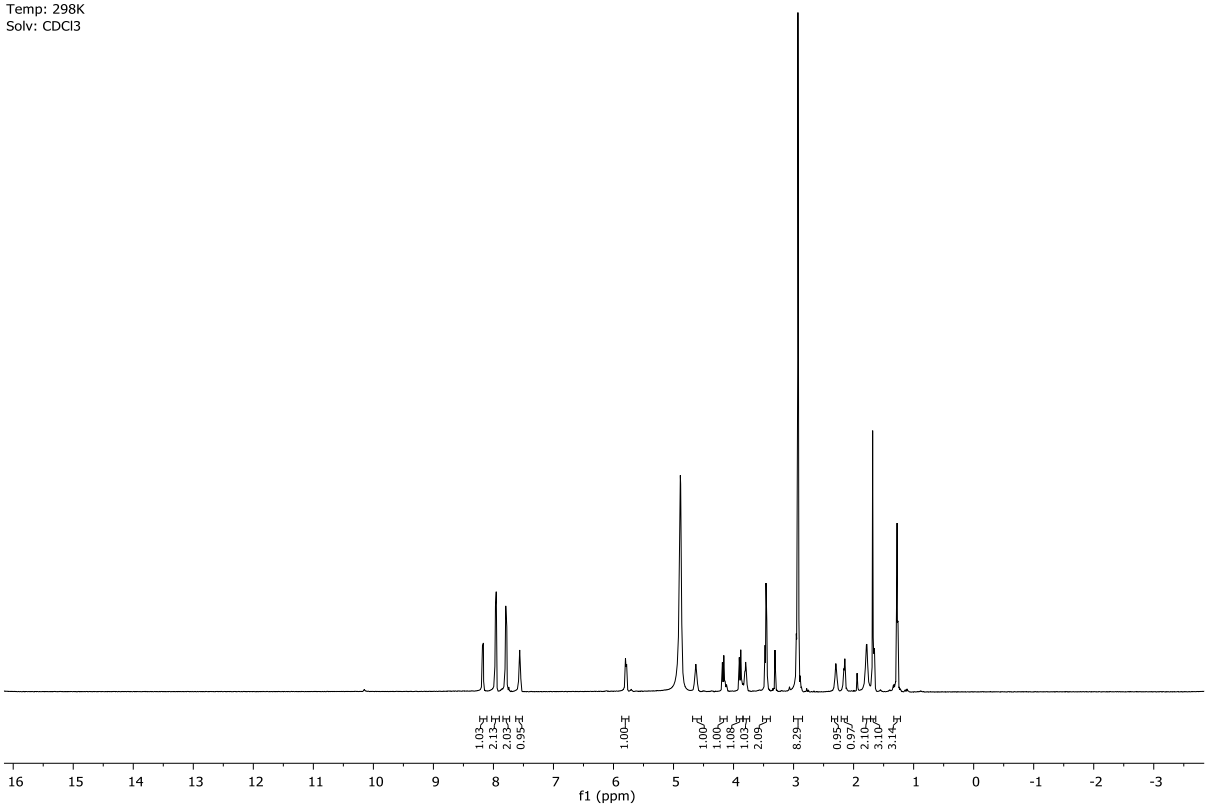

C37LL-281_500.2.1.1r
Av500: 13C{1H} of
Temp: 298K
Solv: CDCl3
Head: mTXI

171.07
170.38
168.13
164.66
157.10
146.37
143.63
130.26
130.10
121.32
98.84
84.44
77.34
74.42
65.53
63.60
54.19
43.74
43.71
30.80
30.07
28.79
18.84
18.81
18.35
18.32

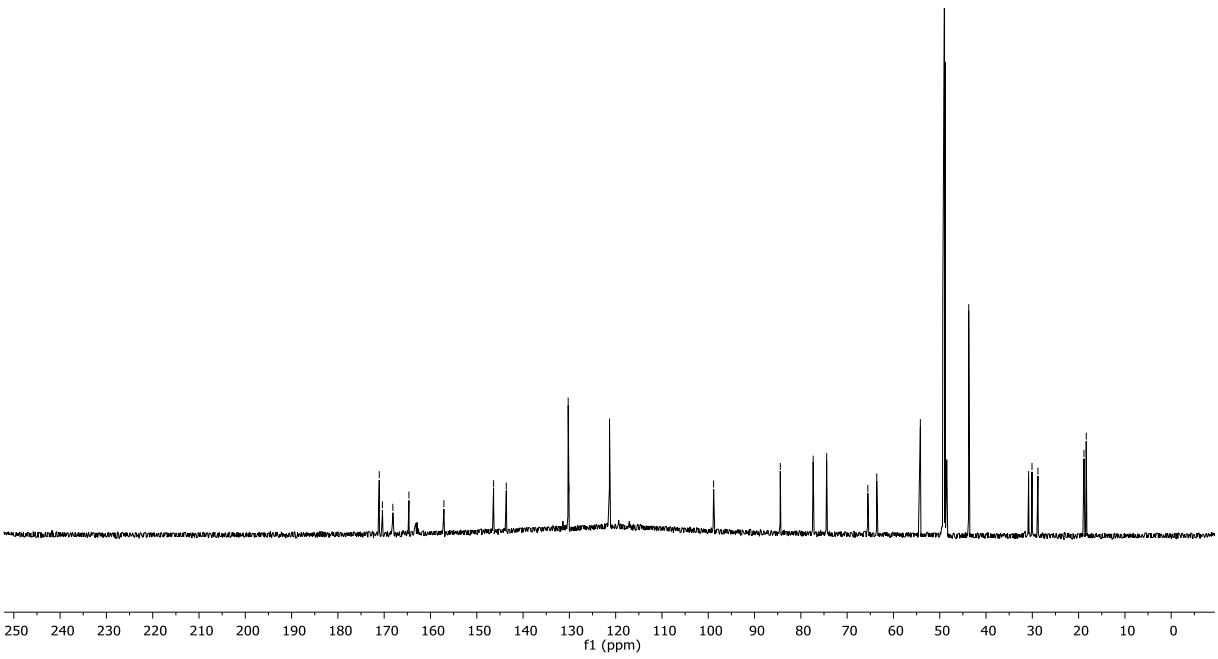

A-216 (2R,3S,6R)-6-(4-(4-((S)-2-amino-3-hydroxy-2-methylpropanamido)benzamido)-2-oxopyrimidin-1(2H)-yl)-2-methyltetrahydro-2H-pyran-3-yl 4-(dimethylamino)butanoate

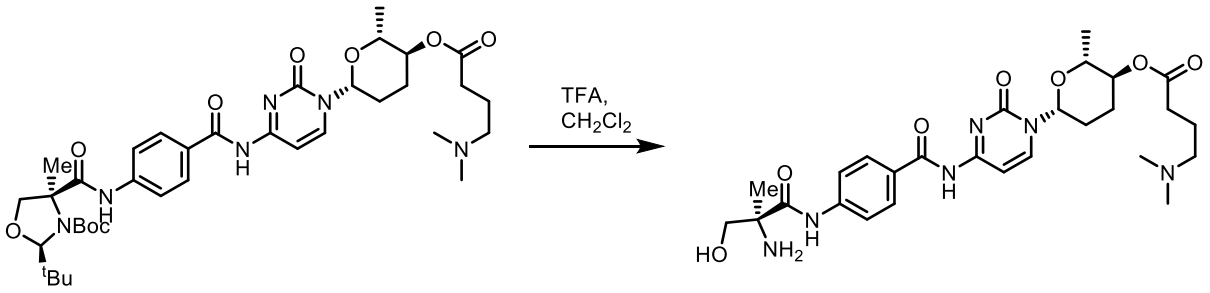

Assay: A-209 (4.6 mg, 6.3 µmol, 1.0 equiv.) was dissolved in CH_2Cl_2 (0.4 mL) and TFA (41 µL, 0.53 mmol, 74.0 equiv) was added in one portion at room temperature. The reaction mixture was stirred for 180 min and meanwhile monitored via TLC. The reaction mixture was then directly concentrated under diminished pressure to obtain a crude brown oil. Purification by HPLC (RP-semiPrep 2 min isocratic 5/95 followed by 5/95 to 90/10 ACN/H_2O) gave the title compound as a white solid (2.45 mg, 0.44 µmol, 70%).

Analytics: **^{1}H NMR** (400 MHz, Methanol-d_4) δ 8.21 (d, *J* = 7.6 Hz, 1H), 8.01 (d, *J* = 8.9 Hz, 2H), 7.84 (d, *J* = 8.9 Hz, 2H), 7.62 (d, *J* = 7.5 Hz, 1H), 5.87 – 5.72 (m, 1H), 4.63 (td, *J* = 9.9, 4.6 Hz, 1H), 4.09 (d, *J* = 11.8 Hz, 1H), 3.91 – 3.68 (m, 2H), 3.24 – 3.14 (m, 2H), 2.92 (s, 6H), 2.53 (t, *J* = 7.1 Hz, 2H), 2.33 – 2.26 (m, 1H), 2.17 (dt, *J* = 8.5, 2.4 Hz, 1H), 2.09 – 1.97 (m, 2H), 1.89 – 1.72 (m, 2H), 1.65 (s, 3H), 1.28 (d, *J* = 6.1 Hz, 3H). **^{13}C NMR** (126 MHz, Methanol-d_4) δ 171.63, 168.87, 166.84, 163.39, 155.83, 144.97, 142.28, 128.88 (2 C), 128.82, 119.94 (2 C), 97.50, 83.14, 76.12, 72.46, 64.09, 62.18, 56.68, 42.09 (2 C), 30.07, 29.50, 27.54, 19.44, 17.48, 17.00. **$[\alpha]^{20}_D$** = +86.19 (c = 0.058, MeOH). **HRMS (ESI)**: 559.2871 $[M+H]^+$; calculated for $[C_{27}H_{39}N_6O_7]$: 559.2875. **IR** [ATR, neat]: ν = 1671.98 s, 1601.59 m, 1482.99 m, 1397.17 w, 1305.57 w, 1250.61 w, 1186.97 s, 1131.05 s, 1095.37 m, 1006.66 m, 835.03 m, 800.31 m, 720.28 m cm^{-1}.

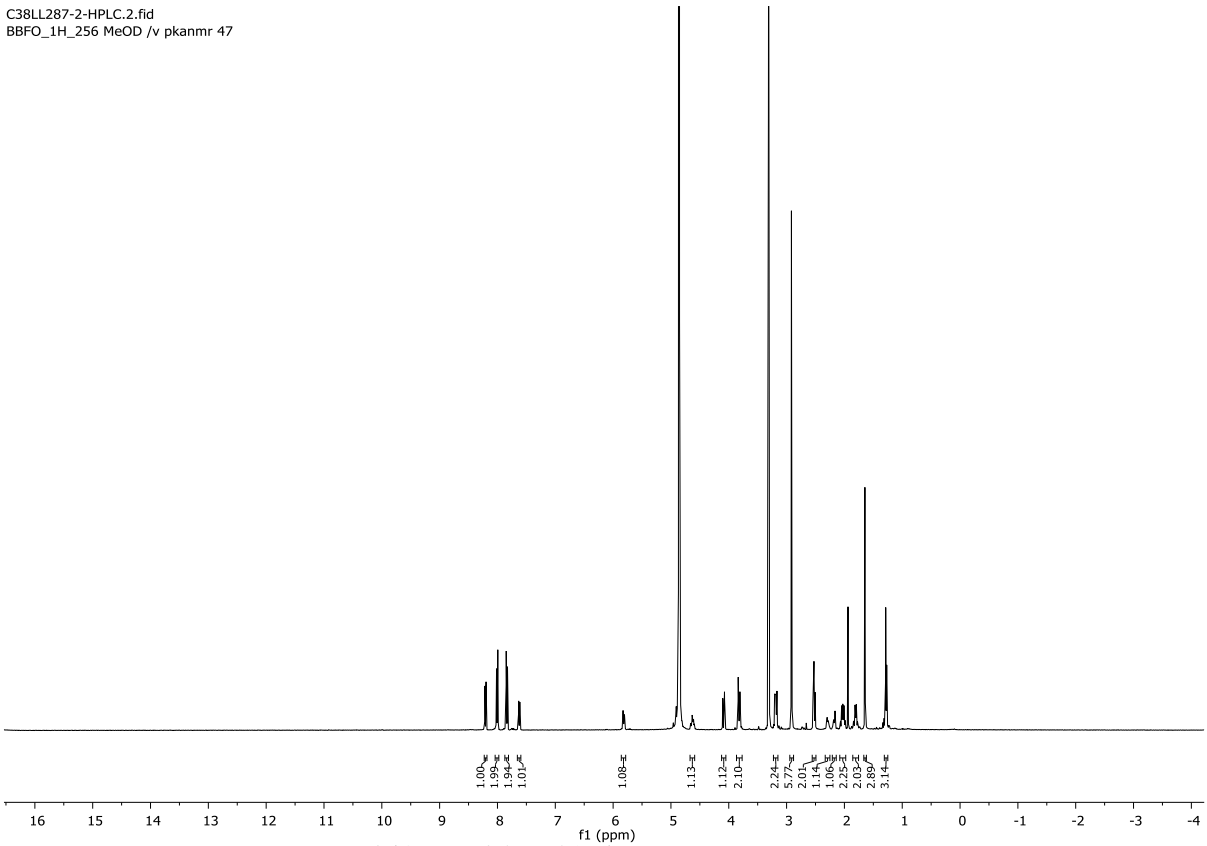
C38LL287-2-HPLC.2.fid
BBFO_1H_256 MeOD /v pkanmr 47
1.00
1.99
1.94
1.01
1.08
1.13
1.12
2.10
2.24
5.77
2.01
1.14
1.06
2.25
2.03
2.89
3.14
f1 (ppm)

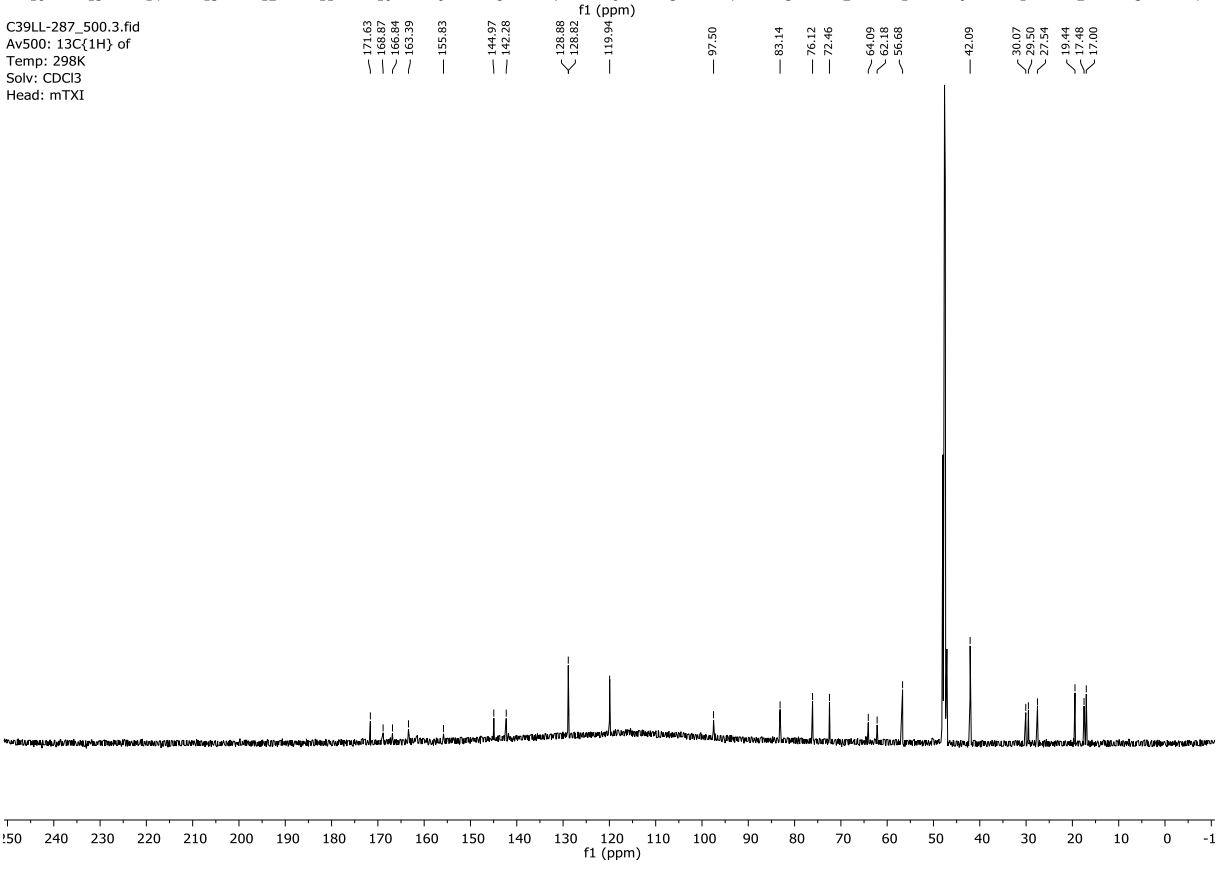
C39LL-287_500.3.fid
Av500: 13C{1H} of
Temp: 298K
Solv: CDCl3
Head: mTXI
171.63
168.87
166.84
163.39
155.83
144.97
142.28
128.88
128.82
119.94
97.50
83.14
76.12
72.46
64.09
62.18
56.68
42.09
30.07
29.50
27.54
19.44
17.48
17.00
f1 (ppm)

3.2.2 Nummularine H (N-1)

N-32 5-hydroxy-2-methoxybenzaldehyde

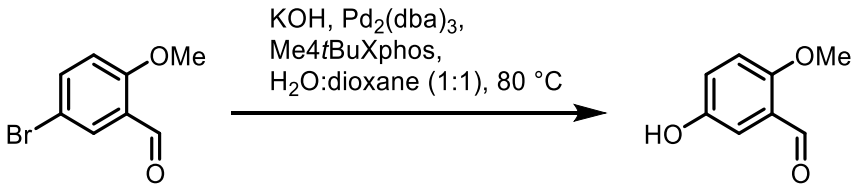

Assay: In a microwave vial, **N-31** (106 mg, 0.49 mmol, 1.0 equiv), Pd_2dba_3 (9.0 mg, 9.9 µmol, 2 mol%), phosphine ligand (1.9 mg, 3.9 µmol, 1 mol%) and KOH (55.3 mg, 0.99 mmol, 2.0 equiv) were combined. The reaction vessel was set under vacuum and refilled with argon (3 times) followed by the addition of degassed dioxane (0.4 mL) and H_2O (0.4 mL). The reaction mixture was then heated up in an oil bath to 80 °C and was stirred as such for 18 h. Filtration over Celite and evaporation of solvents gave a yellowish crude which was then purified by FC (EtOAc:hexane, 1:2) to give an impure mixture of the desired product as a yellow solid.

Analytics: **^{1}H NMR** (400 MHz, Chloroform-*d*) δ 10.41 (s, 1H), 7.09 (dd, *J* = 9.0, 3.2 Hz, 1H), 6.90 (d, *J* = 9.0 Hz, 1H), 6.75 (d, *J* = 8.7 Hz, 1H), 4.65 (s, 1H), 3.89 (s, 3H).

Compound literature known

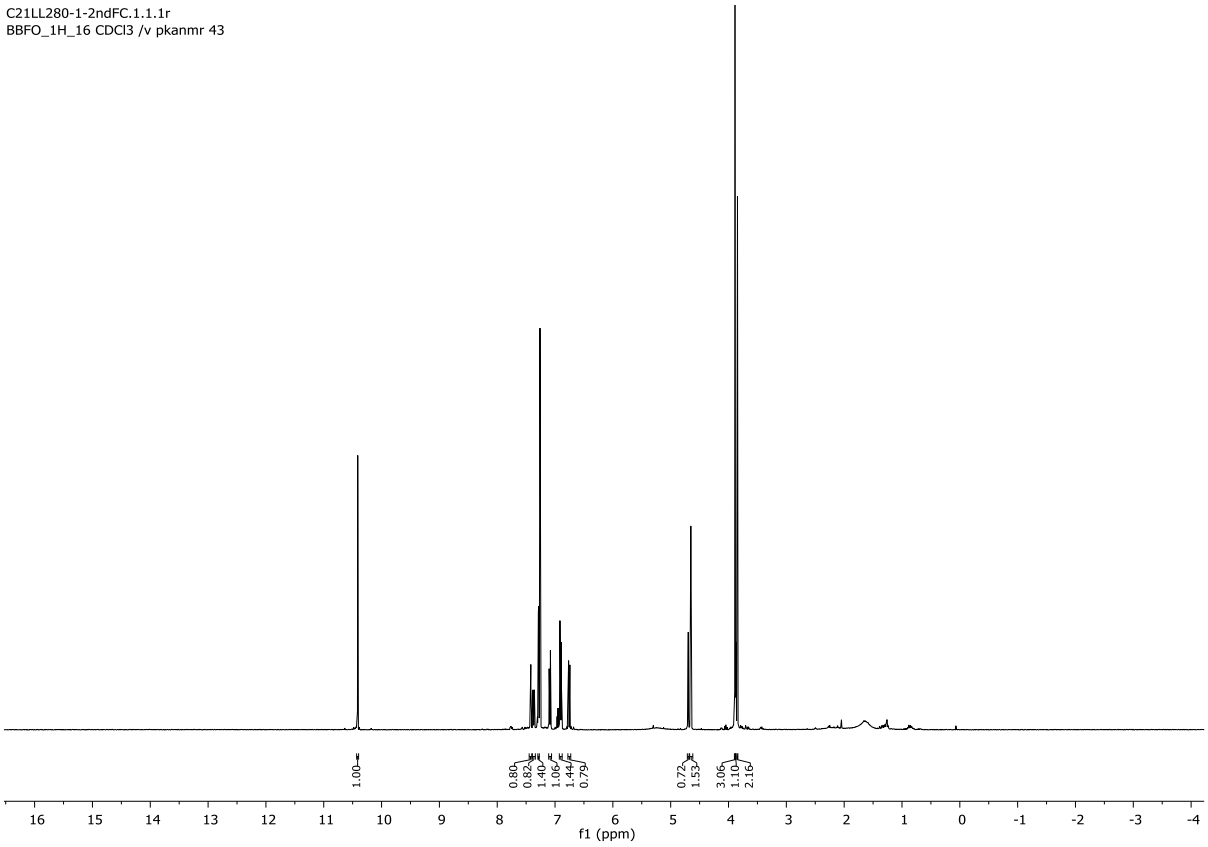
C21LL280-1-2ndFC.1.1.1r
BBFO_1H_16 CDCl3 /v pkanmr 43
1.00
0.80
0.82
1.40
1.06
1.44
0.79
0.72
1.53
3.06
1.10
2.16
16 15 14 13 12 11 10 9 8 7 6 5 4 3 2 1 0 -1 -2 -3 -4
f1 (ppm)

N-33 5-(benzyloxy)-2-methoxybenzaldehyde

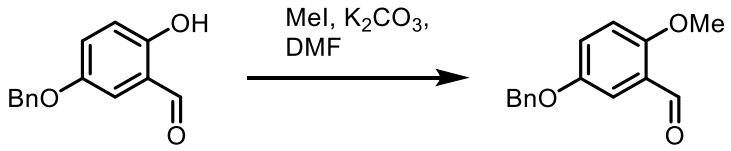

Assay: To a solution of **N-65** (913.0 mg, 4.0 mmol, 1.0 equiv) in DMF (10.0 mL) was added K_2CO_3 (829.0 mg, 6.0 mmol, 1.5 equiv) and the reaction was stirred at ambient temperature for 30 min before MeI (375.0 µL, 6.0 mmol, 1.5 equiv) was added dropwise. The reaction mixture was stirred as such over the weekend and meanwhile turned yellow. Full consumption of starting material was observed. The solvents were then fully removed under diminished pressure. The crude was purified by FC (EtOAc:hexane, 1:10 -> 1:5) to give the target compound as a white crystalline solid (953 mg, 3.933 mmol, 98%).

Analytics: $\mathbf{R_f}$ = 0.14 (EtOAc:hexane, 1:10). **^{1}H NMR** (400 MHz, Chloroform-*d*) δ 10.44 (s, 1H), 7.49 – 7.30 (m, 6H), 7.21 (dd, *J* = 9.1, 3.3 Hz, 1H), 6.95 (d, *J* = 9.1 Hz, 1H), 5.05 (s, 2H), 3.90 (s, 3H). **^{13}C NMR** (101 MHz, Chloroform-*d*) δ 189.67, 157.01, 152.90, 136.81, 128.77 (2C), 128.23, 127.73 (2C), 125.13, 124.40, 113.49, 112.01, 70.83, 56.30. **HRMS (ESI)**: 265.0836 $[M+Na]^+$; calculated for $[C_{15}H_{14}NaO_3]$: 396.9433. **IR** [ATR, neat]: ν = 3035.41 w, 2875.34 w, 1679.69 s, 1609.31 w, 1585.20 w, 1492.63 s, 1454.06 s, 1421.28 s, 1395.25 s, 1382.71 m, 1313.29 m, 1274.72 s, 1220.72 s, 1159.97 s, 1104.05 w, 1024.98 s, 1011.48 s, 873.60 m, 848.53 m, 823.46 m, 762.71 m, 723.18 s cm^{-1}.

Compound literature known

C27LL284-2-FC.1.fid
BBFO_1H_16 CDCl3 /v pkanmr 34

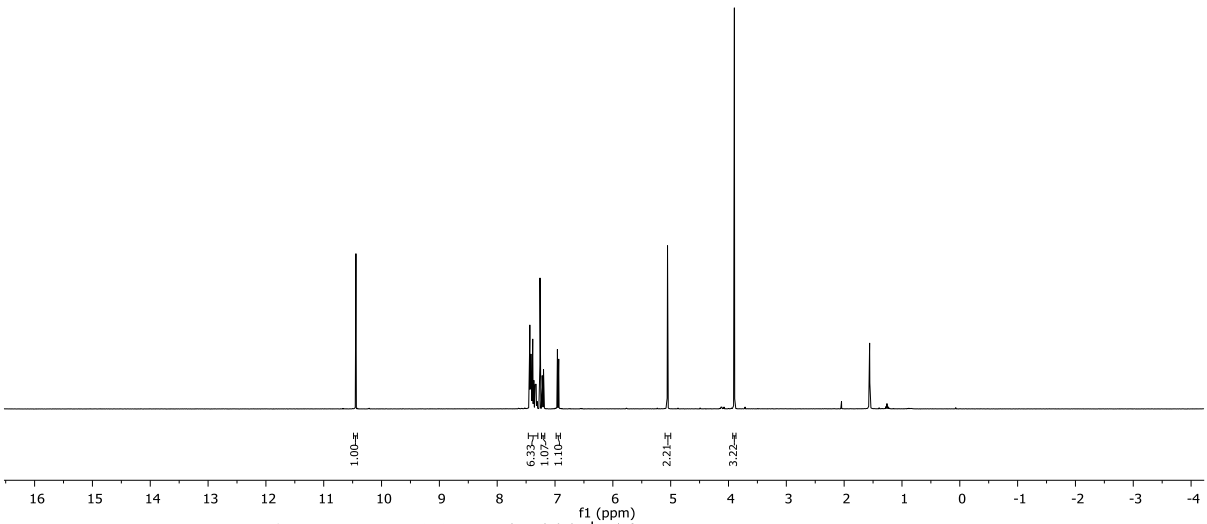

C27LL284-2-FC.2.fid
BBFO_13C{1H}_256 CDCl3 /v pkanmr 34

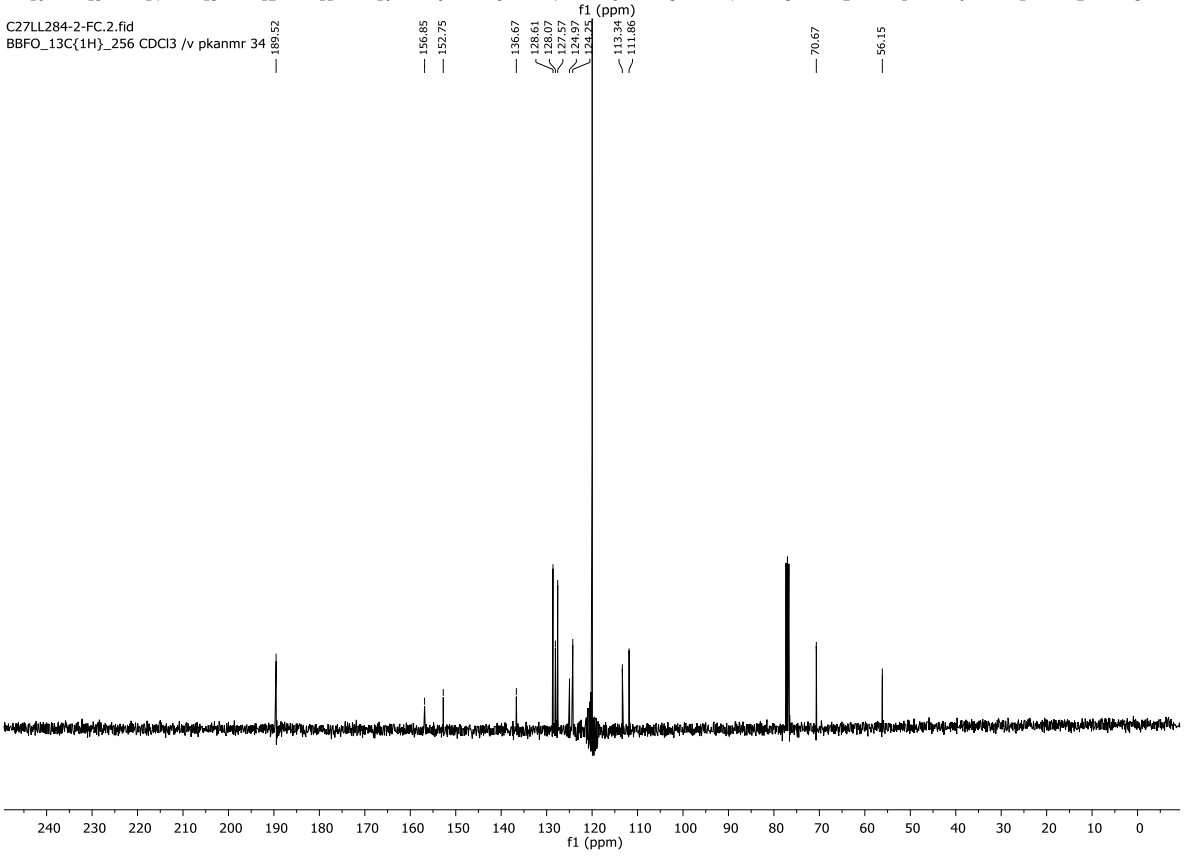

N-30 4-(benzyloxy)-2-(2,2-dibromovinyl)-1-methoxybenzene

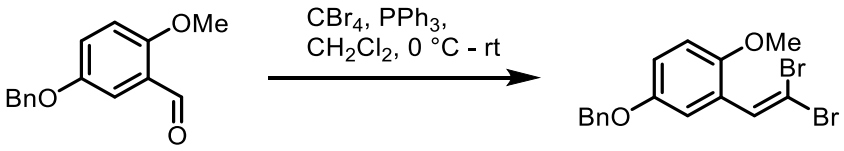

Assay: To a solution of aldehyde **N-33** (953 mg, 3.93 mmol, 1.0 equiv) in CH_2Cl_2 (30 mL) at 0 °C was added CBr_4 (2.61 g, 7.87 mmol, 2.0 equiv) followed by the addition of PPh_3 (4.13 g, 15.73 mmol, 4.0 equiv). The reaction was allowed to slowly warm to ambient temperature and meanwhile turned from yellow to orange. After stirring for 1.5 h the reaction mixture was diluted with hexane and filtered over a pad of Celite/silica (pre-washed with CH_2Cl_2) in order to remove the triphenylphosphine oxide. The filtrate was concentrated and purified via FC (EtOAc:hexane, 1:10) to give the title compound as a brown oil (1.16 g, 2.9 mmol, 74%) which crystallized after exposing to air to a slightly yellow solid.

Analytics: $\mathbf{R_f}$ = 0.39 (EtOAc:hexane, 1:10). **^{1}H NMR** (400 MHz, Chloroform-*d*) δ 7.59 (s, 1H), 7.45 – 7.28 (m, 6H), 6.94 (dd, *J* = 8.9, 3.1 Hz, 1H), 6.79 (d, *J* = 9.0 Hz, 1H), 5.04 (s, 2H), 3.79 (s, 3H). **^{13}C NMR** (101 MHz, Chloroform-*d*) δ 152.29, 151.30, 137.23, 132.66, 128.74 (2C), 128.08, 127.60 (2C), 124.99, 116.59, 115.81, 111.72, 90.03, 70.96, 56.20. **HRMS (ESI)**: 396.9438 $[M+H]^+$; calculated for $[C_{16}H_{15}Br_2O_2]$: 396.9433. **IR** [ATR, neat]: ν = 2938.02 w, 2835.81 w, 1578.45 w, 1487.81 w, 1283.39 m, 1214.93 s, 1180.22 s, 1026.91 s, 874.56 m, 798.39 s, 730.89 s cm^{-1}. **m.p.**: 77.1 °C.

C09LL285.1.1.1r
BBFO_1H_16 CDCl3 /v pkanmr 1

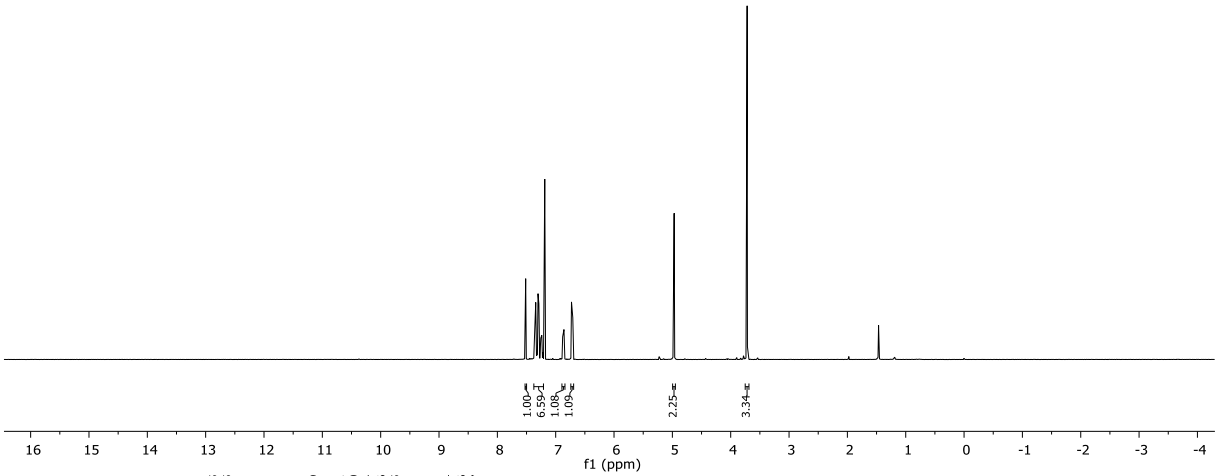

C27LL285-3-FC.2.1.1r
BBFO_13C{1H}_1024 CDCl3 /v pkanmr 28

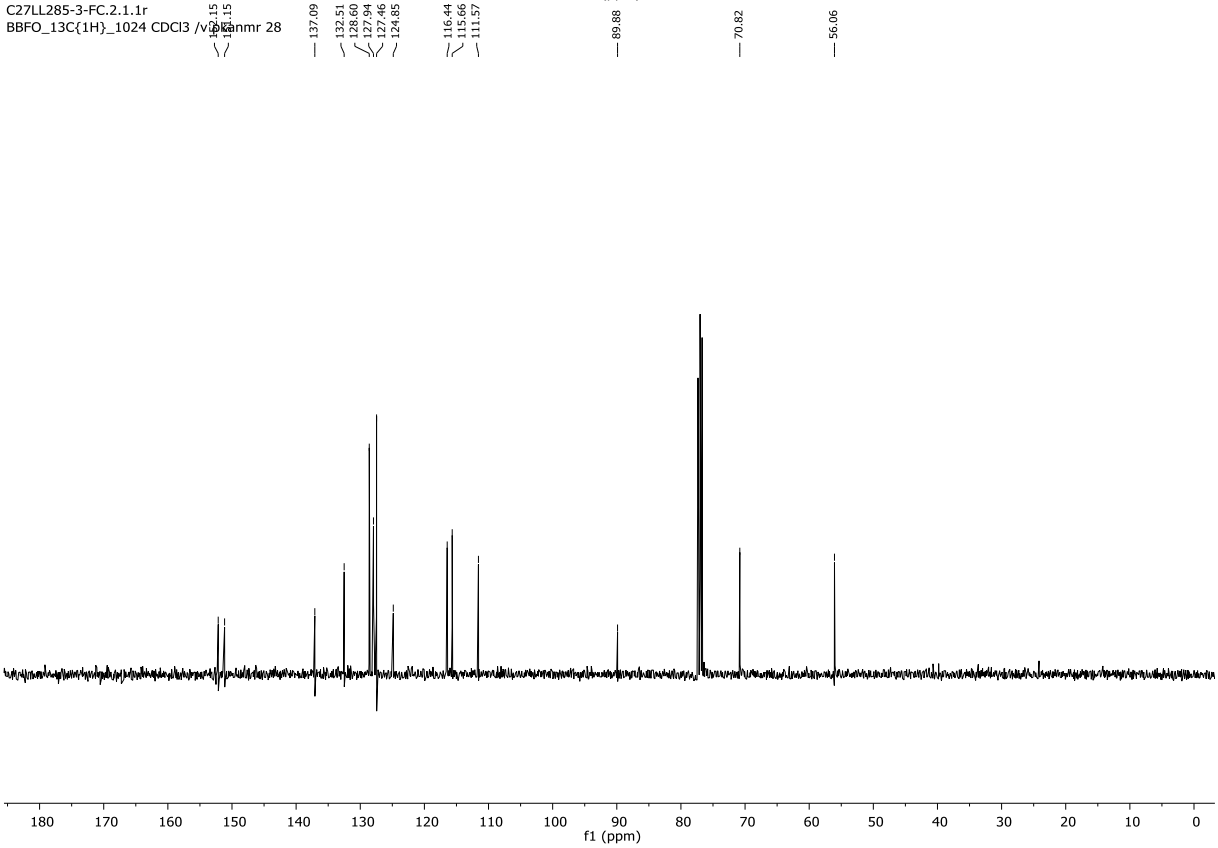

N-34 4-(benzyloxy)-2-(bromoethynyl)-1-methoxybenzene

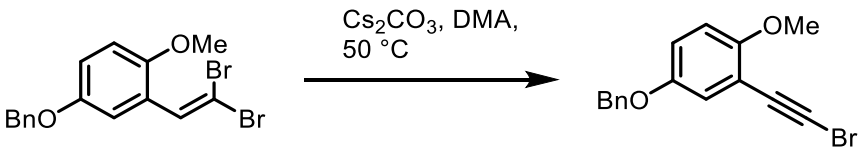

Assay: To dibromovinyl compound **N-30** (151 mg, 0.38 mmol, 1.0 equiv) in DMA (1.8 mL) was added Cs_2CO_3 (247.2 mg, 0.76 mmol, 2.0 equiv) and the reaction mixture was heated up to 50 °C and stirred as such for 16 h. The reaction mixture was then diluted with distilled H_2O (3 mL) and EtOAc (3 mL). The phases were separated and the aqueous phase was extracted with EtOAc (3 x 3 mL). The combined organic phases were dried over $MgSO_4$ and concentrated under reduced pressure. Purification by FC (EtAOc:hexane, 1:10) gave the title compound as a yellow solid (needles) (52.3 mg, 0.17 mmol, 44%).

Analytics: $\mathbf{R_f}$ = 0.36 (EtOAc:hexane, 1:10). **HRMS (ESI)**: 334.0441 $[M+NH_4]^+$; calculated for $[C_{16}H_{17}BrNO_2]$: 334.0437. **^{1}H NMR** (400 MHz, Chloroform-*d*) δ 7.47 – 7.29 (m, 5H), 7.05 (d, *J* = 3.1 Hz, 1H), 6.93 (dd, *J* = 9.1, 3.1 Hz, 1H), 6.79 (d, *J* = 9.1 Hz, 1H), 5.00 (s, 2H), 3.84 (s, 3H). **^{13}C NMR** (101 MHz, Chloroform-*d*) δ 155.54, 152.41, 137.01, 128.74 (2C), 128.15, 127.62 (2C), 119.99, 117.36, 112.45, 112.07, 76.49, 70.89, 56.51, 53.41. **IR** [ATR, neat]: ν = 1497.45 s, 1455.99 w, 1282.43 w, 1229.40 s, 1027.87 m, 736.67 m, 696.18 m cm^{-1}. **m.p.**: 76.3 °C.

C23LL258-1-FC.1.fid
BBFO_1H_16 CDCl3 /v pkanmr 49

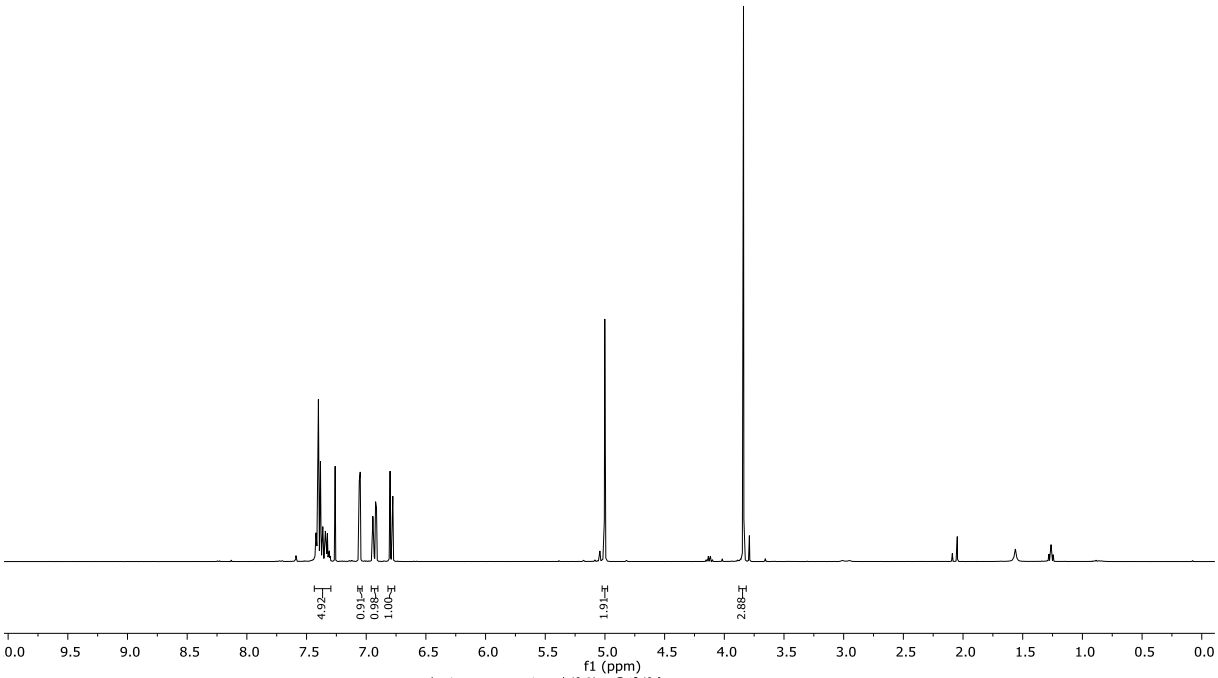

C23LL258-1-FC.2.1.1r
BBFO_13C{1H}_256 CDCl3 /v pkanmr 49

155.54
152.41
137.01
128.74
128.15
127.62
119.99
117.36
112.45
112.07
76.49
70.89
56.51
53.41

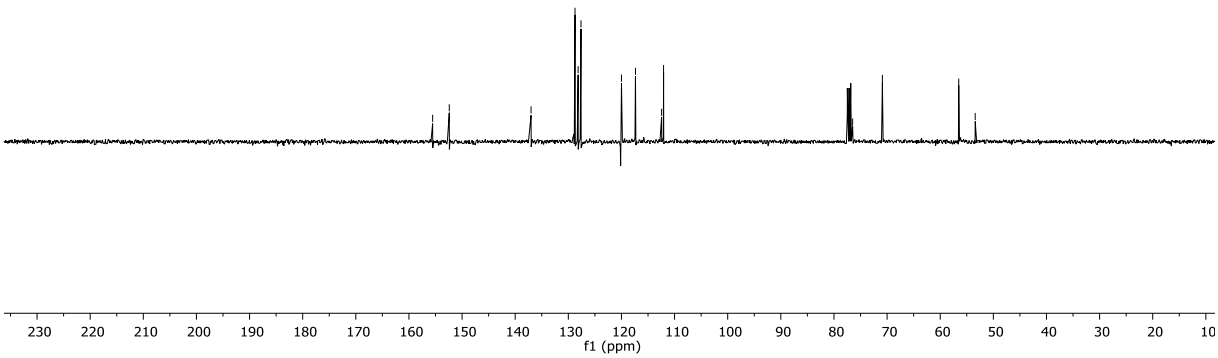

N-36 N-benzyl-N-((5-(benzyloxy)-2-methoxyphenyl)ethynyl)-4-methylbenzenesulfonamide

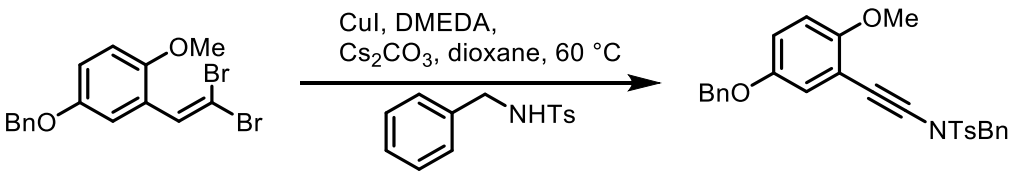

Assay: A flame dried Schlenk tube was charged with N-benzyl-4-methylbenzenesulfonamide (450 mg, 1.72 mmol, 1.0 equiv) and dibromovinyl **N-30** (754 mg, 1.89 mmol, 1.1 equiv). It was then evacuated under high vacuum and backfilled with argon (5 times). The Schlenk tube was then channeled into the glovebox where CuI (41 mg, 0.22 mmol, 0.13 equiv) and Cs_2CO_3 (2.24 g, 6.89 mmol, 4.0 equiv) were added. Again outside the glovebox, degassed dioxane (6 mL) was added followed by DMEDA (35.0 µL, 0.32 mmol, 0.19 equiv) which was prior bubbled through by a stream of argon over 15 min. The reaction mixture was stirred for 25 h at 60 °C resulting in a green suspension. The mixture was filtered over a pad of Celite and was subsequently concentrated under reduced pressure. Purification by FC (EtOAc:hexane, 1:5) gave the target compound (753.5 mg, 1.51 mmol, 88%) along with existing starting material (sulfonamide – slightly impure, 100.0 mg, 0.25 mmol, 15%).

Analytics: $\mathbf{R_f}$ = 0.2 (EtOAc:hexane, 1:5). **^{1}H NMR** (400 MHz, Chloroform-*d*) δ 7.83 (d, *J* = 8.4 Hz, 2H), 7.42 – 7.26 (m, 12H), 6.84 – 6.80 (m, 2H), 6.73 (d, *J* = 9.8 Hz, 1H), 4.96 (s, 2H), 4.59 (s, 2H), 3.76 (s, 3H), 2.43 (s, 3H). **^{13}C NMR** (101 MHz, Chloroform-*d*) δ 154.47, 152.51, 144.57, 137.15, 134.96, 134.67, 129.73 (2 C), 129.14 (2 C), 128.72 (2 C), 128.57 (2 C), 128.37, 128.12, 128.00 (2 C), 127.63 (2 C), 118.96, 115.72, 113.20, 112.33, 86.73, 70.86, 67.93, 56.61, 55.95, 21.80.

C27LL289-2-FC.1.1.1r
BBFO_1H_16 CDCl3 /v pkanmr 3

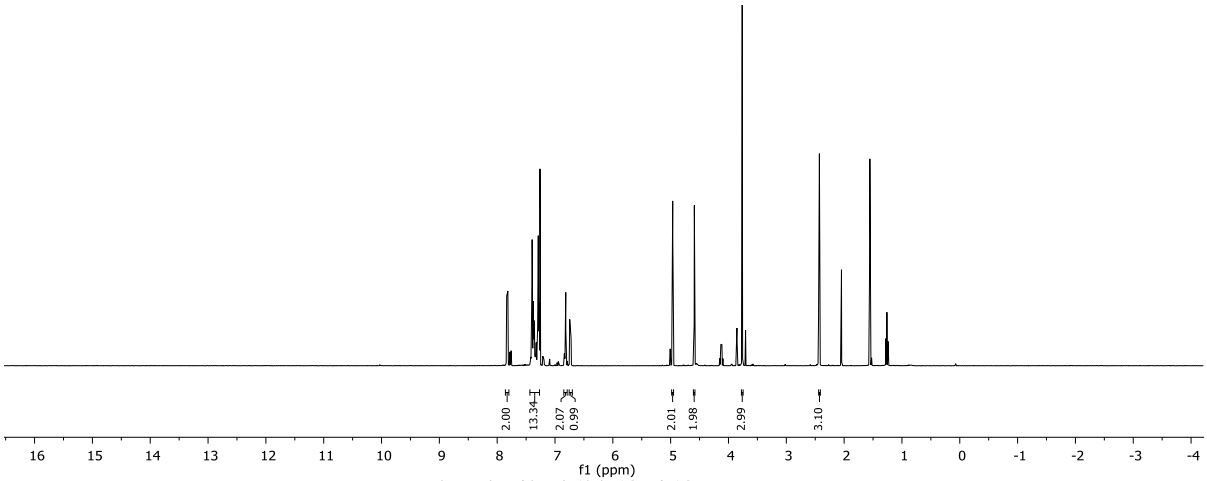

C27LL289-2-FC.2.1.1r
BBFO_13C{1H}_1024 CDCl3 /v pkanmr 3

154.47
152.51
144.57
137.15
134.96
134.67
129.73
129.14
128.72
128.57
128.37
128.12
128.00
127.63
118.96
115.72
113.20
112.33
86.73
70.86
67.93
56.61
55.95
21.80

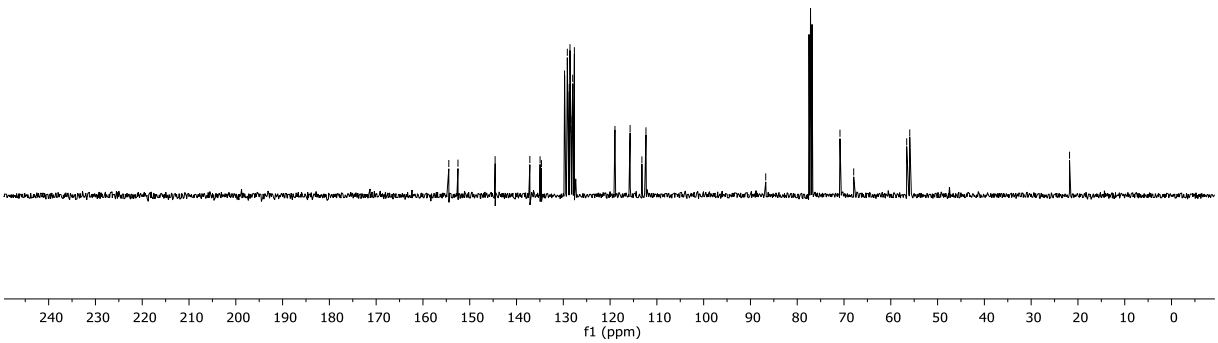

N-36 N-benzyl-N-((5-(benzyloxy)-2-methoxyphenyl)ethynyl)-4-methylbenzenesulfonamide

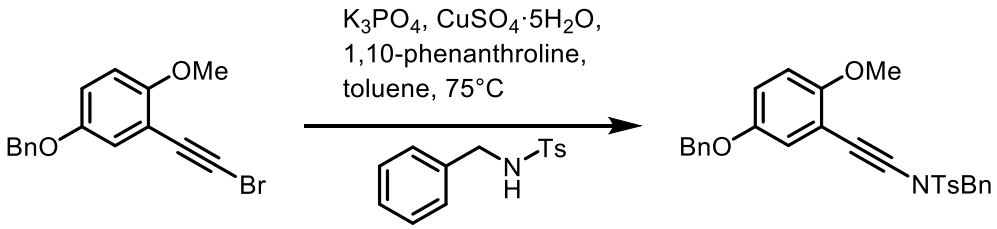

Assay: A flame dried microwave vial was charged with sulfonamide (40 mg, 0.15 mmol, 1.0 equiv), alkyne **N-34** (53.4 mg, 0.17 mmol, 1.1 equiv) and K_3PO_4 (39 mg, 183.7 mmol, 1.2 equiv), phenantroline (55 mg, 30.6 µmol, 0.2 equiv) and $CuSO_4{\cdot}5H_2O$ (3.8 mg, 15.3 µmol, 0.1 equiv) the reaction vessel was then evacuated under high vacuum and backfilled with argon. Toluene (1.5 mL) was then added and again; the reaction vessel was evacuated under high vacuum and backfilled with argon. The microwave vial was sealed with a lid. The reaction mixture was stirred for 18 h at 75 °C resulting in a brown suspension. The mixture was filtered over a pad of Celite and was subsequently concentrated under reduced pressure. Purification by FC (EtOAc:hexane, 1:5) gave the desired title compound (76.1 mg, 0.15 mmol, 83%).

N-37 N-benzyl-N-((5-(benzyloxy)-2-methoxyphenyl)ethynyl)-4-nitrobenzenesulfonamide

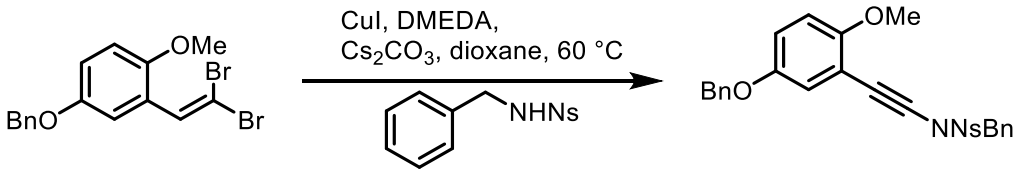

Assay: A flame dried Schlenk tube was charged with sulfonamide (130 mg, 0.45 mmol, 1.0 equiv) and dibromovinyl **N-30** (195 mg, 0.49 mmol, 1.1 equiv). It was then evacuated under high vacuum and backfilled with argon (5 times). The Schlenk tube was then channeled into the glovebox where CuI (10.6 mg, 55.6 µmol, 0.13 equiv) and Cs_2CO_3 (579.6 mg, 1.78 mmol, 4.0 equiv) were added. Outside the glovebox, degassed dioxane (1.6 mL) was added followed by DMEDA (9.0 µL, 83.4 µmol, 0.19 equiv) which was prior bubbled through by a stream of argon over 15 min. The reaction mixture was stirred for 24 h at 60 °C resulting in a brown suspension. The mixture was filtered over a pad of Celite and was subsequently concentrated under reduced pressure. Purification by FC (EtOAc:hexane, 1:5) gave the target compound (as a yellow oil, slightly impure) along with existing starting material (sulfonamide).

Analytics: $\mathbf{R_f}$ = 0.23 (EtOAc:hexane, 1:5). **^{1}H NMR** (400 MHz, Chloroform-*d*) δ 8.24 (d, *J* = 8.9 Hz, 2H), 8.01 (d, *J* = 8.9 Hz, 2H), 7.45 – 7.24 (m, 10H), 6.91 – 6.85 (m, 2H), 6.79 (t, *J* = 9.5 Hz, 1H), 4.99 (s, 2H), 4.69 (s, 2H), 3.80 (s, 3H).

C31LL302-1-FC.1.fid
BBFO_1H_16 CDCl3 /v pkanmr 12

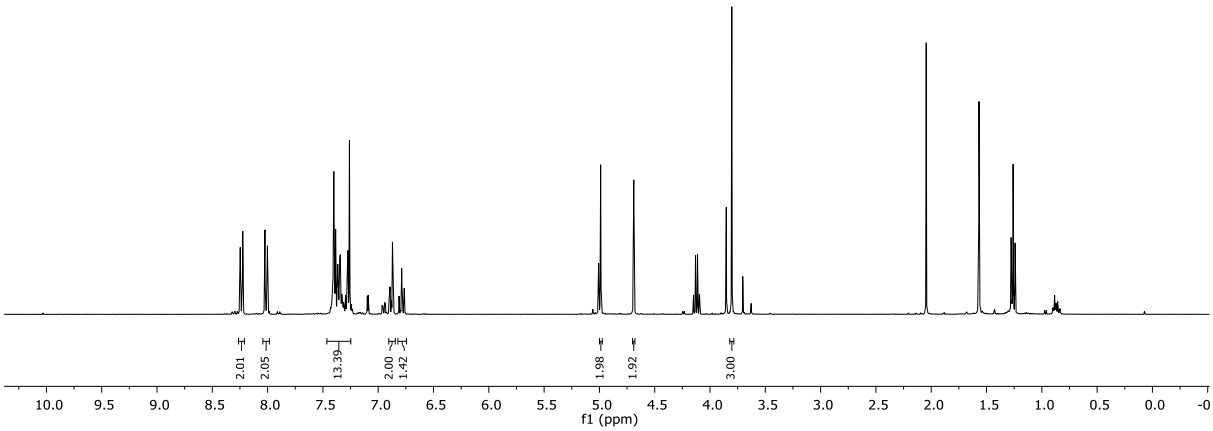

N-38 N-((5-(benzyloxy)-2-methoxyphenyl)ethynyl)-N-(4-methoxybenzyl)-4-nitrobenzenesulfonamide

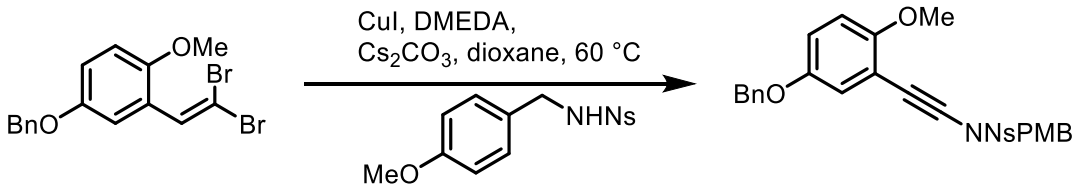

Assay: A flame dried microwave tube was charged with sulfonamide **N-41** (12 mg, 37 µmol, 1.0 equiv) and dibromovinyl **N-30** (16 mg, 41 µmol, 1.1 equiv). It was then evacuated under high vacuum and backfilled with argon (5 times). CuI (1.0 mg, 4.7 µmol, 0.13 equiv) and Cs_2CO_3 (48.5 mg, 0.15 mmol, 4.0 equiv) were added followed by the addition of DMEDA (1 µL, 7 µmol, 0.19 equiv) which was prior bubbled through by a stream of argon over 15 min. The reaction mixture was stirred over the weekend. The brown suspension was allowed to cool to ambient temperature and was then filtered over a pad of Celite. The brownish crude was then purified by FC (1:3, EtOAc:hexane) to give the title compound in low yields as a yellow oil (2.46 mg, 4.4 µmol, 12%).

Analytics: $\mathbf{R_f}$ = 0.26 (EtOAc:hexane, 1:5). **^{1}H NMR** (400 MHz, Chloroform-*d*) δ 8.30 – 8.18 (m, 2H), 8.08 – 7.98 (m, 2H), 7.47 – 7.24 (m, 9H), 6.91 – 6.84 (m, 1H), 6.81 – 6.73 (m, 2H), 4.99 (s, 2H), 4.63 (s, 2H), 3.81 (s, 3H), 3.77 (s, 3H). **^{13}C NMR** (101 MHz, Chloroform-*d*) δ 160.08, 154.65, 152.50, 150.40, 143.36, 137.04, 130.66 (2 C), 129.12 (2 C), 128.74 (2 C), 128.16, 127.60 (2 C), 126.04, 124.04 (2 C), 119.15, 116.26, 114.46, 114.00 (2 C), 112.08, 85.73, 70.86, 68.55, 56.48, 56.31, 55.43. **HRMS (ESI)**: 581.1350 $[M+Na]^+$; calculated for $[C_{30}H_{26}N_2NaO_7S]$: 581.1353. **IR** [ATR, neat]: ν = 1682.59 w, 1604.48 w, 1530.24 m, 1512.88 m, 1499.38 m, 1462.74 w, 1422.24 w, 1370.18 m, 1313.29 m, 1248.68 m, 1171.54 s, 1085.73 m, 1026.91 s, 883.24 m, 853.35 m, 736.67 s, 697.14 m, 683.64 m, 601.68 s cm^{-1}.

C39LL312-3,4-2ndFC.1.fid
BBFO_1H_16 CDCl3 /v pkanmr 41

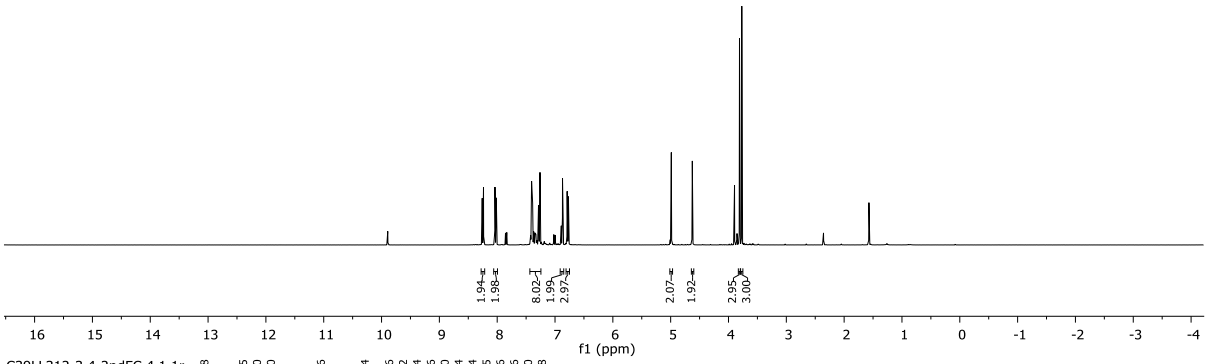

C39LL312-3,4-2ndFC.4.1.1r
BBFO_13C{1H}_1024 CDCl3 /v pkanmr 41

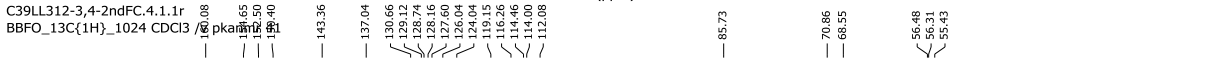

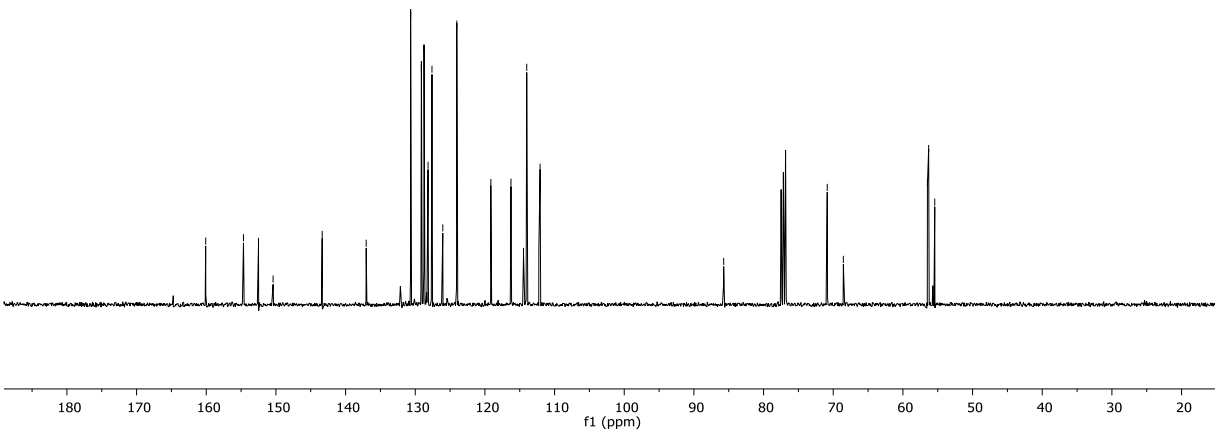

N-41 N-(4-methoxybenzyl)-4-nitrobenzenesulfonamide

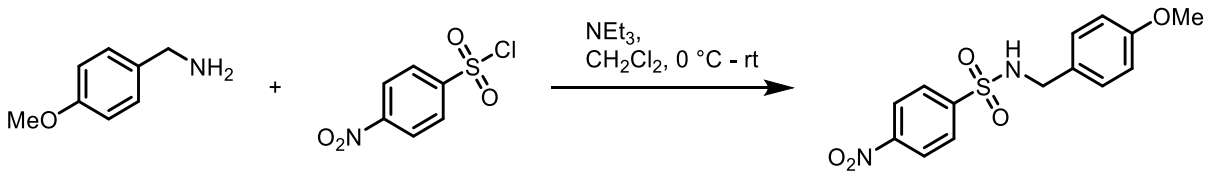

Assay: To a solution of 4-methoxybenzylamine (0.1 mg, 0.73 mmol, 1.0 equiv) in CH_2Cl_2 (6.5 mL) at 0 °C was given NEt_3 (81.0 µL, 1.09 mmol, 1.5 equiv). Nosylchloride (242.3 mg, 1.5 mmol, 1.5 equiv) was then added in one portion whereas the reaction mixture turned yellow/orange. The mixture was allowed to warm to ambient temperature and was stirred as such over night. After stirring for 16 h. The reaction mixture was concentrated under reduced pressure and the orange crude was purified by FC (EtOAc:hexane; 1:3) to give the target compound as a white solid (183.1 mg, 0.57 mmol, 78%).

Analytics: $\mathbf{R_f}$ = 0.19 (EtOAc:hexane, 1:3). **^{1}H NMR** (400 MHz, Chloroform-*d*) δ 8.40 – 8.06 (m, 2H), 8.00 (d, *J* = 8.9 Hz, 2H), 7.13 – 7.00 (m, 2H), 6.79 (d, *J* = 8.7 Hz, 2H), 4.78 (t, *J* = 5.7 Hz, 1H), 4.17 (s, 1H), 4.16 (s, 1H), 3.77 (s, 3H). **^{13}C NMR** (101 MHz, Chloroform-*d*) δ 159.75, 146.29, 129.50 (2 C), 128.47 (2 C), 127.56, 124.45 (2 C), 114.35 (2 C), 55.47, 47.14. **HRMS (ESI)**: 345.0520 $[M+Na]^+$; calculated for $[C_{14}H_{14}N_2NaO_5S]$: 335.345.0516. **IR** [ATR, neat]: ν = 3289.96 w, 1610.27 w, 1528.31 s, 1348.0 s, 1250.61 m, 1161.9 s, 1031.73 m, 850.45 m, 740.53 m, 613.25 m cm^{-1}.

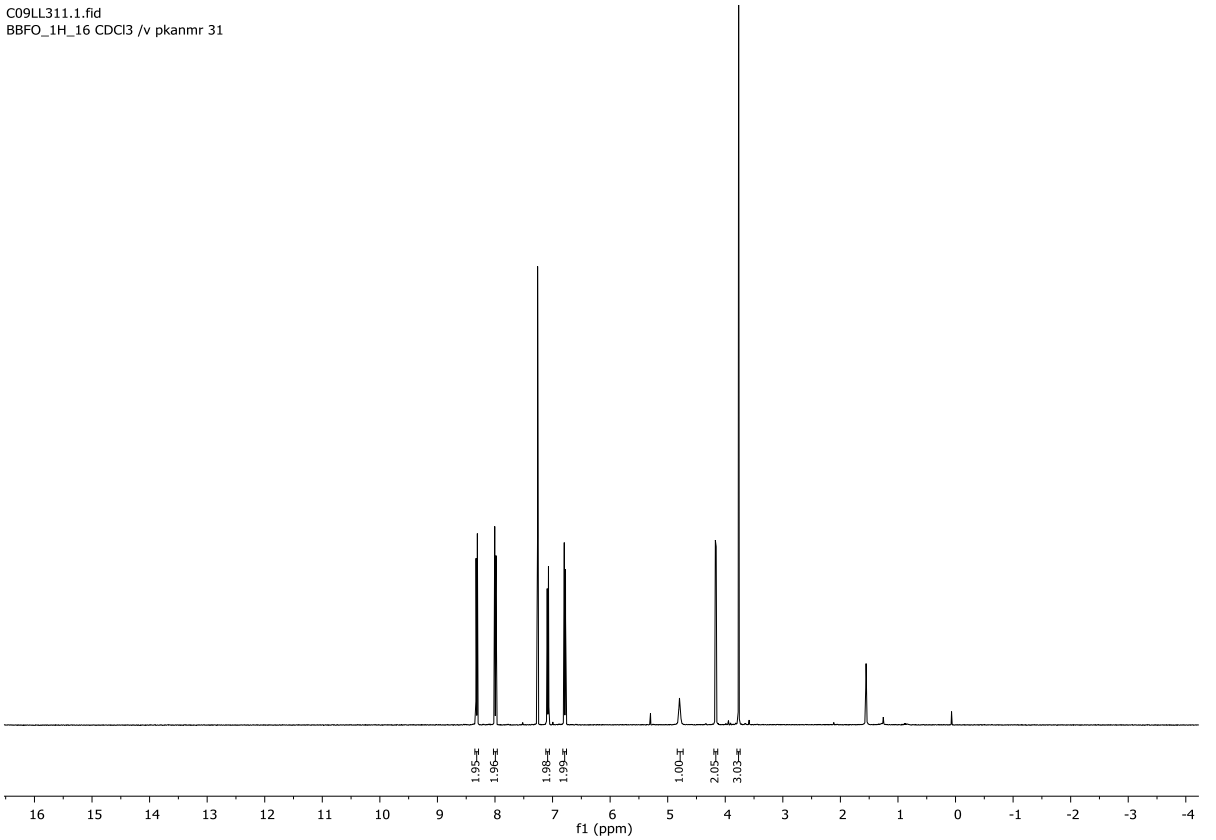
C09LL311.1.fid
BBFO_1H_16 CDCl3 /v pkanmr 31
1.95
1.96
1.98
1.99
1.00
2.05
3.03
f1 (ppm)

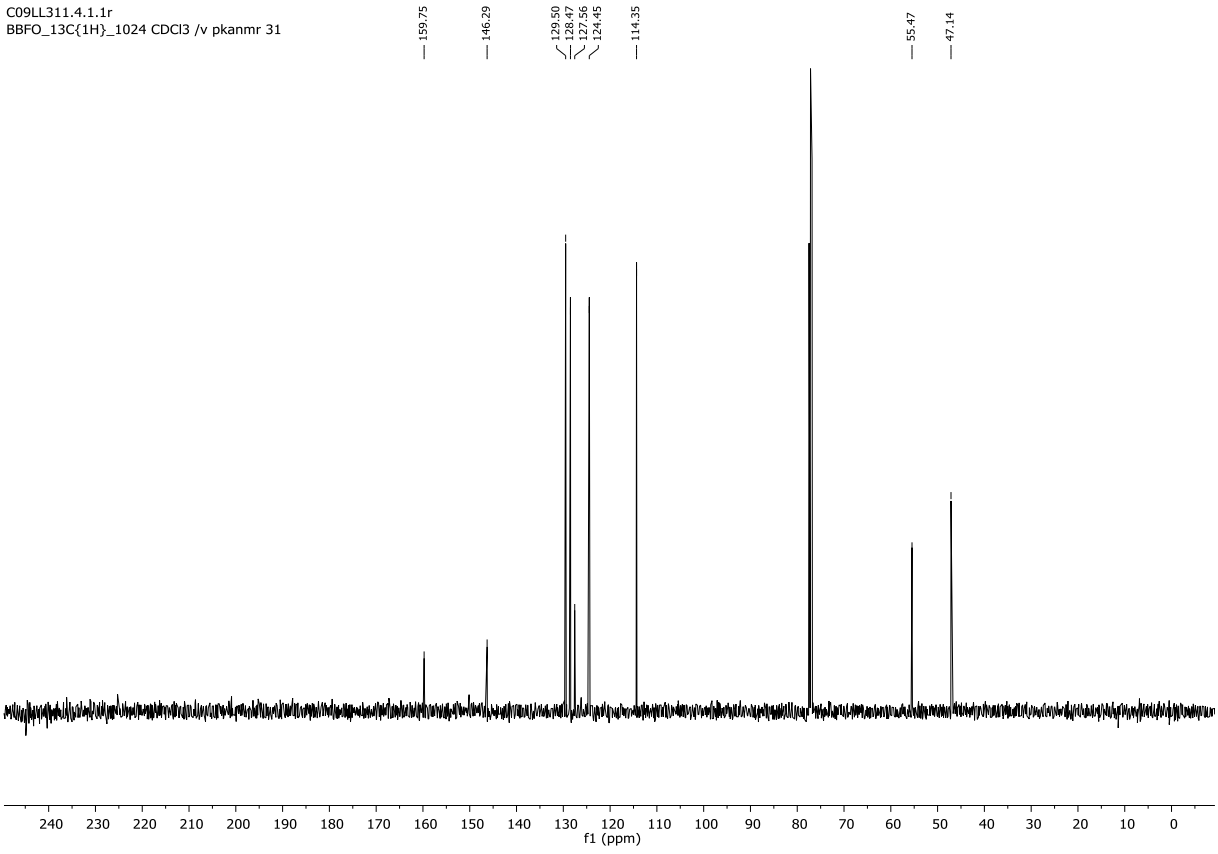
C09LL311.4.1.1r
BBFO_13C{1H}_1024 CDCl3 /v pkanmr 31
159.75
146.29
129.50
128.47
127.56
124.45
114.35
55.47
47.14
f1 (ppm)

N-56 (Z)-N-benzyl-N-(5-(benzyloxy)-2-methoxystyryl)-4-methylbenzenesulfonamide

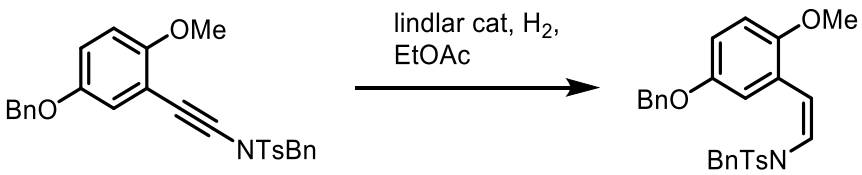

Assay: To a solution of sulfonamide **N-36** (97 mg, 0.19 mmol, 1.0 equiv) in EtOAc (2 mL) was given Lindlar cat. (6.2 mg, 29 µmol, 15 mol %) and the reaction vessel was set under hydrogen atmosphere (balloon). The reaction mixture was stirred over the weekend but no full conversion was observed after 63 h. Therefore another portion of Lindlar cat. (6.2 mg, 29 µmol, 15 mol %) was added and the reaction was stirred at 40 °C for another 5 h to achieve full conversion. The reaction was filtered over a pad of Celite and concentrated under reduced pressure. Purification by FC (EtOAc:hexane, 1:3) gave the target compound as a turbid oil (68 mg, 0.14 mmol, 70%) along with reisolated SM (not quantified).

Analytics: $\mathbf{R_f}$ = 0.48 (EtOAc:hexane 1:3). **^{1}H NMR** (400 MHz, Chloroform-*d*) δ 7.76 (d, *J* = 8.3 Hz, 2H), 7.41 (d, *J* = 4.4 Hz, 4H), 7.38 – 7.31 (m, 1H), 7.29 (d, *J* = 8.1 Hz, 2H), 7.19 – 7.08 (m, 3H), 6.96 – 6.89 (m, 2H), 6.81 (dd, *J* = 9.0, 3.1 Hz, 1H), 6.66 (d, *J* = 8.9 Hz, 1H), 6.63 (d, *J* = 3.1 Hz, 1H), 6.21 (d, *J* = 9.1 Hz, 1H), 6.14 (d, *J* = 9.1 Hz, 1H), 4.77 (s, 2H), 4.34 (s, 2H), 3.57 (s, 3H), 2.32 (s, 3H). **^{13}C NMR** (101 MHz, Chloroform-*d*) δ 152.08, 151.44, 143.72, 137.19, 136.28, 135.90, 129.82, 128.58, 128.28, 128.04, 127.99, 127.75, 127.36, 127.28, 124.78, 124.46, 118.70, 116.01, 115.83, 111.45, 70.49, 55.83, 51.59, 21.48. **HRMS (ESI)**: 522.1705 $[M+Na]^+$; calculated for $[C_{30}H_{29}NNaO_4S]$: 522.1710. **IR** [ATR, neat]: ν = 1492.63 m, 1455.03 m, 1343.18 m, 1219.75 m, 1159.97 s, 1090.55 m, 1027.87 m, 733.78 m, 695.21 s, 681.71 s cm^{-1}.

C28LL299-1-fr20,24.1.1.1r
BBFO_1H_16 CDCl3 /v pkanmr 48

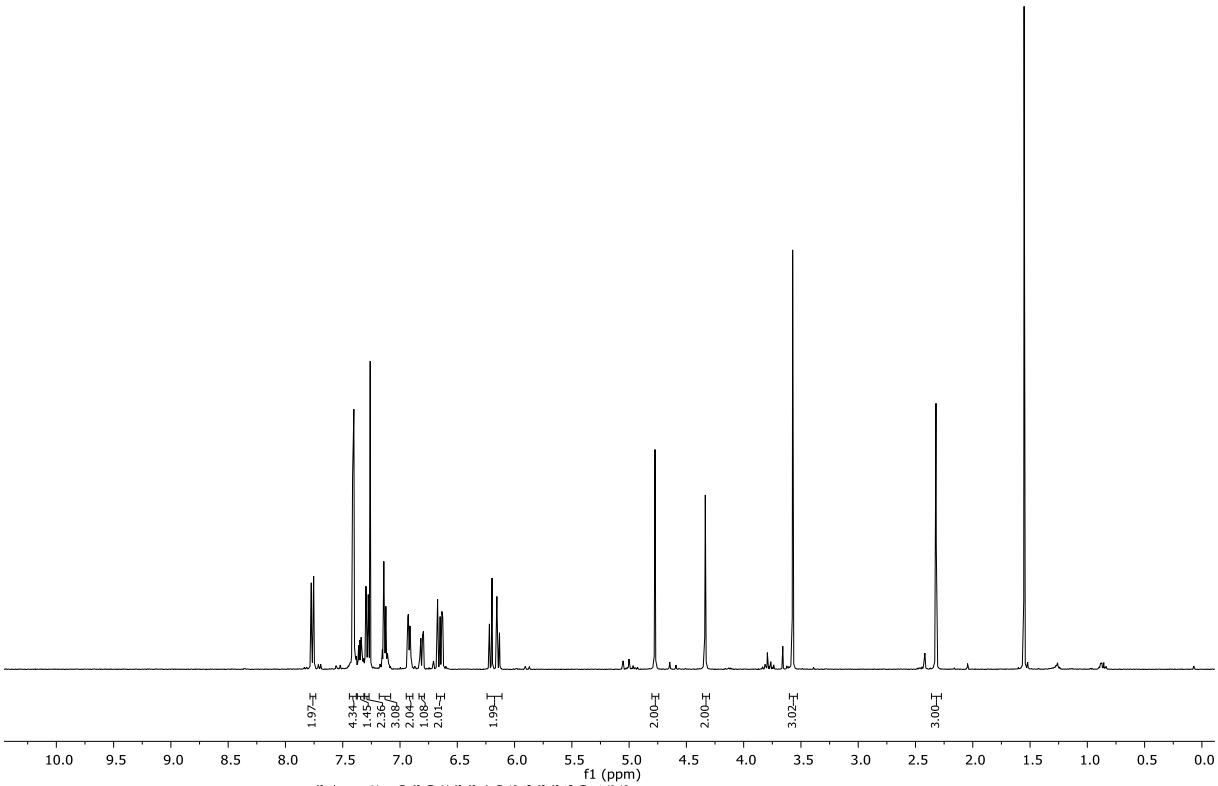

C09LL299.2.1.1r
BBFO_13C{1H}_256 CDCl3 /v pkanmr 56

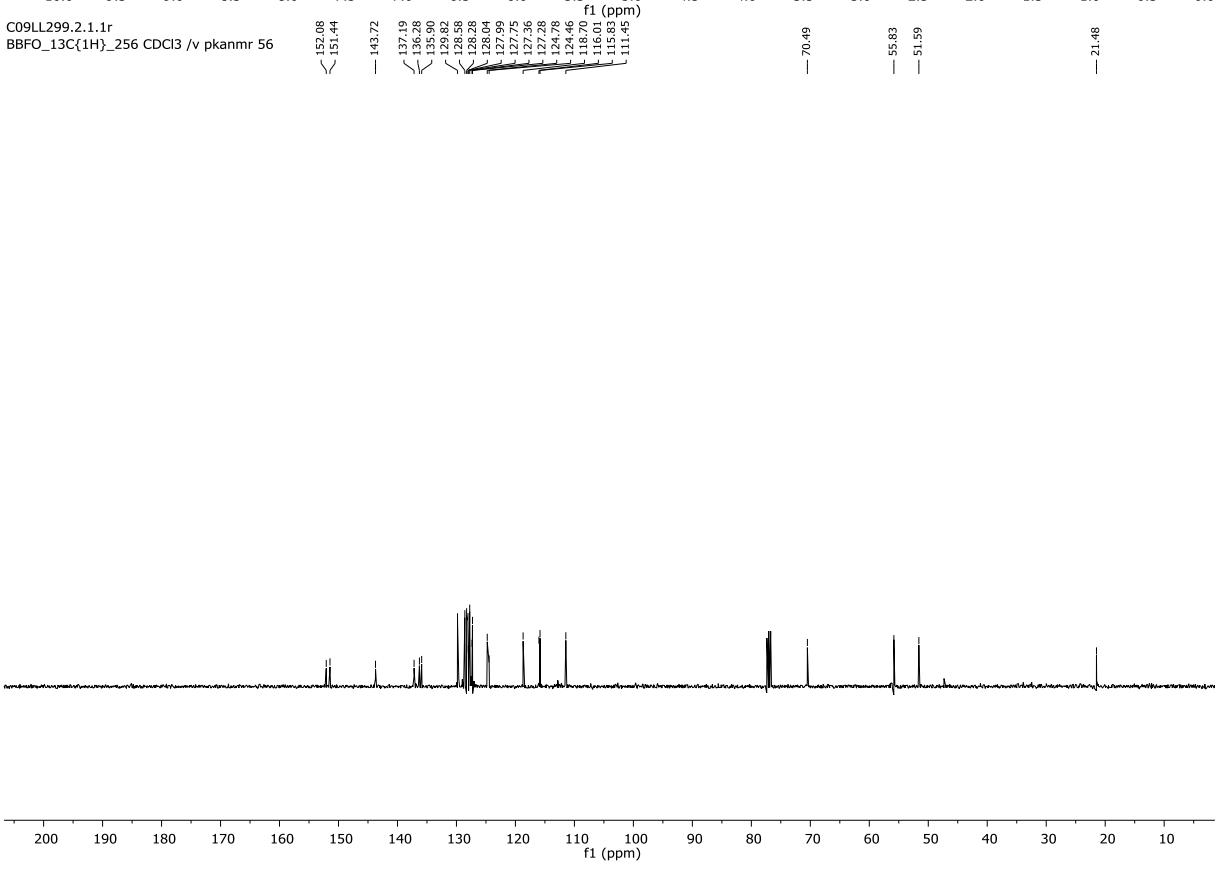

N-65 5-(benzyloxy)-2-hydroxybenzaldehyde

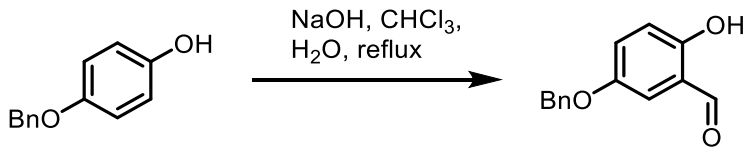

Assay: To a suspension of **N-64** (20 g, 99.88 mmol, 1.0 equiv) in water (80.0 mL) was added sodium hydroxide (26.37 g, 659.2 mmol, 6.6 equiv) carefully. The suspension became greyish and the white solid started to dissolve slowly. The reaction mixture was heated up to 70 °C. Chloroform (16.11 mL, 199.76 mmol, 2.0 equiv) was then carefully (extremely slowly) added whereas a strong bubbling and a change in color (to yellow) was observed. The reaction mixture was kept as such for 4 h. The reaction was then allowed to cool to ambient temperature and acidified with HCl (1 M, to a pH of 4) and extracted with EtOAc (3 x 80 mL). Combined organic layers were dried over $MgSO_4$ and concentrated under reduced pressure. Purification by FC (EtOAc:hexane, 1:10 -> 1:5) gave the target compound as a yellow solid (4.78 g, 20.94 mmol, 21%) and recovered SM (9.81 g, 48.99 mmol, 49%).

Analytics: $\mathbf{R_f}$ = 0.31 (EtOAc:hexane, 1:10). **^{1}H NMR** (400 MHz, Chloroform-*d*) δ 10.66 (s, 1H), 9.84 (s, 1H), 7.45 – 7.31 (m, 5H), 7.22 (dd, *J* = 9.0, 3.1 Hz, 1H), 7.08 (d, *J* = 3.1 Hz, 1H), 6.94 (d, *J* = 9.1 Hz, 1H), 5.07 (s, 2H). **^{13}C NMR** (101 MHz, Chloroform-*d*) δ 196.26, 156.43, 151.97, 136.66, 128.85 (2 C), 128.35, 127.63 (2 C), 126.27, 120.23, 118.92, 117.00, 71.15.

Compound literature known

C26LL283-2-FC.1.1.1r
BBFO_1H_16 CDCl3 /v pkanmr 56

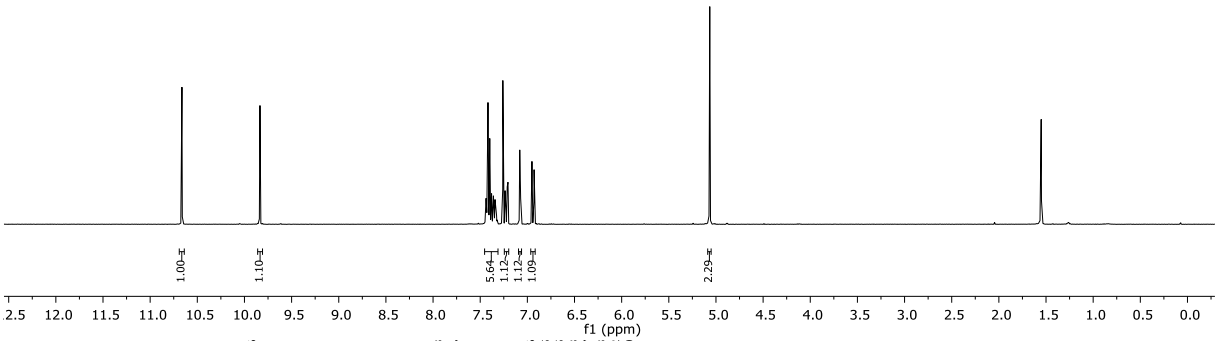

C26LL283-2-FC.5.1.1r
BBFO_13C{1H}_1024 CDCl3 /v pkanmr 46

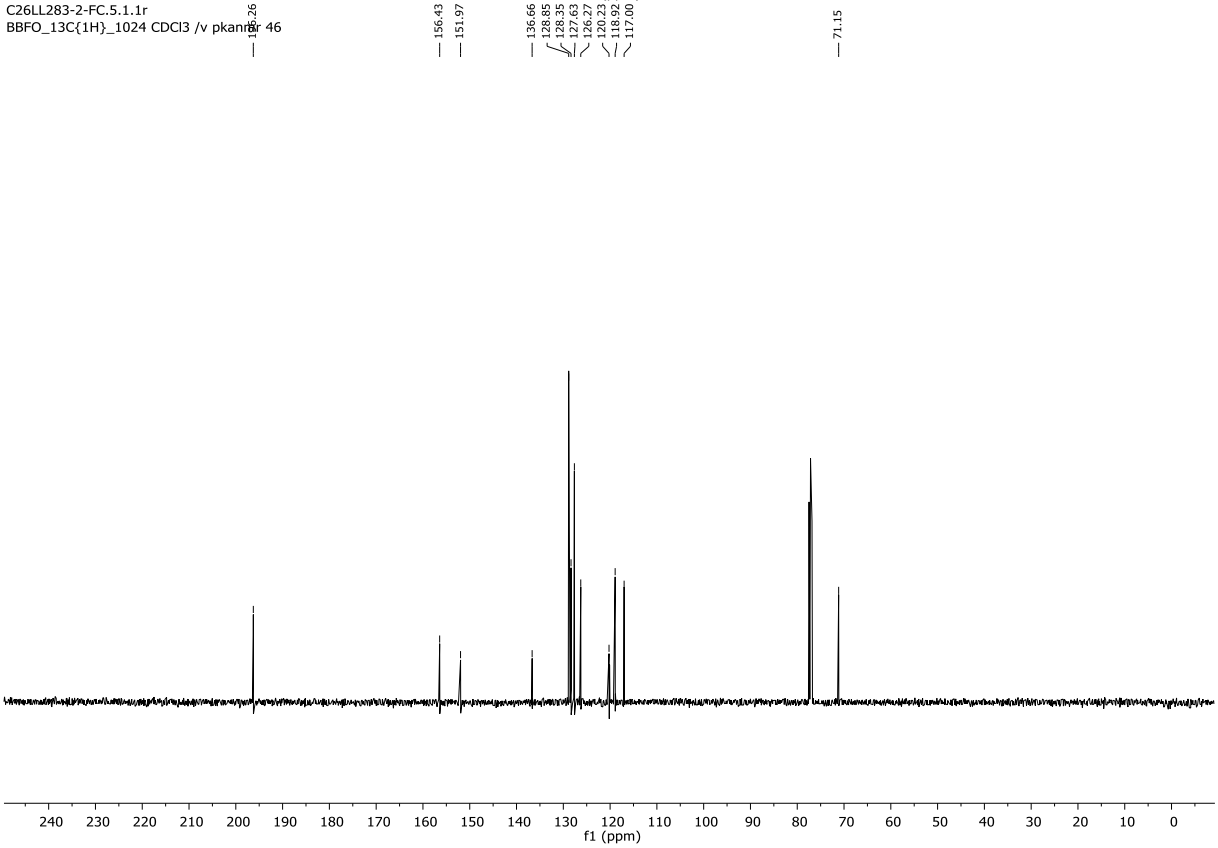

N-66 2-amino-1-(5-(benzyloxy)-2-methoxyphenyl)ethan-1-ol

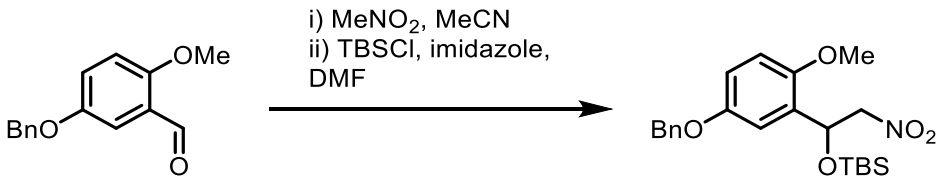

Assay: A stock solution of NaOMe (25 wt% in MeOH, 7.5 mL) in additional MeOH (10 mL) and $MeNO_2$ (11.13 mL, 205.95 mmol, 36.0 equiv) was first prepared. The stock solution (15 mL) was then added dropwise to a stirring solution of **N-33** (1.39 g, 5.72 mmol, 1.0 equiv) in MeOH (60.0 mL). The reaction mixture stayed clear but turned orange. After stirring over night, the starting material was fully consumed. The reaction mixture was carefully quenched with saturated aqueous $NHCl_4$ (60 mL) and extracted with EtOAc (3 x 25 mL). The solvent was evaporated and the crude was taken up in DMF (60 mL). TBSCl (2.24 g, 14.87 mmol, 2.6 equiv) and imidazole (1.95 g, 28.60 mmol, 5.0 equiv) were added in one portion. Starting material was fully consumed after 6 h. The organic solvent was evaporated under diminished pressure and the crude was purified by FC (EtOAc:hexane, 1:10 -> 1:5) to give the desired product (1.40 g, 3.35 mmol, 59% over two steps).

Analytics: $\mathbf{R_f}$ = 0.34 (EtOAc:hexane, 1:1). **^{1}H NMR** ^{1}H NMR (400 MHz, Chloroform-*d*) δ 7.45 – 7.29 (m, 5H), 7.17 (d, *J* = 3.0 Hz, 1H), 6.88 (dd, *J* = 8.8, 3.2 Hz, 1H), 6.78 (d, *J* = 8.9 Hz, 1H), 5.76 (dd, *J* = 9.5, 2.7 Hz, 1H), 5.05 (d, *J* = 11.7 Hz, 1H), 5.00 (d, *J* = 11.8 Hz, 1H), 4.51 (dd, *J* = 11.8, 2.7 Hz, 1H), 4.34 (dd, *J* = 11.8, 9.5 Hz, 1H), 3.83 (s, 3H), 0.88 (s, 9H), 0.04 (s, 3H), -0.10 (s, 3H). **^{13}C NMR** (101 MHz, Chloroform-*d*) δ 153.02, 149.65, 137.12, 128.57 (2C), 128.42, 127.93, 127.40 (2C), 115.58, 113.86, 111.20, 81.19, 70.70, 67.09, 55.75, 25.67, -4.84, -5.65. **HRMS (ESI)**: 440.1865 $[M+Na]^+$; calculated for $[C_{22}H_{31}NNaO_5Si]$: 440.1864 . **IR** [ATR, neat]: ν = 2954.41 w, 2929.34 w, 2857.02 w, 1557.24 s, 1553.38 s, 1497.45 s, 1379.82 w, 1276.65 w, 1254.47 m, 1206.26 m, 1091.51 m, 961.34 m, 829.24 s 780.07 m, 735.71 w cm^{-1}.

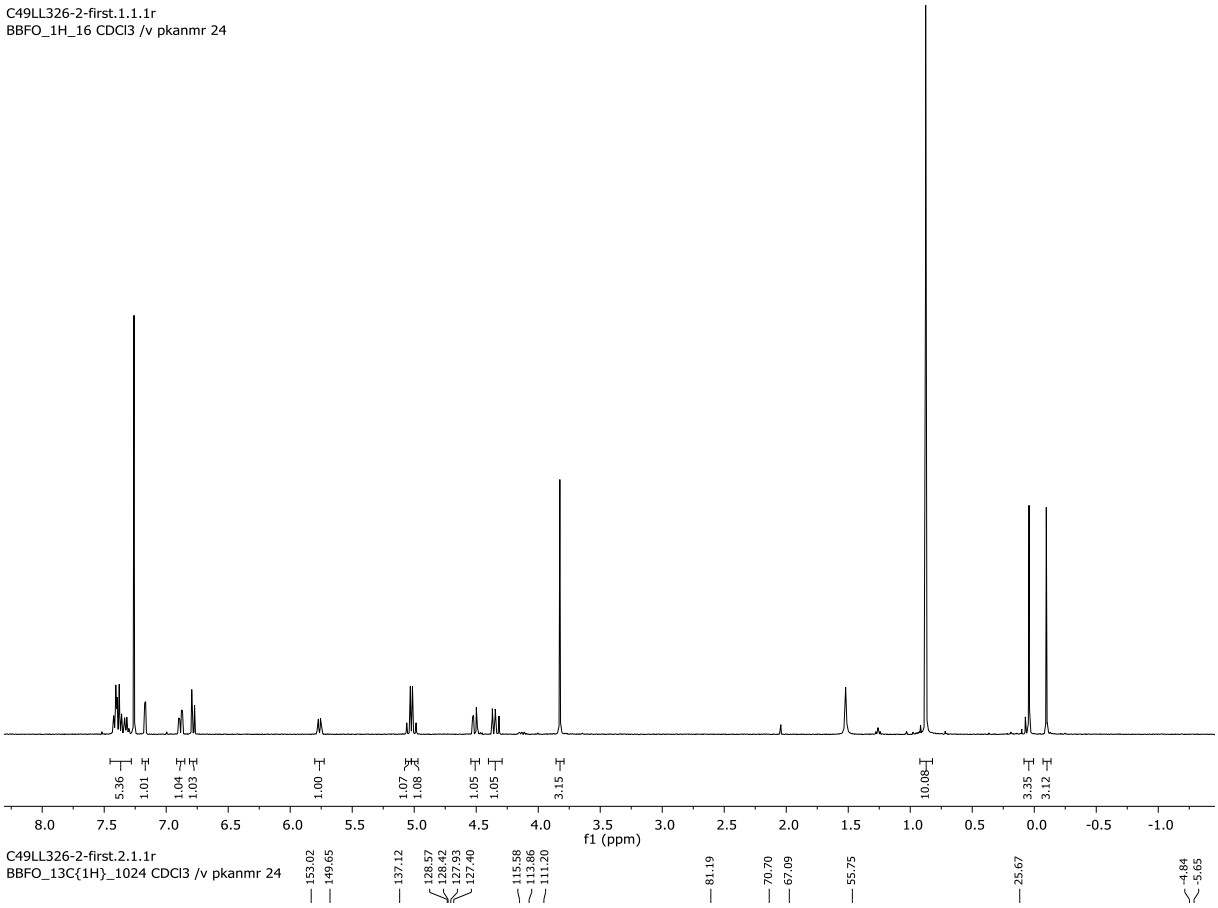
C49LL326-2-first.1.1.1r
BBFO_1H_16 CDCl3 /v pkanmr 24
5.36
1.01
1.04
1.03
1.00
1.07
1.08
1.05
1.05
3.15
10.08
3.35
3.12
f1 (ppm)
C49LL326-2-first.2.1.1r
BBFO_13C{1H}_1024 CDCl3 /v pkanmr 24
153.02
149.65
137.12
128.57
128.42
127.93
127.40
115.58
113.86
111.20
81.19
70.70
67.09
55.75
25.67
4.84
-5.65
f1 (ppm)

N-61 2-(5-(benzyloxy)-2-methoxyphenyl)-2-((tert-butyldimethylsilyl)oxy)ethan-1-amine

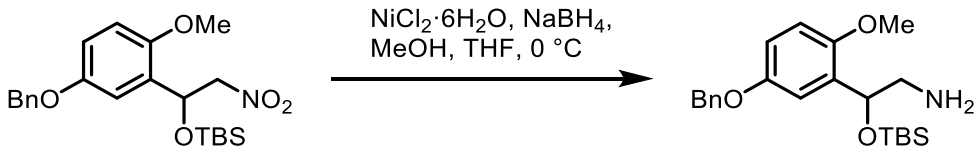

Assay: N-66 (1.15 g, 2.75 mmol, 1.0 equiv) was dissolved in MeOH (30 mL) and THF (15 mL) and cooled to 0 °C. $NiCl_2 \cdot 6H_2O$ (2.62 g, 11.02 mmol, 4.0 equiv) was added followed by stepwise addition of $NaBH_4$ (7 x 111.6 mg, 20.65 mmol, 7.5 equiv). The reaction turns instantly black and a strong effervescent was observed. Product formation was observed rapidly (within 5 min) and full starting material consumption was obtained after 50 min. The reaction mixture was filtered over a pad of Celite and concentrated under reduced pressure. The crude brown/black oil was purified by FC (CH_2Cl_2:MeOH, 9:1) to give the desired product as a yellowish foam/powder (969.1 mg, 2.5 mmol, 91%).

Analytics: $\mathbf{R_f}$ = 0.47 (CH_2Cl_2:MeOH, 9:1). **^{1}H NMR** (400 MHz, Chloroform-*d*) δ 7.45 – 7.28 (m, 5H), 7.12 (d, *J* = 3.0 Hz, 1H), 6.83 (dd, *J* = 8.9, 3.1 Hz, 1H), 6.76 (d, *J* = 8.9 Hz, 1H), 5.40 (dd, *J* = 8.0, 3.4 Hz, 1H), 5.04 (d, *J* = 11.8 Hz, 1H), 5.00 (d, *J* = 11.7 Hz, 1H), 3.78 (s, 3H), 3.48 (s, 2H), 3.13 (dd, *J* = 13.1, 3.4 Hz, 1H), 2.91 (dd, *J* = 13.0, 8.1 Hz, 1H), 0.92 (s, 9H), 0.09 (s, 3H), -0.09 (s, 3H). **^{13}C NMR** (101 MHz, Chloroform-*d*) δ 153.00, 150.03, 137.36, 132.32, 128.53 (2C), 127.84, 127.45 (2C), 114.44, 113.87, 111.33, 70.65, 65.57, 60.54, 55.92, 25.89, -4.75, -5.23. **HRMS (ESI)**: 388.2297 $[M+H]^+$; calculated for [$C_{22}H_{34}NO_3Si$]: 388.2302. **IR** [ATR, neat]: ν = 3419.17 w, 2951.52 w, 2928.38 w, 2856.06 w, 1496.49 s, 1462.74 w, 1254.47 m, 1208.18 m, 1074.16 m, 1027.87 m, 905.42 m, 835.99 m, 779.10 m, 732.82 s cm^{-1}.

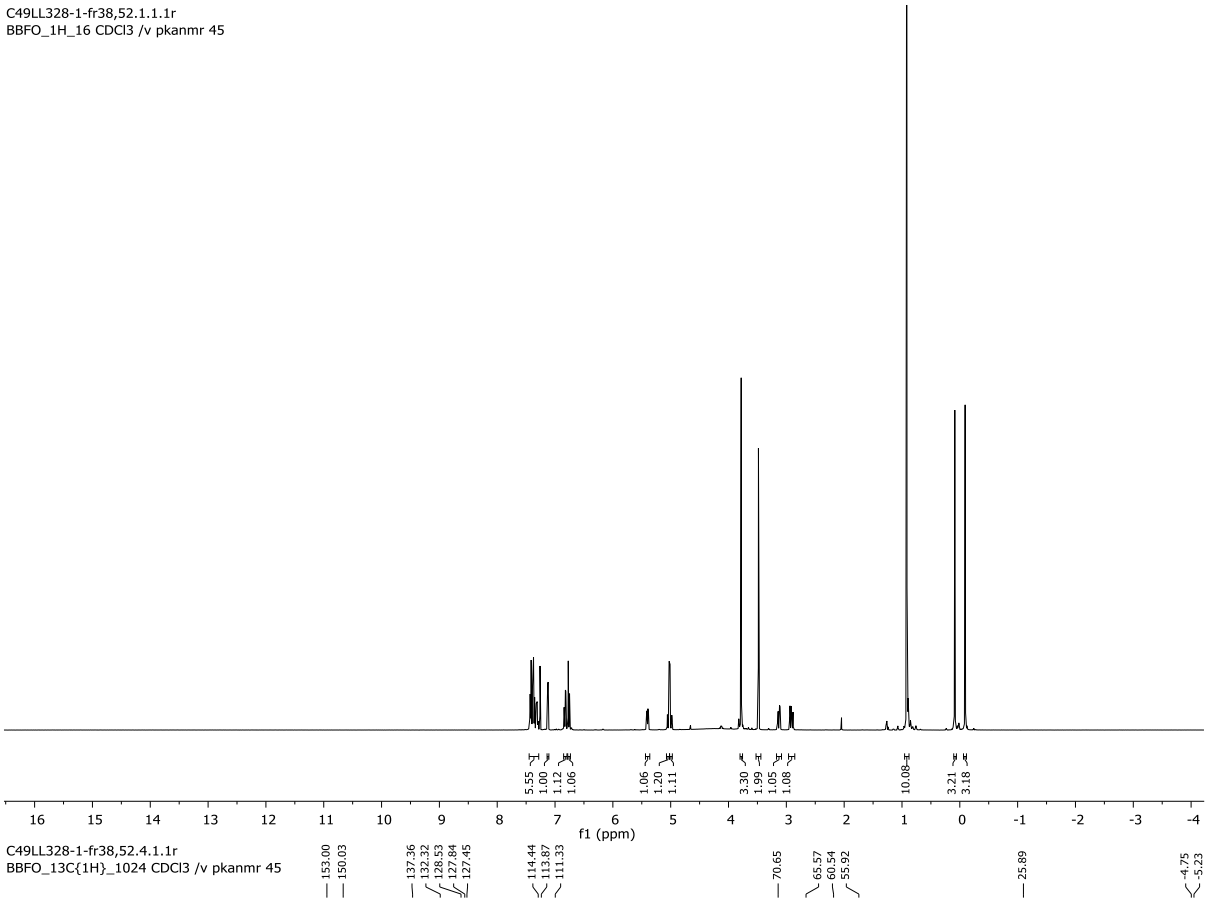
C49LL328-1-fr38,52.1.1.1r
BBFO_1H_16 CDCl3 /v pkanmr 45
5.55
1.00
1.12
1.06
1.06
1.20
1.11
3.30
1.99
1.05
1.08
10.08
3.21
3.18
f1 (ppm)
C49LL328-1-fr38,52.4.1.1r
BBFO_13C{1H}_1024 CDCl3 /v pkanmr 45
153.00
150.03
137.36
132.32
128.53
127.84
127.45
114.44
113.87
111.33
70.65
65.57
60.54
55.92
25.89
-4.75
-5.23
f1 (ppm)

N-67 benzyl ((2S,3R)-1-((2-(5-(benzyloxy)-2-methoxyphenyl)-2-((tert-butyldimethylsilyl)oxy)ethyl)amino)-3-methyl-1-oxopentan-2-yl)carbamate

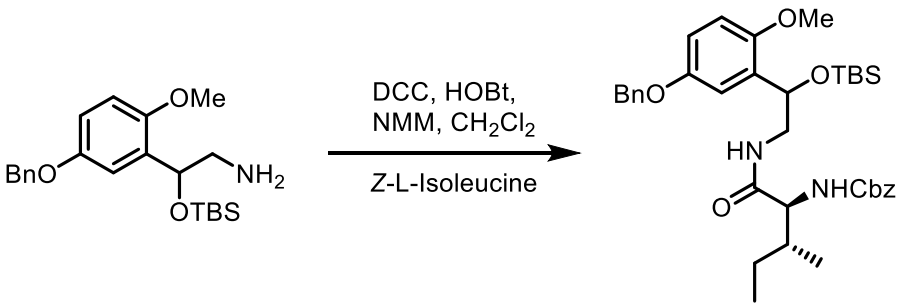

Assay: N-61 (954 mg, 2.46 mmol, 1.0 equiv) and *Z*-L-Ile (718 mg, 2.71 mol, 1.1 equiv) were dissolved in CH_2Cl_2 (20 mL) and cooled to 0 °C. DCC (566 mg, 2.95 mmol, 1.2 equiv), HOBt (432 mg, 3.2 mmol, 1.3 equiv) and NMM (298 µL, 2.77 mmol, 1.1 equiv) were added subsequently and the reaction was allowed to warm to ambient temperature and stirred as such over 16 h. The reaction mixture was filtrated over a pad of Celite and the filtrate was concentrated under reduced pressure. Purification by FC (EtOAc:hexane, 1:3) gave the pure product as a white powder (1.40 g, 2.21 mmol , 90 %).

Analytics: $\mathbf{R_f}$ = 0.2 (EtOAc:hexane, 1:3). **^{1}H NMR** (400 MHz, Chloroform-*d*) δ 7.45 – 7.28 (m, 10H), 7.10 (t, *J* = 2.9 Hz, 1H), 6.82 (dt, *J* = 8.9, 3.7 Hz, 1H), 6.74 (dd, *J* = 9.0, 1.8 Hz, 1H), 5.98 (d, *J* = 6.5 Hz, 1H), 5.30 (dd, *J* = 21.8, 8.8 Hz, 1H), 5.17 (t, *J* = 5.0 Hz, 1H), 5.15 – 4.95 (m, 4H), 4.06 – 3.91 (m, 1H), 3.77 (s, 3H), 3.64 – 3.35 (m, 2H), 1.92 – 1.74 (m, 1H), 1.36 (dq, *J* = 8.0, 4.6, 4.1 Hz, 1H), 1.02 (dtd, *J* = 16.4, 9.4, 8.3, 5.3 Hz, 1H), 0.90 (s, 9H), 0.89 – 0.82 (m, 4H), 0.78 (d, *J* = 6.8 Hz, 2H), 0.06 (s, 3H), -0.07 (d, *J* = 2.7 Hz, 3H). **^{13}C NMR** (101 MHz, Chloroform-*d*) δ 170.85, 170.75, 156.33, 156.22, 152.99, 150.09, 137.45, 136.46, 136.39, 131.20, 128.65, 128.27, 128.18, 127.99, 127.56, 114.61, 114.51, 114.04, 113.97, 111.35, 111.27, 70.67, 67.43, 67.29, 67.12, 67.05, 60.09, 59.98, 55.93, 45.87, 37.81, 37.62, 25.97, 24.84, 24.72, 18.31, 15.56, 15.32, 11.67, -4.70, -4.99. **HRMS (ESI)**: 657.3316 $[M+Na]^+$; calculated for $[C_{36}H_{50}N_2NaO_6Si]$: 657.3330. **IR** [ATR, neat]: ν = 2957.3 w, 2929.34 w, 1711.51 m, 1661.37 m, 1496.49 m, 1248.68 m, 1214.93 m, 1074.16 m, 1040.41 m, 1027.87 m, 908.31 m, 834.06 m, 777.12 m, 729.93 s, 695.21 m cm^{-1}.

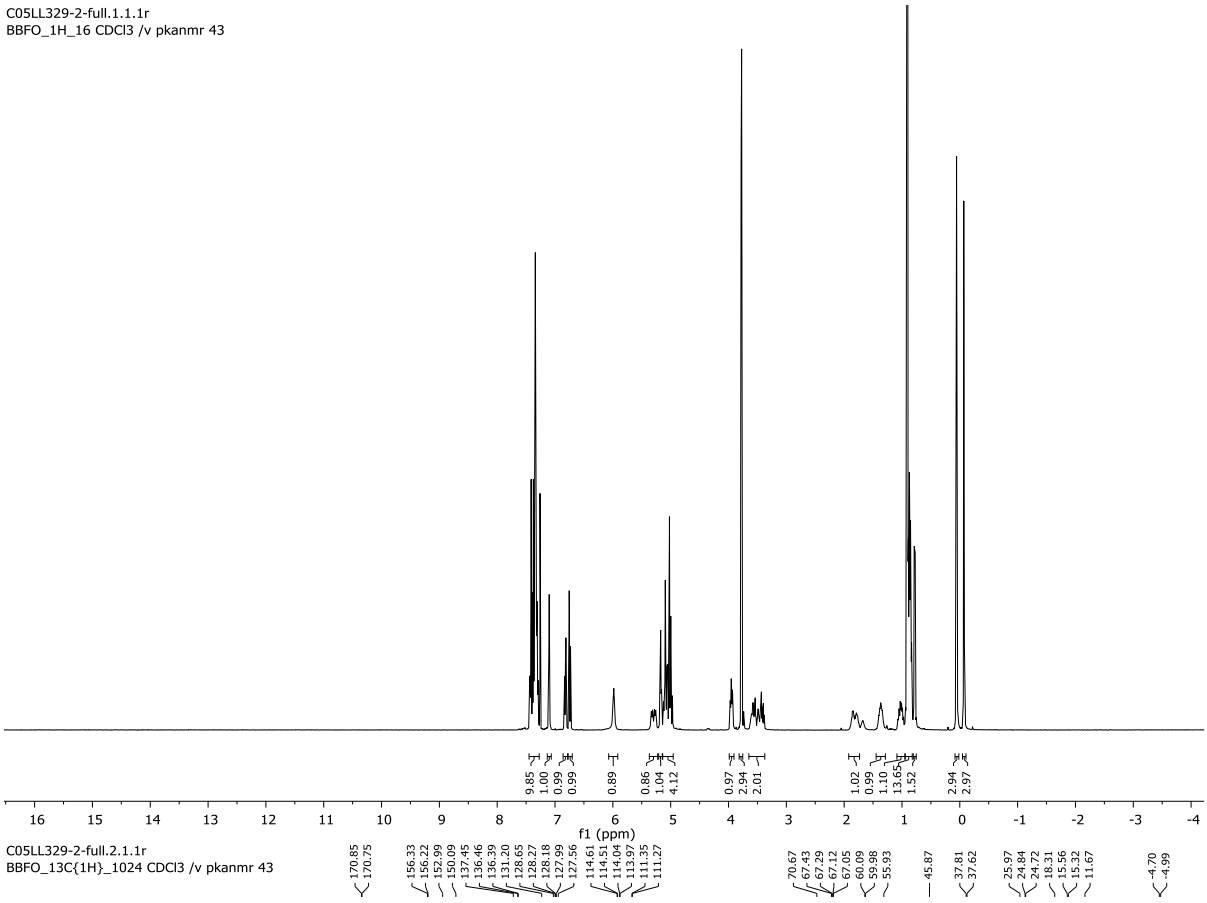
C05LL329-2-full.1.1.1r
BBFO_1H_16 CDCl3 /v pkanmr 43
9.85
1.00
0.99
0.99
0.89
0.86
1.04
4.12
0.97
2.94
2.01
1.02
0.99
1.10
13.65
1.52
2.94
2.97
16 15 14 13 12 11 10 9 8 7 6 5 4 3 2 1 0 -1 -2 -3 -4
f1 (ppm)
C05LL329-2-full.2.1.1r
BBFO_13C{1H}_1024 CDCl3 /v pkanmr 43
170.85
170.75
156.33
156.22
152.99
150.09
137.45
136.46
136.39
131.20
128.65
128.27
128.18
127.99
127.56
114.61
114.51
114.04
113.97
111.35
111.27
70.67
67.43
67.29
67.12
67.05
60.09
59.98
55.93
45.87
37.81
37.62
25.97
24.84
24.72
18.31
15.56
15.32
11.67
-4.70
-4.99
240 230 220 210 200 190 180 170 160 150 140 130 120 110 100 90 80 70 60 50 40 30 20 10 0
f1 (ppm)

N-60 (2S,3R)-2-amino-N-(2-((tert-butyldimethylsilyl)oxy)-2-(5-hydroxy-2-methoxyphenyl)ethyl)-3-methylpentanamide

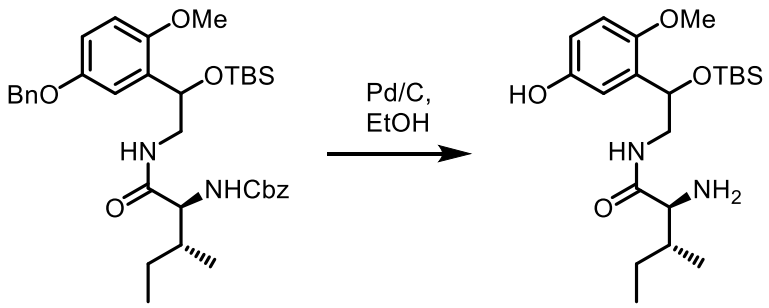

Assay: N-67 (1.4 g, 2.8 mmol, 1.0 equiv) was dissolved in EtOH (28 mL), Pd/C (298.2 mg, 0.28 mmol, 0.1 equiv) was added and the reaction vessel was set under hydrogen atmosphere (balloon). Starting material was fully consumed within 2 h. The mixture was then filtrated over a pad of Celite and the filtrate was concentrated under reduced pressure. Purification by FC (CH_2Cl_2:MeOH, 9:1) gave the desired product as a sticky white foam (884.1 mg, 2.15 mmol, 77%).

Analytics: $\mathbf{R_f}$ = 0.57 (CH_2Cl_2:MeOH, 9:1). **^{1}H NMR** (400 MHz, Chloroform-*d*) δ 7.44 (s, 1H), 6.98 – 6.90 (m, 1H), 6.67 (s, 2H), 5.16 (q, *J* = 5.3, 4.9 Hz, 1H), 3.76 (s, 3H), 3.59 – 3.48 (m, 1H), 3.45 – 3.32 (m, 1H), 3.23 (dd, *J* = 18.5, 3.9 Hz, 1H), 2.01 – 1.83 (m, 1H), 1.39 – 1.16 (m, 1H), 1.12 – 0.97 (m, 1H), 0.91 (m, 9H), 0.89 – 0.80 (m, 6H), 0.06 (s, 3H), -0.07 (s, 3H). **^{13}C NMR** (101 MHz, Chloroform-*d*) δ 174.14, 173.63, 149.79, 149.72, 149.64, 131.63, 131.53, 114.46 (2C), 111.23, 67.32, 67.27, 60.04, 59.94, 55.86, 45.58, 37.79, 37.63, 25.87, 23.64, 18.18, 16.05, 15.94, 11.90, 11.83, -4.78, -5.09. **HRMS (ESI)**: 433.2490 $[M+Na]^+$; calculated for $[C_{21}H_{38}N_2NaO_4Si]$: 433.2493. **IR** [ATR, neat]: ν = 2957.3 w, 2929.34 w, 2857.02 w, 1647.87 m, 1498.42 m, 1461.78 m, 1254.47 m, 1210.11 m, 1075.12 m, 834.06 s, 777.17 s, 734.75 m cm^{-1}.

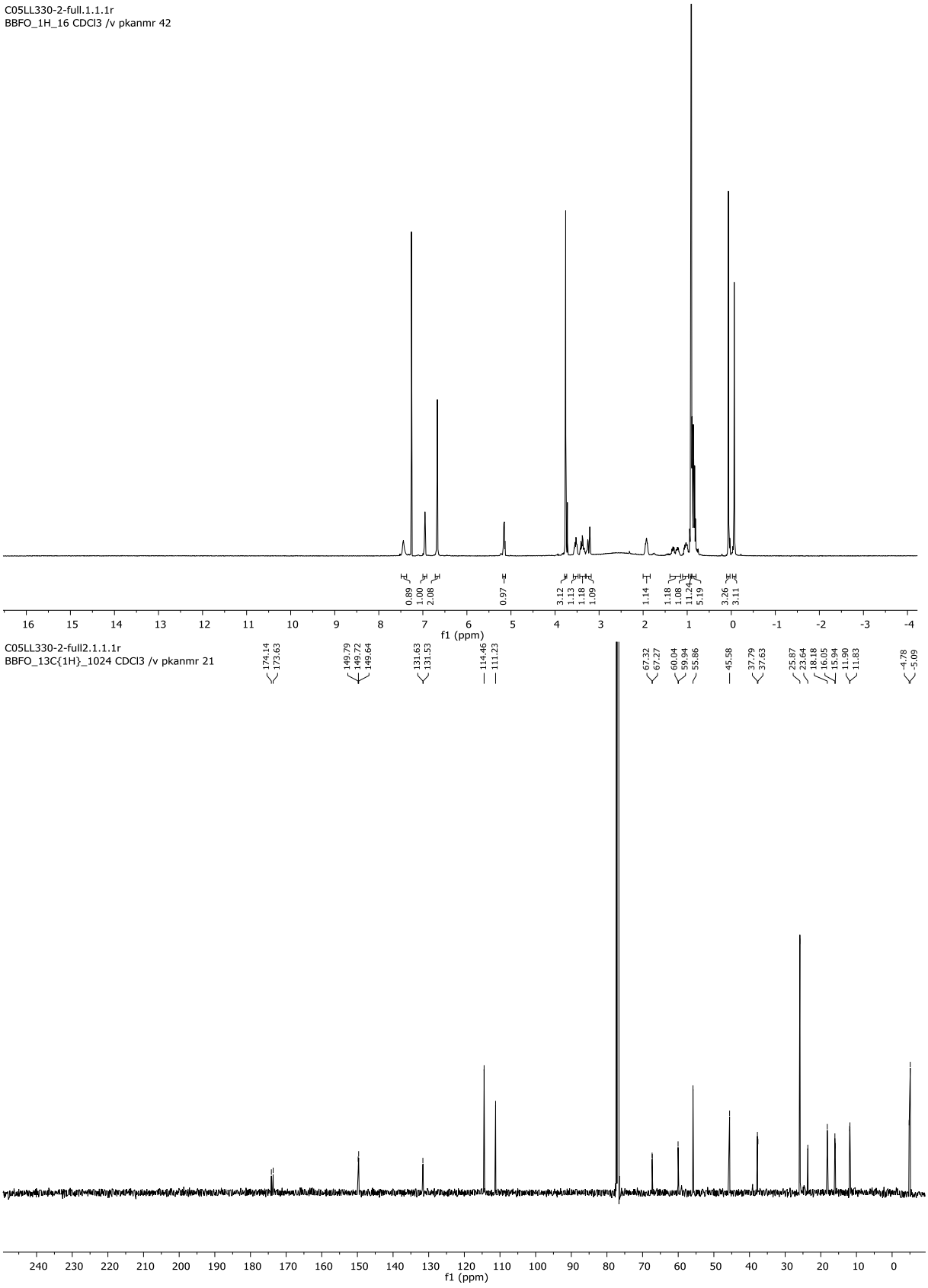
C05LL330-2-full.1.1.1r
BBFO_1H_16 CDCl3 /v pkanmr 42
0.89
1.00
2.08
0.97
3.12
1.13
1.18
1.09
1.14
1.18
1.08
11.24
5.19
3.26
3.11
f1 (ppm)
C05LL330-2-full2.1.1.1r
BBFO_13C{1H}_1024 CDCl3 /v pkanmr 21
174.14
173.63
149.79
149.72
149.64
131.63
131.53
114.46
111.23
67.32
67.27
60.04
59.94
55.86
45.58
37.79
37.63
25.87
23.64
18.18
16.05
15.94
11.90
11.83
-4.78
-5.09
f1 (ppm)

N-59 tert-butyl (2S,3R)-2-(((2S,3R)-1-((2-((tert-butyldimethylsilyl)oxy)-2-(5-hydroxy-2-methoxyphenyl)ethyl)amino)-3-methyl-1-oxopentan-2-yl)carbamoyl)-3-hydroxypyrrolidine-1-carboxylate

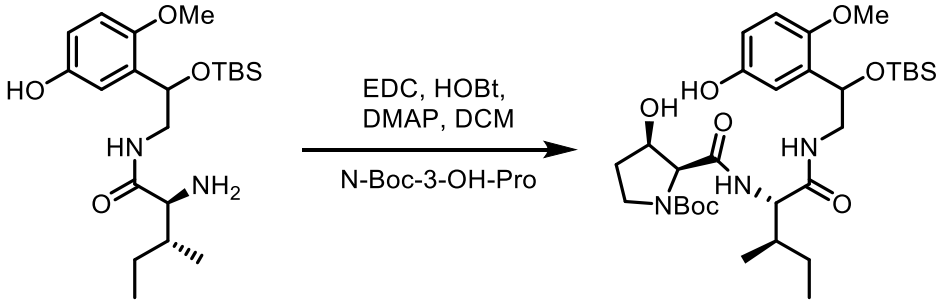

Assay: N-60 (0.81 g, 1.98 mmol, 1.0 equiv), the free acid LL288 (0.54 g, 2.31 mmol, 1.17 equiv), EDC·HCl (0.46 g, 2.37 mmol, 1.2 equiv) and HOBt (0.27 g, 1.98 mmol, 1.0 equiv) followed by DMAP (0.29 g, 2.37 mmol, 1.2 equiv) were suspended in CH_2Cl_2 (20 mL). The reaction mixture was stirred as such over night before being quenched by the addition of saturated aqueous $NaHCO_3$ (15 mL) and diluted with CH_2Cl_2. The two phases were separated and the aqueous phase was extracted with CH_2Cl_2 (3 x 15 mL). The organic phases were dried over $MgSO_4$ and concentrated under reduced pressure. The crude was then purified by FC (CH_2Cl_2:MeOH, 95:5) to give the target compound as a white powder (1.15 g, 1.72 mmol, 87%).

Analytics: $\mathbf{R_f}$ = 0.22 (EtOAc:hexane, 5:1). **^{1}H NMR** (400 MHz, Methanol-d_4) δ 6.91 (d, *J* = 3.1 Hz, 1H), 6.76 (dd, *J* = 8.8, 3.9 Hz, 1H), 6.65 (dt, *J* = 8.8, 2.8 Hz, 1H), 5.28 – 5.14 (m, 1H), 4.58 – 4.46 (m, 1H), 4.39 – 4.24 (m, 2H), 3.77 (s, 3H), 3.63 – 3.54 (m, 1H), 3.51 – 3.32 (m, 3H), 2.15 – 1.88 (m, 3H), 1.40 (s, 10H), 1.18 – 1.06 (m, 1H), 0.96 – 0.83 (m, 15H), 0.06 (s, 3H), -0.09 (s, 3H). **^{13}C NMR** (101 MHz, Methanol-d_4) δ 173.46, 172.63, 156.14, 152.10, 150.94, 132.88, 115.61, 115.48, 112.70, 81.49, 73.19, 68.34, 64.77, 59.77, 56.47, 47.31, 45.08, 37.59, 32.77, 28.68 (3C), 26.49 (3C), 25.31, 19.12, 16.36, 12.08, -4.72 (2C).

IR [ATR, neat]: ν = 3323.71 w, 2959.23 w, 2931.27 w, 1651.73 s, 1501.31 m, 1458.89 m, 1397.17 m, 1254.47 m, 1213.01 m, 1167.69 m, 1075.12 m, 835.99 m, 777.17 m cm^{-1}. **HRMS (ESI)**: 646.3487 $[M+Na]^+$; calculated for $[C_{31}H_{53}N_3NaO_8Si]$: 646.3494.

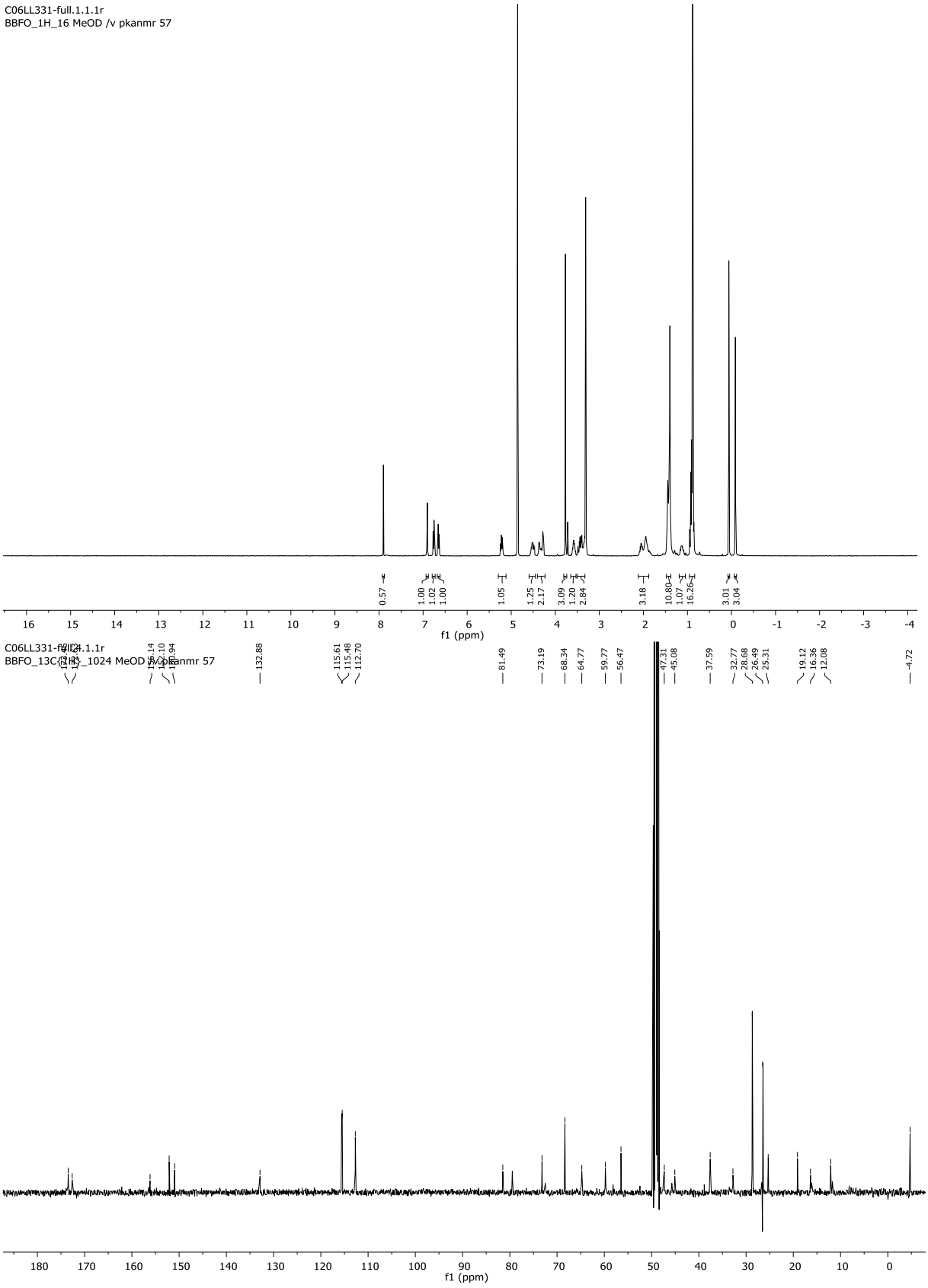
C06LL331-full.1.1.1r
BBFO_1H_16 MeOD /v pkanmr 57
0.57
1.00
1.02
1.00
1.05
1.25
2.17
3.09
1.20
2.84
3.18
10.80
1.07
16.26
3.01
3.04
f1 (ppm)
C06LL331-full.1.1.1r
BBFO_13C{1H}_1024 MeOD /v pkanmr 57
132.88
115.61
115.48
112.70
81.49
73.19
68.34
64.77
59.77
56.47
47.31
45.08
37.59
32.77
28.68
26.49
25.31
19.12
16.36
12.08
-4.72
f1 (ppm)

N-68 tert-butyl (12S,13S,8S)-8-((R)-sec-butyl)-4-((tert-butyldimethylsilyl)oxy)-34-methoxy-7,10-dioxo-2-oxa-6,9-diaza-1(3,2)-pyrrolidina-3(1,3)-benzenacyclodecaphane-11-carboxylate

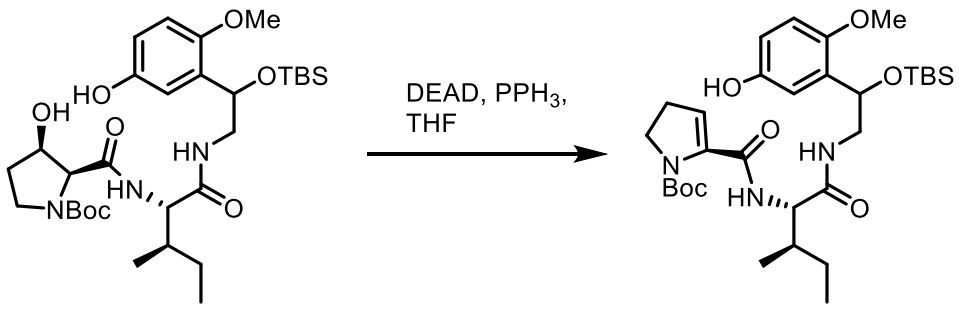

Assay: N-59 (1.07 g, 1.72 mol, 1.0 equiv) was dissolved in THF (18 mL) and PPH_3 (0.56 mg, 2.14 mmol, 1.25 equiv) was added followed by DEAD (0.34 mL, 2.14 mmol, 1.25 equiv). The reaction mixture turned into a soft yellow. Starting material was fully consumed within 30 min. The reaction was quenched by the addition of saturated aqueous $NaHCO_3$ (15 mL) and diluted with CH_2Cl_2 (20 mL). The two phases were separated and the aqueous phase was extracted with CH_2Cl_2 (3 x 15 mL). The organic phases were dried over $MgSO_4$ and concentrated under reduced pressure. Purification by FC (EtOAc:hexane, 1:1) gave the desired macrocycle as a white powder (910 mg, 1.42 mmol, 88%).

Analytics: $\mathbf{R_f}$ = 0.22 (EtOAc:hexane, 1:1). **^{1}H NMR** (400 MHz, Methanol-*d*$_4$) δ 6.93 (dd, *J* = 3.0, 1.8 Hz, 1H), 6.77 (dd, *J* = 8.8, 2.0 Hz, 1H), 6.65 (ddd, *J* = 8.7, 3.1, 1.3 Hz, 1H), 5.64 (dt, *J* = 4.1, 2.9 Hz, 1H), 5.06 (td, *J* = 6.9, 4.1 Hz, 1H), 4.28 (dd, *J* = 6.8, 4.8 Hz, 1H), 3.89 (t, *J* = 9.0 Hz, 2H), 3.76 (d, *J* = 2.2 Hz, 3H), 3.59 – 3.35 (m, 2H), 2.65 (ddd, *J* = 9.7, 7.7, 2.7 Hz, 2H), 1.89 (s, 1H), 1.59 – 1.47 (m, 1H), 1.22 – 1.09 (m, 1H), 0.95 – 0.84 (m, 6H). **^{13}C NMR** (101 MHz, Methanol-*d*$_4$) δ 172.31, 163.93, 152.95, 150.84, 149.67, 138.67, 131.19, 131.12, 116.24, 116.12, 113.95, 113.62, 111.36, 81.07, 67.13, 66.88, 58.30, 58.21, 55.00, 45.32, 45.21, 36.60, 27.78, 27.16, 24.58, 24.50, 14.54, 10.35. **HRMS (ESI)**: 628.3379 $[M+Na]^+$; calculated for $[C_{31}H_{51}N_3NaO_7Si]$: 628.3388. **IR** [ATR, neat]: ν = 3315.03 w, 2959.23 w, 2932.23 w, 2857.99 w, 1655.59 s, 1500.35 m, 1457.92 m, 1393.32 m, 1255.43 m, 1213.01 m, 1137.80 m, 835.99 m, 772.35 m cm^{-1}.

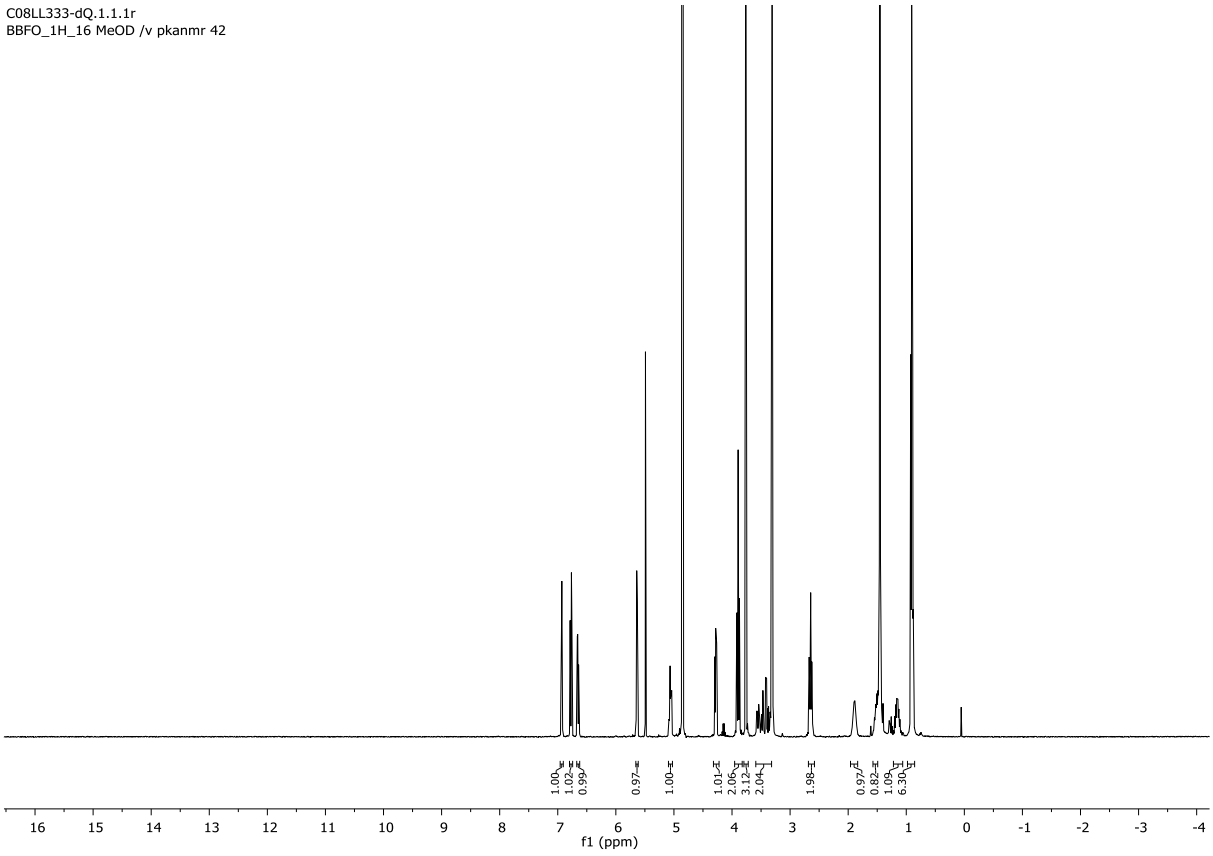
C08LL333-dQ.1.1.1r
BBFO_1H_16 MeOD /v pkanmr 42
1.00
1.02
0.99
0.97
1.00
1.01
2.06
3.12
2.04
1.98
0.97
0.82
1.09
6.30
16 15 14 13 12 11 10 9 8 7 6 5 4 3 2 1 0 -1 -2 -3 -4
f1 (ppm)

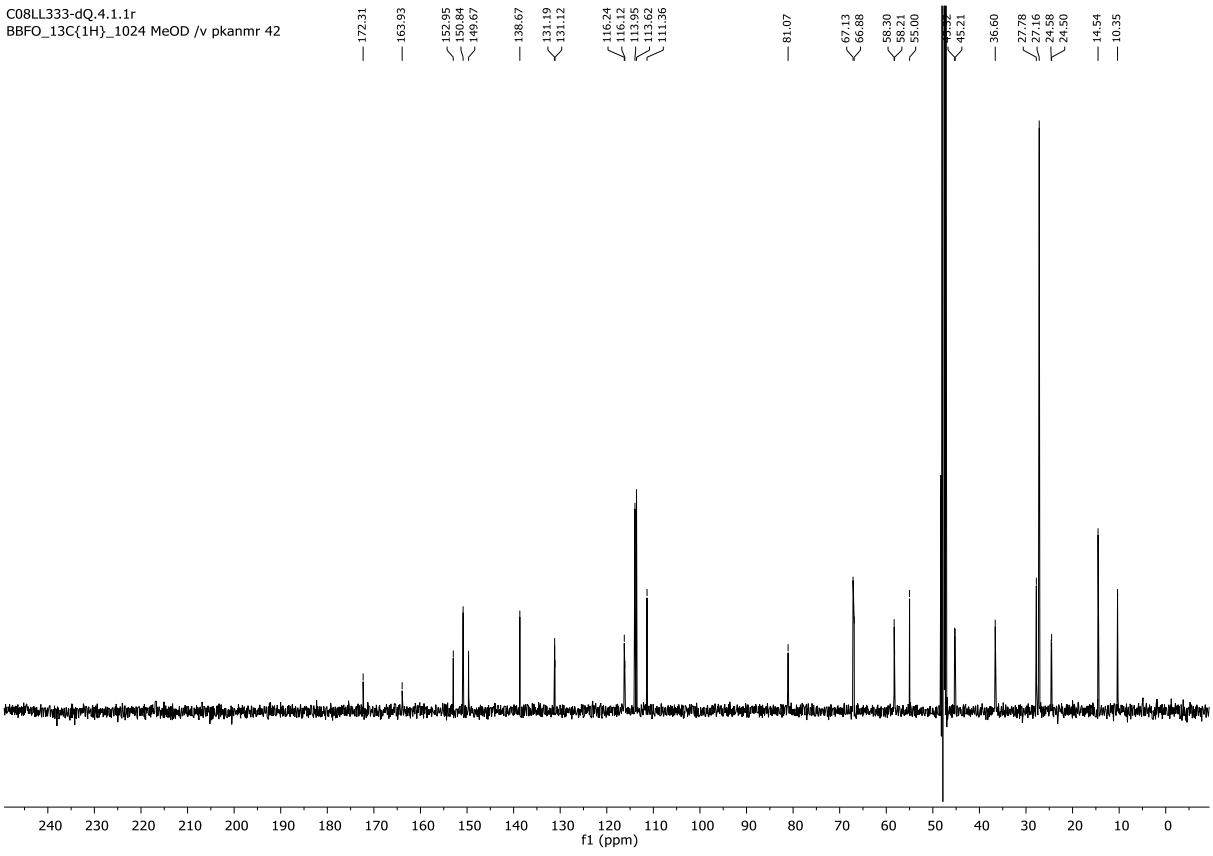
C08LL333-dQ.4.1.1r
BBFO_13C{1H}_1024 MeOD /v pkanmr 42
172.31
163.93
152.95
150.84
149.67
138.67
131.19
131.12
116.24
116.12
113.95
113.62
111.36
81.07
67.13
66.88
58.30
58.21
55.00
45.21
36.60
27.78
27.16
24.58
24.50
14.54
10.35
240 230 220 210 200 190 180 170 160 150 140 130 120 110 100 90 80 70 60 50 40 30 20 10 0
f1 (ppm)

N-72 tert-butyl(1-(5-fluoro-2-methoxyphenyl)-2-nitroethoxy)dimethylsilane

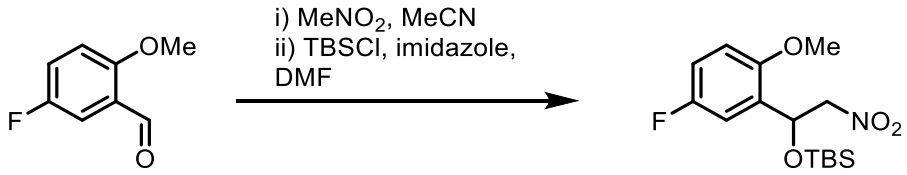

Assay: A stock solution of NaOMe (25 wt% in MeOH, 10.5 mL) in additional MeOH (10 mL) and $MeNO_2$ (14.6 mL, 45 mmol, 18.0 equiv) was first prepared. The complete stock solution was then added dropwise to a stirring solution of **N-71** (2.3 g, 15 mmol, 1.0 equiv) in MeOH (150.0 mL). The reaction mixture stayed clear but turned orange. After stirring overnight, the starting material was fully consumed. The reaction mixture was concentrated to a volume of roughly 10 mL and subsequently carefully quenched with saturated aqueous $NHCl_4$ (60 mL) and extracted with EtOAc (3 x 25 mL). The solvent was evaporated and the crude was taken up in DMF (100 mL). TBSCl (5.88 g, 39 mmol, 2.60 equiv) and imidazole (5.1 g, 75 mmol, 5.0 equiv) were added in one portion. Starting material was fully consumed after 16 h. The organic solvent was evaporated under diminished pressure and the crude was purified by FC (EtOAc:hexane, 1:10 -> 1:5) to give the desired product (21%) along with impure fractions.

Analytics: $\mathbf{R_f}$ = 0.33 (EtOAc:hexane, 1:10). **^{1}H NMR** (400 MHz, Chloroform-*d*) δ 7.23 (ddd, *J* = 9.1, 3.2, 0.8 Hz, 1H), 6.97 (ddd, *J* = 9.0, 7.8, 3.1 Hz, 1H), 6.80 (dd, *J* = 9.0, 4.2 Hz, 1H), 5.75 (dd, *J* = 9.4, 2.5 Hz, 1H), 4.52 (dd, *J* = 11.8, 2.7 Hz, 1H), 4.34 (dd, *J* = 11.8, 9.4 Hz, 1H), 3.86 (s, 3H), 0.89 (s, 9H), 0.05 (s, 3H), -0.08 (s, 3H). **^{13}C NMR** (101 MHz, Chloroform-*d*) δ 157.42 (d, *J* = 240.5 Hz), 151.45, 129.42 (d, *J* = 6.8 Hz), 115.39 (d, *J* = 23.6 Hz), 114.30 (d, *J* = 25.4 Hz), 111.23 (d, *J* = 8.5 Hz), 81.06, 66.97, 56.00, 25.77 3C, 18.23, -4.73, -5.52. **HRMS (ESI)**: 352.1351 $[M+Na]^+$; calculated for $[C_{15}H_{24}FNNaO_4Si]$: 352.1351. **IR** [ATR, neat]: ν = 2954.41 w, 2933.20 w, 2857.99 w, 1555.31 s, 1494.56 s, 1465.63 m, 1425.14 w, 1378.85 w, 1254.47 s, 1197.58 w, 1124.30 m, 1086.69 m, 958.49 m, 832.13 s, 780.07 s cm^{-1}.

C16-KH-157-1_F4-7.1.fid
KH-157-1,Fr.4-7
BBFO_1H_16 CDCl3 /v pkanmr 41

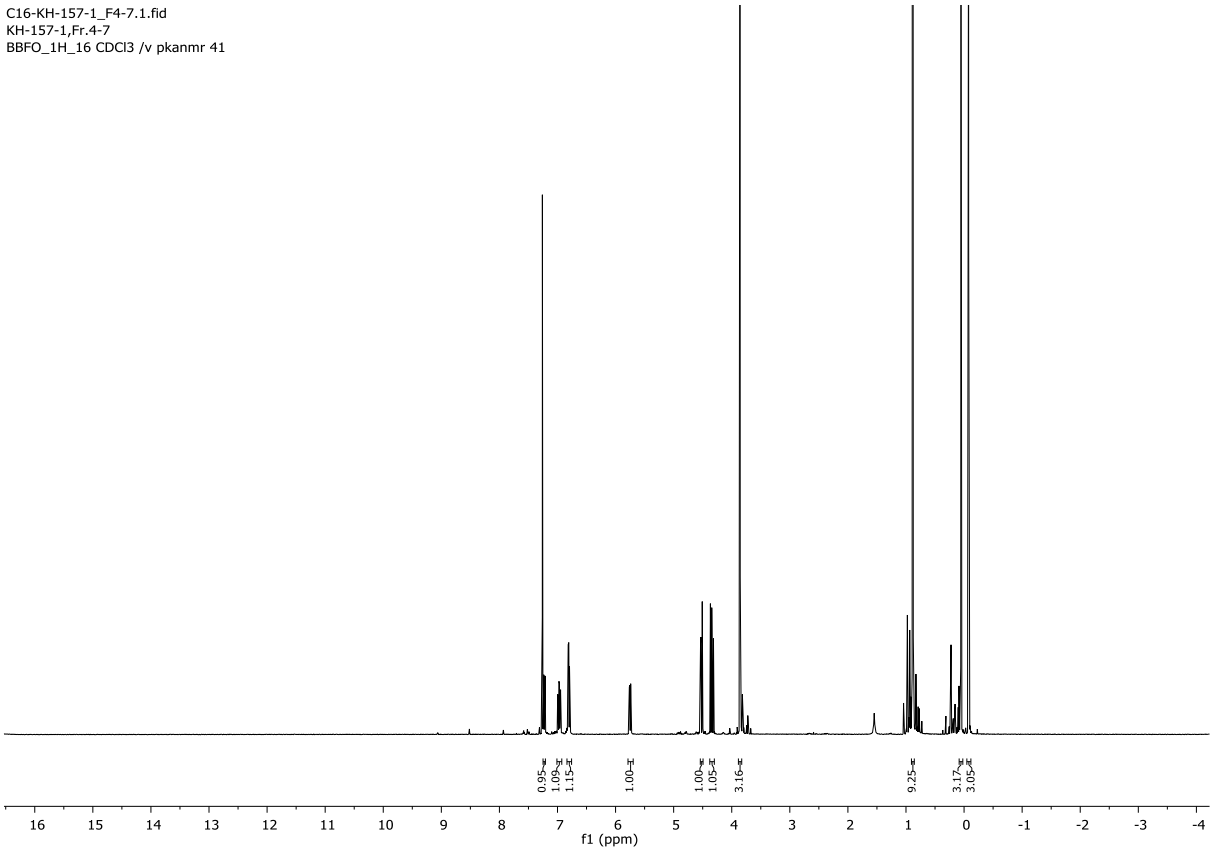

C19LLKH157.2.1.1r
BBFO_13C{1H}_1024 CDCl3 /v pkanmr 4

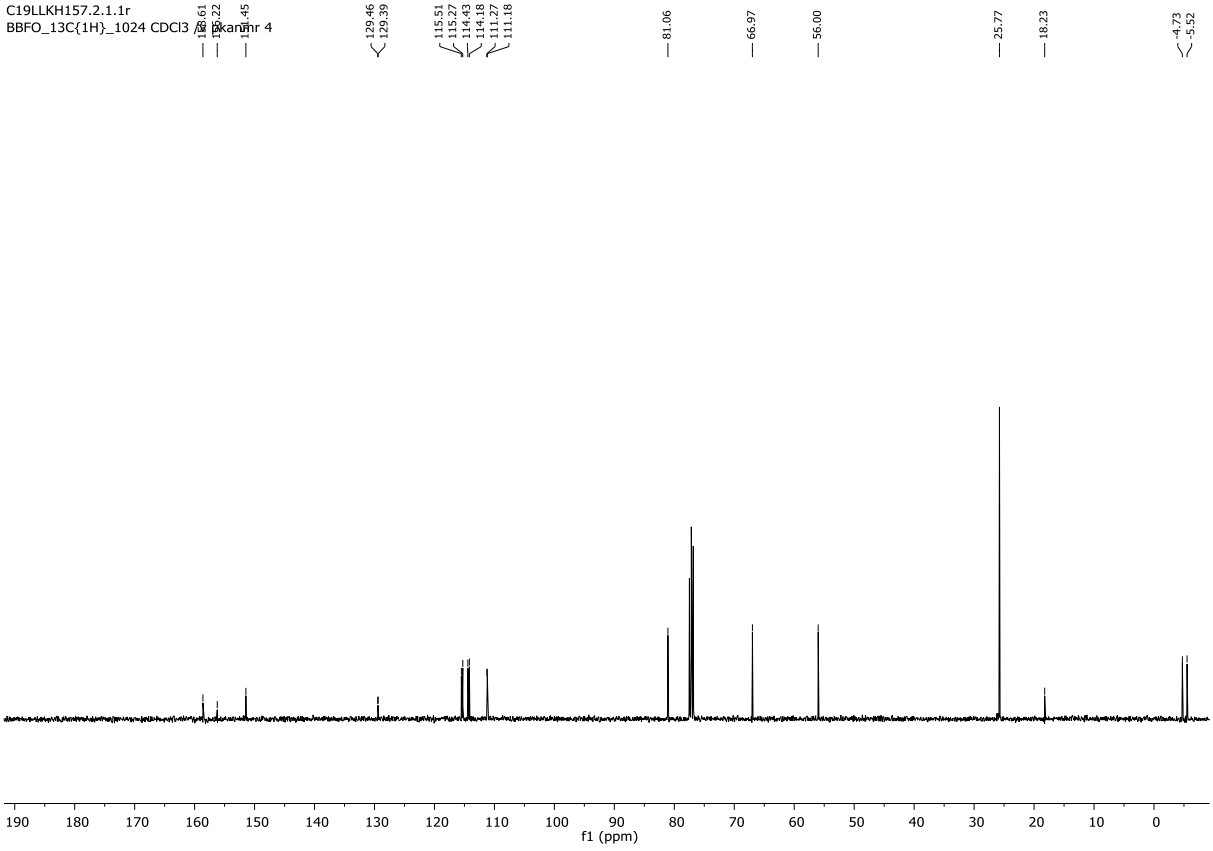

N-73 2-((tert-butyldimethylsilyl)oxy)-2-(5-fluoro-2-methoxyphenyl)ethan-1-amine

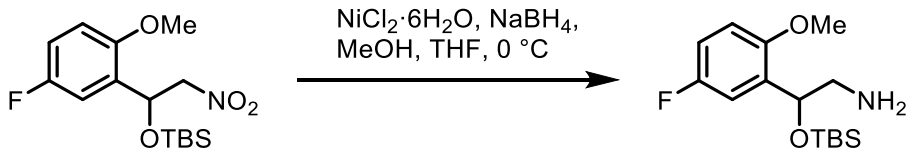

Assay: N-72 (990 0g, 3 mmol, 1.0 equiv) was dissolved in MeOH (30 mL) and THF (15 mL) and cooled to 0 °C. $NiCl_2 \cdot 6H_2O$ (2.62 g, 11.02 mmol, 4.0 equiv) was added followed by stepwise addition of $NaBH_4$ (1.36 g, 36.1 mmol, 12.0 equiv). The reaction turns instantly black and a strong effervescent was observed. The reaction was completed within 50 min. The reaction mixture was cooled to 0 °C and carefully quenched with a solution of saturated $NHCl_4$ (30 mL). The organic solvent was removed under diminished pressure and the aqueous phase was extracted with EtOAc (3 x 30 mL). Combined organic phases were dried over $MgSO_4$ and concentrated under reduced pressure. The crude brown/black oil was purified by FC (CH_2Cl_2:MeOH, 9:1) to give the desired product as a yellowish foam/powder (70%).

Analytics: $\mathbf{R_f}$ = 0.45 (CH_2Cl_2:MeOH, 9:1). **^{1}H NMR** (400 MHz, Chloroform-*d*) δ 7.16 (dd, *J* = 9.3, 3.2 Hz, 1H), 6.89 (ddd, *J* = 8.9, 7.9, 3.2 Hz, 1H), 6.75 (dd, *J* = 9.0, 4.3 Hz, 1H), 5.09 – 5.01 (m, 1H), 3.79 (s, 3H), 2.88 (dd, *J* = 13.0, 3.5 Hz, 1H), 2.76 (dd, *J* = 13.2, 5.8 Hz, 1H), 2.15 (s, 2H), 0.92 (s, 9H), 0.08 (s, 3H), -0.06 (s, 3H). **^{13}C NMR** (126 MHz, Chloroform-*d*) δ 157.34 (d, *J* = 238.0 Hz), 151.68 (d, *J* = 2.0 Hz), 132.88 (d, *J* = 6.4 Hz), 114.37 (d, *J* = 24.5 Hz), 113.96 (d, *J* = 23.1 Hz), 110.97 (d, *J* = 8.1 Hz), 69.80, 55.89, 48.54, 26.04 (3C), 18.37, -4.64, -4.79. **HRMS (ESI)**: 300.1790 $[M+H]^+$; calculated for $[C_{15}H_{27}FNO_2Si]$: 300.1790. **IR** [ATR, neat]: ν = 2953.45 w, 2929.34 w, 2857.02 w, 1493.60 s, 1463.71 s, 1249.65 s, 1199.51 w, 1178.29 w, 1068.37 m, 921.81 w, 834.06 s, 805.14 s, 776.21 s, 712.57 s cm^{-1}.

Remarks: Proton NMR was measured in $CDCl_3$ and not in MeOD as indicated on the spectrum.

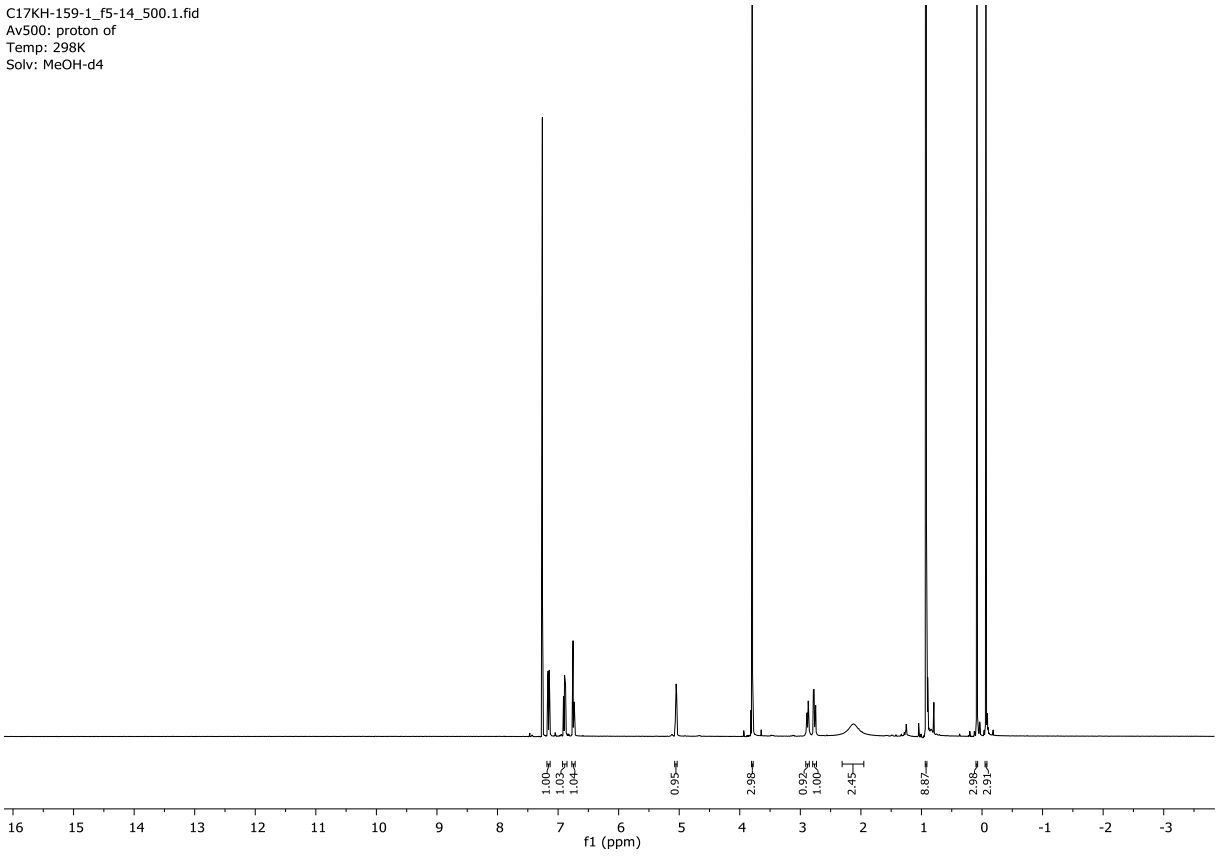
C17KH-159-1_f5-14_500.1.fid
Av500: proton of
Temp: 298K
Solv: MeOH-d4
1.00
1.03
1.04
0.95
2.98
0.92
1.00
2.45
8.87
2.98
2.91
f1 (ppm)

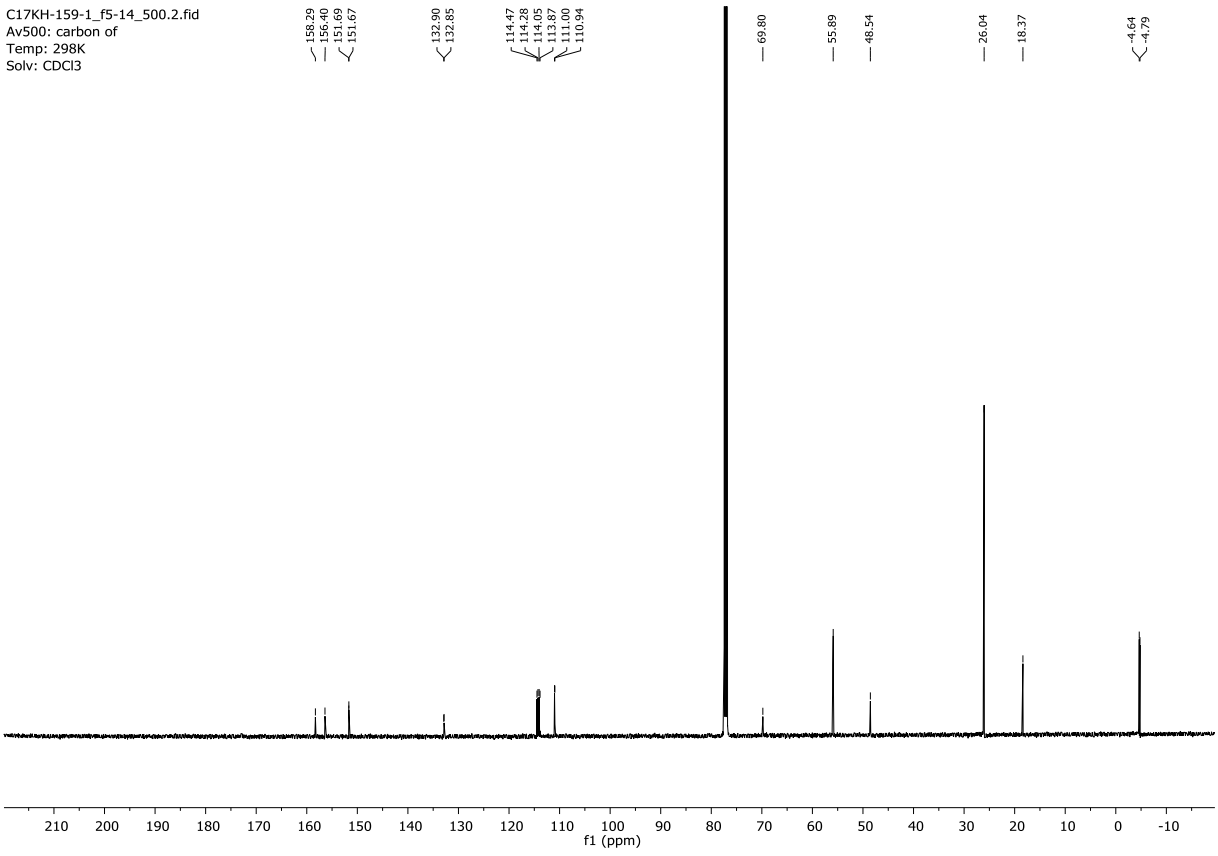
C17KH-159-1_f5-14_500.2.fid
Av500: carbon of
Temp: 298K
Solv: CDCl3
158.29
156.40
151.69
151.67
132.90
132.85
114.47
114.28
114.05
113.87
111.00
110.94
69.80
55.89
48.54
26.04
18.37
-4.64
-4.79
f1 (ppm)

N-74 benzyl ((2S,3R)-1-((2-((tert-butyldimethylsilyl)oxy)-2-(5-fluoro-2-methoxyphenyl)ethyl)amino)-3-methyl-1-oxopentan-2-yl)carbamate

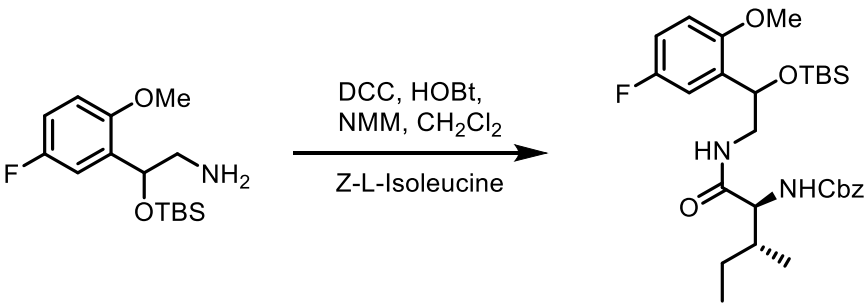

Assay: N-73 (24 mg, 63 µmol, 1.0 equiv) and *Z*-L-Ile (18 mg, 69 µmol, 1.1 equiv) were dissolved in CH_2Cl_2 (0.5 mL) and cooled to 0 °C. DCC (14 mg, 75 µmol, 1.2 equiv), HOBt (11 mg, 82 µmol, 1.3 equiv) and NMM (8 µL, 69 µmol, 1.1 equiv) were added subsequently and the reaction was allowed to warm to ambient temperature and stirred as such over 16 h. The reaction mixture was filtrated over a pad of Celite and the filtrate was concentrated under reduced pressure. Purification by FC (EtOAc:hexane, 3:7) gave the pure product as an oil (93 %).

Analytics: $\mathbf{R_f}$ = 0.45 (EtOAc:hexane, 3:7). **^{1}H NMR** (400 MHz, Chloroform-*d*) δ 7.40 – 7.28 (m, $5H_{ab}$), 7.13 (dd, *J* = 9.3, 3.2 Hz, $1H_{ab}$), 6.89 (dddd, *J* = 8.9, 7.9, 3.2, 2.3 Hz, $1H_{ab}$), 6.74 (ddd, *J* = 8.9, 4.3, 1.7 Hz, $1H_{ab}$), 6.05 – 5.93 (m, $1H_{ab}$), 5.35 – 5.02 (m, $4H_{ab}$), 3.94 (dd, *J* = 8.8, 5.9 Hz, $1H_{ab}$), 3.81 (s, $1.5H_a$), 3.80 (s, $1.5H_b$), 3.61 – 3.43 (m, $2H_{ab}$), 1.91 – 1.72 (m, $1H_{ab}$), 1.40 – 1.29 (m, $1H_{ab}$), 1.09 – 0.95 (m, $1H_{ab}$), 0.92 (s, $4.5H_a$), 0.91 (s, $4.5H_b$), 0.89 – 0.83 (m, $4.5H_{ab}$), 0.76 (d, *J* = 6.8 Hz, $1.5H_{ab}$), 0.06 (s, $3H_{ab}$), -0.05 (s, $1.5H_a$), -0.06 (s, $1.5H_b$). **^{13}C NMR** (101 MHz, Chloroform-*d*) δ 170.96, 170.84, 158.49, 156.13, 151.75, 132.04, 128.68, 128.34, 128.29, 128.23, 114.49, 114.27, 114.02, 111.10, 67.33, 67.21, 60.15, 60.01, 55.99, 45.47, 37.76, 37.39, 25.96, 25.92, 24.81, 24.68, 18.31, 15.62, 15.27, 11.61, -4.76, -4.97. **HRMS (ESI)**: 569.2813 $[M+Na]^+$; calculated for $[C_{29}H_{43}FN_2NaO_5Si]$: 569.2817. **IR** [ATR, neat]: ν = 3310.21 w, 2958.27 w, 2930.31 w, 2857.02 w, 1704.76 m, 1655.59 s, 1494.56 s, 1463.71 m, 1247.72 s, 1071.26 m, 1028.84 m, 834.06 s, 777.17 s, 735.71 m, 697.14 m cm^{-1}.

C17-KH-159-1_F14-25.2.fid
KH-159-1,Fr.14-25
BBFO_1H_256 CDCl3 /v pkanmr 9

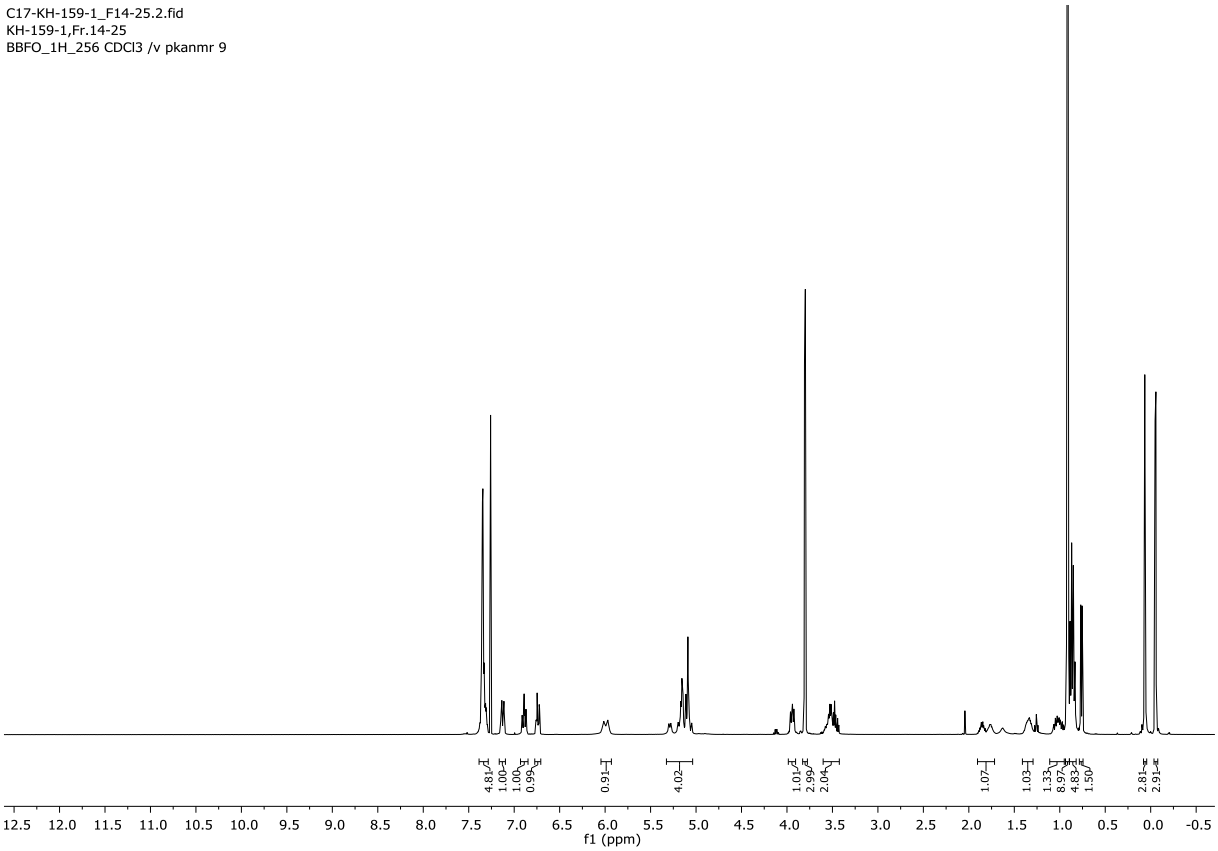

C17-KH-159-1_F14-25.7.1.1r
KH-159-1,Fr.14-25
BBFO_13C{1H}_1024 CDCl3 /v pkanmr 9

170.96
170.84
158.49
156.13
151.75
132.04
128.68
128.34
128.29
128.23
114.49
114.27
114.02
111.10
67.33
67.21
60.15
60.01
55.99
45.47
37.76
37.39
25.96
25.92
24.81
24.68
18.31
15.62
15.27
11.61
-4.76
-4.97

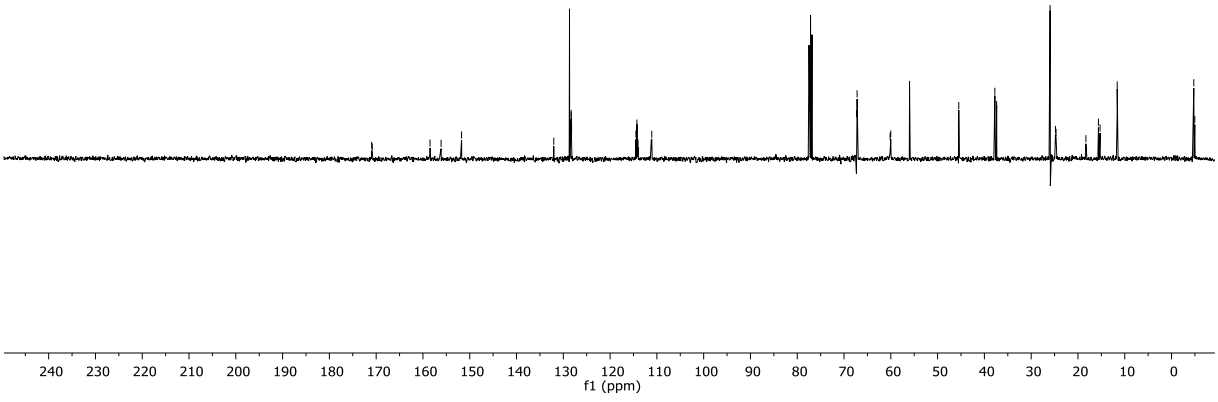

N-75 (2S,3R)-2-amino-N-(2-((tert-butyldimethylsilyl)oxy)-2-(5-fluoro-2-methoxyphenyl)ethyl)-3-methylpentanamide

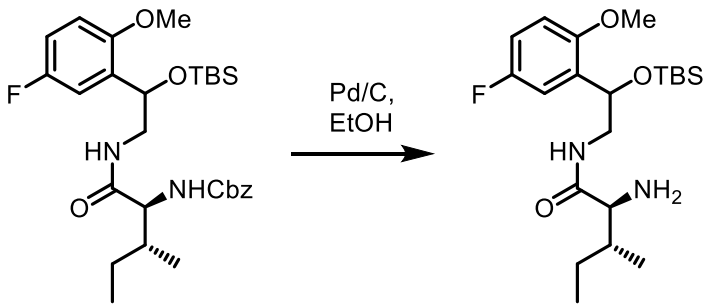

Assay: N-74 (760 mg, 1.39 mmol, 1.0 equiv) was dissolved in EtOH (30 mL), Pd/C (38 mg, 139 µmol, 0.1 equiv) was added and the reaction vessel was set under hydrogen atmosphere (rotavap, balloon). Starting material was fully consumed within 2 h. The mixture was then filtrated over a pad of Celite and the filtrate was concentrated under reduced pressure. Purification by FC (CH_2Cl_2:MeOH, 9:1) gave the desired product (99%).

Analytics: $\mathbf{R_f}$ = 0.63 (CH2Cl2:MeOH, 9:1). **^{1}H NMR** (400 MHz, Chloroform-*d*) δ 7.64 (s, $1H_a$), 7.45 (s, $1H_b$), 7.20 – 7.11 (m, $1H_{ab}$), 6.88 (tt, *J* = 8.0, 3.4 Hz, $1H_{ab}$), 6.74 (ddd, *J* = 9.0, 4.3, 2.4 Hz, $1H_{ab}$), 5.20 – 5.12 (m, $1H_{ab}$), 3.81 (s, $3H_{ab}$), 3.61 – 3.33 (m, $3H_{ab}$), 3.19 (dd, *J* = 18.9, 3.7 Hz, $2H_{ab}$), 1.99-1.88 (m, *J* = 13.7, 8.1, 6.8, 3.4 Hz, $1H_{ab}$), 1.39 – 1.27 (m, $1H_{ab}$), 1.16 – 0.96 (m, $1H_{ab}$), 0.93 (s, $9H_a$), 0.93 (s, $9H_b$), 0.91 – 0.77 (m, $6H_{ab}$), 0.08 (s, $3H_{ab}$), -0.06 (s, $3H_{ab}$). **^{13}C NMR** (101 MHz, Chloroform-*d*) δ 173.75 C_{ab}, 157.29 C_{ab} (d, *J* = 237.2 Hz), 151.80 C_{ab}, 132.52 C_a, 132.45 C_b, 114.32 C_a, 114.25 C_b, 114.07 C_a, 114.02 C_b, 111.10 C_a, 111.02 C_b, 67.57 C_a, 67.45 C_b, 60.12 C_a, 60.01 C_b, 55.99 C_{ab}, 45.29 C_{ab}, 37.83 C_a, 37.60 C_b, 25.96 $3C_{ab}$, 23.86 C_a, 23.49 C_b, 18.30 C_{ab}, 16.17 C_a, 16.04 C_b, 12.04 C_a, 11.97 C_b, -4.72 C_{ab}, -4.93 C_{ab}. **HRMS (ESI)**: 435.2450 $[M+Na]^+$; calculated for $[C_{21}H_{37}FN_2NaO_3Si]$: 435.2450. **IR** [ATR, neat]: ν = 2956.34 w, 2931.27 w, 2857.99 w, 1664.27 m, 1494.56 m, 1464.67 m, 1250.61 s, 1073.19 m, 834.06 s, 777.17 s, 710.64 w cm^{-1}.

C17-KH-160-1_F.1.1.1r
KH-160-1,F
BBFO_1H_256 CDCl3 /v pkanmr 11

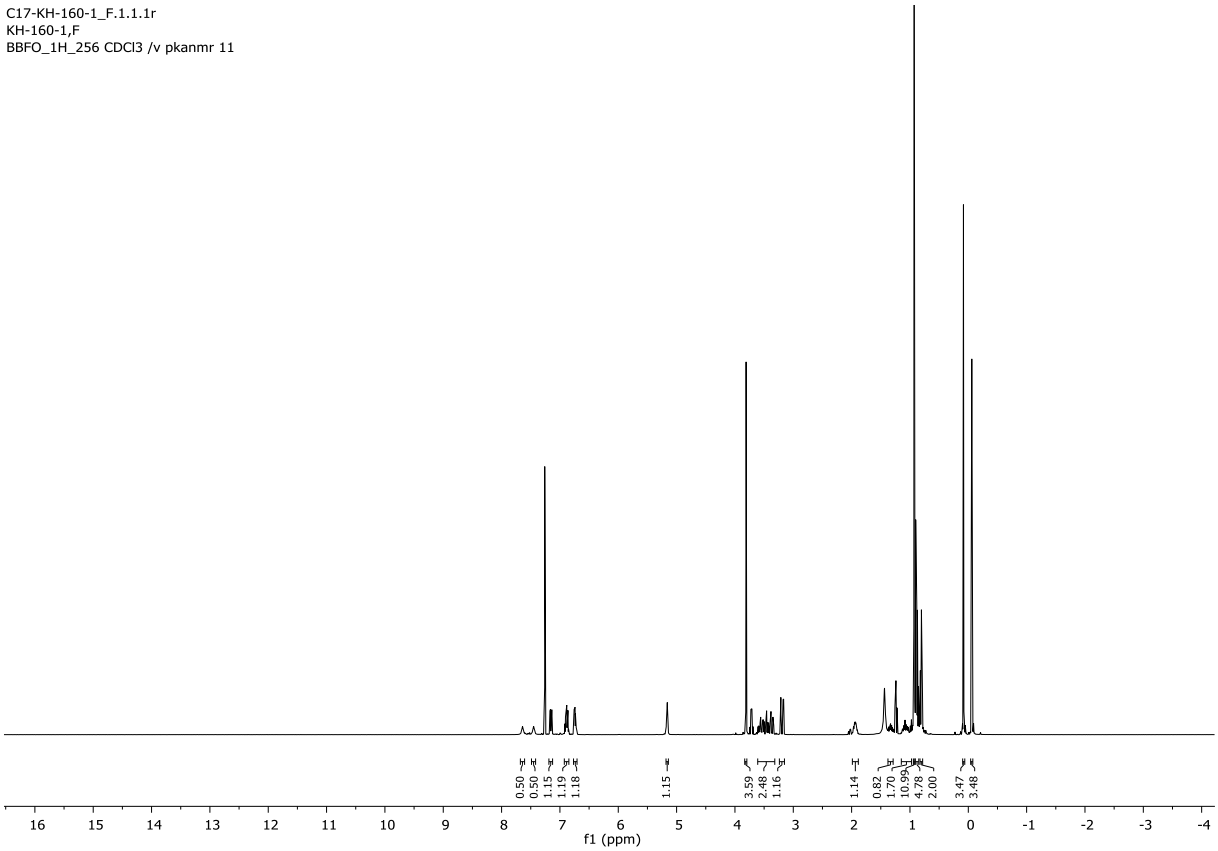

C18-KH-160-1,F.2.1.1r
KH-160-1,F
BBFO_13C{1H}_1024 CDCl3 /v pkanmr 1

173.75
158.47
156.11
151.80
132.52
132.45
114.32
114.25
114.07
114.02
111.10
111.02
67.57
67.45
60.12
60.01
55.99
45.29
37.83
37.60
25.96
23.86
23.49
18.30
16.17
16.04
12.04
11.97
-4.72
-4.93

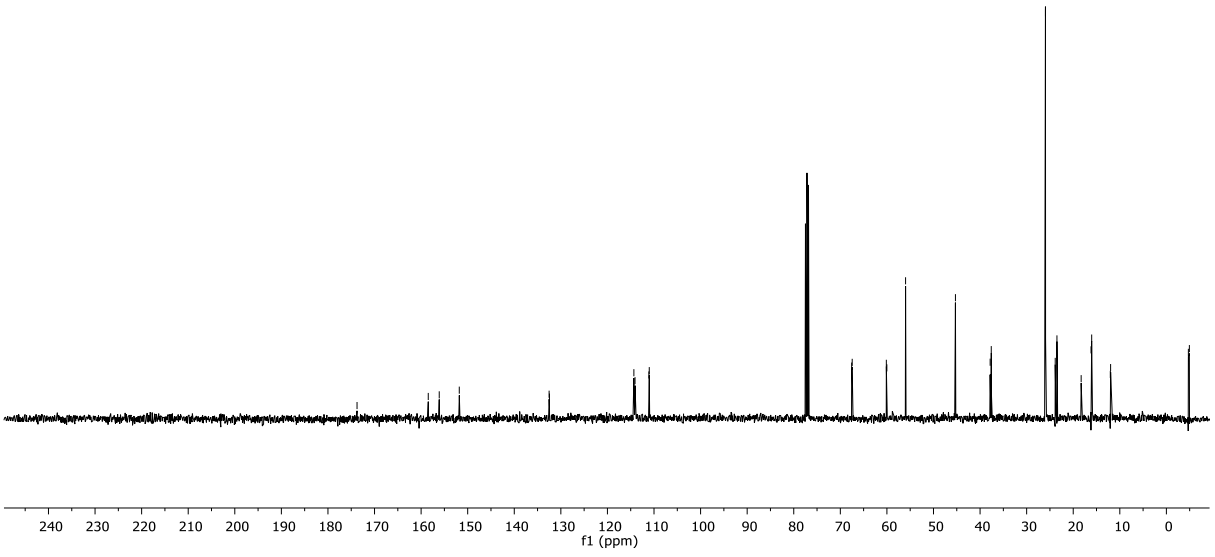

N-76 tert-butyl (2S,3R)-2-(((2S,3R)-1-((2-((tert-butyldimethylsilyl)oxy)-2-(5-fluoro-2-methoxyphenyl)ethyl)amino)-3-methyl-1-oxopentan-2-yl)carbamoyl)-3-hydroxypyrrolidine-1-carboxylate

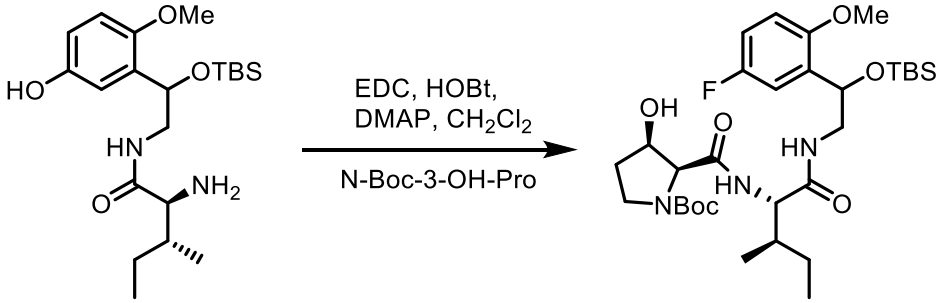

Assay: N-75 (0.55 g, 1.33 mmol, 1.0 equiv), **N-28** (0.36 g, 1.56 mmol, 1.17 equiv), EDC·HCl (0.31 g, 1.6 mmol, 1.6 equiv) and HOBt (0.18 g, 1.33 mmol, 1.0 equiv) followed by DMAP (0.20 g, 1.6 mmol, 1.6 equiv) were suspended in CH_2Cl_2 (20 mL). The reaction mixture was stirred as such over night before being quenched by the addition of saturated aqueous $NaHCO_3$ (15 mL) and diluted with CH_2Cl_2. The two phases were separated and the aqueous phase was extracted with CH_2Cl_2 (3 x 15 mL). The organic phases were dried over $MgSO_4$ and concentrated under reduced pressure. The crude was then purified by FC (CH_2Cl_2:MeOH, 9:1) to give the target compound (98%).

Analytics: **^{1}H NMR** (400 MHz, DMSO-*d*6) δ 7.83 – 7.68 (m, 1H), 7.55 – 7.34 (m, 1H), 7.09 (dd, *J* = 9.6, 2.9 Hz, 1H), 7.07 – 6.99 (m, 1H), 6.95 (td, *J* = 9.1, 4.5 Hz, 1H), 5.30 (dd, *J* = 50.3, 4.6 Hz, 1H), 5.10 (dt, *J* = 10.0, 5.3 Hz, 1H), 4.43 – 4.30 (m, 1H), 4.29 – 4.12 (m, 1H), 3.77 (s, 3H), 3.44 – 3.34 (m, 2H), 3.28 – 3.12 (m, 2H), 1.97 – 1.84 (m, 1H), 1.83 – 1.61 (m, 2H), 1.42 – 1.26 (m, 10H), 1.10 – 0.97 (m, 1H), 0.82 (d, *J* = 5.8 Hz, 9H), 0.80 – 0.72 (m, 6H), 0.03 (d, *J* = 1.3 Hz, 3H), -0.13 (d, *J* = 1.5 Hz, 3H). **^{13}C NMR** (101 MHz, DMSO-d_6) δ 171.42 Ca, 171.35 Cb, 169.96 Ca, 169.85 Cb, 156.84 (dd, *J* = 235.2, 6.2 Hz, Cab), 154.04 Cab, 152.52 Cab, 133.03 – 132.83 (m, Cab), 114.61 (d, *J* = 22.7 Hz, Cab), 114.17 (dd, *J* = 24.0, 5.0 Hz, Cab), 112.66 – 112.34 (m, Cab), 78.86 Cab, 71.78 Ca, 71.73 Cb, 67.09 Cab, 63.49 Ca, 63.37 Cb, 57.68 Cab, 56.56 Ca, 56.49 Cb, 45.56 Cab, 44.21 Cab, 36.75 Cab, 31.66 Cab, 28.41 3Cab, 26.16 3Cab, 24.13 Cab, 18.34 Cab, 16.00 Ca, 15.87 Cb, 12.04 Cab, -4.47 2Ca, -4.63 Cb, -4.76 Cb. **HRMS (ESI)**: 648.3442 $[M+Na]^+$; calculated for $[C_{31}H_{52}FN_3NaO_7Si]$: 648.3451. **IR** [ATR, neat]: ν = 2960.20 m, 2931.27 m, 1698.01 s, 1683.55 s, 1670.05 s, 1652.70 s, 1540.84 s, 1522.52 s, 1496.49 s, 1473.35 m, 1395.25 s, 1366.32 m, 1252.54 s, 1176.36 m, 1119.47 m, 1071.26 m, 836.95 m, 765.60 m, 752.10 m, 669.18 m cm^{-1}.

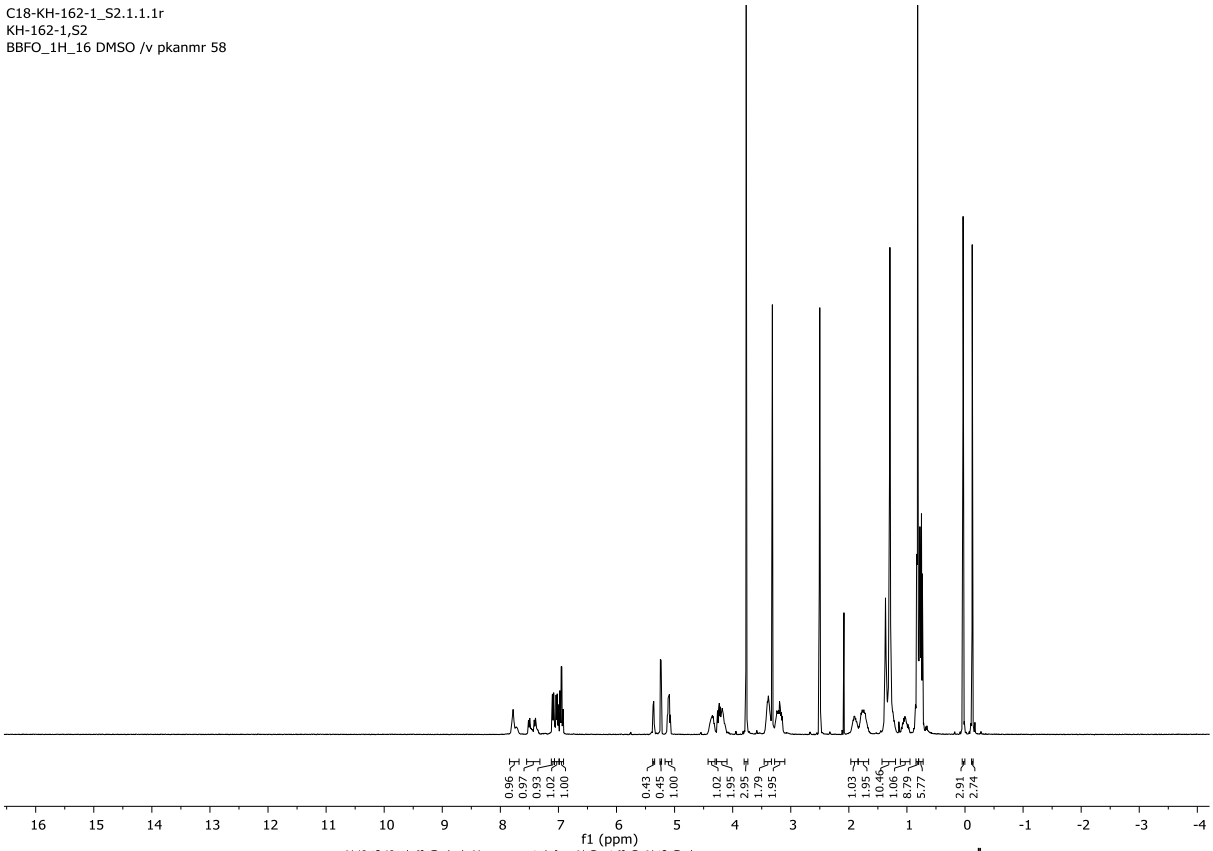
C18-KH-162-1_S2.1.1.1r
KH-162-1,S2
BBFO_1H_16 DMSO /v pkanmr 58
0.96
0.97
0.93
1.02
1.00
0.43
0.45
1.00
1.02
1.95
2.95
1.79
1.95
1.03
1.95
10.46
1.06
8.79
5.77
2.91
2.74
f1 (ppm)

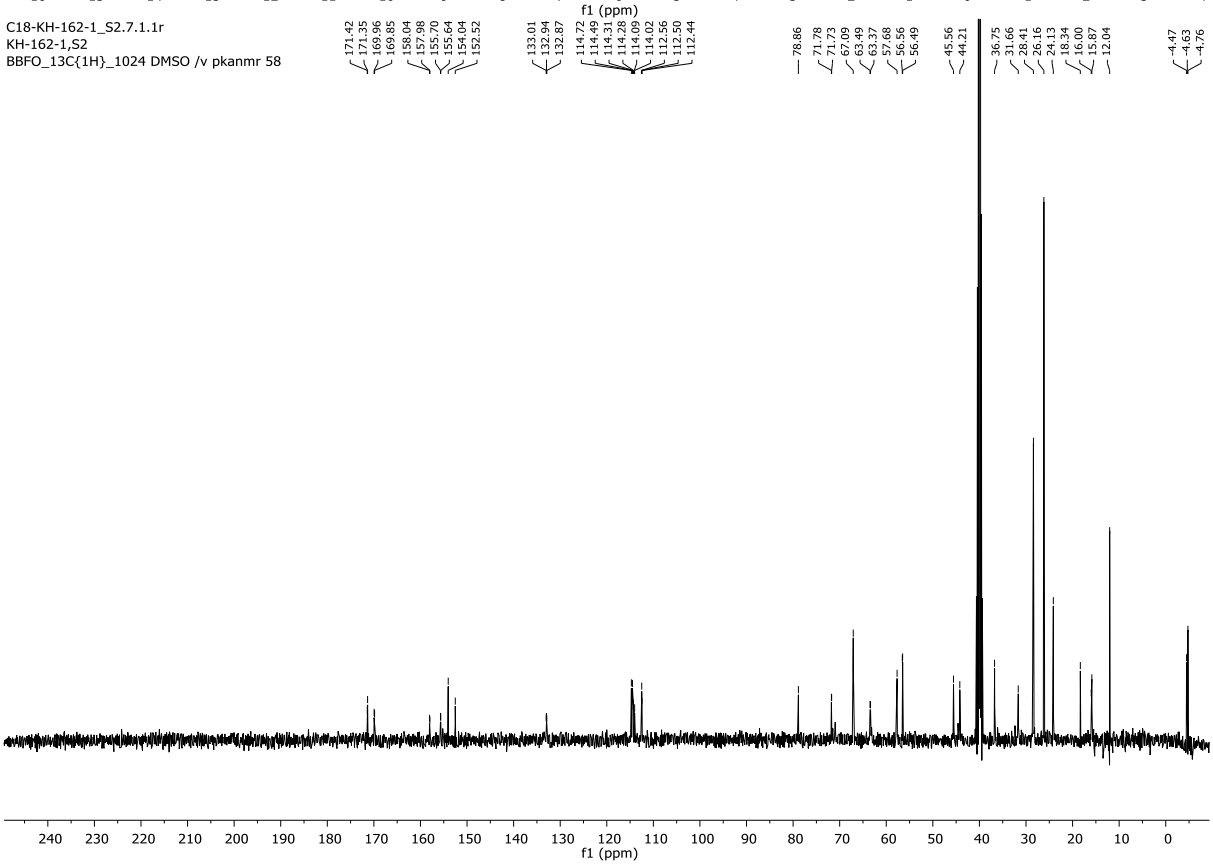
C18-KH-162-1_S2.7.1.1r
KH-162-1,S2
BBFO_13C{1H}_1024 DMSO /v pkanmr 58
171.42
171.35
169.96
169.85
158.04
157.98
155.70
155.64
154.04
152.52
133.01
132.94
132.87
114.72
114.49
114.31
114.28
114.09
114.02
112.56
112.50
112.44
78.86
71.78
71.73
67.09
63.49
63.37
57.68
56.56
56.49
45.56
44.21
36.75
31.66
28.41
26.16
24.13
18.34
16.00
15.87
12.04
4.47
4.63
4.76
f1 (ppm)

N-79 tert-butyl (2S,3R)-2-(((2S,3R)-1-((2-((tert-butyldimethylsilyl)oxy)-2-(5-fluoro-2-methoxyphenyl)ethyl)amino)-3-methyl-1-oxopentan-2-yl)carbamoyl)-3-((trimethylsilyl)oxy)pyrrolidine-1-carboxylate

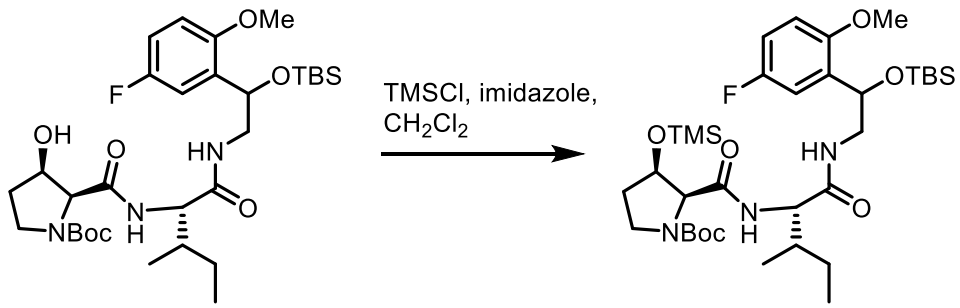

Assay: To a solution of **N-76** (40 mg, 63.9 µmol, 1.0 equiv) in CH_2Cl_2 (0.8 mL) was added imidazole (3 mg, 44.7 µmol, 0.7 equiv) followed by the addition of TMSCl (10 µL, 76.7 µmol, 1.2 equiv) at ambient temperature. The reaction immediately turned turbid after TMSCl addition. After stirring over 16 h product formation was observed along with starting material. Nevertheless, the reaction was quenched by the addition of water. The two phases were separated and the aqueous phase was extracted with CH_2Cl_2 (3 x 3 mL). Combined organic phases were dried over $MgSO_4$ and concentrated under reduced pressure. The blurry crude was purified by FC (EtOAc:Hex, 3:1) to give only undesired products.

4 Bibliography

[1] C. DeBoer, E. Caron, J. Hinman. Amicetin, a new streptomyces antibiotic. *J. Am. Chem. Soc.*, **1953**, *75*, 499–500.

[2] C. L. Stevens, K. Nagarajan, T. H. Haskell. The Structure of Amicetin. *J. Org. Chem.*, **1962**, *27*, 2991–3005.

[3] C. L. Stevens, P. Blumbergs, F. A. Daniher. Stereochemistry and Synthesis of Amosamine: 4,6-Dideoxy-4-Dimethylamino-D-Glucose. *J. Am. Chem. Soc.*, **1963**, *85*, 1552–1553.

[4] C. L. Stevens, N. A. Nielsen, P. Blumbergs. Synthesis of 2,3-Didehydro-2,3-dideoxy and 2,3-Dideoxy Sugar Nucleosides of Known Configuration. *J. Am. Chem. Soc.*, **1964**, *86*, 1894–1895.

[5] S. Hanessian, T. H. Haskell. Configuration of the anomeric linkages in amicetin. *Tetrahedron Lett.*, **1964**, *5*, 2451–2460.

[6] E. H. Flynn, J. W. Hinman, E. L. Caron, D. O. Woolf. The Chemistry of Amicetin, a New Antibiotic. *J. Am. Chem. Soc.*, **1953**, *75*, 5867–5871.

[7] J. L. Smith, M. Sundaralingam. The structure of the antibiotic amicetin consisting of nucleobase, disaccharide and amino acid moieties. *Acta Crystallogr. Sect. B Struct. Crystallogr. Cryst. Chem.*, **1981**, *37*, 1095–1101.

[8] C. Shammas, J. A. Donarski, V. Ramesh. NMR structure of the peptidyl transferase RNA inhibitor antibiotic amicetin. *Magn. Reson. Chem.*, **2007**, *45*, 133–141.

[9] G. Zhang, H. Zhang, S. Li, J. Xiao, G. Zhang, Y. Zhu, S. Niu, J. Ju, C. Zhang. Characterization of the amicetin biosynthesis gene cluster from Streptomyces vinaceusdrappus NRRL 2363 implicates two alternative strategies for amide bond formation. *Appl. Environ. Microbiol.*, **2012**, *78*, 2393–2401.

[10] C. J. Thibodeaux, C. E. Melançon, H. Liu. Natural-Product Sugar Biosynthesis and Enzymatic Glycodiversification. *Angew. Chemie Int. Ed.*, **2008**, *47*, 9814–9859.

[11] M. C. Cone, X. Yin, L. L. Grochowski, M. R. Parker, T. M. Zabriskie. The Blasticidin S Biosynthesis Gene Cluster from Streptomyces griseochromogenes: Sequence Analysis, Organization, and Initial Characterization. *ChemBioChem*, **2003**, *4*, 821–828.

[12] R. Chen, H. Zhang, G. Zhang, S. Li, G. Zhang, Y. Zhu, J. Liu, C. Zhang. Characterizing Amosamine Biosynthesis in Amicetin Reveals AmiG as a Reversible Retaining Glycosyltransferase. *J. Am. Chem. Soc.*, **2013**, *135*, 12152–12155.

[13] *Global Tuberculosis Report 2018*, **n.d.**

[14] R. M. G. J. Houben, P. J. Dodd. The Global Burden of Latent Tuberculosis Infection: A Re-estimation Using Mathematical Modelling. *PLoS Med.*, **2016**, *13*, 1–13.

[15] K. Sakamoto. The Pathology of Mycobacterium tuberculosis Infection. *Vet. Pathol.*, **2012**, *49*, 423–439.

[16] N. A. Knechel. Tuberculosis: Pathophysiology, Clinical Features, and Diagnosis. *Crit. Care Nurse*, **2009**, *29*, 34–43.

[17] S. D. Lawn, A. I. Zumla. Tuberculosis. *Lancet*, **2011**, *378*, 57–72.

[18] L. Ramakrishnan. Revisiting the role of the granuloma in tuberculosis. *Nat. Rev. Immunol.*, **2012**, *12*, 352–366.

[19] L. Helming, S. Gordon. The molecular basis of macrophage fusion. *Immunobiology*, **2008**, *212*, 785–793.

[20] L. Ramakrishnan. Revisiting the role of the granuloma in tuberculosis. *Nat. Rev. Immunol.*, **2012**, *12*, 352–366.

[21] K. Dheda, H. Booth, J. F. Huggett, M. A. Johnson, A. Zumla, G. A. W. Rook. Lung Remodeling in Pulmonary Tuberculosis. *J. Infect. Dis.*, **2005**, *192*, 1201–1209.

[22] H. Ndlovu, M. J. Marakalala. Granulomas and Inflammation: Host-Directed Therapies for Tuberculosis. *Front. Immunol.*, **2016**, *7*, DOI 10.3389/fimmu.2016.00434.

[23] L. . Fu, C. . Fu-Liu. Is Mycobacterium tuberculosis a closer relative to Gram-positive or Gram–negative bacterial pathogens? *Tuberculosis*, **2002**, *82*, 85–90.

[24] F. Ziehl. Zur Färbung des Tuberkelbacillus. *DMW - Dtsch. Medizinische Wochenschrift*, **1882**, *8*, 451–451.

[25] K. A. ABRAHAMS, G. S. BESRA. Mycobacterial cell wall biosynthesis: a multifaceted antibiotic target. *Parasitology*, **2018**, *145*, 116–133.

[26] L. J. Alderwick, J. Harrison, G. S. Lloyd, H. L. Birch. The Mycobacterial Cell Wall—Peptidoglycan and Arabinogalactan. *Cold Spring Harb. Perspect. Med.*, **2015**, *5*, a021113.

[27] E. A. Talbot, B. J. Raffa. Mycobacterium tuberculosis, in *Mol. Med. Microbiol.*, Elsevier, **2015**, pp. 1637–1653.

[28] G. Delogu, M. Sali, G. Fadda. The Biology of Mycobacterium Tuberculosis Infection. *Mediterr. J. Hematol. Infect. Dis.*, **2013**, *5*, 2013070.

[29] M. Achtman. Evolution, Population Structure, and Phylogeography of Genetically Monomorphic Bacterial Pathogens. *Annu. Rev. Microbiol.*, **2008**, *62*, 53–70.

[30] R. P. Morris, L. Nguyen, J. Gatfield, K. Visconti, K. Nguyen, D. Schnappinger, S. Ehrt, Y. Liu, L. Heifets, J. Pieters, G. Schoolnik, C. J. Thompson. Ancestral antibiotic resistance in Mycobacterium tuberculosis. *Proc. Natl. Acad. Sci.*, **2005**, *102*, 12200–12205.

[31] M. C. Kjellsson, L. E. Via, A. Goh, D. Weiner, K. M. Low, S. Kern, G. Pillai, C. E. Barry, V. Dartois. Pharmacokinetic Evaluation of the Penetration of Antituberculosis Agents in Rabbit Pulmonary Lesions. *Antimicrob. Agents Chemother.*, **2012**, *56*, 446–457.

[32] S. A. Munro, S. A. Lewin, H. J. Smith, M. E. Engel, A. Fretheim, J. Volmink. Patient Adherence to Tuberculosis Treatment: A Systematic Review of Qualitative Research. *PLoS Med.*, **2007**, *4*, e238.

[33] WHO. *What Is DOTS? A Guide to Understanding the WHO-Recommended TB Control Strategy Known as DOTS*, **1999**.

[34] S. Asmar, M. Drancourt. Rapid culture-based diagnosis of pulmonary tuberculosis in developed and developing countries. *Front. Microbiol.*, **2015**, *6*, 1184.

[35] K. R. Steingart, H. Sohn, I. Schiller, L. A. Kloda, C. C. Boehme, M. Pai, N. Dendukuri. Xpert® MTB/RIF assay for pulmonary tuberculosis and rifampicin resistance in adults, in *Cochrane Database Syst. Rev.*, (Ed: K.R. Steingart), John Wiley & Sons, Ltd, Chichester, UK, **2013**.

[36] S. E. Dorman, S. G. Schumacher, D. Alland, P. Nabeta, D. T. Armstrong, B. King, S. L. Hall, S. Chakravorty, D. M. Cirillo, N. Tukvadze, N. Bablishvili, W. Stevens, L. Scott, C. Rodrigues, M. I. Kazi, M. Joloba, L. Nakiyingi, M. P. Nicol, Y. Ghebrekristos, I. Anyango, W. Murithi, R. Dietze, R. Lyrio Peres, A. Skrahina, V. Auchynka, K. K. Chopra, M. Hanif, X. Liu, X. Yuan, C. C. Boehme, J. J. Ellner, C. M. Denkinger, S. E. Dorman, S. G. Schumacher, D. Alland, P. Nabeta, D. T. Armstrong, B. King, S. L. Hall, S. Chakravorty, D. M. Cirillo, N. Tukvadze, N. Bablishvili, W. Stevens, L. Scott, C. Rodrigues, M. I. Kazi, M. Joloba, L. Nakiyingi, M. P. Nicol, Y. Ghebrekristos, I. Anyango, W.

Murithi, R. Dietze, R. L. Peres, A. Skrahina, V. Auchynka, K. K. Chopra, M. Hanif, X. Liu, X. Yuan, C. C. Boehme, J. J. Ellner, C. M. Denkinger, Y. C. Manabe, D. Hom, R. Aspindzelashvili, A. David, U. Surve, L. H. Kamulegeya, S. Nabweyambo, S. Surtie, N. Hapeela, K. P. Cain, J. Agaya, K. D. McCarthy, P. Marques-Rodrigues, L. G. Schmidt Castellani, P. S. Almeida, P. P. L. de Aguiar, V. Solodovnikova, X. Ruan, L. Liang, G. Zhang, H. Zhu, Y. Xie. Xpert MTB/RIF Ultra for detection of Mycobacterium tuberculosis and rifampicin resistance: a prospective multicentre diagnostic accuracy study. *Lancet Infect. Dis.*, **2018**, *18*, 76–84.

[37] S. Chakravorty, A. M. Simmons, M. Rowneki, H. Parmar, Y. Cao, J. Ryan, P. P. Banada, S. Deshpande, S. Shenai, A. Gall, J. Glass, B. Krieswirth, S. G. Schumacher, P. Nabeta, N. Tukvadze, C. Rodrigues, A. Skrahina, E. Tagliani, D. M. Cirillo, A. Davidow, C. M. Denkinger, D. Persing, R. Kwiatkowski, M. Jones, D. Alland. The New Xpert MTB/RIF Ultra: Improving Detection of Mycobacterium tuberculosis and Resistance to Rifampin in an Assay Suitable for Point-of-Care Testing. *MBio*, **2017**, *8*, 00812–17.

[38] N. C. Bahr, E. Nuwagira, E. E. Evans, F. V Cresswell, P. V Bystrom, A. Byamukama, S. C. Bridge, A. S. Bangdiwala, D. B. Meya, C. M. Denkinger, C. Muzoora, D. R. Boulware, D. A. Williams, K. Taseera, D. Nyehangane, M. Ivan, P. Orikiriza, J. Rhein, K. H. Hullsiek, A. Musubire, K. Pastick, P. Nabeta, J. Mwesigye, R. Rajasingham. Diagnostic accuracy of Xpert MTB/RIF Ultra for tuberculous meningitis in HIV-infected adults: a prospective cohort study. *Lancet Infect. Dis.*, **2018**, *18*, 68–75.

[39] A. Schatz, E. Bugle, S. A. Waksman. Streptomycin, a Substance Exhibiting Antibiotic Activity Against Gram-Positive and Gram-Negative Bacteria. *Exp. Biol. Med.*, **1944**, *55*, 66–69.

[40] Interview: Fighting resistance. An interview with the late John Crofton. *Bull. World Health Organ.*, **2009**, *87*, 894–895.

[41] G. Sotgiu, R. Centis, L. D'ambrosio, G. B. Migliori. Tuberculosis Treatment and Drug Regimens. *Cold Spring Harb. Perspect. Med.*, **2015**, *5*, a017822–a017822.

[42] A. Koul, E. Arnoult, N. Lounis, J. Guillemont, K. Andries. The challenge of new drug discovery for tuberculosis. *Nature*, **2011**, *469*, 483–490.

[43] J. J. Saukkonen, D. L. Cohn, R. M. Jasmer, S. Schenker, J. A. Jereb, C. M. Nolan, C. A. Peloquin, F. M. Gordin, D. Nunes, D. B. Strader, J. Bernardo, R. Venkataramanan, T. R. Sterling. An Official ATS Statement: Hepatotoxicity of Antituberculosis Therapy. *Am. J. Respir. Crit. Care Med.*, **2006**, *174*, 935–952.

[44] E. J. Forget, D. Menzies. Adverse reactions to first-line antituberculosis drugs. *Expert Opin. Drug Saf.*, **2006**, *5*, 231–249.

[45] T. Schaberg, K. Rebhan, H. Lode. Risk factors for side-effects of isoniazid, rifampin and pyrazinamide in patients hospitalized for pulmonary tuberculosis. *Eur. Respir. J.*, **1996**, *9*, 2026–2030.

[46] A. Zumla, P. Nahid, S. T. Cole. Advances in the development of new tuberculosis drugs and treatment regimens. *Nat. Rev. Drug Discov.*, **2013**, *12*, 388–404.

[47] WHO. WHO treatment guidelines for drug-resistant tuberculosis. **2016**.

[48] A. S. Ginsburg, J. H. Grosset, W. R. Bishai. Fluoroquinolones, tuberculosis, and resistance. *Lancet Infect. Dis.*, **2003**, *3*, 432–442.

[49] T. A. Vannelli, A. Dykman, P. R. Ortiz de Montellano. The Antituberculosis Drug Ethionamide Is Activated by a Flavoprotein Monooxygenase. *J. Biol. Chem.*, **2002**, *277*, 12824–12829.

[50] G. A. Prosser, L. P. S. Carvalho. Kinetic mechanism and inhibition of Mycobacterium

tuberculosis d-alanine: d-alanine ligase by the antibiotic d-cycloserine. *FEBS J.*, **2013**, *280*, 1150–1166.

[51] D. L. Shinabarger, K. R. Marotti, R. W. Murray, A. H. Lin, E. P. Melchior, S. M. Swaney, D. S. Dunyak, W. F. Demyan, J. M. Buysse. Mechanism of action of oxazolidinones: effects of linezolid and eperezolid on translation reactions. *Antimicrob. Agents Chemother.*, **1997**, *41*, 2132–2136.

[52] B. Lechartier, S. T. Cole. Mode of Action of Clofazimine and Combination Therapy with Benzothiazinones against Mycobacterium tuberculosis. *Antimicrob. Agents Chemother.*, **2015**, *59*, 4457–4463.

[53] T. Yano, S. Kassovska-Bratinova, J. S. Teh, J. Winkler, K. Sullivan, A. Isaacs, N. M. Schechter, H. Rubin. Reduction of Clofazimine by Mycobacterial Type 2 NADH:Quinone Oxidoreductase. *J. Biol. Chem.*, **2011**, *286*, 10276–10287.

[54] P. Nahid, S. E. Dorman, N. Alipanah, P. M. Barry, J. L. Brozek, A. Cattamanchi, L. H. Chaisson, R. E. Chaisson, C. L. Daley, M. Grzemska, J. M. Higashi, C. S. Ho, P. C. Hopewell, S. A. Keshavjee, C. Lienhardt, R. Menzies, C. Merrifield, M. Narita, R. O'Brien, C. A. Peloquin, A. Raftery, J. Saukkonen, H. S. Schaaf, G. Sotgiu, J. R. Starke, G. B. Migliori, A. Vernon. Executive Summary: Official American Thoracic Society/Centers for Disease Control and Prevention/Infectious Diseases Society of America Clinical Practice Guidelines: Treatment of Drug-Susceptible Tuberculosis. *Clin. Infect. Dis.*, **2016**, *63*, 853–867.

[55] T. W. Yang, H. O. Park, H. N. Jang, J. H. Yang, S. H. Kim, S. H. Moon, J. H. Byun, C. E. Lee, J. W. Kim, D. H. Kang. Side effects associated with the treatment of multidrug-resistant tuberculosis at a tuberculosis referral hospital in South Korea. *Medicine (Baltimore).*, **2017**, *96*, e7482.

[56] C. Roger, J. A. Roberts, L. Muller. Clinical Pharmacokinetics and Pharmacodynamics of Oxazolidinones. *Clin. Pharmacokinet.*, **2018**, *57*, 559–575.

[57] D. J. Girling. Adverse Effects of Antituberculosis Drugs. *Drugs*, **1982**, *23*, 56–74.

[58] M. R. de Jonge, L. H. M. Koymans, J. E. G. Guillemont, A. Koul, K. Andries. A computational model of the inhibition of Mycobacterium tuberculosis ATPase by a new drug candidate R207910. *Proteins Struct. Funct. Bioinforma.*, **2007**, *67*, 971–980.

[59] M. T. Gler, V. Skripconoka, E. Sanchez-Garavito, H. Xiao, J. L. Cabrera-Rivero, D. E. Vargas-Vasquez, M. Gao, M. Awad, S.-K. Park, T. S. Shim, G. Y. Suh, M. Danilovits, H. Ogata, A. Kurve, J. Chang, K. Suzuki, T. Tupasi, W.-J. Koh, B. Seaworth, L. J. Geiter, C. D. Wells. Delamanid for Multidrug-Resistant Pulmonary Tuberculosis. *N. Engl. J. Med.*, **2012**, *366*, 2151–2160.

[60] L. Guglielmetti, M. Jaspard, D. Le Dû, M. Lachâtre, D. Marigot-Outtandy, C. Bernard, N. Veziris, J. Robert, Y. Yazdanpanah, E. Caumes, M. Fréchet-Jachym. Long-term outcome and safety of prolonged bedaquiline treatment for multidrug-resistant tuberculosis. *Eur. Respir. J.*, **2017**, *49*, 1601799.

[61] J. M. Lewis, P. Hine, J. Walker, S. H. Khoo, M. Taegtmeyer, S. B. Squire, D. J. Sloan. First experience of effectiveness and safety of bedaquiline for 18 months within an optimised regimen for XDR-TB. *Eur. Respir. J.*, **2016**, *47*, 1581–1584.

[62] R. C. Hartkoorn, S. Uplekar, S. T. Cole. Cross-Resistance between Clofazimine and Bedaquiline through Upregulation of MmpL5 in Mycobacterium tuberculosis. *Antimicrob. Agents Chemother.*, **2014**, *58*, 2979–2981.

[63] C. D. Wells, R. Gupta, N. Hittel, L. J. Geiter. Long-term mortality assessment of multidrug-resistant tuberculosis patients treated with delamanid. *Eur. Respir. J.*, **2015**, *45*, 1498–1501.

[64] S. Tiberi, A. Scardigli, R. Centis, L. D'Ambrosio, M. Muñoz-Torrico, M. Á. Salazar-Lezama, A. Spanevello, D. Visca, A. Zumla, G. B. Migliori, J. A. Caminero Luna. Classifying new anti-tuberculosis drugs: rationale and future perspectives. *Int. J. Infect. Dis.*, **2017**, *56*, 181–184.

[65] G. Sotgiu, L. D'Ambrosio, R. Centis, S. Tiberi, S. Esposito, S. Dore, A. Spanevello, G. Migliori. Carbapenems to Treat Multidrug and Extensively Drug-Resistant Tuberculosis: A Systematic Review. *Int. J. Mol. Sci.*, **2016**, *17*, 373.

[66] H. Yao, J. Liu, S. Xu, Z. Zhu, J. Xu. The structural modification of natural products for novel drug discovery. *Expert Opin. Drug Discov.*, **2017**, *12*, 121–140.

[67] D. J. Newman, G. M. Cragg. Natural Products as Sources of New Drugs from 1981 to 2014. *J. Nat. Prod.*, **2016**, *79*, 629–661.

[68] G. M. Cragg, D. J. Newman. Natural Products as Sources of Anticancer Agents: Current Approaches and Perspectives, in *Nat. Prod. as Source Mol. with Ther. Potential*, Springer International Publishing, Cham, **2018**, pp. 309–331.

[69] D. J. Newman, G. M. Cragg. Natural Products As Sources of New Drugs over the 30 Years from 1981 to 2010. *J. Nat. Prod.*, **2012**, *75*, 311–335.

[70] D. J. Newman. Natural Products as Leads to Potential Drugs: An Old Process or the New Hope for Drug Discovery? *J. Med. Chem.*, **2008**, *51*, 2589–2599.

[71] D. J. Newman, G. M. Cragg, K. M. Snader. The influence of natural products upon drug discovery. *Nat. Prod. Rep.*, **2000**, *17*, 215–234.

[72] I. Paterson. The Renaissance of Natural Products as Drug Candidates. *Science (80-.).*, **2005**, *310*, 451–453.

[73] S. Hanessian. *Natural Products in Medicinal Chemistry*, Wiley-VCH Verlag GmbH & Co. KGaA, Weinheim, Germany, **2014**.

[74] T. Henkel, R. M. Brunne, H. Müller, F. Reichel. Statistical Investigation into the Structural Complementarity of Natural Products and Synthetic Compounds. *Angew. Chemie Int. Ed.*, **1999**, *38*, 643–647.

[75] G. M. Cragg, D. J. Newman. Natural products: A continuing source of novel drug leads. *Biochim. Biophys. Acta - Gen. Subj.*, **2013**, *1830*, 3670–3695.

[76] M. Dong, B. Pfeiffer, K.-H. Altmann. Recent developments in natural product-based drug discovery for tuberculosis. *Drug Discov. Today*, **2017**, *22*, 585–591.

[77] K.-H. Altmann. Drugs from the Oceans: Marine Natural Products as Leads for Drug Discovery. *Chim. Int. J. Chem.*, **2017**, *71*, 646–652.

[78] P. Sensi. History of the Development of Rifampin. *Clin. Infect. Dis.*, **1983**, *5*, S402–S406.

[79] B. S. Schuwirth, M. A. Borovinskaya, C. W. Hau, W. Zhang, A. Vila-Sanjurjo, J. M. Holton, J. H. D. Cate. Structures of the Bacterial Ribosome at 3.5 Å Resolution. *Science (80-.).*, **2005**, *310*, 827–834.

[80] C. G. Kurland. Molecular characterization of ribonucleic acid from Escherichia coli ribosomes. *J. Mol. Biol.*, **1960**, *2*, 83–91.

[81] N. Ban. The Complete Atomic Structure of the Large Ribosomal Subunit at 2.4 A Resolution. *Science (80-.).*, **2000**, *289*, 905–920.

[82] V. Ramakrishnan. Ribosome Structure and the Mechanism of Translation. *Cell*, **2002**, *108*, 557–572.

[83] L. L. Kisselev, R. H. Buckingham. Translational termination comes of age. *Trends Biochem. Sci.*, **2000**, *25*, 561–566.

[84] N. Polacek, A. S. Mankin. The Ribosomal Peptidyl Transferase Center: Structure, Function, Evolution, Inhibition. *Crit. Rev. Biochem. Mol. Biol.*, **2005**, *40*, 285–311.

[85] V. I. Katunin, G. W. Muth, S. A. Strobel, W. Wintermeyer, M. V Rodnina. Important Contribution to Catalysis of Peptide Bond Formation by a Single Ionizing Group within the Ribosome. *Mol. Cell*, **2002**, *10*, 339–346.

[86] M. Beringer, M. V. Rodnina. The Ribosomal Peptidyl Transferase. *Mol. Cell*, **2007**, *26*, 311–321.

[87] A. Sievers, M. Beringer, M. V. Rodnina, R. Wolfenden. The ribosome as an entropy trap. *Proc. Natl. Acad. Sci.*, **2004**, *101*, 7897–7901.

[88] E. M. Youngman, J. L. Brunelle, A. B. Kochaniak, R. Green. The Active Site of the Ribosome Is Composed of Two Layers of Conserved Nucleotides with Distinct Roles in Peptide Bond Formation and Peptide Release. *Cell*, **2004**, *117*, 589–599.

[89] W. P. Tate, C. M. Brown. Translational termination: “stop” for protein synthesis or “pause” for regulation of gene expression. *Biochemistry*, **1992**, *31*, 2443–2450.

[90] T. M. Schmeing, V. Ramakrishnan. What recent ribosome structures have revealed about the mechanism of translation. *Nature*, **2009**, *461*, 1234–1242.

[91] A. B. Loveland, G. Demo, N. Grigorieff, A. A. Korostelev. Ensemble cryo-EM elucidates the mechanism of translation fidelity. *Nature*, **2017**, *546*, 113–117.

[92] J. L. Hansen, P. B. Moore, T. A. Steitz. Structures of Five Antibiotics Bound at the Peptidyl Transferase Center of the Large Ribosomal Subunit. *J. Mol. Biol.*, **2003**, *330*, 1061–1075.

[93] J. Lin, D. Zhou, T. A. Steitz, Y. S. Polikanov, M. G. Gagnon. Ribosome-Targeting Antibiotics: Modes of Action, Mechanisms of Resistance, and Implications for Drug Design. *Annu. Rev. Biochem.*, **2018**, *87*, 451–478.

[94] F. Schlünzen, R. Zarivach, J. Harms, A. Bashan, A. Tocilj, R. Albrecht, A. Yonath, F. Franceschi. Structural basis for the interaction of antibiotics with the peptidyl transferase centre in eubacteria. *Nature*, **2001**, *413*, 814–821.

[95] R. HOLT. THE BACTERIAL DEGRADATION OF CHLORAMPHENICOL. *Lancet*, **1967**, *289*, 1259–1260.

[96] D. Moazed, H. F. Noller. Chloramphenicol, erythromycin, carbomycin and vernamycin B protect overlapping sites in the peptidyl transferase region of 23S ribosomal RNA. *Biochimie*, **1987**, *69*, 879–884.

[97] A. Nozaka, A. Nishiwaki, Y. Nagashima, S. Endo, M. Kuroki, M. Nakajima, M. Narukawa, S. Kamisuki, T. Arazoe, H. Taguchi, F. Sugawara, T. Kamakura. Chloramphenicol inhibits eukaryotic Ser/Thr phosphatase and infection-specific cell differentiation in the rice blast fungus. *Sci. Rep.*, **2019**, *9*, 9283.

[98] J. Marks, K. Kannan, E. J. Roncase, D. Klepacki, A. Kefi, C. Orelle, N. Vázquez-Laslop, A. S. Mankin. Context-specific inhibition of translation by ribosomal antibiotics targeting the peptidyl transferase center. *Proc. Natl. Acad. Sci.*, **2016**, *113*, 12150–12155.

[99] J. A. Ippolito, Z. F. Kanyo, D. Wang, F. J. Franceschi, P. B. Moore, T. A. Steitz, E. M. Duffy. Crystal Structure of the Oxazolidinone Antibiotic Linezolid Bound to the 50S Ribosomal Subunit ‖. *J. Med. Chem.*, **2008**, *51*, 3353–3356.

[100] S. Takeuchi, K. Hirayama, K. Ueda, H. Sakai, H. Yonehara. Blasticidin S, a new antibiotic. *J.*

Antibiot. (Tokyo)., **1958**, *11*, 1–5.

[101] M. Kimura, I. Yamaguchi. Recent Development in the Use of Blasticidin S, a Microbial Fungicide, as a Useful Reagent in Molecular Biology. *Pestic. Biochem. Physiol.*, **1996**, *56*, 243–248.

[102] D. N. Wilson. On the specificity of antibiotics targeting the large ribosomal subunit. *Ann. N. Y. Acad. Sci.*, **2011**, *1241*, 1–16.

[103] E. Svidritskiy, C. Ling, D. N. Ermolenko, A. A. Korostelev. Blasticidin S inhibits translation by trapping deformed tRNA on the ribosome. *Proc. Natl. Acad. Sci.*, **2013**, *110*, 12283–12288.

[104] D. L. KALPAXIS, D. A. THEOCHARIS, C. COUTSOGEORGOPOULOS. Kinetic studies on ribosomal peptidyltransferase. The behaviour of the inhibitor blasticidin S. *Eur. J. Biochem.*, **1986**, *154*, 267–271.

[105] G. David, P. D. Shaw. *Antibiotics*, Springer Berlin Heidelberg, Berlin, Heidelberg, **1967**.

[106] J. C. LACAL, D. VÁZQUEZ, J. M. FERNANDEZ-SOUSA, L. CARRASCO. Antibiotics that specifically block translation in virus-infected cells. *J. Antibiot. (Tokyo).*, **1980**, *33*, 441–446.

[107] T. Ruusala, C. G. Kurland. Streptomycin preferentially perturbs ribosomal proofreading. *MGG Mol. Gen. Genet.*, **1984**, *198*, 100–104.

[108] I. G. Leviev, C. Rodriguez-Fonseca, H. Phan, R. A. Garrett, G. Heilek, H. F. Noller, A. S. Mankin. A conserved secondary structural motif in 23S rRNA defines the site of interaction of amicetin, a universal inhibitor of peptide bond formation. *EMBO J.*, **1994**, *13*, 1682–1686.

[109] R. Karimi, M. Ehrenberg. Dissociation rates of peptidyl-tRNA from the P-site of E.coli ribosomes. *EMBO J.*, **1996**, *15*, 1149–1154.

[110] J. Panecka, C. Mura, J. Trylska. Interplay of the Bacterial Ribosomal A-Site, S12 Protein Mutations and Paromomycin Binding: A Molecular Dynamics Study. *PLoS One*, **2014**, *9*, e111811.

[111] N. Vázquez-Laslop, A. S. Mankin. Context-Specific Action of Ribosomal Antibiotics. *Annu. Rev. Microbiol.*, **2018**, *72*, 185–207.

[112] E. C. Böttger, B. Springer, T. Prammananan, Y. Kidan, P. Sander. Structural basis for selectivity and toxicity of ribosomal antibiotics. *EMBO Rep.*, **2001**, *2*, 318–323.

[113] J. Berg, T. John, S. Lubert. *Biochemistry*, W.H. Freeman, **2002**.

[114] D. Wiegmann, S. Koppermann, M. Wirth, G. Niro, K. Leyerer, C. Ducho. Muraymycin nucleoside-peptide antibiotics: uridine-derived natural products as lead structures for the development of novel antibacterial agents. *Beilstein J. Org. Chem.*, **2016**, *12*, 769–795.

[115] T. D. H. Bugg. Nucleoside Natural Product Antibiotics Targetting Microbial Cell Wall Biosynthesis, in *BC Med. J.*, **2017**, pp. 1–25.

[116] L. P. Jordheim, D. Durantel, F. Zoulim, C. Dumontet. Advances in the development of nucleoside and nucleotide analogues for cancer and viral diseases. *Nat. Rev. Drug Discov.*, **2013**, *12*, 447–464.

[117] K. Stokowa-Sołtys, M. Jeżowska-Bojczuk. A rice fungicide blasticidin S efficiently binds Cu(II) ions and prevents DNA from metal-induced damage. *J. Inorg. Biochem.*, **2013**, *127*, 73–78.

[118] K. ISONO. Nucleoside antibiotics: Structure, biological activity, and biosynthesis. *J. Antibiot. (Tokyo).*, **1988**, *41*, 1711–1739.

[119] J. F. Fisher, S. Mobashery, M. M. J. *Antibacterials*, Springer International Publishing, Cham, **2018**.

[120] G. Niu, H. Tan. Nucleoside antibiotics: Biosynthesis, regulation, and biotechnology. *Trends Microbiol.*, **2015**, *23*, 110–119.

[121] K. Isono. Current progress on nucleoside antibiotics. *Pharmacol. Ther.*, **1991**, *52*, 269–286.

[122] A. Bloch, C. Coutsogeorgopoulos. Inhibition of Protein Synthesis by Amicetin, a Nucleoside Antibiotic *. *Biochemistry*, **1966**, *5*, 3345–3351.

[123] H. F. Noller. Ribosomal RNA and Translation. *Annu. Rev. Biochem.*, **1991**, *60*, 191–227.

[124] C. Coutsogeorgopoulos. Amino Acylaminonucleoside Inhibitors of Protein Synthesis. The Effect of Amino Acyl Ribonucleic Acid on the Inhibition *. *Biochemistry*, **1967**, *6*, 1704–1711.

[125] J. Donarski, C. Shammas, R. Banks, V. Ramesh. NMR and Molecular Modelling Studies of the Binding of Amicetin Antibiotic to Conserved Secondary Structural Motifs of 23S Ribosomal RNAs. *J. Antibiot. (Tokyo).*, **2006**, *59*, 177–183.

[126] C. Shammas, J. A. Donarski, V. Ramesh. NMR structure of the peptidyl transferase RNA inhibitor antibiotic amicetin. *Magn. Reson. Chem.*, **2007**, *45*, 133–141.

[127] J. King, C. Shammas, M. Nareen, M. Lelli, V. Ramesh. NMR characterisation of a highly conserved secondary structural RNA motif of Halobacterium halobium 23S rRNA. *Org. Biomol. Chem.*, **2013**, *11*, 3382.

[128] J. Donarski, C. Shammas, R. Banks, V. Ramesh. NMR and Molecular Modelling Studies of the Binding of Amicetin Antibiotic to Conserved Secondary Structural Motifs of 23S Ribosomal RNAs. *J. Antibiot. (Tokyo).*, **2006**, *59*, 177–183.

[129] C. Shammas, J. A. Donarski, V. Ramesh. NMR structure of the peptidyl transferase RNA inhibitor antibiotic amicetin. *Magn. Reson. Chem.*, **2007**, *45*, 133–141.

[130] A. P. Carter, W. M. Clemons, D. E. Brodersen, R. J. Morgan-Warren, B. T. Wimberly, V. Ramakrishnan. Functional insights from the structure of the 30S ribosomal subunit and its interactions with antibiotics. *Nature*, **2000**, *407*, 340–348.

[131] J. L. Hansen, J. A. Ippolito, N. Ban, P. Nissen, P. B. Moore, T. A. Steitz. The Structures of Four Macrolide Antibiotics Bound to the Large Ribosomal Subunit. *Mol. Cell*, **2002**, *10*, 117–128.

[132] C. L. Stevens, J. Nemec, G. H. Ransford. Total synthesis of the amino sugar nucleoside antibiotic, plicacetin. *J. Am. Chem. Soc.*, **1972**, *94*, 3280–3281.

[133] T. H. Haskell. Amicetin, Bamicetin and Plicacetin. Chemical Studies. *J. Am. Chem. Soc.*, **1958**, *80*, 747–751.

[134] H. Sugimura, K. Watanabe. FORMAL SYNTHESIS OF CYTOSAMINE—A COMPONENT OF NUCLEOSIDE ANTIBIOTICS, THE AMICETIN FAMILY. *Synth. Commun.*, **2001**, *31*, 2313–2321.

[135] R. J. Ferrier, N. Prasad. Unsaturated carbohydrates. Part IX. Synthesis of 2,3-dideoxy-α-D-erythro-hex-2-enopyranosides from tri-O-acetyl-D-glucal. *J. Chem. Soc. C*, **1969**, 570–575.

[136] K. C. Nicolaou, S. P. Seitz, D. P. Papahatjis. A Mild and General Method for the Synthesis of O-Glycosides. *J. Am. Chem. Soc.*, **1983**, *105*, 2430–2434.

[137] K. Fukase, A. Hasuoka, I. Kinoshita, Y. Aoki, S. Kusumoto. A stereoselective glycosidation using thioglycosides, activation by combination of N-bromosuccinimide and strong acid salts. *Tetrahedron*, **1995**, *51*, 4923–4932.

[138] J. Fu, S. Laval, B. Yu. Total Synthesis of Nucleoside Antibiotics Plicacetin and Streptcytosine A. *J. Org. Chem.*, **2018**, *83*, 7076–7084.

[139] Y. Li, Y. Yang, B. Yu. An efficient glycosylation protocol with glycosyl ortho-alkynylbenzoates as donors under the catalysis of Ph3PAuOTf. *Tetrahedron Lett.*, **2008**, *49*, 3604–3608.

[140] Y. Zhu, B. Yu. Characterization of the Isochromen-4-yl-gold(I) Intermediate in the Gold(I)-Catalyzed Glycosidation of Glycosyl ortho-Alkynylbenzoates and Enhancement of the Catalytic Efficiency Thereof. *Angew. Chemie Int. Ed.*, **2011**, *50*, 8329–8332.

[141] Y. Tang, J. Li, Y. Zhu, Y. Li, B. Yu. Mechanistic Insights into the Gold(I)-Catalyzed Activation of Glycosyl ortho -Alkynylbenzoates for Glycosidation. *J. Am. Chem. Soc.*, **2013**, *135*, 18396–18405.

[142] F. Yang, Y. Zhu, B. Yu. A dramatic concentration effect on the stereoselectivity of N-glycosylation for the synthesis of 2'-deoxy-β-ribonucleosides. *Chem. Commun.*, **2012**, *48*, 7097.

[143] C. L. Stevens, P. Blumbergs, D. L. Wood. Stereochemical Identification and Synthesis of Amicetose and the Stereochemical Identification of Rhodinose and the Sugar from Streptolydigin. *J. Am. Chem. Soc.*, **1964**, *86*, 3592–3594.

[144] C. L. Stevens, N. A. Nielsen, P. Blumbergs. Synthesis of 2,3-Didehydro-2,3-dideoxy and 2,3-Dideoxy Sugar Nucleosides of Known Configuration. *J. Am. Chem. Soc.*, **1964**, *86*, 1894–1895.

[145] C. M. Serrano, R. E. Looper. Synthesis of Cytimidine through a One-Pot Copper-Mediated Amidation Cascade. *Org. Lett.*, **2011**, *13*, 5000–5003.

[146] C. L. Stevens, J. Nemec, G. H. Ransford. Total synthesis of the amino sugar nucleoside antibiotic, plicacetin. *J. Am. Chem. Soc.*, **1972**, *94*, 3280–3281.

[147] K. Toshima. Glycosyl fluorides in glycosidations. *Carbohydr. Res.*, **2000**, *327*, 15–26.

[148] G. Lian, X. Zhang, B. Yu. Thioglycosides in Carbohydrate Research. *Carbohydr. Res.*, **2015**, *403*, 13–22.

[149] R. R. Schmidt, J. Michel. Facile Synthesis of α- and β-O-Glycosyl Imidates; Preparation of Glycosides and Disaccharides. *Angew. Chemie Int. Ed. English*, **1980**, *19*, 731–732.

[150] Z. Wang. Schmidt Glycosylation. *Compr. Org. Name React. Reagents*, **2010**, 2498–2502.

[151] X. Zhu, R. R. Schmidt. New Principles for Glycoside-Bond Formation. *Angew. Chemie Int. Ed.*, **2009**, *48*, 1900–1934.

[152] M. S. Anson, H. F. Clark, P. Evans, M. E. Fox, J. P. Graham, N. N. Griffiths, G. Meek, J. A. Ramsden, A. J. Roberts, S. Simmonds, M. D. Walker, M. Willets. Complementary Syntheses of N , O -Protected-(S)-2-methylserine on a Multikilogram Scale. *Org. Process Res. Dev.*, **2011**, *15*, 389–397.

[153] E. W. Dean, D. D. Stark. A Convenient Method for the Determination of Water in Petroleum and Other Organic Emulsions. *J. Ind. Eng. Chem.*, **1920**, *12*, 486–490.

[154] M. Brunner, P. Saarenketo, T. Straub, K. Rissanen, A. M. P. Koskinen. Stereocontrolledα-Alkylation of Fully ProtectedL-Serine. *European J. Org. Chem.*, **2004**, *2004*, 3879–3883.

[155] F. Fülöp, K. Pihlaja. Ring-chain tautomerism of oxazolidines derived from serine esters. *Tetrahedron*, **1993**, *49*, 6701–6706.

[156] I. McMillan, R. J. Stoodley. The absolute stereochemistry at C-2 of thiazolidines derived from R-penicillamine and aldehydes. *Chem. Commun.*, **1968**, 11–12.

[157] F. Fülöp, K. Pihlaja, J. Mattinen, G. Bernáth. Stereochemical studies 130 saturated heterocycles 132. *Tetrahedron*, **1987**, *43*, 1863–1869.

[158] D. Seebach, J. D. Aebi, M. Gander-Coquoz, R. Naef. Stereoselektive Alkylierung an C(α) von Serin, Glycerinsäure, Threonin und Weinsäure über heterocyclische Enolate mit exocyclischer Doppelbindung. *Helv. Chim. Acta*, **1987**, *70*, 1194–1216.

[159] D. Hocková, A. Holý, M. Masojídková, D. T. Keough, J. de Jersey, L. W. Guddat. Synthesis of branched 9-[2-(2-phosphonoethoxy)ethyl]purines as a new class of acyclic nucleoside phosphonates which inhibit Plasmodium falciparum hypoxanthine-guanine-xanthine phosphoribosyltransferase. *Bioorganic Med. Chem.*, **2009**, *17*, 6218–6232.

[160] P. Liu, E. N. Jacobsen. Total Synthesis of (+)-Ambruticin. *J. Am. Chem. Soc.*, **2001**, *123*, 10772–10773.

[161] A. Klapars, X. Huang, S. L. Buchwald. A general and efficient copper catalyst for the amidation of aryl halides. *J. Am. Chem. Soc.*, **2002**, *124*, 7421–7428.

[162] N. Ibrahim, M. Legraverend. Synthesis of 6,7,8-Trisubstituted Purines via a Copper-Catalyzed Amidation Reaction. *J. Org. Chem.*, **2009**, *74*, 463–465.

[163] D. R. Vutukuri, P. Bharathi, Z. Yu, K. Rajasekaran, M.-H. Tran, S. Thayumanavan. A Mild Deprotection Strategy for Allyl-Protecting Groups and Its Implications in Sequence Specific Dendrimer Synthesis. *J. Org. Chem.*, **2003**, *68*, 1146–1149.

[164] P. Boullanger, P. Chatelard, G. Descotes, M. Kloosterman, J. H. Van Boom. Use of the Allyloxycarbonyl Protective Group in Carbohydrate Chemistry. *J. Carbohydr. Chem.*, **1986**, *5*, 541–559.

[165] H. Frauenrath, T. Arenz, G. Raabe, M. Zorn. A Diastereoselective Synthesis of ?-(N-Acylamino)aldehydes by Rearrangement ofO-Vinyl-N,O-Acetals. *Angew. Chemie Int. Ed. English*, **1993**, *32*, 83–85.

[166] J. W. Tye, Z. Weng, A. M. Johns, C. D. Incarvito, J. F. Hartwig. Copper Complexes of Anionic Nitrogen Ligands in the Amidation and Imidation of Aryl Halides. *J. Am. Chem. Soc.*, **2008**, *130*, 9971–9983.

[167] B. Schmidt, A. Biernat. The tandem ring-closing metathesis-isomerization approach to 6-deoxyglycals. *Chemistry*, **2008**, *14*, 6135–41.

[168] U. Ramulu, D. Ramesh, S. Rajaram, S. P. Reddy, K. Venkatesham, Y. Venkateswarlu. Stereoselective total synthesis of clonostachydiol. *Tetrahedron: Asymmetry*, **2012**, *23*, 117–123.

[169] G. Yonghong, Z. Fangning, P. Xinfu. A Novel Route to Stereoselective Synthesis of (4R,5S)-O-Acetylosmundalactone and (4S,5R)-O-Acetylosmundalactone. *J. Chem. Res.*, **1999**, 488–489.

[170] M. Carda, S. Rodríguez, F. González, E. Castillo, A. Villanueva, J. A. Marco. Stereoselective Synthesis of the Naturally Occurring Lactones (−)-Osmundalactone and (−)-Muricatacine Using Ring-Closing Metathesis. *European J. Org. Chem.*, **2002**, *2002*, 2649–2655.

[171] S. V. Ley, A. Armstrong, D. Díez-Martín, M. J. Ford, P. Grice, J. G. Knight, H. C. Kolb, A. Madin, C. A. Marby, S. Mukherjee, A. N. Shaw, A. M. Z. Slawin, S. Vile, A. D. White, D. J. Williams, M. Woods. Total synthesis of the anthelmintic macrolide avermectin B1a. *J. Chem. Soc., Perkin Trans. 1*, **1991**, 667–692.

[172] M. Nakata, T. Ishiyama, S. Akamatsu, Y. Hirose, H. Maruoka, R. Suzuki, K. Tatsuta. Synthetic Studies on Oligomycins. Synthesis of the Oligomycin B Spiroketal and Polypropionate Portions. *Bull. Chem. Soc. Jpn.*, **1995**, *68*, 967–989.

[173] W. R. Roush, K. Koyama, M. L. Curtin, K. J. Moriarty. Studies on the synthesis of nargenicin A1: Highly stereoselective synthesis of the complete carbon framework via the transannular Diels-Alder reaction of an 18-membered macrolide. *J. Am. Chem. Soc.*, **1996**, *118*, 7502–7512.

[174] M. Chérest, H. Felkin, N. Prudent. Torsional strain involving partial bonds. The stereochemistry of the lithium aluminium hydride reduction of some simple open-chain ketones. *Tetrahedron Lett.*, **1968**, *9*, 2199–2204.

[175] H. B. Burgi, J. D. Dunitz, E. Shefter. Geometrical reaction coordinates. II. Nucleophilic addition to a carbonyl group. *J. Am. Chem. Soc.*, **1973**, *95*, 5065–5067.

[176] S. Wakabayashi, H. Ogawa, N. Ueno, N. Kunieda, T. Mandai, J. Nokami. Synthesis of Optically Active Litsenolide C. *Chem. Lett.*, **1987**, *16*, 875–878.

[177] A. K. Chatterjee, J. P. Morgan, M. Scholl, R. H. Grubbs. Synthesis of Functionalized Olefins by Cross and Ring-Closing Metatheses. *J. Am. Chem. Soc.*, **2000**, *122*, 3783–3784.

[178] A. E. Sutton, B. A. Seigal, D. F. Finnegan, M. L. Snapper. New Tandem Catalysis: Preparation of Cyclic Enol Ethers through a Ruthenium-Catalyzed Ring-Closing Metathesis−Olefin Isomerization Sequence. *J. Am. Chem. Soc.*, **2002**, *124*, 13390–13391.

[179] B. Schmidt. An Olefin Metathesis/Double Bond Isomerization Sequence Catalyzed by an In Situ Generated Ruthenium Hydride Species. *European J. Org. Chem.*, **2003**, *2003*, 816–819.

[180] C. Cadot, P. I. Dalko, J. Cossy. Olefin isomerization by a ruthenium carbenoid complex. Cleavage of allyl and homoallyl groups. *Tetrahedron Lett.*, **2002**, *43*, 1839–1841.

[181] B. Alcaide, P. Almendros, J. M. Alonso. Ruthenium-Catalyzed Chemoselective N-Allyl Cleavage: Novel Grubbs Carbene Mediated Deprotection of Allylic Amines. *Chem. - A Eur. J.*, **2003**, *9*, 5793–5799.

[182] S. Krompiec, M. Pigulla, T. Bieg, W. Szczepankiewicz, N. Kuźnik, M. Krompiec, M. Kubicki. Isomerisation of N-allyl-N-arylethanamides catalysed by ruthenium complexes. *J. Mol. Catal. A Chem.*, **2002**, *189*, 169–185.

[183] W. A. L. van Otterlo, E. L. Ngidi, C. B. de Koning. Sequential isomerization and ring-closing metathesis: masked styryl and vinyloxyaryl groups for the synthesis of benzo-fused heterocycles. *Tetrahedron Lett.*, **2003**, *44*, 6483–6486.

[184] H. Wakamatsu, M. Nishida, N. Adachi, M. Mori. Isomerization Reaction of Olefin Using RuClH(CO)(PPh 3) 3. *J. Org. Chem.*, **2000**, *65*, 3966–3970.

[185] T. M. Trnka, J. P. Morgan, M. S. Sanford, T. E. Wilhelm, M. Scholl, T.-L. Choi, S. Ding, M. W. Day, R. H. Grubbs. Synthesis and Activity of Ruthenium Alkylidene Complexes Coordinated with Phosphine and N-Heterocyclic Carbene Ligands. *J. Am. Chem. Soc.*, **2003**, *125*, 2546–2558.

[186] D. V. McGrath, R. H. Grubbs. The mechanism of aqueous ruthenium(II)-catalyzed olefin isomerization. *Organometallics*, **1994**, *13*, 224–235.

[187] G.-J. Boons. Recent developments in chemical oligosaccharide synthesis. *Contemp. Org. Synth.*, **1996**, *3*, 173.

[188] anomeric effect, in *IUPAC Compend. Chem. Terminol.*, IUPAC, Research Triagle Park, NC, **n.d.**

[189] E. Juaristi, G. Cuevas. Recent studies of the anomeric effect. *Tetrahedron*, **1992**, *48*, 5019–5087.

[190] T. B. Johnson, G. E. Hilbert. THE SYNTHESIS OF PYRIMIDINE-NUCLEOSIDES. *Science (80-.).*, **1929**, *69*, 579–580.

[191] G. E. Hilbert, T. B. Johnson. Researches on pyrimidines. CXVII. A method for the synthesis of nucleosides. *J. Am. Chem. Soc.*, **1930**, *52*, 4489–4494.

[192] T. Nishimura, B. Shimizu, I. Iwai. A New Synthetic Method of Nucleosides. *Chem. Pharm. Bull. (Tokyo).*, **1963**, *11*, 1470–1472.

[193] L. Birkofer, P. Richter, A. Ritter. „Aktivierung" N-haltiger Heterocyclen durch Silylierung. *Chem. Ber.*, **1960**, *93*, 2804–2809.

[194] U. Niedballa, H. Vorbrüggen. A General Synthesis of Pyrimidine Nucleosides. *Angew. Chemie Int. Ed. English*, **1970**, *9*, 461–462.

[195] H. Vorbrüggen, G. Höfle. Nucleoside Syntheses, XXIII1) On the Mechanism of Nucleoside Synthesis. *Chem. Ber.*, **1981**, *114*, 1256–1268.

[196] U. Niedballa, H. Vorbrueggen. Synthesis of nucleosides. 9. General synthesis of N-glycosides. I. Synthesis of pyrimidine nucleosides. *J. Org. Chem.*, **1974**, *39*, 3654–3660.

[197] M. Böhringer, H.-Jör. Roth, J. Hunziker, M. Göbel, R. Krishnan, A. Giger, B. Schweizer, J. Schreiber, C. Leumann, A. Eschenmoser. Warum Pentose- und nicht Hexose-Nucleinsäuren??. Teil II. Oligonucleotide aus 2',3'-Dideoxy-β-D-glucopyranosyl-Bausteinen ('Homo-DNS'): Herstellung. *Helv. Chim. Acta*, **1992**, *75*, 1416–1477.

[198] M. Karplus. Vicinal Proton Coupling in Nuclear Magnetic Resonance. *J. Am. Chem. Soc.*, **1963**, *85*, 2870–2871.

[199] D. M. Whitfield. In a glycosylation reaction how does a hydroxylic nucleophile find the activated anomeric carbon? *Carbohydr. Res.*, **2015**, *403*, 69–89.

[200] I. Braccini, C. Derouet, J. Esnault, C. H. de Penhoat, J.-M. Mallet, V. Michon, P. Sinaÿ. Conformational analysis of nitrilium intermediates in glycosylation reactions. *Carbohydr. Res.*, **1993**, *246*, 23–41.

[201] T. Hansen, L. Lebedel, W. A. Remmerswaal, S. van der Vorm, D. P. A. Wander, M. Somers, H. S. Overkleeft, D. V. Filippov, J. Désiré, A. Mingot, Y. Bleriot, G. A. van der Marel, S. Thibaudeau, J. D. C. Codée. Defining the SN1 Side of Glycosylation Reactions: Stereoselectivity of Glycopyranosyl Cations. *ACS Cent. Sci.*, **2019**, acscentsci.9b00042.

[202] L. Ayala, C. G. Lucero, J. A. C. Romero, S. A. Tabacco, K. A. Woerpel. Stereochemistry of Nucleophilic Substitution Reactions Depending upon Substituent: Evidence for Electrostatic Stabilization of Pseudoaxial Conformers of Oxocarbenium Ions by Heteroatom Substituents. *J. Am. Chem. Soc.*, **2003**, *125*, 15521–15528.

[203] J. A. C. Romero, S. A. Tabacco, K. A. Woerpel. Stereochemical Reversal of Nucleophilic Substitution Reactions Depending upon Substituent: Reactions of Heteroatom-Substituted Six-Membered-Ring Oxocarbenium Ions through Pseudoaxial Conformers. *J. Am. Chem. Soc.*, **2000**, *122*, 168–169.

[204] H. H. Jensen, M. Bols. Stereoelectronic Substituent Effects. *Acc. Chem. Res.*, **2006**, *39*, 259–265.

[205] R. J. Woods, C. W. Andrews, J. P. Bowen. Molecular mechanical investigations of the properties of oxocarbenium ions. 2. Application to glycoside hydrolysis. *J. Am. Chem. Soc.*, **1992**, *114*, 859–864.

[206] A. J. Birch. 117. Reduction by dissolving metals. Part I. *J. Chem. Soc.*, **1944**, 430.

[207] T. J. Donohoe, R. E. Thomas. The partial reduction of electron-deficient pyrroles: procedures describing both Birch (Li/NH3) and ammonia-free (Li/DBB) conditions. *Nat. Protoc.*, **2007**, *2*,

1888–1895.

[208] T. Mukaiyama, Y. Murai, S. Shoda. An efficient method for glucosylation of hydroxy compounds using glucopyranosyl fluoride. *Chem. Lett.*, **1981**, *10*, 431–432.

[209] K. C. Nicolaou, T. J. Caulfield, H. Katoaka. Total synthesis of globotriaosylceramide (Gb3) and lysoglobotriaosylceramide (lysoGb3). *Carbohydr. Res.*, **1990**, *202*, 177–191.

[210] W. Koenigs, E. Knorr. Ueber einige Derivate des Traubenzuckers und der Galactose. *Berichte der Dtsch. Chem. Gesellschaft*, **1901**, *34*, 957–981.

[211] T. Mukaiyama. Explorations into New Reaction Chemistry. *Angew. Chemie Int. Ed.*, **2004**, *43*, 5590–5614.

[212] H. T. Clarke, H. B. Gillespie, S. Z. Weisshaus. The Action of Formaldehyde on Amines and Amino Acids 1. *J. Am. Chem. Soc.*, **1933**, *55*, 4571–4587.

[213] W. Eschweiler. Ersatz von an Stickstoff gebundenen Wasserstoffatomen durch die Methylgruppe mit Hülfe von Formaldehyd. *Berichte der Dtsch. Chem. Gesellschaft*, **1905**, *38*, 880–882.

[214] K. C. Nicolaou, R. E. Dolle, D. P. Papahatjis. Practical synthesis of oligosaccharides. Partial synthesis of avermectin B1a. *J. Am. Chem. Soc.*, **1984**, *106*, 4189–4192.

[215] C. H. Heathcock, R. Ratcliffe. A Stereoselective Total Synthesis of the Guaiazulenic Sesquiterpenoids α-Bulnesene and Bulnesol. *J. Am. Chem. Soc.*, **1971**, *93*, 1746–1757.

[216] W. H. Hartung, R. Simonoff. Hydrogenolysis of Benzyl Groups Attached to Oxygen, Nitrogen, or Sulfur, in *Org. React.*, John Wiley & Sons, Inc., Hoboken, NJ, USA, **2011**, pp. 263–326.

[217] A. M. Felix, E. P. Heimer, T. J. Lambros, C. Tzougraki, J. Meienhofer. Rapid Removal of Protecting Groups from Peptides by Catalytic Transfer Hydrogenation with 1,4-Cyclohexadiene. *J. Org. Chem.*, **1978**, *43*, 4194–4196.

[218] N. Ikemoto, S. L. Schreiber. Total synthesis of (-)-hikizimycin employing the strategy of two-directional chain synthesis. *J. Am. Chem. Soc.*, **1992**, *114*, 2524–2536.

[219] D. R. Williams, D. L. Brown, J. W. Benbow. Studies of Stemona Alkaloids. Total Synthesis of (+)-Croomine. *J. Am. Chem. Soc.*, **1989**, *111*, 1923–1925.

[220] T. Akiyama, H. Hirofuji, S. Ozaki. AlCl3-N,N-dimethylaniline: A new benzyl and allyl ether cleavage reagent. *Tetrahedron Lett.*, **1991**, *32*, 1321–1324.

[221] M. S. Congreve, E. C. Davison, M. A. M. Fuhry, A. B. Holmes, A. N. Payne, R. A. Robinson, S. E. Ward. Selective Cleavage of Benzyl Ethers. *Synlett*, **1993**, *1993*, 663–664.

[222] K. D. Philips, J. Žemlička, J. P. Horwitz. Unsaturated sugars I. Decarboxylative elimination of methyl 2,3-di-O-benzyl-α-D-glucopyranosiduronic acid to methyl 2,3-di-O-benzyl-4-deoxy-β-L-threo-Pent-4-enopyranoside. *Carbohydr. Res.*, **1973**, *30*, 281–286.

[223] A. Hense, S. V. Ley, H. M. I. Osborn, D. R. Owen, J.-F. Poisson, S. L. Warriner, K. E. Wesson. Direct preparation of diacetals from 1,2-diketones and their use as 1,2-diol protecting groups. *J. Chem. Soc. Perkin Trans. 1*, **1997**, 2023–2032.

[224] R. J. Ferrier, R. W. Hay, N. Vethaviyasar. A potentially versatile synthesis of glycosides. *Carbohydr. Res.*, **1973**, *27*, 55–61.

[225] K. C. Nicolaou, S. P. Seitz, D. P. Papahatjis. A Mild and General Method for the Synthesis of O-Glycosides. *J. Am. Chem. Soc.*, **1983**, *105*, 2430–2434.

[226] M. H. Clausen, M. R. Jørgensen, J. Thorsen, R. Madsen. A strategy for chemical synthesis of selectively methyl-esterified oligomers of galacturonic acid. *J. Chem. Soc. Perkin Trans. 1*, **2001**, 543–551.

[227] B. Yu, H. Tao. Glycosyl trifluoroacetimidates. Part 1: Preparation and application as new glycosyl donors. *Tetrahedron Lett.*, **2001**, *42*, 2405–2407.

[228] B. A. Granger, D. G. Brown. Design and synthesis of peptide-based macrocyclic cyclophilin inhibitors. *Bioorg. Med. Chem. Lett.*, **2016**, *26*, 5304–5307.

[229] W. J. Choi, H. S. Ahn, H. O. Kim, S. Kim, M. W. Chun, L. S. Jeong. Stereoselective synthesis of amino-substituted apio dideoxynucleosides through a distant neighboring group effect. *Tetrahedron Lett.*, **2002**, *43*, 6241–6243.

[230] S. Inuki, K. Sato, Y. Fujimoto. Visible-light-mediated decarboxylative benzoyloxylation of β-hydroxy amino acids and its application to synthesis of functional 1,2-amino alcohol derivatives. *Tetrahedron Lett.*, **2015**, *56*, 5787–5790.

[231] D. M. Coe, R. Perciaccante, P. A. Procopiou. Potassium trimethylsilanolate induced cleavage of 1,3-oxazolidin-2- and 5-ones, and application to the synthesis of (R)-salmeterol. *Org. Biomol. Chem.*, **2003**, *1*, 1106–1111.

[232] K. L. Bhat, M. M. Joullie. Cyclopeptide alkaloids. *J. Chem. Educ.*, **1987**, *64*, 21.

[233] E. Tuenter, V. Exarchou, S. Apers, L. Pieters. Cyclopeptide alkaloids. *Phytochem. Rev.*, **2017**, *16*, 623–637.

[234] D. C. Gournelis, G. G. Laskaris, R. Verpoorte. Cyclopeptide alkaloids. *Nat. Prod. Rep.*, **1997**, *14*, 75.

[235] R. Tschesche, M. Elgamal, G. Eckhardt. Alkaloide aus Rhamnaceen, XXVIII. Nummularin-G, -H und -K, weitere Peptidalkaloide ausZiziphus nummularia. *Chem. Ber.*, **1977**, *110*, 2649–2655.

[236] S.-S. Lee, W.-C. Su, K. C. S. C. Liu. Cyclopeptide alkaloids from stems of Paliurus ramossisimus. *Phytochemistry*, **2001**, *58*, 1271–1276.

[237] U. Schmidt, A. Lieberknecht, H. Boekens, H. Griesser. Total synthesis of zizyphine A. Synthesis of peptide alkaloids. 8. Amino acids and peptides. 40. *J. Org. Chem.*, **1983**, *48*, 2680–2685.

[238] P. Panseeta, K. Lomchoey, S. Prabpai, P. Kongsaeree, A. Suksamrarn, S. Ruchirawat, S. Suksamrarn. Antiplasmodial and antimycobacterial cyclopeptide alkaloids from the root of Ziziphus mauritiana. *Phytochemistry*, **2011**, *72*, 909–915.

[239] U. Schmidt, U. Schanbacher. Total Synthesis of Mucronin B. *Angew. Chemie Int. Ed. English*, **1983**, *22*, 152–153.

[240] U. Schmidt, M. Zäh, A. Lieberknecht. The total synthesis of frangulanine. *J. Chem. Soc., Chem. Commun.*, **1991**, 1002–1004.

[241] J. C. Lagarias, R. A. Houghten, H. Rapoport. Cyclopeptide alkaloids. Synthesis of the ring system and its ion affinity. *J. Am. Chem. Soc.*, **1978**, *100*, 8202–8209.

[242] R. J. Heffner, M. M. Joullié. Studies directed toward the total synthesis of 14-membered cyclopeptide alkaloids: Synthesis of a cyclic precursor to nummularine-F. *Tetrahedron Lett.*, **1989**, *30*, 7021–7024.

[243] B. H. Lipshutz, B. E. Huff, K. E. McCarthy, S. M. J. Mukarram, T. J. Siahaan, W. D. Vaccaro, H. Webb, A. M. Falick, T. A. Miller. Oxazolophanes as masked cyclopeptide alkaloid equivalents: cyclic peptide chemistry without peptide couplings. *J. Am. Chem. Soc.*, **1990**, *112*, 7032–7041.

[244] M. Toumi, V. Rincheval, A. Young, D. Gergeres, E. Turos, F. Couty, B. Mignotte, G. Evano. A General Route to Cyclopeptide Alkaloids: Total Syntheses and Biological Evaluation of Paliurines E and F, Ziziphines N and Q, Abyssenine A, Mucronine E, and Analogues. *European J. Org. Chem.*, **2009**, *2009*, 3368–3386.

[245] M. Toumi, F. Couty, G. Evano. Total Synthesis of Paliurine F. *Angew. Chemie*, **2007**, *119*, 578–581.

[246] G. He, J. Wang, D. Ma. Highly convergent route to cyclopeptide alkaloids. Total synthesis of ziziphine N. *Org. Lett.*, **2007**, *9*, 1367–1369.

[247] S. Chen, J. Xu. Pentafluorophenyl diphenylphosphinate a new efficient coupling reagent in peptide chemistry. *Tetrahedron Lett.*, **1991**, *32*, 6711–6714.

[248] M. Toumi, V. Rincheval, A. Young, D. Gergeres, E. Turos, F. Couty, B. Mignotte, G. Evano. A General Route to Cyclopeptide Alkaloids: Total Syntheses and Biological Evaluation of Paliurines E and F, Ziziphines N and Q, Abyssenine A, Mucronine E, and Analogues. *European J. Org. Chem.*, **2009**, *2009*, 3368–3386.

[249] G. Stork, K. Zhao. A stereoselective synthesis of (Z)-1-iodo-1-alkenes. *Tetrahedron Lett.*, **1989**, *30*, 2173–2174.

[250] M. Toumi, F. Couty, G. Evano. Total Synthesis of the Cyclopeptide Alkaloid Paliurine E. Insights into Macrocyclization by Ene−Enamide RCM. *J. Org. Chem.*, **2008**, *73*, 1270–1281.

[251] K. W. Anderson, T. Ikawa, R. E. Tundel, S. L. Buchwald. The Selective Reaction of Aryl Halides with KOH: Synthesis of Phenols, Aromatic Ethers, and Benzofurans. *J. Am. Chem. Soc.*, **2006**, *128*, 10694–10695.

[252] D. C. M. Chan, H. Fu, R. A. Forsch, S. F. Queener, A. Rosowsky. Design, Synthesis, and Antifolate Activity of New Analogues of Piritrexim and Other Diaminopyrimidine Dihydrofolate Reductase Inhibitors with ω-Carboxyalkoxy or ω-Carboxy-1-alkynyl Substitution in the Side Chain. *J. Med. Chem.*, **2005**, *48*, 4420–4431.

[253] X. Zhang, Y. Zhang, J. Huang, R. P. Hsung, K. C. M. Kurtz, J. Oppenheimer, M. E. Petersen, I. K. Sagamanova, L. Shen, M. R. Tracey. Copper(II)-Catalyzed Amidations of Alkynyl Bromides as a General Synthesis of Ynamides and Z -Enamides. An Intramolecular Amidation for the Synthesis of Macrocyclic Ynamides. *J. Org. Chem.*, **2006**, *71*, 4170–4177.

[254] A. Coste, G. Karthikeyan, F. Couty, G. Evano. Copper-Mediated Coupling of 1,1-Dibromo-1-alkenes with Nitrogen Nucleophiles: A General Method for the Synthesis of Ynamides. *Angew. Chemie Int. Ed.*, **2009**, *48*, 4381–4385.

[255] A. J. Zapata, J. Rúiz. Palladium-catalyzed coupling reactions of functionalized styryl bromides with 1-propenyltributyltin. *J. Organomet. Chem.*, **1994**, *479*, c6–c8.

[256] R. S. Narayan, M. S. VanNieuwenhze. Versatile and Stereoselective Syntheses of Orthogonally Protected β-Methylcysteine and β-Methyllanthionine. *Org. Lett.*, **2005**, *7*, 2655–2658.

[257] Y. Mao, Y. Liu, Y. Hu, L. Wang, S. Zhang, W. Wang. Pd-Catalyzed Debenzylation and Deallylation of Ethers and Esters with Sodium Hydride. *ACS Catal.*, **2018**, *8*, 3016–3020.

[258] K. Reimer. Ueber eine neue Bildungsweise aromatischer Aldehyde. *Berichte der Dtsch. Chem. Gesellschaft*, **1876**, *9*, 423–424.

[259] A. G. M. Barrett, C. D. Spilling. Transfer hydrogenation: A stereospecific method for the conversion of nitro alkanes into amines. *Tetrahedron Lett.*, **1988**, *29*, 5733–5734.

[260] C. A. Brown, V. K. Ahuja. Catalytic hydrogenation. VI. Reaction of sodium borohydride with

nickel salts in ethanol solution. P-2 Nickel, a highly convenient, new, selective hydrogenation catalyst with great sensitivity to substrate structure. *J. Org. Chem.*, **1973**, *38*, 2226–2230.

[261] J. O. Osby, B. Ganem. Rapid and efficient reduction of aliphatic nitro compounds to amines. *Tetrahedron Lett.*, **1985**, *26*, 6413–6416.

[262] P. M. Wovkulich, K. Shankaran, J. Kiegiel, M. R. Uskokovic. Total synthesis of 1233A. *J. Org. Chem.*, **1993**, *58*, 832–839.

[263] L.-J. Cheng, J.-H. Xie, Y. Chen, L.-X. Wang, Q.-L. Zhou. Enantioselective Total Synthesis of (−)-Δ8-THC and (−)-Δ9-THC via Catalytic Asymmetric Hydrogenation and SNAr Cyclization. *Org. Lett.*, **2013**, *15*, 764–767.

[264] M. V. Westphal, M. A. Schafroth, R. C. Sarott, M. A. Imhof, C. P. Bold, P. Leippe, A. Dhopeshwarkar, J. M. Grandner, V. Katritch, K. Mackie, D. Trauner, E. M. Carreira, J. A. Frank. Synthesis of Photoswitchable Δ 9 -Tetrahydrocannabinol Derivatives Enables Optical Control of Cannabinoid Receptor 1 Signaling. *J. Am. Chem. Soc.*, **2017**, *139*, 18206–18212.

[265] M. Sefkow, H. Kaatz. Selective protection of either the phenol or the hydroxy group in hydroxyalkyl phenols. *Tetrahedron Lett.*, **1999**, *40*, 6561–6562.

[266] S. Hanessian, G. J. Reddy, N. Chahal. Total Synthesis and Stereochemical Confirmation of Manassantin A, B, and B 1. *Org. Lett.*, **2006**, *8*, 5477–5480.

[267] G. M. Atkins, E. M. Burgess. The reactions of an N-sulfonylamine inner salt. *J. Am. Chem. Soc.*, **1968**, *90*, 4744–4745.

[268] E. M. Burgess, H. R. Penton, E. A. Taylor. Thermal reactions of alkyl N-carbomethoxysulfamate esters. *J. Org. Chem.*, **1973**, *38*, 26–31.

5 Curriculum Vitae

Lukas Leu

Date of Birth: 19th September 1989

Place of Birth: Horgen, ZH

Hometown: Hohenrain, LU, Switzerland

Nationality: Swiss

Scientific Experience

01/2015 – 08/2019 **PhD Thesis** with Prof. Dr. Karl-Heinz Altmann, ETH Zürich

01/2013 – 07/2013 **Intern**, Novartis Pharma AG, Basel, Switzerland

Planning and chemical synthesis of potential active compounds in drug discovery. Systematic documentation and communication of scientific data.

Education

01/2015 – 08/2019 **Doctoral Studies**, ETH Zürich, Switzerland

09/2013 – 09/2014 **Master of Science in Biology**, ETH Zürich, Switzerland

Master thesis in the group of Prof. Dr. Antognio Togni; "Silyl-Promoted Trifluoromethylation of Amides"

09/2009 – 08/2012 **Bachelor of Science in Biology**, ETH Zürich, Switzerland

08/2002 – 08/2008 **Matura**, Gymnasium Freudenberg, Zurich, Switzerland

Emphasis on languages; Latin, English, French

Teaching Experience

- Supervision of two semester students.
- Lab course Pharmaceutical Biology: Isolation and quantification of natural products (annually in April/May, 2015, 2016, 2017, 2018, 2019).
- Lab course General Chemistry: Introductory lab course (October 2018).

Publication

Schäfer, G.; Leu, L.; Bode, J. W. "Synthesis of Unsymmetrical, gem-Disubstituted Bisamides" *Heterocycles* **2015**, *90*, 1375–1386

Presentations

1. Leu, L.; Altmann K.-H., poster presentation "Studies Towards the Total Synthesis of Amicetin" September 7th, 2018, SCS Fall Meeting, EPFL, Switzerland.
2. Leu, L.; Altmann K.-H., poster presentation "Studies Towards the Total Synthesis of Amicetin" May 20th - 25th, 2018, European Workshop in Drug Synthesis, Sienna, Italy. Winning the "best poster presentation" award.
3. Leu, L.; Altmann K.-H., oral presentation "Studies towards the total synthesis of the antimycobacterial natural product amicetin" February 14th, 2018, Doktorandentag, ETH Zürich.